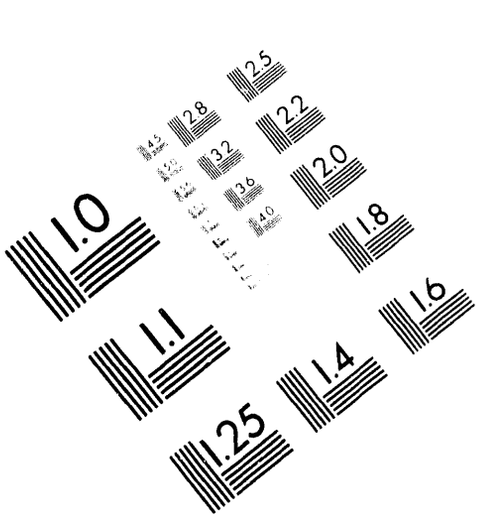

Association for Information and Image Management
1100 Wayne Avenue, Suite 1100
Silver Spring, Maryland 20910
301/587-8202

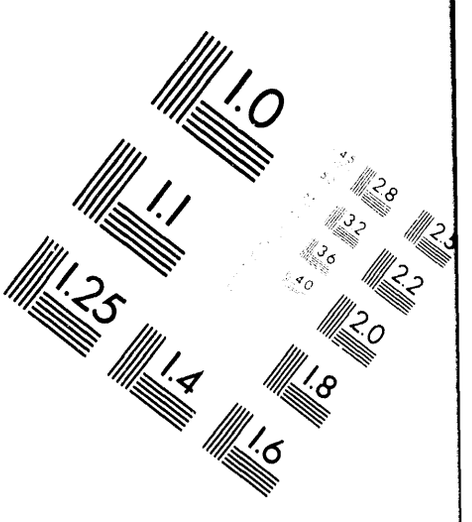

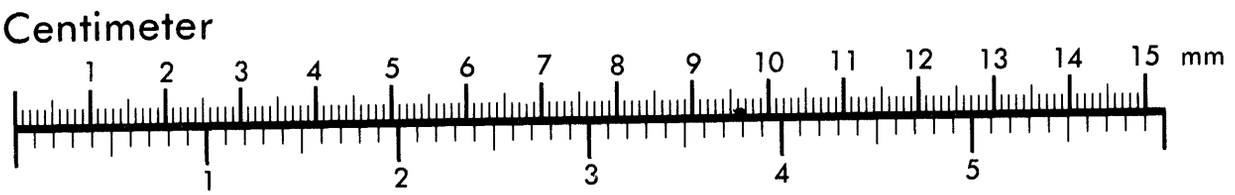

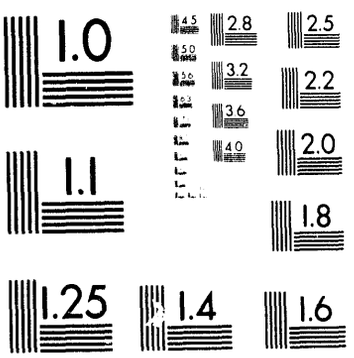

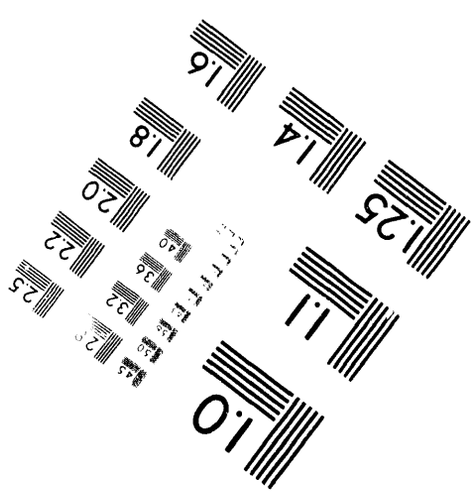

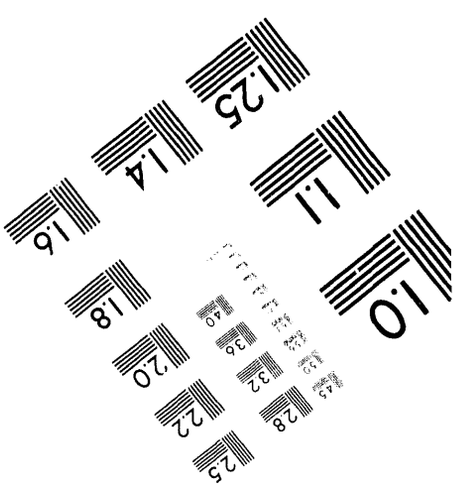

MANUFACTURED TO AIIM STANDARDS
BY APPLIED IMAGE, INC.

1 of 6

DOE/METC-94/1008, Vol. 1
(CONF-9406131)-Vol.1
(DE94012252)
Distribution Category UC-103
UC-106
UC-111

Proceedings of the Coal-Fired Power Systems 94 -- Advances in IGCC and PFBC Review Meeting Volume I

Editors
Heather M. McDaniel
Ronald K. Staubly
Venkat K. Venkataraman

Sponsored by
U.S. Department of Energy
Office of Fossil Energy
Morgantown Energy Technology Center
P.O. Box 880
Morgantown, West Virginia 26507-0880
(304) 291-4764
FAX (304) 291-4403/4469

June 21-23, 1994

MASTER

Foreword

The Coal-Fired Power Systems 94 -- Advances in IGCC and PFBC Review Meeting was held June 21-23, 1994, at the Morgantown Energy Center (METC) in Morgantown, West Virginia. This Meeting was sponsored and hosted by METC, the Office of Fossil Energy, and the U.S. Department of Energy (DOE).

METC annually sponsors this conference for energy executives, engineers, scientists, and other interested parties to review the results of research and development projects; to discuss the status of advanced coal-fired power systems and future plans with the industrial contractors; and to discuss cooperative industrial-government research opportunities with METC's in-house engineers and scientists. Presentations included industrial contractor and METC in-house technology developments related to the production of power via coal-fired Integrated Gasification Combined Cycle (IGCC) and Pressurized Fluidized Bed Combustion (PFBC) systems, the summary status of clean coal technologies, and developments and advancements in advanced technology subsystems, such as hot gas cleanup. A keynote speaker and other representatives from the electric power industry also gave their assessment of advanced power systems.

This meeting contained 11 formal sessions and one poster session, and included 52 presentations and 24 poster presentations. The papers printed in this document have been produced from camera-ready manuscripts provided by the authors. They have been neither refereed nor extensively edited.

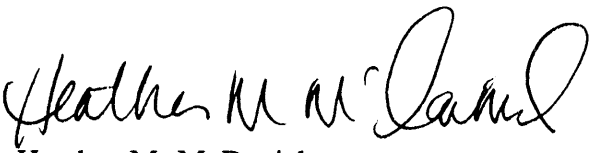

Heather M. McDaniel
Conference Technical Coordinator
Coal Conversion and Cleanup Branch

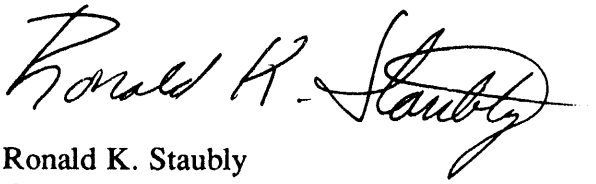

Ronald K. Staubly
Conference Technical Coordinator
Coal Conversion and Cleanup Branch

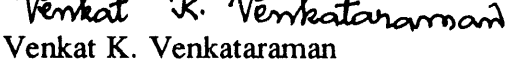

Venkat K. Venkataraman
Conference Technical Coordinator
Technology Base Projects Management Division

Acknowledgments

This document was made possible by the efforts of many dedicated individuals who participated in the Coal-Fired Power Systems 94 -- Advances in IGCC and PFBC Review Meeting. We thank those participants who presented project status summaries, those who made the poster session true technology exhibits, and those who contributed to the interesting and lively discussions during the course of the meeting.

A note of thanks is extended to the session chairpersons: Harvey M. Ness, Rita A. Bajura, Justin L. Beeson, Dale K. Schmidt, Donald L. Bonk, Randall J. Dellefield, Richard A. Dennis, Ronald K. Staubly, Darren J. Mollot, Theodore J. McMahon, Peter E. Botros, Lee D. Gasper-Galvin, and Susan K. Joines. Special recognition is given to J. Wayne Leonard, Vice-President and Chief Financial Officer of PSI Energy, for an interesting keynote speech on "Evolving Utility Business Structure and Impact on New Technology Application" and to Thomas F. Bechtel, Director of the Morgantown Energy Technology Center, for an informative speech on "The Role of Advanced Technology in the Future of the Power Generation Industry." We also thank Ron Wolk from the Energy Power Research Institute, Dale Simbeck from SFA Pacific, the presenters from the various offices of DOE, and the research contractors for their presentations.

Special thanks are extended to the Conference Services staff, the Graphics staff, and the Technical Writing staff of EG&G, Technical Services of West Virginia. These individuals are gratefully acknowledged for providing excellent coordination of and support services at the meeting.

Contents

Volume I

Session 1 -- Opening Commentaries

1.1 The Role of Advanced Technology in the Future of the Power Generation Industry -- Thomas F. Bechtel 3

1.2 Evolving Utility Business Structure and Impact on New Technology Application -- J. Wayne Leonard 12

Session 2 -- Changes in the Market and Technology Drivers

2.1 Overview of Global Utility Market for Advanced Coal Fired Systems -- Ronald H. Wolk and Neville A. Holt 27

2.2 Overview of the Independent Power Producer (IPP) Market for Advanced Coal-Fired Systems -- Dale R. Simbeck, Stan Vejtasa, and Alan Karp 48

2.3 The Search for Innovative Technology -- C. Lowell Miller 58

Session 3 -- Advanced IGCC Systems

Integrated Gasification Combined Cycle - A View to the Future -- Dale K. Schmidt 61

3.1 IGCC System Studies -- Lawrence K. Rath, George T. Lee, and Patrick H. Le 65

3.2 Transport Reactor Development Status -- Randall E. Rush, Martin O. Fankhanel, and William M. Campbell 73

3.3 Gasification Product Improvement Facility Status -- R. Don Carson, Vijay B. Dixit, Richard S. Sadowski, William H. Skinner, Robert A. Lisauskas, and Stephen A. Johnson 83

Session 4 -- Advanced PFBC Systems

4.1 PFBC System Studies -- Michael E. Reed 93

Contents

(Continued)

4.2 Second-Generation PFBC Systems Research and Development - Phase 2: Circulating PFBC Test Results -- Archie Robertson, James Van Hook, Frank Burkhard, Giovanni Carli, Rich Conn, Paul Crooker, Dave Kulcsar, Chongqing Lu, Anthony Mack, Aydemir Nehrozoglu, Mark Torpey, and Frank Zoldak 104

4.3 Status of the Advanced PFBC at the Power Systems Development Facility -- Randall E. Rush, Darrell L. Moore, Zia Haq, Timothy E. Pinkston, P. Vimalchand, James D. McClung, and Michael T. Quandt 127

Session 5 -- Advanced Filter Systems

5.1 Status of the Morgantown Energy Technology Center's Particulate Cleanup Program: Enabling Technology for Advanced Coal-Based Power Systems -- Richard A. Dennis 141

5.2 Potential Industry Use of Continuous Fiber Ceramic Composites -- Jill Jonkouski 144

5.3 Ceramic Fiber Ceramic Matrix Filter Development -- Roddie R. Judkins, Melvin A. Leitheiser, David P. Stinton, Robert G. Smith, and Edward M. Fischer 145

5.4 Westinghouse Advanced Particle Filter System -- Thomas E. Lippert, Gerald J. Bruck, Zal N. Sanjana, and Richard A. Newby 152

5.5 IF&P Fibrosic™ Filters -- Paul M. Eggerstedt 166

5.6 Multi-Contaminant Control Granular Bed Filter -- Keith B. Wilson, John C. Haas, and Cheryl Anne Olivo 176

5.7 Westinghouse Standleg Moving Granular Bed Filter Development Program -- Richard A. Newby, Wen-Ching Yang, Eugene E. Smeltzer, and Thomas E. Lippert 186

5.8 MTCI Acoustic Agglomeration Particulate Control -- Ravi R. Chandran, Momtaz N. Mansour, Alan W. Scaroni, Gary H. Koopmann, and John L. Loth 195

Contents

(Continued)

Session 6 -- Desulfurization Systems

6.1 METC Hot Gas Desulfurization Program Overview -- Daniel C. Cicero 219

6.2 Integrated Operation of a Pressurized Gasifier, Hot Gas Desulfurization System and Turbine Simulator -- Steve Bevan, David Najewicz, Eli Gal, Anthony H. Furman, Raul Ayala, and Alan Feitelberg 222

6.3 Enviropower Hot Gas Desulfurization Pilot -- Kari Salo, Reza Ghazanfari, Gabor Feher, Jukka Konttinen, Arto Lehtovaara, and Wahab Mojtahedi 236

6.4 Slipstream Testing of the Direct Sulfur Recovery Process -- Santosh K. Gangwal, Jeffrey W. Portzer, Gary B. Howe, Daniel H. Chen, and Michael H. McMillian 246

6.5 METC Fluid-Bed Hot-Gas Desulfurization PDU -- Larry A. Bissett 256

Session 7 -- Turbine Systems

7.1 Development of Topping Combustor for Advanced Concept Pressurized Fluidized Bed Combustion -- William F. Domeracki, Thomas E. Dowdy, and Dennis Bachovchin 265

7.2 Development and Testing of Low Btu Fuel Gas Turbine Combustors -- Stephen Bevan, Nesim Abuaf, Alan S. Feitelberg, Stephen L. Hung, Martin S. Samuels, and Anil K. Tolpadi 280

7.3 Advanced Turbine Systems Program Overview -- Holmes A. Webb 290

Poster Session

P1 High Temperature Electrochemical Separation of H_2S from Coal Gasification Streams -- E. Faith Gleason and Jack Winnick 295

P2 Characterization and Fixed-Bed Testing of a Nickel-Based Hot Gas Desulfurization Sorbent -- Lee D. Gasper-Galvin, James H. Swisher, and Kurt Hammerbeck 308

Contents

(Continued)

P3 Pilot Gasification and Hot Gas Cleanup Operations -- John M. Rockey, Edwin Galloway, Teresa A. Thomson, Jay Rutten, and Alain Lui 321

P4 Coal Ash Behavior in Reducing Environments -- Steven A. Benson, Thomas A. Erickson, David W. Brekke, Bruce C. Folkedahl, James E. Tibbetts, and Jan W. Nowok 322

P5 Hot Coal Gas Desulfurization with Manganese-Based Sorbents -- Malcolm T. Hepworth and Rachid Ben-Slimane 337

P6 A Calcium Oxide Sorbent Process for Bulk Separation of Carbon Dioxide -- Douglas P. Harrison and C. Han 351

P7 COMPCOAL™: A Profitable Process for Production of a Stable High-Btu Fuel from Powder River Basin Coal -- Verne E. Smith and Norm W. Merriam 361

P8 Development of Biological Coal Gasification (MicGAS Process) -- Daman S. Walia and Kailash C. Srivastava 376

P9 Simultaneous Removal of H_2S and NH_3 in Coal Gasification Processes -- K. Jothimurugesan, Adeyinka A. Adeyiga, and Santosh K. Gangwal 398

P10 Granular Filtration in a Fluidized Bed -- J. S. Mei, P. C. Yue, and J. S. Halow 403

P11 Dust Cake Behavior in Filters With High Surface Area to Volume Ratios -- Douglas Straub, Ta-Kuan Chiang, and Richard A. Dennis 405

P12 Computer Simulations of IGCC/PFBC Components -- Edward J. Boyle, Thomas J. O'Brien, Lawrence J. Shadle, Madhava Syamlal, and Suresh Venkatesan 411

P13 Scaling of Pressurized Fluidized Beds -- Susan Guralnik and Leon R. Glicksman 413

P14 Evaluation of Options for CO_2 Capture/Utilization/Disposal -- David K. Schmalzer, Richard D. Doctor, and C. David Livengood 422

P15 Absorption of Hydrogen Sulfide by Zinc Ferrite in the Temperature Range 315 to 538 °C (600 to 1,000 °F) -- Thomas Grindley and C. Elaine Everitt 431

Contents

(Continued)

P16 High Temperature Hydrogen Sulfide Removal with Stannic Oxide -- Michael E. Karpuk, Robert J. Copeland, D. Feinberg, D. Wickham, B. Windecker, and J. Yu 444

P17 Fossil Fuel Conversion - Measurement and Modeling -- Peter R. Solomon, L. Douglas Smoot, Michael A. Serio, David G. Hamblen, B. Scott Brewster, and Predrag T. Radulovic 458

P18 CeraMem Filters for Removal of Particles from Hot Gas Streams -- Bruce A. Bishop and Robert L. Goldsmith 469

P19 Development of Disposable Sorbents for Chloride Removal from High-Temperature Coal-Derived Gases -- Gopala N. Krishnan, B. J. Wood, A. Canizales, R. Gupta, S. D. Sheluker, and R. Ayala 478

P20 PyGas Design Support -- Lawrence J. Shadle, Abolghasem Shamsi, Guo-Qing Zhang, Edward J. Boyle, Yau-Hsin Wang, Madhava Syamlal, and Kalkunte Seshadri 490

P21 Chloride and Mercury Monitors for Air Toxics Measurements -- William H. Buttermore, Glenn A. Norton, Colin D. Chriswell, Dave E. Eckels, and Rachel E. Peters 492

P22 Cooperative Research and Development Agreements at METC -- J. Christopher Ludlow, Lisa A. Jarr, and William F. Lawson 498

P23 Optimal Design and Synthesis of Advanced Power Systems under Uncertainty -- Urmila M. Diwekar, Edward S. Rubin, and H. Christopher Frey 499

P24 Development of a Radio Frequency Surface Contour Mapping System -- William H. Buttermore, Robert J. Weber, and Warren E. Straszheim 513

Contents
(Continued)

Volume II

Session 8a -- Filter Technical Issues

8a.1 Tidd PFBC Hot Gas Filter Operating Experience: July 1993 - April 1994 -- Michael J. Mudd and John D. Hoffman 519

8a.2 Karhula Hot Gas Cleanup Test Results -- Thomas E. Lippert, Gerald J. Bruck, and Juhani Isaksson 535

8a.3 Durability of Ceramic Filters -- Mary Anne Alvin, Richard E. Tressler, Thomas E. Lippert, Edward S. Diaz, and Eugene E. Smeltzer 545

8a.4 Properties of Ceramic Candle Filters -- Duane H. Pontius and H. Stuart Starrett 572

8a.5 Results of Patch Tests -- Duane H. Pontius 575

8a.6 PFBC Dust Cake Studies -- Thomas E. Lippert, Richard A. Newby, Mary Anne Alvin, Dennis M. Bachovchin, and Eugene E. Smeltzer 580

Session 8b -- Hazardous Air Pollutants

8b.1 Comprehensive Assessment of Toxic Emissions From Coal-Fired Power Plants -- Thomas D. Brown 591

8b.2 Trace Element Emissions -- Steven A. Benson, Thomas A. Erickson, Edward N. Steadman, Christopher J. Zygarlicke, William B. Hauserman, and David J. Hassett 592

8b.3 HAP Sampling at Tidd PFBC -- Michael J. Mudd and Patrick A. Dal Porto 607

8b.4 Trace Species Emissions for IGFC -- A. Ed Pigeaud and J. J. Helble 616

8b.5 Hazardous Air Pollutant Sampling for Advanced Power Systems -- Gwen Eklund, Robert G. Wetherold, Al Williams, David P. Maxwell, Robert M. Mann, and Don B. Burrows 627

8b.6 Instrumentation for Trace Emission Measurements -- William P. Chisholm 632

Contents
(Continued)

Session 9a -- Sorbents and Solid Wastes

9a.1 Development of Sorbents for High-Temperature Desulfurization in Moving-Bed Systems -- Raul E. Ayala, Timothy Chuck, Eli Gal, and Raghubir P. Gupta 637

9a.2 Fluidized-Bed Sorbents -- Santosh K. Gangwal and Raghubir P. Gupta 646

9a.3 Fluidization Studies Using Phillips Z-SORB Sorbent -- Santosh K. Gangwal, Raghubir P. Gupta, Gyanesh P. Khare, Gary A. Delzer, and Don H. Kubicek 654

9a.4 Desulfurization Sorbent Development at the Morgantown Energy Technology Center -- Ranjani V. Siriwardane, Ulrich Grimm, James Poston, and Steven Monaco 662

9a.5 Stabilization of Spent Calcium-Based Sorbent -- Philip J. Shires, Satyan Katta, and Gunnar B. Henningsen 668

9a.6 Market Assessment and Technical Feasibility Study of PFBC Ash Use -- Verne E. Smith, Alan E. Bland, Terry H. Brown, Demetri N. Georgiou, and John Wheeldon 679

9a.7 Co-Firing Waste Materials in an Advanced Pressurized Fluidized-Bed Combustor -- Lynn N. Rubow, Michael R. DeLallo, and Roman Zaharchuk ... 690

Session 9b -- Membranes

9b.1 High Temperature Size Selective Membrances -- Stephen F. Yates, S. James Zhou, David J. Anderson, and Alan E. van Til 703

9b.2 A Catalytic Membrane Reactor for Facilitating the Water-Gas Shift Reaction at High Temperature -- David J. Edlund 709

9b.3 New Developments in Hydrogen Permselective Membranes -- George R. Gavalas 714

9b.4 Preparation and Characterization of Composite Membrane for High Temperature Gas Separation -- Shamsuddin Ilias, Franklin G. King, and Nan Su 721

Contents
(Continued)

9b.5 Development of Hollow Fiber Catalytic Membrane Reactors for High Temperature Gas Cleanup -- Y. H. Ma, W. R. Moser, S. Pien, and A. B. Shelekhin 727

9b.6 Thermal/Chemical Degradation of Inorganic Membrane Materials -- Gopala N. Krishnan, Angel Sanjurjo, Ashok S. Damle, Bernard J. Wood, and Kai-Hung Lau 736

Appendices

Appendix A. Agenda 747

Appendix B. Meeting Participants 758

Appendix C. METC Participants 774

Session 1

Opening Commentaries

1.1 The Role of Advanced Technology in the Future of the Power Generation Industry

Thomas F. Bechtel
Morgantown Energy Technology Center

My talk today will attempt to portray a vision for the future of the electric power generation industry that has advanced technology as a key element. Given today's highly competitive markets, the demands on capital to meet environmental regulation on existing plants, and the technology risk adversity of the industry, you might be inclined to treat this vision as a fantasy conjured up by a gypsy fortune teller with a faulty crystal ball. However, if you grant me 30 minutes or so to look at how the industry's history has defined its culture, how today's economic and regulatory climate has constrained its strategy, and how certain technology options might give some of the players an unfair advantage, you might give the vision some credibility.

As William Faulkner so aptly put it; "The past is never past; it is always with us." With that in mind, I'd like to take you on a short "Back to the Future" look at the power generation industry. The electric power generation industry in the United States, as we know it today, can trace its roots to September, 1882, and Thomas Edison's Pearl Street Generating Station, which lighted a square mile of New York City with direct current produced by six 100-KW steam engine-driven dynamos. Edison's partner in that enterprise was Samuel Insull, his private secretary. They would eventually dominate the industry, Edison on the equipment side - Insull on the operating side. The steam engine/dynamo combination offered few economies of scale and many initial customers preferred self-generation, an approach that Edison feared would never provide the cost edge he wanted over the "hated gas industry".

A letter written by Insull to friends in England just before Pearl Street opened, while he was still Edison's secretary is most illuminating. Let me read you an excerpt:

> "You ask me about electric light. Well, I have seen 700 lights burning, the current generated from the same dynamo-electric machine for the whole lot, all of them getting their current from the same main (i.e., street cables) of no less than eight miles in length. Edison gets eight lights or thereabouts of 16 candles each per indicated horse-power, which allows of his competing with gas. Into the details of the cost I cannot go, as it is not told to anybody.[1] Suffice to say that here in New York he can produce light and get a handsome profit on it at a charge to the consumer which would ruin the gas companies. There is not, however, that vast difference between the cost of the two lights which will allow him to be utterly oblivious of his friends, the gas producers; but his estimates show that he can compete with them and do it at a handsome profit. Besides he can furnish power by means of electric motors, which will give him an enormous pull over the gas companies as he will not have the greater part of his plant lying idle during 365 working days of the year, as the gas companies with but very slight exception must, as the business is at night; but he can sell electricity for power purposes by day, which means that his plant is never

idle, his capital is never running to waste, but is always earning money by night and by day alike. Edison will work just as the gas companies do. He will have central stations where the current will be generated (probably one station of about 15,000 lights to each square mile). This current will be conveyed along the streets underground by means of copper wire embedded in two-inch iron pipes insulated with a special form of insulation of his own invention. Branch pipes will be led into each house, and the electricity, whether for light or power (to us it is all the same), will be sold by means of a registration on an electric meter, which is the most ingenious and yet the simplest thing imaginable.[2] The district which he will light up first in New York has about 15,650 lights in the various buildings in the district and a great deal of power in varying amounts. He is getting contracts just as fast as his canvassers apply for them, and we have large gangs of men wiring the houses in anticipation of the time when we can lay our mains, erect our dynamo machinery and light up. I suppose this district will be all lighted up in from three to four months, and then you will see what you will see. - - -

"Menlo Park is practically abandoned. All experiments are finished[3]; all speculation on the probable results are dismissed; and Edison thinks, and so does everyone else who has looked into the matter, that success is assured. Of course, time alone can prove this. As for myself, I am not competent to judge but I can use my eyes, can see the success with which the houses, the fields, roads and depot have been illuminated here, and I can see nothing to disprove the assertations. His lamps last about 400 hours; at all events that is the estimate by a time test, i.e., by running them at about four times their ordinary candle power until the carbons break; but this estimate is every day falsified, and experience points to the conclusion that the life of his lamps will be much longer than the estimate. As for rivals, Edison has but little to fear, in fact, none, from them. - - -

"To carry out the gigantic undertaking of fighting the gas companies we have much to do. A great difficulty is to get our machinery manufactured. This Mr. Edison will attend to himself. He personally has taken a very large works for this purpose, where he will probably within the next six months have 1500 men at work. The various parts of the machines will be contracted out, one firm making one part in large quantities, another firm another part, and so on. At Mr. Edison's works ("Edison Machine Works"), all these parts will be assembled and put together. Then there is the lamp factory, in which Mr. Edison owns almost all the interest, for manufacturing lamps and which is now turning out one thousand lamps a day, the Electric Tube Company (of which I am secretary and Mr. E. President) for manufacturing our street mains. So you can imagine what Mr. Edison has to do, as he is the mainspring and ruling spirit of everything. And you can imagine also what I have to do as his private secretary. - -"

In 1883, Edison sent Insull out to promote central power stations to mid-sized town with few large building, customers that fit Edison's vision and equipment. However, the emergence of the electric streetcar and the superiority of Westinghouse's alternating current technology for that application did more than Edison's vision to make the central station a winner. The market boomed and Edison sent Insull to create his Schenectady Works. In 1892, J. P. Morgan created GE by merging Edison's assets with many others and focused it on manufacturing everything electrical. Insull left for Chicago to create the predecessor of the Commonwealth Edison Company and by 1930 controlled one-eighth of the nation's generation capacity, had personal assets exceeding $3 billion, and served as chairman or member of more than 100 corporate boards. His power evaporated in the 1930's, when his Ponzi scheme of overvalued assets, underrecognized costs, and "pegged stock prices" crumbled. He was tried for embezzlement, larceny, securities fraud, and Bankruptcy Act violations. Although he was found "not guilty" by the jury in each case, his notoriety resulted in the Public Utility Holding Company Act, which was just repealed by the Energy Policy Act of 1992, and the creation of a large public power system with TVA as the model.

In spite of the legal tainting, Insull is widely credited with the creation of the electric utility industry that is just now changing its basic structure. His Fisk Street Station, which came on line in October, 1903, with its 5-MW steam turbine-generators, completed the picture started when he broke with his mentor's technical practices, introduced DC-AC conversion, adopted Westinghouse's AC transmission technology, and the Wright peak demand kilowatt-hour meter in the 1890's. Prices dropped from 20 cents/kilowatt-hour in the 1890's to 8 cents/kilowatt-hour in 1910, fulfilling Edison's vision that "they would make electric power so cheap, that only the rich could afford to burn candles". His focus on building volume and using technology to cut cost made him an industry advocate for "cost-shifting" as a way to make electric living available to the general public. Thus he contributed to the massive growth of the electrical appliance industry and broad public support for the electric utilities. He also promoted the idea of state regulation, an umbrella for his monopolies to operate under. That structural and technical foundation drove the industry to great growth and, with evolutionary development, sustained it on a declining cost curve until the 1950's; it "ran out of steam" (Figure 1) when the supercritical units turned out not to be cost effective. Nuclear power promised to change the paradigm; the boiler was dead and efficiency was not critical to the nuclear system's financial success. Variable cost would be so low that metering would be unnecessary; only a capacity charge for capital recovery would be needed. Thus ended a 70-year period in which equipment-supplier investments in technology reduced cost, grew volume, and fostered new product applications for an industry that was permitted to absorb new technology at a high rate because of its monopoly umbrella.

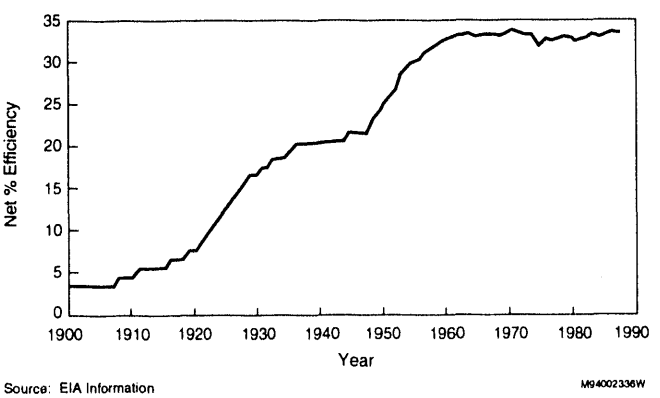

Figure 1. Average Net Efficiency of Coal-Fired Power Plants

Every decade from the 1950's to the 1990's has seen defining events that have irreversibly changed this industry. The 1950's saw the massive supplier price-fixing scandals that coupled with technology glitches to convince many customers and regulators that dependence on highly profitable vendors to deliver the industry's technology diet in response to competitive pressure was bad policy. The industry reacted by aggressively prosecuting these anti-trust violations, opening up the market to off-shore vendors, and creating the Electric Research Council to fund and manage a user-industry driven research and development program. These actions reduced supplier profits and put the funding burden for technology development and the control of research priorities on the equipment users, the electrical utilities.[4]

The 1960's also saw the emergence of commercial nuclear power and major blackouts, which put the integrity of the whole supply system in doubt. The peaking gas turbine solution to providing reliability through increased reserve margins looked good, but became a nuisance in the 1970's as gas turbines proved to be less reliable than desired in this cyclic load environment. When costs are declining and the supply is reliable, the customer tolerates minor transgressions; not so when the reverse is true. One broad-based industry action to counter customer reaction was the formation of the North American Electric Reliability Council to promote enhancements to generation and transmission reliability.

The shortage mentality and increased fuel costs, aided and abetted by the Arab oil boycott, the cost of compliance with the Clean Air Act (CAA), and the onerous interest rates in the 1970's sealed the coffin on the era of declining costs. These increased costs combined with the rate-basing of unneeded capacity in a period of slow economic growth, affectionately called "stagflation", led to unparalleled consumer "rate-shock". It also brought us the Public Utility Regulatory Policies Act (PURPA) and over-building by those with cheap money and limited operating competence, the Rural Electricification Administration (REA). But its defining moment was Three Mile Island, the beginning of the end (or hiatus depending upon your viewpoint) for nuclear power and its backlash of unrecoverable capital for the industry. Monday morning "prudency reviews" struck fear in the hearts of most utility CEO's, while operating cost "pass-throughs", justified by the Arab oil boycott, eliminated much of the incentive for efficient operations.

The 1980's saw Independent Power Producers (IPP), bidding, PURPA saturation, anxiety over new CAA revisions, very limited construction of new plants as the industry tried to work off excess capacity, and pressures for utilities to invest in demand-side management to reduce market growth[5].

The 1990's have already brought CAA revisions to capture the grandfathered capacity already in place when the 1977 act passed, climate change and electromagnetic fields (EMF) fear-mongering, pressure for open access to transmission capacity ("retail wheeling" to the in-crowd), an increasing involvement of the unregulated arms of the traditional electric utilities in the IPP market, and an emergence of the natural gas-fired gas turbine combined cycle as the technology of choice for new generation capacity.

What is the point of all this discussion of the past? We could cite the trite; i.e. "The past is prologue!" or "Those who ignore the lessons of history are doomed to repeat them." Moreover, it is with a sense of déjà vu that we point out that more than 100 years after Edison and Insull created this "bullet-proof" structure to nurture an infant industry, it is the "hated gas

industry" working with and as independent power producers that has broken this "natural monopoly" and created a challenging new environment for those of us who see ourselves as "partners" with that industry.

One doesn't have to be much of a visionary to see a first decade of the next century where inter-utility price competition for baseload customers between the generating arms of newly unbundled (or as I prefer, "dis-integrated") electric utilities leads to further cost pressures on the small consumer and the associated backlash from this public on the regulatory structure. The analogy to the telephone system history is clear, although I'm not sure you'll get to choose who supplies electric power to your individual hotel room. As you know, the deregulation process is already underway in California, targeted to hit industrial users by 1996 and homeowners by 2002. Its particularly threatening to the California utilities, who charge electrical rates 50 percent higher than the national average. Experiments may come slower in the Northeast, where New England's utilities have a 20 percent variable production cost disadvantage, compared to mid-Atlantic competitors, and a 50 percent retail cost disadvantage; an untenable competitive environment for residential customers in New England if the capital cost recovery is on their backs instead of being written off as excess, with stockholders bearing the burden.

The traditional part of the electric power industry as it exists today has some classical textbook attributes:

- Low growth.
- Many, many, many competitors.
- Many low-margin vendors.
- Little, if any, product differentiation.
- Great difficulty in finding sites for new manufacturing capacity, even if needed.
- Severe price competition becoming even more so with open access.
- A distribution system that is difficult to expand.
- An aging manufacturing plant.
- High capacity utilization levels, approaching 85 percent at peak.

Put simply, we're dealing with a "mature" industry which is dependent on "mature" technology provided by "mature" suppliers for its bread and butter. It has all the characteristics classically attributed to "maturity" and as such is not inclined to invest in technology for future capacity growth. Instead, the emphasis is on getting the most from existing business assets, working on the marginal cost of existing operations and eliminating base cost, all with minimal investment (Figure 2). That translates into a focus on product cost reduction, improved reliability to enhance capacity utilization, excellent customer service, and shortening cycle time for responding to customer needs. That usually drives organizations to spend their limited research and development (R&D) funds working at the end of the product life cycle curve, where the emphasis is on risk reduction; one can't take much product development or application risk with small profit margins. A business in that situation literally "bets the business" in attempting rejuvenation through R&D on "paradigm shifting" products. Since dis-integration, read that divestiture, emphasizes owning only those assets that contribute directly to short-term profit, there is almost no attention to major system improvements. What power generation investor in that situation will take a potential bottom-line hit to bring new capacity on line, knowing that the incremental capacity cost will necessarily be borne by the captive customers, if there is such a thing? The lure of increasing capacity factors on existing assets by price-cutting to win base load customers from competitors will be irresistible. The transition will be difficult and the short-term profitability impact will be substantial and, in fact, unacceptable to

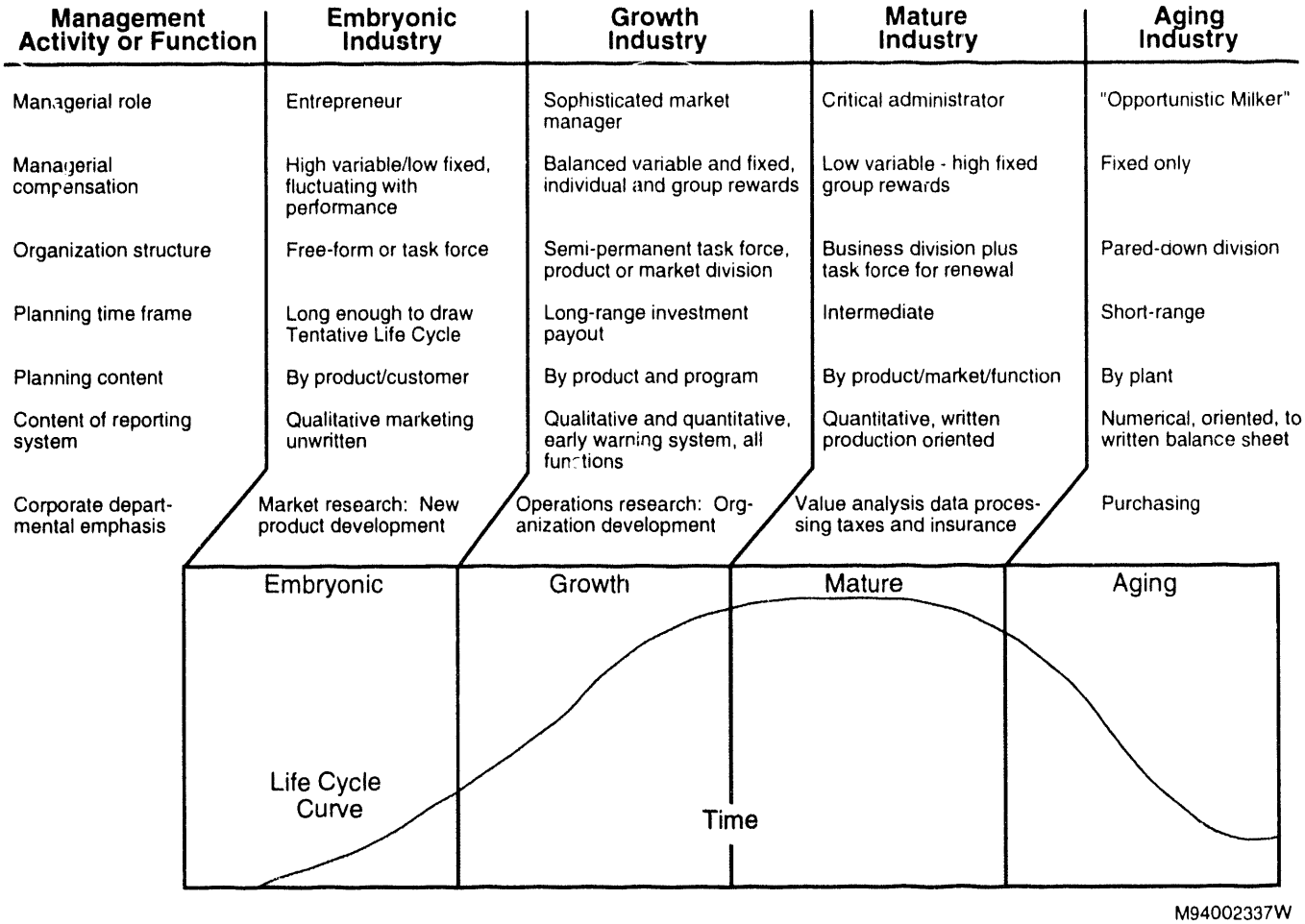

Figure 2. Product Life Cycle

many utilities captive to this industry's traditional high equity capital structure as a consequence of their regulatory situation.

We're faced with the basic question: What does technology have to offer this deregulated, dis-integrated industry with extremely tight constraints on siting, discharges, and product distribution?

In our minds, the most important asset in this future is existing permitted sites, both the aged plants of the utilities and the industrial sites of their customers, both relatively free of Nimbyism. We see the traditional utilities fighting IPP's to invest to build capacity on the potential customer's site. If the customer company is young and healthy and looking to vertically integrate production, it may build its own capacity and in effect compete with the utility. If, on the other hand, the customer is in a mature industry situation, it may welcome the opportunity to divest a steam supply facility and let the utility play out its "customer-retention" strategy in competition with other potential suppliers.

METC's program is committed to helping the industry exploit this asset to the fullest; we're convinced that repowering is the most attractive technology-driven answer to the industry's current dilemma. Repowering offers

a way to upgrade existing assets, coincidently grow capacity, and reduce the cost of electricity relative to other alternatives. For the neophyte, repowering is usually most cost-effective when it uses the steam turbine-generator, condenser, coal storage and handling facilities, and waste handling facilities at the existing location. Although specific requirements are sometimes less severe, one generally needs to meet the steam turbine's design point steam conditions, require no more coal, generate no more waste, and require no additional electrical transmission right-of-way. The opportunity is great. While only 18 GW of new coal capacity is projected by 2010, more than 60 GW of existing capacity will be more than 50 years old by that time, with more than 30 GW in the 65 to 250-MW range of interest for repowering. All of these plants are eligible for the CAA's 4-year compliance bonus if repowered with Clean Coal Technology.

The technologies in the METC portfolio that fit the bill in the repowering game are integrated gasification combined cycle (IGCC), pressurized fluidized bed (PFB), externally fired combined cycle (EFCC), and the advanced gas turbine system (ATS). Each option offers enhanced efficiency that promises increased dispatch hours, helping to write-off the capital investment while displacing an older, less environmentally attractive generation. A few examples of how the various options could work help to make the point.

The IGCC, which in its most cost-effective configuration increases plant output by 150 to 200 percent over its original steam turbine rating, can be a bad match in fuel, waste and transmission capacity unless we're talking about a multiple steam turbine plant. For example, if we start with two 100-MW steam turbines operating at 30 percent efficiency and convert one of them into an IGCC and retire the other, we end up with a 250 to 300-MW combined cycle at 50+ percent efficiency. That translates into a 25 to 50 percent increase in output and a 25 to 10 percent decrease in fuel use. The waste reduction could be even higher, depending on the pollution control option that would have been required for retrofit technology-based CAA compliance.

The PFB approach results in an output increase in the 35 to 50 percent range, resulting in an excellent repowering option. If we repower an existing 200-MW plant with first generation PFB, we end up with 250 to 300-MW plant operating at 40 percent efficiency; a 25 to 50 percent increase in output and a -6 percent/+12.6 percent change in fuel use. The big advantage vis-á-vis IGCC is in cost; we use the entire steam turbine capacity and add a gas turbine that is one-third to one-half the size of that employed on the IGCC. A second-generation PFB plant could do even better in the two turbine situation. If one turbine is converted and the other retained, the output increases by 70 to 100 MW at a system efficiency of 40 to 41 percent. A 35 to 50 percent increase in output while the fuel use change is in the +1/+10 percent range. Both steam turbines are used, and the gas turbine is only half that used in the IGCC case. Both PFB approaches are environmentally attractive because of excellent in-bed sulfur capture and excellent NO_x performance.

The EFCC is most attractive in smaller industrial applications, where it can be used with an atmospheric fludized bed (AFB) primary combustor and a coal fines-fueled topping combustor to meet a broad range of process steam needs without significant loose in cycle efficiency. Although the system tends to cost-optimize at the 70 to 100 percent power increase level, it also provides extreme fuel flexibility, which heavily impacts the definition of optimum.

Using the advanced gas turbine to do natural gas repowering can be extremely attractive, particularly if we employ staged construction to preserve the IGCC option and employ a gasifier that is not a net user or producer of steam. However, it suffers from the same deficiency as IGCC in producing a 150 to 200 percent increase in output relative to the existing steam demand.

We know that the global power generation market will be focused on new generation. We know that these same technologies will dominate these global new-plant markets, but that the relative competitive situation between technologies will change. However, we cannot ignore the role that low-cost electrical power plays in keeping the United States economy globally competitive. Repowering is the key to meeting this objective as the power generation industry transitions toward open markets. Recent Electric Power Research Institute (EPRI) and Gas Research Institute (GRI) studies reach the same conclusion; however, in keeping with Edison's original theme, they disagree on fuel choice. Natural gas retains its capital cost edge in repowering, so the fuel cost differential debate is critical for decision makers. By focusing our R&D effort at METC on gas turbine-based systems, we are striving to keep the fuel option open.

The policy question on DOE's table is clear: Once we've helped the electric power industry through the minefield of clean air and water regulation, natural gas deregulation, and electric power deregulation, all of which government created as beneficial public policy, is our involvement in funding R&D to meet the technology needs of a mature industry warranted in a free-market economy? Liquid fuel security, maybe; but is cheap electric power in the same league, even if we can tie it to global competitiveness and jobs? I don't know the answer, but with EPRI and GRI already in distress as a result of role-definition conflicts in a world where their supporting members are competitors, and DOE's role in question, our industry needs to find sound answers that are salable in today's tight budget climate.

Some of my associates in government are inclined to "hand wring" with you and focus their attention on the "mature end" (Figure 2) of the product life-cycle curve. However, we believe you can do that without us. You know your operations best and know where to best leverage investments to improve them. The university community will do its usual good job in understanding "what is", i.e. the "art-into-science" area, and training students to do what you already do even better. You may even become comfortable working cooperatively with your new competitors to understand new generic issues such as EMF and air-toxic health effects. We believe that government must be in league with the "paradigm shifters" that can remake your industry and offer attractive investment opportunities. We must focus on forging the future, not preserving the past.

If you look closely at our past and current performance, you won't find METC working on better pulverized coal boilers, better steam turbines, or better scrubbers; you'll find us working on the AFB which gets rid of two out of three of those components. You'll find us working to make gas turbines reliable base load generators that break the 40 percent efficiency barrier in a cost effective way with fuel flexibility that even gas turbine devotees wouldn't promise. You'll find us working on fuel cells, the ultraclean, ultraefficient, quiet, direct conversion machine that eliminates the concept of working fluid. To sum it up, when we find a pile of horse manure, we look for the pony and plan to raise race horses; others choose to get in the fertilizer business. We need your leadership in making sure the product focus is correct, the development cycle time is appropriate, and that

the job we do is complete enough that your application risks are acceptable. The "new DOE" is more than open to your feedback; it will assertively seek it and will commit to reflect it in our actions. Unless our customers succeed, we have no reason for being. Thanks for your attention and hopefully your comments and questions.

REFERENCES

DRI/McGraw-Hill; "Repowering Potential in the Electric Utility Sector"; GRI-93/0169.

EPRI Journal; January/February, 1993.

General Electric Company; "Electric Utility Systems and Practices"; GEZ-2587A; 1969.

Gorowitz, B.; "A Century of Progress"; November, 1981.

Heppenheimer, T.A.; "American Prometheus"; AUDACITY Magazine; Summer, 1994.

Hewson, T.: "Potential Role of Fluid Bed Combustion Technologies for Utility Repowering"; Energy Ventures Analysis, Inc.; EPRI Fluid Bed Combustion for Power Generation Conference: Atlanta, Georgia; May 17, 1994.

Lubove, S.; "Another Monopoly Bites the Dust"; FORBES Magazine; May 23, 1994.

Newton, T.U. and J.D. Burkett; "PFBC Repowering - A Clean Air Act Driven Choice; EPRI Fluid Bed Combustion for Power Generation Conference: Atlanta, Georgia; May, 17, 1994.

THE ECONOMIST; "California Unplugged"; May 21, 1994.

The KIPLINGER WASHINGTON LETTER; April 29, 1994.

ENDNOTES

1. An astute observer would note that GE hasn't changed a bit in those hundred plus years.

2. When Edison and friends wanted to insult someone, they noted that "He lies like a gas meter.."

3. That man understood commercialization; no research for the fun of it.

4. This effort culminated in the early 1970's in the creation of an industry-controlled R&D coordinator-manager, the Electric Power Research Institute. The Congressional response to the "blackouts", with threats of forming a Federal agency to manage the industry's technology future, added impetus for the industry to act. Some pundits have noted that subsequent events have demonstrated that the concern that led them to act was well placed.

5. Insull probably spun in his grave on that last one.

TBECHT\2:940781A

1.2 Evolving Utility Business Structure and Impact on New Technology Application

J. Wayne Leonard
PSI Energy, Inc.

I was asked to speak on the topic of the evolving business structure in the electric power industry and the effect on technology development. What is interesting about that premise is that for years many have believed and, in fact argued, just the opposite. That is, it is technology development that determines (or should determine) the business structure. And, the simple fact was that technology largely dictated that the electric power industry was a natural monopoly. That is, production conditions lead to a lower unit cost with ever increasing levels of output, resulting in a condition where costs are subadditive, so that a single firm can supply the entire market at a lower cost than can two or more firms. Thus competition can only increase costs and thus is not desirable. And, thus see vertically integrated electric utilities with partial or complete territorial integrity of exclusive franchise rights in return for accepting the obligation to serve all within that franchise territory at prescribed regulated prices.

And today, some are still locked into that debate, but right or wrong the idea of the electric power industry, as a natural monopoly and immune from competition, is not likely to survive to see the turn of the century. I will spend some time this morning explaining the views of economists, customers, and the financial markets on this subject, and why I think public policy and technology development is best served by this approach. And right up front, I should say mine is a minority opinion in the industry, particularly because I do not believe any of us are really prepared for the challenges we face.

From an economist viewpoint, it is important to keep mind that there are various services we receive in today's society which qualify for public utility status, but have never been regulated as such, or have been deregulated over the years. They provide essential services, exhibit scale or scope economies, are capital intensive, and have costs that vary by time of use (examples could be transportation sector or electric equipment companies). But to economists, what must justify public utility regulation is the necessity for the regulation, not the necessity of the services. Even with scale economies, a market with free entry need not have regulation to attain competitive pricing. The mere threat of rapid and substantial entry by potential competitors may do the job quite nicely.

Regulation is almost universally regarded as a questionable substitute for competition under conditions of a natural monopoly and is a poor substitute indeed when an industry is naturally competitive. Regulation carries with it the potential for anti-competitive effects even when there is a true natural monopoly. Many economists share this view, well stated by Clair Wilcox, who in 1966 wrote, "Regulation, at best, is a pallid substitute for competition. It cannot prescribe quality, force efficiency, or require innovation, because such action would invade the sphere of management. Competition does so, and the high-cost company is compelled to discover means whereby its costs can be reduced. Regulation fails to encourage performance in the public interest by offering rewards and penalties. Competition offers both."

What economists prefer and what generally promotes public policy interests is the replacement of effective regulation with effective competition. Effective competition puts strong pressures on firms to perform well by minimizing costs, holding prices to marginal costs, and by innovating rapidly in order to survive. But as technological conditions change to permit deregulation and the condition of effective competition, there are always public policy concerns that it may never actually take place if deregulation is allowed to occur. Even though the technology exists for effective competition, without proper controls, former monopoly firms may now be free to perpetuate their dominance without any constraint at all. As someone once said, regulation is like growing old, we would rather not do it, but consider the alternative.

With that in mind, do not expect totally unfettered competition in this country. In order to alleviate the possibility of neither effective regulation nor effective competition, you may well expect to see an ultimate industry structure whereby the electric grid is separated, heavily regulated, treated as a natural monopoly, and paid a largely fixed lease fee with incentives for good performance. A second natural monopoly would continue to exist as separate regional central dispatch, pooling, and economy trading processes. The pool company would, in effect, be an agent for the system users and decide how best to raise the required money to pay the grid co. They would do that through energy traders using basic market concepts to minimize the cost of meeting dispersed demand with dispersed production and determining when and how to expand the grid.

You then have generation companies and retail companies competing for the customers business. All with equal access to required natural monopoly services who would not have any vested or conflicting interests that come from having a private property interest in the outcome.

While there is considerable debate over whether all or any of this is needed from an economic efficiency standpoint, a new argument as to the benefits of retaining franchise utilities is now emerging and that is that the regulatory assurance of cost recovery affords utilities greater freedom to adopt new technologies, to innovate, and to lead in the implementation of other worthwhile endeavors like energy efficiency or global warming initiatives.

When this assertion is made by those outside the industry (and it has been), it creates a thoughtful discussion of the trade-offs and alternatives. When it is repeated by those in the industry, it sounds more like the child who kills his parents and then begs for mercy because he is an orphan. This is not an industry that voluntarily embraced either one of these initiatives or many others for that matter until long after the handwriting was on the wall.

You have to remember, this is an industry that argued wholesale wheeling could not/should not be done. And now says it is a matter of price, the higher of embedded or replacement. And has a large contingent promoting loop flow compensation at embedded cost, ignoring the fact that (1) your path was not chosen because your embedded price was higher than your neighbors, and (2) loop flows generally occur because your facilities are less utilized than your neighbors and to most people, underutilized capacity means you discount not raise your price. And, in any event, loop flow compensation at these prices will likely end many of the perfectly economic transactions we see today.

How credible will we be if we are seen promoting this as the outcome? Do we reasonably expect that we can use transmission pricing to thwart the purpose of the Energy Policy Act? And doesn't this type of debate and logic just help assure that we will ultimately be required to spin-off the grid co. and the dispatch and pooling process as separate companies.

This is industry that said SO_2 legislation was not needed and would raise rates 15 to 25 percent. After the bill was passed, very few utilities did not half their cost estimate and some (who previously said no harm to the environment) actually reversed their position and said they would not purchase allowances because they wanted to personally reduce SO_2 to protect the environment. Instead, they built rate base in the form of scrubbers.

It is an industry that says all the right things about global warming, signs up for the President's voluntary reduction program and in stark contrast to the priorities of foreign utilities, just weeks later a survey of the CEO's indicates an overwhelming majority ranked global warming near the bottom of their priorities, indicating it was not in the public interest. How does the industry argue before the U.S. Senate that competition is BAD because it will thwart our voluntary efforts to comply with global warming initiatives when the majority openly admits they do not even think global warming initiatives make sense, and it is not one of our priorities anyway.

It is an industry that took the position in the early 1980's that it would not build capacity anymore because the returns were too low and, when Independent Power Producers (IPPs) said they would and Congress moved to allow that to happen, the industry fought to maintain its monopoly position in the market, and keep others from accepting a role we appeared to not want just a few years earlier.

This is an industry that is currently arguing that retail wheeling is bad, but just the threat has prompted hundreds of millions of dollars of cost cuts. How do you convince a customer that that would have happened anyway or that there is not more to come as pressure is increased? If competition is not needed, why is it after years of arguing for 20 to 25 percent reserves, many are now announcing numbers as low as 6 percent. How is it that experiments with retail wheeling in other countries have not turned up the massive problems envisioned here?

It is an industry that argues to its customers "I had a deal" with regard to my past investment. I believed that you would be here, and it is unfair for you to leave and burden others with the stranded costs. But has little sympathy when the customer counters that "unfairness" to him is when his competitor just down the road is charged prices less than half what he pays—that he never signed up for that deal.

One utility is trying to charge a 165-MW customer an exit fee of $235 million for stranded investment (costs presumably left behind if the customer leaves). Doesn't the size of that number alone make it obvious why the customer wants to leave? How long will regulators listen to stranded investment arguments if that is the size of numbers we are going to put on the table? Is it credible to argue that you reasonably believed that customer would remain regardless of price? In the June 1 issue of Public Utility Fortnightly, 11 of 17 CEO's surveyed said the determining factor on who should pay for stranded investment is the "regulatory compact." In other words—it is the customer—plain and simple. "I have a deal" with regulators.

It is an industry that says all the right things about customer satisfaction and shows incredible numbers in this area, but understands very little about customer loyalty. And routinely finds itself in the fourth and last phase of the account death cycle, that is, lawsuits or litigation with its own customers. When a retail wheeling bill was recently proposed in Ohio, one utility immediately announced it was just another attempt of the large industrial user to take advantage of the poor residential consumer. Does this attitude create customer loyalty?

Why is it that when power outages occurred in the PJM pool in January, the industry was so surprised when a myriad of investigations were launched to determine what happened? Was it price or capability or what? When we routinely deliver the highest reliability levels in the world, why is it no one seems to trust us? And why was it that in the crisis, we discovered the transfer capability of one line in particular, was almost three times what we had previously said was possible?

For all the talk of wanting to be more competitive to cut costs, why do the majority of the CEO's still indicate in surveys that mergers are BAD—not in the public interest—when there is strong evidence as to benefits to customers and shareholders? How open minded do we appear to the outside world when it really comes down to it?

At the same time, there is little question that the industry has legitimate arguments on many issues related to past promises or a less-than-level playing field. There is no question utilities have been used as everything from a revenue collector for state Government to a vehicle to levy social costs on customers to facilitate public policy objectives. For example, you have seven states who assign externality values to resource choices.

More broadly, we are expected to invest hundreds of millions of dollars in demand side management equipment to be put in customer homes or businesses without any security they will even be our customer in the years ahead. The playing field is not level, and there are legitimate positions regarding the fairness of allowing third parties (who do not bear these types of costs) to cherrypick the system or allowing large industrials (for example) to escape with lower costs after the utility built facilities, legitimately and reasonably, expecting the customer to be there, leaving potentially billions of dollars in stranded investment to oe borne by shareholders or other less elastic customers. The question is, given positions the industry has taken in the past on issues, the hard-line positions they are likely to take on these issues in the future, and the relationship we have established with customers and regulators, will anybody listen to any legitimate argument? Have we earned a seat at the bargaining table?

Meanwhile on Wall Street, in the last 6 months, we have seen stories by all the major business magazines signalling the dangers to the industry from competition. Typical of this was a story that appeared in Business Week on January 10 that quoted Vice President of Airco Gas & Gear plant in Joliet, Illinois, who pays twice as much per kilowatt-hour in Illinois as in Indiana, as wanting to import cheap Indiana power to Joliet. "Competition works in every other industry," he says "Why not electricity?"

At the same time, there seems to have been some sudden concern in the industry over what all this talk means and a sudden recognition that these changes are occurring not because rating agencies, Wall Street analysts, or even because renegade CEO's like PSI's Jim Rogers are predicting them, but because we are part of a global economy, and we have a regulatory system in

this country that has produced industrial rates that vary from 3.0 to over 10¢ per kWh across the country, with self generation now below 4¢. Customers want choices and they want low cost. And they believe that a system that relies on market forces and competition (the same thing that has made them more efficient) will produce better results in the electric sector. As the Albuquerque city counselor said, "No other business in the world mismanages itself and then forces its customers to buy their product at exorbitant prices."

Every week, some business magazine is warning investors that the party is over for utility stocks. While the industry has outperformed the S&P 500 over the last 5 years, the fundamentals paint a very different picture. Book value has increased less than 1 percent per year. Earnings growth was negative from 1988 through 1992, up 11 percent in 93 due primarily to refinancing and extreme weather. Authorized ROE's by regulators have declined 9 of the last 10 years. Credit quality has continued its 20-year decline.

And dividend payout ratios are setting new records. And many would say poor fundamentals are the least of our problems. In the last 8 months or so, we have seen major announcements or papers written by all the rating agencies (in particular S&P) outlining the increased risks of competition and what that will mean to credit ratings. S&P now has over half the industry on negative outlook.

At the industries financial conference last November, the focus was on the changing business structure and competition, leaving Doug Preiser of Kidder Peabody to question whether the industry was prepared strategically and financially to deal with the changes that are likely to occur since many continued to deny the problems existed, and no one seemed to have a clear vision of what the new industry would look like.

At the financial conference, the speakers reminded you a great deal of Woody Allen's "speech to the graduates" when he said, "more than any other time in history, mankind faces a crossroads. One path leads to despair and utter hopelessness. The other, to total extinction. Let us pray we have the wisdom to choose correctly." He goes on to say that with regard to the predicament of modern man that "it can be stated one of two ways, though certain linguistic philosophers prefer to reduce it to a mathematical equation where it can be easily solved and even carried around in a wallet."

The point of this is that just as Woody Allen factiously wrote about modern man, there is a growing perception on Wall Street that our predicament in the electric utility is to choose between paths of hopelessness or extinction. And a growing concern that we believe the uncertainties and risks facing the industry can be reduced to a mathematical equation and then easily solved. And those that have seen competition develop in other regulated industries clearly realize it is not that simple. There is no black and white. There are no absolute answers. And those that seek such clarity before making decisions are doomed to spend eternity buried at the starting gate.

Most of the sell-side analysts are developing models to separate the winners from losers in a more competitive environment. Barry Abramson of Prudential recently concluded in his research report that there are no winners and losers from increased competition, only big losers and small losers, leading others to question why those in

the industry who are promoting competition would engage in a kind of fratricide/suicide game.

The fact is competition is inevitable. The fact also is that two-thirds of the CEO's in the industry believe not just competition is inevitable, but retail wheeling is inevitable. As a result, in the words of Sandy Cohen's at Morgan Stanley, "the future is going to require a unique blend of communication, political, cost management, and operation skills combined with a clear, consistent focused strategy and an attitude of not only acceptance, but encouragement of change."

Leading me to the premise that the greatest risk we may well be facing is neither poor fundamentals nor increased competition, but whether or not we have the management skills, capabilities, and attitudes to not just manage the change, but change ourselves. It is our belief that without making commitment to shape the outcome and making the necessary compromises to be a part of the solution, we will end up with a porous monopoly franchise without any lessening of the obligation to serve and pricing at the lower of cost or market. That is what investors should see as the worst of all worlds— regulated competition. That may not be the path to extinction, but in our mind, it is damn close to utter despair. Asked to play the same game with two different sets of rules, increased competition and increased regulation.

We all need to understand that even with all the competitive pressures, (the injection of market forces) regulation is not fading, it is evolving. Regulators are no longer just in the business of trying to keep rates just and reasonable. They are playing a legitimate role of using their powers to prompt specific changes in utility behavior to facilitate broader public policy objectives. The regulator is still the 800-pound gorilla. And if you choose to wrestle the gorilla, you need to remember the old adage that the game is over when the gorilla gets tired, not when you do.

While it may be easier to appreciate why customers would not mind seeing a little cut-throat competition and short-term prices that could, as some have hypothesized, drop to 2 to 3¢ per kWh, or why intellectual economists who have never worked a day in the real-world of business would push to test their "theories" on how monopolies destroy consumer surplus through a real-world laboratory experiment in the mother of all monopolies, why should policymakers be so quick to want to fix what is not broken, particularly, at the potential risk to the financial health of the industry or to programs like energy efficiency and global warming initiatives?

For policymakers, there is a continual search for how to create a competitive advantage for your nation and your nation's people so that they prosper and continue to enjoy a rising standard of living. While there are not too many issues economists can not debate either side of, virtually all agree that society's wealth is determined by its supply of physical resources. That means that life is a zero sum game, one person's gain is another's loss. Over the centuries, this view has been responsible for numerous wars, revolutions, and Government policies.

As evidence of this, let us recall the enormously influential 1972 study, The Limits to Growth. This was a study performed by the Club of Rome—a collection of distinguished scientists, economists, and sociologists from 25 countries. Using the most sophisticated computer modeling available, the experts predicted that with the world's population growing at about 2 percent per year, the world's physical resource would be exhausted in the next few

decades, with humanity wiped out by 2100. The study was widely accepted almost without question and, in fact, events of the next few years--soaring energy prices, shortages of energy, brownouts, and long lines at gasoline pumps--seemed to reinforce the premise.

But as we sit here today, the world did not come to an end. In fact, our effective supply of resources is greater today than it was then and is increasing. We have probably twice the oil resources that were estimated in 1973, three times the natural gas reserves, and prices reflect that abundance. In fact, the U.S. Office of Technology Assessment concluded that America's future has probably never been less constrained by the cost of natural resources.

All of this is true today because of technology. While society's wealth is still a function of our physical resources, we now recognize that technology controls the definition and the supply of those resources. Technology determines our supply of physical resources by fixing the efficiency with which we use those resources and our ability to find, obtain, distribute, and store them.

What makes resources valuable are their usefulness. And again technology gains that enhance either supply (like improved drilling or mining techniques) or demand (like fuel injection carburetors or high efficiency furnaces) increase the effective supply and the usefulness of our world's resources.

Peter Drucker once called John Maynard Keynes the legitimate heir and the liquidator of Adam Smith, but what we have learned over the years is that contrary to Keynes' predictions that increasing affluence stifles demand, in fact, we now know that people's needs are not absolute, but defined by technology. What people want is a function of what is available.

We increasingly have an economy made better off by demand-driven innovations. That is, imagine a need beyond the physiological limits and rely upon technology to satisfy it. Often used examples of this include President Roosevelt's ordering of a nuclear device that many experts doubted would ever be feasible, or President Kennedy's commitment to put man on the moon by the end of the 1960's, or to a lesser extent President Carter's declaration of the energy crisis during the 1970's as the moral equivalent of war.

The point is, we now accept the general premise that anything is possible and that technology is the great lever that can, in fact, move the world. Technology has given firms and nations the power to circumvent scarce factors via new products and new processes. It has nullified the importance of certain perceived constraints that once loomed large, such as those identified in The Limits to Growth study that predicted the end to mankind, and at the same time it has produced great wealth and power for its creators. And it has changed the standard of living forever for much of the world.

Relatedly, it is widely accepted that trade among nations is based, in part, on differing labor productivity in producing particular goods due again, in part, to technology differences. The technology gap theory says nations will export in industries in which firms lead in technology and then exports inevitably fall as the gap closes over time.

But even if we can all agree that technology development is the key to a nation's wealth and its competitive advantage, these theories still leave unanswered the questions as to why a productivity gap or technology difference emerges in the first place. Michael Porter

in his work, *The Competitive Advantage of Nations*, seeks to answer this question--why some nations succeed and others fail in international competition. It is one of the most frequently asked economic questions of our time and is one of the central preoccupations of Government and industry in every nation.

No nation's pool of resources is unlimited, and the ideal is that they be deployed in the most productive uses possible. What Mr. Porter explores is the way a firm's proximate environment shapes its competitive success over time or why some organizations prosper and others fail. This is not the superficial bathroom reading material that popular business authors often turn out. This is based upon exhaustive scientific research which makes it more complex and technical than most people have the time or inclination to get through. To some, it's conclusions are controversial. To others, it stands alone as the most robust holistic theory explaining the creation of competitive advantage.

Porter's research clearly shows that companies with the same national home base appear to thrive, prosper, and dominate specific industry competition internationally. They do this in a way that is not explained by comparative factors of production—like rich endowments of natural resources, for example. In fact, many resource poor nations have been among the most successful trading nations.

And wage rates do not explain these differences either. Why is Germany, for example, home base for so many of the world leaders in making printing presses, luxury cars, or chemicals? Why does Sweden lead in heavy trucks and mining equipment? Why do the Japanese dominate consumers electronics or robotics?

The globalization of industries and the internationalization of companies would tempt one to conclude that this is a thing of the past, that the nation has lost its role in the international success of its firms, that companies have transcended countries. But in fact, Mr. Porter's work concludes that the role of the home nation seems to be as strong as or stronger than ever before.

The home base is where the essential competitive advantages are created. It is where the firms' strategy is set and the core process technologies are maintained. It will be the location of many of the most productive jobs and most advanced skills.

A key determinant of success in any industry was found to be strong competition on the domestic level, i.e., large numbers of strong domestic competitors. For example, the Japanese have 112 domestic rivals in machine tools and 34 in semi-conductors.

Another key determinant was found to be the existence of sophisticated, demanding domestic buyers. Buyers that constantly pressure suppliers to innovate and again, while the global theory of competition is intuitively appealing and certainly has some truth, the study reveals that physical and cultural proximity to these sophisticated buyers helps anticipate and satisfy their needs and creates an international competitive advantage.

In addition, early large home demand leads to scale economics in production and in learning. It leads to similar competitive advantages in related industries and it creates localized spin-offs and start-ups by former employees who create technological breakthroughs on their own. The silicon valleys, for example.

Toughened by domestic rivalry, firms are better able to compete abroad. Porter found that it is rare that companies succeed internationally

in an industry without strong domestic competition. Domestic rivalry forces a nation's firms to seek higher order and ultimately more sustainable sources of competitive advantage. Domestic rivalry keeps each other honest in seeking Government support or Government protection which tends to slow the rate of change or product innovation.

Direct cooperation among competitors, an approach sometimes advocated as a means of avoiding duplication or achieving economics of scale, undermines competitive advantage by sapping incentives and eliminating diversity. Dr. Porter's theory emphasizes that market pressure and competition create innovation and technological advantages that can overcome inherent factor cost advantages.

Mr. Porter's work takes a very dim view of short-term investor's pressures to cut costs in lieu of making technological investments or upgrades, of financial stewards harvesting cash from entities for unrelated diversification efforts, of public policies or business structures that reduce the cost of failing to innovate or financially discourages technological advances because it makes obsolete the current fixed investment, and of horizontal mergers that reduce domestic rivalry. He views loss of domestic rivalry as a dry rot that slows the pace of innovation.

It is survival of the fittest, evolutionary biology, and what economist Joseph Sumpter called the constant creative destruction of capital, that is, the positive displacement of older obsolete capital equipment.

As to Government's role in all this, Mr. Porter believes Government should focus on education, setting high standards and assuring teaching is a prestigious and valued profession, and set policies that encourage research, including Government laboratories that focus on innovation and not just science and technology, with substantial dollar commitments to research universities.

The Government should stimulate commercial innovation by public policies directed toward domestic competition with strong antitrust regulation. The "national champion theory" fails the test of logic and history. Competition is neither wasteful nor excessive, but the essence of national competitive advantage.

Government as a buyer, should set stringent product specifications (particularly in anticipating standards that will spread internationally) and create an early demand for advanced products.

Suffice it to say deregulation of monopoly services or privatization of Government services are seen by Mr. Porter as obvious areas for immediate spurs to national advantage.

The electric utility industry fairs very badly under Michael Porter's theory. We have sophisticated technologies and suppliers that can not get to market. We have demanding, sophisticated customers who compete in world markets, but we have a system that basically ignores their needs. We had a case last week where service to a group of industrial customers of another utility was being interrupted under their tariff. They called PSI directly to buy power. We agreed to sell it to them for a price they accepted. The host utility, when contacted by the customer, refused to buy from us as opposed to interrupting the customer because under the tariff they had the right to curtail service. We actually did make an off-system sale last week to another out-of-state utility because customers who had been interrupted called us on their own to find power that was available.

Electricity is a service related to almost any product or service we hope to sell in world markets, but we have a system that has provided almost no rewards to encourage the utilities to be aggressive, to innovate or take risks, or if this example is any indication of how we routinely do business, penalties for failing to do so.

In the June 1 issue of Public Utility Fortnightly, Dr. Charles Studness, a respected researcher on electric utilities, wrote in response to consumer concerns that competition in the industry will thwart energy efficiency gains, "the progress of energy efficiency under the command-and-control process of regulation has been dismal. The heat rate of the electric utility industry is virtually the same now as it was during the energy crisis 20 years ago. Meanwhile, energy efficiency in the economy has risen 37 percent. Replacement of current generating facilities with new plant could reduce the energy used in electric generation by over 25 percent and the nation's overall energy consumption by 11 percent. However, these potential gains will not be realized unless there is strong incentive to replace obsolete plant. That incentive can be expected to develop under competition, but is unlikely to emerge under regulation. After all, regulation has done little to promote utility heat efficiency in the past, and is now leading utilities in the opposite direction."

As we speak, Norway, Chile, Argentina, and the United Kingdom have all moved to more rational regulatory schemes for electric service. Schemes that more closely resemble Michael Porter's prescription for achieving competitive advantage. Schemes that will likely mean greater rewards for innovation, greater imperative for technological change, greater pressures to improve—to be better, faster, or cheaper. Systems that will force electric utilities to be more demanding customers to their suppliers and more attentive suppliers to their customers. And as the rest of the world innovates, not only will the electric utility industry in this country lose competitive advantage, but (if you believe Michael Porter's theory on home base advantage) so will U.S. domestic suppliers to the industry and so will our customers.

Economists speak of the technology gap, the difference between the best production practice possible with current knowledge and the practice in actual use. How well a society does at closing that gap goes a long way to explain its national competitive advantages. But what is just as critical is the multiplier effect of technology. As all of you know, every new technological breakthrough or successful application is a link in a continuing chain of innovation. They are building blocks for tomorrow's successes.

Technology determines the value of our physical resources whether we are imagining superconductivity, super efficient batteries, cold fusion, or even the clean coal technology that DESTEC and the DOE are bringing to the Wabash River Station at PSI. The new world order is knowledge and technology based. A nation's wealth, its standard of living, the value of its physical resources are determined by its technological progress, its ability and willingness to invest in new technologies, to replace obsolete ways of doing business, and to constantly innovate.

The regulatory and business structure in this country for the electric utility industry, creates by nature, stewards of the existing assets. The desire to preserve and protect entrenched positions, to live off existing value and wealth instead of making new contributions. And, as I previously indicated, it has resulted in dismal financial fundaments for the industry—no earnings growth in 5 years and 80 percent of earnings.

But maybe more importantly, large industrial customers do not like the deal they have gotten, they do not like how they are treated, and regulators are under pressure to address these concerns. The industry has no choice but to change for its own self-preservation (if nothing else). But sometimes we are our own worst enemy.

We need to begin to back up the talk about wanting to be more competitive with more actions. We need to get the base case that we compare alternative scenarios to right, and for most, it is not full recovery of everything I have invested on the sole basis "I have a deal."

We need to start thinking about sunk costs and market forces, and we need to start thinking longer-term than today. And, quit declaring war on our own customers. It is a war you can not possibly win.

Peter Drucker says one of the five deadly sins is slaughtering tomorrow's opportunity on the altar of yesterday. Or as a more popular philosopher 40-year-old rock and roller, Meat Loaf, sings as he reflects on a simpler period of his youth that "Objects in the rear view mirror may appear closer than they are." And that regulatory compact train, that we missed during the last building cycle, and that some are still looking to ride on again, left the station a long time ago and it is not coming back.

And as someone once observed, an indication of insanity is doing the same thing over and over again, but expecting different results.

Our fear is that this is an industry headed down a path of tragic proportions. It is tragic because few industries in the nation have the competitive advantage the electric industry does over the rest of the world. We have as fine an infrastructure as exists in the entire world and we enjoy a substantial positive technology gap created by the fact that we have sophisticated suppliers and customers right at our door step.

And somewhere in the debate we have forgotten that and gotten lost in the forest. At times, seems as much a part of the problem as we are the solution. And, we have far more to offer.

What policymakers are looking for is not intellectually appealing philosophies that sound like they could have been conceived by old world philosophers, Hegal or Kant—pompous and pedantic, and with every statement qualified. They want industry that sounds more like American William James who made philosophy relevant by abandoning the search for the absolute in favor of a "Will it cut down trees?" approach to ideas, the belief that truth is tantamount to effectiveness and that philosophy should stick to answering questions that have "cash value," i.e., will make a significant difference in people's lives.

As electricity is an essential service—if your philosophy does not make people's lives better (and there are clearly trade-offs and conflicts), you are destined to be on the losing end (or at least left out of) the debate. And, technical reasons why something can not or should not be done just does not ring true from an industry that has proven time and time again when push comes to shove, we can always come up with a way to get it done.

This is an industry that needs to get on with life—to plan for the future instead of reminiscing about the past. We need to get past the feeling that suggesting change is tantamount to disloyalty. We need to deal with endings, with

the potential mortality of the industry, and move on to create a compelling vision for the industry consistent with the new realities.

While Martin Luther King rallied people with "I have a dream," we have offered very little beyond the rhetoric of the constant "I have a deal." William James once observed that as human beings, we typically lead lives inferior to ourselves. That we are capable of so much more. Maybe no industry is more guilty of that than ours.

In his movie *Love & Death*, Woody Allen says about life that "The important thing is not to be bitter. You know if it turns out there is a God, I do not think He is evil. I think the worst that you can say about him is that, basically, he is an underachiever." And at the end of the day, I hope that is the worst you can say the regulatory system and business structure we have built over the last 75 years. It is not inherently evil, but it does produce, basically, underachievers.

In the end, the real reward for all of us comes from doing the right thing. being a business with a conscience, and finding a balance that satisfies the ambitions of the powerful (like our large institutional shareholders or our large industrial customers) without sacrificing the dreams of others and the rights of future generations to inherit a planet still capable of supporting life as we know it without the limits to growth some once predicted.

The industry is truly facing some potentially difficult times and difficult problems. As an industry, we need to get off this endless search for the absolute truth, whether it is global warming, transmission loop flows or retail wheeling, and develop a vision consistent with public policy issues and become a part of the solution.

As a last thought, you should consider that this is an industry increasingly populated by those coming from competitive environments. Like many of you out there today, they are risk takers. While they do not always understand the risks they may be taking, when you walk in a regulated world with multiple competing public policy interests, nonetheless they play not "to survive" but "to win."

They are analogous to professional card players, and I once heard a professional card player brag he could clean out any local game without ever looking at his cards. All he needed to do was observe how the "amateurs" played their hands. Because competition is externally focused, it is game theory. It is about knowing the difference between bluffing and believing. And most people are not very good or experienced at that.

You should all recall the scene in the movie where Butch Cassidy and the Sundance Kid are trapped on side of a mountain, 100 feet above a raging river on the one side, and a posse of sharp shooters on the other. In seconds, Sundance, the best fighter who ever held a gun, made the decision to jump into the river. Butch who could not swim, (and later admitted he had never actually shot anybody) at first chose to fight it out alone while clinging to the side of the mountain, but eventually chose to jump also.

That is what will happen in our industry. Surrounded by competitive pressures on the one side and the potential world of regulated competition or lower of cost or market prices on the other, the experienced fighters will instantly choose to seize control of their destiny, to voluntarily jump into the competitive world—recognizing they may be killed by the fall or drown in the river. But, preferring that to a certain future of a long, slow death clinging to

the side of the mountain until you run out of bullets and food while the vultures circle overhead.

For those that do not believe policymakers have the votes to create full-scale competition, the question is how long anybody will be able to remain on the side of that mountain once others voluntarily start down the path of retail competition.

And I firmly believe while there may be some lean times for the industry in the near term and some unpleasant trade-offs in our future, that change is in our long-term best economic interest. The future is one of investment and technological innovation. Long-term competitive advantage emerges from pressure, challenge and adversity, rarely from the easy life.

And I would even go as far to say we have an almost moral obligation to future generations to change how we do business today. For throughout history, there may not be two more underestimated forces than the power of competition and the ability of technological change to exceed our expectations and even our imaginations. The challenge is there. We have only to accept it.

JLEONA\1:940879

Session 2

Changes in the Market and Technology Drivers

2.1 Overview of Global Utility Market for Advanced Coal Fired Systems

Ronald H. Wolk
Neville A. Holt

Abstract

Coal reserves represent the major fossil energy storehouse of the earth. The most important current use for coal in the economically developed nations (OECD) is for electricity production. Increased production of electricity throughout the world is anticipated as the standard of living of developing nations approaches that of OECD nations. Coal is most likely to be the fuel for this additional production since it is widely distributed and will remain lower in cost than competitive fuels.

There are many technologies which can be used for the conversion of coal to electricity. Almost all current coal fueled electricity production is based on conventional combustion to produce high temperature, high pressure steam which is passed through expansion turbines which drive generators. Newer technologies based on atmospheric (AFBC) and pressurized fluidized bed combustion (PFBC) and gasification (IGCC) are beginning to penetrate the power generation market. The incentives for these technologies are the ability to use low quality fuel (AFBC), to achieve higher efficiencies (PFBC, IGCC) and to minimize all types of effluents and waste products (IGCC). Demonstrations of improved variations of these technologies are planned under the Department of Energy's (DOE) Clean Coal Technology program and by other organizations around the world.

This paper will discuss some of the criteria that must be considered by those responsible for selecting a coal fueled generating technology for a new power plant. These includes technology cost, maturity, environmentally detrimental emissions, waste products, supplier guarantees and subsidization. While the market for new coal fired power plants is likely to be very large during the next twenty to thirty years, it is impossible at this time to identify a clearly dominant technology parameter for selection. Both existing and advanced technology will share the market. Successful demonstrations, significant cost reductions, and new business approaches are required for advanced technology to capture a significant share of this market.

INTRODUCTION

Over the past 25 years the share of primary energy provided by electricity has steadily increased in the OECD countries even as the energy usage per unit of Gross National Product (GNP) has declined. This can be attributed to the increased use of more efficient industrial processes, automobiles, and power generation technology. There is also a strong positive correlation of electrical usage per capita with the GNP per capita. As the developing nations of the World seek to expand their economies, increased and efficient use of electric power is the key to achievement of this goal.

The fears of imminent exhaustion of fossil energy resources that were widely held 20 years ago now appear, at least for the moment, to be of little concern. Oil and gas continue to experience a reasonably constant ratio of annual production to reserves. Coal continues its long-held position as the world's most widely available fossil energy source with reserves available for several hundred years' consumption.

Although a significant expansion of natural gas use for electricity production is forecast for most OECD countries, regional imbalances between supply and demand are increasing and the need to transport gas over ever longer distances will raise costs. Despite the recent loss of some markets to gas, coal is expected to maintain its basic position as the mainstay of OECD power generation.

However, the main growth of electricity demand will be in the emerging economies. It is expected that about two thirds of the additional power generation capacity will be in those nations, most of it concentrated in China, India and the Pacific Rim. Projections by EIA are that coal usage in these regions will probably double in the next 30 years. In order to minimize the environmental impact, the adoption of the newer "clean coal technologies" assumes greater importance. In the near term time frame and in the emerging economies capital will be scarce and the tendency will be to adopt the lowest initial capital cost technology available. Technology transfer to these countries is probably best focused on the current state-of-the-art direct coal fired plant emissions control technology and the establishment of an infrastructure in these countries to supply equipment components, parts and services. As the new clean coal technology projects, based on Integrated Coal Gasification Combined Cycle (IGCC) Pressurized Fluidized Combustion (PFBC), complete their demonstration periods at commercial size over the next few years, wider deployment of advanced coal technology will begin. The most likely market segments for each technology are summarized in Table 1

Fuel Supplies

Coal constitutes the world's largest available supply of fossil energy. Reserves total about 300,000 Q (quadrillion BTU's of energy; 1500 billion tons) compared with 6000 Q (1000 billion barrels) of oil and 4000 Q (4000 trillion cubic feet) of natural gas. These reserve estimates represent an averaged view of the estimates of information that is available in the literature. The definition of reserves is also not precise but is usually accepted as the amount that can be extracted from the earth under present and expected local economic conditions with existing available technology. In 1990, the world consumed 136 Q of oil, 74 Q of natural gas and 93 Q of coal along with 21 Q of hydroelectric power and 20 Q of nuclear power.

These reserve and consumption figures indicate that the supply of fossil fuel in total could supply the needs of today's world population for hundreds of years. However the world's population continues to increase. The world's highly industrialized countries use far more energy per capita than the less developed countries. For example, in 1989 the United States used about 312, West Germany about 172, Japan about 130 and China about 23 million Btu per capita. The Energy Intensity of industrialized societies, which annually represents the ratio of the amount of energy consumed to the value of the goods produced, has historically risen during the early stages of their industrialization and then fallen. Most industrialized societies utilize an Energy Intensity of 0.3 - 0.4 metric tons of petroleum per $1000 of Gross Domestic Product. Improvements in efficiency of both the energy production and consumption processes drive these changes. As societies begin to industrialize they first use scarce capital resources to maximize the yield of products rather than to maximize fuel efficiency. As the level of technical sophistication increases, mechanical power is replaced by electricity which leads to more efficient means of production. The ratio of electrical energy to total energy consumed is an excellent measure of technical sophistication of a society. In the U.S. for example, this ratio has been increasing as the total energy required per unit of GNP has decreased. As a result of these offsetting trends - more efficient industrialized societies reducing their Energy Intensity and developing countries increasing theirs -- it is difficult to calculate the energy needs of the world's future population. It is clear though that for the near term, fossil fuel consumption will increase as the world's population and its standard of living increase simultaneously.

While at least for the near-term, the world supply of fossil fuels is adequate, the distribution of these fuels is very uneven. In 1990 the United States, China, and the USSR produced and consumed almost 50% of the world's energy.

In 1990 the United States consumed about 17.0 million barrels/day (MB/day) of petroleum or about 26% of the world's consumption, but produced only 9.0 MB/day (including 1.6 MB/day of natural gas liquids). The U.S. accounted for 12% of the world's production of petroleum in 1989 from only 3% of the world's reserves,. More than 80% of the world's oil reserves are contained in only eight countries, Saudi Arabia, Iraq, United Arab Emirates, Kuwait, Iran, Venezuela, USSR and Mexico. About 65% of the total is found in the Middle East.

Natural gas reserves are also narrowly distributed among the world's nations. About 37% is in the former USSR and 32% in the Middle East. Algeria, Venezuela, Canada, Indonesia, and Norway account for about 15%. The U.S. holds only about 4% of the world's reserves. The balance of the reserves are distributed throughout the world. Coal reserves, which by far represent most of the world's fossil fuel reserves, are concentrated in the U.S., the former USSR, and China with other significant reserves in Australia Germany, South Africa, India, Poland, Hungary and Columbia.

Technology Status - Current State Of The Art For Direct Coal Firing And Flue Gas Desulfurization (FGD)

The main competition for advanced clean coal technology particularly in Europe and Japan, are the direct pulverized coal supercritical units with FGD fueled with readily available, low sulfur, high ash fusion coals from Australia, Colombia, South Africa etc. and which incorporate low cost once through ocean cooling. These coals and cooling methods are particularly advantageous for technologies based on the Rankine steam cycle and are of lesser benefit to Brayton (i.e. gas turbine) cycles. Papers by ELSAMPROJEKT describe such plants in Denmark with efficiencies of 45-47% Lower Heating Value (LHV) basis. Conversion to U.S. conditions of 2.5 inches Hg condenser back pressure lowers the range to 42-4% LHV in line with the latest EPRI estimates.

Several technologies are available for reducing emissions of sulfur and nitrogen oxides and particulate matter from direct coal-fired power plants that are generally classified as:

- Pre Combustion— where sulfur and other impurities are removed from the fuel before it is burned.
- Combustion - where techniques to prevent pollutant emissions are applied at the boiler.
- Post Combustion—where the boiler flue gas is treated to reduce pollutants.

Current information for SO_X and NO_X control technologies are summarized in Tables 2 and 3. The mature status of these technologies

make them formidable competitors with emerging IGCC and PFBC technologies.

Advanced Clean Coal Technologies

Currently about 56% of U.S. power is generated from coal, but increasingly stringent emission regulations are being enacted for coal-based power stations. The U.S. Department of Energy's (DOE) Clean Coal Technology (CCT) program of demonstration projects is being conducted in response to this urgent need for the commercial development of technologies which can provide confidence for the continued use of coal for power generation and to maintain the use of valuable existing generating sites and equipment. The demonstration projects noted in this paper cover both Integrated Gasification Combines Cycle (IGCC) and Pressurized Fluidized Bed Combustion (PFBC) technology. If operated successfully, these plants (and those in Europe, and Japan) should provide the basis for deployment of commercial plants about the year 2000.

However, the current coal technology of direct firing with flue gas desulfurization has also continued to improve and for low sulfur coals and at sites with sea water cooling its established history and low capital costs are at this point still quite competitive. Nevertheless, gasification, gas clean-up, PFBC, gas turbines and fuel cells are all technologies which have significant improvement and growth potential. In addition gas turbines can be designed to handle both natural gas and coal derived syngas. Gasification, if developed as planned, can provide the technology to ensure the continued operation of the considerable investment in gas turbine combined cycles in the event that natural gas is no longer economically available and thereby provide a smooth transition to coal use. This "Phased Construction" approach can also be applied to the "Repowering" of valuable existing sites and equipment.

Obtaining operating permits for new sites is an increasingly lengthy and problematic procedure in many OECD countries. Therefore perhaps the most valuable existing resources of power generating companies are the ownership of, use permits for, and the precedent of operation at existing sites. If space is available the addition of new generation at existing sites is often easier and the "Repowering" or reuse of some of the existing site equipment and infrastructure can represent significant cost savings.

IGCC

The next most important event in the schedule for IGCC commercialization is the recently initiated operation of the highly integrated SEP 253 MW GCC plant in the Netherlands using the Shell Coal Gasification Technology and a Siemens-KWU V94.2 1100°C gas turbine. This has a design

efficiency of about 43% (LHV basis) and is designed to meet stringent emission standards. Single train IGCC plants using 1260°C firing temperature gas turbines are being designed and constructed for demonstration in 1995-2000 both in the U.S. under the DOE CCT program and in Europe.

The results from these demonstration plants will provide the basis for commercial IGCC plants anticipated to be deployed in the 2000+ time frame. The IGCC technology will also benefit greatly from advances made in gas turbine technology from both the DOE ATS program and other manufacturers' improvements which are expected to lead 1370-1425°C gas turbines being available in this same time frame. It is anticipated that increases in output and efficiency with such turbines will provide substantial capital and operating cost reductions for IGCC.

Six U.S. IGCC projects have been selected under DOE's CCT program. Three of these projects are proceeding PSI/Destec, Tampa Electric (TECO), and Sierra Pacific. The other three (ABB, TAMCO and Duke) are currently seeking to secure power purchase agreements and new sites. Information about the major ongoing IGCC projects is summarized in Tables 4a and 4b.

Pressurized Fluid Bed Combustion (PFBC)

Recent EPRI engineering studies of PFBC systems have projected that the capital costs of 320 MW PFBC units using modern supercritical steam cycles will be lower than IGCC in many applications and at similar efficiencies of 40-43%. PFBC technology is particularly suitable for moderate- to low-sulfur coals where the additional costs of handling the limestone required for SO_2 control and its associated solid waste products are sufficiently low to not offset the capital cost advantage. The smaller physical size of PFBC units is expected to provide an advantage over direct PC fired boilers, particularly in certain repowering applications at space constrained existing sites. Also, the added increment of power in repowering applications is 25% - 30% for PFBC compared to 200% for gasification which may make PFBC repowering more suitable for sites constrained by transmission capacity or not needed large incremental power additions.

Five 80 MW first-generation PFBC bubbling bed units using ABB Carbon technology are operating today in Sweden (2 units), Spain (1 unit), the United States (1 unit) and Japan (1 unit). The next major step for commercialization of bubbling PFBC is to scale the technology to 340 MW. Several bubbling PFBC projects at the 80 MW scale and one at the 340 MW scale are planned in Japan. Two additional 80 MW scale projects are being developed in Europe.

Circulating PFBC technology, which promises lower capital and

operating costs, better operating characteristics and further emissions improvements, is in the pilot scale of development. A 150 MW demonstration which utilizes Ahlstrom/Pyropower technology, is planned by Midwest Power in 1997. The two developers of circulating PFBC, Ahlstrom/Pyropower and Deutsche Babcock/LLB, use ceramic hot gas filtration in their systems which requires considerable development before it is able to achieve utility-required reliability levels.

Both bubbling and circulating PFBC should be commercially available from three to five manufacturers at the 300-400 MW scale by 2000.

Advanced PFBC

The integration of gasification with Pressurized Fluidized Bed Combustion (IGPFBC) has the potential to achieve high efficiency and a reduction in capital costs over IGCC albeit at some sacrifice in environmental performance with regard to solid waste. Partial gasification of the coal yields a char which is fed to the PFBC unit. Supercritical steam cycles can be used with PFBC to give substantial efficiency gain to the steam cycle and the combined effect of integrating this with the coal gas fired Brayton Cycle (i.e., gas turbine) results in high efficiency. As with PFBC this technology will find its preferred application using low to moderate sulfur coals.

In Europe Ahlstrom and Deutsche-Babcock have pilot plants exploring this configuration. British Coal's Topping Cycle is similar but plans to use an Atmospheric FBC rather than PFBC on the char from a spouted fluid bed partial gasifier.

In the U.S. Foster Wheeler has been testing this IGPFBC concept at their 2.5 MWTh pilot plant in Livingston, NJ. Under DOE, Southern Company Services and EPRI sponsorship, scale-up to a 15 MWTh pilot plant is planned for the Power Systems Development Facility (PSDF) to be located at Wilsonville, Alabama. A 90 MWe project based on this technology, proposed by Air Products for a Kentucky location was recently selected by DOE under the CCT program. It plans to start-up in 1998.

Integration Of Gasification With Other Advanced Cycles (IGAC)

Power plants based on the integration of gasification with advanced gas turbine cycles such as the Humid Air Turbine (IGHAT) offer the potential of significant cost savings over IGCC while maintaining the low emission and high efficiency characteristics. In IGCC plants expensive syngas coolers are used at the gasifier outlet to raise steam. However with humid air cycles, a lower cost quench gasification system can be

used with the quench providing hot water for use in air humidification. IGHAT will also have better part load efficiency that IGCC.

The Integration of Gasification with Compressed Air Storage combined with Humidification (IGCASH) can provide a very competitive intermediate load plant with low emissions and flexible operating characteristics. The lower cost quench gasification systems can also advantageously be used in this application. The gasification system and gas turbine operate continuously 24 hours/day typically delivering power to the grid about 16 hours/day and using the power about 8 hours/day (during the night) to compress air into a storage cavern. During the day air is withdrawn from the cavern to supply the combustion air to the gas turbine. The addition of natural gas fired turbo-expanders to operate off the same compressed air storage cavern as the IGCASH, can also provide additional low cost peaking capability (the CASHING concept).

It is anticipated that major components of currently available gas turbines and other equipment can be combined to produce these advance cycles. EPRI is continuing to study these concepts but no actual demonstration projects have yet been put together.

Integration Of Gasification With Fuel Cells (IGFC)

Studies conducted by DOE, EPRI and others in Europe show that the integration of gasification with molten carbonate or solid oxide Fuel Cells (IGFC) offers the potential of power plants with the lowest emissions and highest efficiency (> 54% LHV basis) of any coal based technology yet defined. However, at the current state of development and under the current standard economic least cost of electricity criteria the capital cost is still estimated to be too high, and the current R&D effort is therefore primarily aimed at obtaining crucial exposure experience of fuel cells to coal derived gas and at IGFC cost reduction. Early in 1994, EPRI completed a test of a 30 kW Molten Carbonate Fuel Cell on a slipstream of the syngas at the Destec 160 MW GCC plant in Plaquemine, LA.

The major fuel cell project currently underway is the 2 MW natural gas fired Molten Carbonate Fuel Cell (MCFC) demonstration plant due to begin operation in Santa Clara, CA in early 1995. Additional important projects are aimed at reducing the cost for fuel cell module assembly, gas manifolding and Balance of Plant (BOP) for multiple stack arrangements.

The demonstration of the IGFC concept at the ~ 10 MW scale, operating on a slip stream of a larger IGCC plant will probably occur in the late 90's to be followed

by demonstration of a stand alone IGFC plant in the first decade of the 21st century with subsequent commercialization beyond that time frame. In the longer term the integration of biomass gasification with fuel cells could be a very effective way of efficiently using the dispersed biomass resource.

Market Penetration of New Technology

Outside the United States the market for new coal fired power plants will be very large over the next several decades. It will be primarily driven by the rate of economic growth of the developing nations. Rough estimates of the size of the market are in the range of 20,000 to 40,000 MW per year through 2020. This is based on 1992 World Energy Council projections, which are summarized in Table 5, of increases in worldwide electricity production in that time period from 11,500 TWh in 1990 to 22,700 TWh in 2020 which can be converted into a total capacity increase of about 100,000 MW/year and an assumption that 20-40% would be coal fueled. The percentage growth in each of the markets in presented in Table 6. These estimates can be cross-checked against coal production estimates. EIA projected coal production increasing from 5100 to 6400 million short tons per year from 1991 to 2010. This would support an annual increase of about 25,000 MW of coal fired generation. EIA data on world wide coal consumption is summarized in Table 7.

Obviously these are only projections. They were developed from historical trend lines which involve population growth, Energy Intensity, GNP increase and a likely host of other factors. The key question is how will the responsible parties in each national(or local) situation decide on what their next power plant will be and what will it be fueled with?

The China Market

China is the key example that is focused on here to illustrate some of the challenges of bringing new technology to new markets. The market for new coal fired power plants in China will probably continue to be the largest in the world during the next two or three decades. China is the world's largest producer of coal. In 1990 production was 1.08 billion tons which equaled about 25% of world production. About 29% of this was used for power production which resulted in 75.6% of total generation. Generating capacity at end of 1992 totaled 166 GW. Current plans are to increase capacity at a 9% annual rate with the objectives of reaching production levels of 980 TWh in 1995 and 1500 TWh in 2000 with installed capacities of 200 and 300 GW respectively.

The principles for development of power production in China have been stated as

follows-" develop thermal power vigorously, exploit hydropower energetically and develop nuclear power appropriately". The implications are that the current high percentage of coal fueled thermal power will likely increase. The great distances between coal mines and markets for coal and power result in 40% of all rail traffic committed to the movement of coal.

As a result, there is a desire to develop large mine mouth power plants to free up the rail system .

As shown in Table 8, a large number of relationships with international organizations have been developed to facilitate technology transfer into this huge market. It is apparent that these relationships will facilitate the introduction of new technologies from companies and countries that have taken the initiative. Because foreign exchange resources have been limited in the past, there has also been a major effort to develop the capability to manufacture much of the required equipment domestically.

Recently completed thermal power projects and those planned for the next eight years are listed in Table 9. It is most likely that those planned for the beginning of that period will be conventional stations. However, toward the end of that time it is anticipated that advanced technologies will be considered. Texaco Development Corporation recently reported that it had entered into its tenth license for gasification technology in China. These are all syngas plants but the experience being gained now will support IGCC technology in the future.

Decision Factors

There are a large number of factors involved in choosing the technology for a new power plant. Some of these can be approached analytically but others will be approached on a qualitative basis. The major factors are:

Analytically based

Projected heat rate
Emissions
Capital costs
Fuel costs
Labor costs and staffing requirements
Other operating costs
Degree of subsidization offered

Qualitatively based

Maturity of Technology(i.e., number of commercial installations, success of existing units, status of demonstration programs,)
Quality of vendor team
Quality of vendor commitment and guarantees
Complexity(perceived ability of local people to successfully operate the plant)
Country of origin of the technology and vendors
State-of-the-art versus outdated technology

As in all other aspects of life, it is always easier to deal with analytical assessments. It is fairly simple to put together a proposal which describes a coal fired plant in detail. Cost, performance, and reliability projections which have been developed can be defended on the basis of background data, calculations and assumptions However, the relative probability of success of a specific customer making a technical decision on strictly analytical grounds is unknown and will vary with the situation. Therefore dependence on analytical work to sell technology to a new customer is usually inadequate. Marketing advanced coal technology will be a daunting task.

The key unresolved issue with these new technologies is that their immaturity as measured by few current commercial installations is real. Costs have not yet been substantially reduced through elimination of redundancy based on successful commercial operation. Few vendors are willing to take on the risk of delivering a fixed price power plant project. New approaches to competing in this market should be developed.

New Project Approaches

The traditional categories used in calculating the cost of electricity for a planned project are the capital investment, fuel, fixed and variable operating expenses, and byproduct revenue and disposal costs In order to meet competitive market requirements, it is suggested that a new approach be used in which projects are developed from the top down rather than the bottom up. What this means is setting targets for each of the cost categories so that the total cost meets the market need. The typical vendor or A/E in the power plant supply business historically develops a design to meet the clients capacity requirement , then calculates the total investment required in a business as usual fashion. If the COE computation doesn't meet the market requirement, the first response is to see how one of the other participants in the project can cut their costs. In discussions with individual vendors, it is usual to hear statements about how they have cut their costs to the bone but are sure that the other participants have a lot of fat in their estimates.

The traditional practice of treating each project as a one-of-a-kind design which is developed sequentially is very expensive and perhaps outdated. Is it possible to think more in terms of a product development rather than a project development approach? In that way concurrent efforts by the process design, mechanical design, procurement, construction planning and operating teams could be integrated from the beginning of the project to minimize ultimate costs. This approach requires bringing together a team of selected vendors who will coordinate their efforts to put together a market priced

offering. Whether the costs of such a product can meet market needs is open to question. If it does not, the parties involved can come to a decision on whether to offer the product or not. Since many of the costs involved would not have to be repeated for subsequent projects, the subsequent projects could be profitable enough to offset the potential losses resulting from subsidization of the initial project.

Repowering

Existing power plants sites are very valuable assets to power companies. All permits required for operation of the existing equipment are in hand. Tie-ins with the transmission system to move power from the site exist. However, many of the sites are equipped with inefficient generation equipment that results in a very low utilization factor. This situation represents a financial opportunity for those utilities that would like to add power capacity to meet load growth. Depending on the site, the incremental investment cost may be low enough to allow the utility to develop a project that is competitive with its other alternatives. In this way coal fueled projects may be able to compete with green-field natural gas combined cycle projects. A very careful analysis is required to determine if the potential savings from utilization of old equipment with a finite remaining life is attractive. However, as was stated previously, the most valuable attribute of an existing coal fired power generation site is its acceptance by the surrounding community.

Minimizing the Risk

Perhaps the single greatest concern facing the potential buyer of an new coal technology plant is how to minimize his risk. The key issues are whether the plant will meet its performance, reliability, availability and maintenance goals so that the project investment criteria can be met. This of course assumes that the fuel and electricity prices meet their market projections.

Most of the components in fluidized bed combustion and in gasification plants are in conventional use in other industries and their performance and reliability can be predicted with a fair degree of uncertainty. This information should be used in rigorous reliability analyses in the same way that process engineers can carefully calculate plant heat rate to four significant figures. The reliability should be designed into the plants, with weak components eliminated and redundancy used only where it is cost effective.

Personnel training should be very formal and long term utilizing tours of duty at existing IGCC and PFBC demonstration plants as well as simulators which have been validated to the extent possible in existing plants, and video archives which have

captured the experience of previous plant operations.

If all of the elements above can be accomplished properly then the probability of a minimum period startup and smooth transition into commercial operation can be enhanced. It is vital that the efforts of all teams that get involved are integrated from the beginning. If they are not, the risk of an unsuccessful project is greatly increased.

There is a cliché often used when discussing a new technology project with utility personnel (or indeed with others in any industrial organization), that pioneers usually get shot in the back. In addition the rewards to the early adopters of new technology often disappear in the fog of startup problems, poorer than design performance, and higher than predicted O&M expenses. It is far safer to be the owner of the second or third plant rather than the first.

The question is how to increase the comfort factor so that the project owner is more willing to take on the risk. There is a clear market reward for plants with an 8 — 10 point higher fuel efficiency if base load coal plants are the least cost option. Risk acceptance and minimization requires that the major components in the plant have been demonstrated elsewhere at a scale that is close to the new plant. Even more important is a successful demonstration of the integrated operation of those components. One of the key benefits of the DOE Clean Coal Technology program is that it provides an opportunity for these demonstrations. Most buyers have a rational "show me" attitude where a visit to a successfully operating demonstration plant is worth many visionary presentations.

New financial approaches are also likely to have an important market impact. For example the concept of Build—Own—Operate—Transfer may be appealing to utilities in developing countries and their bankers since the risk of performance and project cost is transferred to the project developers rather than the ultimate owners. It should also be presumed that in return for acceptance of the risks that many of the rewards would also flow to the developers. Perhaps a more equitable arrangement of risk and rewards between the initial developers and ultimate owners would encourage new coal technology projects to be formulated and consummated.

Conclusions

Although there may be a few near term opportunities for some of the new clean coal technologies in Eastern Europe and other regions of the world, in this time frame technology transfer to these countries is probably best focused on the current state of the art direct coal fired plant with emissions control technology and the establishment of an infrastructure

in these countries to supply equipment, components, parts and services. As the new clean technology projects complete their demonstration periods in OECD nations over the next few years, there will then be an infrastructure in place to support the wider deployment of advanced coal technology.

More efficient and cleaner power plants are being offered commercially for both natural gas and coal. Higher firing temperature and innovative gas turbine systems continued to evolve and are entering the market place. Coal fueled systems which utilize total gasification or pressured fluidized bed combustion both promise to provide efficiencies of about 45% when combined with those gas turbines with firing temperatures of 2300 to 2500°F which will be available prior to the year 2000. Major demonstration projects are underway in the United States of America and Europe at the 250-310 MW scale which will qualify these technologies for acceptance in the utility market.

Significant improvements are also underway with high temperature aeroderivative gas turbines and fuel cells. While the early market for each of these appears to be natural gas fired power plants, they can be utilized with clean coal gas when the economics are appropriate. Sophisticated gas turbine based cycles and simpler fuel cycles can generate electricity at over 60% efficiency on natural gas and over 50% on coal.

Marketing new coal fired technology to developing nations will require that vendors from the OECD countries develop business strategies that reduce the cost of the delivered power plant to the buyer, perhaps by subsidization, and more importantly reduce the risks involved. A few of the ways to reduce risk are to successfully complete current and planned demonstration project, design reliability into the project at the beginning since retrofits will be difficult and expensive, establish relationships with people and institutions in developing countries that can facilitate communication with the objective of avoiding misunderstanding, and carefully train, at existing plants, those people who will be involved in new technology projects.

Table 1. Markets—PC+FGD, PFBC & IGCC

	PC+FGD	PFBC	IGCC
Low S coal	√	√	—
Medium S coal	√	√	√
High S coal		—	√
Environmental Site constraints			√
Size < 200 MW		√	?
200-350 MW	√	√	√
500 MW	√		√
Repowering Need significant new power	N/A		√
Modest increment only required		√	
Site T&D constraint		√	
Stringent site environmental constraints			
—Air			√
—Solid waste			√

Table 2. Direct Coal Fired Plants

SO_2 Control Options

Option	% S Removal	Capital Costs $/kW
Physical Coal Cleaning	30-50 (Pyritic S only)	Australia
Furnace Sorbent Injection + Economizer & Duct Injection	20-40 (Limestone) 40-60 (Lime) Up to 70	50-100
Wet Limestone FGD + Additives	90-95 Up to 98	200 (1-3 times more for Retrofit)
Regenerable FGD		> Limestone FGD
Spray FGD		< Limestone FGD

Table 3. Direct Coal Fired Plants

NOx Control Options

		Costs	
Option	% NOx Removal	Capital Costs $/kW	Operating Mills/kWh
Low NOx Burner + Reburn	40-60	5-25	
SCR + Low NOx Burner	80 90	60-90	4-6
SNCR	30-55	5-15	0.5-2.0

Table 4a. DOE CCT GCC Projects in Progress

Project	Technology	Efficiency % LHV	MWe	Application	Start-up
PSI/Destec -Wabash River	Destec 2 stage Entrained O_2 Blown Cold Gas GE 7 FA	40	265	Repowering	Mid 1995
Tampa Electric Polk County	Texaco Entrained O_2 Blown Hot & Cold Gas Clean up GE 7 FA	42	260	Greenfield	Mid 1996
Sierra Pacific -Pinon Pine	KRW Fluid Bed Air Blown Hot Gas Clean up GE 6 FA	42	95	Existing Site	Late1996

Table 4b. European GCC Projects In Progress

Project	Technology	Efficiency % LHV	MWe	Applications	Start-up
SEP —Buggenum, Netherlands	Shell Entrained O2 Blown Cold Gas Clean up V.94.2	43	284 (Gross) 253 (Net)	Green Field	Early 1994
ELCOGAS —Puertollano, Spain	PRENFLO Entrained O2 Blown Cold Gas Clean up V.94.3	45	335 (Gross) 300 (Net)	Green Field	Mid 1996
RWE —KOBRA Hurth, Germany	HT Winkler Fluid Bed Air Blown Cold Gas Clean up V.94.3	45	357 (Gross) 312 (Net) (+27 from Residues in FBC)	Green Field	Post 2000

Table 5. Total Electricity Generation, TWh (Not as Primary Energy)

TWh	1960	1970	1980	1990	2020*
North America	958.0	1844.4	2731.4	3534.7	4700
Latin America	72.0	160.5	385.0	624.6	2500
Western Europe	611.7	1238.6	1892.1	2427.3	3850
Central Eastern Europe	74.5	184.1	336.0	372.8	600
Newly Independent States of Former USSR	292.1	735.6	1274.9	1722.1	2400
Middle East & N. Africa	10.2	36.6	117.2	273.4	1150
Sub Saharan Africa	30.2	74.2	148.2	220.5	700
Pacific (inc. Central Planned Asia)	230.0 (70.3)	615.1 (140.4)	1196.9 (354.6)	1997.7 (680.9)	5500 (2650)
South Asia	22.8	71.2	139.9	318.6	1250
World	2301.5	4960.3	8221.6	11490.9	22700

Table 6. Growth Rates in Electricity Generation, %p.a.

	1960-1970	1970-1980	1980-1990	1990-2020	(1960-1990)
North America	6.8	4.0	2.6	1.0	4.4
Latin America	8.3	9.1	5.0	4.7	7.6
Western Europe	7.3	4.3	2.5	1.5	4.6
Central Eastern Europe	9.5	6.2	1.0	1.7	5.4
Newly Independent States of Former USSR	9.7	5.7	3.1	1.1	5.9
Middle East & N. Africa	13.6	12.3	8.8	5.0	11.9
Sub Saharan Africa	9.4	7.2	4.1	3.8	6.9
Pacific (inc. Central Planned Asia)	10.3 (7.2)	6.9 (9.7)	5.3 (6.7)	3.4 (4.6)	7.4 (7.8)
South Asia	12.1	7.0	8.6	4.7	9.3
World	8.0	5.2	3.4	2.3	5.4

* Projection by WEC
Sources: UN Energy Statistics Yearbook, WEC

Table 7. World Coal Comsumption
(Million Short Tons)

			U.S. EIA Base Projections		
Market Economies		1991	1995	2000	2010
OECD		(2015)	(2094)	(2150)	(2285)
	U.S.	888	947	987	1135
	Canada	56	68	83	90
	Japan	127	134	134	136
	Europe	832	825	821	795
	Other	112	120	124	128
OPEC		11	13	14	18
Other Developing Countries		575	585	646	744
Total Market Economies		(2601)	(2692)	(2810)	(3047)
Centrally Planned Economies		(2501)	(2746)	(2988)	(3432)
	China	1192	1441	1685	2113
	Former Soviet Union	725	720	723	741
	Other	585	586	580	578
World Total		5102	5439	5798	6479

Table 8. Cooperative Agreements/Memoranda of Understanding Signed with Foreign Partners

Chinese Partnership	Foreign Partnership	Country
DIC, MEP	TEPCO	Japan
DIC, MEP	EDF	France
DIC, MEP	ENEL	Italy
DIC, MEP	DPIE	Australia
Northeast China Power Group Corp.	Hokuriku Electric Power Company	Japan
Northeast China Power Group Corp.	SECV	Australia
Jilin Electric Power	Hokuriku Electric Power Company	Japan
Heilongjiang Electric Power Company	Tohoku Electric Power Company	Japan
East China Power Group Corp.	KEPCO	Japan
Central China Power Group Corp.	Chuba Electric Power Company	Japan
Northwest China Power Group Corp.	Shikoku Electric Power Company	Japan
Zhejiang Electric Power Co.	EDF	France
Shandong Electric Power Co.	Pacific Power Company	Australia
Shandong Electric Power Co.	CESP	Brazil
Shandong Electric Power Co.	Kyushu Electric Power Company	Japan
EPPEI	EDF	France
EPIRI	JEPIC	Japan

DIC: Dept. of Int'l Cooperation
MEP: Ministry of Electric Power
DPIE: Dept. of Primary Industries & Energy
TEPCO: Tokyo Electric Power Company
EDF: Electricité de France
KEPCO: Kansai Electric Power Company
CESP: Companhia Energetica de Sao Paulo
SECV: State Electricity Commission of Victoria

Table 9. The Sino-Foreign Joint Venture Thermal Power Projects Completed and Planned (1986-2002) (BOT, BOO)

Completed Projects

No	Projects	Installed Capacity (Nox x MW)	Schedule	Estimated Loan U.S. ($M)	Source of Loan	Location (Province, Municipality,Region)
1.	Beilungang	2 x 600	1986-1993	390.00	World Bank	Zhejiang
2.	Ligang	2 x 350	1988-1992	245.00	Spain & Italy	Jiangsu
3.	Wujing	2 x 300	1988-1992	190.00	World Bank	Shanghai
4.	Shidongkou	2 x 600	1988-1992	413.06	EDC, USA	Shanghai

Planned Projects

	Projects	Installed Capacity (Nos x MW)	Location (Province, Municipality, Region)
1.	Waigaoquiao (phase 2)	2 x 800 or 2 x 1000	Shanghai
2.	Jiaxing (phase 2)	4 x 600	Zhejiang
3.	Ligang (phase 2)	2 x 350	Jiangsu
4.	Ligang (phase 3)	2 x 600	Jiangsu
5.	Shidongkou (phase 2)	2 x 600	Shanghai
6.	Yangcheng	4 x 600	Shanxi
7.	Tuoketuo No. 2	4 x 600	Inner Mongolia
8.	Daihai	4 x 600	Inner Mongolia
9.	Datong No. 2	2 x 600	Shanxi
10.	Shalingzi (phase 2)	2 x 600	Hebei
11.	Shuangyashan	2 x 600	Heilongjiang
12.	Zhuhai	2 x 600	Guangdong
13.	Beihai	2 x 350	Guangzi
14.	Xidu	2 x 660	Jiangsu
15.	Rizhao	2 x 350	Shandong
16.	Shjiliquan	2 x 300	Shandong
17.	Laicheng	2 x 600	Shandong
18.	Shiheng (phase 2)	2 x 300	Shandong
19.	Heze (phase 2)	2 x 300	Shandong
20.	Meizhouwan	2 x 350	Fujian
21.	Songyu	2 x 350	Fujian
22.	Hanchuan (phase 2)	2 x 300	Hubei
23.	Pingu	2 x 600	Beijing
24.	Expansion of Liaoning	2 x 300	Liaoning
25.	Shenmu	2 x 350	Shaanxi
26.	Dalian (phase 2)	2 x 350	Commissioned in the early "Ninth Five-year Plan" period
27.	Dandong	2 x 350	Commissioned in the early "Ninth Five-year Plan" period
28.	Nantong (phase 2)	2 x 350	Commissioned in the early "Ninth Five-year Plan" period
29.	Fuzhou (phase 2)	4 x 660	Commissioned in the early & middle "Ninth Five-year Plan" period
30.	Yueyang (phase 2)	2 x 350	Commissioned in the middle "Ninth Five-year Plan" period
31.	Shidongkou No. 2 (phase 2)	2 x 600	Commissioned in the middle & latter "Ninth Five-year Plan" period
32.	Luohuang (phase 2)	2 x 350	Commissioned in the middle & latter "Ninth Five-year Plan" period
33.	Shantou (phase 2)	2 x 350	Commissioned in the middle & latter "Ninth Five-year Plan" period
34.	Yingkou (phase 2)	2 x 600	Commissioned in the middle & latter "Ninth Five-year Plan" period

BOT: Build-Own (Operate) - Transfer BOO: Build-Own-Operate

2.2

Overview of the Independent Power Producer (IPP) Market for Advanced Coal-Fired Systems

by

Dale R. Simbeck, Vice-President - Technology
Stan Vejtasa, Manager - Power Technology
Alan Karp, Senior Chemical Engineer

SFA Pacific, Inc.
444 Castro Street, Suite 920
Mountain View, CA 94041

Presented at:
"Coal-Fired Power Systems 94 -- Advances in IGCC and PFBC"

Morgantown Energy Technology Center
Morgantown, West Virginia
June 21, 1994

INTRODUCTION

U.S. electric utilities traditionally are granted exclusive franchises to sell retail electricity in given geographical service areas. In return, the utilities agree to be regulated by public utility commissions (PUCs) that determine electricity prices for different classes of customers based on the utility's "cost of service," which includes a return on the utility's undepreciated capital investment (the "rate base"). With most large utilities being integrated, the regulatory structure covers electricity generation, transmission, and distribution through retail sales.

Regulation initially helped to stabilize the electric utility business, but ultimately inhibited it from reacting to the competitive changes now occurring worldwide for nearly all businesses. This fact and the subsequent deregulation of the electric power industry now are driving the growth of independent power producers (IPPs) and dramatically impacting the technology mix of new power generation capacity.

THE EVOLUTION OF THE U.S. ELECTRIC POWER INDUSTRY [1]

The rapid growth of the nascent U.S. electric power business during the late 19th and early 20th centuries soon attracted government regulation. Thus insulated from "ruinous competition," the industry quickly became concentrated. Stronger utilities absorbed their weaker neighbors and investor-owned utilities consolidated into even fewer holding

companies. By 1932, three such holding companies controlled over 44% of U.S. electricity production. Holding company abuses led to the Public Utility Holding Company Act (PUHCA) of 1935, causing many holding companies to break up and extending control over the interstate transmission and sale of electricity to what is now the Federal Energy Regulatory Commission (FERC).

U.S. utilities thrived following World War II, as new technologies -- such as large, high-efficiency pulverized coal (PC) plants and high voltage transmission -- drove down power costs. Between 1945 and 1965, the average electricity price fell by nearly 50% in real terms to about 1.5¢/kWh. Demand grew by 7% a year, and regulatory reviews usually were short proceedings to reduce rates as costs declined.

However, in the late 1960s and early 1970s, events reversed the decline in power costs and irreversibly altered the electric utility industry's future course. These events included:

- increased environmental regulations
- increased fuel costs
- unexpected expenses with nuclear technology
- declining load growth
- changes in regulatory practice

Many utilities had looked to nuclear power to solve their environmental problems and alleviate their dependence on fossil fuels. However, nuclear plants' economies of scale dictated large units having long construction lead times and lacking operating flexibility. These characteristics clashed with uncertain load growth and with future load-following and cycling capacity needs. Three Mile Island effectively eliminated nuclear as a generation option in the United States, stalling construction of many nuclear plants and exacerbating the financial repercussions for utilities.

Low (≈ 2%) annual load growth and eventual completion of many nuclear plants subsequently created widespread excess capacity. Inclusion of high-capital-cost nuclear plants in the rate base also threatened to significantly increase power costs. To minimize such "rate shock," PUCs disallowed or deferred recovery of nuclear plant investments, imposing severe financial strain on utilities.

THE EMERGENCE OF DEREGULATION AND COMPETITION [1]

In 1978, the Public Utility Regulatory Policies Act (PURPA) was passed, requiring utilities to buy power from Qualifying Facilities (QFs) -- unregulated cogeneration units and small power producers using waste or renewable fuels. Cogeneration QFs had to meet specific operating, efficiency, and ownership standards. Small power producers had to meet size, fuel use, and ownership standards. PURPA regulations were to be established by FERC and administered by state PUCs.

Local utilities were compelled to buy power from QFs at "avoided costs," as determined by PUCs, that ranged from marginal operating costs for utilities having excess capacity to cases that included the full capital and fuel charges for a new generation unit. California's Standard Offer No. 4, since discontinued, based avoided costs on $38/barrel oil and years of built-in escalation. After gas prices fell, such contracts became "gold mines" for organizations operating gas-fired QFs. Some utilities have since bought back these contracts, finding this option cheaper than buying the expensive power.

In 1978, concerns over oil and natural gas shortages precipitated the Fuel Use Act. This law prohibited utilities from building oil- or gas-fired capacity if planned operation exceeded 1,000 hours annually, thereby confining new oil and gas use to peaking units. Consequently, only high capital cost alternatives -- coal or nuclear -- remained available to utilities for baseload power capacity. QFs, however, were not similarly restricted and, when gas prices began falling in the early 1980s, were able to sell power at avoided costs based on the utility's "next new coal plant."

To correct this imbalance, the Fuel Use Act was amended in 1987 to allow utilities to build gas- or oil-fired generation capacity if it included provision for future conversion to coal. Successful demonstration of coal gasification, led by the Electric Power Research Institute (EPRI), in the mid-1980s made coal conversion a credible option for gas-fired combustion turbines and combined cycles.

PUCs, following guidelines proposed by FERC, subsequently took regulatory actions that were key to the emergence of competition in the electric power industry. These actions included the following key elements:

- Limiting avoided costs to the utility's least expensive alternative

- Allowing competitive bidding to establish avoided costs (-- a practice currently endorsed by most PUCs)

- Creating IPPs, a class of non-utility power producers that are not QFs but can sell unregulated power to electric utilities.

IPPs had a strong interest in building power plants but were severely constrained by two limitations -- PUHCA requirements and transmission access

PUHCA was the biggest legal obstacle to IPPs. To avoid regulation as a utility under PUHCA, IPPs either had to be a QF under PURPA or have a complicated ownership structure limiting a non-utility partner to a maximum of 10% ownership. Without guaranteed transmission access, IPPs also could be stranded with no place to sell power if the local utility refused to take it. Since utilities had to accept power from QFs, non-utility generators (NUGs) developed cogeneration projects -- so-called "PURPA machines" -- having only token thermal loads -- e.g., heating a greenhouse -- in order to obtain QF status.

As Figure 1 indicates, NUGs built an increasing amount of new generating capacity throughout the 1980s. In 1989, the capacity added by NUGs -- 7,000 MW -- equaled that added by regulated utilities. Figure 2 shows that, over the same period, the overall constant dollar retail price of electricity sold by U.S. electric utilities declined significantly.

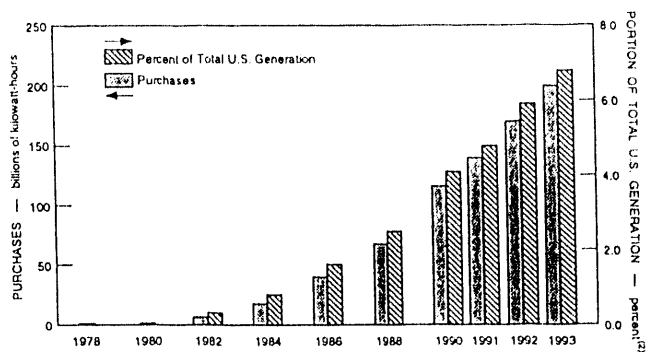

[1]Total non-utility power producer generation is approximately 50% larger than these figures. [2]SFA Pacific, Inc. estimate

Source: DOE and SFA Pacific, Inc.

Figure 1. Electricity Purchased From Non-Utility Power Producers by Electric Utilities in the U.S.[1] [Billion (10^6) Kilowatt-Hours]

The Energy Policy Act of 1992 facilitated NUG projects and reduced the associated regulatory burden and business risks by:

• creating a new class of unregulated power producers -- Exempt Wholesale Generators (EWGs)

• directing FERC to allow transmission access by EWGs to sell wholesale electricity in interstate markets

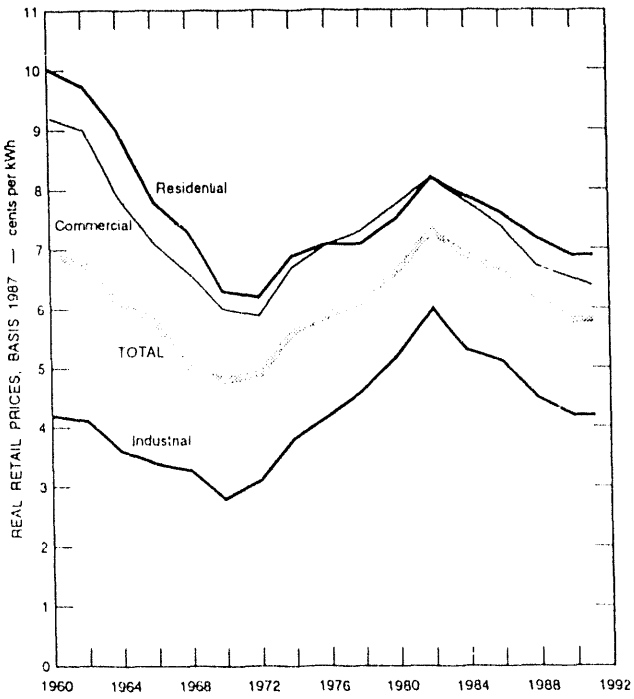

Source: DOE/Energy Information Administration

Figure 2. Real Retail Prices of Electricity Sold By Electric Utilities in the U.S., 1960-1991

• allowing companies generating and selling both wholesale and retail power in foreign markets exemption from PUHCA regulations

• eliminating PURPA's restriction of 50% utility ownership of a NUG facility

The Energy Policy Act portends an increasingly competitive wholesale power market that can be supplied by EWGs selling power without price regulation. Utilities that purchase the power for retail sales remain regulated, and PUCs may play a role in approving wholesale power sales agreements. To date, most power sales prices are being determined by bidding systems whereby utilities request proposals and select winners based on cost and other factors such as dispatchability. NUGs have responded to such solicitations in large numbers, with offers to supply power often exceeding the requested amount by a factor of ten.

LOOKING AHEAD: THE 'NEW ORDER' OF ELECTRIC POWER GENERATION [1]

Experience has shown that many unregulated power producers are:

• aggressive in developing projects
• undeterred by environmental regulations
• willing to adopt new technology
• not biased against gas, as many utilities are or have been

Deregulation of electric power generation will continue, with EWGs and cogenerators supplying most new baseload capacity. Clean-burning natural gas will be the fuel of choice because it eases facility siting and lowers capital costs. Gas also will be preferred for new peaking capacity, even if its price rises significantly, because utilities want to minimize their capital investment in equipment having a low capacity factor. Peaking capacity most likely will be built by utilities, although unregulated companies have bid to supply peaking units.

NERC forecasts that the net growth of new generation capacity will average only 1.2%

Table 1
Current Status of U.S. Electric Power Generation
(Nameplate Capacity)

	Capacity, MW January 1992	Capacity, MW January 1993	Increase, % 1992-1993
Type of Facility			
Electric Utility	740,000	742,300	0.3
Non-Utility			
Cogenerators	37,100	40,700	9.7
Small Power Producers	10,000	10,200	2.0
Other (EWGs)	2,900	4,300	48.3
Total Non-Utility	50,000	55,200	10.4
Total U.S. Capacity	**790,000**	**797,500**	**0.9**
Type of Fuel--Non-Utility			
Coal	7,600	8,600	2.6
Oil	1,400	1,500	7.1
Natural Gas	21,800	24,900	14.2
Biomass (Wood)	9,300	9,600	3.2
Waste Fuels	3,600	3,800	5.5
Hydro, Wind, Solar, Other	6,300	6,800	7.9
Total	**50,000**	**55,200**	**10.4**

Source: Edison Electric Institute (EEI) and SFA Pacific, Inc.

over the next decade. Although a somewhat higher growth rate -- 1.7% -- is anticipated for peak demand, the higher rate can be absorbed by the current excess capacity.

As Table 1 shows, the total net (nameplate) generation capacity added by U.S. electric utilities grew by only 2,300 MW, or 0.3%, in 1992. However, new capacity added by NUGs increased by 5,200 MW, or 10.4%. Over half the new NUG capacity uses natural gas.

NUG power has grown so much in some parts of the United States that utilities cannot always absorb the power produced. Most new power contracts with larger NUG facilities therefore allow the utility to reduce power purchases when demand is low. At such times, the NUG typically receives a payment to cover fixed costs. According to EEI, of the 55,000 MW of NUG capacity, 12% is fully dispatchable, 22% is partly dispatchable.

The other major area addressed by the Energy Policy Act, transmission access, will be more difficult to implement. Key issues are the price to be charged for wheeling power and the management of electricity load flows.

Although the Energy Policy Act prohibits interstate sales by NUGs to retail customers, some PUCs want to allow retail wheeling within their state. If successful on an intrastate basis, interstate retail wheeling undoubtedly will be implemented.

New technology has facilitated unregulated power generation. The emergence of highly efficient and reliable combustion turbines and combined cycles with low environmental emissions has allowed the siting of power generation and cogeneration facilities at numerous industrial sites. While electric utilities have been reluctant to install combustion turbines because of bad experiences with early models in the late 1960s and early 1970s, combustion turbines are the technology of choice for NUGs.

NUGs also have embraced new technologies promising lower cost operation -- and greater profits. For example, NUGs essentially commercialized atmospheric pressure circulating fluidized bed combustion (CFBC) in the 1980s. NUGs also have been receptive to new emission control technology, such as selective catalytic reduction, to avoid regulatory siting delays and bring facilities on line faster. Utilities, however, sell power on a cost-of-service basis and reap no reward for taking technical risks. They therefore tend to be extremely risk averse, avoiding new technologies.

A CASE FOR ADVANCED COAL-BASED POWER [2-5]

In most locales, making an economic case for coal-based power of any kind currently is difficult due to low prices and ample supplies of natural gas. Moreover, near-term capacity requirements in the United States and Europe are largely for cycling and peaking service, for which coal is not competitive with combustion turbine systems having far lower capital costs.

However, as erosion of the supply/demand balance drives natural gas prices up and new baseload capacity needs emerge, coal-based power will again become economic. Based on recent technical and commercial successes and on current commercial demonstration programs, coal gasification will dramatically challenge direct-coal-fired power for this market. Coal gasification has fundamental advantages over direct coal-firing in environmental performance, efficiency, and flexibility.

Coal gasification has demonstrated superior environmental performance with respect to air, water, and solid waste. A coal gasification combined cycle (CGCC) power plant can match the emissions levels of a natural gas combined cycle plant. A CGCC's aqueous effluents are significantly less than for direct coal-fired steam cycles because a CGCC's steam cycle produces less than 40% of the system's overall power generation. Most coal gasification processes produce a granular, non-leachable slag having little or no fly ash. This is the only solid waste, since sulfur is recovered and sold in purified elemental form. Direct combustion systems produce 2-3 times the amount of solid waste.

With CGCC, 65-80% of overall power output is generated from the high temperature combustion turbine-based topping cycle. This provides high overall efficiencies and much higher power-to-cogenerated heat ratios, compared to steam cycles. Several coal gasification developer/vendors (e.g., Texaco, Destec, Shell) now offer CGCC designs, based on commercially proven technology, having electric power efficiencies greater than 40% (HHV) for standalone power plants. This equates to a heat rate of 8,500 Btu/kWh. If cogeneration is considered, the electric power

and overall efficiencies can exceed 50% and 80%, respectively.

Flexibility to meet the market requirements of competitive power production will be essential for individual generators. Self-generation and cogeneration, both already widely practiced, will expand greatly in response to the economics of deregulated generation. Combustion turbine-based technology has clear flexibility advantages for both. Combustion-turbine based systems using natural or coal-derived gas are more flexible in terms of size and configuration than direct coal-fired systems. For example, aeroderivative combustion turbines can be built in various smaller sizes and produce the highest electric power-to-cogenerated heat ratio. Fuel gas also can be transported to numerous small combustion turbines located at a distance from one large coal gasification plant.

Since the majority of new generation capacity now being installed is natural gas combined cycle, coal-derived fuel gas replacement, another aspect of CGCC flexibility, could be important in the future. Medium-BTU coal gas produced in oxygen-blown coal gasification processes is easily fired in combustion turbines originally designed to fire natural gas. For maximum benefit, future conversion to CGCC should be planned in advance. SFA Pacific's evaluations indicate that coal-based power generation again becomes economical when natural gas prices reach the range of $5-6 per million BTU.

In view of U.S. environmental mandates, repowering of old coal-fired power plants with coal-derived gas may be an attractive option, especially in high-sulfur-coal regions. The use of coal gasification/combustion turbine-based repowering to achieve environmental compliance currently is being commercially demonstrated as part of DOE's Clean Coal Technology program.

Synthesis gas coproduction is another potentially attractive option for improving CGCC's flexibility and economics, especially for new power plants that could be required to operate in cycling service in the future.

Pressurized fluidized bed combustion (PFBC) currently is being demonstrated, even as promoters are transforming PFBC designs to improve efficiency. The "advanced" PFBC designs essentially are highly integrated, air-blown CGCC designs with hot gas cleanup aimed at increasing PFBC's low gas turboexpander-to-steam turbine power ratio, thereby improving efficiency. However, PFBC, advanced PFBC and advanced CGCC systems all face major technical and economic challenges in achieving their potential advantages relative to well-designed conventional PC or CGCC plants. The key issues are environmental performance (NO_x, HAPs, solid waste), turboexpander operation with dirty high-temperature gas, and the impact of deregulation on competitive power generation options, especially cogeneration. The lack of short-term markets for advanced coal technologies makes continued government support critical if these challenges are to be resolved.

INTERNATIONAL POWER GENERATION [5]

NUGs in the United States have built new power plants on time and on budget. This success has been carefully observed by the international community, and independent power production has recently spread to many areas of the world. Unlike regulated utilities, NUGs receive no allowances for funds used during construction, thus having a strong incentive to build and commission plants

quickly. They also have strong incentives to keep them running, since they receive no revenue if no power is sold (-- unlike regulated utilities, which can earn a return on a rate-based plant even if it is idle). This efficiency of plant construction and operation convinced the World Bank to require any country requesting a loan for power generation facilities to offer the option of private ownership and operation.

Over 125 IPPs now are active in about 50 countries. Table 2 shows the leading IPPs. Exxon Energy, with nearly 6,000 MW, leads the list because of its large holdings in China Light & Power in Hong Kong. However, Mission Energy, an affiliate of Southern California Edison, has the greatest diversity of projects. Five of the top ten IPPs are from Europe and Asia.

Table 2
Top Independent Power Firms
by Net Project Ownership

Net Ownership, MW	Company
>5,000	Exxon Energy
2,000-3,000	Mission Energy
	National Power Int'l.
	Enron Power
1,000-2,000	PowerGen
	Sithe Energies
	AES
	Hopewell Holdings
	Destec Energy
	British Gas
	CMS Generation
	U.S. Generating
	Cogen Technologies
500-1,000	Cogentrix
	Dominion Energy
	Southern Electric Int'l.
	Wheelabrator
	Intercontinental
	J. Makowski
	Texaco
	Tractebel
	Trans Alta Energy

Source: Independent Power Report (McGraw-Hill) and SFA Pacific,Inc.

IPPs are closely watching the countries having the greatest need for new power generation capacity. Private power needs outside the United States and Canada reportedly grew by 64% in 1993 to 487,000 MW. China's booming economy and increased interest in private sector participation have, over the last year, doubled some estimates of that country's potential private power needs, although such estimates may be inflated by many projects that will never be built.

The enormous overall growth in coal-fired utility power plants in China -- perhaps by as much as 17-20 GW per year between 1995 and 2000, 70-80% of it coal-based -- provides the current market for vendors of large coal-fired power plant technology. The corresponding market in developed nations is bleak due to excess capacity and the proliferation of NUG capacity using primarily natural gas.

The growth in coal-fired generation in China also is well timed for IPPs. According to various reports, over 60 GW of electric power generation capacity in China now is being solicited for IPP ownership of build-own-operate-transfer (BOOT). The IPPs' capital and construction and operating expertise will be invaluable to China. The IPPs' biggest challenge will be financing and payment terms.

China currently is building "world class" 300-600 MW PC power plants. These plants include low-NO_x burners and electrostatic precipitators, but usually are without SO_2 controls due to the low sulfur content of Chinese coals.

In the future, the Chinese electric utility industry will want coal-fired plants based on advanced technologies such as CFBC, pressurized fluidized bed combustion (PFBC), and CGCC. All three technologies offer higher efficiency and lower emissions than current Chinese coal-fired power plants. Fluidized bed systems are advantageous for use in China due to the high ash content and variability of its coals. Also, the low sulfur content of most Chinese coals greatly reduces solid waste disposal problems. However, all three advanced coal technologies also require technology transfer, additional imported components, higher capital cost, and the highest quality construction, operation, and maintenance. The success of these advanced coal-fired power plant technologies in China will be greatly enhanced by the presence of IPPs and BOOT.

Though generally of less interest to the international coal technology community, industrial sector coal use in China is perhaps more important than utility sector use, for the following reasons:

- the annual tonnage increase in industrial coal use, currently about 550 million tons per year and over half of total coal use, will equal the growth in utility consumption

- industrial coal use is China's largest source of air pollution

- industrial cogeneration -- using either simple domestic or advanced coal technology -- potentially can far exceed the efficiencies of the most advanced standalone power plants

- many parts of China's industrial sector are experienced in international trade and technology licensing

- "hard currency" is available to the industrial sector, making IPP and BOOT financing and payment terms much easier than those for utility projects.

CFBC is clearly favored for new industrial boilers in China due to fines content, coal variability, low sulfur content -- and the highly successful CFBC boiler experience in the United States. SFA Pacific's FBC database shows 19 licensed CFBC units -- based on Ahlstrom/Pyropower and Riley/Deutsche Babcock technology -- at 10 locations in China with a total steam generation capacity of 2,700 tons/hour. Longer-term, coal gasification will be even better for industrial cogeneration in China. Texaco already has several coal gasification projects in China's industrial sector in conjunction with combustion turbine-based cogeneration, industrial fuel gas, and synthesis gas chemicals. The industrial use of coal gasification will greatly expand as China converts from an oil exporter to an oil importer. [6]

The U.S. government's current efforts to assist development of clean coal technology projects in China constitute a win-win" situation. They help China improve its environment while furthering commercialization of the most promising U.S. clean coal technologies.

OUTLOOK

The deregulation of electric power generation will continue to expand worldwide. Problems relating to transmission access in the United States will be resolved, once pricing mechanisms are worked out. Retail wheeling likely will be allowed in several states and could result in a nationwide power brokering system with the transmission lines serving as common carriers. Electric utilities still interested in operating generation facilities will

set them up as EWGs to maximize profitability.

Combustion turbine-based technology increasingly will dominate fossil generation in the developed nations. Coal gasification combined cycle is the only coal technology that is synergistic with natural gas-fired combustion turbine systems and will therefore find markets when coal-based power generation again becomes economic after the year 2000.

Markets for IPP power generation are expanding worldwide, particularly among the developing nations. China provides the current market for vendors of large coal-fired power plant technology, currently in the form of "world class" PC plants. In the future, China will seek advanced coal-based power generation options. The U.S. government's assistance to advanced coal technologies assures that the U.S. will continue to be the world leader in both independent power production and clean coal technology.

REFERENCES

1. S. Vejtasa, "The 'New Order' of Electric Power Generation," *The SFA Quarterly Report*, a private multisponsored report, SFA Pacific, Inc. April, 1994.

2. R.L. Dickenson and D.R. Simbeck (SFA Pacific, Inc.), "Coal Gasification-Based Electric Power -- The Present and Future," technical keynote presentation at the JSME-ASME International Conference on Power Engineering - 93 (ICOPE - 93), Tokyo, September 12-16, 1993.

3. *Combustion Turbine Power Systems: Analysis of Technology, Fuels, and Economics*, SFA Pacific, Inc., a private multisponsored analysis, August 1993.

4. A.D. Karp and D.R. Simbeck (SFA Pacific, Inc.), "The Future of Combustion Turbine Technology for Industrial and Utility Power Generation," presented at the 16th National Industrial Technology Conference, Houston, April 13-14, 1994.

5. D.R. Simbeck et al, *Coal Gasification Guidebook: Status, Applications, and Technology*, EPRI Report TR-102034, December, 1993.

6. D.R. Simbeck and R.L. Dickenson (SFA Pacific, Inc.) and L.D. Carter (U.S. Department of Energy), "Coal Utilization in China: Technology Options by Sector," presented at the IEA Second International Conference on the Clean and Efficient Use of Coal and Lignite: Its Role in Energy, Environment, and Life," Hong Kong, November 30 - December 3, 1993.

2.3 The Search for Innovative Technology

Dr. C. Lowell Miller
Associate Deputy Assistant Secretary
Office of Clean Coal Technology

ABSTRACT

The Clean Coal Technology Demonstration Program is but one phase of a research and development effort embarked on a continuous search for innovative technologies that over the years have been needed to overcome the barriers that have threatened the continued use of coal as an energy source. The significance of past technology development in coal utilization is perhaps best evident in the historic trends in thermal efficiency and output capacity of coal-fired plants. The thermal efficiency of these facilities has increased from 5 percent in the late 1800s to nearly 45 percent by the early 1990s. This increase has resulted in an 86 percent reduction in fuel consumption per kilowatt hour of power produced. During this same period, boiler size has increased from 50 kilowatts to 1,200 megawatts, causing the cost of new generating capacity to drop by over 60 percent.

While these significant achievements were being made in thermal efficiency and cost of generation, however, new societal and institutional demands have been evolving. The fundamental changes in the technology of coal utilization are now being driven by another significant factor--environmental control requirements. As a result, environmental performance criteria have been raised over the past decade to a level equivalent with the classical criteria of cost and reliability. It is now necessary to consider each of these criteria also in the search for new innovative concepts. In spite of these new requirements, continued progress in the development of coal utilization technology is not only expected, but is in progress. Such concepts as Integrated Gasification Combined Cycle, Pressurized Fluidized-Bed Combustors, fuel cells, magnetohydrodynamics, etc., hold the promise of being able to connect thermal energy into electrical energy at efficiencies of 55 to 60 percent. At the same time, these systems in themselves and as part of advanced cycles will reduce any associated environmental impact.

It is possible through the continued development, demonstration, and commercialization of clean coal technology to establish coal in the 21st century as a fuel that can be stored and transported in an environmentally clean and aesthetically acceptable manner, that supplies reliable competitively priced power, that can be a source of industrial steam and power, and that serves as a feedstock for value-added refined fuels and products that can be used cleanly and efficiently.

Continued development of innovative advances in coal utilization will reverse the inaccurate, negative image of coal, replacing it with an updated public view of coal as an economic, stable, efficient, and environmentally responsive fuel of choice.

Session 3

Advanced IGCC Systems

Integrated Gasification Combined Cycle - A View to the Future

Dale K. Schmidt
Morgantown Energy Technology Center

INTRODUCTION

DOE is involved in research, development, and demonstration (RD&D) of Integrated Gasification Combined Cycle (IGCC) because of a strong belief that it will result in widespread commercialization that will be of great benefit to this Nation. METC's long-range vision comprises (1) product goals that require improvements to known technical advantages, and (2) market goals that are based on expectations of market pull.

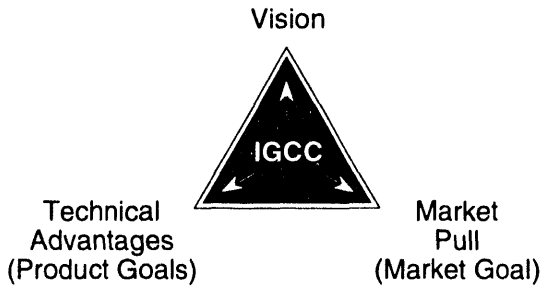

Figure 1. Vision and Goals for IGCC

The first IGCC plant in the United States was build for about $3,000 per kilowatt (kW) in the mid 1980s and operated at an efficiency comparable to conventional coal-fired plants. The six IGCC clean coal projects scheduled for startup from the mid to late 1990s will demonstrate significant reductions in capital cost ranging from $1,500 to $2,000 per kilowatt and impressive increases in efficiency of around 40 percent, based on higher heating value (HHV). The METC vision for IGCC is that over the next 20 years R&D-based technology advances and plant learning curve cost reductions will yield even more dramatic improvements resulting in plant efficiencies of over 50 percent and cost reductions to nearly $1,000 per kilowatt.

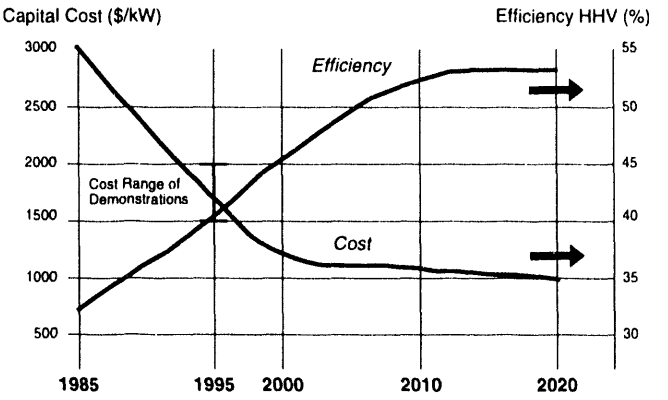

Figure 2. IGCC Vision: Cost versus Efficiency

Specific goals (Table 1) are that by the year 2010, capital cost as low as $1,050/kW and efficiencies as high as 52 percent HHV are viable along with superior coal-based environmental performance, resulting in possibly the lowest cost electricity option. Commercial-scale demonstration of multiple IGCC technologies that will result in healthy competition is critical to this goal.

Fossil Energy research and development (R&D) is interactively supporting the IGCC product goals. The year 2000 goal of 45 percent efficient IGCC plants is aided by over 50 METC contracted and in-house projects that are topics of these conference proceedings. Major

initiatives are underway in advanced gasifier systems and advanced turbine systems toward achievement of the more ambitious year 2010 goal of 52 percent efficiency.

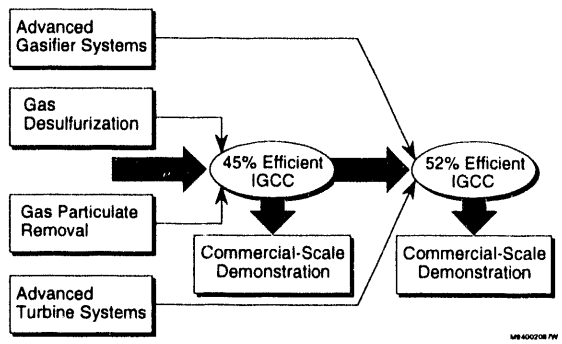

Figure 3. Interaction of IGCC Product Improvements

DOE projections of our Nation's electricity needs are provided by the Energy Information Administration-Annual Energy Outlook (AEO). (See Table 2.) Considering the AEO-1994 projection for coal-based and gas turbine-based electricity production, modest assumptions about the IGCC market share of three market segments are made. These market segments are: (1) coal plant additions, (2) coal plant repowerings, and (3) staged addition of gasifiers to natural gas combined cycle plants. It is expected that the IGCC investment could exceed $150 billion by the year 2030.

The combination of these IGCC technology goals and market goals suggest great benefit to our Nation. The IGCC dollar investment, as projected through the year 2000, has the potential of millions of person/year construction jobs, thousands of permanent operating jobs related to domestic projects, and thousands of U.S. jobs related to overseas projects.

Six IGCC commercial-scale demonstration projects costing nearly $3 billion are underway

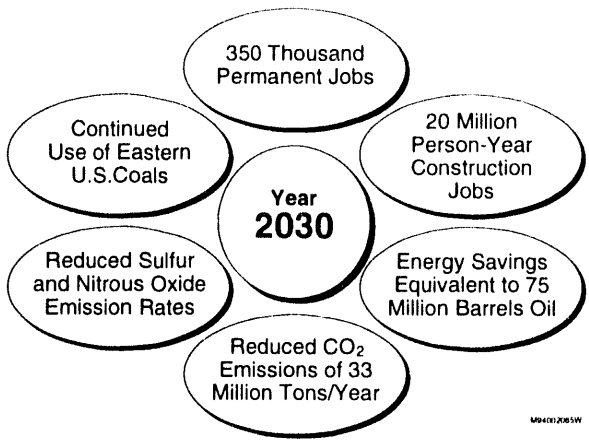

Figure 4. National Benefits of IGCC

in DOE's Clean Coal Technology (CCT) program. The Government is cost sharing about one-third of these CCT demonstrations. METC's strategy is to link RD&D via a product improvement concept so that (a) the CCT projects will benefit from the latest R&D results, and (b) R&D will be focused toward technical breakthroughs that shortcut achievement of the longer range IGCC goals.

The IGCC R&D budget (Table 3) necessary to accomplish these purposes projects a modest growth for FY 1995 to about $28.2 million. Additionally, there is about $2 million of IGCC-related funding in two other budget categories: advanced research and environmental technology (AR&ET), and advanced research and technology development (AR&TD).

Within the IGCC budget (Table 4), about 40 percent is allocated to the Power Systems Development Facility, about 25 percent to Gasifier Product Improvement, about 20 percent to two large-scale hot gas cleanup systems test facilities, one at General Electric and one at METC, and the balance of about 15 percent to other hot gas cleanup (HGCU) activities. Essentially, all of these projects are described in these conference proceedings.

Table 1. IGCC Product Goals by Year 2010

Capital Cost:
$1,050 per kW to build

Efficiency:
Operating at 52 percent efficiency

NO_x Emissions:
0.06 lb. per million Btu

SO_2 Emissions:
0.06 lb. per million Btu

Commercial-Scale Demonstrations:
Six U.S. technologies

Table 2. IGCC Market Goals

Market Area	By 2010	By 2030	By 2050
Added or Replaced Plants IGCC Share	1%	20%	30%
Aged Plants > 30 IGCC Repowered	0.5%	20%	80%
Nat. Gas CC Plants Conversions to IGCC	0%	10%	50%
Cumulative IGCC Capacity (Thousand Megawatts)	6	155	450

Table 3. R&D Budget - IGCC Related

Budget Category	FY93	FY94	FY95*	
AR&ET	5.3	3.7	2.9	~ $2 Million per Year is IGCC Related
AR&TD	3.6	2.5	2.7	
IGCC	19.5	27.2	28.2	

Dollars in Millions

** Proposed to Congress*

Table 4. IGCC R&D Budget

	FY 93	FY 94	FY 95*
Power Systems Development Facility	6.8	10.2	12.9
Gasifier Product Improvement Facility	4.2	6.0	7.8
GE/METC PDUs	3.4	5.9	5.2
Other HGCU	5.1	5.1	2.3
IGCC Total	19.5	27.2	28.2

** Proposed to Congress* *Dollars in Millions*

DSCHMI\2:940804

3.1 IGCC System Studies

Lawrence K. Rath
George T. Lee
Patrick H. Le
Morgantown Energy Technology Center

OBJECTIVE

Systems studies are performed on both the currently available, but not fully demonstrated, integrated gasification combined-cycle (IGCC) technologies and the future technologies. The objective of these studies is to support and guide the Morgantown Energy Technology Center's (METC) Strategic Product Planning efforts. Through these efforts, the research, development and demonstration (RD&D) needs of various alternative gasification and power island components can be quantified and factored into the overall planning processes.

BACKGROUND

IGCC product plans have established the following RD&D goals:

- Net system efficiency of 45% by 2000 and 52% by 2010.
- Capital costs in 1990 dollars of $1,200/kilowatt (kW) in 2000 and $1,050/kW in 2010.
- Cost of electricity (COE) 80% of conventional pulverized coal (PC) plant with flue gas desulfurization in 2000; COE 75% of PC plant by 2010.
- Nitrogen oxide (NO_X) and oxides of sulfur emission values of 0.06 pound per million British thermal unit in 2000 and less than 0.06 by the year 2010.

Ideally a number of IGCC systems will be able to meet these goals in the noted time periods. Results of system studies conducted by METC are discussed in this paper relating to these goals.

IGCC STUDIES BASED ON CURRENT GAS TURBINE TECHNOLOGY

Two U.S. organizations are currently offering gas turbines that feature 2,300°F to 2,350°F turbine inlet temperatures. Each organization also has sufficient experience or data to guarantee performance on fuel gas supplied via coal gasification. This guarantee allows these "F-technology offerings" to be a basis for METC's current view of nominal 250-megawatt (MW) IGCC modules representing a spectrum of gasification technologies, as shown in Table 1. The predicted exhaust gas temperatures exiting the turbine of approximately 1,100°F would readily allow a heat recovery steam generator with 1,450 pounds force per square inch, absolute (psia), 1,000°F generation and 1,000°F reheat for the steam turbine portion of a combined cycle.

An IGCC based on a fluidized-bed gasifier would operate at 1,850 to 1,900°F and 400 psia with air supplied from the gas turbine and a booster compressor as the oxygen source. Limestone added to the coal inlet stream would calcine and provide in-bed sulfur capture of hydrogen sulfide as it is released from the coal. Carbon conversion in the gasifier is 96.5% with residual carbon present primarily in overhead fines. Fuel gas from the gasifier passes through

Table 1. Today's View

IGCC Efficiency Using F-Type Technology
1,450 P/1,000/1,000°F Steam Cycle

Gasifier Type	Fluidized Bed	2-Stage Entrained Flow	Fixed-Bed Slagging	Slurry Feed Entrained Flow
Oxidant	Air	Air	Oxygen (Partial Integrated ASU)	Oxygen (Partial Integrated ASU)
Gasifier C-Conv.	96.5%	98.7%	99.2%	98.9%
Gasifier Pressure	400 psia	325 psia	395 psia	615 psia
Type of Gas Cleanup	1,210°F ZnTi, HGCU, Fixed Bed	1,250°F ZnTi, HGCU, Fluid Bed	100°F Selexol, Claus/ Scot, CGCU	1,250°F ZnTi, HGCU, Moving Bed
Sulfur Recovery or Conversion	Atmospheric Sulfation (Disposal)	Sulfuric Acid	Elemental Sulfur	Sulfuric Acid
Net Power	275 MW	260 MW	248 MW	268 MW
Overall Efficiency, % of HHV	43.3%	43.9%	41.8%	42.8%
Cost of Electricity, mills/ kW, Constant $	55.6	53.9	64.4	58.5

cyclones and is cooled to 1,210°F, where it is filtered of all particulates and chlorine is removed. The fuel gas is then desulfurized to less than 20 parts per million by volume (ppmv) in a fixed bed of a regenerable zinc-based sorbent. The clean gas can then be directed to the combustors of the gas turbine. Sulfur dioxide (SO_2) generated in the regeneration process along with the calcium sulfide underflow from the gasifier is converted to calcium sulfate. Any residual carbon from the gasifier is burned to produce additional steam in an atmospheric sulfation unit. All residue from this unit is disposed by landfill.

The steam turbine contribution to the combined cycle is increased by the steam generated from the atmospheric sulfation unit. The overall net efficiency on an higher heating value (HHV) basis for this 275-MW net IGCC is 43.3%. The COE in constant 1992 dollars is 55.6 mills per kW/hr.

An alternative air-blown, gasification concept is a two-stage entrained flow unit, where the dried coal feed and some limestone is split 85/15 between a slagging bottom stage at 2,800 to 3,000°F (partial combustion gases flow upward) and the second stage, where steam is added to promote carbon conversion at 2,000°F and 325 psia. Fuel gas and fines carried over

from the second stage are cooled to 1,250°F. Fines are separated and recycled to the bottom stage. With the higher operating temperatures, carbon conversion is predicted to be 98.7% A ceramic filter removes the last traces of fines prior to a chloride removal guard bed. A fluidized-bed desulfurization process reduces the hydrogen sulfide level to less than 50 ppmv, and sorbent regeneration produces an SO_2 stream that is converted into byproduct sulfuric acid.

Without the steam generated from sulfation in the previous IGCC system, the overall net power generation from this IGCC system is 260 MW. The higher carbon conversion of the gasifier contributes to a net efficiency on a HHV basis of 43.9%. COE in constant 1992 dollars is 53.9 mills per kW/hr.

Overall coal gasification efficiency is enhanced by counterflow of coal against the rising product gases generated in fixed-bed gasification of the oxygen-blown, slagging type. Partial integration of the air separation unit (ASU) with the gas turbine is utilized to enhance overall plant efficiency. A substantial portion of the coal sulfur is released in the form of coal tars in the uppermost region of the gasifier. To achieve overall sulfur capture in gasification of 99% as a common basis for all of the system studies discussed in this paper, the coal tars in the product gas had to be quenched to facilitate recycle to extinction in the slagging zone of the gasifier. The overall carbon conversion of the gasifier was 99.2%. With tars in the raw gas, no heat recovery of raw gas is considered feasible. Cold gas cleanup of the product gas at 100°F was utilized with a Selexol System, followed by elemental sulfur recovery using the Claus with a SCOT tail gas treatment.

The overall power production of this IGCC system was only 248 MW for two reasons: inability to utilize raw-gas heat recovery, and higher miscellaneous power usage of the partial ASU supplying oxygen and cold gas cleanup. As a result, the IGCC efficiency was 41.8% on a HHV basis, and COE was substantially higher at 64.4 mill per kW/hr than other cases studied.

The final IGCC case simulated with the current version of gas turbine technology is a slurry-feed, entrained-flow, slagging gasifier operated in excess of 2,400°F and 615 psia, followed by heat recovery/chloride removal and moving-bed, hot-gas cleanup at 1,250°F using zinc-based sorbents. The overall power requirements for oxygen supply to the gasifier are reduced via partial integration of the ASU with the gas turbine air compressor. Power is recovered in an expander on the fuel gas between the chloride guard and the moving-bed desulfurizer. Gasifier carbon conversion is 98.9%. The moving-bed desulfurization system produces an enriched SO_2 stream that can be integrated to a sulfuric acid plant. A final cyclone after the moving-bed system provides particulate removal before the combined cycle.

The steam generated from the raw-gas heat recovery adds substantially to the steam turbine portion of power generation and helps to compensate for the high oxygen plant power requirements. The result is a net power output of 268 MW and a net efficiency of 42.8% on an HHV basis. The resulting COE of 58.5 mills per kW/hr on a constant 1992 dollar basis reflects a 10% or more higher capital cost of this case over the first two cases.

ENHANCED IGCC EFFICIENCIES WITH ADVANCED TURBINE SYSTEMS

DOE/METC is currently managing an Advanced Turbine Systems (ATS) Program to develop a new generation of gas turbines that, on natural gas, are expected to achieve

efficiencies of greater than 60% on a lower heating value (LHV) basis in a combined cycle. These gas turbines will likely incorporate improved cooling of the first stator airfoils in addition to rotor stage cooling enhancements. Closed cycle cooling is being considered to reduce parasitic air cooling requirements. For the IGCC performance simulations performed by METC, closed-loop steam cooling of the stator and nozzles other than the first is utilized to minimize total parasitic airflow. With fuel gas supplied from the gasifier, the gas turbine pressure ratio of 18:1 with a turbine inlet temperature of 2,600°F yielded an exhaust temperature of 1,215°F.

The higher exhaust temperature permitted selection of a 2,465-psig, 1,140°-F steam turbine inlet conditions with a reheat temperature of 1,110°F for the intermediate pressure section. European pulverized-coal plants under development now are utilizing similar steam temperatures at higher pressures. The gasifier heat recovery was also used to produce the high-pressure superheated steam; this is not currently being practiced in all worldwide IGCC demonstrations (most demos produce saturated stream in the gasifier heat recovery) and may require metallurgy developments over the next 10 years.

As shown in Table 2, the fluidized-bed gasifier system previously discussed, when adapted to the future ATS cycle, will produce a net power output of 441 MW at an efficiency of 51.2% on an HHV basis. The calculation of the simple cycle efficiency of the gas turbine on an LHV basis is 45.3%. The two-stage, entrained-flow slagging gasifier previously presented, but adapted to the advanced turbine systems IGCC configuration, yielded an efficiency of 52.2% HHV for a 423-MW plant. With a capital cost per MW that is 12% lower than current technology with hot gas cleanup and the higher operating efficiencies, the COE for this configuration in constant 1992 dollars is 14% lower. Therefore, a substantial benefit to IGCC will be obtained from the ATS Program.

The fixed-bed slagging gasifier with ATS cycle gave an efficiency of 48.1% HHV for a 378-MW IGCC plant.

IMPACTS OF IMPROVED GASIFICATION CONCEPTS

METC is exploring ways in which improved concepts for gasification can improve the overall COE for IGCC applications while still maintaining excellent environmental performance. One concept is the PYGAS concept of CRS Sirrine Engineers, Inc., which currently is the focus of a preliminary engineering design effort for testing in a Gasification Product Improvement Facility. As soon as the conceptual design phase of this project was completed, METC attempted to model the PYGAS reaction zones utilizing ASPEN. The most optimistic of the simulations is presented to illustrate the potential of the gasification reactor if all the combined processes work together synergistically.

The METC ASPEN simulation assumed a pyrolyzer exit temperature of 1,650°F at 600 psig and 86% capture of coal sulfur by the limestone feed simultaneously with the coal. Carbon conversion in the pyrolyzer was assumed to be 68% of incoming carbon. An upper combustion zone above the pyrolyzer elevates the products of pyrolysis to 2,300°F. The gases and char then flow downward in a packed column, and gasification occurs until the char reaches 1,500°F or until the char reaches a larger fixed-bed gasifier zone. The remaining carbon is consumed by the gasification reactions above the fixed-bed air/steam rotating grate. The products of gasification from both the upper and the lower bed exit the gasifier at 1,500°F. The coal

Table 2. Tomorrow's View

IGCC Efficiency Using ATS Technology
2465 P/1142/1100°F Steam Cycle

Gasifier Type	Fluidized Bed	2-Stage Entrained Flow	Fixed-Bed Slagging
Oxidant	Air	Air	Oxygen
Gasifier C-Conv.	96.5%	99.0%	99.2%
Gas Cleanup/ Sulfur Recovery	HGCU, Sulfation	HGCU, Sulfuric Acid	CGCU, Elemental Sulfur
Net Power	441 MW	423	378
Overall Efficiency, % of HHV	51.2%	52.2%	48.1%

sulfur picked up by the limestone in the pyrolyzer is assumed to remain as calcium sulfide as it passes through the ash grate region and exits the gasifier at 700°F. The reactor is constructed with metal internals that must be cooled to maintain structural strength. If the cooling of the internals of the gasifier can be substantially converted into steam for power generation, the net loss of reactor input heat can be kept to less than 2.5% of total coal heating value.

The exit gas from the gasifier passes through a cyclone at 1,500°F and is expanded down to 255 psia to generate power prior to the final desulfurization of the product gas. A fluidized-bed desulfurization system is used at 1,270°F to increase the overall sulfur capture to 99%, and regeneration of the sorbent produces SO_2 that is converted to sulfuric acid.

As shown in Table 3, the net power production of the PYGAS-based IGCC with current gas turbine technology is 278 MW and yields an efficiency of 45.1% on an HHV basis. The 1.0 to 1.5% increased efficiency of this best case PYGAS IGCC simulation does not translate into a lower COE, since the number of gasifier trains is doubled from those of other IGCC systems. The COE for this case is 61 mills per kW/hr based on capital costs that are 10 to 12% higher than the cases with the next highest efficiencies. This gasifier throughput per train may be less significant in repowering applications on the COE, where the repowering is of the type in which the exhaust from a smaller gas turbine (40 to 80 MW) is used to repower an existing coal-fired boiler and its associated steam turbine. In this way, 30% more capacity can be added to a nominal 100-MW boiler with an overall 20 to 25% efficiency improvement for minimum dollars per kW.

Another promising study case of future gasification technology shown in the table is a transport gasifier that operates at potentially 1,600°F with coal and limestone pulverized to less than 100 micrometers in size. The gasifier operates at substantial velocities with high recirculation of char and calcined limestone. The possibility of a single moderate temperature gasifier supplying a 420-MW IGCC plant is plausible, but two gasifiers were considered as

Table 3. Improving Gasification Concepts Impacts IGCC Efficiency

	With Current Technology		With ATS Technology		
	Fluid Bed	PyGas	Fluid Bed	Transport w/Ext. Desulf.	Transport w/o Ext. Desulf.
Oxidant	Air	Air	Air	Air	Air
Sulfur Capture, In Gasifier	86.5%	86.0%	86.5%	96.0%	96.0%
With Ext. Desulf.	99.0%	99.0%	99.0%	99.0%	-
Carbon Conversion	96.5%	98.5%	96.5%	98.2%	98.2%
Sulfur Recovery or Conversion	Atmospheric Sulfation	Atmospheric Sulfation	Atmospheric Sulfation	Pressurized Sulfation	Pressurized Sulfation
Overall Efficiency, % of HHV	43.3%	45.1%	51.2%	52.5%	52.5%
Cost of Electricity, mills/kW, Constant $	55.6	61.0	48.0	46.9	43.3

part of this analysis. Claims of 96.0% sulfur capture and 98.2% carbon conversion will be confirmed in testing at the Wilsonville Power Systems Development Facility. The overall IGCC concept as viewed by METC is shown in Figure 1 for the gasifier concept integrated with the gas turbine, and in Figure 2 for the heat-recovery steam generator/steam turbine integration. Fixed-bed desulfurization increases overall sulfur capture to 99% with regeneration gases recycled to the gasifier. Final sulfation and carbon burnout of the gasifier underflow material is performed in a pressurized sulfator, the exhaust gas of which provides some of the oxidant requirements for gasification.

With the ATS power module, this IGCC concept is projected to have an efficiency of 52.5% on an HHV basis. Equally important to the higher efficiency is a 47 mills per kW/hr COE for a system that has excellent environmental performance. Since the in-bed desulfurization performance is already 96% with a low calcium to sulfur ratio, tests at Wilsonville could prove that 97% plus sulfur capture is possible. This could eliminate the need for external desulfurization, lowering the capital cost and COE to $1,100/kW and COE to the 43 mills per kW/hr range on a constant dollar basis. Alternately, lower capital cost, external desulfurization systems can be explored in DOE's RD&D program to lower overall capital costs to the $1,050/kW goal.

CONCLUSIONS

The following conclusions can be made when one reviews METC's projected performance with current gas turbine combined cycles and the suite of gasifiers currently included in planned demonstrations in the U.S. DOE Clean Coal Technology Demonstration Program or undergoing demonstration elsewhere in the world.

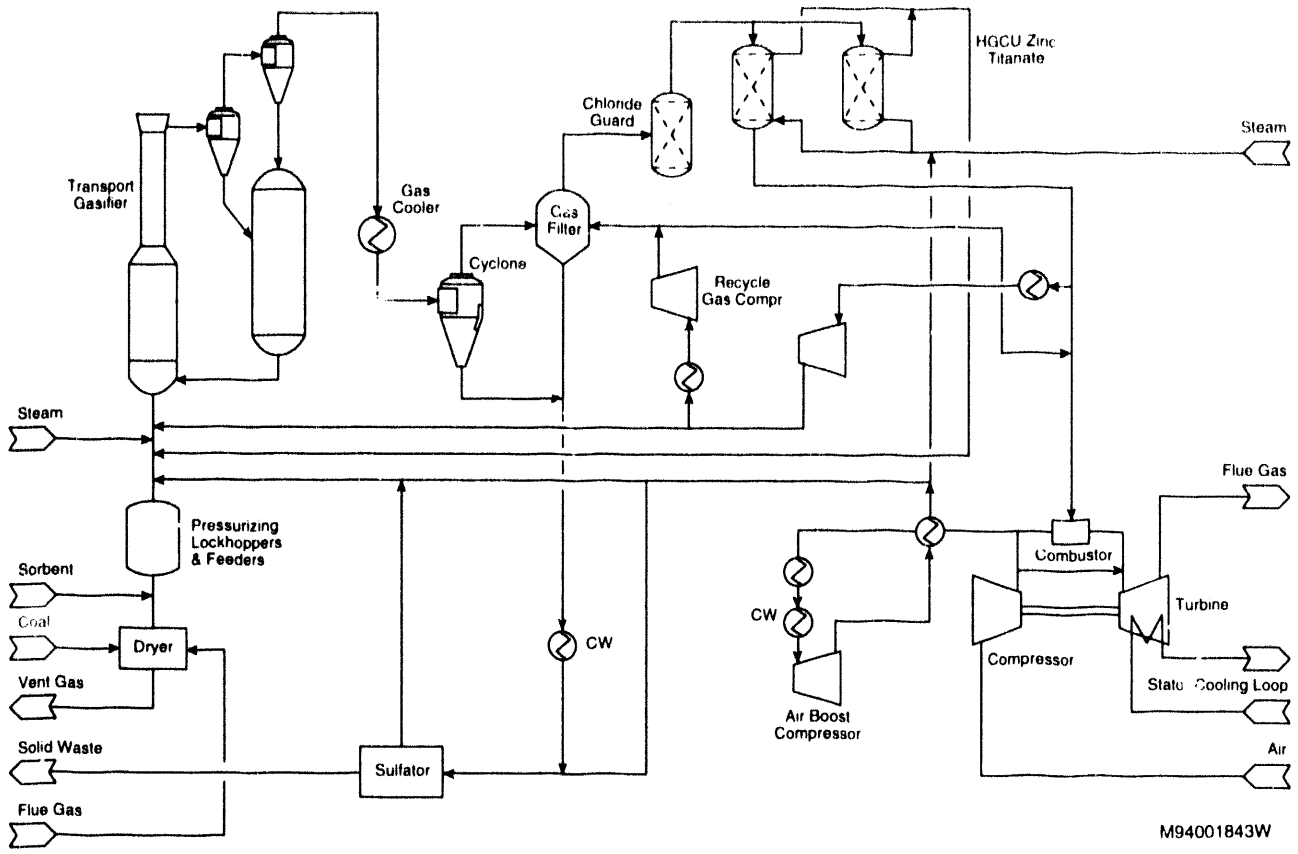

Figure 1. Transport Gasifier Advanced IGCC - Gasifier Island and Gas Turbine

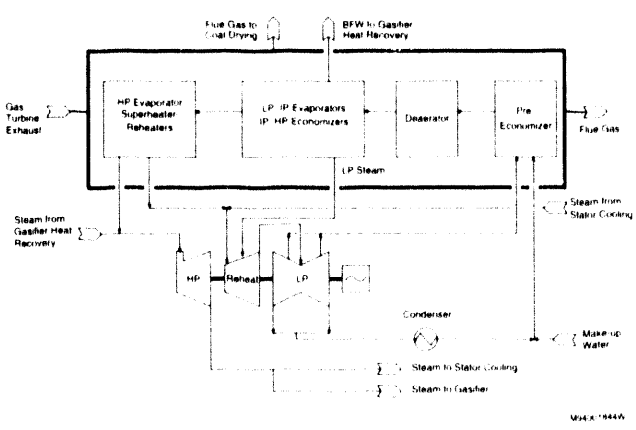

Figure 2. Transport Gasifier Advanced IGCC Heat Recovery and Steam Turbine

- All of today's gasifier type when coupled with hot gas cleanup technology should be able to achieve an efficiency of 43 plus/minus 1% on an HHV basis and give excellent environmental performance relative to a PC plant with low NO_x burners and scrubbers.
- When coupled to cold gas cleanup technology, the IGCC efficiency range of 41 plus/minus 1.5% (HHV basis) is predicted with environmental performance close to or equal to a natural gas combined cycle (without carbon dioxide externalities).

With the results of DOE's Clean Coal Technology Demonstration Program and demonstrations of utility-size ATS machinery likely in place shortly after the turn of the century, the following conclusions about the future of IGCC can be made.

- The goal of an IGCC with an efficiency of 52% on an HHV basis for the year 2010 appears achievable with initial demonstration projects of the initial high efficiency IGCC systems occurring around 2005.
- The 27% gain in efficiency over those IGCC systems undergoing demonstration today translates into 28% COE reductions.

Additional gains of 3.2 efficiency points over today's best IGCC system with cold gas cleanup (2.0 efficiency points over today's demonstration with hot gas cleanup) are plausible if the advanced gasification PYGAS process is proven capable of high pyrolysis yields at moderate temperatures. However, the COE for a grassroots IGCC application of this gasifier can only be reduced to those of alternate gasification concepts if capacity gains per unit gasifier volume are doubled over the current basis.

The transport gasifier concept integrated with an ATS cycle has the greatest potential to achieve simultaneously a 52% efficiency goal along with a 33% COE savings over the IGCC systems currently planned or undergoing demonstrations.

METC goals for the year 2000 and 2010 in the IGCC product area are demanding but clearly achievable with diligent research, focused engineering development, and prudent and cost effective demonstrations.

LRATH\1:940761c

3.2 Transport Reactor Development Status

CONTRACT INFORMATION

Cooperative Agreement	DE-FC21-MC25140
Contractor	Southern Company Services, Inc.
Subcontractor	The M.W.Kellogg Company 601 Jefferson Avenue P.O.Box 4557 Houston, Tx 77210
Contractor Project Director	Randall E. Rush
Subcontractor Project Manager	Martin O. Fankhanel
Subcontractor Development Manager	William M. Campbell
METC Project Manager	James R. Longanbach
Period of Performance	November 1990 to March 1996

OBJECTIVES

This project is part of METC's Power Systems Development Facility (PSDF) located at Wilsonville, Alabama. The prime contractor for the program is Southern Company Services, Inc. The M.W.Kellogg Company will supply the technology for the Advanced Gasifier module. This module includes Kellogg's Transport reactor technology for combustion and gasification of coal.

The primary objective of the Advanced Gasifier module is to produce vitiated gases for intermediate-term testing of Particulate Control Devices (PCDs). The Transport reactor potentially allows particle size distribution, solids loading, and particulate characteristics in the off-gas stream to be varied in a number of ways. Particulates in the hot gases from the Transport reactor will be removed in the PCDs. Two PCDs will be initially installed in the module; one a ceramic candle filter, the other a granular bed filter. After testing of the initial PCDs they will be removed and replaced with PCDs supplied by other vendors.

A secondary objective is to verify the performance of a Transport reactor for use in advanced Integrated Gasification Combined Cycle (IGCC), Integrated Gasification Fuel Cell (IG-FC), and Pressurized Combustion Combined Cycle (PCCC) power generation units.

This paper discusses the development of the Transport reactor design from bench-scale testing through pilot-scale testing to design of the Process Development Unit (PDU-scale) facility at Wilsonville.

BACKGROUND

In the PSDF, Kellogg's Transport reactor will produce either an oxidizing or reducing gas for parametric testing of the PCDs. The Transport reactor was selected as the gas generator due to its flexibility for producing particulate-containing test gases. The reactor operates at pressure in either the gasification or combustion mode over a wide range of temperatures and particle residence times. The feed coal to the reactor consists of fine particles similar to entrained reactor gasification systems while the reactor operates at temperatures characteristic of fluidized bed systems.

The Transport reactor concept is modelled on the Fluid Catalytic Cracking (FCC) process which has been used for about 50 years in petroleum refineries to upgrade heavy oils to transportation fuels. Kellogg built a one ton per day (TPD) Transport combustor at its Technology Development Center in Houston, Texas, and operated it on bituminous coal and petroleum coke under a wide variety of test conditions. Subsequently, a bench-scale Transport Reactor Test Unit (TRTU) was built to develop the kinetic data required for design of coal gasification units.

An intermediate-size Transport Reactor Development Unit (TRDU) was built at the University of North Dakota, Energy and Environmental Research Center (UND/EERC) in Grand Forks, ND, to verify the scale-up factors that were being used in the design of the Wilsonville facility. The UND/EERC unit is designed to process 2.4 TPD of coal in the gasification mode and 1.8 TPD in the combustion mode. To date, the TRDU has operated only on Wyodak coal.

PROJECT DESCRIPTION

The Wilsonville Transport Reactor

The Wilsonville Transport reactor is sized to process 38 TPD of coal in the gasification mode and 27 TPD in the combustion mode, delivering 1000 ACFM of particulate-laden gas to the PCD units over a temperature range of 1000-1800°F at 300 psig. The design coal for the facility is Illinois No. 6 bituminous coal with a Powder River subbituminous coal as an alternate feed. Longview limestone, available locally, has been chosed as the sulfur sorbent.

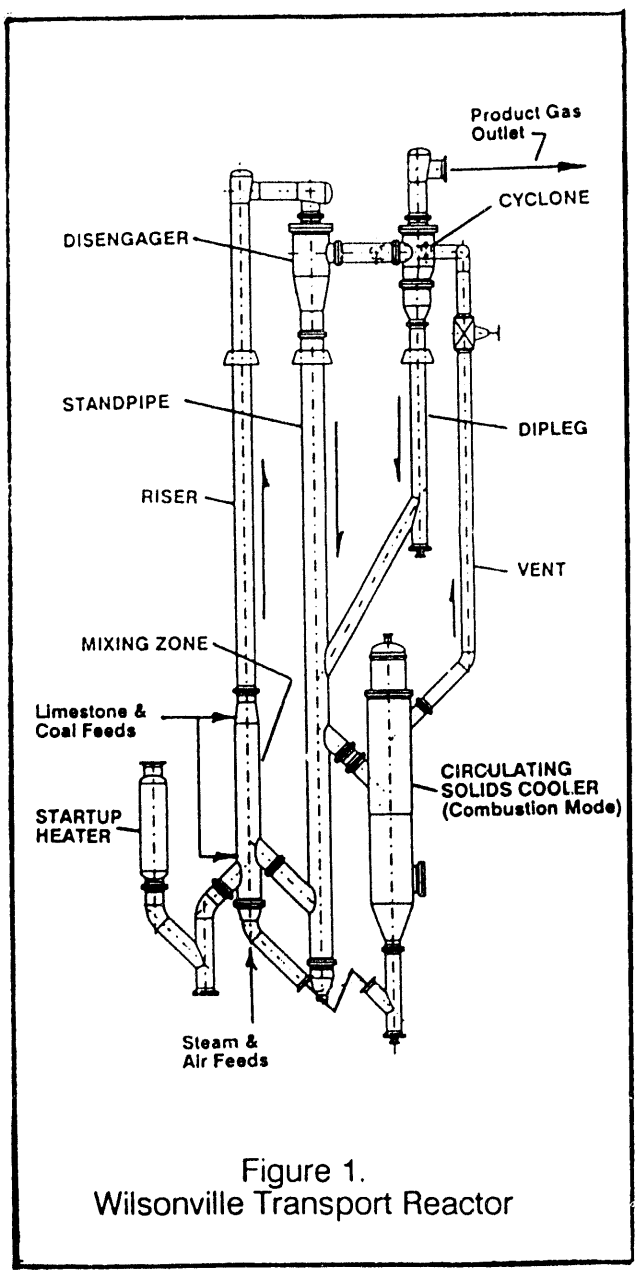

Figure 1.
Wilsonville Transport Reactor

In gasification mode, pulverized coal and limestone are fed into the top of the mixing zone of the reactor where they mix with a much larger quantity of hot circulating char. See Figure 1. The coal immediately devolatilizes and, in the presence of steam, the volatiles pyrolyze and the char gasifies in the Riser section of the reactor. The velocity in the Riser is about 35 feet per second (fps) providing 1-2 seconds of contact time for each pass of the solids through the system.

The product fuel gas passes through a disengager and a cyclone where the bulk of the solids are removed and become part of the circulating inventory of the system. The disengaged solids build up in the downcomer providing the hydraulic head to recirculate the solids through the reactor. Air injected into the bottom of the mixing zone substoichiometrically combusts a small portion of the char in the circulating solids providing the heat for the pyrolysis and gasification reactions.

Product fuel gas coolers are provided to accomodate whatever temperature is desired for the PCD being tested. The expected amount of particulate matter in the gas is about 4000 ppm and can be increased, if desired, by online spoiling in the cyclone.

In combustion mode, the coal is fed to the bottom of the mixing zone and the combustion air is staged to reduce the formation of NOX. Circulation of solids is substantially higher in combustion mode to control the temperature rise of the solids. Heat is removed from a slipstream of the circulating solids in an external bayonet-type heat exchanger. Circulating solids temperature is affected by controlling the amount of solids flowing through the heat exchanger.

The design of the Wilsonville Transport reactor is based upon data developed in bench-scale and pilot-scale facilities which are briefly described below.

The CFBC, TRTU and TRDU Reactors

In 1985 Kellogg built a 1-TPD Circulating Fluid Bed Combustor (CFBC) to verify the performance predicted by the model that had been developed during previous studies. The design of this atmospheric pressure reactor included a mixing zone with staged combustion, and a Riser designed to operate at velocities up to 60 fps. See Figure 2. The physical design is very similar to the design for the Wilsonville facility.

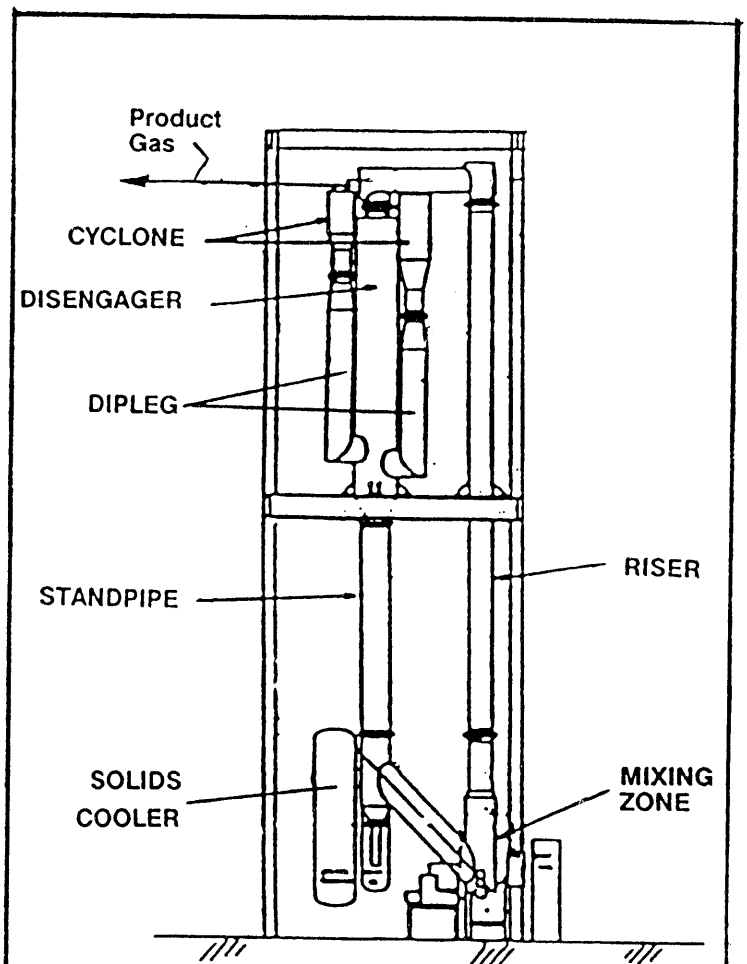

Figure 2.
Circulating Fluid Bed Combustor

In 1990 Kellogg built a bench-scale Transport Reactor Test Unit (TRTU) to verify the performance predicted by the Transport gasification model which had been developed. Gasification tests at small scale require a reactor system in which heat leak is essentially nil, so that actual commercial oxidant/coal ratios can be tested. The TRTU is a 0.6 inch diameter, 30 feet high reactor totally enclosed in a multi-section clam-shell heater. See Figure 3. This heater assures that there is no data bias caused by system heat leak.

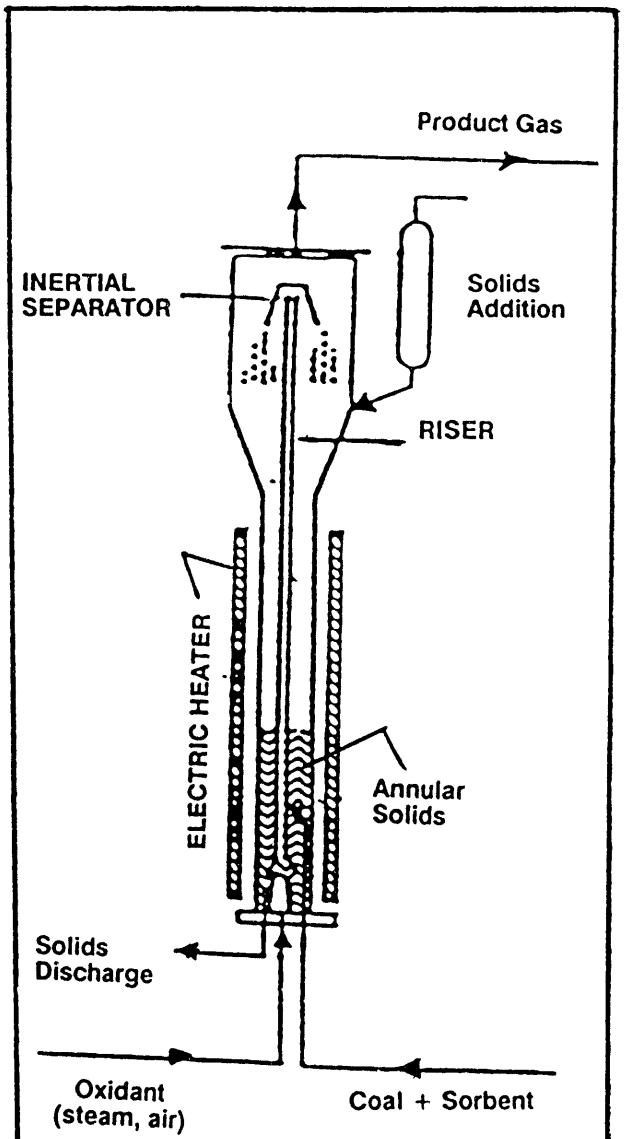

Figure 3.
Bench-Scale Transport Reactor

The TRTU processes up to 10 pounds per hour of coal feed and is capable of operation at high pressure in combustion, pyrolysis or gasification modes. For accurate modelling, reaction rates associated with the three stages of Transport gasification; i.e., substoichiometric combustion, pyrolysis and steam gasification, need to be separately measured.

In 1992 Kellogg designed a pilot-scale Transport Reactor Development Unit (TRDU) which was installed at UND/EERC. See Figure 4, overleaf. This reactor was designed to process 2.4 TPD of coal feed and special care was taken to assure that the reactor heat leak was minimized. This required addition of substantially greater refractory thicknesses than are required in a commercial unit. Although this extra refractory is needed to assure minimum heat leak and proper oxidant/coal ratios are achieved during testing, it does add substantially to the size of the reactor and the heat-up time whenever the unit is started.

An overview of the results of testing in the CFBC, TRTU and TRDU is presented next along with some comments on the applicability of the data to the Wilsonville reactor design.

RESULTS

The development of the Transport reactor concept which is incorporated in the Wilsonville PSDF has been a protracted process, influenced by the background and experience of many participants and by data produced in a number of test facilities. The application of this test data to the design of the Advanced Gasifier module is now discussed.

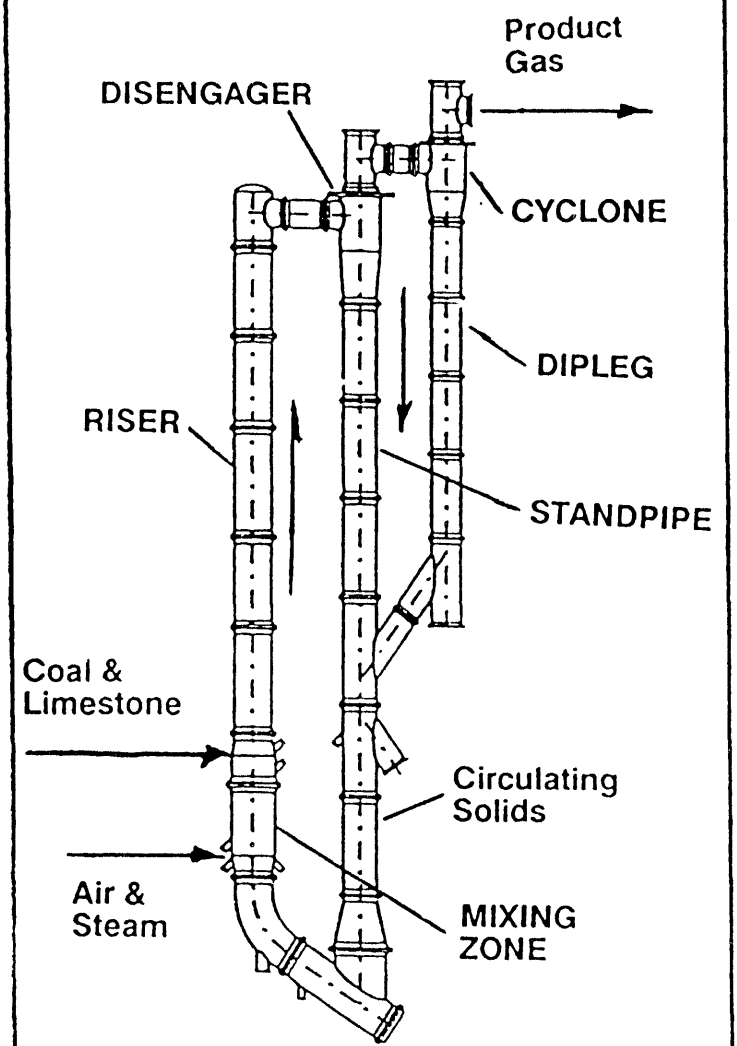

Figure 4.
Transport Reactor Development Unit

The Conceptual Design Models

The Transport combustion and gasification models were initially based on literature data available from a wide variety of reactor designs, none of which represented the Transport concept very closely. The prototype for the concept was the ubiquitous Fluid Catalytic Cracking (FCC) unit which is a combination of a Transport gasifier and a fluid bed combustor processing heavy oils. Reaction rates in fluid beds are substantially different from those in Transport reactors. Typically, the particle size in fluid beds is much larger and superficial gas velocities are lower. The oxidants and product gases are imperfectly mixed with the reacting solids in the emulsion phase in the bed.

In the Transport reactor the particles are much smaller and are totally surrounded by the gas phase. The combination of high surface area, high turbulence and lower gas diffusion resistances results in substantially higher reaction rates and requires a smaller reactor volume. The gas residence in these reactors is 1-2 seconds but the high solid recirculation rate increases the residence time of the reacting solids many fold.

Kellogg's models predict that in gasification the particle size and solid recirculation rate has a very substantial effect on carbon conversion and sulfur capture. Staging introduction of coal and oxidants was expected to affect both carbon conversion and sulfur removal. In combustion, the models predict that staging the oxidant addition affects NOX, CO and SO_2 emissions. Each of these predictions needs to be verified for a range of operating conditions and for several types of coal.

Testing in the Circulating Fluid Bed Combustor (CFBC)

Testing was carried out in the CFBC in 1986. Table 1 shows the range of variables in the test program and Table 2 indicates the range of results. Some 56 runs were carried out. It is apparent that the combustion reaction rate at about 1600°F is more than adequate to complete carbon conversion, even with the relatively refractory petroleum coke. No uncontrolled reactor exotherms were experienced, indicating that it is possible to circulate adequate quantities of solids in a 40-50 feet tall reactor. No apparent difference was noted between the two coal particle sizes tested.

Table 1.
Circulating Fluid Bed Combustor
Design Basis

Feed Rate	1.0 TPD
Temperature	1550-1650oF
Pressure	atmospheric
Velocity	20-60 Ft/sec
Contact Time	1-3 Seconds
Riser Dia.	6 inches
Rxr Height	64 feet

Table 2.
Circulating Fluid Bed Combustor
Test Results

Feeds	West Kentucky #6 Petroleum Coke	
Limestone	Greer	
Riser Velocity	36-60 ft/sec	
Riser Temperature	Coal: Petcoke:	1550oF 1650oF
Carbon Conversion	Coal: Petcoke:	99.5 % 99.2 %
Calcium/Sulfur Ratio	1.3 - 1.6	
Sulfur Capture	Coal: Petcoke:	96 - 99% 93 - 97%
NOx Emission	0.04 - 0.07	#/MM Btu

Sulfur capture was substantially higher than reported in the literature on fluid bed combustors. Sulfur capture is affected by Riser velocity and by solid recirculation rate, indicating that the sulfur/sorbent reaction rate is relatively slow and particle and pore surface dependent. Sorbent utilization, or the amount of excess sorbent available, did not seem to affect the sulfur leakage within the range tested. It is apparent that the Transport reactor is an effective combustion device.

Testing in the Transport Reactor Test Unit (TRTU)

As a result of the successful combustion tests Kellogg decided to proceed with the development of a Transport gasifier model. Subsequent economic studies also indicated that substantial capital cost savings could be realized compared to fluid bed gasifier designs if results of testing verified the model predictions.

Testing was carried out in the TRTU in 1991. Table 3 indicates the range of variables in the test program and Table 4 shows the test results. Western Kentucky #6 and Illinois #6 bituminous coals and Wyodak subbituminous coal were tested. Transport gasification is a staged reaction. Circulating char is first combusted substoichiometrically to supply reaction heat, then coal is introduced, devolatilizes, the volatiles pyrolyze and, finally, the residual char is steam gasified. This staging forces the air to react with char rather than volatiles, as is characteristic in fluid bed gasifiers. If staging is effective, then the amount of char to be gasified by the very slow reaction with steam is reduced substantially.

A typical staged test sequence in the TRTU is as follows: (1) coal is fed into the circulating solids (which are alumina or ash initially) in a steam/nitrogen atmosphere. The coal pyrolyzes and the volatiles crack, laying down carbon on the circulating solids. The solids are allowed to build up to 20-30 wt% carbon; (2) the coal feed is stopped and air is introduced into the reactor, simulating substoichiometric combustion of char; and (3) before the char is completely oxidized, the air is replaced by steam and gasification rates are measured.

Table 3.
TRTU - Bench-Scale Gasification
Test Variables

Coals	Wyodak, subbit. West Kentucky #6, bit. Illinois #6, bit.
Limestones	Greer, Longview
Riser Velocity	28 - 38 fps
Riser Temp.	1600 -1850°F *
Pressure	85 psig
Ca/S Ratio	1.5

* Temperature range depended upon actual coal tested

In this test sequence the rates of devolatilization/pyrolysis, substoichiometric combustion and steam gasification are each separately measured. By raising or lowering the reactor temperature (via the external clam shell heaters) during steps (2) and (3), the effect of temperature on reaction rates can be determined. Figure 5 presents an Arrhenius-type plot of carbon conversion rate against operating temperature for the coals examined.

Tests were also carried out in which all three reactions occur simultaneously as in a commercial reactor system. Coal was fed continuously and the char level in the recirculating solids was monitored to permit establishing operating conditions where the char level remained constant. In practice this is not easy to achieve in the TRTU and in a number of cases the carbon level increased or decreased during the testing.

The TRTU testing indicated that both bituminous and subbituminous coals could be effectively gasified without agglomerating in the reactor and that acceptable sulfur emission levels could be expected.

Table 4.
TRTU - Bench-Scale Gasification
Test Results

Riser Temp.	Subbit: Bit:	1600-1750°F 1600-1850°F
Carbon Conv.	Subbit: Bit:	95+ % 90+ %
Sulfur Capture	Subbit: Bit:	70 - 80% 70 - 95%

Referring to Arrhenius-type plot in Figure 5. it can be seen that in the operating range of interest, the rate of conversion for the subbituminous coal is 2 - 3 times higher than for the bituminous coal at the same temperature. Expressed another way, there is about 150°F lower operating temperature for the subbituminous coal equivalent gasification rate.

Testing in the Transport Reactor Development Unit (TRDU)

The Wilsonville project team proposed building a Transport reactor at a size somewhere between the TRTU bench scale and the Wilsonville plant size. It was determined that such a reactor could be readily inserted into the existing infrastructure at UND/EERC. After reviewing the facility at UND/EERC it was decided to build the 2.4 TPD unit previously described. The reactor was designed in multiple sections to facilitate installation into the existing high bay structure. The design basis for this unit is given in Table 5.

Initial shakedown of the TRDU was started in October 1993. Cold circulation of solids was established for about 70 hours while operators familiarized themselves with the unit and checked out instrumentation. The unit was initially heated with natural gas and then gradually switched over to coal feed.

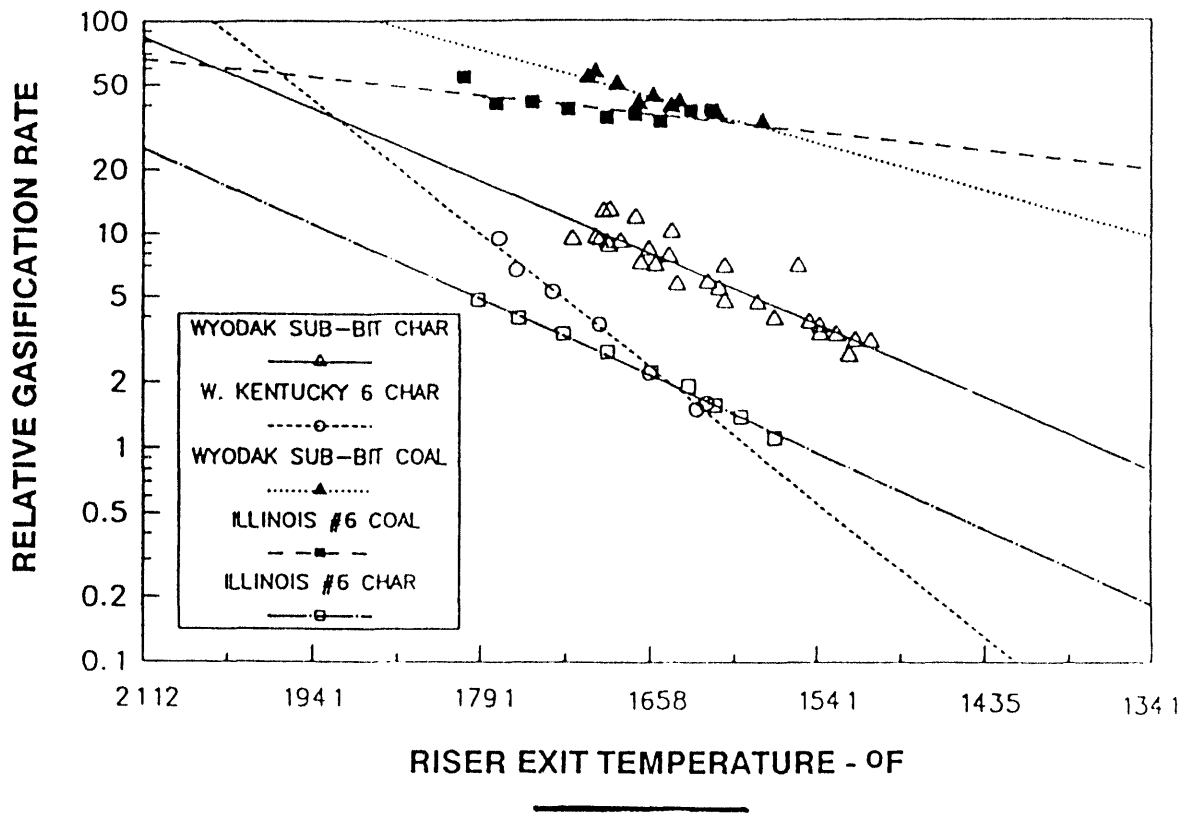

Figure 5.
Arrhenius-type Plot - Gasification Transients

Table 5.
TRDU - Pilot-Scale Gasification
Design Basis

Coal	Wyodak subbituminous
Limestone	Longview
Riser Velocity	28 - 30 fps
Pressure	120 psig
Ca/S Ratio	1.5

Table 6.
TRDU - Pilot-Scale Gasification
Test Results

Riser Temperature	1520 - 1565°F
Carbon Conversion	92 - 97%
Sulfur in Outlet Gas	100-300 ppmv
Product gas HHV*	83 - 104 Btu/Scf

* Adjusted to reflect corrections for heat leak, excess water in coal feed and miscellaneous purges.

There were some problems with the ash removal augers and solids were purged batchwise from the unit. Operation was not sufficiently stable and solids carryover to the gas recovery system forced shutdown of the unit before gasification was initiated.

Repairs to the unit were made and a second shakedown was started in early December. During this test campaign the TRDU operated for over 250 hours in hot circulation mode, for 46 hours in combustion mode, and for 34 hours in gasification mode during which two steady-state periods of about eight hours each were analyzed in detail. Selected steady state test data is presented in Table 6. The test successfully met pre-set conditions for capacity, operating pressure, carbon conversion and heating value of the product gas. Reactor heat losses were essentially as predicted in the design calculations.

Table 7.
Design Basis for Wilsonville
Transport Reactor

	Gasification	Combustion
Coal Feed, TPD	38.0	19.3
Limestone, TPD	5.2	2.7
Mean Particle Size, microns	100	100
Riser Vel., fps	36	30
Pressure, psig	295	295
Riser Temp., ^{o}F	1770	1600

Application of the Test Data to the Wilsonville Design

The design bases for the Wilsonville Transport reactor in gasification and combustion modes are given in Table 7. Figure 1 is a sketch of the Wilsonville reactor. The disengager on the design is a cyclone with the gas inlet and outlet positions reversed to permit higher dust loadings in the product gas to the PCDs. Spoiling gas is available on the cyclone to permit varying the quantity of dust for the PCD testing.

There are a number of significant differences between Transport and fluid bed reactors that the development program described above was designed to address and verify.

Common to both Transport gasification and combustion is the need to circulate large quantities of solids to assure effective mixing of reactants and to dissipate the large amount of heat evolved within a small reactor volume. The Transport concept is based upon maintaining the temperature of the reactants below the point where ash melting is detrimental. This is done by avoiding a hot gas jet and by circulating large quantities of "dry" solids compared to the coal feed rate.

The ashes and chars circulated in the CFBC, the TRTU and the TRDU gave no indication that there was a problem in circulating these materials. There were no hot spots detected in operation and no indication of significant ash agglomeration during processing. TRTU testing indicated that high conversion of bituminous coals could be achieved at moderate operating temperature. Bituminous coal has not been tested in the TRDU yet.

Product gas desulfurization is expected to be very efficient in the Transport reactor because of the high sorbent surface area and continuous contact of the product gas with the sorbent until it leaves the reactor.

Testing in the CFBC and the TRTU confirmed high sulfur removal and calcium utilization. Sulfur emission with subbituminous coal in the TRDU gasification testing was low but the the Wyodak coal contains only 0.5 %S.

The full advantage of staged gasification has not been tested in the TRDU since the carbon conversion on Wyodak coal was very high and the carbon level in the circulating solids did not build up to the desired level to prove the concept. The advantage of staging will not be demonstrasted until bituminous coal is tested in the unit.

Although the TRDU was designed for pressurized combustion operation, the circulating solids cooler required to remove the exothermic heat of combustion was not initially installed. Coal combustion did take place during each startup of the TRDU in the reactor heat up cycle. There was no indication that ash agglomeration took place during this operation. The TRDU operates at only 120 psig pressure and requires use of enriched air to simulate the effect of higher pressure and prove that excessive temperature exotherms do not occur. Enriched air tests are planned but have not yet been carried out.

There was no indication of refractory damage during the CFBC testing at KTDC. During the two short test campaigns carried out at UND/EERC there was no indication of excessive refractory wear in any section of the reactor.

Kellogg is confident that the design of the Wilsonville Transport reactor will meet the design criteria established for the facility. Sufficient flexibility has been built into the unit to permit operation of the reactor with a variety of coals and over a wide range of operating conditions.

ACKNOWLEDGEMENTS

This paper was prepared with the support of the U.S. Department of Energy, Morgantown Energy Technology Center, under Cooperative Agreement No. DE-FC21-90MC25140. The authors wish to thank the many colleagues in the DOE, SCS, UND/EERC, EPRI, SRI and Kellogg who have counseled and assisted in the Transport reactor development program. Any opinions, findings, conclusions or recommendations expressed herein are those of the authors and do not necessarily reflect the views of the DOE, SCS. or UND/EERC.

REFERENCES

Campbell; Development of a Transport Mode Pressurized Circulating Fluid Bed Combustor; Power-Gen 88.

Gbordzoe et al; Development of a Pressurized Transport Gasifier by The M.W.Kellogg Company; Pittsburgh Coal Conference 1992.

Gbordzoe et al; Development of The M.W.Kellogg's Pressurized Transport Combustor for Power Applications; Pittsburgh Coal Conference 1992.

3.3 Gasification Product Improvement Facility Status

CONTRACT INFORMATION

Contract Number	DE-RP21-91MC28202
Contractor	CRS Sirrine Engineers, Inc. 1041 East Butler Road P. O. Box 5456 Greenville, South Carolina 29606-5456 (803) 676-5082
Contractor Project Managers	R. Don Carson, CRS Sirrine Engineers, Inc. Vijay B. Dixit, Riley Stoker Corporation
Principal Investigators	Richard S. Sadowski, CRS Sirrine Engineers, Inc. William H. Skinner, CRS Sirrine Engineers, Inc. Robert A. Lisauskas, Riley Stoker Corporation Stephen A. Johnson, PSI PowerServ
METC Project Manager	Richard A. Johnson
Period of Performance	October 1, 1992 to March 31, 1996
Schedule and Milestones	**FY94 Program Schedule**

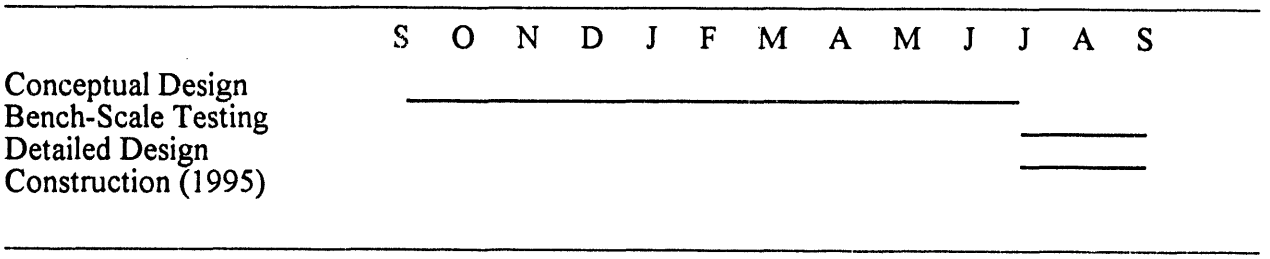

OBJECTIVE

The objective of the Gasification Product Improvement Facility (GPIF) project is to provide a test site to support early commercialization of the Integrated Gasification Combined Cycle (IGCC) technology. The design of this facility will be based on PyGas™, a patented air blown fixed bed gasification process. The GPIF will be capable of processing run of mine high swelling coals that comprise 87% of all Eastern U.S. coals. A team consisting of CRS Sirrine Engineers, Inc., Riley Stoker Corporation and PSI PowerServ has been formed to execute the program.

BACKGROUND INFORMATION

Success of any technology hinges on its cost competitiveness in the market place. The GPIF project is expected to deliver a gasifier design that will satisfy the criteria for good process performance and cost effectiveness. For utility applications, IGCC offers the potential benefits of achieving higher efficiencies than those possible in conventional coal-fired systems. IGCC systems are also capable of meeting the stringent environmental regulations which will be promulgated in the early part of the next century.

The PyGas™ process was conceived to handle high swelling coals, crack tars, and reduce ammonia and trace metal emissions. The GPIF program will generate useful scale up data.

Initially, the PyGas™-IGCC systems will be offered as modular units for the repowering markets which will reduce the financial burden on utilities in comparison to large plants. In addition, modular designs will also reduce the plant construction schedules.

PyGas™ Process

Sticky coal agglomerates can form during the heating process in a fixed bed gasifier using highly swelling coals. The PyGas™ process deals with this situation by carrying out the devolatilization by rapid heating and gasification at two separate locations in a single vessel.

Figure 1 schematically describes different steps in the PyGas™ process. Coal is pneumatically injected into the pyrolyzer section of the gasifier vessel. Steam can also be added to the pyrolyzer bottom if needed. The temperature in the pyrolyzer is maintained between 1500-1800°F. The intent is to decake the coal and maximize devolatilization in this region with some tar cracking.

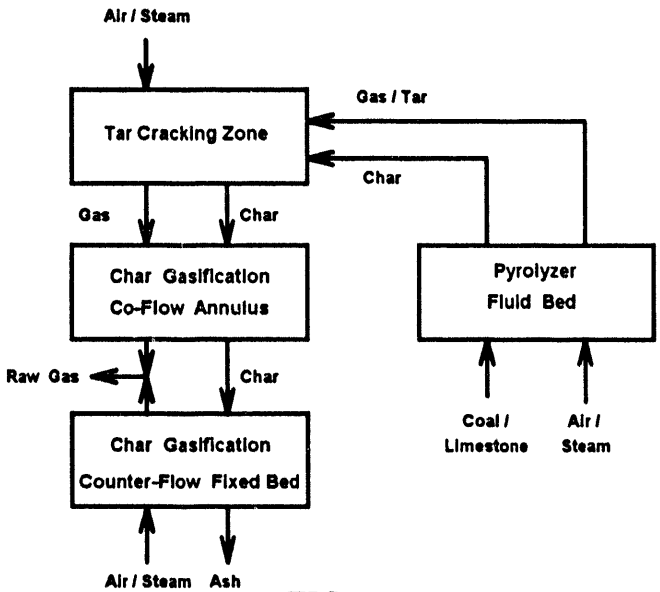

Figure 1. PyGas™ Process Schematic

The remaining tars are cracked in the tar cracking zone down stream of the pyrolyzer. The gases and char then move down a co-flow annular section and to the top of the fixed bed where the final gasification of char takes place.

The combined gasification products from the fixed bed and the co-flow region exit the gasifier at approximately 1150°F and enter a cyclone for removal of particulates. The clean gases go through pressure reduction and enter the combustion chamber of a Heat Recovery Steam Generator (HRSG) to produce steam for the process.

In a fully implemented IGCC system, the gas generated will be combusted in a combustion turbine to generate power and the HRSG will be located down stream of the combustion turbine.

The Fort Martin Project Site

Selection process of a site for the GPIF project was based on the following criteria:

- An existing utility site to reduce permitting requirements
- A utility with interest in the IGCC technology
- Close vicinity to Morgantown Energy Technology Center (METC) to reduce operating costs
- Infrastructure for steam and other utility tie-ins with the GPIF

Near perfect conditions exist at Monongahela Power's Ft. Martin (subsidiary of Allegheny Power System) project site. This 1100 MW_e pulverized coal-fired electric utility facility is providing several key utility interfaces which would otherwise become added project costs.

The following utilities have been combined with the main site to minimize both the capital and operating costs:

- High and medium voltage power interconnects
- 600± psig backup steam for startup
- No. 2 oil interconnect for preheat

- Coal dryer and coal gas combustion sustaining flame use
- Cooling water
- Wastewater treatment
- Potable water supply
- Flue gas breeching tie to the existing electrostatic precipitator
- Coal sourcing
- Permitted ash disposal site
- Electricity production from the steam byproduct

The integration of the PyGas™ process at Fort Martin has alleviated several process and environmentally related concerns, which has led to an approval of the required National Environmental Protection Act (NEPA) permit.

PROJECT DESCRIPTION

Team

The project team consists of CRS Sirrine Engineers, Inc., Riley Stoker Corp. and PSI PowerServ.

This partnering arrangement has added significant advanced gasifier and control system technology engineering, design, fabrication, and field construction expertise as well as an in-place marketing capability to commercialize PyGas™.

The Multi Phase Project

The GPIF project will be executed in two phases. Phase I consists of design and construction of a fixed bed gasifier based on the PyGas™ process. The plant will operate at 600 psi and will be capable of processing 150 tons/day of high swelling Eastern coals. During Phase I, Cooperative Research And Development Agreement (CRADA) work will be performed to support the gasifier design. Another CRADA related to the testing on the GPIF plant will be executed at the conclusion of Phase I.

The Phase I work will address process and coal based issues associated with fixed bed gasification. These include the handling of high swelling coals, pressure scaleup and system integration.

Phase II consists of the design, construction and operation of a hot gas cleanup unit integrated with the gasifier. Provisions for the major peripheral equipment such as storage, piping, material handling, electricals, interconnects, control room, building, and foundations will be made in the Phase I - General Arrangement.

GPIF Schematic

The following major sub-systems comprise the GPIF as shown in Figure 2:

- Air Compressor
- Day Silo/Coal Dryer/Crusher
- Coal Pressure Lock
- PyGas™ Coal Gasifier
- Hot Gas Cyclone
- Pressure Reducing Station
- Emergency Flare Stack
- Fixed Heat Recovery Steam Generator (HRSG)
- Ash Depressurization Lock
- Wet Sulfation Tank/Pumps/Vacuum Filter
- Enclosed Ash Temporary Storage Slab
- Tarpaulin Covered Test Coal Pile Slab
- Limestone Storage Silo
- Administration Buildings/Facilities

RESULTS

Conceptual Design

The "Conceptual Design" task, which was the major effort in the past year, can be broken into what we term process and mechanical areas.

Process Design

The major focus of the conceptual design effort was to develop a thorough understanding of the processes occurring in different parts of the gasifier. To examine these parts independently, the gasifier was divided into four major sections as shown previously. This allowed us to study how individual parameters operate within these blocks to influence the overall performance.

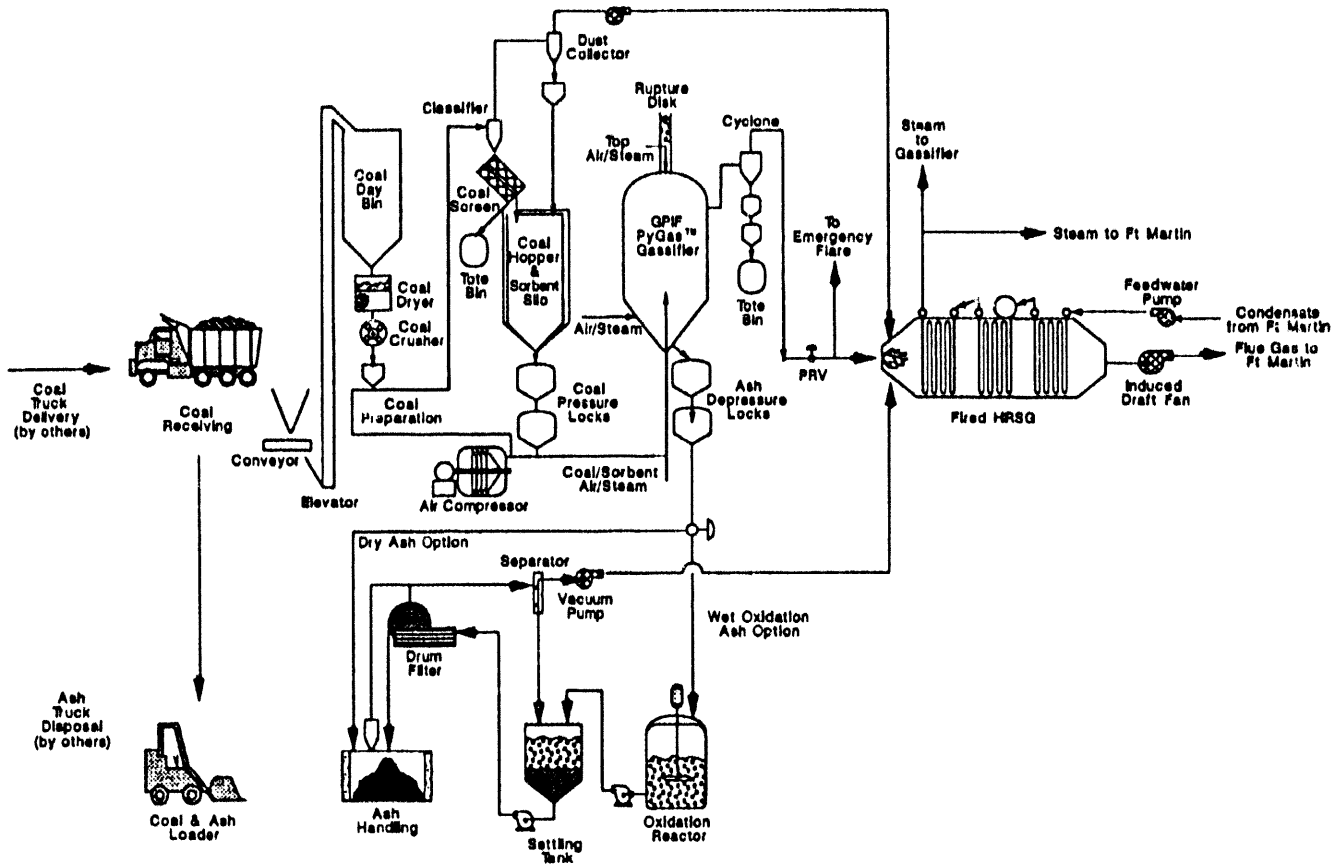

Figure 2. GPIF System Schematic

The sections down stream of the pyrolyzer are strongly influenced by the exit conditions of the pyrolyzer. Therefore, during the conceptual design stage considerable effort was spent on analyzing the pyrolyzer design. A wide range of process and mechanical parameters were selected to predict fluid dynamics in the pyrolyzer. Pressure, particle sizing, local/superficial velocities, fuel injection nozzle design, air distribution were among the variables studied.

The design approach employed for the gasifier also focused on building sufficient mechanical flexibility to carry out development work in support of current and future IGCC systems. The gasifier is equipped with a reversing/rotating type grate. Also, the pyrolyzer bottom was arranged outside of the gasifier vessel for ease of accessibility.

Heat and mass balance calculations were performed for the design case in which all the conversion outside of the pyrolyzer was carried out in the fixed bed gasifier. Figure 3 shows the major flows for this case. The coal analysis used for this design is shown in Table 1.

Table 1. COAL ANALYSIS: FORT MARTIN STATION

Ultimate Analysis	Wt%	Proximate Analysis	Wt%
Carbon	68.7	VR Matter	30.0
Hydrogen	4.6	Fixed Carbon	52.0
Nitrogen	1.2	Moisture	3.0
Oxygen	4.7	Ash	15.0
Sulfur	2.8		100.0
Ash	15.0		
Moisture	3.0		
	100.0		
HHV (Btu/lb)	12,500		

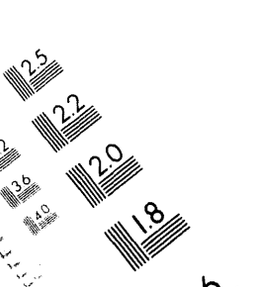

Association for Information and Image Management

1100 Wayne Avenue, Suite 1100
Silver Spring, Maryland 20910

301/587-8202

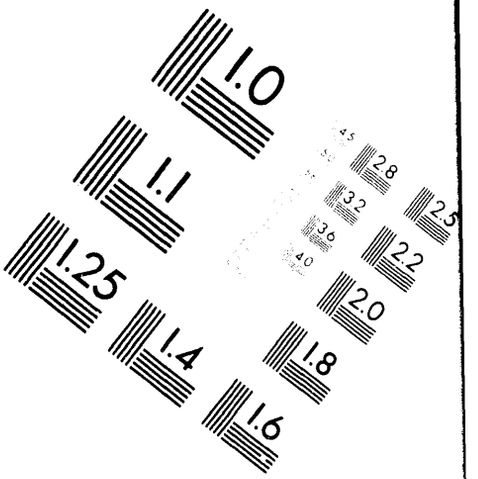

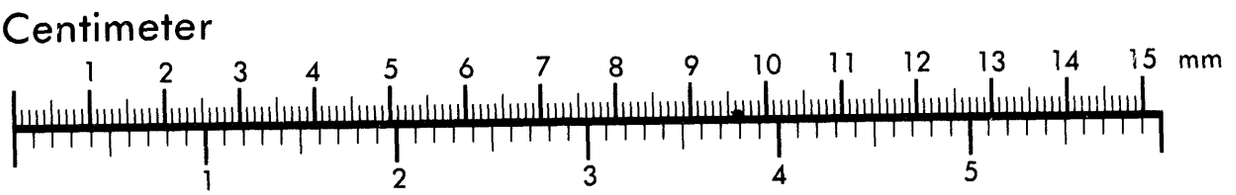

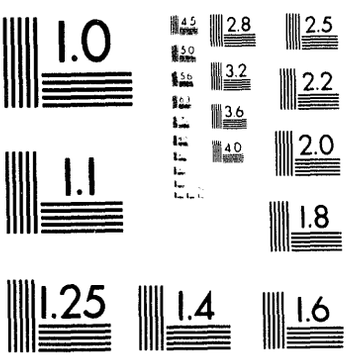

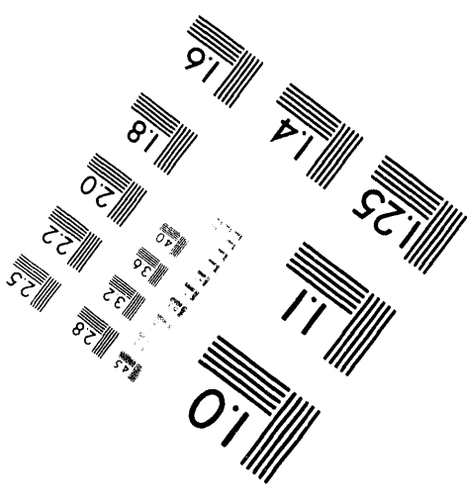

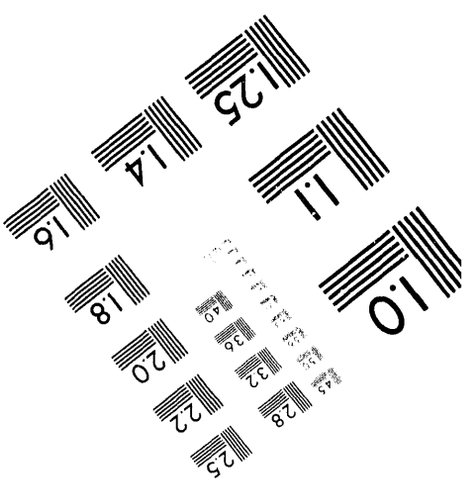

MANUFACTURED TO AIIM STANDARDS
BY APPLIED IMAGE, INC.

2 of 6

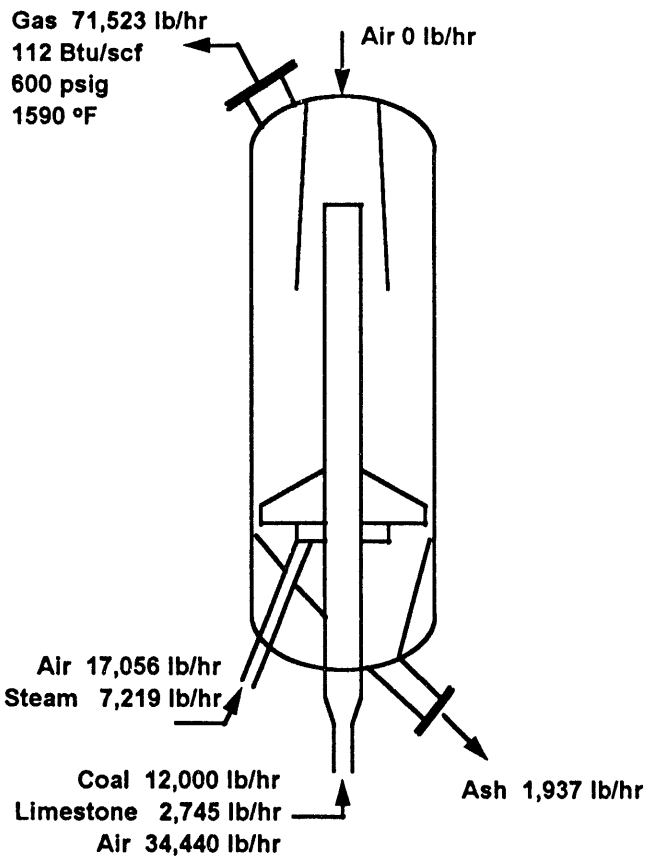

Figure 3. PyGas^{TM} Gasifier Process Flows

It is important that the devolatilized coal particles be well dispersed in the pyrolyzer to avoid agglomeration due to the caking characteristics of the coal. Maintaining a good jet penetration length in the bed facilitates this process. Using jet penetration correlations that incorporate pressure effects, jet lengths were estimated for the 600 psi and 200 psi operations. To avoid any stagnation of solids as they move down the walls of the pyrolyzer, fluidizing air was included on the conical sections of the pyrolyzer. Earlier gasifier designs have employed such an arrangement to improve the down flow of solids.

The amount of fines leaving the pyrolyzer and how it would impact the total throughput was an issue that received tremendous attention during the conceptual design task. Another critical issue related to the estimated superficial gas velocities at different locations, especially in the fixed bed and the outer annulus of the gasifier. It is very important that the particle size in the bed should be coarse enough to maintain a fixed bed. Also, if considerable amount of carbon is elutriated from the gasifier due to high velocities in the outer annulus, recycling of the fines to improve efficiency would be necessary. Different ideas for internal and external recycling of fines were considered during the conceptual design. A strong focus on these issues will be maintained during the final design phase.

Mechanical Design

The conceptual gasifier arrangement is shown in Figure 4. The pressure vessel has flanged construction which will permit mechanical modifications to different parts of the gasifier without affecting other parts. It is equipped with a reversing/ rotating type grate with provision for breaking large agglomerates. It also has a water cooled ledge at the bottom that restricts the uncontrolled flow of fine ash from the gasifier. The outer jacket is cooled with an evaporative circuit. The pyrolyzer has membrane wall construction cooled with an economizer circuit. Because of reducing conditions in the pyrolyzer, its walls are lined with refractory to protect them against corrosion and abrasion.

The pneumatically conveyed solids are injected at the bottom of the pyrolyzer. The fuel nozzle is designed with an annular space around it to provide additional air to meet the process needs of the pyrolyzer. The same annular space will be used for draining ash from the pyrolyzer on an intermittent basis. The pyrolyzer bottom is arranged outside of the main gasifier vessel to provide additional access. The conical section has fluidizing air streams at three levels to help avoid any stagnation of solids at the bottom of the pyrolyzer. To maintain proper fluidization and jet penetration in the pyrolyzer at 600 and 200 psi, the two operating pressures for the gasifier, separate sets of removable nozzles have been designed.

Preliminary stress analysis was performed to start work on selecting material thickness for the inner and outer walls of the water jacket and the flanges.

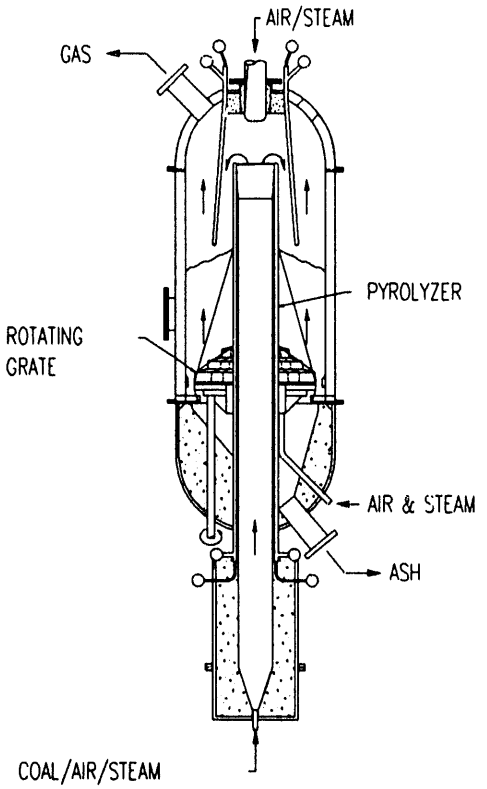

Figure 4. PyGasTM Gasifier Arrangement

Work was also initiated on detailing the control philosophy for operating the plant and instrumentation needs for monitoring temperatures and pressures at strategic locations. More work is ongoing in that area.

In the GPIF the low BTU gas will be combusted in a Heat Recovery Steam Generator (HRSG) to produce steam using a multi nozzle burner. The performance of the HRSG is presented in Table 2.

Other Results

An important milestone was reached with the formal NEPA approval for the project by the government. Without this we could not perform any site specific plant design work. Preliminary site work activities were also initiated. Among them was soil testing for plant foundations and other site construction.

Table 2. GPIF HRSG PREDICTED PERFORMANCE

Coal Gas Fuel:	112 BTU/dscf
Supplemental Fuel:	No. 2 Oil
Steam Generation (lb/hr)	96,473
Temp. of water ent. econ., °F	227
Water press. drop thru econ., psi	20
Temp. of air entering FD fan, °F	80
Steam temp. at SH outlet, °F	700
Steam press. at SH outlet, psig	900
Steam press. drop thru SH, psi	30
Boiler drum press., psig	730

FUTURE WORK

GPIF Tasks

The next step in the project is to proceed to the final design phase for the GPIF. Data available on other similar systems will be evaluated to refine the process issues related to the PyGas design. The CRSS/Riley team will also participate in a number of CRADA activities at METC to generate information to understand fluidization characteristics and pressure scaling issues facing the PyGas technology.

Immediate attention will be given to the pressure vessel design along with the control philosophy. This will require a thorough examination of all the process issues related to the technology.

Work on the design for the balance of plant and on the preparation of specifications for the auxiliary systems will be started. This will proceed along with the site work.

Operating CRADA

An operating CRADA will be executed to generate data to optimize process conditions and to provide scale up data for the commercialization of the PyGas™ technology.

Commercialization

A commercialization plan was also conceived during the conceptual design phase to identify markets that would initially benefit from this technology. The CRSS/Riley strategy calls for taking a step approach, starting with the repowering markets that are expected to open up in late nineties. This would be followed by greenfield installations in the first decade of the next century. Initially, in the repowering area, partial repowering options will be considered where existing utility site infrastructure and major power generating equipment will be used to enhance the efficiency and generation capacity at the site. The technical challenge forcing this approach will be the successful integration of new and existing equipment based on economics, efficiency, reliability and emission criteria. Hot windbox, partial fuel substitution, feed water heating were among the repowering options considered.

REFERENCES

1. "Advanced Hybrid Gasification Facility", R.S. Sadowski, et al., Coal-Fired Power Systems '93-Advances in IGCC & PFBC Review Meeting, June 28-30, 1993.

2. "Gasification Product Improvement Facility (GPIF)", 1992 DOE/METC Annual Contractors Meeting.

3. "Repowering: Special Report", Electric World, March 1994.

4. Forecast, The Electric Power Industry, Electrical World, November, 1993.

5. New Thermodynamic Cycles for Cogeneration Plants, R.S. Sadowski, et. al., 1994 ASME Industrial Power Conference.

6. Solids Circulation Patterns and Particles Mixing on a Large Jetting Fluidized Bed, W, Yang, et. al., AIChE Journal, December 1986.

7. Cold Flow Scale Up Facility Experimental Results and Comparison of Performance at Different Bed Configurations, DOE Contract DE-AC21-82MC19122, Vol 1, Topical Report, Jan-Dec 1983.

Session 4

Advanced PFBC Systems

4.1 PFBC System Studies

Michael E. Reed
Morgantown Energy Technology Center

ABSTRACT

The U.S. Department of Energy (DOE) has been involved in research, development and demonstration (RD&D) of pressurized fluidized-bed combustion (PFBC) systems since the 1970's. PFBC's success in the Clean Coal Program is the start of the demonstration phase of PFBC's life cycle. Because the DOE's emphasis has shifted to the commercialization of systems, the focus of PFBC system studies at the Morgantown Energy Technology Center (METC) has changed from the evaluation of new systems to the improvement of present commercial concepts.

Thermal efficiency is a key factor in the commercialization of power generation systems. Studies are being conducted to assess the impact of the Advanced Turbine Systems (ATS) Program and the use of advanced bottoming cycles in second-generation PFBC systems. Preliminary results show that systems using these advanced technologies will have efficiencies of 2-7 percent (%) higher than the baseline efficiency. The baseline of 46.5% higher heating value (HHV) is based on a Foster Wheeler system using a Westinghouse 501F gas turbine and a conventional 2,400-pound steam cycle.

Environmental performance is another key factor in defining the commercial potential of a system. Quantitative assessments are limited to the quality of data available on a system. Tools are being developed and used at METC that will perform quantitative studies on the environmental performance of a system taking into account the uncertainty associated with preliminary data. These studies will provide the guidance for targeted efforts to improve the environmental performance of PFBC systems. Specific studies addressing nitrous-oxide production, hazardous air pollutants (HAP's), co-firing of wastes, and very low sulfur emissions systems will be discussed.

Efforts are underway to develop operating philosophies for utility-sized systems. Dynamic models are under development to simulate systems and test control strategies. These efforts will also suggest changes to the system to enhance the operability of the system without detrimental effects to the rest of the system.

INTRODUCTION

METC's Process and Project Engineering Branch is responsible for performing systems analysis of the products under development by METC. A major portion of the systems studies are designed to support the METC Product Managers as they decide budget priorities and perform marketing functions in behalf of their specific system. These studies range from economic analysis of competing filter technologies to a technical assessment of selected nitrogen oxide (NO_x) control technologies. This paper gives a summary of the major PFBC systems studies performed during the past year and analysis that will be done during the next year. The topics covered are thermal efficiency, stochastic analysis of NO_x formation and control, dynamic modeling, HAP's, co-firing of wastes, systems with very low sulfur emissions, and future work.

THERMAL EFFICIENCY

Improvements to the thermal efficiency are an important area of study involving PFBC systems. A recent study addressed the effect of the ATS Program and the use of supercritical steam cycles in second-generation PFBC systems.

Baseline System

The baseline system used to test the effect of changing the gas turbine and the steam cycle is a Foster Wheeler second-generation PFBC system. A process diagram of the system is shown in Figure 1. Coal, steam, air, and limestone are fed using a dry, pneumatic system to a pressurized carbonizer. The carbonizer operates at a temperature of 1,700°F, and a portion of the coal is turned into a fuel gas. The limestone captures sulfur compounds that are evolved in this reducing environment. The solids left, after the fuel gas is produced, are sent to a pressurized, circulating, fluidized combustor. More air is added to create an oxidizing environment in the combustor, where the remaining combustible solids are burned. The limestone captures sulfur compounds that are created during the combustion process. The bed is operated at a temperature of 1,600°F. This temperature is maintained by generating steam in heat exchange tubes imbedded in a fluidized-bed heat exchanger. The non-combusted solids are withdrawn from the combustor as an ash and disposed. The ash has been shown to have beneficial uses as a roadbed filler, a strip mine reclamation material and other uses. This is an area of continuing research.

The fuel gas produced in the carbonizer and the flue gas from the combustor are combined in a topping combustor and burned. The outlet temperature of the topping combustor is 2,300°F. This is the inlet temperature of the Westinghouse 501F gas turbine. The gas turbine expander drives the compressor, providing the pressurized air for the combustor and carbonizer and a generator set producing electricity.

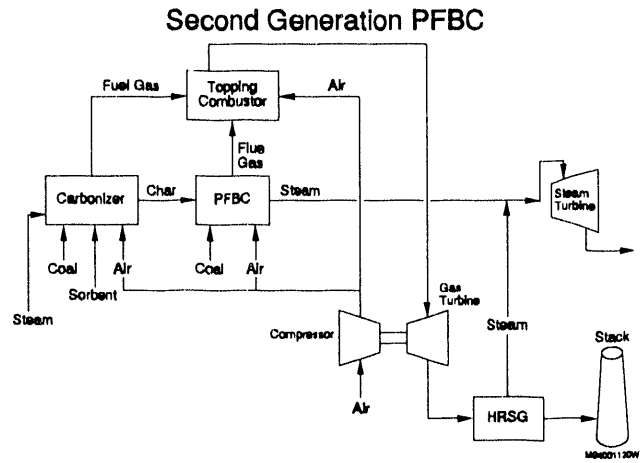

Figure 1. Second-Generation PFBC System

The gas exiting the gas turbine is fed to a heat recovery steam generator providing heat to the steam cycle. The steam cycle is a conventional 2,400 pounds force per square inch, absolute (psia)/1,000°F/1,000°F/2.5 millimeters of mercury single reheat steam cycle.

A summary of the performance of this system is in Table 1. The items to note in this table are the net power of 269.3 megawatt electrical (MWe) and the HHV efficiency of 46.5%.

ATS Gas Turbine

Starting in 1992, the Office of Fossil Energy and the Office of Energy Efficiency and Renewable Energy have been working with industry and academia in an 8-year program to develop the next generation of gas turbines. The turbines developed in this RD&D program are to have efficiencies such that a natural gas-fired combined cycle utility system will have a lower heating value efficiency greater than 60% (Webb 1994). In order to simulate an ATS turbine,

Table 1. Performance of Base System

Gas Turbine	139.4 MWe
Steam Turbine	138.3 MWe
Miscellaneous	-3.5 MWe
Auxillary	-5.0 MWe
Total Net Power	269.3 MWe
Net Efficiency (HHV)	46.5%

assumptions had to be made concerning the performance of the ATS-like turbine to change the natural gas-fired goals to coal-based performance. The assumption was made that advances in materials and air cooling schemes would allow a turbine inlet temperature of 2,450°F while using the same amount of cooling air as used in the present 501F machine. The efficiency of the expander and compressor sections are kept the same in the ATS-alike turbine as the present efficiencies in the 501F machine. These are conservative assumptions.

The ATS Program has a goal to produce inlet temperatures of 2,600°F+. However, these advances are expected to translate into coal-based systems only after development as a natural gas-fired system. As the ATS Program progresses, the gas turbine models will be updated and incorporated into future studies.

Supercritical Steam Cycles

During the 1950's and 1960's, development work was done in the U.S. on supercritical steam cycles. Because there was no economic need for efficient power and some technology problems with materials, the systems were shelved. However, steam system improvements have been shown to result in improved PFBC systems (Rubow et al. 1992). Supercritical steam cycles are an attractive way to boost the efficiency of coal-based power plants. The steam systems used in this study are based on two EPRI reports (EPRI CS-2555, EPRI CS-2223). Performance parameters are listed in Table 2. The cycle efficiencies listed in Table 2 are calculated using the Advanced System for Process Engineering (ASPEN™) System. The 3,500 psia and 4,500 psia dual reheat cycles are very efficient and capable of enhancing the electricity production of a second-generation PFBC system.

Efficiency Results

The results of different combinations of gas turbine and steam cycle are presented in Table 3. The top efficiency of 53.4% produced with an ATS turbine and a 4,500-psia steam cycle serves as a target for systems to reach for in the 21st century.

NO_x STOCHASTIC ANALYSIS

Because the systems under development at METC have not been fully commercialized, there are uncertainties associated with the performance and economic characteristics of the systems. In order to assess the technical and economic performance of the systems, this uncertainty must be accounted for in the analysis. It is difficult for a deterministic analysis to account for the uncertainty, so new tools must be developed. Stochastic analysis methods are the tools implemented at METC to analyze systems under uncertainty of technical and economic parameters (Dawes 1988). These tools were used to study the effect of uncertainty on NO_x production and control in a second-generation PFBC system (Reed 1994).

System Definition

The system studied is the same 46.5 efficient cycle used as the base case for the

Table 2. Supercritical Steam Cycle Performance

Throttle Pressure	2400 psi	3500 psi	4500 psi
Throttle Temperature	1000°F	1050°F	1100°F
Reheat 1 Temperature	1000°F	1050°F	1100°F
Reheat 2 Temperature	N/A	1050°F	1100°F
Cycle Efficiency (HHV)	38.67%	47.16%	48.54%

Table 3. Advanced Systems Power Breakout

GT	ST	GT Power (MWe)	ST Power (MWe)	Aux. (MWe)	Misc. (MWe)	Net Power (MWe)	Net Eff. (HHV)
W501F	2400	139.42	138.32	-3.48	-5.00	269.26	46.5%
ATS	2400	156.02	131.39	-3.35	-5.17	278.89	48.2%
W501F	3500	138.83	167.78	-4.84	-5.52	296.25	51.2%
W501F	4500	139.49	173.36	-5.89	-5.63	301.33	52.1%
ATS	3500	155.46	159.48	-4.63	-5.67	304.64	52.6%
ATS	4500	155.46	165.04	-5.64	-5.77	309.09	53.4%

ATS/supercritical steam study discussed above. The NO_X control technologies considered in this study were selective non-catalytic reduction (SNCR) and selective catalytic reduction (SCR). The flow diagram of the system containing the NO_X control technologies is given as Figure 2.

SNCR is based upon the Exxon™ thermal de-NO_X™ process. Ammonia (NH_3) is injected into the freeboard or cyclone of the solids combustor where the NO_X is converted into nitrogen and water. SCR is based upon the same chemical principle as SNCR, but the entire flue gas stream is passed over a catalyst that enhances the conversion of the NH_3 + NO_X reaction at a lower temperature to yield better conversion of NO_X.

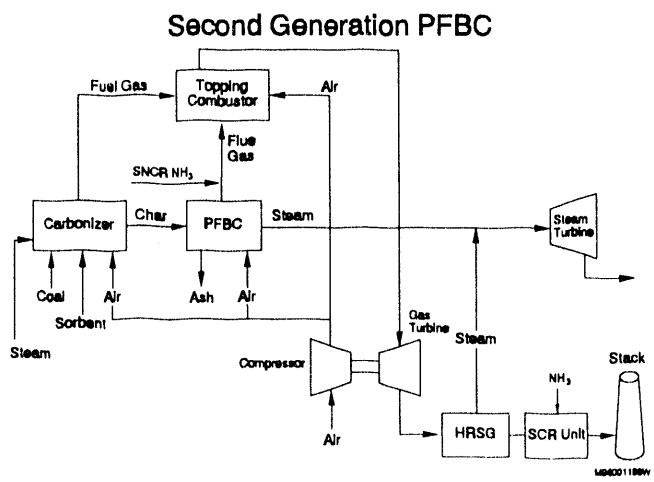

Figure 2. NO_X Controls Flow Diagram

Methodology

Stochastic analysis involves four steps. First, the parameters that will contain uncertainty must be chosen and the distributions modeling the uncertainty must be assigned. Second, a statistically sound method must be used to generate the samples from the distributions assigned in step 1. Third, the generated samples are used as input parameters to the model being studied and the output results are calculated. Finally, the output results are processed to obtain cumulative frequency diagrams and output coefficients.

In order to have a study that yields meaningful results, the parameters assigned uncertainty must be chosen with great care. Also, the distributions placed on the parameters must be carefully considered. The results of the simulation are totally dependent upon these choices. If any variable is added or deleted, or if any of the distributions are changed, the results under the old conditions do not apply. The calculations must start from the beginning in order to be relevant.

The parameters chosen and their distributions are given in Table 4. The first five parameters concern NO_X production within the PFBC system. The first of these parameters is the fraction of coal bound nitrogen converted to NH_3 in the carbonizer. This NH_3 can be turned into NO_X in the topping combustor. The second parameter is an error factor associated with a correlation used to predict the amount of NH_3 converted to NO_X in the topping combustor. This NO_X is called fuel-NO_X because the nitrogen starts in the coal. The third parameter is the ratio of NO to NO_2 formed in the PFBC. This has an effect on the chemistry of the PFBC and was of interest in the study. The fourth parameter is the amount of NO_X created in the PFBC. The fifth parameter of this group is the amount of thermal-NO_X created in the topping combustor. The next four parameters are related to the performance of the SNCR system. The sixth parameter determines the efficiency of NO_X reduction in the SNCR. The next three are related to operational characteristics of the SNCR system and are included to check the amount of NH_3 in the stack gas and the possible efficiency changes related to the SNCR system.

The final three parameters deal with the performance of the SCR system. The first parameter in this group is the efficiency of the SCR system. The other two are operational parameters of the SCR system and are included to check the amount of NH_3 in the stack gas and the possible efficiency changes related to the SCR system.

Latin Hypercube Sampling is the method used to generate random samples from the probability distributions selected. Details of this methodology can be found elsewhere (Iman 1984). The result of the selection process is a set of input vectors used as starting points by the PFBC system.

The PFBC power plant is modeled using the ASPEN™ computer software. This is the software that performs the energy and material balances of the PFBC system. The results of these calculations are further processed into forms used to assess the quantitative effect of uncertainty on the system.

The output results are used to create cumulative frequency diagrams such as Figure 3. The mean and confidence intervals calculated from these diagrams provides insight into the quantitative effect of uncertainty on the system.

The output results are also used to calculate regression coefficients or correlation coefficients, as shown in Figure 4. The coefficients give a

Table 4. Listing of Distributions of Uncertain Variables

Variable	Units	Low	Most Likely	High	Distribution
Coal N to NH_3 in Carbonizer	mole fraction	.1	.3184	.7684	Triangle
NH_3 to NO_x in Topping Combustor Noise	N/A	.9	1.0	1.1	Triangle
NO/NO_2 in PFBC	mole %	.37	.38	.44	Triangle
NO_x in PFBC	lb/MM BTU	.2	.6	1.2	Triangle
Thermal NO_x in Topping Combustor	ppm	24	25	30	Triangle
SNCR outlet NO_x	ppm	35	55	65	Triangle
NH_3 slip in SNCR	ppm	5	10	20	Triangle
NH_3 feed ratio in SNCR	mole %	.75	.85	1.0	Triangle
% carrier air for SNCR NH_3	%	1.0	1.2	2.0	Triangle
SCR NO_x % reduction	%	80	85	87	Triangle
NH_3 feed ratio in SCR	mole %	.71		.89	Uniform
SCR pressure drop	psia	8	8	12	Triangle

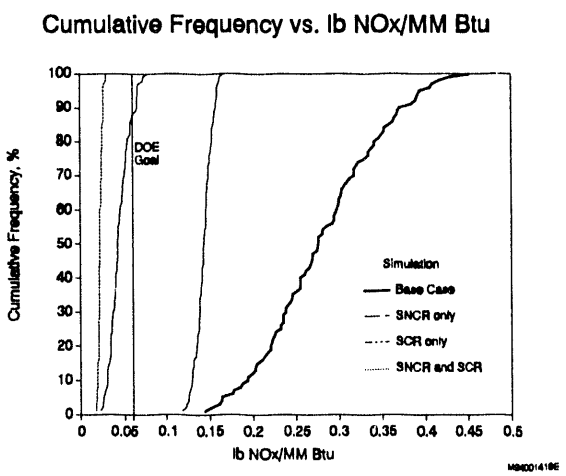

Figure 3. Cumulative Frequency Diagram for NO_x Emissions

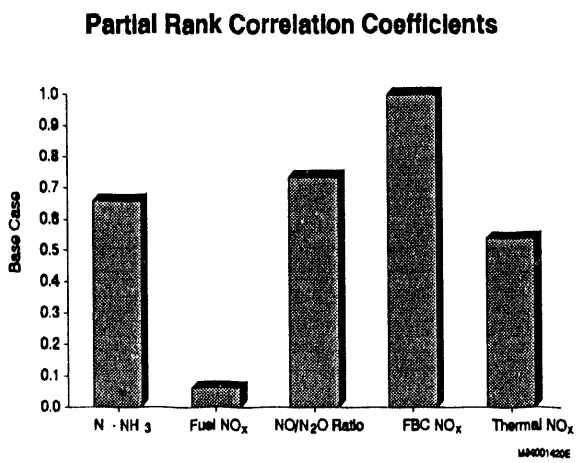

Figure 4. Partial Rank Correlation Coefficients for Base Case System

quantitative comparison of the importance of the input variables effect on the output of interest. Details on the calculation and use of these coefficients can be found elsewhere (Iman 1985).

NO_X Stochastic Study Results

The results of the study are presented in Figures 3 and 4, and in Table 5. Table 5 lists the NO_X emissions under different control schemes. Inspection of this table shows that SCR and SNCR have a significant effect on the total NO_X emissions of the plant.

Figure 3 shows the uncertainty associated with the calculations. The large range presented in the base case curve demonstrates that more work needs to be done to accurately quantify NO_X emissions from this system. Figure 4 shows the importance of the variables under study. These coefficients only apply to the base case configuration. A different set of coefficients must be calculated for each of the four cases because the parameter's given uncertainty changes for each of the different configurations.

NO_X Stochastic Study Conclusions

The largest absolute value in the set of coefficients corresponds to the most important parameter. In this case, NO_X production in the PFBC is the critical parameter. The conclusion from this information is that research should focus on controlling NO_X production in the PFBC first.

This study demonstrates the stochastic simulation methodology that has been implemented into the ASPEN™ simulator at METC. This tool is powerful and will provide input into the evaluation and budget process as METC moves into the 21st century. If research is focused on reducing NO_X production in the PFBC solids combustor, it is possible that the curves in Figure 3 will be shifted to the left and the DOE's goal can be met with only the use of SNCR. This type of advancement in NO_X control technology would make the addition of an extra downstream cleanup system, and the associated capital cost, unnecessary.

DYNAMIC MODELING

Historically, studies done at METC have concentrated on steady-state analysis. Because PFBC technologies are entering the commercialization phase, more emphasis is being placed on the operability of the systems. Operations studies require dynamic analysis.

Starting last summer, Gilbert/Commonwealth and Foster Wheeler have been working under a DOE/METC contract to develop a dynamic model of a second-generation PFBC system to develop an operations control strategy. The objectives of the study are as follows:

- Develop a working dynamic model of the Foster Wheeler second-generation PFBC process.
- Develop a control strategy for the fully integrated system.
- Develop operating strategies for turn-down from 100 to 90% and 90 to 50% power.
- Suggest changes to the system that will improve operating characteristics without an adverse impact on system efficiency.

At this time, the model has been developed using PC Trax™ software. The model has been tested under steady-state and some dynamic conditions. The final report for this task will be delivered in September 1994. This software and modeling knowledge will be used to evaluate other systems and eventually become a part of the technology evaluation process at METC.

HAP's STUDIES

Part of the Clean Air Act Amendments of 1990 is designed to address the emissions of

Table 5. Statistics for Cumulative Frequency Curves

Case	Mean (lb/MM BTU)	90% Low (lb/MM BTU)	90% High (lb/MM BTU)
Base Case	.28	.19	.37
SNCR	.14	.128	.157
SCR	.05	.03	.065
SNCR+SCR	.02	.019	.026

HAP's. Coal-based power plants have the potential to be regulated under this law. In order to assess the potential problems PFBC systems may have with HAP's emissions, a modeling study was performed.

This study was based upon the configuration and operating parameters of the Tidd PFBC plant operating in Brilliant, Ohio. A Lotus 1-2-3™ spreadsheet was developed using basic thermodynamic models. The purpose of the model was to partition HAP's into the flue gas and various solid waste streams leaving the system. A sensitivity study assessed the effects of temperature and pressure in different unit operations.

The sensitivity study shows the potential to reduce HAP's emissions by using lower operating temperatures in particulate cleanup devices such as barrier filters. As shown in Figure 5, the amount of HAP's emissions can be reduced by over 80% if the temperature of the barrier filter is lowered to 600°C (1,112°F). This model will be enhanced and validated as data is obtained from Tidd and other Clean Coal development projects.

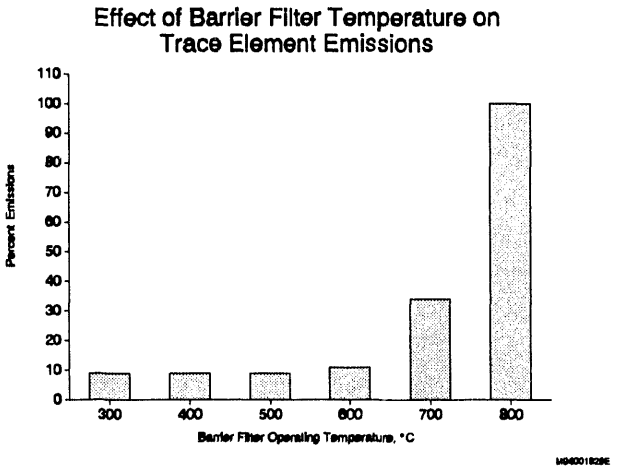

Figure 5. PRCCs for Base Case System

SCOPING STUDIES

Waste Co-Firing

A study assessed the effect of co-firing on the performance of PFBC systems (Bonk et al. 1994) to provide industry with an assessment of PFBC's ability to be as fuel flexible as atmospheric fluidized-bed technology. Results indicate that up to 20% waste by weight can be burned without dramatically changing the performance of first-generation PFBC systems. The

additional cost of waste handling has been studied and was shown not to be prohibitive to the development of these systems.

Low Sulfur Emissions Study

The Clean Air Act Amendments of 1990 place strict requirements on sulfur emissions from future coal-based power plants. In response to the regulations, DOE sponsored a study to determine if second-generation PFBC systems could operate under very strict sulfur (99% capture) requirements (Horazak et al. 1993). Results indicate that a system could be configured to meet this requirement. However, using limestone to capture sulfur compounds in the carbonizer and PFBC as the only sulfur capture method is not sufficient to reach 99% capture. Additional sulfur clean-up methods, such as Zinc Titinate, must be used.

FUTURE ACTIVITIES

Optimization and Process Synthesis

Work is continuing that will add new capabilities to the ASPEN™ simulator at METC. A contract with Carnegie Mellon University will add optimization and process synthesis sections to the simulator software. By the end of fiscal year (FY) 94 these advanced programming techniques will be installed. Plans for FY 95 include testing and implementation of these enhancements on PFBC systems.

With the optimization capability, we plan to perform an economic optimization on the NO_x control study discussed above. SCR is expensive and SNCR is less costly. The optimization capability allows for an objective function to be used as the basis for optimizing the system. In this case, the cost of electricity will be the objective function. This technique could also be used to explore how the compressor air should be used. The amount of air heated in the solids combustor instead of by-passed to the topping combustor is one option that could be optimized for efficiency or cost.

The process synthesis techniques will be used to address the problem of NO_x control. Several techniques are available to reduce the amount of NO_x emitted from a PFBC system. The process synthesis capability will consider all of these techniques at the same time, and determine which techniques should be used and where they should be placed in the system. An optimization algorithm based on an objective function is used to determine the optimum system. This technique could be used for other studies where unit operations need to be moved within the system as part of the study.

Advanced Bottoming Cycles

Supercritical steam cycles are one way to improve the efficiency of bottoming cycles. METC is also active in analyzing other bottoming cycles to take advantage of the unique heat characteristics of the second-generation PFBC cycle. The two sources of heat for a bottoming cycle may make alternative cycles, such as the Kalina ammonia-water cycle, very attractive. This cycle and alternate configurations of steam cycles are being investigated.

Economic Modeling

Most of the analysis at METC is focused on the technical side of problems. As commercialization becomes a larger issue, the economics of the system become more important to decision makers. We are addressing this by developing an economic data base that will cost the advanced coal systems METC is commercializing. Then economic factors can be directly integrated into calculations with the ASPEN™

simulation system. The economics will be involved in optimization and synthesis criteria. Also economic uncertainty for advanced processes can be accounted for when calculating cost associated with these systems.

CONCLUSIONS

System studies of PFBC systems are summarized in this paper. These studies are being used for various reasons: to validate the economic and environmental benefits that this technology offers the country, to identify issues associated with the commercialization of PFBC technology, and to help the DOE and its industrial partners focus on those RD&D activities which produce the "biggest bang for the buck," an increasingly important goal in the present climate of increasingly tight Federal and corporate budgets.

This year, the conclusion that NO_X generation in the solids combustor is the most important factor in determining NO_X production in an uncontrolled system was of particular significance. The initial assessment of HAP's, showing a possible reduction in HAPs emissions if the barrier filter is operated below 600°C in a first-generation PFBC, was the first time this type of data was produced on the ability of PFBC systems to be a low HAP's emission technology. Work will continue to improve these analytical tools used in these system studies useful for both DOE and its industrial partners.

REFERENCES

Bonk, D., H. McDaniel, M. DeLallo, R. Zaharchuk, 1994, "Co-Firing a Pressurized Fluidized-Bed combustion System with Coal and Refuse Derived Fuels and/or Sludges," Task 16 of Contract No. DE-AC21-89MC25177.

Dawes, R.M., 1988, *Rational Choice in an Uncertain World*, Harcort Brace Jovanovich, San Diego.

Iman, R.L., and M.J. Shortencarier, 1984, "A FORTRAN 77 Program and User's Guide for the Generation of Latin Hypercube and Random Samples for Use with Computer Models," *Nuclear Regulatory Commission Report*, NUREG/CR-3624, Albuquerque, New Mexico.

Iman, R.L., M.J. Shortencarier, and J.D. Johnson, 1985, "A FORTRAN 77 Program and User's Guide for the Calculation of Partial Correlation coefficients and Standardized Regression Coefficients," *Nuclear Regulatory Commission Report*, NUREG/CR-4122, Albuquerque, New Mexico.

General Electric Company, Stone & Webster Engineering Corporation, and Babcock & Wilcox Company, August 1982, *Engineering Assessment of an Advanced Pulverized-Coal Power Plant*, Final Report EPRI CS-2555.

Horazak, D.A., J.S. White, P.M. Whitman, and T.L. Buchanan, 1993, *Very Low Sulfur Emission (VLSE) PFBC System*, Final Report for Task 6, Contract No. DE-AC01-88FE61657.

Reed, M.E., "Stochastic Analysis of Nitrous Oxide (NO_X) Formation and Control in a Second-Generation Pressurized Fluidized-Bed Electric Generation Plant," AIChE 1994 Spring National Meeting, April 17-21, 1994, Atlanta, Georgia.

Rubow, L.N., D.A Horazak, M.R. Hyne, and T.L. Buchanan, 1992, *PFBC Concepts Analysis for Improved Cycle Efficiency and Cost*, Final

Report for Task 2, Contract No. DE-AC01-88FE61657.

Webb, H.A., and W.P. Parks, "Department of Energy Program to Develop Advanced Turbine Systems," *Advanced Combustion Turbines — Technology, Applications and the Global Marketplace*, January 27-28, 1994, Washington, D.C.

Westinghouse Electric Corporation, Combustion Engineering, Inc., and Gilbert Associates, Inc., January 1982, "Engineering, Assessment of an Advanced Pulverized-Coal Power Plant," Final Report, EPRI CS-2223.

MREED\1:940761a

4.2

Second-Generation PFBC Systems Research and Development—Phase 2
Circulating PFBC Test Results

CONTRACT INFORMATION:

Contract Number:	DE-AC21-86MC21023
Contractor:	Foster Wheeler Development Corporation 12 Peach Tree Hill Road Livingston, NJ 07039 (201) 535-2328
Contractor Program/Project Manager:	Archie Robertson
Contractor Project Engineer:	James Van Hook
Principal Investigators:	Frank Burkhard, Giovanni Carli, Rich Conn, Paul Crooker, Dave Kulcsar, Chongqing Lu, Anthony Mack, Aydemir Nehrozoglu, Mark Torpey, Frank Zoldak
METC Project Manager:	Donald Bonk
Phase 2 Period of Performance:	April 1988 through May 1995

Schedule and Milestones:

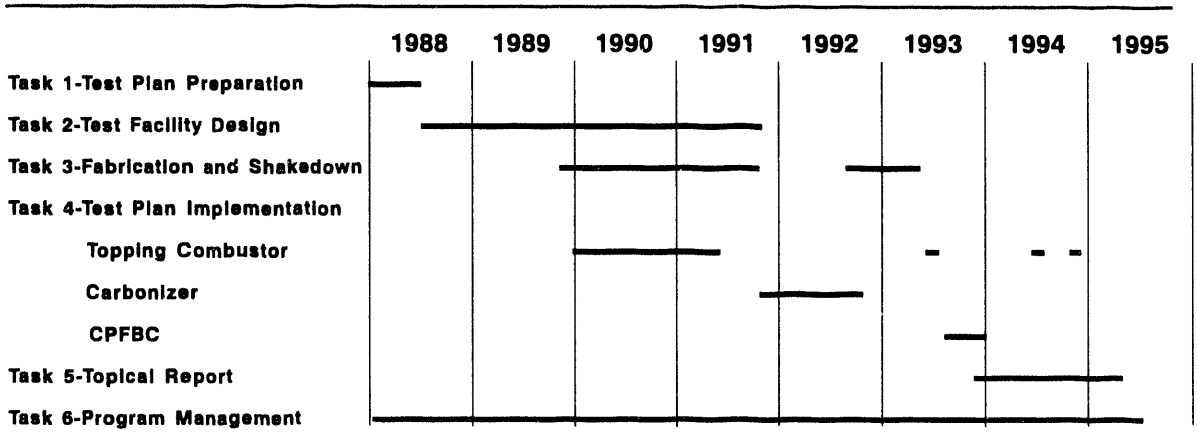

OBJECTIVES—PHASE 2

Three major objectives of Phase 2 are: ■ Separately test key components [the carbonizer, circulating pressurized fluidized bed combustor (CPFBC), particle-capturing ceramic barrier filter, and topping combustor] of second-generation PFB combustion plants at laboratory scale to ascertain their performance characteristics ■ Revise the commercial plant performance and economic predictions where necessary ■ Prepare for a 1.2-MWe equivalent Phase 3 integrated subsystem test of the key components.

BACKGROUND INFORMATION

Second-generation pressurized fluidized bed (PFB) combustion plants that generate electricity offer utilities the potential for significantly increased efficiencies with reduced costs of electricity and lower emissions, while burning the Nation's abundant supply of high-sulfur coal. Figure 1 is a simplified process block diagram of a second-generation PFB combustion plant.

In the plant, coal is fed to a pressurized carbonizer that produces a low-Btu fuel gas and char. After passing through a cyclone and ceramic barrier filter to remove gas-entrained particulates, the fuel gas is burned in a topping combustor to produce the energy required to drive a gas turbine. The gas turbine drives a generator and a compressor that feeds air to the carbonizer, a CPFBC, and a fluidized bed heat exchanger (FBHE). The carbonizer char is burned in the CPFBC with high excess air. The vitiated air from the CPFBC supports combustion of the fuel gas in the topping combustor. Steam generated in a heat-recovery steam generator (HRSG) downstream of the gas turbine and in the FBHE associated with the CPFBC drives the steam turbine generator that furnishes the balance of electric power delivered by the plant.

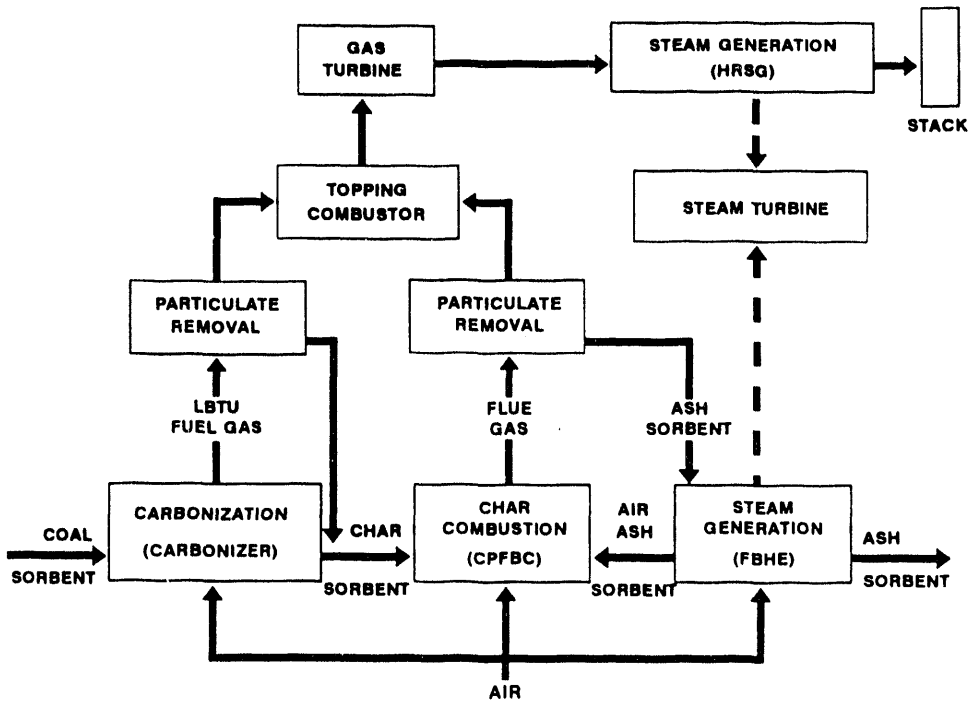

Figure 1. Simplified Process Block Diagram—Second-Generation PFB Combustion Plant

The low-Btu gas is produced in the carbonizer by pyrolysis/mild devolatilization of coal in a fluidized bed reactor. Because this unit operates at temperatures much lower than gasifiers currently under development, it also produces a char residue. Left untreated, the fuel gas will contain hydrogen sulfide and sulfur-containing tar/light oil vapors; therefore, lime-based sorbents are injected into the carbonizer to catalytically enhance tar cracking and to capture sulfur as calcium sulfide. Sulfur is captured in situ, and the raw fuel gas is fired hot. Thus the expensive, complex, fuel gas heat exchangers and chemical or sulfur-capturing bed cleanup systems that are part of the coal gasification combined-cycle plants now being developed are eliminated.

The char and calcium sulfide produced in the carbonizer and contained in the fuel gas as elutriated particles are captured by high-temperature filters, rendering the fuel gas essentially particulate free and able to meet New Source Performance Standards (NSPS). The captured material, with carbonizer bed drains, is collected in a central hopper and injected into the CPFBC through a nitrogen-aerated nonmechanical valve. The high excess air in the combustor transforms the calcium sulfide to sulfate, allowing its disposal with the normal CPFBC spent sorbent.

In the CPFBC, the burning char heats the high-excess-air flue gas to 1600°F; any surplus heat is transferred to the FBHE by the recirculation of solids (sorbent and coal fly ash) between the two units. Controlled recirculation is accomplished with cyclone separators and nonmechanical valves. The FBHE contains tube surfaces that cool the circulating solids. Because of the low fluidizing velocity in the FBHE ($\leq 1/2$ ft/s), the risk of tube erosion is virtually eliminated.

The exhaust gases leaving the carbonizer and the CPFBC contain sorbent and fly ash particles—both of which can erode and foul downstream equipment. A hot gas cleanup (HGCU) system, consisting of ceramic cross-flow filters preceded by cyclone separators, cleans these gases to <20 ppm solids loading before they enter the fuel gas topping combustor and the gas turbine and cause erosion and fouling. Ceramic candle filters, screenless granular-bed filters, and others, are candidate alternatives for the cross-flow filter should their performance and economics be found superior. All these devices are currently under development for first-generation PFB combustion cycles. They should also be applicable to the second-generation plant.

The topping combustor, which consists of metallic-wall multiannular swirl burners (MASBs), will be provided in two external combustion assemblies (topping combustors) on opposite sides of the gas turbine. Each MASB contains a series of swirlers that aerodynamically create fuel-rich, quick-quench, and fuel-lean zones to minimize NO_x formation during the topping combustion process. The swirlers also provide a thick layer of air at the wall boundary to control the temperature of the metallic walls.

A team of companies led by Foster Wheeler Development Corporation (FWDC)—with ■ Foster Wheeler Energy Corporation and Foster Wheeler USA ■ Gilbert/Commonwealth, Inc. ■ Institute of Gas Technology ■ Westinghouse Power Generation Business Unit (PGBU) and Science & Technology Center (STC)—has embarked upon a DOE-funded three-phase program to develop the technology for this new type of plant. A conceptual design of a 3-percent-sulfur Pittsburgh

No. 8 coal-fired second-generation PFB plant with a conventional 2400 psig/1000°F/1000°F/ 2-1/2 in. Hg steam cycle was prepared, and its economics were determined [1]. In 1987 we estimated that, when operated with a 14-atm/ 1600°F carbonizer, the plant efficiency would be 44.9 percent (based on the higher heating value of the coal) and its cost of electricity would be 21.8 percent lower than that of a conventional pulverized coal-fired plant. Tests conducted in our pilot-scale carbonizer (described later) yielded performance superior to that estimated in 1987. As a result, we now expect a more energetic fuel gas and a plant efficiency of 46.2 percent with a 1600°F carbonizer [2].

PROJECT DESCRIPTION

The second-generation PFB combustion plant development effort is divided into three phases, the first of which has already been completed and documented in a series of reports available through the National Technical Information Service [3-4].

The first phase of the DOE program was aimed at plant conceptualization and optimization and identification of plant R&D needs. The second phase, involving laboratory-scale tests of the key plant components, is under way.

The R&D needs of this new type plant were presented in the Phase 1 Task 2 Report issued under this contract [3]; an integrated program plan for meeting these needs was presented in the Task 3 Report [4]. In accordance with that plan, the key components of this new plant are being tested separately in Phase 2 of this contract to ascertain their individual performance characteristics. A series of topping combustor tests has already been conducted at the University of Tennessee Space Institute (UTSI) under the direction of Westinghouse PGBU [5-7]. These tests were successful, proving the combustor concept.

CARBONIZER TEST PROGRAM

In November 1991 FWDC began operating a PFB pilot plant at its John Blizard Research Center in Livingston, New Jersey. The facility had a multipurpose reactor and a ceramic barrier filter. The reactor was designed to test a second-generation plant carbonizer and then, after modification, a CPFBC/FBHE. Ceramic barrier filters provided by Westinghouse STC were used with both of these units to demonstrate particulate control capabilities.

Because a new facility and a new process (carbonization) were involved, the pilot plant began operation with a two-cyclone HGCU system. After completing the planned carbonizer test matrix and ascertaining that the carbonizer fuel gas composition was compatible with a ceramic barrier filter (no tars or oil vapors in the gas), the second-stage cyclone was replaced by a ceramic cross-flow filter.

The carbonizer was a 30-in.-OD × 34 ft-6 in.-tall refractory-lined pressure vessel. It had a 19-ft-deep jetting fluidized bed and a 9 ft 5-3/4 in.-tall freeboard (Figure 2). The carbonizer ID increased from the bottom to the top in three steps to enhance solids circulation and limit slugging and elutriation. The ID was 10 in. for the first 3 ft-7 in. of bed height, 12 in. to the top of the bed, and 14 in. in the freeboard. Air, coal, and lime-based sorbent were injected into the unit at a 40- to 60-ft/s jet velocity through a central, vertical, 1-in., Sch 80, stainless steel feed pipe at the bottom of the unit. Low-Btu fuel gas left through a 3-in. ID radial nozzle at the top. Spent bed material and char drained through the annulus that surrounded the feed pipe, entered the packed

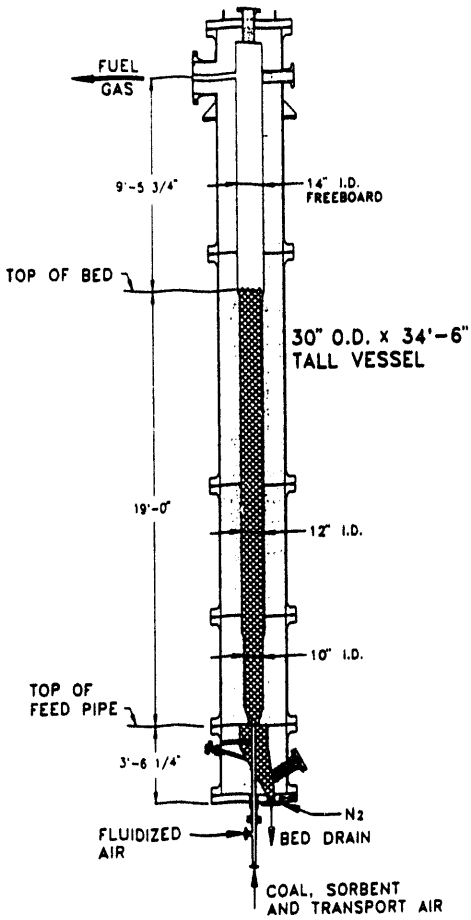

Figure 2. 10-in. Carbonizer Test Unit

bed, and were cooled to 300°F by counter-flowing nitrogen before leaving through a 4-in. drain. A pressurized screw feeder in the drain line controlled the material drain rate/bed height and discharged to a lock hopper for de-pressuring and ultimate drum disposal.

The first carbonizer test program consisted of eight bubbling fluidized bed test runs. It encompassed 37 setpoints/533 hours of operation. Portions of the collected data have been discussed in other publications [8-10]. Although highly caking Pittsburgh No. 8 coal and Ohio Plum Run dolomite were most frequently used, Illinois No. 6 and Wyoming Eagle Butte coals and Alabama Longview limestone were also tested. The Pittsburgh coal typically had a 3.5-percent sulfur content and a Free Swelling Index of 6.5; the Eagle Butte coal contained 0.7-percent sulfur and 27-percent moisture.

The bubbling bed carbonizer shown in Figure 2 was operated at approximately 3 ft/s superficial gas velocity (measured in the 10-in. ID section). Pressures, temperatures, and steam injection rates ranged from 10 to 14 atm, 1500 to 1800°F, and 0 to 0.4 lb steam/lb coal respectively.

From the standpoint of fluidized bed combustors, circulating bed performance (e.g., combustion efficiency, sulfur-capture efficiency, NO_x emissions) is generally accepted to be superior to bubbling bed performance. Although the bubbling bed carbonizer demonstrated excellent performance, an exploratory test run was made with a circulating bed carbonizer to determine whether it also offered improved performance. To achieve the higher gas velocity required for circulating bed operation, ceramic inserts were installed in the carbonizer, reducing its cross section to a constant top-to-bottom 8-in. ID, as shown in Figure 3. Four circulating bed carbonizer test points were completed at a nominal velocity of 10 ft/s at 5 to 9 atm pressure, with Pittsburgh No. 8 coal and limestone. Because a comparison of the circulating and bubbling bed data showed little difference in performance, no further circulating bed tests were completed.

At no point in the program have any tar or oil vapors been found/condensed from the fuel gas. This finding is very important because their presence might jeopardize barrier filter operation by causing filter blinding and blocking. The high carbonizer operating temperature, relatively long in-bed gas residence time (approximately 8 seconds), high pressure, exposure to lime-based sorbents, and method

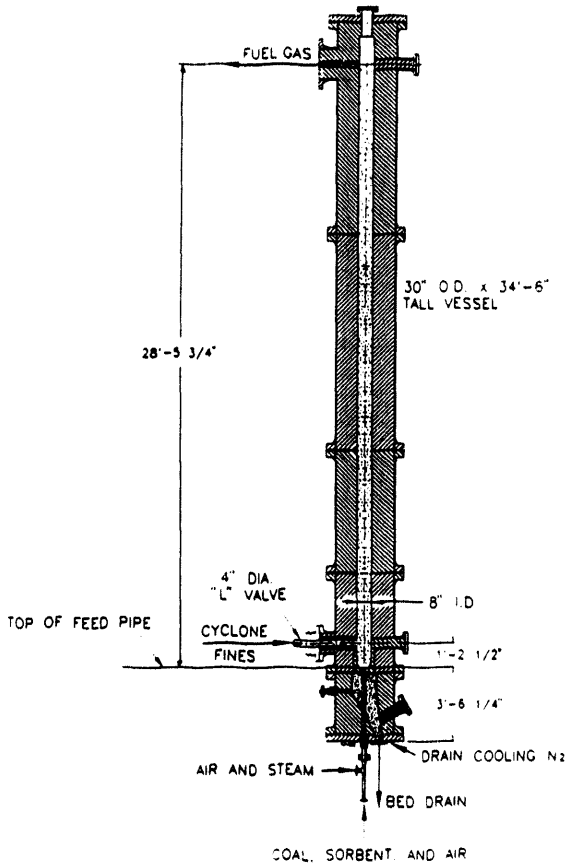

Figure 3. 8-in. Circulating Bed Carbonizer Test Unit

of coal/air feed (coal and air injected at the same point) destroy all tar and oil vapors in the bed.

The solids residue from the process is a char/sorbent mixture containing fine carbon particles. The residue is free flowing and not sticky, except possibly at very low sorbent-to-coal ratios with highly caking coals. It is captured by the primary cyclone and returned hot to the base of the carbonizer via the refractory-lined L-valve arrangement shown in Figure 4.

Ceramic cross-flow and ceramic candle filters were used in the bubbling bed and circulating bed carbonizer tests respectively. All four program fuels and two program sorbents were used, and the cross-flow filter inlet temperature reached a high of about 1500°F. Filter test results were discussed by R. Newby, et al. [11]. Briefly, residue from the four different fuels posed no problem to the barrier filter; the filter cakes were easily cleaned, there was little change in filter permeability, and there were no indications of significant particle reentrainment during pulse cleaning.

In summary, the carbonizer test program has been very successful. It has demonstrated that carbonizer operation is smooth and controlled, emissions are lower than were previously estimated for a commercial plant, and the char/sorbent residue and fuel gas from the process appear compatible with the particle-capturing ceramic barrier filters.

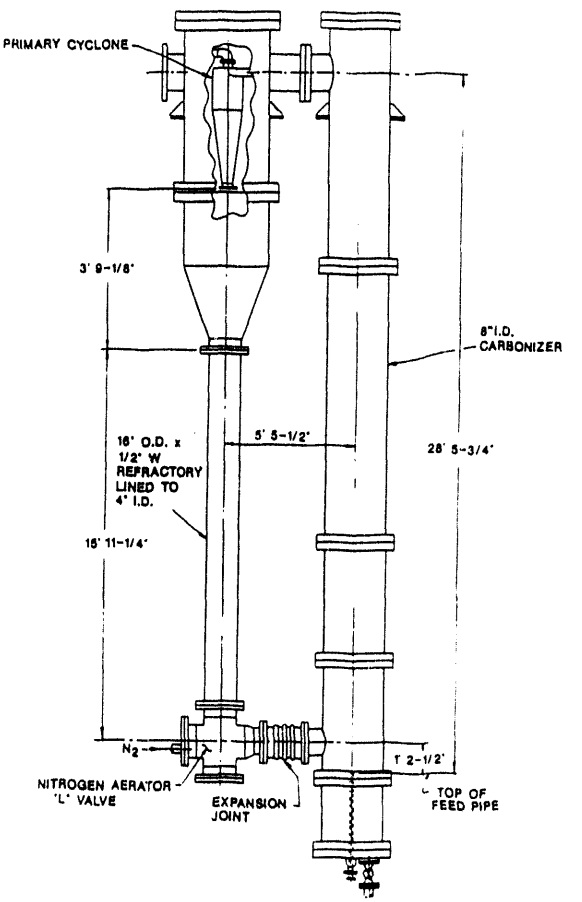

Figure 4. Circulating Bed Carbonizer General Arrangement

CPFBC PILOT PLANT

Having successfully completed the carbonizer test program, the pilot plant was modified for CPFBC operation.

A schematic of the CPFBC pilot plant is shown in Figure 5. Crushed coal and sorbent are loaded into and stored in separate 10-ton silos adjacent to the outside wall of the laboratory. A series of bucket elevators, vibrating feeders, belt conveyors, etc., load and transfer these materials into the building into separate lock hopper systems that are pressurized to approximately 200 psig with 70°F nitrogen. From the pressurized hoppers, the coal and sorbent are fed into a pneumatic transport line via screw feeders and injected into the CPFBC.

The CPFBC is a vertical, 30-in.-OD, 34 ft-6 in.-tall pressure vessel, shown in Figure 6. The CPFBC primary zone is 12 ft-6 in. tall, and the secondary zone is 16 ft tall. The vessel is refractory lined to an 8-in. diameter. Coal, sorbent, and pneumatic transport air are injected at the bottom of the unit at a 40- to 60-ft/s jet velocity through a central, vertical 1-in. Sch 80 stainless steel pipe. At a point 10-3/4 in. below the feed pipe discharge, an outer, concentric, 2-in. Sch 40 pipe injects fluidized air around and at the base of the feed pipe. A nitrogen-aerated packed-bed cooler at the bottom of the CPFBC cools spent bed material to 300°F before lock-hopper depressuring and disposal. Two diametrically opposed secondary air injection ports are provided 12 ft-6 in. above the point of fluidized air entry.

The heat released during the combustion process is absorbed by a sorbent/fly ash mixture continuously circulated between the CPFBC and the FBHE. A cyclone separator atop the FBHE and a nonmechanical L-valve at the bottom control the circulation of solids entering the CPFBC 14-3/8 in. above the fluidizing air.

The FBHE, also shown in Figure 6, is a 42-in.-OD by 34 ft-6 in.-tall pressure vessel, refractory lined to yield a 18-in. square bed and freeboard section. A 39-in.-tall (bottom-to-top tube centerline height) water-cooled tube bundle in the bed consists of eight 1-in.-OD Incoloy 800H tubes. City water is used as the coolant, and its flow rate is adjusted as required to keep the water outlet temperature below 140°F. An air-sparger pipe injects fluidized air at the bottom of the bed and allows solids to flow downward into the L-valve or through the bed-drain cooling section. A screw feeder immediately below the FBHE controls the bed drain rate and bed height. Raising and lowering the bed height controls the amount of tube surface immersed in the bed and hence the bed and CPFBC solids return temperature. The fluidized air leaves the top of the FBHE and enters the CPFBC as secondary air.

The combustion gas/solids mixture exits the combustor and passes through a 3-in. connecting pipe into the cyclone atop the FBHE. The hot solids are separated from the gas and fall by gravity into the 6-in. Sch 40 standpipe. At the end of the standpipe, an aerated J-valve provides a gas seal between the FBHE and cyclone separator. After passing through the J-valve, the solids fall into the FBHE bed, containing tube bundles, where part of the secondary air fluidizes the solids. After passing over the heat exchanger coils, the solids are recycled to the combustor via the nitrogen-aerated L-valve. Pressure, temperature, and pressure differential ports are provided on the standpipe, J-valve, heat exchanger, and L-valve. The cyclone exhaust gas exits the FBHE and enters a ceramic barrier candle filter for final particulate cleanup.

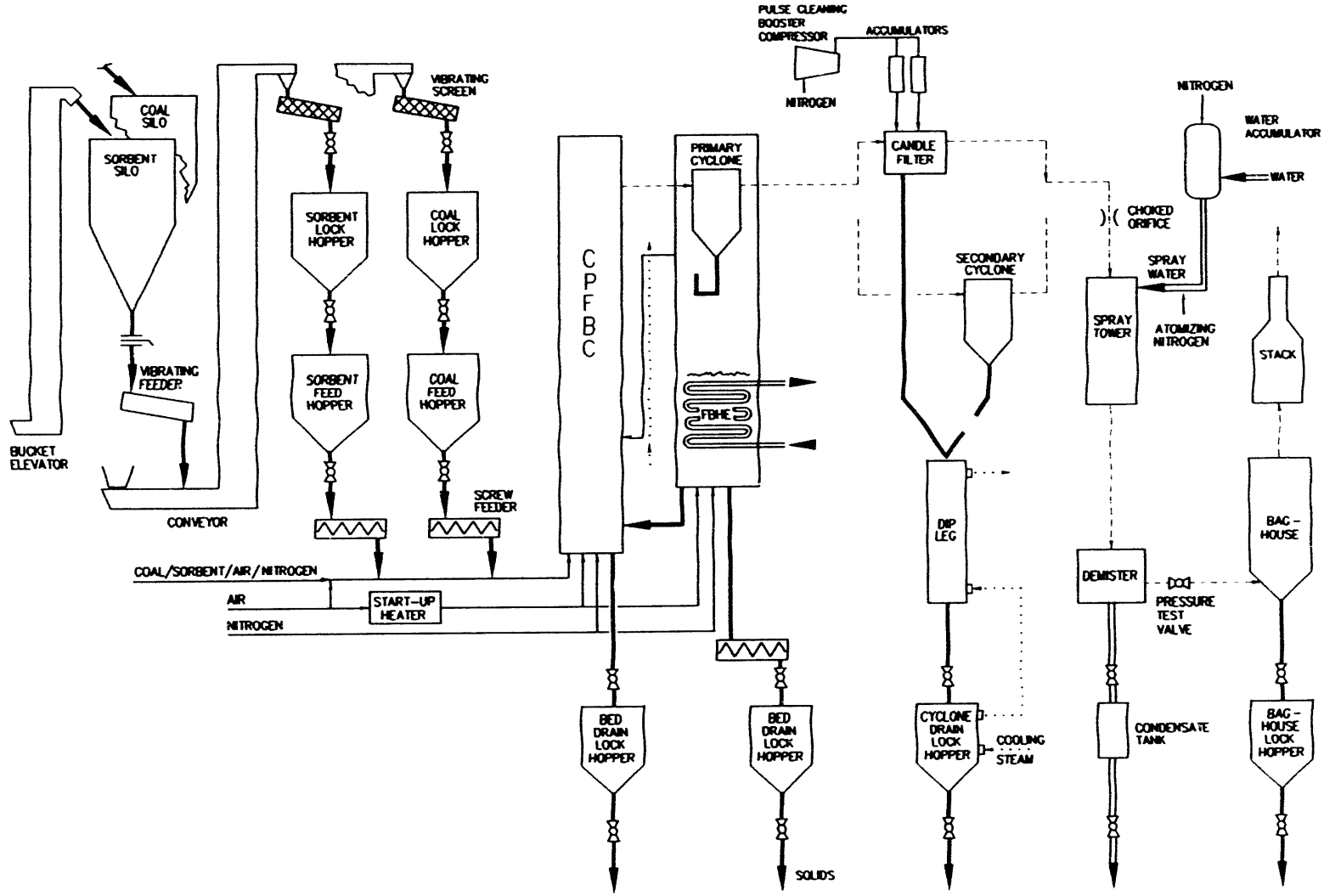

Figure 5. CPFBC Pilot Plant Schematic

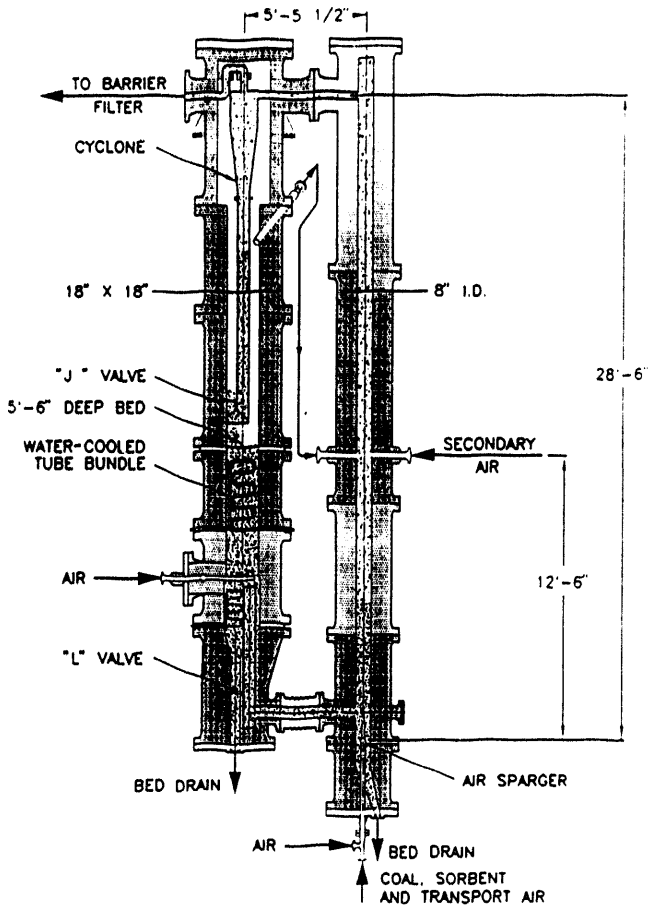

Figure 6. Integrated CPFBC/FBHE Unit—Phase 2

The gas exhausting from the ceramic-candle filter is lowered to atmospheric pressure as it passes through a choked-flow orifice. The high-velocity orifice jet discharges into an Incoloy-shrouded refractory-lined chamber, where a nitrogen-atomized nozzle injects spray water to cool the gas to approximately 350°F. Although the cooling is accomplished by a dry quench, a wire mesh demister is provided at the base of the spray tower to remove any water droplets that may be present in the gas. The cooled gas passes through a baghouse filter and is then discharged to the atmosphere via an elevated stack.

Flue gas is sampled both periodically and continuously. The periodic samples are taken from the CPFBC freeboard and from a point downstream of the demister; the continuous measurements are made at the stack via continuous emissions monitors.

CPFBC TEST RESULTS

A total of 23 steady-state setpoint periods were obtained from over 300 hours of operation while firing the test fuels. The coals tested in the pilot plant included Pittsburgh No. 8, Illinois No. 6, and Kentucky Andalex, all high-volatile bituminous and Eagle Butte subbituminous. A setpoint period was also conducted with petroleum coke, which served as the pilot plant start-up fuel. Char-sorbent residues from the carbonizer test program were also tested; they included Eagle Butte with limestone, three Illinois No. 6 blends with limestone, and a Pittsburgh No. 8 with dolomite. Proximate and ultimate analyses of the test fuels are shown in Tables 1 and 2.

Sulfur contents ranged from 0.5 to 3.53 percent for the Eagle Butte subbituminous and Kentucky Andalex coals respectively. All of the coals were relatively low in ash content, with the Kentucky Andalex having the highest ash content (11.66 percent). The low ash content of some of these fuels was important from a bed maintenance standpoint; consequently, sorbent feed was often dictated by CPFBC system inventory requirements.

All of the chars contained Longview limestone sorbent, except for the Pittsburgh No. 8 which contained Plum Run dolomite. As shown in Table 2, all of the chars were relatively low in volatile content (less

Table 1. Fuels Tested in CPFBC

Description	Petroleum Coke	Pittsburgh No. 8 (HVB)	Illinois No. 6 (HVB)	Kentucky (HVB)	Eagle Butte
Proximate Analysis, wt%					
Fixed Carbon	86.34	51.30	47.37	46.65	34.11
Volatile Matter	11.85	35.96	33.13	35.71	30.92
Ash	1.30	10.16	11.14	11.66	4.86
Moisture	0.51	2.58	8.36	5.98	30.11
Ultimate Analysis, wt%					
Carbon	90.34	71.48	62.37	66.49	47.21
Hydrogen	3.72	4.74	3.80	3.98	3.37
Oxygen	0.77	5.60	9.84	6.77	13.04
Nitrogen	1.32	1.92	1.35	1.59	0.90
Sulfur	2.04	3.52	2.84	3.53	0.51
Ash	1.30	10.16	11.14	11.66	4.86
Moisture	0.51	2.58	8.36	5.98	30.11
HHV, Btu/lb	15,382	12,799	11,532	12,216	8,245

Table 2. Char Proximate and Ultimate Analysis

Description	Eagle Butte Limestone	Pittsburgh No. 8/ Dolomite	Illinois No. 6/ Limestone Blend 2	Illinois No. 6/ Limestone Blend 3	Illinois No. 6/ Limestone Blend 10
Proximate Analysis, wt%					
Fixed Carbon	60.16	46.39	35.98	46.91	45.75
Volatile Matter	8.08	5.55	10.73	7.76	14.86
Ash	28.64	47.15	53.06	44.67	34.74
Moisture	3.12	0.91	0.23	0.66	4.65
Ultimate Analysis, wt%					
Carbon	63.54	45.97	39.33	48.31	51.25
Hydrogen	0.52	0.50	0.65	0.54	0.65
Oxygen	1.78	0	0.32	0	4.36
Nitrogen	0.90	0.96	0.70	0.81	0.89
Sulfur	1.50	4.51	5.71	5.01	3.46
Ash	28.64	47.15	53.06	44.67	34.74
Moisture	3.12	0.91	0.23	0.66	4.65
HHV, Btu/lb	9,407	8,156	5,961	8,364	8,527
Sulfide S, %	0.80	3.03	4.30	4.19	1.80

than 15 percent). The higher heating values of the chars ranged from 5961 Btu/lb for an Illinois No. 6 char to 9407 Btu/lb for the Eagle Butte char. The sulfide sulfur content of the chars ranged from 0.80 percent for the Eagle Butte to 4.30 percent for an Illinois No. 6 blend.

The major operating variables evaluated in the test program included combustor bed temperature, combustor pressure, primary air stoichiometry, and excess air. The range of these operating variables is shown below:

Combustor temperature, °F	1600 to 1700
Combustor pressure, psig	90 to 190
Primary air stoichiometry, %	60 to 90
Excess air, %	30 to 80

The target sulfur capture for all test points was 92 percent or greater. Sorbent feed rate was often dictated by system inventory requirements, not the desired level of sulfur capture.

Heat and material balances were performed for all setpoint periods to ensure the validity of efficiency and emissions calculations. Material balances were calculated based on measured and calculated input and output streams from the combustor. Input streams included measured air and nitrogen input flows and calculated fuel and sorbent rates. Output streams included measured stack gas flow and calculated ash drain rates. Both total mass flow and elemental rates (C, H, O, and N) generally showed excellent closure of less than 5 percent.

Carbon conversion efficiencies were in excess of 99.5 percent for the diverse types of fuels tested. Carbon conversions were determined by measuring the organic carbon content of the ash drains and calculating the ash drain rates. The organic carbon content of all ash drains was very low and never exceeded 0.5 percent.

A plot of carbon conversion vs. combustor bed temperature is shown in Figure 7 for the coals and chars. As shown in this figure, there appeared to be little effect from bed temperature on carbon conversion since conversions were all in excess of 99.5 percent. These data are consistent with those from the literature for other pressurized CFB pilot plants [12, 13]. Extremely high carbon conversion in the CPFBC was probably a result of the high oxygen partial pressure compared with atmospheric CFBs.

Average CO, SO_2, and NO_x emissions were determined for the steady-state test periods. These emissions were calculated from averages of 1-minute data over a setpoint period of between 2 and 4 hours.

Carbon monoxide emissions were very low for all the fuels tested and generally ranged between 0.01 and 0.02 lb/10^6 Btu. Low CO emissions are usually an indication of high carbon combustion efficiency. A plot of CO emissions vs. combustor bed temperature is shown in Figure 8. CO emissions decreased by a factor of two as the bed temperature was increased from 1500 to 1600°F. These data are consistent with atmospheric CFBC experience, which also shows a strong temperature dependence on CO emissions.

The sorbents utilized in this test program included two limestones (Genstar and Three Rivers) and one dolomite (Plum Run). Important chemical and physical properties of these sorbents are summarized in Table 3. At the beginning of each test run, the bed was sulfated by a nitrogen-SO_2 gas mixture for a

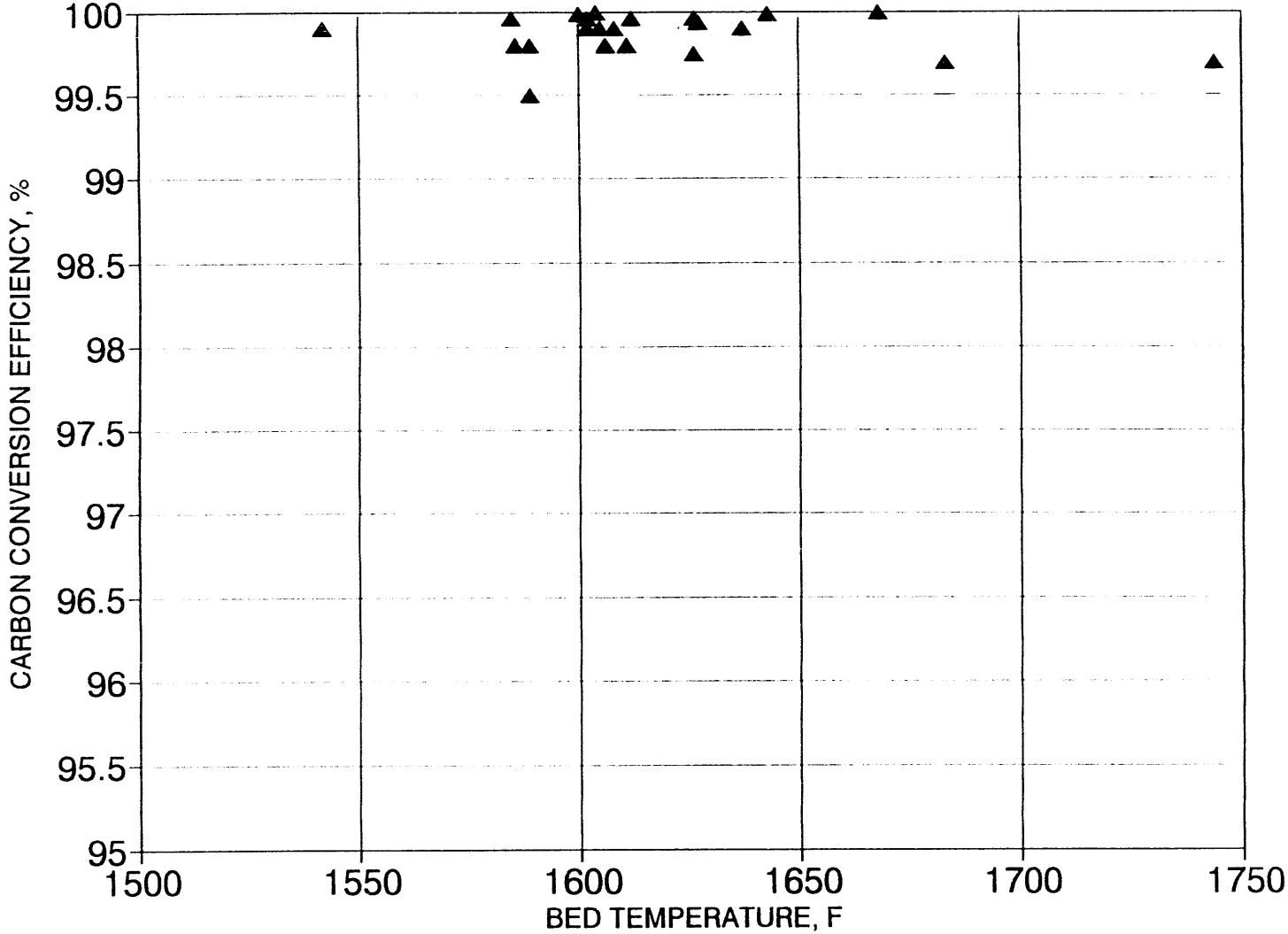

Figure 7. Carbon Combustion Efficiency Vs. Combustor Bed Temperature

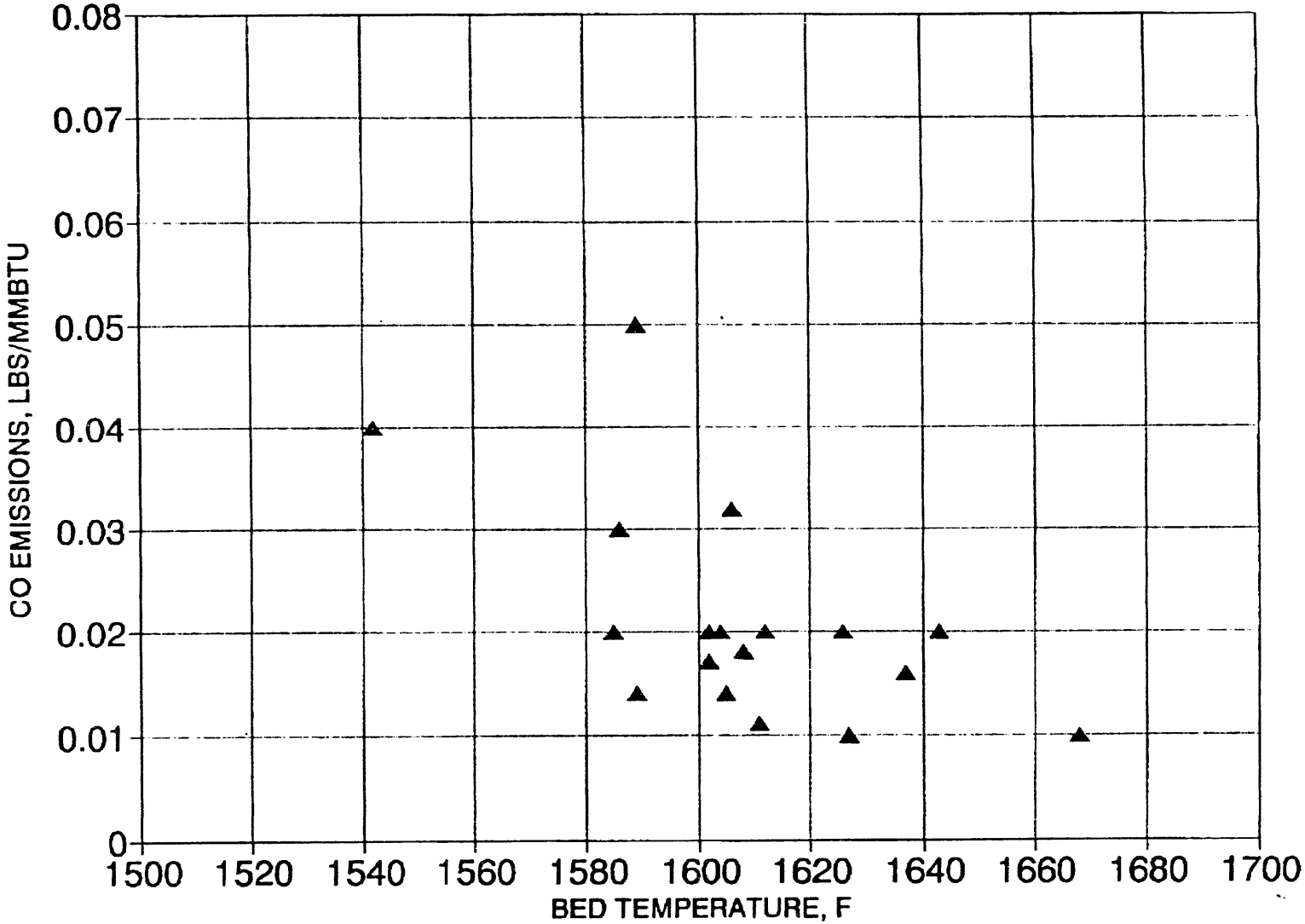

Figure 8. Carbon Monoxide Emission as a Function of Combustor Bed Temperature

Table 3. Sorbents Tested in CPFBC

Analyses	Genstar Limestone	Three Rivers Limestone	Plum Run Dolomite
Chemical Analysis, wt%			
$CaCO_3$	98.1	98.0	55.5
$MgCO_3$	0.7	1.1	42.7
Inerts	1.2	0.9	1.8
Hardgrove Index	53	49	91
TGA Ca Utilization, %	49	40	88

period of up to 20 hours to mature the bed and provide reasonable sulfur-capture data.

Sulfur-capture data for all of the test points are shown in Figure 9 as sulfur-capture efficiency vs. feed Ca/S ratio. A sulfur-capture efficiency greater than 96 percent was usually achieved with Ca/S ratios ranging from 1:1 to 2:1. In some cases system inventory maintenance dictated sorbent feed rate instead of targeted sulfur capture. This was particularly true for very low ash fuels such as petroleum coke and Eagle Butte subbituminous coal. The carbonizer chars all revealed very high sulfur capture from inherent calcium and did not require additional sorbent.

NO_x emissions generally ranged from 0.3 to 0.6 lb/10^6 Btu for the test fuels. Of all the operating parameters, primary zone stoichiometry appeared to have the greatest impact on NO_x emissions. Over the range of operating temperatures and excess air levels, no strong dependence was observed. Some of the test chars showed exceptionally high conversions of fuel nitrogen to NO_x. This phenomenon has been observed in atmospheric CFBC systems and has been attributed to the inability to control NO_x formation from nonvolatile nitrogen by air staging.

The effect of primary-zone stoichiometry on NO_x emissions is shown in Figure 10. Although there is considerable scatter in the data, NO_x emissions did reveal a moderate dependence on primary air stoichiometry, particularly for the Illinois No. 6 coal tests. Most of the other fuels did not show a strong dependence of primary air stoichiometry on NO_x. However, the range of primary air stoichiometries was not very great for these tests (65 to 75 percent).

To discern the effect of fuel type, the same emissions data are shown in Figure 11 as the percentage of fuel nitrogen converted to NO_x. These data show similar trends with primary zone stoichiometry, with the exception of the test chars. In particular, the Pittsburgh No. 8 and Eagle Butte chars showed much higher conversions of nitrogen to NO_x than the parent coals. This trend was also observed for the Illinois No. 6 chars, but was not quite as pronounced.

As mentioned earlier, there was considerable scatter in the NO_x data correlation with primary zone stoichiometry. This scatter may be because of the variation of other operating parameters, particularly excess air level. Because of the intricate coupling of the FBHE with the combustor, difficulty was often encountered in varying one operating parameter at a time while holding all others constant. However, from some limited data, excess air level did not appear to have a significant effect on NO_x emissions. Figure 12 shows the effect of excess air on NO_x emissions for Illinois No. 6 coal over a narrow range of primary air stoichiometries. NO_x emissions remained fairly constant even though excess air was increased by over a factor of three (25 to 83 percent).

A major issue involving the performance of the CPFBC is the extent of char calcium sulfide conversion. Conversion of sulfide was evaluated for four different char blends (Pittsburgh No.8/dolomite and three Illinois No. 6/limestones). The sulfide sulfur contents of the chars varied from 1.8 to 4.3 percent, as shown in Table 4. The sulfide conversion ranged from 68 to 82 percent, with the high-sulfide Illinois No. 6 char having the highest conversion. As expected, the candle filter drains had the lowest concentrations of sulfide (about 1 percent). The sulfide sulfur levels were considerably higher in the FBHE and combustor drains, with the latter having the highest.

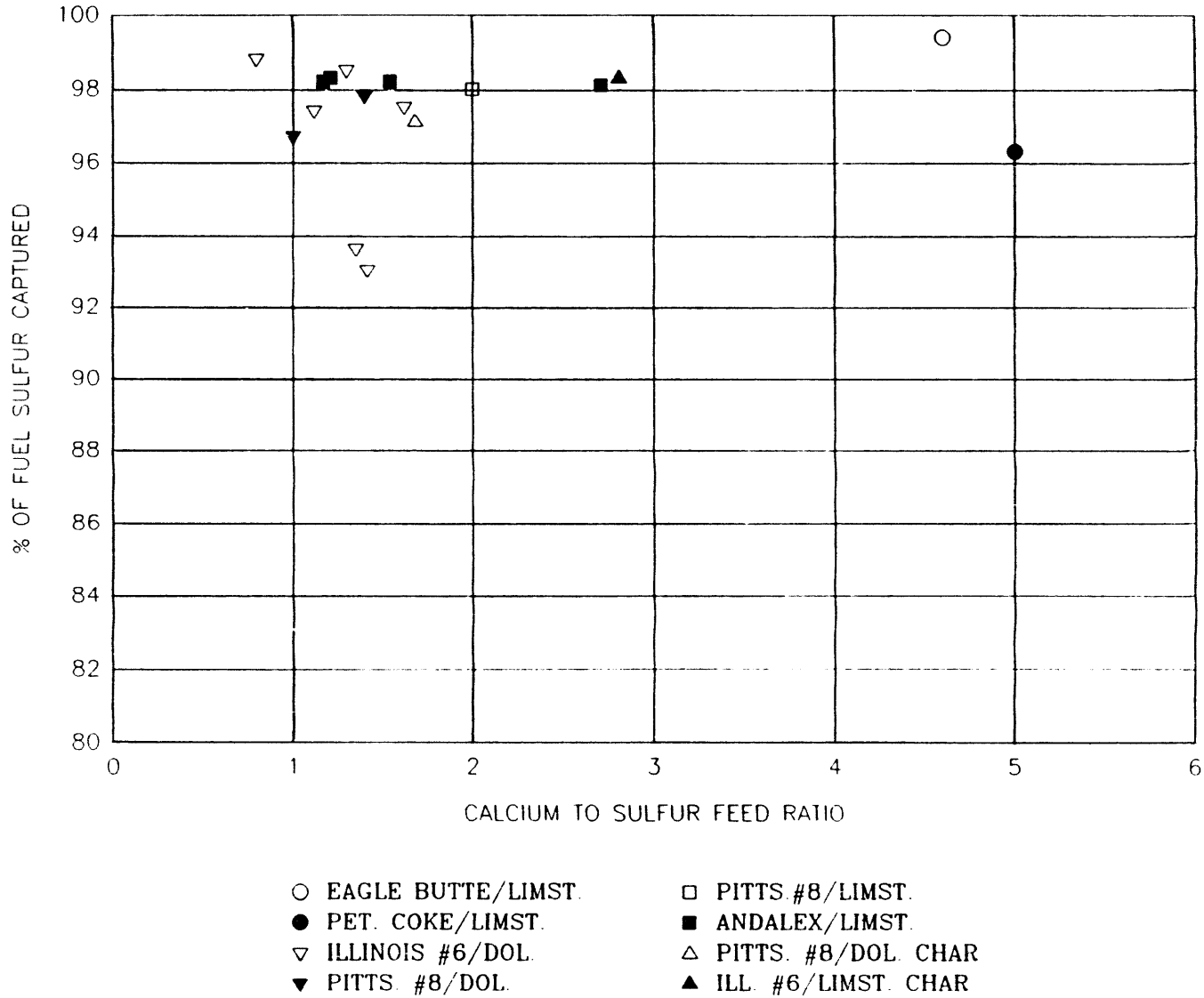

Figure 9. Sulfur Capture Vs. Ca/S Ratio

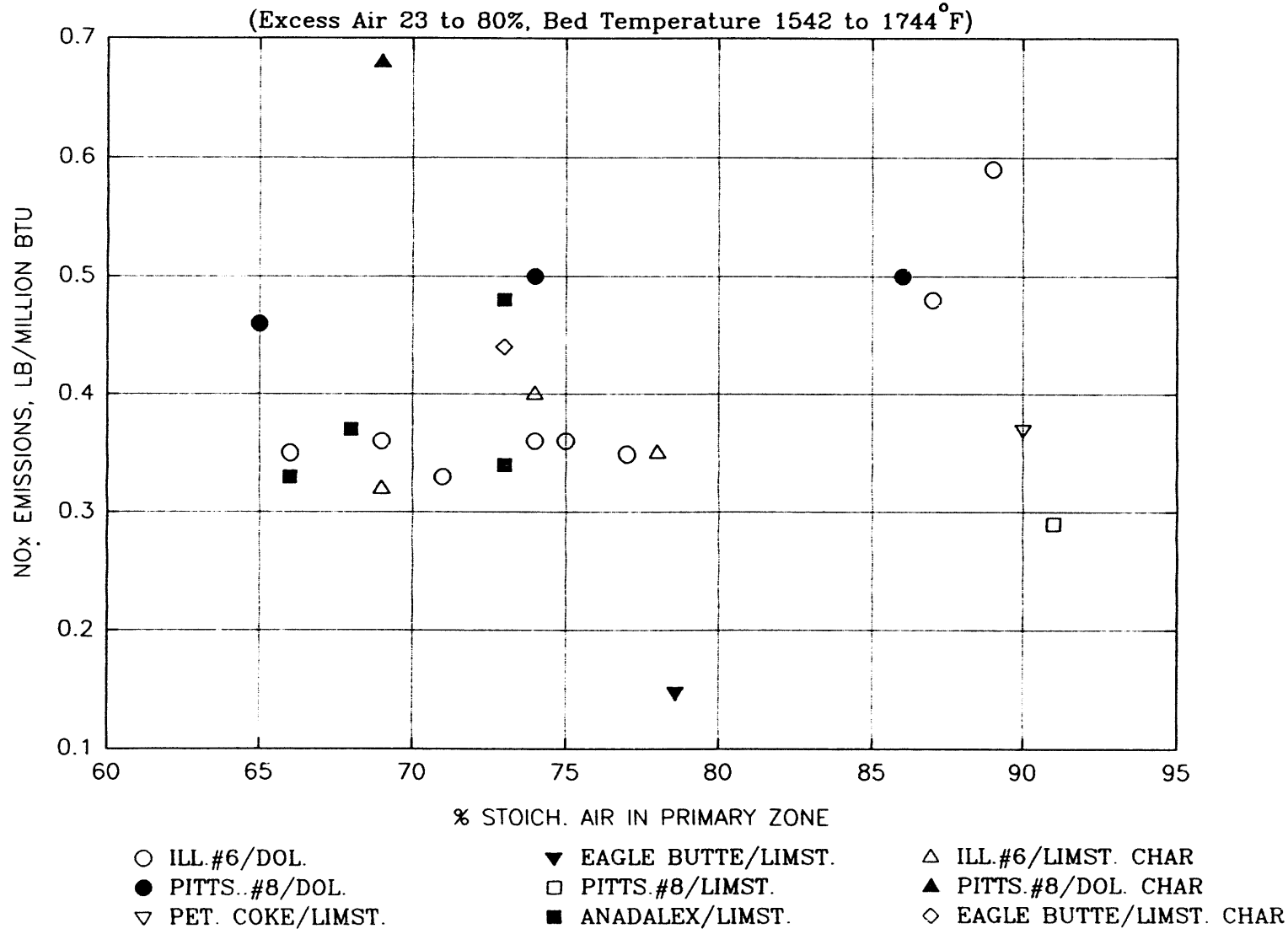

Figure 10. NO_x Emissions Vs. Primary Zone Stoichiometry

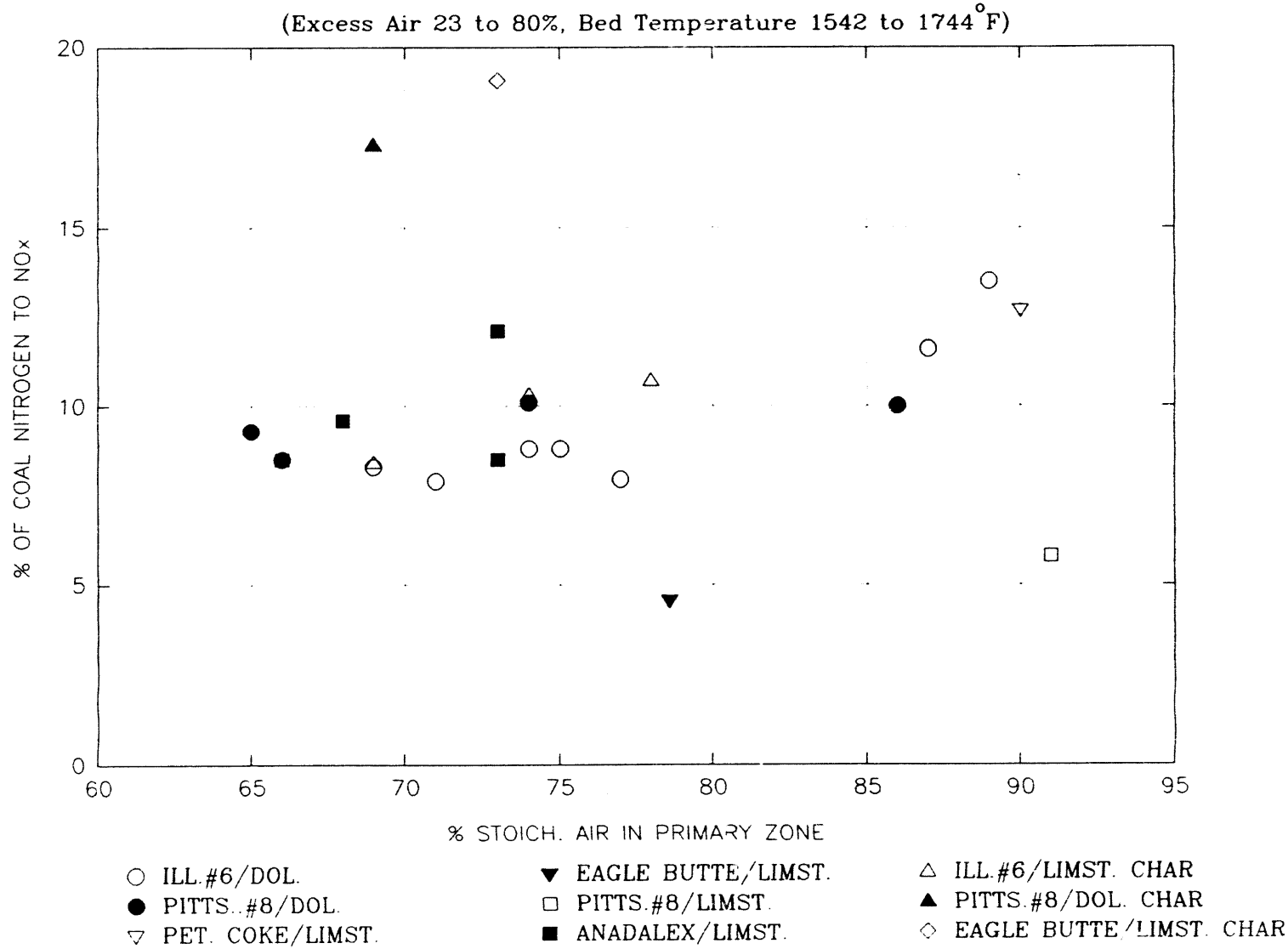

Figure 11. Nitrogen in Fuel Conversion to NO_x Vs. Primary Zone Stoichiometry

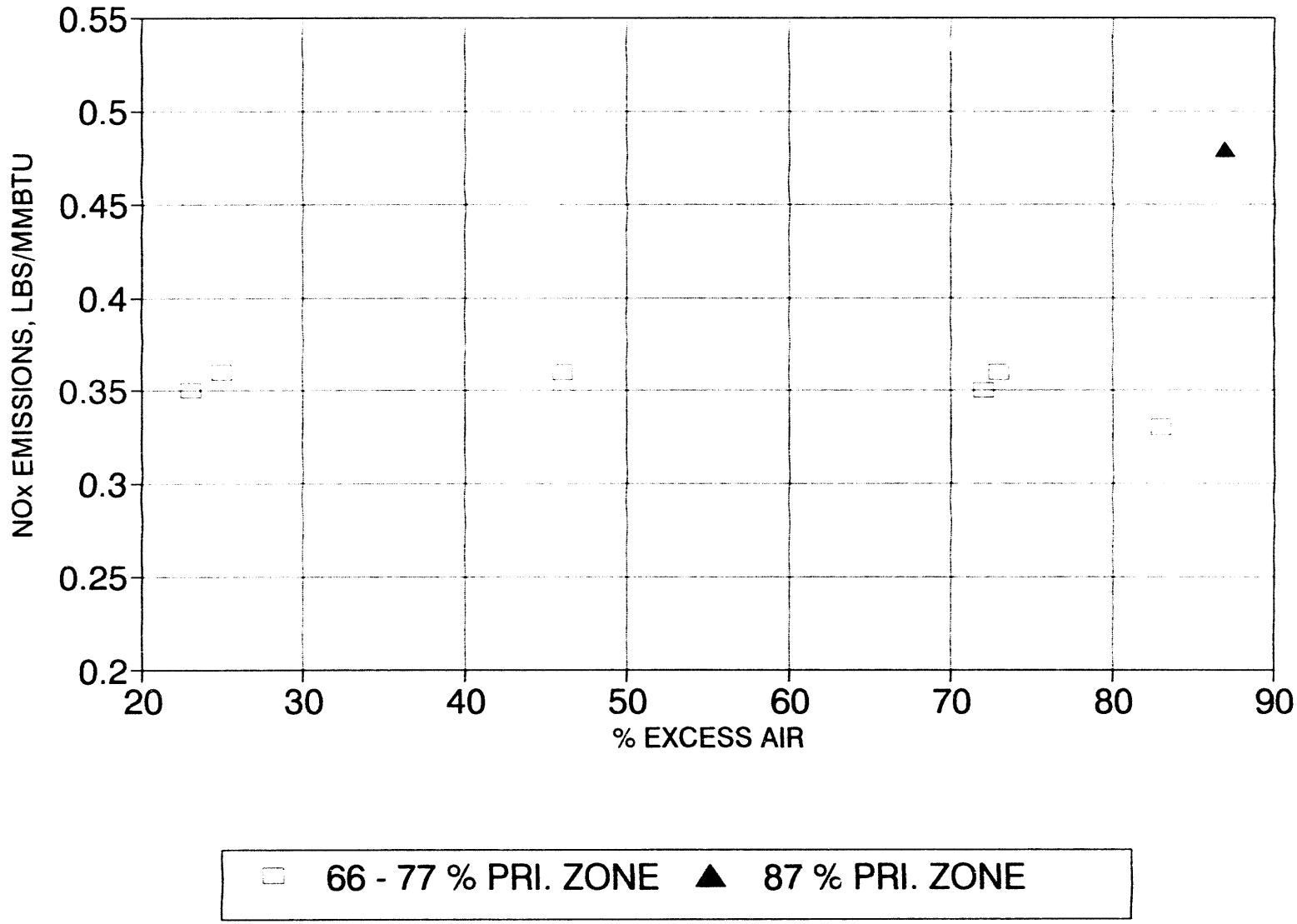

Figure 12. Effect of Excess Air on NO_x Emissions for Illinois No. 6

Table 4. PFB Char Sulfide Conversion Data—Run TRC-5

Description	Pittsburgh No. 8 (Dolomite)	Illinois No. 6 (Limestone)		
Char Rate, lb/h	200	190	195	165
Sulfide S, %	2.68	4.19	4.3	1.8
Sulfide S (in), lb/h	5.36	7.96	8.39	2.97
Filter Drain, lb/h	43	29	21	18
Sulfide S, %	1	1	1	1
Sulfide S, lb/h	0.43	0.29	0.21	0.18
Bed Drain, lb/h	21	12	8	8
Sulfide S %	1.82	1.96	2.88	1.71
Sulfide S, lb/h	0.38	0.23	0.23	0.14
Heat Exchanger Drain, lb/h	30	55	73	57
Sulfide S, %	1.7	1.61	1.62	1.89
Sulfide S, lb/h	0.51	0.89	1.91	1.08
Sulfide S (out), lb/h	1.32	1.41	2.35	1.4
Sulfide Conversion, %	75.4	82.3	72	52.9
Bed Temperature, °F	1627	1612	1626	1626
Primary Air Stoichiometry, %	69	78	74	69
Excess Air, %	51	68	39	41

Some of the major operating parameters affecting the level of sulfide in the system inventory include temperature, excess air, and solids circulation rate. In all the char tests, relatively low firing rates and solids circulation rates (< 10,000 lb/h) were used because of the limited supply of carbonizer chars. Higher circulation rates may have resulted in higher sulfide conversions for two major reasons. First, higher circulation rates increase the inventory residence time in the oxidizing region of the combustor secondary zone. Second, increased circulation also promotes particle attrition, which can break down the calcium sulfate shell of spent sorbent particles and allow further reaction of the exposed calcium sulfide layer. Higher solids circulation rates will be utilized in Phase 3 testing of the CPFBC to assess their effect on sulfide conversion.

The CPFBC tests were conducted in the multipurpose reactor vessel. Since this vessel was primarily designed to support the carbonizer test program, its short height resulted in a relatively short secondary/oxidizing zone. With secondary gas residence times being only approximately 1 second, NO_x and sulfide conversion levels were less than optimum. In Phase 3, a larger CPFBC will be used, and we expect both reduced NO_x levels and increased sulfide conversion levels.

PHASE 3 TEST PROGRAM

The carbonizer and CPFBC have been tested separately to ascertain their individual performance characteristics. In Phase 3, the multipurpose reactor will be returned to the bubbling bed carbonizer configuration, and a larger CPFBC will be installed to facilitate integrated performance tests. The CPFBC will have a 13-in. ID and, being 38 ft-3 in. tall, should exhibit improved NO_x and sulfide conversion performance. In addition, the dry lock-hopper pneumatic transport feed systems will be supplemented with a coal/water paste feed system to study the effect of a coal/water paste feed on carbonizer performance.

Construction of the Phase 3 pilot plant began on January 3, 1994, and shakedown/commissioning is expected to begin in July 1994.

REFERENCES

1. A. Robertson, et al. 1988. Second-Generation PFB Combustion Plant Performance and Economics. *1988 Seminar on Fluidized-Bed Combustion Technology for Utility Applications,* Palo Alto, CA.

2. A. Robertson, et al. 1993. Second-Generation PFBC Systems Research and Development—Phase 2, Best Efficiency Approach in Light of Current Data. *Proceedings of the Coal-Fired Power Systems 93—Advances in IGCC and PFBC Review Meeting*, Don Bonk (ed.), DOE/METC 93/6131.

3. A. Robertson, et al. 1989. Second-Generation Pressurized Fluidized Bed Combustion Plant: Research and Development Needs. Foster Wheeler Development Corporation, Livingston, NJ. Phase 1 Task 2 Report FWC/FWDC-TR-89/06 to the U.S. DOE under Contract DE-AC21-86MC21023.

4. A. Robertson, et al. 1989. Second-Generation Pressurized Fluidized Bed Combustion Plant: Integrated R&D Program Plan. Foster Wheeler Development Corporation, Livingston, NJ. Phase 1 Task 3 Report FWC/FWDC-

TR-89/08 to the U.S. DOE under Contract DE-AC21-86MC21023.

5. A. Robertson, et al. 1991. Carbonizer, CPFBC and Topping Combustor Testing for Second-Generation PFB Combustion Plants. *Proceedings of the 1991 International Conference on Fluidized Bed Combustion,* Vol. 1, E. J. Anthony (ed.), ASME, New York.

6. W. Domeracki, et al. 1993. Second-Generation PFBC Systems Research and Development. Phase 2 Topping Combustor Development *Proceedings of the Coal-Fired Power Systems 93,* Don Bonk (ed.), DOE/METC 93/6131.

7. W. Domeracki, et al. 1992. Second-Generation PFBC Systems Research and Development. *Proceedings of the Ninth Annual Coal-Fueled Heat Engines, Advanced Pressurized Fluidized Bed Combustion and Gas Stream Cleanup Systems Contractors Review Meeting,* DOE/METC 93/6129.

8. A. Robertson, et al. 1992. Second-Generation PFBC Systems Research and Development. *Proceedings of the Twelfth Annual Gasification and Gas Stream Cleanup Systems Contractors Review Meeting*, Vol. 1, DOE/METC 92/6128.

9. A. Robertson, et al., 1992. Initial Second-Generation PFBC Carbonizer Pilot Plant Test Results. *Proceedings of the Ninth Annual International Pittsburgh Coal Conference,* University of Pittsburgh.

10. J. Van Hook, A. Robertson, and D. Bonk. 1992. Carbon Conversions Measured in a Second-Generation PFB Pilot Plant Carbonizer. *Proceedings of the 12th International Conference on Fluidized Bed Combustion*, Vol. 2, L. N. Rubow (ed.), ASME, New York.

11. R. Newby, et al., 1992. Hot Gas Clean-up and Gas Turbine Aspects of an Advanced PFBC Power Plant. *Proceedings of the Ninth Annual Coal-Fueled Heat Engines, Advanced Pressurized Fluidized Bed Combustion and Gas Stream Cleanup Systems Contractors Review Meeting,* DOE/METC 93/6129.

12. K. M. Sellakumar, et al. 1993. Process Performance of Ahlstrom Pyroflow PCFB Pilot Plant. *Proceedings of the 12th International Conference on Fluidized Bed Combustion,* San Diego, pp. 423-429.

13. G. von Wedel, et al. 1993. Pressurized Fluidized Bed Combustion in a 15 MWth Test Facility—Bubbling and Circulating Experience and Future Development. *Proceedings of the 12th International Conference on Fluidized Bed Combustion,* San Diego, pp. 403-423.

4.3 Status of the Advanced PFBC at the Power Systems Development Facility

CONTRACT INFORMATION

Cooperative Agreement DE-FC21-90MC25140

Contractor
Southern Company Services, Inc.
P.O. Box 2625
Birmingham, AL 35202-2625
(205) 870-6011

Contractor Project Manager Randall E. Rush

Principal Investigators
Darrell L. Moore, Zia Haq, Timothy E. Pinkston, and P. Vimalchand, SCS
James D. McClung, FWDC
Michael T. Quandt, FWEC

METC Project Manager James R. Longanbach

Period of Performance June 16, 1993 to June 6, 1994

Schedule and Milestones

FY '94 & '95 Program Schedule

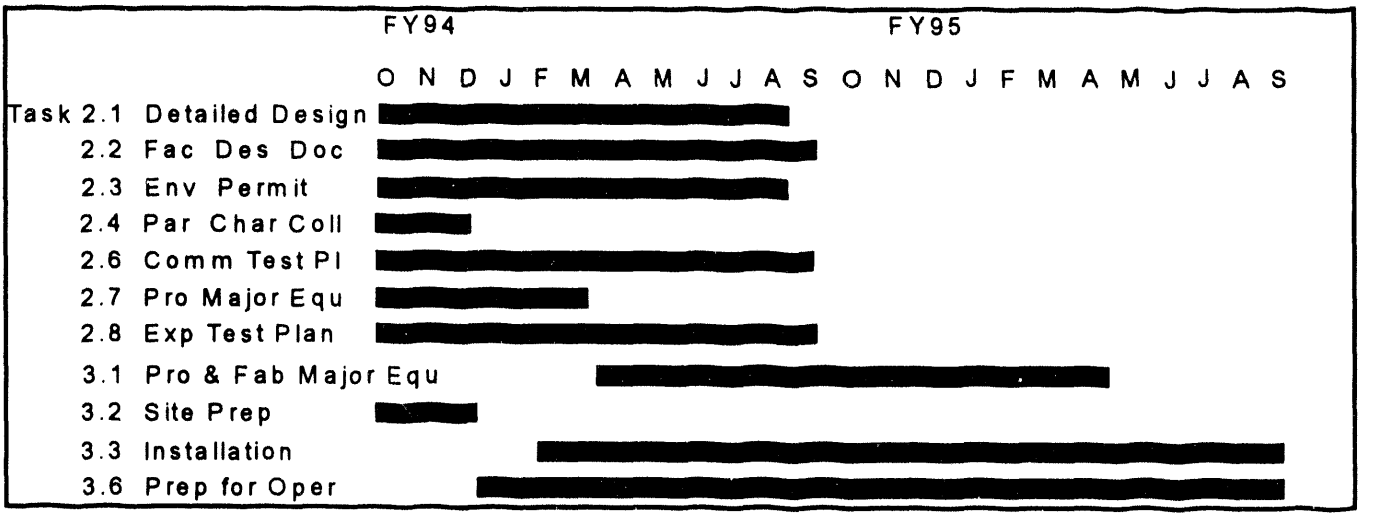

OBJECTIVES

The objectives of the Power Systems Development Facility (PSDF) are to develop advanced coal-fired power generation technologies through the testing and evaluation of hot gas cleanup systems and other major components at the pilot scale and to assess and demonstrate the performance of the components in an integrated mode of operation and at a component size easily scaled to commercial systems. This will entail the design, construction, installation, and use of a flexible test facility, which can operate under realistic gasification and combustion conditions. The major particulate control device issues to be addressed include the integration of the particulate control devices (PCDs) into coal utilization systems, on-line cleaning techniques, chemical and thermal degradation of components, fatigue or structural failures, blinding, collection efficiency as a function of particle size, and scale-up of particulate control systems to commercial size.

BACKGROUND INFORMATION

Coal is the primary fuel source for the generation of electricity in the United States. Due to The Southern Company's commitment to be a major supplier of electricity and the continued use of coal as a primary fuel source throughout the Southern electric system, Southern Company Services (SCS) has entered into a cooperative effort with the U. S. Department of Energy (DOE) Morgantown Energy Technology Center (METC) to develop a facility where component and system integration tests can be carried out for advanced coal-based power plants. The PSDF is being designed to be a flexible facility that will address the development of the PCDs and an advanced second-generation pressurized fluidized-bed combustion technology. A key element of the program is the testing and assessment of the technical issues for PCDs in an integrated test facility that directly supports DOE's Clean Coal program. Test conditions - such as gas pressure, temperature, and particulate loading - are variable over a range of values to facilitate the assessment of the PCDs.

PROJECT DESCRIPTION

The Power Systems Development Facility will be located 40 miles southeast of Birmingham, Alabama, at the Southern Company's Clean Coal Research Center in Wilsonville, Alabama. The PSDF location is adjacent to Alabama Power Company's 1,900 MW Plant Gaston. The PSDF utilizes the site of the decommissioned Selective Oil Agglomeration Facility in addition to a greenfield area west of the agglomeration site.

A simplified diagram of the PSDF is shown in Figure 1. The facility is divided into two trains, an advanced gasifier train for parametric testing of the PCDs and an Advanced Pressurized Fluidized Bed Combustion (APFBC) train for integration of the PCDs into a power generation system for longer term testing. The PSDF will be sized to feed 104 tons/day of Illinois No. 6 bituminous coal with a Powder River subbituminous coal as an alternate coal. Longview Limestone, which is obtained locally near Wilsonville, has been chosen as the sorbent for sulfur removal during the initial testing. The estimated project value is $150 million with 80 percent of the funding being provided by DOE and 20 percent being cost shared by industry.

The project team for the PSDF is comprised of DOE/METC, SCS, the Electric Power Research Institute (EPRI), The M. W. Kellogg Company (MWK), Foster Wheeler USA (FW), Westinghouse, Southern Research Institute (SRI), Industrial Filter & Pump, Combustion Power Company and Nolan Multimedia. SCS Research

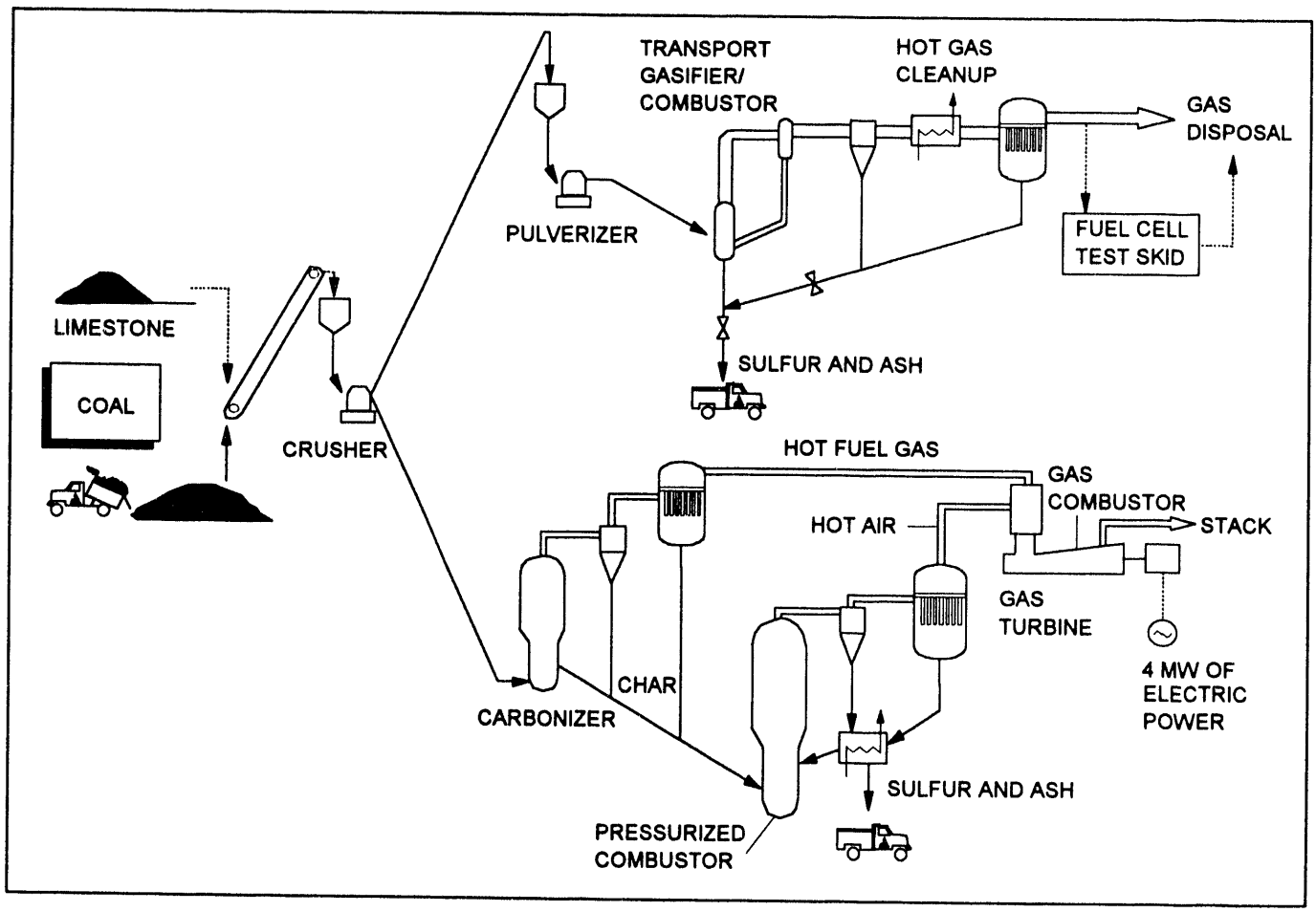

Figure 1. Simplified Diagram of the Power Systems Development Facility

and Environmental Affairs is responsible for overall project management and procurement of the PCDs. SCS Engineering is responsible for coordinating the design of the facility as well as plant layout and balance-of-plant design. SCS will provide construction management through the construction and installation phases of the project and will also be the facility operator, with a site staff of approximately 90.

The process engineering and detail design for the APFBC train is being done by FW. The APFBC system is designed to accommodate long-term testing of the PCDs and other system components, as well as evaluation of turbine system configurations. FW also has the lead in integrating a carbonizer and a circulating pressurized fluidized-bed combustor (CPFBC) with the topping combustor (supplied by Westinghouse Electric Corporation) and the gas turbine/air compressor (supplied by Allison Engine Company). MWK is providing the process engineering and detail design for the Advanced Gasifier train, which includes a transport reactor unit. The MWK transport train is designed to

The process engineering and detail design for the APFBC train is being done by FW. The APFBC system is designed to accommodate long-term testing of the PCDs and other system components, as well as evaluation of turbine

accommodate parametric testing of the PCDs and other system components. Southern Research Institute will conduct particulate and alkali sampling to evaluate PCD performance. In addition to providing cost sharing, EPRI is also providing technical guidance for the project.

FOSTER WHEELER'S APFBC SYSTEM

In the Foster Wheeler Second-Generation PFBC concept, coal is fed to a pressurized carbonizer, where it is converted to a low-Btu fuel gas and char. The relatively low carbon conversion in the carbonizer results in a simpler sulfur-removal process than is typically required in coal gasification processes. The char produced in the carbonizer is transferred to a CPFBC where it is subsequently burned. The carbonizer fuel gas and CPFBC flue gas are cleaned of particulates in separate ceramic filters, after which the fuel gas is fired in a specially designed topping combustor outside a high-temperature gas turbine using the CPFBC flue gas as the oxidant. Steam is raised and superheated in the fluidized bed heat exchanger (FBHE) with heat extracted from the CPFBC.

Most of the Second-Generation PFBC components will be tested in the Wilsonville configuration as an integrated system. An exception is that a steam turbine is not incorporated in the design. Instead, heat from the CPFBC will be rejected to condensate supplied by and returned to the balance of plant areas. A major component to be evaluated will be the pressurized FBHE integral to the CPFBC, to prove the use of an integrated heat exchanger to remove heat from the CPFBC under pressurized conditions. The APFBC plant will also provide the first full integration of the gas side of the power island, allowing operation of a gas turbine topping combustor with hot pressurized fuel gas from the carbonizer and hot pressurized flue gas from the CPFBC. Periodic examination of the gas turbine will demonstrate the merits of hot gas cleanup for the APFBC systems.

APFBC PROCESS DESIGN

A process flow diagram of the APFBC plant is shown in Figure 2. Dry coal and sorbent with steam are fed to the pressurized carbonizer, where the coal is converted to a low-Btu fuel gas and char. The design coal and sorbent are Illinois No. 6 and Longview limestone. Eagle Butte subbituminous coal is an alternate fuel. The plant is designed for a coal feed rate of about 5500 lb/hr, and a sorbent feed rate of about 1050 lb/hr. Provision has been made in the design to test the CPFBC under low excess-air conditions, feeding coal (either paste or dry) and sorbent directly to the CPFBC. Low-Btu fuel gas exits the top of the carbonizer and is cleaned of particulates in a single-stage cyclone and PCD (ceramic filter), and of alkalies in an alkali getter in series with the cyclone and PCD. Solids collected in the carbonizer cyclone and PCD combine in a surge hopper with char and reacted/unreacted sorbent exiting the side of the carbonizer, and are fed by gravity with pneumatic assist through an N-valve to the CPFBC, where the balance of carbon conversion occurs.

The flue gas from the CPFBC is also cleaned of particulates and alkali in a single-stage cyclone, PCD (ceramic filter), and alkali getter. Solids captured by the cyclone are fed to the FBHE via a J-valve for heat removal and returned to the CPFBC. Ash collected by the CPFBC PCD is cooled via a screw cooler and discharged through lock hoppers. Solids are removed from the CPFBC bottoms by an oxidizer/cooler, which fluidizes and cools the ash from 1600 to about 400°F, discharging bed ash to a depressurizing hopper, which operates at system pressure during charging and at atmospheric pressure during

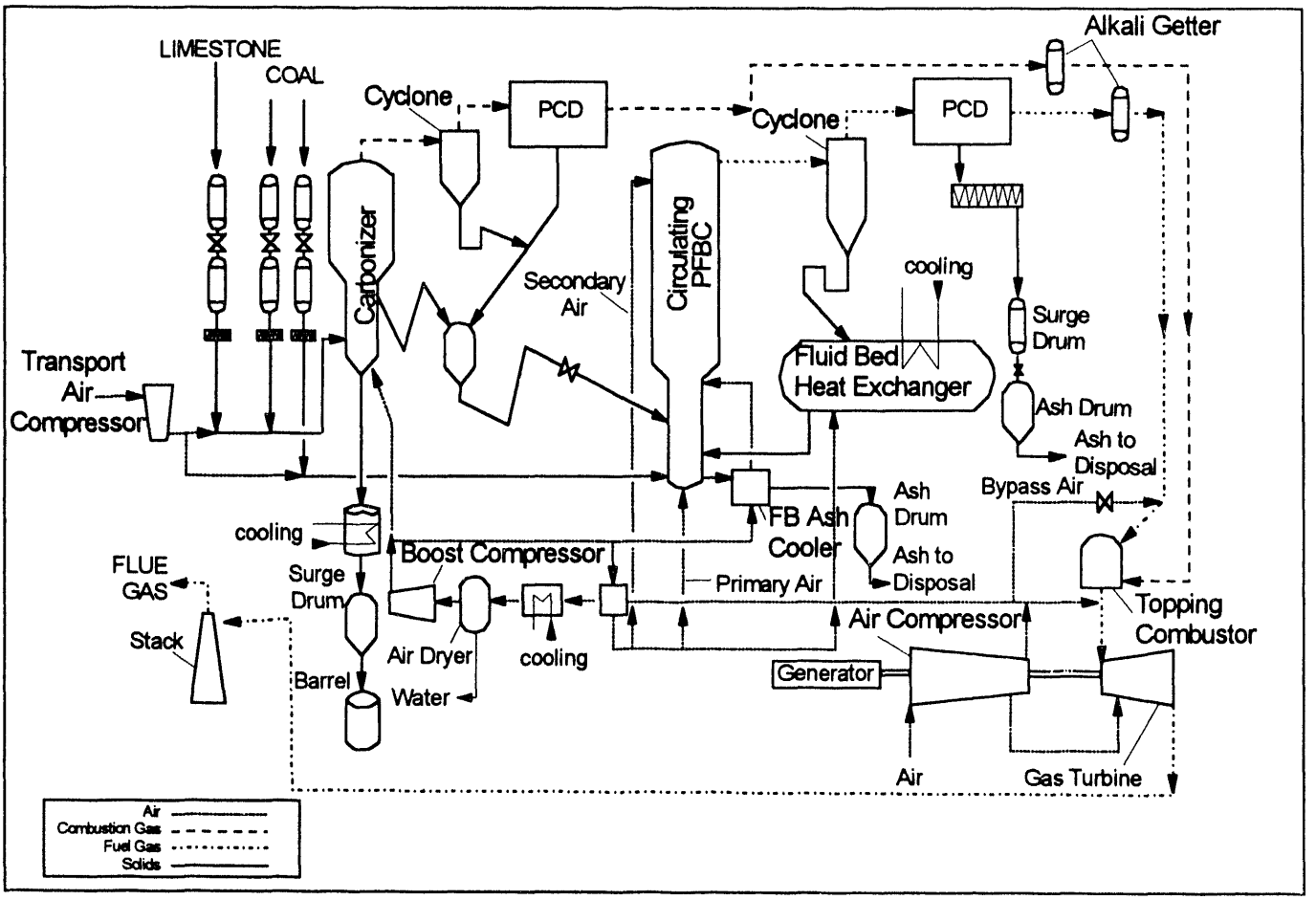

Figure 2. Advanced Pressurized Fluidized-Bed Combustion

discharge. The cleaned fuel gas from the carbonizer is burned in a topping combustor, utilizing clean flue gas from the CPFBC as the oxidant. The hot topping combustor exhaust is expanded in the gas turbine driving the air compressor and generator, and discharged to atmosphere via a stack.

Carbonizer

The carbonizer is a spouting fluidized bed without heat-transfer surface. The 175 psia/1700°F carbonizer is a vertical, approximately 48 ft. in height, refractory-lined vessel comprising the bed section (lower part - I.D. approximately 3 ft.) and a disengagement section (upper part - I.D. approximately 4 ft.). Coal and sorbent are fed into the carbonizer pneumatically under pressure, entering axially through the bottom. The carbonizer has been provided with additional nozzles to allow for alternately feeding coal and sorbent radially at varied in-bed and above-bed elevations. Provision has also been made in the design to feed a coal/water paste. Bed temperature is maintained by the air-to-coal ratio.

Circulating Pressurized Fluidized Bed Combustor (CPFBC)

The CPFBC, shown in Figure 3, is a refractory-lined vessel with a 33 in. I.D. upper section. The vessel is lined with two-layer refractory, 4 in. of light castable refractory and 4.8 in. of hard-face refractory for erosion resistance. The main functions of the CPFBC are char combustion and conversion of CaS in the char to $CaSO_4$, while combining effective capture of SO_2 to achieve >95 percent sulfur removal with reduced NO_x formation through staged combustion. The major operating parameters controlling these functions are:

- Bed Temperature - Based on bubbling bed PFBC technology, bed temperature is limited to about 1600°F. A higher bed temperature improves carbon conversion, but also results in higher alkali release, which increases the potential for bed agglomeration and corrosion of downstream components.

- Ca/S Molar Ratio - A Ca/S molar ratio of 2 is assumed to attain 95 percent sulfur capture with Illinois No. 6 coal and Longview limestone. This assumption will be verified during operation.

- Bed Stoichiometry - To control NO_x formation, the combustion process is staged. The lower part of the CPFBC operates in a reducing mode with approximately 70 percent stoichiometry, while the upper portion operates in an oxidizing mode.

The CPFBC bed temperature is controlled by the amount of heat-transfer surface in the unit, and the load to the gas turbine is controlled by the fuel feed rate. The unit has been designed so it can operate between 20 and 300 percent excess air to test both first-generation and advanced PFBC concepts. Primary air is fed into the CPFBC from the plenum below the grid. Nozzles distribute the air flow evenly for optimum air/solids mixing in

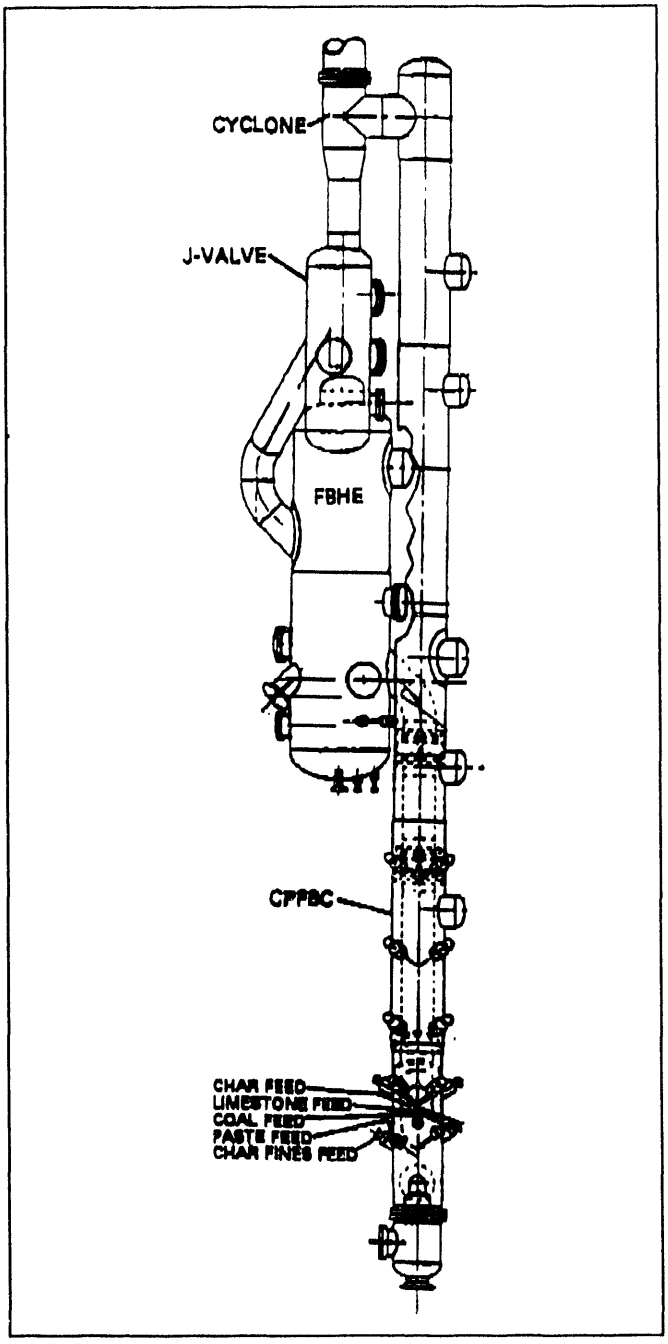

Figure 3. Circulating Pressurized Fluidized-Bed Combustor (CPFBC)

the CPFBC. Secondary air to the CPFBC can be fed above the grid at four different elevations, and can be adjusted between the elevations to determine the best emissions control and carbon burnup. Hot flue gas exits at the top of the vessel.

Oxidizer/Cooler

Solids are withdrawn from the CPFBC bottoms via an oxidizer/cooler, which assures sulfation of the CPFBC bottoms ash and cools the ash from 1500 to 400°F. Drawoff from this system may be either on a batch basis or a continuous basis. The design also provides for two bed ash drain locations, with the higher elevation drain for continuous operation.

Fluidized Bed Heat Exchanger (FBHE)

The FBHE is a refractory-lined vessel containing four cells - an inlet, an outlet, and two heat exchanger cells. The FBHE receives recycled ash from the CPFBC cyclone/J-valve. The flow of recycled material to the FBHE will be dependent on the load of the unit (fuel flow). Material enters the inlet cell, underfeeds to the heat exchanger cells, and discharges through the outlet cell back to the CPFBC. Heat is removed from the FBHE by a once-through condensate system. The FBHE is designed to allow the heat duty to be changed for different case studies in the test plan. This FBHE design has been tested and commercially accepted in CFB designs.

High-Temperature Gas Cleaning (HTGC)

The carbonizer and CPFBC have independent HTGC systems consisting of three cleaning stages in series - a cyclone, PCD, and alkali-removal system. The cyclone design is based on the use of a single, standard cyclone stage to remove the bulk of the relatively coarse particles from the gas streams and protect the downstream PCD from process upsets.

The PCDs are used for final particulate removal. An Industrial Filter & Pump Mfg. Co. low-density fiber ceramic candle design will be used as the initial carbonizer PCD. The refractory-lined filter vessel has a 60 in. diameter and contains 78 candles arranged in six groups of 13 each for jet pulse cleaning. The 54 mm O.D. x 1.5 m long candles are of an aluminosilicate fiber construction (with binders of silica and alumina). The monolithic flared flange and end cap of the candle are of densified ceramic fiber construction, as are the tubesheet and the candle retainer plate. The six pie-shaped jet pulse plenums are constructed of a high-alumina castable material for maximum strength. For effective cleaning, individual jet pulse nozzles are provided to each candle. An Enhancer™ consisting of an orifice-type device at the outlet of the candle increases jet pulse intensity and also serves as a fail-safe plug in case of a candle failure. A back-pulse tank, designed for 1500 psig, will provide back-pulse gas to the filter.

The CPFBC PCD will be a Westinghouse ceramic candle filter consisting of a refractory-lined 10.2 ft. O.D. pressure vessel containing six arrays ("clusters") of 60 mm O.D. x 1.5 m long candle elements. The individual clusters are supported from a common high-alloy tubesheet and expansion assembly that spans the pressure vessel and divides it into the "clean" and "dirty" gas sides. The Westinghouse cluster arrays are formed by attaching individual filter elements to a common plenum and discharge pipe. The arrays are cleaned from a single pulse nozzle source. For efficient packaging, several of the individual plenum assemblies are arranged vertically from a common support structure forming a filter cluster. The cluster concept permits maintenance and replacement of individual filter elements and provides a modular approach to scale-up.

The last stage, alkali removal, captures sodium and potassium vapor-phase species. The

alkali-removal systems are simple, packed beds of emathlite pellets contained in vertical, refractory-lined pressure vessels. The emathlite material reacts irreversibly with sodium and potassium vapor-phase compounds at high temperature. Nozzles are provided for gas inlet and outlet at the top and bottom of the vessels, respectively, as well as for pellet loading and unloading. The alkali getter in the CPFBC flue gas stream is being installed as a safety measure since the alkali content expected in the CPFBC flue gas is lower than the turbine tolerance. Following particulate and alkali removal, fuel gas and flue gas are conveyed to the topping combustor by refractory-lined piping. A metallic lining between the alkali getters and topping combustor isolates the refractory and prevents any spalled refractory from entering the cleaned gas streams.

The HTGC systems are designed to achieve sufficient levels of particle and alkali removal to protect the gas turbine from erosion, deposition, and corrosion damage as well as satisfy plant emissions standards. The HTGC systems must meet the following performance levels:

- Achieve particle-removal efficiency to meet both environmental and turbine protection standards.
- Meet performance standards - outlet particulate loadings less than 20 ppm(w) with no more than 1 wt% particles exceeding 10 μm and no more than 10 wt% exceeding 5 μm.
- Control alkali content (total sodium plus potassium vapor) to less than 50 ppb(w).
- Limit the maximum pressure drop across each HTGC train to 10 psi.
- Limit the temperature drop to less than 100°F across the carbonizer HTGC train and to less than 10°F across the CPFBC train.

Topping Combustor

The topping combustor assembly consists of carbon steel spools which form the pressure vessel. A concentric, stainless steel cylinder inside each steel spool piece provides the temperature boundary. A layer of insulation fills the void between the concentric cylinders. The multiannular swirl burner (MASB) is constructed from an Inconel or Hastelloy-type alloy with a diameter of about 18 in., which is a commercial size. Flue gas from the CPFBC enters the topping combustor at approximately 150 psia and 1400°F. About 11,600 lb/hr of carbonizer fuel gas, entering at approximately 1650°F, is burned in the MASB to produce an exhaust gas temperature of 2350°F, which is the optimum firing temperature for a commercial plant at this carbonizer temperature. The gas is cooled to about 1975°F with compressor bypass air before entering the gas turbine.

Gas Turbine

The gas turbine generator set is a modified Allison 501-KB5 gas turbine, which drives a synchronous generator through a speed-reducing gearbox. The hot exhaust gas from the topping combustor is expanded through the gas turbine, powering both the electric generator and the air compressor. Exhaust gases from the gas turbine are discharged hot through a stack. Air from the compressor supplies all APFBC plant process air requirements. Approximately 8 percent of the air flow is used for gas turbine blade cooling and approximately 22 percent for tempering the topping combustor exhaust gas from 2350 to 1975°F before it enters the turbine. Most of the

compressed air, approximately 63 percent, is used in the CPFBC system for fluidizing the FBHE and as primary and secondary air. The remaining 7 percent provides air to the carbonizer.

CHANGES IN PSDF APFBC DESIGN

Carbonizer Operation and Char Flow

The carbonizer train design has been reviewed to ensure that operation up to 1800°F is possible. The PSDF design originally removed char from the bottom of the carbonizer, cooling the char via a screw cooler, and reducing oversized particles with a delumper. Particles were then dumped into a holding vessel and pneumatically conveyed to the CPFBC. This design has been replaced with a system which withdraws char from a bed overflow nozzle from the side of the carbonizer, instead of withdrawing from the bottom, so hot char will feed directly to the PFBC by gravity and differential pressure. In addition, the carbonizer bottoms has been modified to allow occasional batchwise rejection of oversized char through a double pipe heat exchanger, where cooling is effected by the heating of low pressure steam, to a lock hopper for discharge. Nitrogen is introduced below the heat exchanger to keep the exchanger clear and sweep fuel gas from the discharged solids. These changes should improve reliability of the plant, reduce heat loss and maintenance, and decrease capital equipment costs.

CPFBC Solids Withdrawal

Earlier PSDF design provided for ash removal from the CPFBC primarily from the FBHE and from overhead (PCD) fly ash with incidental removal from the bottom of the CPFBC. Alternate operating lock hoppers with combined feeds from both the FBHE and the CPFBC PCD were provided for continuous removal of the ash. Because the design required multiple, relatively expensive and potentially problematic ash coolers and other factors, this design was abandoned in favor of a more simplified design. Bed ash removal from the FBHE was deleted, and bed ash removal and cooling is now accomplished at the bottom of the CPFBC. Continuous flyash removal and cooling below the PCD using a screw cooler, surge drum and lock hopper was retained. Solids are withdrawn from the CPFBC bottoms via an oxidizer/cooler, which has been added to assure sulfation of the CPFBC bottoms ash and cool the ash from 1600 to 400°F. In addition, there is an increase in fuel burnup efficiency and limestone utilization, as well as classifying of the ash particles, which results in longer residence time for small particles and removal of very coarse particles from the system.

Full-stream Booster Compressor

A full-stream booster compressor has been incorporated into the PSDF design to increase the air pressure to both the carbonizer and the CPFBC. This was effected due to the thrust bearing limitation of the Allison gas turbine. Due to the type (aircraft derivative) and size of the gas turbine employed in the APFBC plant, the turbomachinery was not sufficiently robust to accommodate the pressure drop of the plant without significant rework. Conversely, a more "rugged" gas turbine would reduce the turbine efficiency in the simple cycle mode (propane firing). Consequently, it was decided to boost the air pressure in the CPFBC process flow stream in addition to the carbonzier process flow stream to reduce the overall system pressure drop. Another advantage of the full-stream booster compressor is that it can be used for a more rapid cool down and heat up of the CPFBC. Heat exchange between the hot air flowing to the booster compressor suction and the booster compressor discharge gas feed to the CPFBC was provided to minimize the effect on the heat and material balance of the unit.

Transport Air Compressor

Pneumatic feed systems are pressure sensitive and with minimum pressure drop through the feed system, minor surges in pressure have a significant effect on the operation of the system. Review of pilot plant operation indicated multiple cases where pressure surges led to feed system upsets which in turn led to thermal excursions and in some cases to plant shutdown. As a result, the Wilsonville APFBC design was revised to provide more conventional solid to gas loading rates and respectively higher pressure drop, necessitating the need for a transport air compressor. Since pneumatic transport systems prefer dry air it was decided to use plant instrument air as the source of transport air. The instrument air will be boosted by the transport air compressor to desired pressures, a less expensive option than boosting some of the flow from the full-stream booster compressor.

Burners

An additional startup burner was added to the Combustor because the original single burner resulted in an excessive pressure differential across the grate in the Combustor which would have required a redesign of the grid floor. Also, the above Grid Burner will help the Combustor and cyclone heat up evenly during startup. In addition, a startup burner has been added to the oxidizer cooler.

Other Design Changes Under Consideration

A simplified char transfer system is being evaluated, which consists of separate down legs from the carbonizer, carbonizer cyclone, and carbonizer PCD feeding a common up leg, and final down leg to the CPFBC. Aeration gas would be supplied to the bottom of the up leg as well as to various alternative positions on each down leg.

Deletion of the fugitive dust baghouse and blower is being reviewed. This system currently services the coal and limestone surge and pressurization drums, the ash depressurization drums, and the oversized char drum. If the system is deleted, the fugitive dust collection system would be revised to vent the coal and sorbent surge and feed drums to their respective feed hoppers, which are equipped with filters. The ash depressurization drums would vent to the ash transfer system, and ultimately to the balance-of-plant storage silo. A new filter would be installed on the oversized char drum.

Particulate Sampling

Past hot particulate removal demonstration projects have shown that particulate size distribution and morphology determine particle penetration and energy loss (pressure drop), and play an important role in the durability of filtration devices. Particle mass loading, size distribution, morphology, and levels of alkali metals, both in particulates and in the vapor phase, play distinct roles in subjecting turbine components to erosion and corrosion. Characterization of alkali vapor is also needed to quantify turbine exposure and to assess the performance of the alkali getter beds that will be installed to protect the topping combustor and gas turbine. Therefore, on-line sampling for both particulates and alkali species will be conducted at the PSDF. Particulate sampling will be done at the inlet and outlet of the PCDs. Alkali sampling will be done at the inlet and outlet of the alkali getter beds for the APFBC system.

Project Status

Currently, the PSDF schedule consists of a 22 month design period overlapping with a 24 month installation period to better accommodate the design and construction of the facility.

Detailed design for the base facility commenced in July 1992 and construction began in September 1993. At present, the FW APFBC system design and the PCD designs are nominally 50% complete. Procurement of long-lead equipment is in progress. Site grading and preparation are complete and steel erection will start in July. The construction phase will be followed by three months of shakedown and an additional three months of characterization test runs. The commissioning of the test facility will be completed by the third quarter of 1995 and will be followed by a two year operations period.

Summary

The Power Systems Development Facility offers a unique opportunity for government and the utility industry to focus on the developmental needs of advanced coal-based power generation systems. The critical need in advanced power generation processes is to improve the reliability and performance of hot particulate removal systems. This continues to be the primary focus for the PSDF. The testing and operation of the second-generation APFBC system at the PSDF will generate data and operational experience that will be helpful in the evaluation of newer process and equipment design and concepts. The facility will be instrumental in testing and advancing the PFBC technology. The PSDF is an investment in the development of more efficient, cost effective, and environmentally sound advanced coal-based power plants. The results should be a reduction or stabilization in the cost of electricity and a reduction in environmental emissions for new coal-based power plants.

ACKNOWLEDGEMENTS

We would like to acknowledge Thomas J. Boyd, EPRI Project Manager; C. J. Crumm, FWUSA Project Manager; Robert E. Froehlich, FWUSA Sr. Process Supervisor; and George H. Griswold, SCS Engineering Project Manager, for their contributions to the project.

Session 5

Advanced Filter Systems

5.1 Status of the Morgantown Energy Technology Center's Particulate Cleanup Program -- Enabling Technology for Advanced Coal-Based Power Systems

Richard A. Dennis
Morgantown Energy Technology Center

Advanced coal-based power systems, such as integrated gasification and pressurized fluidized-bed combustion (PFBC), require particulate removal at high temperatures and high pressure (HTHP) to achieve their high efficiencies. In this enabling role, HTHP cleanup systems must provide particulate removal efficiencies greater than 99 percent, with high availability, and while operating under adverse conditions. These conditions include corrosive gases, thermal fatigue, and thermal transients. To facilitate the development of advanced coal-based power systems, the Morgantown Energy Technology Center (METC) has assembled a Particulate Cleanup Program, which conducts technology demonstration projects and applied research to address the adverse filtration conditions and filter system issues, as well as the future performance demands of these systems. A brief status of the program follows.

A look at past accomplishments will provide a good perspective for evaluating the present status of the METC particulate cleanup program. For discussion purposes, the past is viewed in a 10-year time frame where accomplishments of others establish bench marks. These bench marks can indicate the relative progress of the program.

Between 1985 and 1992, the Grimethorpe PFBC Establishment operated the largest ceramic filter system in the world on the exhaust from a nominal 10 megawatt-thermal (MW_{th}) PFBC (1). The filter system utilized up to 130 1.5-meter long, clay bonded silicon carbide candle filters suspended from a single tube sheet. Actual gas-flow rates were nominally 1.085 cubic meters per second. During several test campaigns 2300 hours of definitive operation were obtained. During this test program the limited filter failures were typically a result of a faulty filter hold-down and sealing assembly or failure of filter cleaning pulse valves. Candle filter elements used in these tests showed a significant loss in strength, which was attributed to high thermal stresses as a result of back-pulse cleaning with cold gas.

From 1986 to 1989, HTHP particulate control tests were conducted at the Department of Energy's New York University PFBC Test Facility. In this program three particulate control devices were tested, including an electrostatic precipitator (ESP), a granular bed filter (2), and cross flow filter systems (3). Gas-flow rates were nominally 0.5663 actual cubic meters per second from the 5-MW_{th} PFBC. Two-hundred hours of testing was planned for each device. Test results indicated delamination and sealing problems with the cross flow filter, voltage discharge problems with the ESP, and control and erosion problems with the granular bed filter.

During 1987 and 1988, HTHP particulate cleanup tests were conducted at the KRW fluidized-bed gasifier with ceramic candle filters (4). During this test period, over 650 hours of exposure were obtained on the clay bonded silicon carbide filter element. The filter vessel housed 33 1-meter long filter elements from a

single tube sheet and filtered up to 0.160 actual cubic meters per second of dirty gas. During this test period, filter failure was attributed to system upsets and the candle filter hold-down assembly.

During 1992, eleven separate filter tests were conducted with the Texaco slagging entrained-flow gasifier located at Montebello, California (5). A total of 678 hours of test time was accumulated, with flow rates to the filter vessel ranging between 0.0472 and 0.0755 actual cubic meters per second. Tests were split between either four or eight cross-flow filters or nineteen candle filters. Both clay bonded silicon carbide and alumina/mullite candle filters were used. Candle filters were suspended from a single tube sheet. When the cross-flow filters were used, they were mounted to plenums and then suspended from a single tube sheet. Significant strength reduction was measured in all candle filter materials. The cross-flow filter showed signs of delamination.

In summary, past tests, both under PFBC and IGCC conditions, have been conducted at the pilot and sub-pilot scale. These tests clearly established the ability of the proposed technology to meet particulate removal, pressure drop, and heat loss requirements for the advanced coal-based power systems. It was through the success of these tests that the technical issues facing this technology were firmly established. In general, test results indicated a significant reduction in strength of both the clay bonded silicon carbide and alumina/mullite ceramic filter materials; a need for a better filter hold-down and sealing assembly; a need for longer and more continuous test times; the importance of coal, sorbent, and coal conversion process on dust cake performance; and a need to test and evaluate filter systems that exhibit commercial-scale features. These results established the issues and questions that needed to be addressed in order to bring HTHP particulate cleanup technology to fruition.

The present status of the particulate cleanup program is best ascertained by reading the papers presented in the Advanced Filter Systems and Filter Technical Issues sections of this conference's proceedings. These papers will show that significant accomplishments have been made towards the commercialization of HTHP particulate filter systems by addressing the technical issues developed over the past several years. Briefly these accomplishments include the long duration testing of candle filter systems, which represent commercial-scale subassemblies; the demonstrated ability to clean multiple filter elements from a single blow back nozzle; the development of a candle filter fail-safe and thermal regenerator device; an improved understanding of dust cake behavior; a better understanding of candle filter strength degradation mechanisms; the advancement of alternate particulate control technologies; and the utilization of improved materials for ceramic filters. These advances will minimize the risk of future demonstration-scale testing of HTHP particulate control systems.

Our vision for the future is being shaped by our best made plans from the past and present. These plans include the demonstration of particulate cleanup technology at Southern Company Service's Power Systems Development Facility and the Clean Coal Demonstration Projects. The near-term aspect of these projects has set the cadence towards our future goals. The success of development and testing over the next 2 years will be critical to achieving these goals.

REFERENCES

1. Burnard, G., Leitch, A., Stringer, J., Clark, R., and Holbrow, P., "Operation and Performance of the EPRI Hot Gas Filter at Grimethorpe PFBC Establishment: 1987-1992," 2nd International Symposium on Gas Cleaning at High Temperatures, University of Surrey, Gilford U.K., September 1993.

2. Zakkay, V. Sellakumar, K., Dellefield, R., and Bossart, S., "Advanced Particle Control Research at the New York University Coal-Fired Pressurized Fluidized-Bed Combustion Facility," Electric Power Research Institute FBC Seminar Palo Alto, California, May 1988.

3. Lippert, T., Haldipour, G., Smeltzer, E., and Meyer, J., *Performance Evaluation of a Cross Flow Filter on a Subpilot-Scale Pressurized Fluidized Bed Combustor*, Final Report DE-AC21-85MC22136, NTIS/DE90000477, Springfield, Va.: National Technical Information Service.

4. Haldipour, G., Schmidt, D., and Smith, K., *A 50-Month Gasifier Mechanistic Study and Downstream Unit Process Development Program for the Pressurized Ash-Agglomerating Fluidized-Bed Gasification System*, Volumes I and II, Final Report DE-AC21-84MC21063, NTIS/DE89011704, Springfield, Va.: National Technical Information Service.

5. Lippert, T., Alvin, M., Smeltzer, E., Bachovochin, D., and Meyer, J., *Subpilot Scale Gasifier Evaluation of Ceramic Cross Flow Filter*, Final Report DE-AC21-88MC24021, NTIS/DE89011704, Springfield, Va.: National Technical Information Service.

RDENNI\1:940781B

5.2 Potential Industry Use of Continuous Fiber Ceramic Composites

Jill Jonkouski
DOE Chicago Operations Office

ABSTRACT

This presentation will introduce the Continuous Fiber Ceramic Composite (CFCC) Program, whose goal is to develop, in industry, the primary processing methods for the reliable and cost-effective fabrication of CFCC components for industrial applications. CFCC components are expected to be used in gas turbines, heat exchangers, radiant burners, and hot gas filters. The main focus of the presentation will be on how CFCC components in industry will benefit the environment and the economy, and the technical progress made by team members to date. The presentation will also cover the program strategies, status, and structure. The last section will discuss the impact of CFCC components on the market.

5.3 Ceramic Fiber Ceramic Matrix Filter Development

CONTRACT INFORMATION

Contract Numbers

DE-AC05-84OR21400 (ORNL)
Field Work Proposal FEAA028

93X-SB482C (3M)

Contractors

Oak Ridge National Laboratory
Metals and Ceramics Division
1 Bethel Valley Road; P.O. Box 2008
Oak Ridge, TN 37831-6084
615-574-4572

3M Company
3M Center
St. Paul, MN 55144-1000
612-733-2564

Contractor Project Managers

Roddie R. Judkins (ORNL)
Melvin A. Leitheiser (3M)

Principal Investigators

Roddie R. Judkins (ORNL)
David P. Stinton (ORNL)
Robert G. Smith (3M)
Edward M. Fischer (3M)

HQ Program Manager

James P. Carr

METC Project Manager

Richard A. Dennis

Period of Performance

October 1986 to Present

Schedule and Milestones

FY 1993/94 Program Schedule

	M	A	M	J	J	A	S	O	N	D	J
1st Filter Tests	———										
Design Modifications			———								
Filter Fabrication							———				
2nd Filter Test										———	

OBJECTIVES

The objectives of this project were to develop a novel type of candle filter based on a ceramic fiber-ceramic matrix composite material, and to extend the development to full-size, 60-mm OD by 1-meter-long candle filters. The goal is to develop a ceramic filter suitable for use in a variety of fossil energy system environments such as integrated coal gasification combined cycles (IGCC), pressurized fluidized-bed combustion (PFBC), and other advanced coal combustion environments. Further, the ceramic fiber ceramic matrix composite filter, hereinafter referred to as the ceramic composite filter, was to be inherently crack resistant, a property not found in conventional monolithic ceramic candle filters, such as those fabricated from clay-bonded silicon carbide. Finally, the adequacy of the filters in the fossil energy system environments is to be proven through simulated and in-plant tests.

BACKGROUND INFORMATION

The successful development and deployment of several advanced coal-fueled gas turbine technologies depend greatly on the ability to clean fuel or combustion gas streams of particulates prior to these gases being passed through the turbines. These technologies include IGCC, PFBC, and direct coal-fired turbines. Rigid ceramic filters of a variety of designs are either commercially available or under development in programs around the world. Several filter designs are in use or are being developed. The most popular is the candle filter, which resembles a laboratory test tube in having one end closed and a flanged opening at the other.

Rigid ceramic candle filters are currently being developed to remove particulates from gas streams being introduced into hot-gas turbines. Filter systems large enough to handle the volume of gases for typical IGCC or PFBC systems will be extremely expensive. For example, a 300-MW(e) oxygen-blown IGCC power plant has a gas flow of about 8 m^3/s. In order to filter such a large volume of gas, approximately 130 m^2 of filter area or 1660 candle filters would be required. An air-blown gasifier would generate twice the gas flow and, therefore, require approximately 3300 candle filters. PFBC systems generate five times the volume of gas of an air-blown gasifier and would require 16,000 candle filters. Assuming candle filters could be purchased in large quantities for $300 to $600 each, the cost of one set of candles would range from $0.5 to $1.0 million for an oxygen-blown gasifier and from $5 to 2$10 million for a PFBC.[1]

Many different materials – oxides, nonoxides, and mixed – may be used for any of these ceramic filter types. The most popular oxide ceramics include alumina/mullite, cordierite, aluminosilicate foam/fibers, clay-bonded alumina, fireclay, and continuous fiber ceramic composites produced by chemical vapor infiltration (CVI). Nonoxide ceramics include clay-bonded silicon carbide, sintered silicon nitride, reaction-bonded silicon nitride, recrystallized silicon carbide, and CVI silicon carbide fiber-reinforced composite filters. Fabric filter materials include various grades of silica-alumina-boria, alumina-silica, and silicon carbide-silica. Most commercial and near-commercial ceramic filters are made of bonded ceramics. Several advanced concepts are being investigated and developed, including a ceramic composite filter developed at Oak Ridge National Laboratory (ORNL), which is being scaled to full-size by 3M Company of St. Paul, Minnesota. Ceramic composites have several properties that make them attractive for this application. They do not fail catastrophically as do monolithic ceramics; equivalent strengths can be achieved with much thinner and lighter

structures; they have greater mechanical and thermal shock resistance; and they have greater resistance to chemical degradation compared to clay-bonded materials. In addition, they retain other properties of ceramics such as high strength (due to a silicon carbide matrix); refractoriness; good abrasion and corrosion resistance; and good oxidation resistance. Figure 1 provides a comparison of the failure characteristics of monolithic and fiber-reinforced composite ceramics.

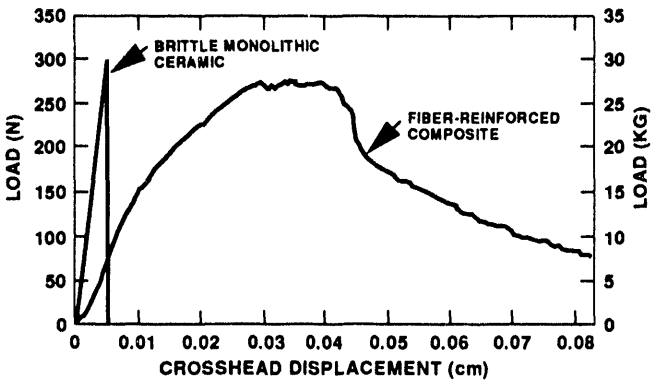

Figure 1. Load-displacement curves for monolithic and fiber-reinforced ceramics

PROJECT DESCRIPTION

This project was begun in FY 1986 as an exploratory effort derived from a project at ORNL on the development of dense ceramic composites for heat exchange applications. This project, which was funded by the U.S. DOE Office of Fossil Energy Advanced Research and Technology Development (AR&TD) Materials Program, involved the production of ceramic composites by CVI of a ceramic matrix into a structural form, hereinafter preform, of ceramic fibers. Several concepts for ceramic composite filters were examined at ORNL. Figure 2 is a schematic of the CVI process.

Based on initial results, the ORNL filter work was continued under DOE-Morgantown Energy Technology Center (METC) Surface Gasification Materials Program sponsorship in FY 1987, and the AR&TD Materials Program

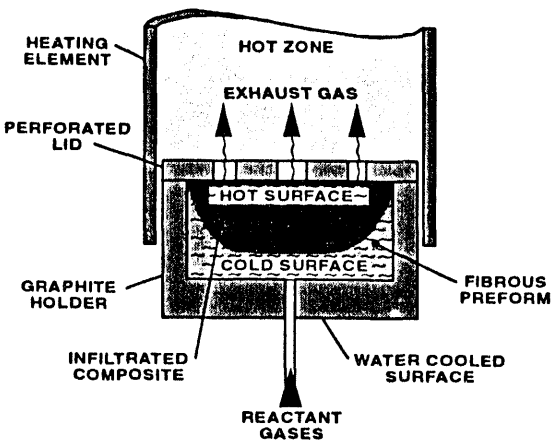

Figure 2. Chemical vapor infiltration process schematic

also continued to support CVI process development and the evaluation of the filters. Tests of filter specimens were conducted at ORNL, Acurex Corporation, and the Coal Research Establishment (United Kingdom). The ORNL work was continued from FY 1988 through 1991 under METC Advanced Research funding. In FY 1989, the 3M Company was awarded a contract on the AR&TD Materials Program through competitive bidding to scale the ORNL invention (Patent No. 5,075,160) to full-size candle filters.

To aid the project in addressing relevant issues, a project was conducted by Acurex Corporation and Virginia Polytechnic Institute and State University to assess the causes of failure of ceramic filters.[2] Several common failure modes were identified. These included thermal and mechanical shock, strength degradation during use, plugging, cracking/breaking at the flange/candle body junction, and binder degradation due to chemical attack. Suspect causes of these failures were improper mounting techniques, tubesheet design, pulse cleaning, candle design,

system transients, and corrosive contaminants in gas streams. Information from this project was incorporated into the 3M project to ensure that the filter developed by 3M would not suffer from the same deficiencies of other ceramic filters.

Many other tests and investigations of the suspected modes and causes of failures of ceramic candle filters as well as ceramic materials in other applications have been conducted.[3-16] The results of those investigations were also considered in the present work.

RESULTS

In mid-FY 1993, 3M Company completed the development of its first-generation ceramic composite candle filter. This first-generation filter, shown in Fig. 3, was a filament-wound structure with three plies of Nextel 312 with a filter surface on the exterior of the candle. The filter surface is a barrier layer of chopped fibers or felt. The binder for the filter is a silicon carbide matrix deposited by chemical vapor deposition (CVD).

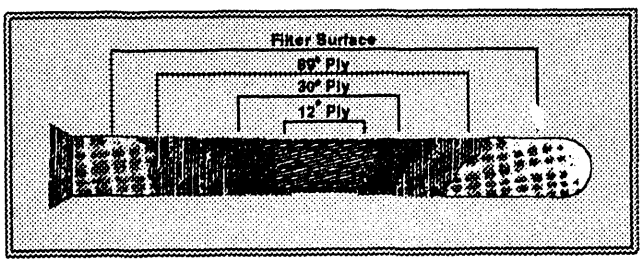

Figure 3. First-generation 3M Company Ceramic Composite Filter

Two of the first-generation 3M Company filters were tested at the Westinghouse Science and Technology Center (STC) in March 1993. These tests were conducted in a simulated PFBC environment at 815 to 830°C for a total of 136.4 operating hours. Ten turbine trip simulation thermal transients were made and the filters withstood these transients without cracking or failure. Filter performance was good and consistent with other ceramic candle filters. However, one candle filter experienced patchy cleaning and partial (≈75%) loss of the filter surface. Details of this phase of the filter development are presented in a 3M Company report entitled *Fabrication of Full-Scale Fiber Reinforced Hot-Gas Filters by Chemical Vapor Deposition.*[17]

Improvements in filter construction and fabrication processing were made by 3M. Among the most significant changes were strengthening of the flange seal area; elimination of the filament-wound structure; and the incorporation of a loosely woven outer layer to address the problem of sloughing off of the filter surface. The resultant structure incorporates a filter surface sandwiched between a tightly woven inner layer and the loosely woven outer layer of Nextel fibers. This loosely woven outer layer is evident in Fig. 4, which is a photograph of the 3M Company Ceramic Composite Filter and a clay-bonded silicon carbide filter.

Testing of six of the 3M Company's second-generation filters was conducted at Westinghouse STC in December 1993. As in the tests of the first-generation filters, these filters were tested in a simulated PFBC environment at 820°C and 0.7 MPa. Tests were conducted for 172 total operating hours using two lots of ash from the Grimethorpe (United Kingdom) PFBC. The first lot, from Grimethorpe Run 132, has been used in many filtration tests at Westinghouse STC and is generally considered to be a typical and relatively easy to filter PFBC ash. The second lot, from Grimethorpe Run 129, is a red ash that is particularly difficult to filter. As before, thermal transients were produced by simulated turbine trips. In these tests, 14 thermal shock tests were conducted.

The new, second-generation design 3M Ceramic Composite Filters met or exceeded all performance criteria for a successful test. They

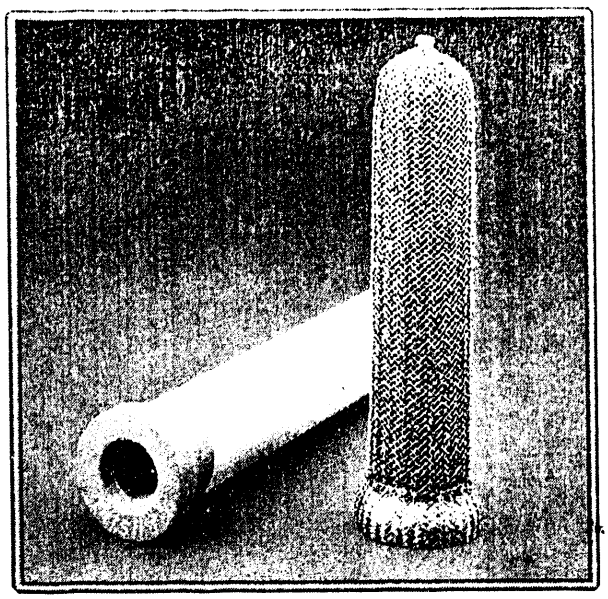

Figure 4. Second-generation 3M Ceramic Composite Filter and a clay-bonded silicon carbide filter

proved to be more durable than the previous design, and none of the filter surface came off during the tests. Dust removal efficiencies exceeded 99.8% with <4 wppm dust in the exit gas from the filters. The filters reached stable, conditioned permeability after 50 cleaning cycles. Permeance values and trends were consistent with clay-bonded filters. Acceptable cleaning of the filters was maintained using up to 300-psig pulses of cleaning gas. Mounting and gasketing maintained dust seals without apparent leakage. Post-test examination indicated significant but not excessive strength reductions. There was no damage (breakage, cracks, distortion, etc.) apparent to the 3M filters as a result of the test.

Based on the development and test results presented here, as well as additional studies at ORNL and elsewhere,[18] we have concluded that the 3M Company Ceramic Composite Filter is a viable filter for PFBC and IGCC applications, as well as other advanced coal combustion applications.

FUTURE WORK

The 3M Company Ceramic Composite Filter has performed well in PFBC simulation tests. Additional tests are needed in an operating PFBC and in an IGCC. To this end, three of the filters have been placed in the filter vessel at the Tidd PFBC for testing. At Tidd, approximately 7% of the process gas stream is diverted to the filter system. Filters have been, and are being, provided to many companies for testing in their specific applications. Testing in the Ahlstrom Pyropower Circulating Pressurized Fluidized Bed (CPFB) pilot plant in Karhula, Finland, is also being pursued. This would be an excellent test of the filters. The Karhula plant is a 10-MW(t) CPFB in which 100% of the process gas stream is directed through the filters, as opposed to the situation at the Tidd PFBC in which a small portion of the process gas flows through the filter vessel.

The 3M Company Ceramic Composite Filter is near to commercialization. It offers a viable and preferred alternative to clay-bonded ceramic filters for PFBC and IGCC applications.

This project provides an excellent example of cooperation between the Department of Energy-Fossil Energy AR&TD Materials Program, Coal Technology Programs, and industry. It also is a most successful example of technology transfer from a national laboratory to the industrial sector. This project also confirms the validity of the research and development (R&D) approach which involved good technical assessments of requirements and a disciplined approach to the R&D needed to satisfy those requirements.

REFERENCES

1. M. Epstein, "Overview of Dust Filtration From Coal-Derived Reducing Gases at High Temperature," in *Proceedings: Second EPRI Workshop on Filtration of Dust from Coal-Derived Reducing and Combustion Gases at High Temperature*, March 11-13, 1992, ed. R. C. Bedick, M. Epstein, and R. A. Brown, Electric Power Research Institute, Palo Alto, Calif, 1992.

2. J. Sawyer, *Assessment of the Causes of Failure of Ceramic Filters for Hot-Gas Cleanup in Fossil Energy Systems and Determination of Materials Research and Development Needs*, ORNL/Sub/86-57964/01, Acurex Corporation, Mountain View, CA, January 31, 1989.

3. R. Clark, et al., "Some Recent Experiences with the EPRI Hot-Gas Rigid Ceramic Filter at Grimethorpe PFBC Establishment," pp. 1251-58 in *Proceedings of the 12th International Conference on Fluidized-Bed Combustion*, American Society of Mechanical Engineers, New York, 1993.

4. K. R. Valentino, et al., "Durability Testing of Ceramic Candle Filters in PFBC Environments," pp. 1375-83 in *Proceedings of the 12th International Conference on Fluidized-Bed Combustion*, American Society of Mechanical Engineers, New York, 1993.

5. R. E. Tressler, "High-Temperature Stability of Non-Oxide Structural Ceramics," *MRS Bull.*, **XVIII**(9), 58-63 (1993).

6. M. A. Alvin, J. E. Lane, and T. E. Lippert, *Thermal-Chemical Degradation of Ceramic Cross-Flow Filter Materials-Phase 1*, DOE/MC/25034-2967, Westinghouse Electric Corporation Science and Technology Center, November 1989.

7. N. S. Jacobson, "Corrosion of Silicon-Based Ceramics in Combustion Environments," *J. Am. Ceram. Soc.* **76**(1), 3-28 (1993).

8. N. S. Jacobson and J. L. Smialek, "Hot Corrosion of Sintered α-SiC at 1000°C," *J. Am. Ceram. Soc.* **68**(8) 432-39 (1985).

9. J. L. Smialek and N. S. Jacobson, "Mechanism of Strength Degradation for Hot Corrosion of α-SiC," *J. Am. Ceram. Soc.* **69**(10), 741-52 (1986).

10. D. S. Fox and J. L. Smialek, "Burner Rig Hot Corrosion of Silicon Carbide and Silicon Nitride," *J. Am Ceram. Soc.* **73**(2), 303-11 (1990).

11. D. S. Fox, N. S. Jacobson, and J. L. Smialek, "Hot Corrosion of Silicon Carbide and Silicon Nitride at 1000°C," in *Corrosion and Corrosive Degradation of Ceramics*, ed. R. E. Tressler, and M. McNallan, American Ceramic Society, Westerville, Ohio, 1990 [also *Ceram. Trans.* **10**, 227-49 (February 1990)].

12. M. A. Alvin, et al., "Evaluation of Ceramic Filter Material, Selection for Application," presented at the *Coal-Fired Power Systems '93/Advances in IGCC and PFBC Contractor's Review Meeting, Morgantown, WV, 1993.*

13. M. A. Alvin, et al., *Degradation of Cross-Flow Filter Material*, DOE/METC-90/6110, DOE Morgantown Energy Technology Center, Morgantown, W. Va., March 1990.

14. J. Sawyer, R. J. Vass, N. R. Brown, and J. J. Brown, *Corrosion and Degradation of Ceramic Particulate Filters in Direct Coal-*

Fired Turbine Applications, ASME Paper 90-GT-347, American Society of Mechanical Engineers, New York, June 1990.

15. H. W. Carpenter, "SiC Tubes Exhibit Excellent Performance in Fluidized-Bed Heat Exchanger Tests," pp. 1-4 in *Materials & Components in Fossil Energy Applications*, DOE/FE-0054/54, U.S. DOE, Washington, D. C., Feb. 1, 1985.

16. J. Stringer, "Ceramic Filter Experience at the Grimethorpe PFBC," presentation without publication at the *36th ASME International Gas Turbine and Aeroengine Congress and Exposition, Brussels, Belgium, June 12, 1990.*

17. R. G. Smith, J. H. Eaton, and M. A. Leitheiser, *Fabrication of Full-Scale Fiber Reinforced Hot-Gas Filters by Chemical Vapor Deposition*, ORNL/Sub/89-SB482C/02, Martin Marietta Energy Systems, Inc., Oak Ridge Natl. Lab., April 1994.

18. R. R. Judkins, D. P. Stinton, and J. H. DeVan, *A Review of the Efficacy of Silicon Carbide Hot-Gas Filters in Coal Gasification and Pressurized Fluidized-Bed Combustion Environments*, ASME Paper 94-GT-314, American Society of Mechanical Engineers, New York, 1994.

5.4

Westinghouse Advanced Particle Filter System

CONTRACT INFORMATION

Contract Number	DE-FC21-89MC21023 DE-FC21-89MC26042 DE-FC21-90MC25140
Contractor	Westinghouse Electric Corporation Science & Technology Center 1310 Beulah Road Pittsburgh, PA 15235 (412) 256-2210
Contractor Project Manager	Thomas E. Lippert
Principal Investigators	Gerald J. Bruck Zal N. Sanjana Richard A. Newby
METC Project Manager	Richard A. Dennis
Period of Performance	October 1992 thru September 1997

Schedule and Milestones

Schedule and Milestones FY94

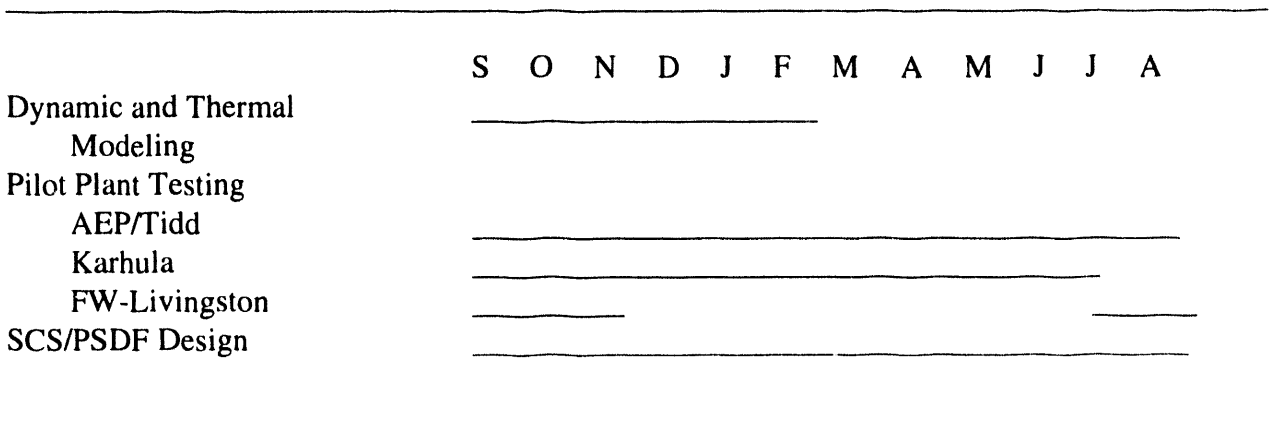

OBJECTIVES

Integrated Gasification Combined Cycles (IGCC) and Pressurized Fluidized Bed Combustion (PFBC) are being developed and demonstrated for commercial, power generation application. Hot gas particulate filters are key components for the successful implementation of IGCC and PFBC in power generation gas turbine cycles. The objective of this work is to develop and qualify through analysis and testing a practical hot gas ceramic barrier filter system that meets the performance and operational requirements of PFBC and IGCC systems.

BACKGROUND INFORMATION

High temperature particulate filters are a key component in advanced, coal based gas turbine cycles (IGCC and PFBC) that are currently under development by DOE/METC for clean coal demonstration. In these applications the hot gas particulate filter protects the downstream heat exchanger and gas turbine components from particle fouling and erosion effects and cleans the gas to meet particulate emission requirements. Both PFBC and IGCC plants benefit because of lower cost downstream components, improved energy efficiency, lower maintenance and the elimination of additional and expensive flue gas treatment systems.

In IGCC systems, the hot gas particulate filter must operate in reducing gas conditions (i.e., presence of H_2, CH_4, CO), high system pressure (150 psi to 350 psi) and at operating temperatures usually determined by the method of sulfur removal, i.e., in bed, external or by cold gas scrubbing. Typically, these temperatures range around 1650°F (in bed), 900 to 1200°F (external) and 1000°F to 500°F (cold scrubbing).

In gasification applications, cold scrubbing of the fuel gas has been demonstrated as effective in cleaning the fuel gas to meet turbine and environmental requirements. However, with this process, plant energy efficiency is reduced, and higher capital costs are incurred. Incorporating a hot particulate filter upstream of the scrubbing unit reduces heat exchanger costs and provides for dry ash handling.

Hot fuel gas cleaning concepts (in bed and external) have also been proposed that utilize reactive solid sorbents to remove gas phase sulfur and hot gas filters to collect the ash and sorbent particles. This approach in IGCC provides for highest energy efficiency and lowest cost of electricity.

IGCC systems may utilize air or oxygen blown entrained or fluid bed gasifiers. Specific operating conditions of the hot gas particulate filter will vary depending on these choices. In general, hot gas filter pilot plant test experience suggests that gasifier ash/char is noncohesive with relatively high flow resistance. Thus, the potential for fines reentrainment and high filter pressure drop are reduced by selecting a relatively low design filter operating face velocity (<5 ft/min). Since the filter treats only the fuel gas component of the total gas flow, the choice of a low filter face velocity does not adversely impact economics. Typically, for a 100 MW_e IGCC system, the filter is required to treat only 6000 to 12,000 acfm, depending if the gasifier is oxygen or air blown. Inlet dust loadings may also vary widely, ranging from <1000 ppmw to 10,000 ppmw.

Bubbling bed PFBC technology is currently being demonstrated at commercial scale. Two PFBC units are located in Sweden (Stockholm Energi, Vartan Plant), another one at the Endesa's Escatron Plant in Spain and one in the United States at the American Electric Power's (AEP) Tidd Plant located in Brilliant, Ohio. The Tidd PFBC is a 70 MW_e demonstration plant awarded through the Round 1 U.S. DOE Clean Coal Technology Demonstration Program. Currently, all four plants utilize high efficiency cyclones to remove greater than 95% of the ash and a ruggedized gas turbine to tolerate ash carried over from the upstream cyclones. Economic and performance improvements in these first generation type PFBC plants can be realized with the application of hot gas particulate filters. Both the secondary cyclone(s) and stack gas ESP(s) could be eliminated saving costs and providing lower system pressure losses. The cleaner gas (basically ash free) provided with the hot gas filter, also permits a wider selection of gas turbines with potentially higher performance.

For these bubbling bed PFBC applications, the hot gas filter must operate at temperatures of 1580°F and system pressures of 175 psia (conditions typical of the Tidd PFBC plant). Inlet dust loadings to the filter are estimated to be about 500 to 1000 ppm with mass mean particle diameters ranging from 1.5 to 3 μm. For commercial applications typical of the 70 MW_e Tidd PFBC demonstration unit, the filter must treat up to 56,600 acfm of gas flow. Scaleup to about 320 MW_e would require filtering over 160,000 acfm gas flow. For these commercial scale systems, multiple filter vessels are required. Thus, the filter design should be modular for scaling.

An alternative to the bubbling bed PFBC is the circulating bed concept. In this process the hot gas filter will in general be exposed to higher operating temperatures (1650°F) and higher (factor of 10 or more) particle loading. Although the inlet particle loading is high, it contains a significantly coarser fraction (mass mean generally >15 μm) which helps mitigate the effect of the higher mass loading. For a 75 MW_e commercial scale circulating bed PFBC plant, gas flow to the filter is approximately 70,000 acfm. At this scale, multiple vessels with modular filter subassemblies are required.

Second generation (or advanced) PFBC is being developed and planned for demonstration and commercialization. In this plant, higher (than first generation PFBC) turbine inlet temperatures are achieved by partially devolatilizing the coal in a carbonizer unit producing a fuel gas. The char produced is transferred and burned in a circulating PFBC unit with high excess air. The hot (1600°F) vitiated air produced is used to combust the hot fuel gas to raise the combustion gas temperature to as high as 2350°F (Robertson, et al., 1989). With second generation PFBC, two hot gas filters are required. One filter is used to collect the ash and char material carried over from the carbonizer unit with the hot fuel gas. The second filter is used to remove ash and sorbent particles carried over with the hot vitiated air leaving the circulating pressurized fluidized bed combustor (CPFBC). Both filter units are required to operate at high temperatures (1200 to 1600°F) and high particle loading. The fuel gas filter will operate in reducing gas while the CPFBC filter operates in oxidizing conditions. A 95 MW_e second generation PFBC demonstration plant requires a hot fuel gas flow to its filter of about 8000 acfm and hot vitiated air flow to its filter of approximately 64,000 acfm.

Westinghouse is currently evaluating candle and cross flow filter devices in subpilot and pilot scale PFBC facilities. These units are designed and operated to support the scaleup of these filters to commercial scale. Table 1 identifies the subpilot and pilot scale facilities that are currently operating (or plan to operate) with a ceramic barrier filter test system supplied by Westinghouse.

Foster Wheeler Advanced PFBC Facility

This testing is taking place at the Foster Wheeler Development Corporation (FWDC) pilot plant facility located at the John Blizard Research Center in Livingston, New Jersey. The second-generation PFBC development is divided into three phases. The first phase, already completed, developed a conceptual design of the commercial scale plant and identified R&D needs (Robertson et al., 1989). The second phase, completed in 1993, involved separate subscale pilot tests of the carbonizer/filter and circulating fluid bed combustor/filter components. The carbonizer/filter testing was initiated in June 1992 and completed in September (Newby et al., 1993). Following this test program, the facility was modified for CPFBC operation, utilizing the candle filter unit. Shakedown tests on the combustor/filter components were initiated in

February 1993. Initial results from this testing have been reported (Lippert et al., 1993). A brief summary of the final test run made in the Phase II activity is reported herein. In phase three of the project, an integrated second generation PFBC pilot plant facility is being constructed and operated. The integrated facility includes both carbonizer and combustor filter units. This testing is scheduled to begin in June 1994.

Advanced Particle Filter Hot Gas Filter Slipstream (AEP/APF)

In August 1989 a cooperative agreement was signed between Ohio Power Company, through its agent, the American Electric Power (AEP) Service Corporation and the U.S. DOE to assess the readiness and economic viability of high temperature and high pressure (HTHP) particulate filter systems for PFBC. The test facility is a one-seventh (1/7) slipstream taken from the Tidd 70 MW (electric) PFBC Clean Coal Demonstration Plant located in Brilliant, Ohio (Mudd et al., 1992). Results of this testing are reported in a companion paper.

Ahlstrom PCFB Facility

Ahlstrom Pyropower has built a 10 MW (thermal) pressurized circulating fluidized bed combustor (PCFB) - ceramic barrier filter test facility located in Karhula, Finland. Through the AEP-PFBC hot gas cleanup cooperative agreement, the U.S. DOE/METC, AEP, Pyropower, EPRI and Westinghouse have embarked on a program to test the Westinghouse candle filter system under PCFB conditions. Results of this work are reported in a companion paper.

Power System Development Facility (PSDF)

Southern Company Services, under a DOE Cooperative Agreement (DE-FC21-90MC25140), is designing and constructing a Power Systems Development Facility that is intended to test and evaluate advanced coal based power generation systems and components. One test module is a 4 MW_e, Advanced Pressurized Fluidized Bed Combustion (APFBC) System including hot gas filters and gas turbine components. A second test module is a dedicated hot gas filter test leg consisting of the M. W. Kellogg transport technology for pressurized combustion and gasification to provide either an oxidizing or reducing gas environment. The full description of the PSDF is given in a companion paper. Westinghouse is providing two hot gas filters for installation and operation at the PSDF. One filter is intended for the combustor leg of the APFBC module. The second filter will be installed on the M. W. Kellogg transport reactor module.

PROJECT DESCRIPTION

Westinghouse is developing a high temperature particulate filter system for application in IGCC and PFBC, advanced power generation systems.

The Westinghouse hot gas filter design, shown in Figure 1, consists of stacked arrays of filter elements supported from a common tubesheet structure. In this design, the arrays are formed by attaching individual candle elements (Item 1) to a common plenum section (Item 2). All the dirty gas filtered through the candles comprising this single array is collected in the common plenum section and discharged through a pipe to the clean side of the tubesheet structure. Each array of filter elements is cleaned from a single pulse nozzle source. The individual plenum assemblies (or arrays) are stacked vertically from a common support structure (pipe), forming a filter cluster (Item 3). The individual clusters are supported from a common, high alloy tubesheet structure and expansion assembly (Item 4) that spans the pressure vessel and divides the vessel into its "clean" and "dirty" gas sides. Each cluster attaches to the tubesheet structure by a specially designed split ring

assembly. The cluster is free to grow down at temperatures. The plenum discharge pipes ducting the filtered gas to the clean gas side of the tubesheet structure are contained within the cluster support pipe and terminate at the tubesheet. Each discharge pipe contains an eductor section. Separate pulse nozzles are positioned over each eductor section. The eductors assist pulse cleaning. During cleaning, the pulse gas is contained within and ducted down the discharge pipe and pressurizes the respective plenum section.

The plenum assembly and cluster (stacked plenums) form the basic modules needed for constructing large filter systems indicative of PFBC requirements. The scaleup approach is:

- Increasing plenum diameter (more filter elements per array)
- Increasing the number of plenums per cluster
- Increasing the vessel diameter to hold more clusters

In general, vessel diameter will be limited by the tubesheet structure and desire to shop fabricate the vessel. Larger PFBC plants would utilize multiple vessels.

The pulse gas used to clean the filters is provided from a pressurized source and delivered and controlled through a series of pipes and valves that comprise the pulse delivery subsystem. The key operating component is the fast acting solenoid valve that controls the pulse action. Figure 2 shows a simplified schematic of a single back pulse module. The module consists of a pressurized gas source, the pulse gas control function and the pulse gas distribution manifold. The cleaning pulse is initiated by first selecting and opening (through the control logic) one of the pneumatic activated ball valves on the pulse gas distribution manifold. The control solenoid valve is then activated allowing a short, high pressure pulse to travel through the opened ball valve and discharge through the pulse nozzle. High reliability and maintainability of this system is obtained by providing a redundant pulse gas control leg and associated isolation valves that allow on-line maintenance. The control logic is developed to automatically switch to the redundant line should a failure signal be received. Control of the pulse cleaning system will be based on either a timing sequence or filter pressure drop signal. The practical operation of this system has been demonstrated in the Tidd PFBC 10 MW_e hot gas filter slipstream.

This paper updates the assessment of the Westinghouse hot gas filter design based on ongoing testing and analysis. Results are summarized from recent computational fluid dynamics modeling of the plenum flow during back pulse, analysis of candle stressing under cleaning and process transient conditions and testing and analysis to evaluate potential flow induced candle vibration.

RESULTS

Computational Fluid Dynamics Modeling. A transient flow analysis was conducted to evaluate the flow conditions within the clean gas plenum section during a pulse cleaning event. The objective of the analysis was to determine the time when the pressure drop (given criteria) across the ash cake of each candle (during cleaning) was sufficient to remove the cake deposit. Also of interest is how the flow field is affected after the first candle is cleaned. A fifty-two (52) candle element plenum array was chosen for analysis. Computations were carried out using a general purpose computational fluid dynamics code. The symmetry of the flow field permitted solution in only half the domain. The major physical features of the candle/plenum arrangement are illustrated in Figure 1. The flow

solution was three-dimensional and included the effects of compressibility and turbulence. Figure 3 shows the three dimensional CFD model. For this initial analysis, it was assumed the dust cake to be uniform and that cleaning of any single candle was uniform over its length.

Results of the analysis show all 52 candles (considering symmetry) are cleaned within a 48.4 to 49.0 ms after start of the pulse cleaning event. Table 2 shows the sequence of candle element cleaning. It was found that the velocity and temperature fields did not vary significantly in the time interval when the candles are cleaned. The flow field is not affected in a manner that would disrupt the cleaning of the other candles and that the candles are all cleaned at relatively the same time. Additional analysis is being considered to evaluate effects of nonuniform candle cleaning, nonuniform cleaning between candles, assumptions on ash properties and impact of broken candles.

Flow Induced Vibrations. The Westinghouse hot gas filter design utilizes free hanging candles fixed at one end to a metal plenum section. The possibility of damaging flow included vibration in the candle element caused by either normal gas filtration or pulse cleaning has been evaluated. The natural frequencies of the candle and mounting system were calculated and measured. The measurement was conducted by fastening accelerometers to the end of one of the candle elements mounted in the Westinghouse filter unit installed at the AEP/Tidd PFBC plant. Experiments were performed by "bumping" the candle and recording response; including frequencies and damping characteristics. From this testing, the largest spikes on the power spectra occurred at 84.37 and 114.45 Hz. Results of finite element mode frequency analysis that modeled the candle/holder system confirmed the measured natural frequencies. Four potential flow included effects were evaluated; Vortex shedding, jet switching, circumferential skimming and turbulence, Table 3. Failure criteria for each mode was established and then compared to the estimated effect based on the filter flow conditions, geometry and natural frequency. The turbulence parameter was estimated based on the results of computational fluid modeling done for one specific installation and flow arrangement. Results of the analysis show that the estimated effect of each flow mode fall significantly below the failure criteria. In general, therefore, flow induced vibration during the normal filtration process is not expected to be a significant factor in the mechanical durability of the candle filter system.

Following the "bump" tests on the accelerometer instrumented candle element in the Tidd filter unit, a series of cold back pulse tests were conducted to measure the candle acceleration and damping as a function of pulsing pressure. In these tests, as expected, the maximum acceleration (e.g., loading) increases with increased pulse tank pressure, Figure 4. The maximum measured acceleration was 0.7 g's at 700 psi under ambient conditions.

Since the g acceleration is expected to vary directly with modulus of elasticity, actual g loading under operating conditions are expected to be decreased. Calculations show that the reaction force at the candle caused by a 1-g loading results in a candle bending stress of less than 200 psi, well within the modulus of rupture limits of candidate candle materials.

Filter Thermal Stressing. Thermal stressing of the filter media occurs with cold backpulsing and whenever there is a sudden and rapid change in the process gas temperature. Such changes may be associated with plant startup, shutdown, plant trip or some unanticipated plant upset.

During filter cleaning, relatively large quantities of (cold) pulse gas flow through the porous ceramic wall causing rapid cooling within the ID wall region and high local tension stressing. Westinghouse calculations, given in Figure 5, show that local wall stresses are well in excess of the modulus of rupture (MOR) of current commercial candle filters. However, the ID wall stresses quickly, dissipate as the pulse gas is heated by the filter. As a result, microcracking of the ID surface may occur. The propensity of these microcracks to grow quickly and cause catastrophic filter failure is a property of the material (critical threshold stress intensity, K_{1c}). K_{1c} values are estimated by using a combination of two experimental techniques – the stressing rate dependence of strength and interrupted static fatigue tests.

Accelerated pulse cycling tests are currently being conducted to identify microcracking and confirm the integrity of candle elements.

Process thermal transients generally last several minutes or longer, subjecting the full filter body to temperature change. Pilot plant testing has shown that process thermal transients may range from $< \pm 10\,^{\circ}$C/min to over $\pm 100\,^{\circ}$C/min. Thermal process transients that cycle, i.e., first increase temperature then decrease temperature, even through relatively low in magnitude, cause the filter body (from OD to ID) to cycle between tension and compression stressing, Figure 6. Such conditions may cause pre-existing flaws or cracks to grow, causing catastrophic failure of the filter element. Although large demonstration and commercial PFBC and IGCC plants are expected to be well controlled and process upsets minimized, tolerance to process thermal transients is a primary requirement of any filter material.

Pilot Plant Testing - Foster Wheeler APFB. The Phase II APFB pilot testing was completed in early December 1993. Filter testing has included separate operation on both the carbonizer and circulating pressurized fluid bed (CPFB) units (Lippert et al., 1993). The same 22-element candle filter unit was utilized for both the carbonizer and CPFB testing, Figure 7. The CPFB testing included a significant shakedown period (approximately 400 hours, representing nine different test runs) to evaluate CPFB operation and control. During this period the CPFB was tested on both coke and coal and the filter was exposed to severe upset events and process conditions that would vary widely. Candle breakage was incurred in some of the shakedown runs.

The final CPFB test run, following shakedown in the Phase II program, included a 180 hour continuous test period in which the CPFB and filter operated under char and coal fired conditions, Table 4. In this test, the filter was configured with 14 candle elements to operate at a face velocity of about 7.8 ft/min. the filter inlet dust loading ranged from about 1000 ppmw to 40,000 ppmw (depending on coal/char feedstock). Filter operating pressure drop was stable throughout the test run. The CPFB operated smoothly and without major upset. Inspection of the filter following completion of the test run showed the 14 candle element to be undamaged. No indication of dust leaks to the clean side could be identified. The residual filter cake was relatively uniform in appearance and did not show any crusty sublayer of sodium or potassium sulfate eutectic that had been experienced in one of the earlier shakedown runs.

Following the Phase II component testing, Foster Wheeler has now reconfigured the pilot plant to include integrated carbonizer and CPFB operation. The Westinghouse Phase II candle filter unit will be integrated with the carbonizer. A second hot gas candle filter unit has been designed and supplied for the CPFB. Table 5

summarizes the design and expected operating conditions for the two Westinghouse filter units. Phase II operation is expected to be initiated in late June or early July, 1994.

SCS/PSDF - Hot Gas Filters.
Westinghouse is designing two hot gas particle control devices (PCD) for installation at the Southern Company Services Power System Development Facility located in Wilsonville, Alabama. Table 1 summarizes the basis for the two PCD designs. PCD 352 will be installed and integrated with the Foster Wheeler circulating PFBC unit. The filer is designed to utilize candle filter elements. Operating experience gained from the Karhula PCFB and Tidd PFBC filter testing have been factored into the PCD 352 design. Improvements include increased spacing between the candle elements and plenum pipe support structure, redesign of the plenum dust shields to enlarge and improve the path for ash discharge; recessing the candle filter holders into the clean gas plenum sections thus eliminating the region where dust can bridge and form clumps that ultimately can break off and get trapped between the candle elements. A steeper cone angle and large outlet flange are also employed in the vessel ash hopper region to promote ash discharge. The PCD 352 is scheduled to be delivered to the PSDF in the first quarter of 1995.

The PCD 301 unit will be initially installed and operated on the M. W. Kellogg transport reactor test module. The PCD 301 is designed to interchange the test cluster to accommodate a variety of filter types including:

- Advanced Candles
- Cross Flow
- CeraMem Axial Cross Flow
- Ceramic Bags

FUTURE WORK

Continued testing of Westinghouse hot gas filter system is planned this summer at the Foster Wheeler APFBC pilot plant facility. Testing of the Advanced design PCD 301 and 352 at the SCS/PSDF is scheduled to be initiated in the second or third quarter in 1995. Results of these and other ongoing filter testing will be utilized to demonstrate and qualify the Westinghouse Advanced Particle Filter for Clean Coal and commercial application.

REFERENCES

Lippert, T. E. et al., 1993. Specific Filter Designs for PFBC. Companion paper - In *Proceedings of Coal Fired Power Systems 93 – Advances in IGCC and PFBC Contractors Review Meeting*DOE/METC June 28-30, 1993.

Mudd, M. J. et al., 1992. Initial Operation of the Tidd PFBC HGCU Test Facility. In *Proceedings of the Ninth Annual Coal-Fueled Heat Engines, Advanced Pressurized Fluidized-Bed Combustion (PFBC), and Gas Stream Cleanup Systems Contractors Review Meeting,* p. 27, DOE/METC-93/6129.

Newby, R. A. et al., 1993. Cross Flow Filter Performance with Second-Generation PFBC Carbonizer Fuel Gas. Paper presented at the 1993 International Fluidized Bed Combustion Conference, May 18-23, 1993 in San Diego, CA.

Robertson, A. et al., 1989. Second-Generation Pressurized Fluidized Bed Combustion Plant: Research and Development Needs. Foster Wheeler Development Corporation, Livingston, NJ. Phase 1 Task 2 Report FWC/FWDC-TR-89/06 to the U.S. DOE under contract DE-AC21-86MC21023.

Table 1. Hot Gas Filter Pilot Plant Test Facilities

	Advanced PFBC (Foster Wheeler)				Southern Companies Services Power Systems Development Facility	
	Carbonizer	Combustor	PFBC (AEP-Tidd)	PCFB Ahlstrom	APFB Foster Wheeler	Transport Reactor, MWK
Facility Size	2 MWt	1.2 MWt	10 MWe	10 MWt	4 MWe	2 MWt
Coal Feed	Dry	Dry	Paste	Paste	Dry	Dry
Operating Temperature	1400-1600°F	1400-1650°F	1300-1550°F	1500-1650°F	1650°F	1800°F
Operating Pressure	100 - 200 psi	100 - 200 psi	130 - 150 psi	130 - 150 psi	200 psi	350 psi
Gas	Reducing	Oxidizing	Oxidizing	Oxidizing	Oxidizing	Reducing (Oxidizing)
Gas Flow (Nominal)	120 acfm	750 acfm	7500 acfm	3100 acfm	6000 acfm	1000 acfm
Precleaning	None	None	Cyclone	None	Cyclone	Cyclone

Table 2. Candle Cleaning Times

Time (sec)	Candle Numbers
0.04844	4
0.04845	5
0.04847	6
0.04848	1
0.04850	7
0.04852	8
0.04853	9, 16, 20
0.04855	10, 17, 19
0.04857	11, 21, 22
0.04858	12, 18
0.04859	13
0.04861	14
0.04862	15
0.04873	3
0.04877	2
0.04880	27
0.04882	26
0.04886	25
0.04884	28
0.04893	24
0.04899	23

Table 3. Summary of Candle Flow Induced Vibration Evaluation

Flow Mode	Criteria	Estimated	Comment
Vortex Shedding	At Critical Frequency (84 Hz)	~0.34 Hz	0.34<<84 Hz No Issue
Jet Switching	u/fD ≥100	0.2	0.2<<100 No Issue
Circumferential Skimming	Velocity >590 ft/s	<<590 ft/sec	No Issue
Turbulence ($0.5\ m^2/sec^2$)	Work Energy From Turbulence >Energy Lost in Damping	$W_T<2\%W_D$	No Issue

Table 4. Summary of CPFB TR5 Test Run

Operating Temperature	1550° F (Nominal)
Pressure	100 to 130 psi
Face Velocity	7 to 8 ft/min
Baseline ΔP	25 - 30 in wg
Dust Loading	1000 to 40,000 ppmw
Test Hours	183

Table 5. Summary of Hot Gas Filter Design and Operating Conditions for Phase III APFBC Testing

PHASE 2 FILTER - CARBONIZER

- Design Gas Flow (acfm) - 120
- Number Candles: 14 (max. 22)
- Face Velocity (ft/min): 2 - 3
- Pressure (psig): 100 - 200
- Temperature (° F): 1400 - 1600
- Dust Loading (ppmw): 2,000 - 20,000

CPFB FILTER

- Design Gas Flow (actual = 750)
- Number Candles: 36 (max 48)
- Face Velocity (ft/min): 5 - 8
- Pressure (psig): 100 - 200
- Temperature (° F): 1400 - 1650
- Dust Loading (ppmw):

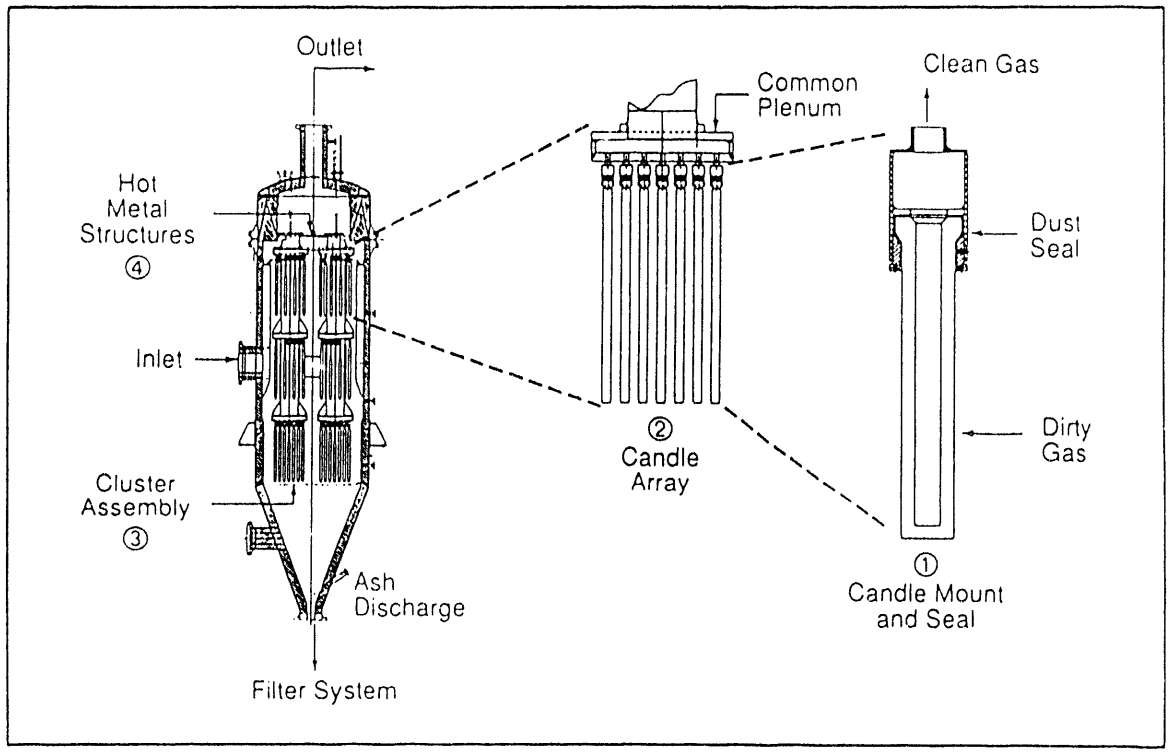

Figure 1. Hot Gas Cleaning Systems - Westinghouse Candle Filter System

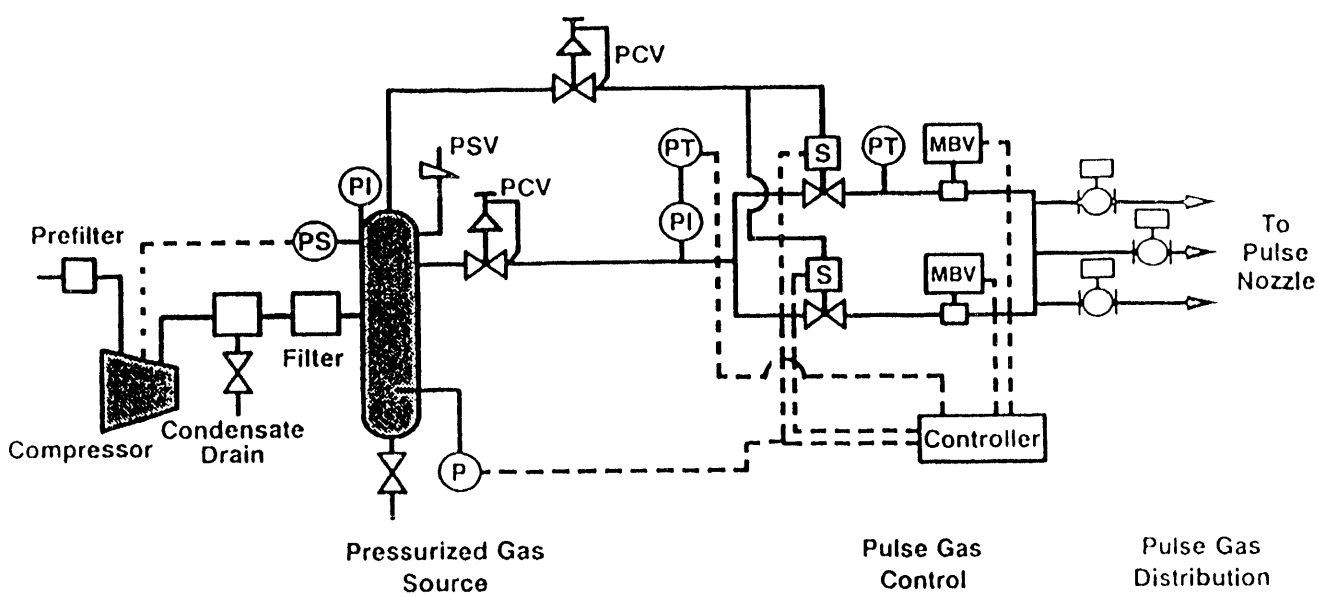

Figure 2. Pulse Gas System Schematic

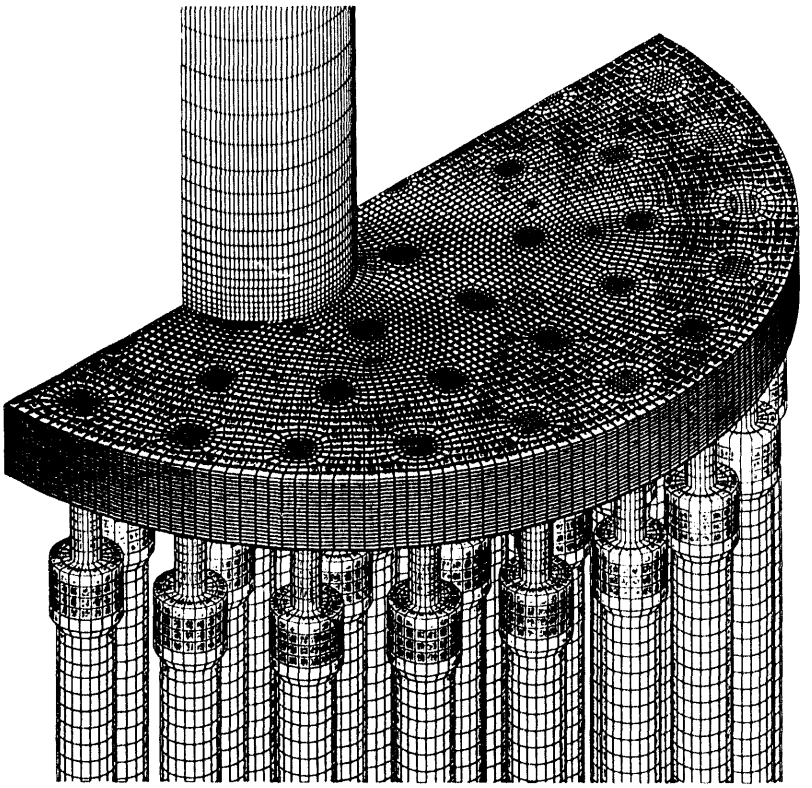

Figure 3. Westinghouse Candle Filter System

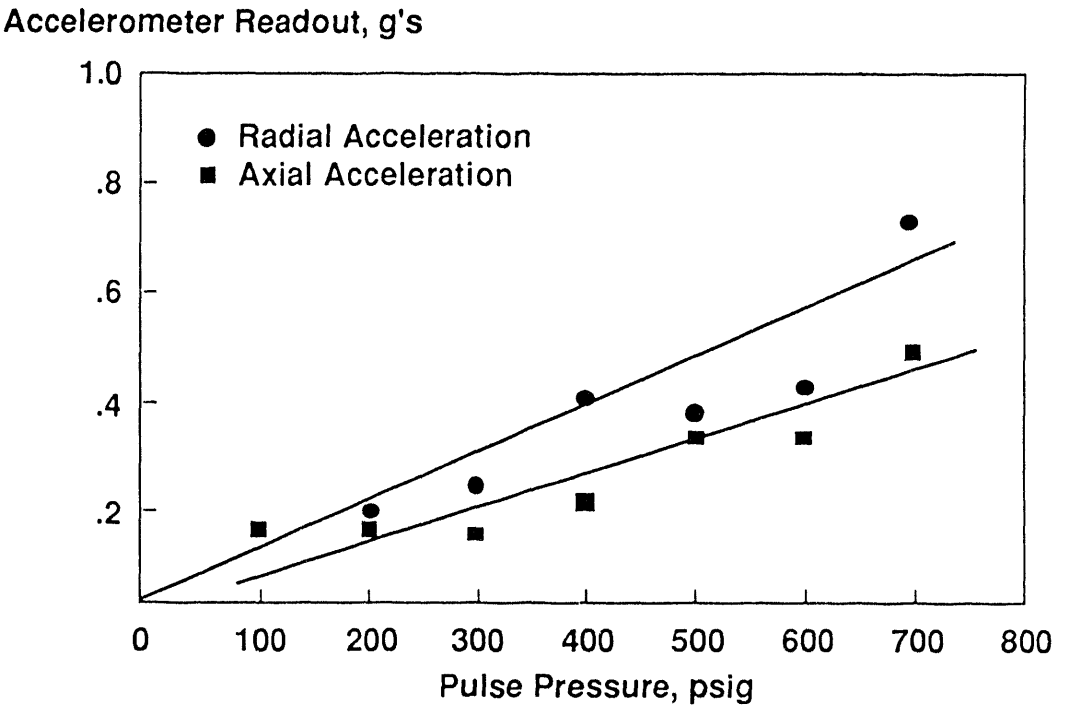

Figure 4. Pulse Induced Vibrations - Test Results

- High Candle ID Wall Tension Stresses - > MOR
- Potential ID Wall Damage (i.e. Microcracks)
- High Stressing Limited to 1 mm Wall Thickness
- Bulk of Filter Wall in Compression

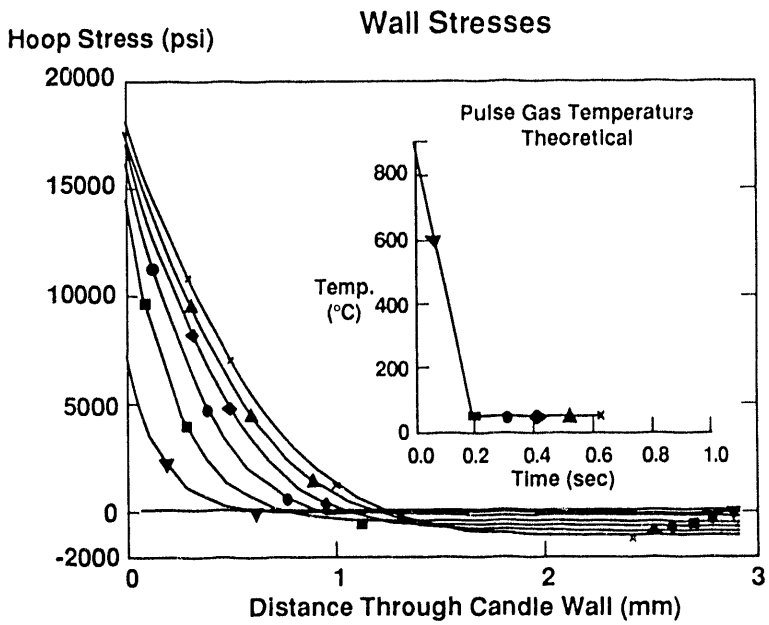

Figure 5. Filter Element Stressing - Cold Pulse Cleaning

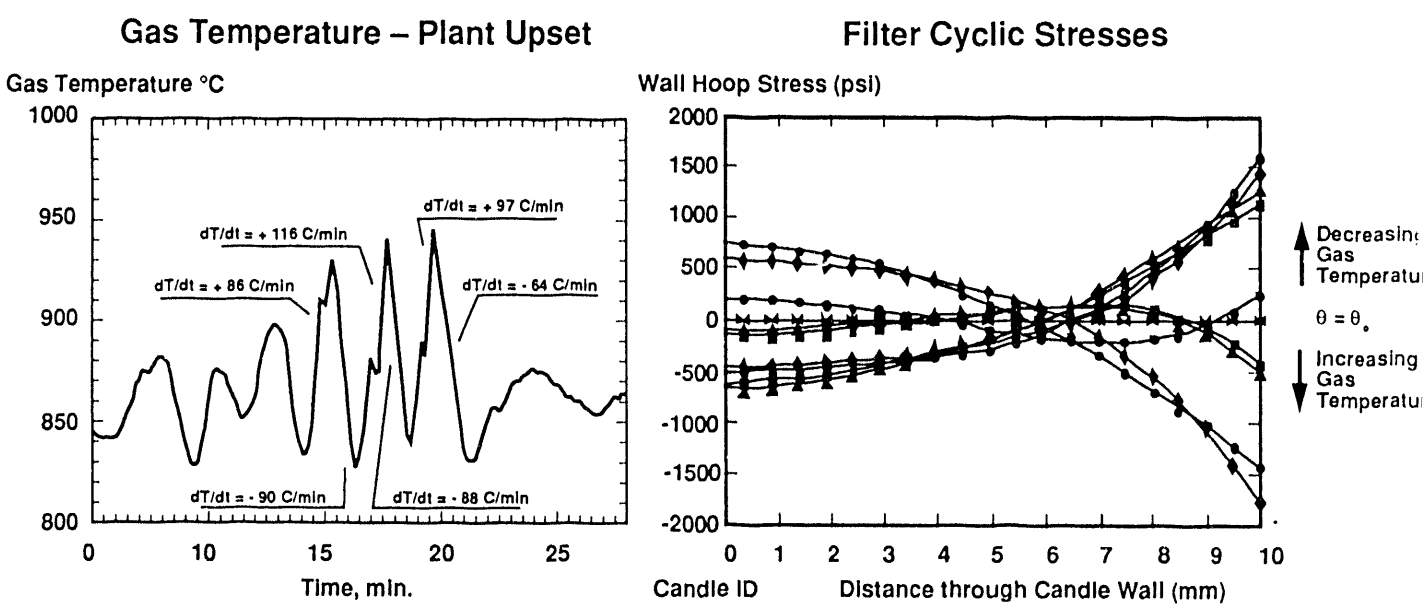

Figure 6. Filter Element Stressing - Process Transients

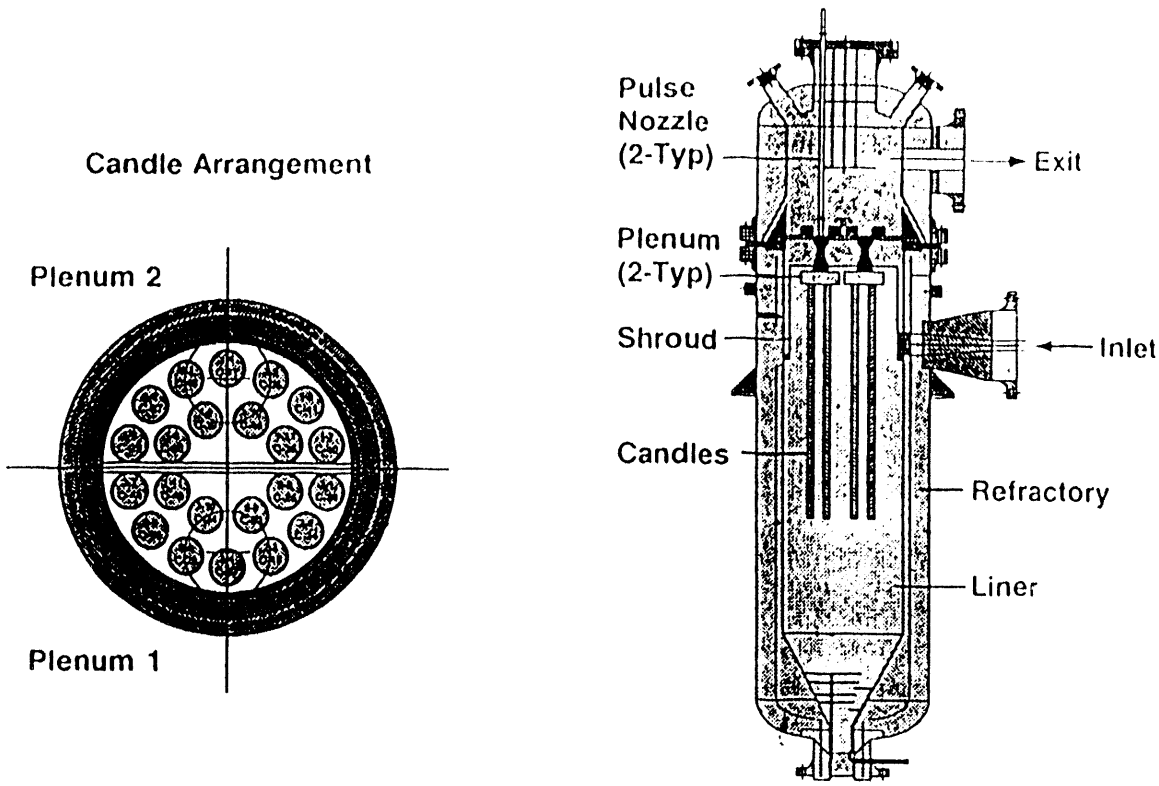

Figure 7. Schematic of 22-Element Candle Filter Installation

5.5

IF&P Fibrosic™ Filters

CONTRACT INFORMATION

Contract Number DE-FG02-92ER81349

Contractor Industrial Filter & Pump Mfg. Co., Inc.
5900 Ogden Avenue
Cicero, IL 60650
(708)656-7800

Contract Project Manger Paul M. Eggerstedt

Principal Investigator Paul M. Eggerstedt

METC Project Manager Norman T. Holcombe

Period of Performance July 27, 1992 to February 17, 1995

Schedule of Milestones

Program Schedule

	1992	1993	1994	1995
Phase 1	**********			
Phase 2	**********	**********	**********	
Candle Strength Testing		**********	**********	
Tubesheet Strength Testing		**********	**********	
Corrosion Studies			**********	*****

OBJECTIVES

The primary objective of this SBIR research program is to increase the performance, durability, and corrosion resistance of lightweight filter candles and filter tubesheet components (Fibrosic™), fabricated from vacuum formed chopped ceramic fiber (VFCCF), for use in advanced coal utilization applications. Phase I results[1] proved that significant gains in material strength and particle retentivity are possible by treatment of VFCCF materials with colloidal ceramic oxides. Phase II efforts will show how these treated materials tolerate high temperature and vapor-phase alkali species, on a long-term basis. With good durability and corrosion resistance, high temperature capability, and a low installed and replacement cost, these novel materials will help promote commercial acceptance of ceramic candle filter technology, as well as

increase the efficiency and reliability of coal utilization processes in general.

BACKGROUND INFORMATION

Ceramic candle filtration is an attractive technology for particulate removal at high temperatures. Due to their simple and cost effective design, temperature capability, and high filtration efficiency, ceramic candles are one of the few clean-up technologies which can consistently meet gas turbine manufacturer's inlet particulate requirements and Clean Air Act mandates. Unfortunately, traditional ceramic candles, made from granular silicon carbide, etc., can be prone to failure from physical and thermal shock as well as chemical attack. These candles also tend to be expensive and, owing to their weight, present internal filter design problems.

VFCCF Filter Materials

Unlike traditional filter candles, VFCCF filter candles offer unique properties for use in HGCU applications, as shown below:

VFCCF Filter Candle Properties:

- Formed from stable ceramic oxides
- Lightweight
- High temperature capability
- Fibers & binder share similar thermochemical properties
- "Knitted" pore matrix

Typically, VFCCF filter candles are formed from commercially available fibers and binders, using existing vacuum forming technology, resulting in a low cost product with excellent manufacturing uniformity and quality control. Because the fibers and binders are essentially a blend of stable, pure ceramic oxides, such as alumina and aluminosilicate materials, the amount of contaminants, organics, etc. which might be reactive in certain applications is negligible.

With apparent density values in the range of 17-22 lbs/ft^3, VFCCF candles are much lighter in weight than their granular ceramic counterparts. This low density, which translates into a weight savings of 70-80% over isostatically pressed silicon carbide filter elements, results in a highly permeable filter with roughly twice the pore volume as granular filter candles. Additionally, as a direct result of the weight savings, the design and construction of the tubesheet and supporting hardware becomes a much easier task, not to mention the reduced stress on the filter candle flange.

VFCCF fibers and binders are typically rated for a maximum temperature of 2600°F to 2800°F, and do not exhibit significant physical changes, such as shrinkage, until a temperature of about 2300°F. is reached. As a result, they are suitable for use in nearly all IGCC and PFBC applications, where temperatures are generally 2000°F. or lower.

Because VFCCF binders are nearly identical in chemical composition to that of the fibers, differences in thermochemical properties between the binder and fiber are negligible, resulting in excellent thermal shock and thermal spalling resistance, as well as resistance to microcracking caused by differences in the thermal expansion coefficients of the fiber and binder. As a consequence of the fiber geometry within the VFCCF matrix, these candles also have an inherently high crack resistance, due to the "knitting" tendency of the fibers during fabrication, and their random orientation which tends to blunt microcrack propagation. Table 1 summarizes these important properties of VFCCF materials.

In the course of fabrication of VFCCF candles, it was found that such materials respond extremely

well to treatment with colloidal ceramic oxide materials, which can increase strength, add corrosion resistance to suit a given application, and allow for the particle retention of the filter element to be controlled, all of which have led to the research effort discussed in this report. With their combined high temperature capability, low thermal expansion, corrosion resistance, and resistance to catastrophic failure, VFCCF materials show promise for use as filter candles and other internal filter hardware, such as a tubesheet, with proper colloidal treatment.

Table 1. VFCCF Material Properties

Typical Chemistry	35-60% Al_2O_3 40-65% SiO_2
Apparent Density	17-22 lbs/ft^3
Maximum Use Temperature	2800°F
Thermal Conductivity (1500°F)	1.26 BTU-in/ft^2-°F-hr
Permanent Lineal Shrinkage (2000°F)	less than 0.8%
Coefficient of Thermal Expansion	2.8 x 10^{-6} in/in-°F

PROJECT DESCRIPTION

Phase 1 Efforts

The overall objective of the Phase 1 effort was to determine which colloidal ceramic oxides of those tested exhibited the greatest increase in the strength of VFCCF filter candle and tubesheet specimens. In the case of VFCCF filter candles, strength increases were valued as important, but not at the expense of acceptable permeability. A total of five different colloidal ceramic oxides, applied using two distinctly different methods, were investigated as shown in Table 2.

Table 2. Colloidal Ceramic Oxide Tests

Materials Tested	Application Methods
Silica Alumina Zirconia Yttria Ceria	Spray Infusion

The materials above were selected on the basis of their temperature capability, corrosion resistance, thermal expansion compatability with VFCCF materials, commercial availability, and cost. Application methods were approached from the standpoints of reproducibility of results, relative cost, and minimal complexity. In both application methods, variations in the colloidal material concentrations as well as the total amount of material applied to the candle and tubesheet test specimens were evaluated in an effort to optimize a technique for producing filtration components with superior performance characteristics.

Phase 2 Efforts

Several goals of the Phase 2 effort are expected to be met as a result of this ongoing research, namely:

- Selection of the most suitable colloidal ceramic oxide material for use in increasing VFCCF material strength and corrosion resistance, without greatly sacrificing permeability (in the case of filter candle applications);
- Development and optimization of the most promising colloidal ceramic oxide

application methods, suitable for mass production of VFCCF components;

- Development and refinement of other means of increasing strength and durability of VFCCF materials, including such techniques as:

  -Filter candle flange, end-cap, and forming die modifications;
  -Investigating the effect of varying fiber type and fiber length on VFCCF material strength;
  -Investigation of lamination and joining techniques for structural VFCCF uses.

Descriptions of each of the above aspects of this research effort follow.

Colloidal Ceramic Oxide Material Selection. In addition to the colloidal oxide materials cited earlier, Phase 2 tests involving colloidal mullite were performed, and appear to be particularly promising. Colloidal mullite has good thermochemical properties and corrosion resistance, adds considerable strength, and tends to form a desirable divergent, acicular pore structure within the VFCCF candle matrix after infusion and subsequent curing. Several VFCCF filter candle specimens prepared in this manner were tested in a PFBC application at Argonne National Laboratory, through funding from the Illinois Clean Coal Institute (ICCI), with excellent results[2], other similarly prepared candles are being tested for permeability decay and durability at Acurex Corp. in Mountain View, CA.

Colloidal Ceramic Oxide Treatment of VFCCF Materials; Spray Application Trials. In continuation of the Phase 1 effort, colloidal ceramic oxides have been applied to aluminosilicate VFCCF matrices, both singularly and in combination, by spraying and immersion application techniques in the Phase 2 effort. In the case of application of colloidal oxides by spraying directly onto VFCCF specimens, a number of problems were encountered, including clogging of the spray nozzles due to drying of the ceramic oxide solids within the nozzle during application. Another problem noted during spraying was a gradual but evident dimensional change of the spray nozzle, presumably due to erosion caused by the ceramic oxide's high velocity through the nozzle orifice. This resulted in an increase in deposited material on subsequent samples, over time.

A third problem noted with the spraying technique was that it provided only a very superficial coating of ceramic oxide material onto the sample. This was alleviated partially by the use of a slight amount of vacuum on the downstream side of the specimen, but the additional amount of ceramic oxide coating observed on each specimen was very small. Efforts were made to produce very fine spray patterns for greater penetration of the colloidal oxides into the VFCCF matrices, but this was found to be troublesome and produced substantial amounts of "overspray" due to the fineness of the spray droplets.

Immersion (Infusion) Application Trials. By comparison, application of the colloidal ceramic oxides by means of simple immersion (infusion) was much more successful and easier to control. Limited to only a few variables, namely the concentration of the ceramic oxide material and the infusion duration, the application from one specimen to the next was found to be much more uniform and predictable than application by spraying techniques.

VFCCF Filter Candle Development Program. In addition to the work involving colloidal ceramic oxides, other means of increasing the durability of VFCCF filter candles has been

ongoing, as part of this research grant. Geometry changes in the critical flange and end cap zones has been one successful approach. A female vacuum forming die was constructed to permit forming of an integral candle flange, in order to eliminate the original bonded flange design, which subjected the flange joint to shear when positioned in a tubesheet. In so doing, it was believed that the filter element would be inherently stronger in the flange area, by the complete elimination of the ceramic adhesive joint. Several dozen filter candles were made using the new forming die, but it was found that in every case, the tapered flange section of the filter candles did not form sufficiently thick to permit machining to the traditional (rectangular or hemispherical) flange shapes which are accepted commercially. In spite of repeated attempts using different vacuum forming pressures, flowrates, and slurry concentrations, a wall thickness of only 7-10mm resulted in the tapered (flange) section of the die.

In view of the above, the approach whereby the outside flange taper would simply be machined to the desired flange geometry was modified. Numerous designs and procedures were tested, but the most promising approach involved the following flange assembly steps:

- Truncating of the "as formed" filter candle at a point 25mm from the onset of the flange taper;

- Machining of a flange "ring" from VFCCF board stock. The outside surfaces of the flange ring can be easily machined into a hemispherical, reverse hemispherical, or rectangular flange geometry from the flat (board) stock, while the inner surface of the ring is machined to the same pitch as the outer taper of the filter candle flange. In so doing, it was found that machining from VFCCF flat stock, subjected to an immersion (infusion) treatment of colloidal ceramic oxide material resulted in a smoother outer machined surface, as compared to flanges machined from untreated VFCCF flat stock;

- "Roughing" the filter candle tapered surface as well as the flange ring inner surface to provide the best "bite" for the ceramic adhesive, followed by vacuuming of fiber debris;

- Affixing the flange ring to the tapered section of the filter candle by slipping it across the distal candle end and into place at the candle taper. A properly selected aluminosilicate ceramic adhesive, designed specifically for VFCCF materials is applied to both mating surfaces, which are first prewetted with colloidal silica for maximum adhesive penetration.

- Compression is applied to the flange joint during the curing step, at temperature, per the adhesive manufacturer's recommendations.

By following the above procedure, a substantially stronger filter flange results, since the flange adhesion joint is no longer subjected solely to shear and tension but is instead in compression, due to the flange taper. Also, unlike the "integral" flange concept, turning of the filter candle flanges to their desired final geometry (on a lathe) is not required.

In destructive testing of the compressive flange joint described above, a downward (shear) load of 73 lbs. was applied to the filter candle flange before failure occurred. Additionally, as hoped, the failure did not occur at the glue joint seam but instead failed within the porous section of the candle. This compares quite favorably to earlier flange designs tested in Phase 1, which had an average flange strength of 53 lbs. Further efforts

are underway to increase the flange strength to an even greater degree; ceramic adhesives using reconstituted fiber, for example, appear to show promise in creating a unique "ceramic weld" between the joined surfaces.

With the above advances made in the flange area of the filter candle, it became apparent that similar candle fabrication techniques would be applicable to the end cap section of VFCCF candles. Capitalizing on the techniques used above, a compressive-state glue joint in the end cap area was developed. By rewetting the open filter candle end temporarily, it became possible to insert a conical VFCCF plug into the softened end to serve as an end cap, much like a stopper in a flask. By inserting the plug backwards (i.e., widest end first), however, the softened cylinder could then be drawn or "puckered" around the conical taper of the plug, after which it would reharden upon drying. Further use of some of the techniques used during flange assembly resulted in a design which places the end cap joint in compression, rather than shear, during the critical jet pulse cleaning of the filter candle.

RESULTS

Phase 1 Efforts

Phase 1 test results showed that the bending and compressive strength characteristics of VFCCF materials can increase substantially as a direct result of the infusion of colloidal ceramic oxide suspensions into the VFCCF matrix. In some instances, it was possible to increase strength of typical VFCCF tubesheet specimens eight-fold, in comparison to the strength of untreated specimens. By variation in colloidal solution application techniques and curing methods, it was also possible to greatly increase VFCCF filter candle strength in critical flange and end cap areas, with a minimal decrease in overall candle permeability. Table 3 provides the highlights of some of the infusion trials, which were quite successful.

Table 3. Results of Phase 1 Testing
Aluminosilicate VFCCF Tubesheet Specimen Strength Test Results After Colloidal Ceramic Oxide Infusions

Infusion Description	Apparent Density (lbs./ft.^{3})	Modulus of Rupture (lbs./in^2)
Untreated Aluminosilicate	17.02	52.68
Single Immersion, SiO_2	36.83	274.11
Single Immersion, Al_2O_3	32.67	127.84
Double Immersion, SiO_2, then Al_2O_3	47.06	440.45
Single Immersion, ZrO_2	32.08	61.79
Single Immersion, Y_2O_3	28.81	168.15
Single Immersion, CeO_2	30.84	86.1

Phase 2 Efforts

Single Infusion Studies. Because of the problems cited earlier with the application of colloidal ceramic oxides by means of spraying, Phase 2 efforts focused primarily on infusion (immersion) as the method of application. Numerous single infusions of VFCCF (aluminosilicate) fiber specimens were made; in each case, the solids concentration of the various colloidal suspensions used was as follows:

- Silica 40% w/w
- Mullite 28% w/w
- Yttria 14% w/w
- Alumina 20% w/w

While it would have been desirable to test using identical concentrations of each suspension, the number and significance of other variables (e.g., pH, viscosity, particle size distribution, etc.), combined with the relative instability of the suspensions, made this an impossible task. Also, unlike Phase 1 testing, ceria and zirconia colloidal ceramic oxides were eliminated in the Phase 2 tests, due to their relatively small resultant strength enhancement of VFCCF matrices.

In the case of silica, a single immersion appeared to increase weight and also strength of the aluminosilicate fiber matrix considerably more than any other material, but at the same time appeared to "seal" the outer pores of each specimen so as to prevent further penetration of colloidal oxides after a subsequent immersion. Although silica is known to increase VFCCF material strength dramatically, because of its susceptibility to corrosion in high temperature environments (from steam, alkali and other corrosive attack mechanisms), it became apparent that another additional ceramic oxide must be applied over the silica layer to produce a durable product. Because of the sealing tendency of the silica, however, it became questionable if suitable penetration by a subsequent corrosion resistant material such as alumina, yttria, or mullite would in fact take place.

Another material which was tested in a single treatment immersion application was that of colloidal mullite. While the mullite applications did not see the rather dramatic weight or strength increases observed with the silica treatment, it was noted that the mullite treatment penetrated very uniformly in each specimen tested, and did not have the tendency to seal or "blind" the pores, as was noted in the silica immersion trials. This observation seems to indicate that subsequent immersions in colloidal mullite, or other colloidal ceramic oxides might lead to greater overall penetration than was noted in the silica trials. Given the advantage mullite has over silica in terms of corrosion resistance, (particularly against vapor phase alkali species in a hot gas environment), combined with good thermal shock resistance and low thermal expansion, mullite is considered to be a choice colloidal material for VFCCF treatment. In each test case involving mullite, a weight increase of 45-85% was noted.

Still another material which was tested in a single treatment immersion study was that of alumina. Alumina has a very high corrosion resistance with regard to vapor phase alkali species, but it was noted that the amount of alumina infused into the VFCCF specimens resulted in a weight increase less than that of mullite, in the range of 45-65%. Based on Phase 1 bending strength test data, alumina did not significantly increase strength, so it was concluded that the use of colloidal alumina for VFCCF materials would be limited to that of a final corrosion resistant treatment only.

The last colloidal ceramic oxide material which was applied by means of single immersion techniques in the Phase 2 effort was that of yttria. Yttria has high thermal stability and good corrosion resistance, but exhibited relatively small weight increases, generally averaging about 40%.

In summary then, the strength of structural VFCCF aluminosilicate materials can be substantially increased by a single immersion in silica, whereas strength and corrosion resistance may be increased in one (or more) immersions using mullite colloidal ceramic oxide material, possibly in conjunction with colloidal yttria or alumina.

For filter candle applications, in contrast to structural ceramic applications, it appears as though the mullite colloidal material also provides a strength increase without a dramatic reduction in pore size,which relates inversely to the pressure differential across a filter candle in operation. Specifically, in the case of the single mullite immersed filter candle specimens, it was found that a weight increase occurred on the order of 60-80%, for immersion durations of 10-15 seconds. Unlike silica, however, it was found that the pore structure of the material did not change dramatically and decreased only from approximately 55 microns to 45-50 microns, from which it can be concluded that filter candle specimens could undergo dramatic increases in strength and durability, as well as corrosion resistance, using a colloidal mullite material, without greatly compromising the pore size (and consequently the pressure differential) across the filter candle. Ongoing tests seem to show that even diluted concentrations (as low as 12%) of mullite are very effective in enhancing candle strength, with almost no loss in permeability.

VFCCF Fiber Length Variation; Mullite and High Alumina Fiber Testing. Efforts involving variations in VFCCF fiber length, as well as forming of filter components using mullite fiber and alumina fiber, rather than aluminosilicate fiber, were performed to see what effect these changes might have on VFCCF material strength. The comparative testing was limited to three-point modulus of rupture (M.O.R.) bend tests, performed on specimens having dimensions of 3" x 2" x 12" (span). The average strength values from these tests are shown in Tables 4 and 5.

Table 4. VFCCF Fiber Length vs. Strength

Nominal Fiber Length (mm)	Modulus of Rupture (psi)
30	55.35
15*	55.65
7.50	85.95

*This material is our VFCCF "standard" material.

Table 5. VFCCF Fiber Type vs. Strength

Fiber Type (Nominal Length, mm)	Modulus of Rupture (psi)
Aluminosilicate, 15mm	55.65
Mullite, 15mm	24.30
High Alumina, 15mm	48.15

The above results indicate that longer aluminosilicate fiber lengths, which produce a lower density product, do not increase strength in comparison to the standard (medium length) aluminosilicate fiber normally used. Shorter, high density aluminosilicate fibers, however, appear to increase strength substantially, by approximately 55%. In the case of the various fiber types tested, both the pure mullite fibers and high alumina fibers show lower strength values than the standard medium length aluminosilicate fiber.

Ceramic Fiber Composite Materials (for structural applications). Investigation of a commercially available pressure-laminated aluminosilicate fiber composite material has also been underway as a result of this research effort, for use as a suitable material for hot gas filter structural components. The composite material closely matches the chemical composition of VFCCF aluminosilicate boards, but has improved properties both in compression (10,000 psi strength) and tension (8,000 psi strength)

Thicknesses are commercially available up to a maximum of 1", and sizes of up to 36" square can be obtained. Because of the size limitations, however, the joining of sections of this material is required to fabricate ceramic tubesheets, etc. in excess of about 36" in diameter. For filter applications involving large tubesheet designs, a joined tubesheet eliminates several drawbacks associated with monolithically formed tubesheets, namely:

- The tendency for formation of air pockets, poor fiber "knitting", etc. in VFCCF specimens thicker than about 2";
- Inability to vacuum form, dry, and cure large diameter specimens, due to existing equipment size limitations (tanks, dies, ovens, etc.);
- Inability to physically handle large specimens while wet, due to their fragility.

In view of the above, the concept of laminating and joining composite ceramic fiber board sections to create a larger final product is being pursued; the 18" x 30" laminated tubesheet specimen shown in Figure 1 is currently being tested for high temperature creep strength at Acurex Corp. of Mountain View, CA.

In addition to high strength, advantages of laminated and joined composite ceramic tubeheets include:

- Utilization of "off-the-shelf" VFCCF and composite board materials for maximum product uniformity, tolerances, etc.;
- No special oversize dies, ovens, tankage, etc. required;
- Attractive cost;
- No special one-of-a-kind tooling required for each particular product design;
- Chemical stability, corrosion resistance, and thermal expansion properties similar to VFCCF materials;
- The need to stock only laminated boards and ceramic adhesive for virtually any tubesheet application.

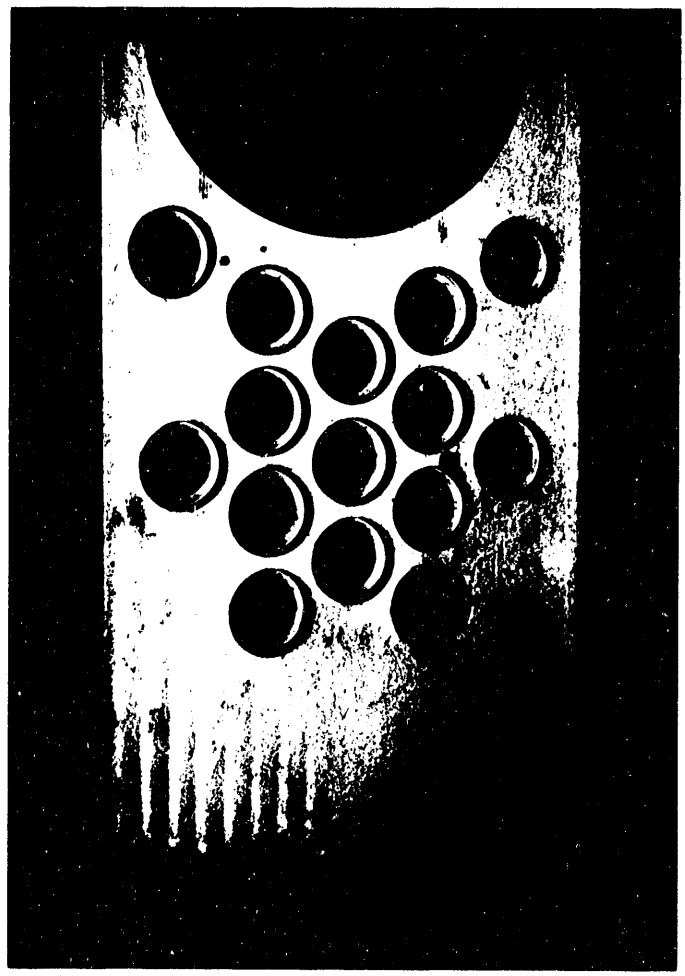

Figure 1. Laminated Composite Ceramic Tubesheet Section

Conclusions

As evidenced from the preceding sections, mullite appears to be the most promising colloidal ceramic oxide treatment material for VFCCF matrices. When applied by means of infusion techniques, considerable process control can be maintained with relative ease, for consistency of final product. Colloidal mullite can be used to increase the strength of VFCCF filter candles without a significant decrease in candle permeability, and creates a desirable divergent, acicular pore geometry during high temperature curing.

The development of a new flange and end cap design approach and joining technique appears to be very promising; continued efforts in ceramic adhesives development should lead to even greater filter candle integrity.

Aluminosilicate fiber composite materials, for use as lightweight ceramic structural components, offer high strength and can be successfully laminated for even greater strength, using proper joining techniques and ceramic adhesives suited for VFCCF materials.

FUTURE WORK

Future VFCCF filter candle developmental efforts will consist of:

- Investigation of multiple infusions of colloidal mullite material, as well as successive mullite/alumina and mullite/yttria infusions, to maximize filter candle strength and corrosion resistance without the premature sealing of pores and possible corrosion, as was noted with colloidal silica;
- Continued development of critical filter flange and end cap areas;
- Further investigation of shorter (7.5 mm) length aluminosilicate VFCCF fibers for use in increasing filter candle strength;
- Application of a finely chopped ceramic fiber "membrane" layer on the filter candle, to produce superior filtration characteristics;
- Corrosion and alkali exposure studies of the most promising filter candle specimens as a result of the above.

Regarding VFCCF and aluminosilicate composite materials, for structural (tubesheet) applications, future efforts will include:

- Development of the optimum lamination, joining, and curing procedures for maximum strength and integrity of these critical components.

REFERENCES

1) Eggerstedt, P. M., (1993) Final Technical Report of Phase 1 Project Entitled: "Durable, Low Cost Ceramic Materials for Use in Hot Gas Filtration Equipment"; USDOE SBIR Grant No. DE-FG02-92ER81349, Cicero, Illinois

2) Lee, S.H.D., (1994), "Evaluate FIBROSIC™ Candle Filter for Particle Control In PFBC", Illinois Clean Coal Institute Final Technical Report for September 1, 1992 through December 31, 1993, Argonne National Laboratory, Argonne, IL.

5.6 Multi-Contaminant Control Granular Bed Filter

CONTRACT INFORMATION

Contract Number	DE-AC21-90MC27423
Contractor	Combustion Power Company 2101 Webster Street #1700 Oakland, CA 94612 510-286-8820
Contractor Project Manager	Keith B. Wilson
Principal Investigators	John C. Haas Cheryl Anne Olivo
METC Project Manager	Heather M. McDaniel
Period of Performance	October 1992 to April 1994

Schedule and Milestones

FY94-96 Program Schedule

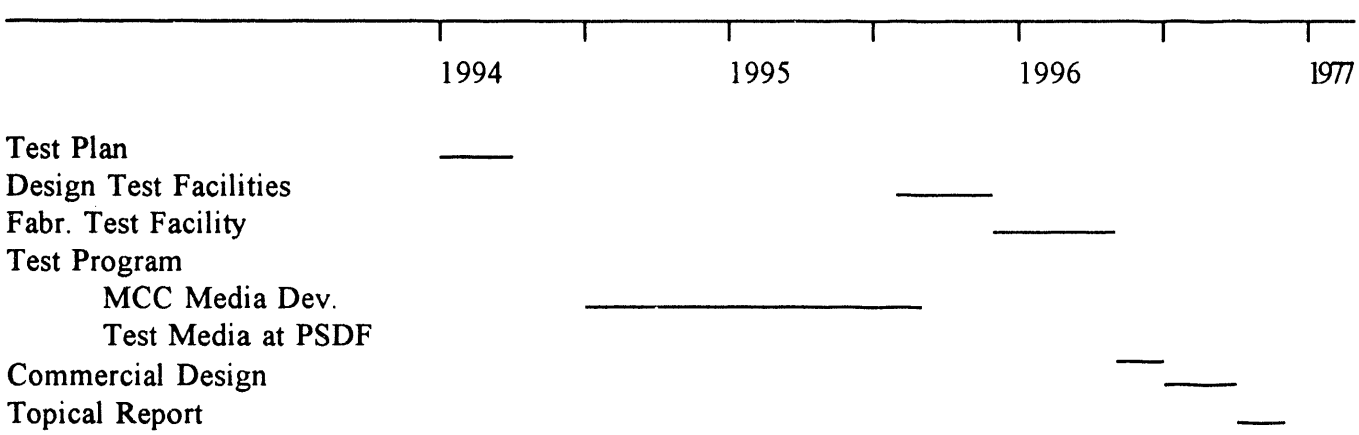

OBJECTIVES

The objective of this phase of the Moving Granular Bed Filter (GBF) Development Program is to develop a GBF for the control of particulates and other contaminants found in high pressure and high temperature coal-derived gas streams. The filter should be able to remove particulates and one or more contaminants such as sulfur compounds, nitrogen compounds, alkali compounds, halogenated compounds, heavy metals and tars. The multi-contaminant control

granular bed filter should be applicable to reducing and/or oxidizing conditions.

Specific objectives of the program are:

- To identify and define an approach to multi-contaminant control using a moving granular bed filter. The approach chosen for multi-contaminant control is justified with supporting data and information from the literature.

- To develop a test plan which includes the conceptual design of component test facilities, a description of tests which includes experimental procedures, operating conditions, duration of tests, number of tests and data to be collected.

- To design, procure and install experimental test facilities.

- To conduct tests to evaluate the moving granular bed filter for multi-contaminant control.

- To develop a commercial-scale design and economic analysis for a multi-contaminant control granular bed filter in PFBC or IGCC applications.

BACKGROUND INFORMATION

The granular bed filter was developed through low pressure, high temperature (1600°F) testing in the late 1970's and early 1980's (Guillory, 1980). Collection efficiencies over 99% were obtained. In 1988, high pressure, high temperature testing was completed at New York University, Westbury, N.Y., utilizing a coal-fired pressurized, fluidized bed combustor. High particulate removal efficiencies were confirmed as it was shown that both New Source Performance Standards and turbine tolerance limits could be met (Wilson, 1989).

The early scale-up work of the granular bed filter indicated potential limitations due to size, cost, and mechanical complexity. These limitations were addressed in the base contract of the present program (Wilson et al, 1992). It is currently proposed to use large diameter filters with 6 mm spherical filter medium to increase filtration capacity and reduce system complexity. Figure 1 shows a granular bed filter designed for a 100 MWe KRW (air) gasifier. The filter has an inside diameter of 14 ft with a nominal bed depth of 5 ft.

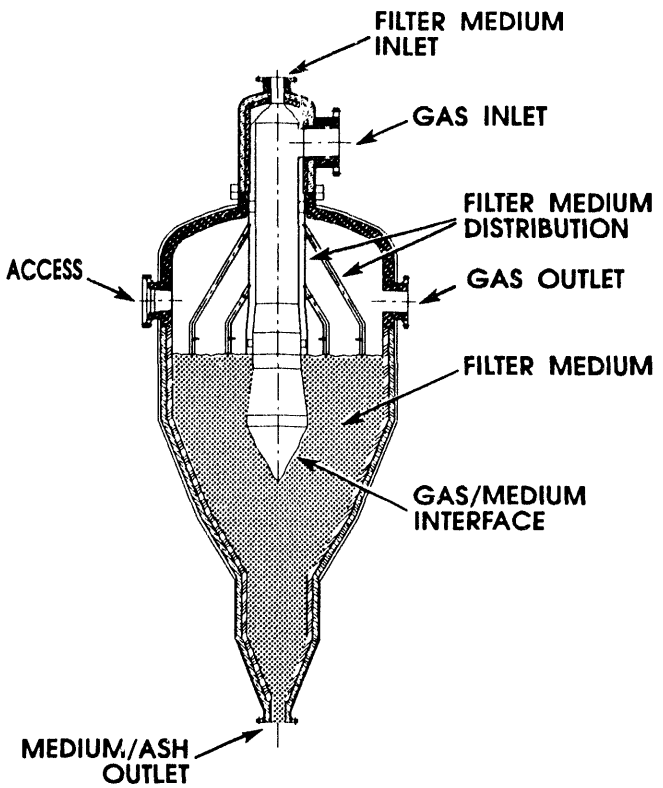

Figure 1. Granular Bed Filter for 100 MWe KRW (Air) Gasifier

PROJECT DESCRIPTION

A multi-contaminant control filter requires that either a chemically reactive sorbent be added to the gas stream and then removed in the filter or that the filter medium itself be chemically reactive. An application in which a fine grained sorbent is added to the gas stream

and is then removed with the filter would be applicable to a granular bed filter as well as other types of filtration processes. We have chosen to use a chemically reactive filter medium to take advantage of the inherent characteristics of a granular bed filter which are long residence times for both the filter medium and the gas which is in contact with the filter medium.

The chemically reactive filter medium can be either a regenerable or non-regenerable sorbent. Others are currently working on the development of regenerable zinc titinate sorbents (Ayala et al, 1992). Such a sorbent would have potential use as a granular bed filter medium if it possesses sufficient strength and attrition resistance for many cycles through a granular bed filter and a sorbent regenerator. Another approach is to use a sorbent which has a finite life and is removed from the filter system after it is spent.

We propose to investigate a non-regenerable filter medium composed of a mixture of limestone and clay for the control of sulfur and alkali contaminants in coal-derived gas streams. Such a sorbent would also have the potential for the control of halogenated compounds, trace metals and tars.

In this concept, the filter medium would be composed of 6 mm chemically reactive spheres which are the same size as the filter medium used for particulate control. The rate of circulation of the filter medium in the GBF for particulate control is much greater than the rate at which reactive filter medium would need to be added to the filter for multi-contaminant control. Fresh reactive filter medium would be added to the circulating filter medium before it enters the filter. After the filter, spent filter medium would be removed from the circulation loop at the rate at which it is added.

Limestone for Sulfur Control

Limestone is widely used for the control of sulfur contaminants in both coal gasification and combustion processes because of its effectiveness, low cost and wide availability. Crushed limestone may not be an effective GBF filter medium because its irregular shape does not have the solids flow characteristics needed for a GBF and may have high attrition rates due to the loss of edges and corners formed in the crushing process.

Rather than using crushed limestone as the filter medium, it will first be pulverized, mixed with clay for alkali control, and then agglomerated into 6 mm spheres using suitable binders. The agglomerated limestone/clay spheres have the advantages of an improved shape for flow in a GBF, an increased micro-pore size and improved attrition properties.

Previous investigators have found that agglomerating finely powdered limestone improved its chemical reactivity and the temperature range of its reactivity, and that the addition of binders during agglomeration could improve mechanical strength. Shen and Albanese (1978), Voss (1983), and Spitsbergen et al. (1988) all demonstrated that calcined agglomerates of powdered limestone have considerably higher reactivity than calcined, similar-sized particles of the naturally occurring stone and may have increased mechanical strength. Zhang et al. (1989) demonstrated that not only is the chemical reactivity of calcined limestone improved by agglomeration, but also the temperature range for chemical reactivity.

Limestone can react directly with H_2S by the reaction route shown in equation 1. If the temperature is high enough, the limestone first calcines to calcium oxide and reacts by the route shown in equations 2 and 3.

$$CaCO_3 + H_2S = CaS + CO_2 + H_2O \quad (1)$$

$$CaCO_3 = CaO + CO_2 \quad (2)$$

$$CaO + H_2S = CaS + H_2O \quad (3)$$

$$CaO + COS = CaS + CO_2 \quad (4)$$

$$CO + H_2O = CO_2 + H_2 \quad (5)$$

Carbonyl sulfide also reacts with calcium oxide as shown in equation 4. The extent of the above reactions are limited by the equilibrium concentrations.

Figure 2 shows the calculated equilibrium concentrations for H_2S and COS in the presence of limestone for fuel gas resulting from the KRW (air) gasifier. The equilibrium H_2S concentration decreases with temperature until a minimum value of 90 ppmv is reached at the calcination temperature of calcium carbonate, 1692°F. After the calcium carbonate calcines to calcium oxide, the equilibrium concentration of

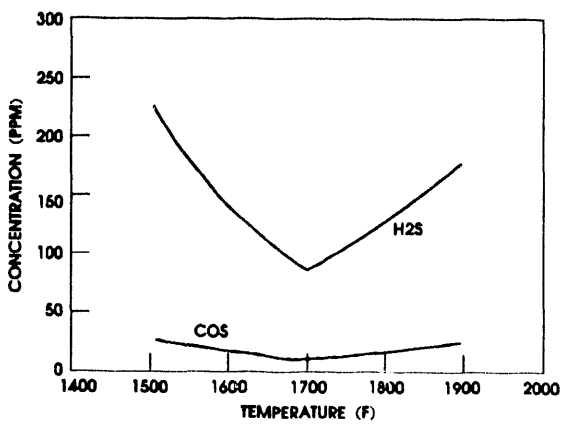

Figure 2 Equilibrium Concentration for H_2S and COS for KRW (Air) Gas

H_2S increases with temperature. The equilibrium concentration of COS depends on the concentration of H_2S. The minimum equilibrium COS concentration is 11 ppmv and it also occurs at 1692°F.

Pilot plant tests conducted at IGT (Goyal, 1988) showed that in their gasifier, it is possible to achieve 85% or more approach to the equilibrium concentration of H_2S. Assuming an 85% approach to the equilibrium concentration of H_2S, the H_2S concentration at the outlet of the GBF would be 106 ppmv. If the COS has the same approach to its equilibrium concentration, its concentration would be 13 ppmv. The combined concentration of H_2S and COS would be 119 ppmv which corresponds to 97.3% sulfur removal for the 2.68% sulfur coal used in the Wansley study (Southern Company Services, 1991).

Unlike the control of hydrogen sulfide with limestone, the control of sulfur dioxide is not thermodynamically limited in a pressurized fluidized-bed combustor operating at 10 atmosphere pressure at temperatures below 1050°C (Newby et al., 1989). Assuming that the PFBC has a limestone bed, a GBF with limestone medium would be used as a polishing sulfur dioxide absorber and as a particulate filter. In such an application, the limestone/clay medium would circulate through the GBF many times since the inlet concentration of sulfur dioxide would be low. The medium would have to have a high attrition resistance to be able to circulate many times through the filter.

Clay for Alkali Control

Several investigators have reported successful alkali removal from high temperature gas streams with sorbents of activated bauxite, attapulgus clay, calcium montmorillonite clay, diatomaceous earth, kaolin clay, and emathlite clay.

Emathlite, a type of fullers earth, was found to be a leading getter of alkali (Bachovchin et al., 1986). The clay had a high capacity for sodium and binds the sodium irreversibly. At extreme conversions, the clay was found to become sticky. This could be a problem but is unlikely to occur as these extreme conversions are not realistically obtained and the anticipated fraction of clay within the agglomerated pellet is small. Kaolin, bauxite, and emathlite were all found to be capable of removing alkali from coal conversion streams (Uberoi et al., 1990). Kaolin and emathlite sorption of alkali was an irreversible process. The maximum sorption capacity of the kaolin was about 25% while that of bauxite and emathlite was about 15%. During screening of alkali sorbents, calcium montmorillonite clay was found to be superior and was chosen for further investigation (McLaughlin, 1990).

All of these sorbents are capable of alkali removal but only a few can be considered within the scope of this program. Of these alkali sorbents tested, bauxite was reported to be fractionally irreversible with alkali removal being 10% chemical sorption and 90% physisorption (physically absorbed as water soluble alkali) (Lee and Johnson, 1980) while only kaolin and emathlite were reported to react irreversibly with alkali (Bachovchin et al., 1986; Uberoi et al., 1990). Because bauxite is also a relatively expensive sorbent which would not be suitable as a non-regenerable sorbent. Work on limestone agglomeration found attapulgus clay to be an effective binding agent (Voss, 1983). With these points in mind, an alkali sorbent of kaolin, attapulgus or emathlite clay in conjunction with limestone will be investigated.

Trace Metal Control

Work at the University of Arizona indicates the potential of porous solids such as bauxite, kaolin or activated alumina for the absorption of heavy metals such as lead or cadmium (Uberoi and Shadman, 1991a). Results have shown that bauxite was considerably more effective than kaolinite for the sorption of cadmium vapors (Uberoi and Shadman, 1991b). The lower effectiveness of kaolinite was explained during examination of the particle which showed an almost completely reacted surface with an unreacted interior. This surface reaction is also typical of dense, natural limestones reacting with sulfur. Therefore, the use of kaolinite in an agglomerated pellet with large micro-pores may allow higher utilization just as it does for the sorption of sulfur species by limestone agglomerates. The kaolinite had a lower water soluble fraction of sorbed cadmium than the bauxite which is desirable from the point of view of ultimate disposal. Also studied was the sorption of lead vapors by various sorbents and kaolinite was found to be the most effective (Uberoi, 1990).

Limestone and dolomite were found to be effective for the removal of zinc and lead vapors from simulated flue gases (Mojtahedi et al., 1989). Dolomite, with its more open pore structure, removed 82% of the lead vapors and 19% of the zinc vapors. Limestone removed 41% of the lead vapors and 81% of the zinc vapors. The sorption of lead vapors may possibly be improved by the agglomeration of limestone to give a more open pore structure similar to dolomite.

From the work of these investigators, a high temperature sorbent composed of kaolinite, bauxite, limestone or dolomite could be capable of heavy metals removal from coal process streams. These same materials have proven to be effective for the capture of alkalies and sulfur species.

Filter Media Preparation, Characterization and Evaluation

In order to evaluate the concept of a GBF multi-contaminant control filter medium, a bench scale laboratory program is planned to be followed by testing in a pilot scale GBF. The bench-scale laboratory program consists of filter media preparation, physical characterization and evaluation of chemical reactivity.

The filter media will be prepared from pulverized limestone, either 80% minus 150 microns or 80% minus 44 microns, an alkali absorbing clay and suitable binders. A disc pelletizer will be used to prepare 6 mm and 2 mm spherical pellets. Major emphasis will be on evaluation of 6 mm media. The 2 mm media will be evaluated only if the 6 mm media does not have suitable properties. Should disk pelletizing not produce a suitable filter medium, extruded pellets which are rounded into spherical shapes with a disc pelletizer would then be evaluated.

The clay to be used in the filter medium as an alkali sorbent will be determined on the basis of a screening test developed by McLaughlin (McLaughlin, 1990). The candidate clays to be evaluated are: kaolin clay, bauxitic kaolin clay, ematholite (calcium montmorillonite clay), attapulgite clay and low swelling bentonite clay. A mixture of clay and NaCl is heated in a thermogravimetric analyzer (TGA). The mixture with the lowest weight loss would be the best alkali sorbent. Mixtures of limestone, clay and NaCl will also be evaluated. The preferred clay will be mixed with limestone at 5% weight concentration to form the multi-contaminant control filter medium.

In order to make a strong, attrition resistant filter medium from the clay and limestone mixture, a binder may be needed. The following lists the binders which will be evaluated and their weight concentration.

- 15% attapulgus clay with 2% boric acid
- 2% and 4% sodium silicate
- 2% and 4% corn starch
- 2% sodium bentonite with 10% calcium sulfate
- 2% and 5% sodium bentonite
- 2% and 5% calcium montmorillonite
- 5% and 10% calcium sulfate hemihydrate
- 10% and 15% portland cement
- 10% and 15% FBC bed ash

The filter media prepared from the above combinations will be evaluated in terms of their physical properties. Pellet green strength is evaluated by a drop test which relates to the ability of the pellet to be handled before curing. After curing, calcined pellets are subjected to a crush test which relates to the ability of the pellets to maintain shape in the GBF. Pellet attrition resistance is measured using ASTM D4164-88 procedure. The attrition resistance of the most promising formulation will be evaluated in a special test apparatus which simulates the particle motion in a GBF. The apparatus consists of a lift pipe and return seal leg.

For the five most promising formulations more extensive physical characterizations will be performed. These include bulk density measurements, measurement of pore volume and pore diameter, determination of optimum pellet moisture for maximum strength and SEM microstructure of reacted pellets.

Media reactivity will be evaluated in sulfidation, sulfation and alkali absorption tests. Initial TGA sulfidation tests will be run on 15 formulations of 6 mm pellets and 3 sample of 2 mm pellets. The five best formulations will then be sulfided in a larger batch apparatus so that the reacted medium can be evaluated for crush strength and ASTM attrition resistance. For the most promising formulation, additional TGA will be run to obtain detailed kinetic data. In these tests, gas composition and temperature

will be varied. A series of pressurized TGA tests will be run to access the effects of pressure on reaction kinetics. A larger scale fixed bed reactor will be used to sulfide filter medium for large scale attrition tests and to obtain kinetic data for comparison with the TGA data. This test series will evaluate the medium's reactivity with respect to the sorption of H_2S.

Prior to disposal, sulfided filter medium will have to be converted to the sulfate form. It is expected that the larger micro-pores of the pelletized limestone will facilitate the conversion of sulfide to sulfate as occurs with dolomite. Atmospheric TGA tests will be used to determine the kinetics of the oxidation of the sulfide filter medium.

The multi-contaminant control GBF could be used with combustion gases to remove particulate, sulfur dioxide, and alkali compounds. The five best formulations determined from the sulfidation tests will be evaluated for SO_2 removal. TGA tests will evaluate the kinetics of the sulfation reaction. Batch sulfation tests will generate sufficient quantities of reacted filter medium for crush strength tests and ASTM attrition tests.

Fixed-bed alkali absorption tests will be used to obtain kinetic data on the reactivity of the prepared sorbents with respect to the absorption of alkali and sulfur compounds. A heated sample holder whose change in weight is monitored with a micro balance heats salt crystals which vaporize into a carrier stream. The rate of evaporation is controlled by the temperature of the sample holder. The alkali vapors are mixed with either a gas stream containing H_2S or one containing SO_2 and are carried into the packed bed of sorbent. The packed bed section will be 3 inches in diameter by 12 inches long, in a tube of alumina which is inert with respect to the alkali vapors. Test durations are between 24 and 100 hours. The first tests use a carrier gas containing N_2, 5% H_2O, and additives of H_2S and HCl. In later tests, the carrier gas contains 95% CO_2 and 5% H_2O with additives of SO_2 and HCl. The first five tests use a shallow bed which will be analyzed for the average alkali and sulfur sorption. After the first five tests, the bed will be sectioned into ninths and analyzed for alkali and sulfur content as a function of the position in the bed. In some of the tests, the carrier gas will contain HCl which is know to inhibit the sorption of alkali.

The kinetic data collected on sorbent reactivity will be used to create a model of the sorbent's chemical reactivity in a GBF. The model will take into account the sorbent reactivity with respect to sulfur species and alkali. The model will provide information on the required bed depth of the GBF, the expected outlet concentration of sulfur and alkali species and the extent of reaction of the sorbent.

Pilot Plant Testing

Bench scale tests are used to develop and evaluate multi-contaminant control media. The developed media is evaluated in terms of its chemical and physical properties in a bench scale environment. The next phase of evaluation will be at the pilot plant scale. Combustion Power Co. is participating in the DOE sponsored tests at the Power Systems Development Facility (PSDF) to be installed in a Southern Company Services Facility in Wilsonville, AL. The first year of testing at the PSDF will be dedicated to the evaluation of the GBF for particulate control. For these tests, the GBF is connected to M.W. Kellogg's transport reactor which can be operated in either a gasification or combustion mode. After the evaluation of a GBF for particulate control, the opportunity exists to evaluate the GBF with a reactive medium for the control of sulfur and alkali compounds.

The modification necessary to allow testing at the PSDF GBF are relatively straight forward. Lock hoppers will be installed for the addition and removal of multi-contaminant control filter medium. The additional feed and removal systems can be accommodated within the existing structure. Nine tons of clay/limestone filter medium will be prepared for the test series which will provide for 80 hours of testing.

Cost Estimate for Production of GBF Multi-Contaminant Filter Medium

To evaluate sorbent feasibility, plant scale processes were developed to estimate the capital and operating costs to produce a GBF medium of limestone and clay at three different production rates. The production rates chosen were 5,000, 50,000 and 500,000 ton/yr.

To develop the plant processes and cost estimates for the three production rates, assumptions were made concerning the medium composition, i.e. the sorbent formulation. Of the 68 possible formulations to be evaluated, a single formulation was chosen as the base case. This formulation is 6 mm pellets of 80% less than 149 micron limestone with 5% montmorillonite clay and 10% dry binder addition of portland cement (PC III). The pellets would be formed by disc pelletization requiring 20% pellet moisture and moist environment curing for 72 hours. Cost estimates were also made for lower and upper limits based on different formulations and pelletizing procedures.

Table 1 shows the cost estimates; for the base case, the production cost for 50,000 tons/year would be $39.72 per ton.

FUTURE WORK

The first task in the GBF multi-contaminant development program of identifying a concept and a test plan is completed. The next phase will be the execution of bench scale tests to determine the feasibility of the proposed approach to multi-contaminant control using a GBF. Following bench scale testing, testing will be conducted on a pilot scale GBF at the PSDF. After completion of testing, the cost and design of a commercial scale GBF with multi-contaminant control will be determined.

Table 1 Cost Estimate for GBF Medium Production

Production Rate ton/yr	Capital Cost M$		Operating Cost $/ton	
	Base	Range	Base	Range
5,000	2.5	2.1 - 2.8	152.0	137.8 - 200.3
50,000	4.3	3.6 - 5.1	39.7	31.1 - 86.0
500,000	15.2	12.3 -17.0	26.9	190.2- 71.9

REFERENCES

Ayala, R.E., E. Gal, and R.P. Gupta. 1992. Enhanced Durability of High-Temperature Desulfurization Sorbents for Moving-Bed Applications, in *Proceedings of the Twelve Annual Gasification and Gas Stream Cleanup Systems Contractors Review Meeting Vol 1*, ed. R.A. Johnson and S.C. Jain, 230-239. DOE/METC--92/6128 (DE93000228) Morgantown, West Virginia.

Bachovchin, D.M., M.A. Alvin, E.A. Dezubay and P.R. Mulik. 1986. "Study of High Temperature Removal of Alkali of a Pressurized Gasification System." Final Report DOE-MC-20050-2226.

Goyal, A. et al. 1988. "In-Situ Desulfurization in a Fluidized Bed Coal Gasifier." *Energy Sources*, Vol. 12, pp. 161-179.

Guillory, J. L. 1980 *High-Temperature Particulate Removal By Moving Bed Granular Filtration.* TR 80-3. Menlo Park CA: Combustion Power Company.

Lee, S.D. and I. Johnson. 1980. "Journal of Engineering Power", ASME Trans. 102, pg. 397.

McLaughlin, J. 1990. "The Removal of Volatile Alkali Salt Vapors from Hot Coal-Derived Gases". PhD Thesis, Guildford, UK, Dept. of Chemical and Process Engineering, University of Surrey, 214 pp.

Mojtahedi, W. and R. Blackman. 1989. "Release of Alkali Metals in Pressurized Fluidized-Bed Combustion and Gasification of Peat." Public Technical Research Center, Finland, 53, March, 48 pp.

Newby, R.A., D.L. Keairns, T.E. Lippert, M.A. Alvin and D.M. Bachovchin. 1989. "Pressurized Fluidized-Bed Combustion at Elevated Temperatures." In *Proceedings of the 1989 International Conference on Fluidized Bed Combustion*, Vol. 2, pp. 873-879.

Shen, M. and A.S. Albanese. 1978. "Regenerative Process for Desulfurization of High Temperature Combustion and Fuel Gases", Quarterly Progress Report No.11, October 1 - December 31. BNL 50992.

Spitsbergen, U., W.C.Van Werven and H.A. Akse. 1988. "Desulfurization Quality of Limestone-Based Sorbents Tested Under Multi-Stage Fluidized Bed Combustion Conditions." Presented at the Fifth Annual International Pittsburgh Coal Conference, September 12-16.

Uberoi, M. 1990. "High-Temperature Removal of Metal Vapors by Solid Sorbents." PhD Thesis, University of Arizona.

Uberoi, M., W.A. Punjak and F. Shadman. 1990. "Kinetics and Mechanism of Alkali Removal from Flue Gases by Solid Sorbents." *Prog. Energy Combustion Science*, Vol. 16, No. 4, pp. 205-211.

Uberoi, M. and F. Shadman. 1991a. "High-Temperature Removal of Cadmium Compounds Using Solid Sorbents." *Environmental Science Technology*, Vol. 25, No. 7, pp. 1285-1289.

Uberoi, M. and F. Shadman. 1991b. "Fundamentals of Heavy Metal Removal by Dry Sorbents." Prepr. Pap. *Am. Chem. Soc., Div. Fuel Chem.*, Vol. 36, No. 4, pp. 1724-1729.

Voss, K.E. 1983. "Limestone-Based Sorbent: Agglomerates for Removal of Sulfur Compounds in Hot Gases and Method of Making." U.S. Patent 4387653.

Wilson, K. B. March 1989. Performance Evaluation of a Screenless (Counter-Current) Granular Bed Filter on a Subpilot-Scale PFBC.

In *Proceedings of the Sixth Annual Coal-Fueled Heat Engines and Gas Stream Cleanup Systems Contractors Review Meeting*, ed. R.C. Bedick, T.P. Dorchak, N.F. Rekos, H.A. Webb, 293-303. Doe/METC-89/6101 (DE89000952) Morgantown, West Virginia.

Wilson, K.B., J.C. Haas, and M.B. Eschelman, 1992. Moving Granular Bed Filter Development Program. In *Proceedings of the Twelve Annual Gasification and Gas Stream Cleanup Systems Contractors Review Meeting Vol 1*, ed. R.A. Johnson and S.C. Jain, 289-296. DOE/METC--92/6128 (DE93000228) Morgantown, West Virginia.

Zhang, H., X. Huang, X. Zhang and B. Wu. 1989. "Development of Advanced Synthetic Sulphur Sorbent for Fluidized Bed Coal Combustion." In *Proceedings of the 1989 International Conference on Fluidized Bed Combustion*, Vol. 1, pp. 591-595.

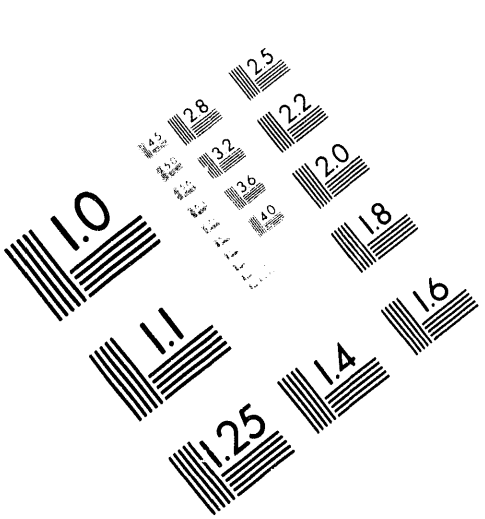

Association for Information and Image Management

1100 Wayne Avenue, Suite 1100
Silver Spring, Maryland 20910

301/587-8202

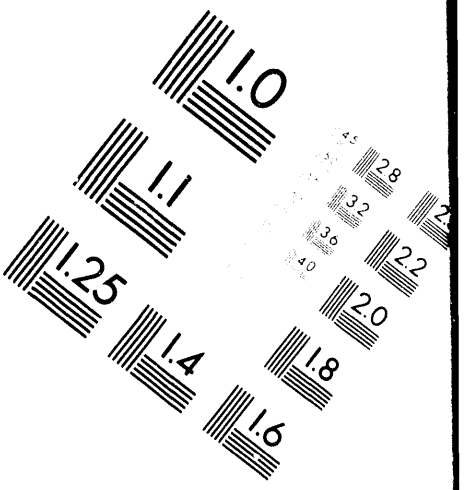

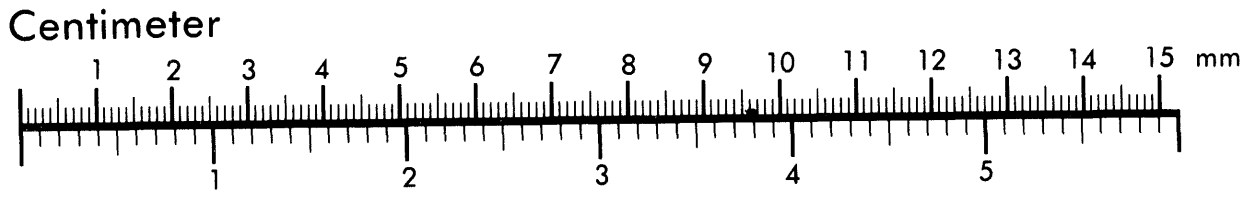

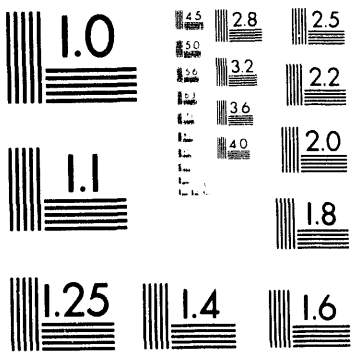

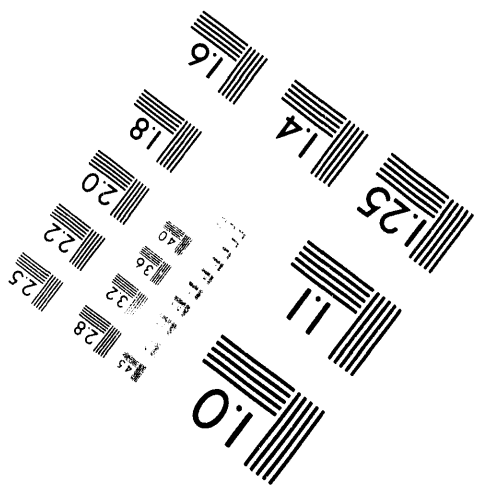

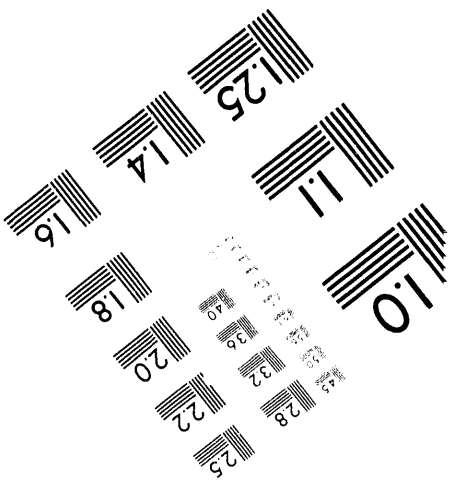

MANUFACTURED TO AIIM STANDARDS
BY APPLIED IMAGE, INC.

3 of 6

5.7 Westinghouse Standleg Moving Granular Bed Filter Development Progam

CONTRACT INFORMATION

Contract Number	DE-AC21-91MC27259
Contractor	Westinghouse Electric Corporation Science & Technology Center 1310 Beulah Road Pittsburgh, PA 15235 (412) 256-2210
Contractor Project Manager	Richard A. Newby
Principal Investigators	Wen-Ching Yang Eugene E. Smeltzer Thomas E. Lippert
METC Project Manager	Heather M. McDaniel
Period of Performance	May 13, 1991 to December 15, 1994

Schedule and Milestones

FY94 Program Schedule

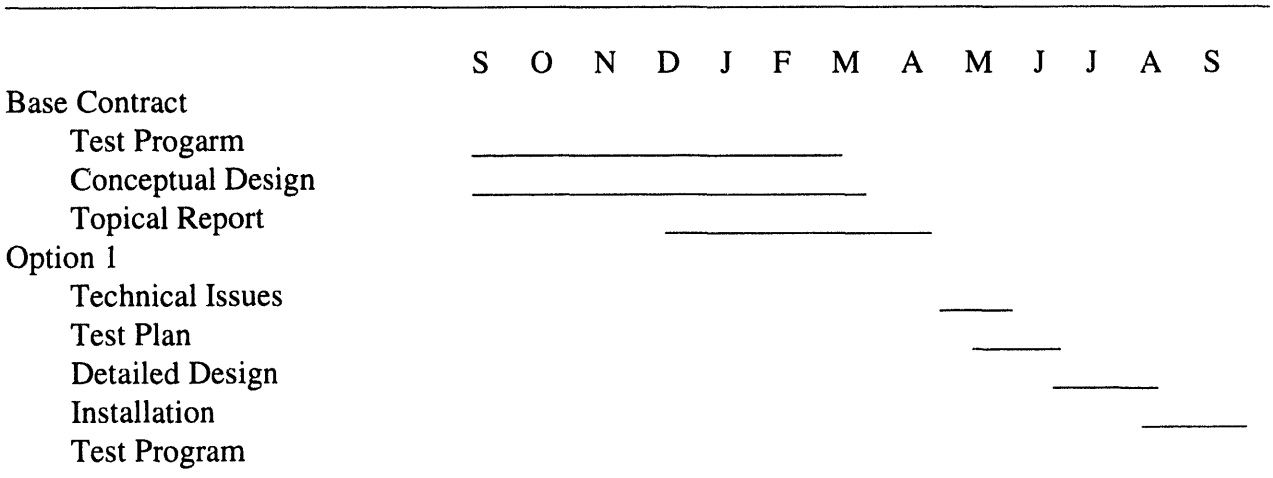

OBJECTIVES

The overall goal of the Standleg Moving Granular Bed Filter (SMGBF) development program is to establish a moving granular bed filter system that meets all of the performance requirements and design constraints imposed by advanced power generation applications, and is economically competitive with ceramic barrier filter systems. In the recently completed, Base Contract period, it was the objective of the program to identify barrier technical issues for

the SMGBF technology and to perform critical testing and evaluation to resolve those key issues. This paper summarizes the activities and conclusions from the Base Contract period.

BACKGROUND INFORMATION

Advanced, coal-based, power plants, such as IGCC and Advanced-PFBC, are currently nearing commercial demonstration. These power plant technologies require hot gas filtration as part of their gas cleaning trains. Ceramic barrier filters are the major filter candidates being developed for these hot gas cleaning applications. While ceramic barrier filters achieve high levels of particle removal, there are concerns for their reliability and operability.

An alternative hot gas filtration technology is the moving granular bed filter. These systems are at a lower state of development than ceramic barrier filters, and their effectiveness as filters is still in question. Their apparent attributes, relative to ceramic barrier filter systems, result from their much less severe mechanical design and materials constraints, and the potential for more reliable, failure-free particle removal operation.

The Westinghouse Science & Technology Center has proposed a novel moving granular-bed filter concept, the Standleg Moving Granular-Bed Filter (SMGBF) system, that may overcome the deficiencies of the current state-of-the-art moving granular-bed filter technology. The SMGBF is a compact unit that uses cocurrent gas-pellet contacting in an arrangement that greatly simplifies and enhances the distribution of dirty, process gas to the moving bed and allows effective disengagement of clean gas from the moving bed.

The SMGBF vessel concept is elucidated in Figure 1. Dirty process gas is introduced into the top chamber of the filter vessel through a tangential entry. The moving bed media is introduced into the same chamber through a single, vertical dipleg pipe, where it spills from the base of the dipleg pipe to form a free surface having the normal media angle of repose. The dirty process gas enters the moving bed media through this free surface. Cocurrent flow of gas and bed media through the short, vertical standleg promotes intimate contact between the flowing gas stream and the moving bed media, resulting in excellent separation of fly ash particles. The cocurrent gas/solids operation also prevents fluidization at the bottom of the standleg and permits high flow throughput (3 to 6 ft/s through the standleg), with relatively small ratios of bed media-to-fly ash (mass ratio of about 10). The cleaned gas is then allowed to flow out through the free surface of the bed formed naturally below the standleg. Special design features are built into the region at the base of the standleg to permit disengagement of the cleaned gas from the moving bed media without significant fly ash re-entrainment. The bed media and captured fly ash withdrawal from the filter vessel is controlled by a water-cooled, rotary valve or screw conveyor located below the vessel. The SMGBF vessel design is relatively simple, and it employs well-known standpipe design technology, making it cost effective, reliable, and easy to scaleup.

Two approaches for handling the bed media can be applied to the SMGBF: "Once-Through" media operation, and "Recycle" media operation. Once-Through media operation applies pelletization technology to generate filter pellets from the power plant solid waste materials, and uses these pellets as a "once-through" filtering media to eliminate the need for costly, complex, and large filter media recycling equipment. This pelletizing step also generates a more environmentally acceptable solid waste product

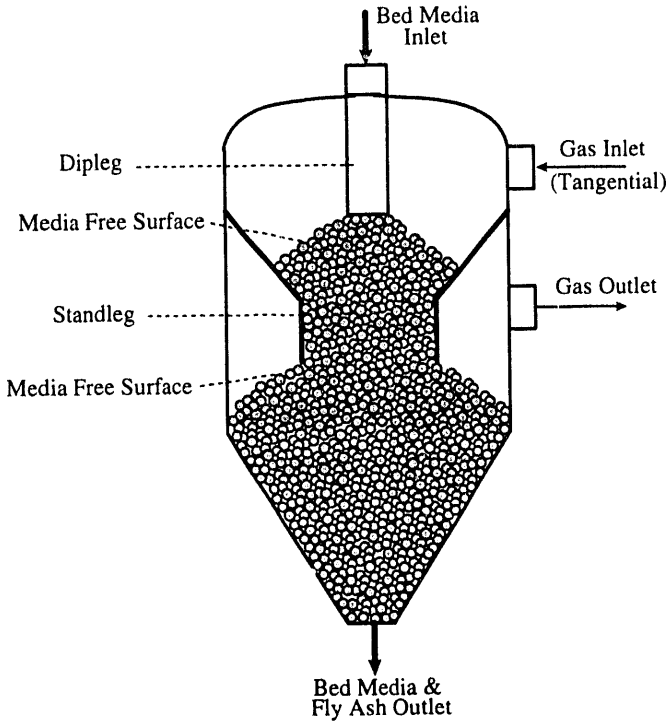

Figure 1. SMGBF Configuration Concept

and provides the potential to incorporate gas-phase contaminant sorbents into the filtering media. Recycle media operation recirculates granules from the SMGBF bottom withdrawal point to a top feed point, much as in the traditional moving granular bed filter approach. The SMGBF system performs this media circulation function by applying standleg, dense-phase flow and pneumatic transport that uses the dirty process gas to carry the granules. The granules are purchased bed media selected for its attrition resistance and it performance as a filtering media.

A general schematic diagram of the Once-Through SMGBF system in PFBC and IGCC applications is shown in Figure 2. The Once-Through SMGBF system is closely integrated with the power plant because of its need to utilize the power plant solid waste as the moving bed filter media while maintaining high power plant performance and economics. The major system components are:

- The SMGBF modules and their connecting piping
- The plant solid waste handling system (solids cooling and heat recovery, depressurization, transport)
- The pelletization system
- The pellet handling system (pressurization, transport, feeding and distribution)
- The pellet/dust cake handling system (cooling and heat recovery, depressurization, transport)

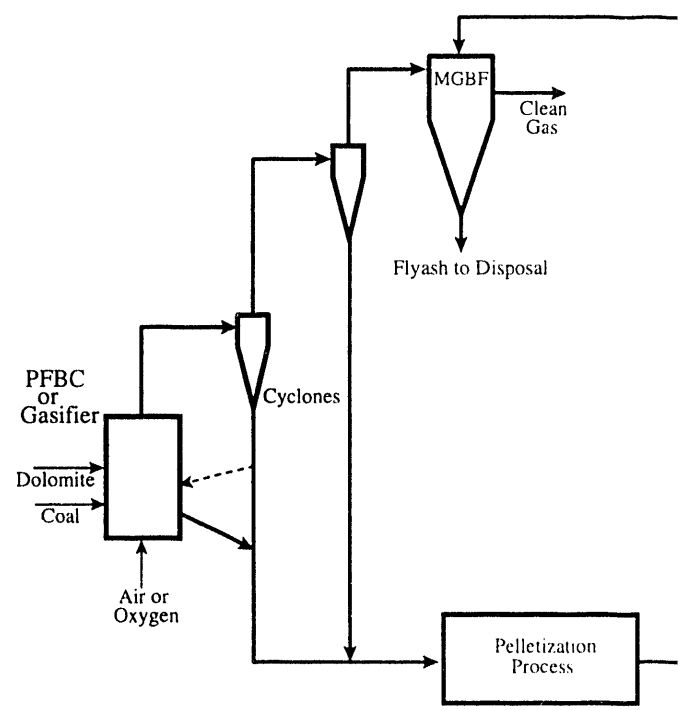

Figure 2. Once-Through SMGBF System Concept

There are several equipment options for each of these system components. The solids handling systems and pelletization system are generally commercially available components, but their selection is highly dependent on the nature of the solid waste streams, and they may need to be adapted to environments (eg., high pressure) where they have not been previously demonstrated. The pelletization system is a key system, and many pelletization techniques are available. The pelletization system must be integrated into the power plant to minimize complexity and to maximize energy efficiency, as well as being selected to produce sufficiently durable pellets for the SMGBF system.

The Recycle SMGBF system is Conceptually illustrated in Figure 3. Granules and captured fly ash are drained from the SMGBF and ash-granule separation is performed to remove a large portion of the captured fly ash.

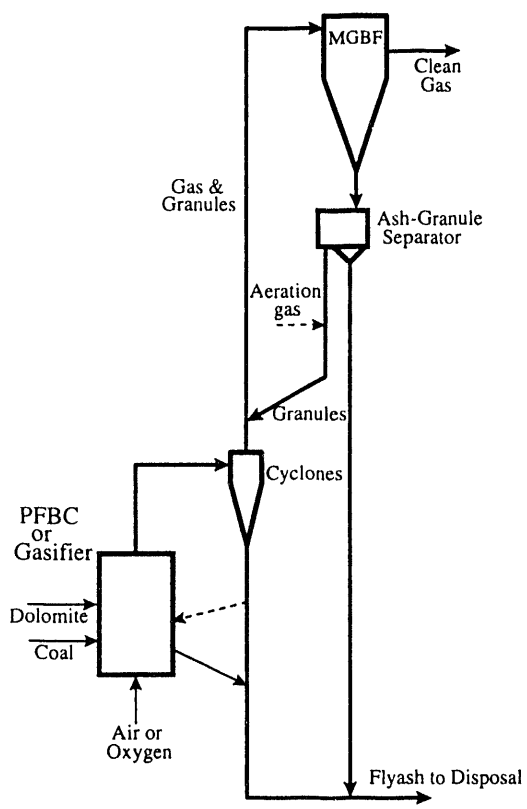

Figure 3. Recycle SMGBF System Concept

the SMGBF. The SMGBF configuration allows the transport to be accomplished by the dirty, process gas, and fly ash not separated from the granules in the ash-granule separator are reintroduced to the SMGBF.

PROJECT DESCRIPTION

The Standleg Moving Granular Bed Filter (SMGBF) development program is a four-phase program, a Base Contract and 3 Optional phases. The program has successfully completed the initial, Base Contract period, identifying and resolving barrier technical issues, and demonstrating conceptual feasibility. The Option 1 program has been initiated, confronting the major technical issues remaining for the SMGBF by conducting key component tests to optimize the SMGBF performance. Option 3 will demonstrate the SMGBF at an advanced, coal-fired power plant, pilot facility to be selected. Option 4 is devoted to development of multi-contaminant control features for the SMGBF, incorporating gas-phase contaminant sorbents into the moving bed media.

RESULTS

The SMGBF development program has completed the initial, Base Contract period. The barrier technical issues identified were:

- The ability to achieve sufficient levels of fly ash removal to meet environmental standards and turbine protection criteria,
- The ability to generate sufficiently durable pellets from plant solid wastes, using commercial, economical pelletization techniques integrated with advanced power plants.

The technical approach applied to achieve the Base Contract objective was to conduct commercial plant conceptual design evaluation, in combination with laboratory and bench-scale testing that focused directly on the barrier issues. These activities were performed in parallel to ensure that each had the appropriate perspective to provide significant results.

Two major test efforts were undertaken to establish the conceptual feasibility of the SMGBF with respect to its ability to achieve sufficient fly ash removal, a cold flow model test program, and a high-temperature, high-pressure (HTHP) test program. The cold flow model test program was conducted first to investigate several design and operating features of the SMGBF in a facility where performance phenomena within the SMGBF unit could be visualized, where detailed probing could be easily performed, and where equipment changes could be easily made. The HTHP testing was then conducted to show that the cold model trends were reproducible at HTHP conditions, and to demonstrate the SMGBF performance at small-scale, prototypic conditions. In parallel to the cold model test program, an effort to identify viable solid waste pelletization techniques, and to test pellet durability was conducted.

A new, cold flow model facility was designed and constructed, as shown in Figure 4. The model was constructed primarily of Plexiglas, with a vessel OD of 36", and a 36" long standleg having 12" OD. The test unit was designed to be highly sectionalized so that internal modifications could easily be performed, and was of a size that represented a reasonable scaling to commercial dimensions. Support facilities for the cold model test included a large bed media feed hopper located above the SMGBF vessel, a screw feeder and weight scale located below the SMGBF vessel to control and record the flow rate of bed media, a fly ash feed system

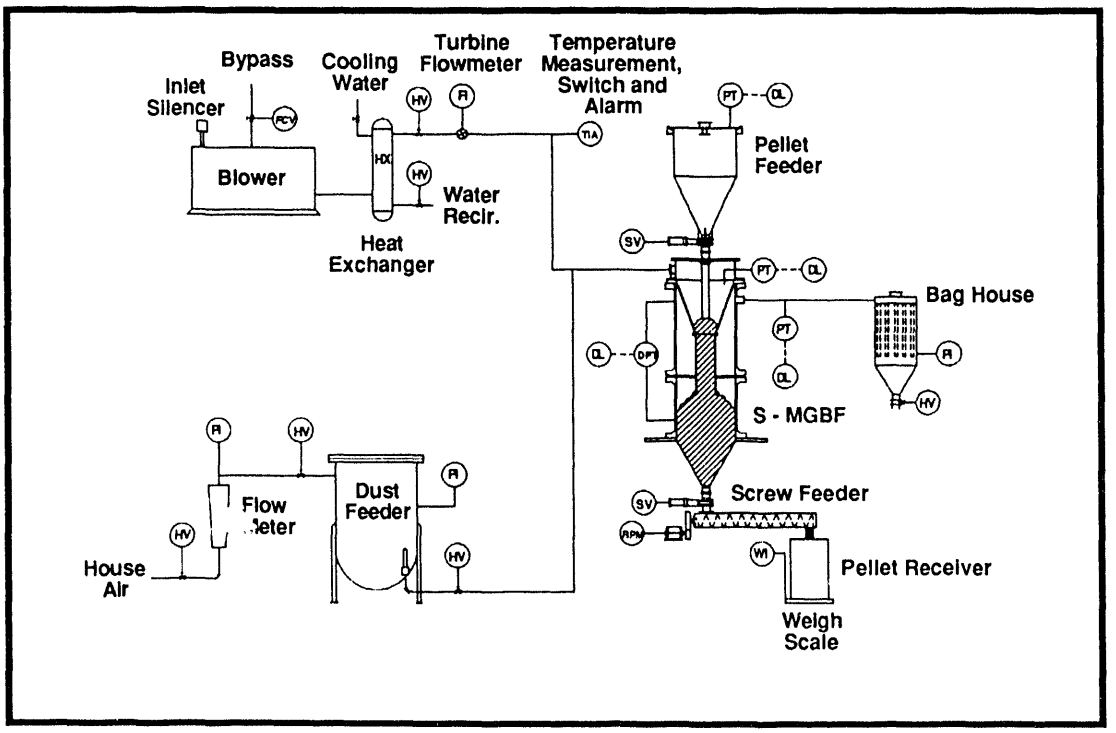

Figure 4. SMGBF Cold Model Facility

(K-Tron, loss-in-weight screw feeder) to inject fly ash into the inlet gas, a fabric filter to capture the fly ash in the SMGBF outlet gas so that its particle removal performance could be monitored, and instrumentation to measure the pressure drop profile within the SMGBF unit.

The cold flow model testing was performed with crushed acrylic particles, having an average diameter of about 3800 μm, as the bed media. The acrylic was selected because it had a density low enough to provide proper scaling to the actual, high-pressure SMGBF environment. A series of cold flow model tests were performed to characterize the gas flow and bed pressure drop characteristics, and the bed media flow characteristics, without fly ash feed. No visible fluidization of the bed media could be detected at standleg velocities up to 6 ft/s, exceeding the bed media minimum fluidization velocity of 5 ft/s. The clean bed pressure drop was consistent with existing packed bed pressure drop correlations. Fly ash injection testing was performed with fly ash from a PFBC pilot plant. Three SMGBF configurations were tested: the simple standleg configuration, a skirt section added at the base of the standleg, and a secondary, or topping bed added to surround the standleg skirt. Operating with a standleg gas velocity of about 3 ft/s, a bed media to fly ash mass feed ratio of about 10, and an inlet fly ash loading of about 6400 ppmw, total unit pressure drop was acceptable at less than 40 in-wg, and the particle removal performance achieved was:

- >97% removal with the simple standleg configuration,
- >99% removal with the added skirt section,
- >99.95% with the added topping bed.

Test durations were extended to relatively long periods of time to ensure that steady levels of performance were achieved. The cold flow model testing identified the key phenomena controlling the SMGBF performance, established the design features needed to achieve high levels of performance, and demonstrated the potential performance capabilities of the SMGBF. The cold flow model testing was representative of both the Once-Through and Recyle SMGBF performance capabilities.

Pelletization studies were performed by collecting representative solid waste samples from various advanced, coal-fired power plant units, and having commercial vendors prepare pellets from these wastes by several commercial techniques. Solid waste samples from both IGCC plants and PFBC plants were collected, as well as from some AFBC plants. All of these were successfully pelletized by several vendors. The generated pellets were then tested for durability by simple furnace heating tests, as well as a standard, rotary pellet attrition test rig that was adapted to high-temperature conditions. The attrition test subjected the pellets to much more severe attrition conditions than they would see in the SMGBF application. The results indicated that sufficiently durable pellets can be produced with advanced power plant solid wastes using conventional pelletization methods, but more evaluation is required to develop optimum techniques for solid waste sizing, water and binder content, mixing, and curing.

An existing HTHP test facility previously used to test ceramic barrier filter elements was adapted to test the SMGBF, as illustrated in Figure 5. The pressure vessel used had an OD of 40" and a total vessel height of about 10 feet. A new vessel head was constructed with a tangential gas inlet nozzle, and the natural gas-fired combustion system was moved to the head gas inlet location. The standleg internals inserted in

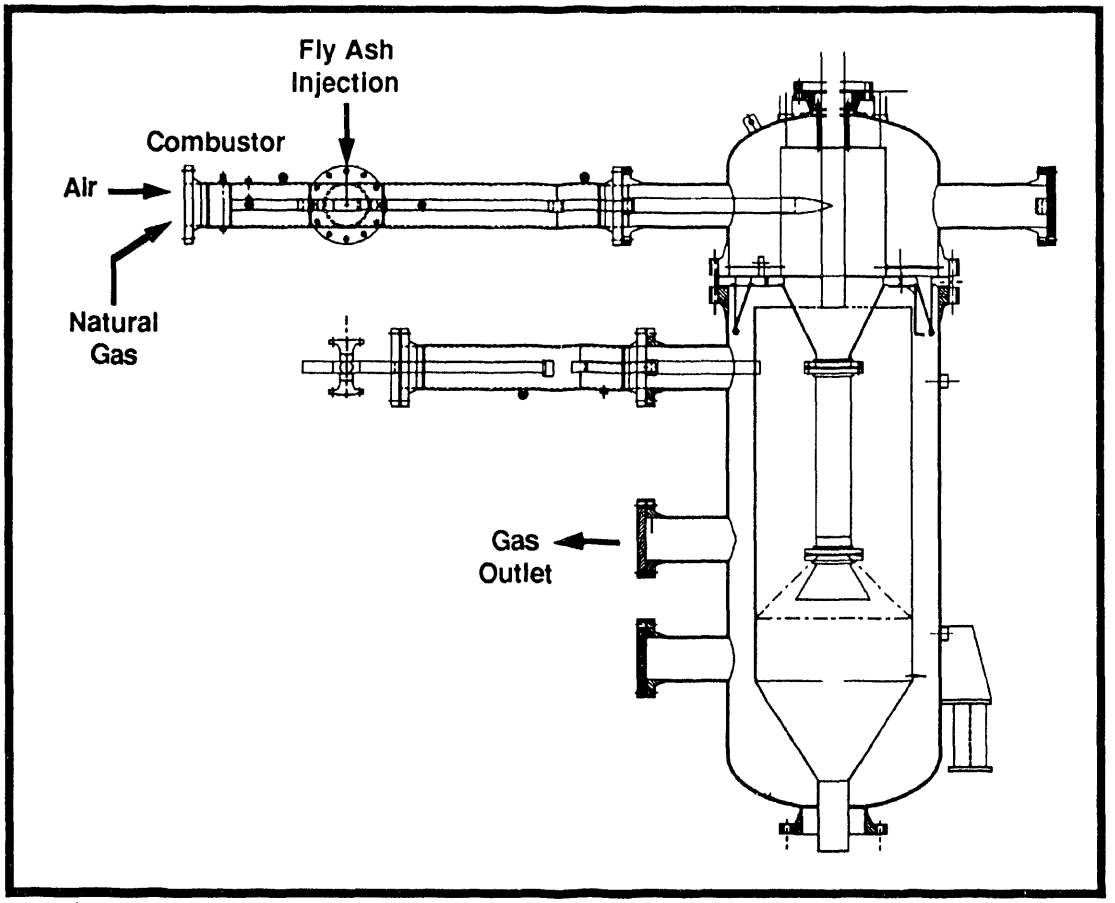

Figure 5. SMGBF HTHP Facility

the vessel had a 6" diameter, and were operated at a standleg velocity of about 3 ft/s in most of the testing. The standleg was constructed with a skirt section attached at its base, with its design based on the cold flow model results. A pressurized, water-cooled screw conveyor was added to the facility to control the flow of bed media through the unit. A batch feed hopper for bed media was located over the SMGBF vessel. The tests were performed under conditions simulating a PFBC application:

- Temperature of 1500 to 1600 ° F,
- Pressure of 100 psig,
- Injected PFBC fly ash at inlet loadings of 1000 to 7000 ppmw.

A total of 18, high-temperature test runs were completed. The tests were arranged in three major series:

1. On-off bed media flow with pelletized fly ash,
2. Continuous bed media flow with alumina beads,
3. Continuous bed media flow with pelletized fly ash.

The pelletized fly ash used in the tests was Aardelite, a commercial, pelletized conventional pulverized coal (PC) power plant fly ash product. The on-off bed media flow testing showed very high levels of particle removal performance, with

outlet loadings of 2 to 20 ppmw, but operational problems would not permit representative, steady operation to be achieved. Subsequent, continuous bed media flow testing with alumina beads, a mixture of 1/4" and 3/8" diameter beads, was performed without operational problems, but the higher density, more uniform sized and shaped alumina beads resulted in poorer particle removal performance, with outlet loadings of 6 to 250 ppmw. The final series of continuous bed media flow, pelletized fly ash tests achieved good performance, with acceptable unit pressure drop and outlet loadings of 8 to 14 ppmw. The HTHP testing showed a clear trend for higher particle removal performance as the mass ratio of bed media to fly ash flow was increased, and demonstrated a particle removal performance acceptable for commercial applications. Mass ratios of bed media to fly ash were in the range of 10 to 20 for acceptable performance.

Conceptual design evaluations were conducted for IGCC and Advanced-PFBC applications of the SMGBF technology, and comparisons were made with ceramic barrier filter technology by applying Reference Studies conducted previously for ceramic barrier filter applications (Ciliberti, et al, 1986; Foster Wheeler Development Corp., 1989). Process flow diagrams and material & energy balances were developed for the IGCC and Advanced-PFBC applications using SMGBF hot gas cleaning. Both Once-Through and Recycle SMGBF were evaluated. The SMGBF system equipment was sized and specified to the extent needed to develop equipment delivered and installed cost estimates and to produce rough plant equipment layouts. The impact of the SMGBF system on the power plant thermal efficiency was estimated based on estimated heat losses, SMGBF system gas pressure drop, and auxiliary power consumption. Finally, total power plant capital requirements, annual operating costs and cost-of-electricity (COE) estimates were made, updating the Reference Studies to the current plant economic premises.

The evaluation results show that the SMGBF system is economically competitive with ceramic barrier filters for IGCC and Advanced-PFBC applications. The installed equipment costs of the SMGBF system are comparable to those of the ceramic barrier filter systems, although the pelletization system adds a significant equipment cost to the Once-Through SMGBF system:

- Installed equipment cost for IGCC application
  - Once-Through SMGBF: 32 - 41 $/kW
  - Recycle SMGBF: 17 - 22 $/kW
  - Ceramic barrier filter:, 11 - 19 $/kW

- Installed equipment cost for Advanced-PFBC application
  - Once-Through SMGBF: 31 $/kW
  - Recycle SMGBF: 18 $/kW
  - Ceramic barrier filter: 17 $/kW

The Once-Through SMGBF system has a higher total power plant capital cost, annual operating cost, and COE than the ceramic barrier filter system for IGCC and Advanced-PFBC, but these cost increases are small, about 1% for IGCC, and about 3-5% for Advanced-PFBC. The waste material issued from the plants using Once-Through SMGBF potentially has a superior environmental character, or even byproduct possibilities. The Recycle SMGBF system total power plant capital cost, annual operating cost and COE is nearly identical with that of the ceramic barrier filter system.

The Base Contract conclusions reached are:

- Design features have been identified in the cold flow model testing that optimize the SMGBF particle removal performance.

- Cold flow model and HTHP testing trends are consistent.

- Particle penetration levels of 6 to 14 ppmw are representative performance levels based on the HTHP testing, with the cold flow model testing indicating that even higher performance levels can be achieved.

- Particle removal performance increases and the unit pressure drop decreases as the mass feed ratio of bed media to fly ash increases. Ratios of 10 to 20 are required for acceptable performance.

- Sufficiently durable pellets can be generated from advanced power plant solid waste using conventional pelletization techniques, but further evaluation of optimum solid waste sizing, water and binder content, mixing, and curing procedures is needed.

- The pelletized solid waste may provide particle removal performance superior to more regular shaped and uniformed sized purchased granules.

- The Once-Through SMGBF total power plant capital requirement and COE are only marginally higher (1 to 5%) than that for ceramic barrier filter systems in both IGCC and Advanced-PFBC applications.

- The Recycle SMGBF system is comparable in capital cost and COE to the ceramic barrier filter system for both IGCC and Advanced-PFBC applications.

REFERENCES

Ciliberti, D. F., et. al., Westinghouse, "Performance Evaluation of a Ceramic Cross-Flow Filter on a Bench-Scale Coal Gasifier", Eighth Quarterly Report and Monthly Status Report for September 1, 1986 - September 30, 1986, Contract No. DE-AC21-86MC21338.

Foster Wheeler Development Corporation, Second-Generation PFBC Plant Conceptual Design and Optimization of a Second Generation PFB Combustion Plant, Phase 1, Task 1, Volume 1, DOE/MC/2023-2825, September 1989.

5.8 MTCI Acoustic Agglomeration Particulate Control

CONTRACT INFORMATION

Contract Number	DE-AC21-89MC26288
Contractor	Manufacturing and Technology Conversion International, Inc. (MTCI) P.O. Box 21 Columbia, MD 21045 (301) 982-1292
Contractor Project Manager	Ravi R. Chandran
Principal Investigators	Ravi R. Chandran Momtaz N. Mansour Alan W. Scaroni (Penn State U.) Gary H. Koopmann (Penn State U.) John L. Loth (West Virginia U.)
METC Project Manager	Darren J. Mollot
Period of Performance	June 15, 1989 to June 1, 1995

Schedule and Milestones

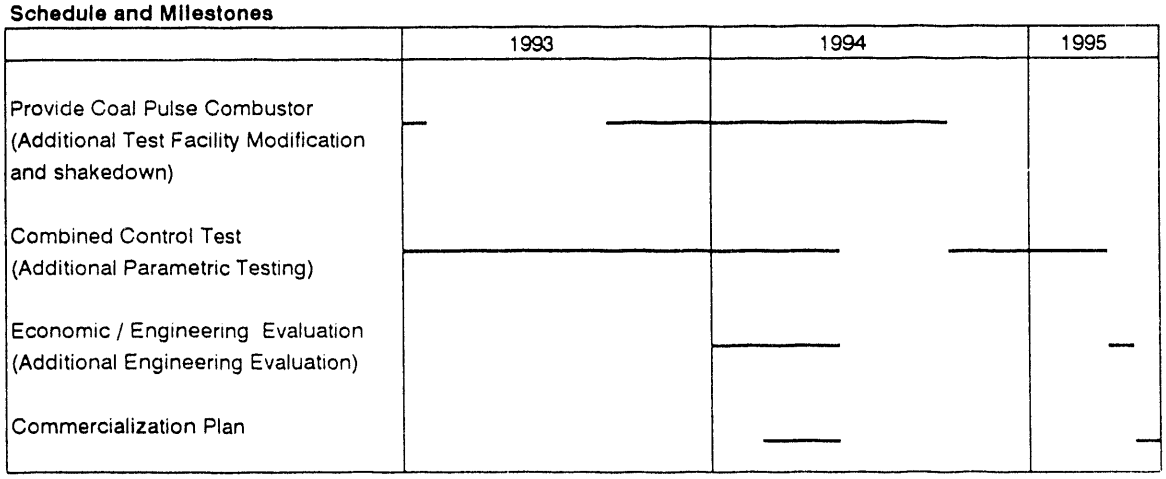

OBJECTIVES

The overall objective of this project is to demonstrate pulse combustion induced acoustic enhancement of coal ash agglomeration and sulfur capture at conditions typical of direct coal-fired turbines and PFBC hot gas cleanup. The goal of the program is to support the mission of the Department of Energy (DOE) for developing coal-fired combustion gas turbines and advanced PFBC systems.

Specifically, the goals are to:

- Demonstrate the pulse coal combustion, ash agglomeration and sulfur capture,
- Achieve/Meet
  - combustion efficiency > 99%
  - turbine tolerance criteria
    - -- particulate loading in the 100 - 150 ppmw range
    - -- particle size
      < 10 microns with 99%
      < 3 microns
    - -- NO_x @ 15% O_2
      < 125 ppm
    - -- SO_2 @ 15% O_2
      < 75 ppm
  - New Source Performance Standards
    - -- SO_2 < 1.2 lb/MMBtu
    - -- NO_x < 0.6 lb/MMBtu
    - -- particulates
      <0.03 lb/MMBtu

BACKGROUND INFORMATION

Growing concern over global warming, dwindling environmental quality, accelerated waste generation rate, and dependence on foreign oil has spawned an interest in and the need for advanced energy technologies in general and advanced combustion technologies in particular. This, together with the interest in increasing the utilization of coal, entails the development of innovative concepts which promise higher combustion efficiency, higher sulfur capture efficiency, lower NO_x emissions, lower particulate emissions, and greater fuel flexibility. The advanced combustion technologies currently under demonstration include Fluidized Bed Combustion (FBC), Staged Slagging Combustion (SSC), and Limestone Injection Multistage Burning (LIMB). While these technologies promise lower SO_2 and NO_x emissions compared to conventional technologies, each possesses one or more of the following limitations:

- Operates either in the combined cycle format but at a lower peak cycle temperature (e.g., 1550°F rather than at ~ 2300°F) or at atmospheric system pressure and therefore not in the combined-cycle format. This results in lower overall cycle thermal efficiency and consequently higher specific fuel consumption and typically higher emissions levels (CO_2, CO, SO_2, NO_x, and particulate) per pound of coal burned.
- Operates in the slagging mode which poses difficulty with regard to design, reliability, material selection, compliance with emissions standards in the absence of downstream particulate collection equipment, and economics.
- Requires barrier filters to control particulate emissions which pose concerns regarding durability, economics, and limited operating range.
- Requires specially prepared sorbents or some process enhancement to improve calcium utilization and achieve 90% SO_2 retention and this significantly increases the operating cost of the unit.

In response to this challenge, MTCI has developed an advanced compact pulse combustor island for direct coal-firing in combustion gas turbines. This combustor island comprises a coal-fired pulse combustor, a combined ash agglomeration and sulfur capture chamber (CAASCC), and a hot cyclone (**Figure 1**). In the MTCI proprietary approach, the pulse combustion-induced high intensity sound waves improve sulfur capture efficiency and ash agglomeration. The resulting agglomerates allow the use of

commercial cyclones and achieve very high particulate collection efficiency.

Many investigations have confirmed the ability of acoustic fields to agglomerate fly ash to increase particle size. However, the majority of this work focused on the agglomeration of unimodal distributions of fine aerosols which were not fully representative of the conditions within a gas turbine combustor utilizing standard grind pulverized coal or coal-water mixtures, particularly in conjunction with lime sorbent injection processes. Therefore, the conclusions drawn from experimental and theoretical investigations to date using fine unimodal distributions, such as the optimum acoustic sound pressure levels and frequency, may not be valid as applied to the MTCI coal-fired gas turbine technology.

In the MTCI proprietary approach, sorbent particles are injected into a gas stream subjected to an intense acoustic field. The acoustic field serves to improve sulfur capture efficiency by enhancing both gas film and intra-particle mass transfer rates. In addition, the sorbent particles act as dynamic filter foci, providing a high density of stagnant agglomerating centers for trapping the finer entrained (in the oscillating flow field) fly ash fractions. The fly ash fractions have particle sizes which fall primarily in the range from less than 1 to 20 microns. Therefore, by introducing sorbent particles which are primarily concentrated in the size range from 20 to 80 microns, a bimodal distribution is created. The bimodal distribution offers several advantages. First, by increasing the density (in the gas) of large stagnant trap centers, an accelerated agglomeration rate can be achieved. Second, agglomeration can be efficiently performed at a significantly lower acoustic frequency range compared to unimodal distributions containing only finer fly ash fractions.

The effectiveness of particle agglomeration at low frequencies is extremely significant. The rate of agglomeration is strongly influenced by the acoustic intensity level. Since low frequencies are attenuated less than high frequencies, lower frequency operation is anticipated to be more effective. Furthermore, low frequencies are not expected to affect performance of turbine blades, while frequencies in the kHz range may couple into the system's natural frequencies. Finally, the cut-off particle diameter for 50% entrainment increases with a decrease in frequency and therefore lower frequency operation results in the entrainment of a larger proportion of a given particle feed size distribution and places less constraint on the upper limit for particle growth.

The major advantage of the MTCI combustor island shown in Figure 1 is the ability to use standard grind, unbeneficiated or partially beneficiated coal as fuel. It offers the following additional benefits:

- Pulse combustion provides for a relatively high volumetric heat release rate and high combustion efficiency in a shorter residence time. This gives rise to a compact combustor.

- The pulse combustor is an inherently low NO_x burner and therefore NO_x emissions are low.

- While a conventional steady flow combustor results in pressure loss, the pulse combustor provides for a combustion-induced pressure boost. The net pressure gain is therefore significant and offers the potential for higher specific power output or lower specific fuel consumption.

- Employs sonic-enhanced coal ash agglomeration and dry ash rejection. This avoids the need for slagging mode of operation which poses difficulty with regard to design, reliability, material selection, compliance with emissions standards, and economics. Ash agglomeration allows the use of conventional cyclones to achieve very high particulate

collection efficiency and eliminates the need for barrier filters which pose concerns regarding durability and economics.

- Efficient in-situ sulfur and alkali capture in sonic-enhanced mode.

PROJECT DESCRIPTION

The overall objectives of this project are to experimentally develop the basic design framework for scale-up of this technology and to experimentally characterize a laboratory-scale gas turbine combustor island.

The specific objectives of this program are to:

- Perform system shakedown and parametric testing;
- Conduct applied studies for the development of a combined acoustic agglomeration and sulfur capture model and an aerodynamic analysis to establish the aerovalve design data base;
- Conduct engineering and economic evaluations of the system; and
- Develop a design code for combustor island scale-up.

A team has been formed with MTCI as the prime contractor and Penn State University (PSU) and West Virginia University (WVU) as subcontractors to MTCI. MTCI is focusing on hardware development and system demonstration, PSU is investigating and modeling acoustic agglomeration and sulfur capture, and WVU is studying aerovalve fluid dynamics.

Apparatus

To demonstrate proof-of-concept, a laboratory-scale bimodal test facility has been designed, fabricated, and integrated for elevated pressure (4 atm.) operation at MTCI (**Figure 2**). It incorporates an advanced tailpipe-agglomeration chamber interface configuration, a coal preheating arrangement, a refractory-lined cyclone to simulate hot gas cleanup, and elaborate instrumentation and controls to enable complete process characterization and safe operation. The test facility comprises the following components/ subsystems:

- Coal and sorbent feed system.
- Air and natural gas supply system.
- Pulse combustor.
- Acoustic agglomeration and sulfur capture chamber.
- Refractory-lined cyclone.
- Fuel preconditioner.
- Heat exchanger.
- Pressure letdown valve.
- Baghouse.
- Steam circuit.
- Cooling water circuit.
- Instrumentation and controls.

Initial tests were performed with one cyclone (primary cyclone) on-line. The design velocity for this cyclone was kept modest (40 to 50 ft/s) to reduce potential agglomerate breakup during transit. This, however, reduced the particulate capture efficiency so that some 10 μm

size particles were leaving with the cyclone exit flue gas. Therefore, a secondary cyclone was added (as shown in Figure 2) to enhance overall solids capture efficiency.

System Tests and Results

At MTCI, system shakedown tests were initially conducted at pressures of 2 and 3 atm. with natural gas and pulverized coal (Seacoal - Pittsburgh No. 8). After verification of satisfactory system operation, 27 screening tests have been performed. The system has been in operation for about 193 test hours.

The parameters varied include pulverized sorbent types, sorbent injection location and Ca/S molar feed ratio. The sorbent types examined include a dolomite (Dolofil by Pfizer), a limestone (Linden Falls), a precalcined lime (Annville by Wimpey Minerals), a pulse combustor calcined and classified (PCC) dolomite (Pfizer Dolofil), and a PCC lime (Annville by Wimpey Minerals).

Tests have been performed with injection of:

- Coal into the pulse combustion chamber and no sorbent injection,
- Premixed coal and sorbent (dolomite or limestone) into the pulse combustion chamber (P.C.),
- Coal into the pulse combustion chamber and sorbent (dolomite, lime, mixture of lime and Baltimore Gas and Electric power plant fly ash, cold air classified lime, PCC dolomite and PCC lime) into the inner section of the agglomeration chamber (A.C.).

The PCC dolomite and PCC lime were generated in the MTCI laboratory-scale pulsed atmospheric fluidized combustion system which integrates a pulse combustor with a bubbling fluidized bed.

The reader is referred to an earlier paper [1] for test results from the initial test series. The overall test results indicated the following:

- Stable pulse combustor operation was achieved with a variation in firing rate from 1.67 MMBtu/hr to 2.52 MMBtu/hr at 3 atm. system pressure.
- The pressure oscillations were robust and the sound pressure level (SPL) varied from 174 to 186 dB with an increase in firing rate.
- The combustion efficiency exceeded 99%.
- The sulfur capture efficiency ranged from 38 to 98.5%. Calcium utilization was the highest with dolomite followed by lime and then by limestone. Limestone was pretty good in capturing sulfur (77%) at low firing rate but inferior (38% sulfur capture) at medium firing rate probably due to sintering. Sulfur capture exhibited an increase with Ca/S feed ratio for PCC dolomite and PCC lime injection into the A.C. (see **Figure 3**). The calcium utilization was low due probably to the high operating temperature (2000-2200°F) in the A.C.
- NO_x emissions were in the 82 to 200 ppm range when corrected to 15% O_2 (**Figure 4**). NO_x emissions tended to increase with dolomite feed rate corroborating the catalytic effect of calcined dolomite on NO_x formation reactions. With PCC lime injection into A.C., the NO_x emissions did not increase from the base case (no sorbent injection) level and remained below the 125 ppm @ 15% O_2 target for turbine tolerance.
- The solids loading in the cyclone exit flue gas ranged from 23 ppmw (with two cyclones) to 450 ppmw (with one cyclone). The highest

loading was obtained with dolomite injection into the P.C. and this is attributed to particle fragmentation and fines generation in the high heating rate environment of the pulse combustor. Penn State University (PSU), in an independent study, similarly found increasing decrepitation with an increasing magnesium oxide content. The high purity limestone (Linden Falls) was tested based on the recommendation of PSU and it also was found to decrepitate albeit to a lesser extent than dolomite. The injection of lime into the agglomeration chamber was therefore attempted and the test results indicate the merit of that option. With one cyclone on-line, the cyclone exit flue gas solids loading was below 150 ppmw and within the target goal for gas turbine particulate tolerance. With one cyclone on-line , the baghouse catch indicated about 30% by weight of particles exceeding 3 microns in size. Turbine tolerance criteria require less than 1% by weight of particles exceeding 3 microns in size and therefore a secondary, high efficiency cyclone was added to the system. Ideally, this secondary cyclone should be located downstream of the primary cyclone and upstream of the heat exchanger. However, due to such considerations as space constraints leading to repiping difficulties and cost factors, it was decided to locate the secondary cyclone downstream of the heat exchanger but upstream of the pressure letdown valve. With two cyclones on-line, coal firing and no sorbent injection, the cyclone exit solids loading dropped to 32 to 44 ppmw range (see **Figure 5**). With PCC dolomite injection, the cyclone exit solids loading was higher (72 ppmw) possibly due to sorbent fines generation. With PCC lime injection, the cyclone exit solids loading dropped to the 23 to 27 ppmw range (see Figure 5) which is good enough to meet the New Source Performance Standards (NSPS).

- The particle size distributions for the primary and secondary cyclone catch material and the secondary cyclone exit solids are shown in **Figure 6**. The data correspond to the coal-fired test with no sorbent injection. The secondary cyclone exit stream was iso-kinetically sampled with a pre-calibrated cascade impactor. The two cyclone catch material were sized by the BAHCO method. The d50 cut sizes for the three streams are also shown in Figure 6. There seems to be room for improvement of the second cyclone performance and thereby decrease both the larger size (> 3 microns) particle population and the total solids loading in the second cyclone exit stream. For example, the "core separator" concept of LSR Technologies, Inc. [2] could be used in lieu of the two cyclones to achieve higher particulate collection efficiency.

- The size distributions of the particles collected by the cascade impactor in the case of tests without and with PCC lime injection are shown in **Figure 7**. The particle sizes are relatively larger and the quantities/weights are smaller for the case of lime injection in comparison to that for no sorbent injection. This is further evidence for the effectiveness of bimodal agglomeration. Note that the ash generated from coal combustion typically has a bimodal particle size distribution and agglomerates in the presence of an acoustic field even without sorbent injection. For example, based on literature data [3], about 30% by weight of ash generated in conventional combustion corresponds to a size below 6.4 microns. Assuming a linear variation in cyclone collection efficiency up to 6.4 microns and 100% capture efficiency beyond that size, a first order estimate for solids loading in the flue gas corresponding to the combustion conditions of Figure 6 is 429 ppmw. The measured loading was in the 32 to 44 ppmw range indicating the advantages of acoustic agglomeration. Let the

acoustic agglomeration enhancement factor (AAEF) be defined as:

$$AAEF = 100 (1 - TMA/TMO)$$

where TMO is the mass loading at the exit of the cyclone without acoustic pretreatment and TMA is the mass loading at the cyclone exit with acoustic pretreatment. Then AAEF for the no sorbent and lime injection cases turn out on average to be 91 and 94%, respectively. This is a substantial improvement and verifies the merit of pulse combustion-induced bimodal agglomeration.

- The measured emissions of SO_2, NO_x and particulates with PCC lime injection were all below the levels stipulated by NSPS as shown in **Figure 8**.

- CO and total hydrocarbon (THC) emissions were generally below 10 and 5 ppm respectively @ 3% O_2.

The test results obtained from the MTCI laboratory-scale combustor island are encouraging and meet gas turbine tolerance criteria and New Source Performance Standards.

PSU STUDY

The objective of the work being conducted at Penn State University is to provide scientific verification of the MTCI pulse combustion technology in the areas of sulfur capture and bimodal agglomeration. The project consists of two parts: 1) investigation of the fundamental behavior of sorbents under pulse conditions, particularly the effect of rapid sorbent particle heat-up and the presence of an acoustic field on calcination and sulfation, and 2) a fundamental investigation of acoustic bimodal agglomeration.

The presence of an acoustic field within the combustion environment influences the mass transfer of SO_2 to particle surfaces and the movement of particles themselves within the gas stream. The result is an enhancement in the rate and extent of sulfation of limestone in the system. Mitigation of SO_2 from the gases produced during the combustion of fossil fuels is necessary given the new SO_2 emission standards. In addition, the agglomeration of very fine particles is necessary for the application of this technology to produce hot combustion gases for gas turbines. Gas turbines have a very low tolerance level for particles within the gas stream. Removal of the coarser size fractions can be accomplished by current technology; however, removal of micron and submicron particles is more difficult. Agglomeration of the micron size ash and sulfated calcine particles forms larger particles that can be removed more efficiently by conventional particle collection technology.

Calcination and Sulfation Studies and PCGC-2 Modeling

Experimental studies in the area of calcination and sulfation have shown that under high heating rates the fragmentation of sorbents is influenced by the sorbent type, particle size and particle temperature. Sorbent type was the most important factor. Dolomites and limestones containing high levels of magnesium fragment to a greater extent during heating producing significantly finer calcine than high purity limestones.

The extent of calcination of sorbents was relatively insensitive to particle size; however, the extent of sulfation was affected by particle size. Particle size affects heat transfer such that smaller particles calcine at a slightly greater rate than larger particles (**Figure 9**). The extent of sulfation was related to particle size as shown in **Figure 10**. An increase in the S/Ca molar ratio of 26 to 32% was observed for a dolomite and a

high purity limestone, respectively, when the average particle size was decreased from 89 to 45 μm. On the basis of sorbent utilization the performance of lower purity stones was not significantly different than that of high purity stones. This may have implications regarding sorbent selection for the MTCI pulse combustor system due to the stringent requirements for low particle loading of fines.

The experimental data from the calcination and sulfation studies was used to modify an existing combustion model, i.e., PCGC-2. PCGC-2 can model gaseous turbulent diffusion flames and pulverized coal combustion. PCGC-2 has been successfully modified to include mechanisms that define the calcination, sintering and sulfation process. Empirically obtained rate equations were used to model the processes of calcination and sulfation. A shrinking core model was used to model calcination. Processes influencing sulfation include: the rate of calcination, product layer diffusivity, pore diffusion, external heat and mass transfer. Pore diffusion dominates for large particles, i.e., 100 μm, whereas product layer diffusion dominates for submicron size particles. Heat and mass transfer effects are more limiting in larger particles. The model assumes that sulfation is irreversible. Sulfur release during combustion is assumed to be proportional to the coal weight loss and local instantaneous equilibrium chemistry is assumed for the conversion of sulfur to sulfur dioxide.

The model was fitted to the experimental data predicting the calcination and sulfation of particles 45, 63, and 89 μm in size (Figures 9 and 10). The model further predicts that the extent of sulfation increases with increasing sound pressure level due to the increase in mass transfer coefficients (**Figure 11**). Modeling by PCGC-2 shows that an acoustic field generates large relative velocities between the particles and the gas stream. The increase in slip velocity between the particle and gas stream increases the heat and mass transfer to and from the particles. The increase in the mass transfer coefficient, i.e., Sherwood number, with increasing sound pressure is shown in Figure 11. An increase in the Sh number results in an increase in the rate at which SO_2 reaches the surface of the calcine, thereby increasing the rate of sulfation. In addition, highly porous calcines ($\epsilon = 0.5$) show a greater increase in the extent of sulfation than less porous calcines ($\epsilon = 0.15$), i.e., approximately 12% at higher sound pressure levels (**Figure 12**).

Another benefit of the presence of the acoustic field is due to the agglomeration of small particles to form larger agglomerates. Calcine particles that agglomerate experience a greater rate of diffusion of SO_2 to the calcine surfaces than smaller calcine particles. The Sh number is proportional to the mass transfer coefficient which determines the rate of SO_2 diffusion to the particle. Therefore, the rate of SO_2 diffusion to the surface of smaller particles that make up an agglomerate is greater than the rate of SO_2 diffusion to individual small particles.

Acoustic Agglomeration

This work has provided new insight into the interaction mechanisms between small particles under the influence of a strong acoustic field. These mechanisms are associated with what is referred to as acoustic agglomeration caused by the relative motion and collisions between particles in a high intensity sound field. The agglomeration process has potential use in air pollution control to enhance the performance of conventional particle filtering devices. A number of existing acoustic agglomeration models are reviewed and presented graphically in **Figure 13**. A quantitative analysis of the proposed theories was conducted with parameters representing those of the physical experiments. The evaluation of the different models leads to the conclusion that mutual scattering interaction, an effect proposed as an important agglomeration volume refill

factor, does not contribute significantly to the agglomeration process if gravitational effects are included in the computations. On the other hand, hydrodynamic effects due to asymmetric flow fields around the particles generate significant particle attraction in the direction of the acoustical axis (**Figure 14**). This so-called "acoustic wake effect" is shown to contradict another mechanism referred to as the mutual radiation pressure interaction. A comparative analysis of the two effects suggest that the competing interaction forces might lead to "pseudo" agglomerates, i.e., pairs of particles held together by an acoustically induced captive force field.

To evaluate these findings, experimental analysis were carried out with a small-scale observation chamber using a CCD camera in conjunction with a high resolution video system. A homogenous acoustic velocity field is generated by two rectangular, flat-membrane loudspeakers which comprise two opposing walls in the observation chamber. Glass microspheres (diameters 8,1 and 22.1 μm) and quartz particles (diameter < 50 μm) are used for the observation of interaction and agglomeration trajectories under the influence of an intense acoustic velocity field (1.2-0.53 m/s at 400-900 Hz). The recorded digitized images show a number of similar-sized particles which come together forming larger agglomerates. It is proposed that similarly sized particles first agglomerate to form larger clusters. These larger clusters then find particles of similar size forming larger agglomerates. This process is enhanced at higher sound frequency levels and pressure levels. For dissimilar particle sizes, the particles displayed an axial change of direction resulting missed collisions. In general, this behavior did not lead to particle agglomerations. The experimental evidence suggests the conclusions given in **Table 1** regarding the various acoustic agglomeration models.

WVU STUDY

The quality of an aerovalve is expressed in terms of diodicity (DIO), defined as the ratio of forward mass flow to reverse mass flow. Thus, diodicity is a strong function of the aerovalve: geometry, size, inlet pressure and temperature and the type of gas used as well as the exit back pressure. The aerovalve operates in a non-steady flow field inside the pulse combustor. The length of the aerovalve (L_a) is at lease ten times shorter than the length of the combustor tailpipe (L_t), the latter controls the combustion pulse frequency. The pulse frequency is approximately equal to $f_v = \frac{1}{2}a/L_t$, where (a) is the speed of sound. Thus the resonance frequency of the short aerovalve by itself is about ten times higher than the combustion pulse frequency. Therefore, non-steady aerodynamic effects are negligible and a quasi-steady state flow analysis can be applied to compute its mass flow rate as a function of pressure differential. This justifies aerovalve diodicity testing using steady flow tests in both the forward and the reverse flow directions. During a pulse combustion cycle, the peak as well as the mean forward and reverse mass flow rates can be calculated by integrating the instantaneous mass flow rates based on pressure as a function of time for any given wave form.

Besides the need for high diodicity and small size, the aerovalve must also have low total pressure loss in forward flow. Next, the pressure differential, where the forward flow starts to choke and the diodicity drops off, should be high. The aerovalve must be easy to manufacture and to keep clean.

The MTCI aerovalves tested incorporate a venturi-type geometry with a rapid contraction to a throat area (A_{th}) with a sharp angle transition to a small angle diffuser where the flow expands to area (A_2). Reverse flow is unable to negotiate the sharp turn at the throat and therefore separates at

the throat without any diffusion type pressure recovery.

For the cold flow ideal subsonic isentropic flow venturi-type aerovalve, the diodicity (DIO) equals the venturi area ratio $\bar{A} = A_2/A_{th}$. This can be explained as follows. In this case there is no loss in total pressure and the flow adjusts itself such that the exit static pressure equals the back pressure. Thus the exit total to static pressure ratio and exit Mach number are identical for both forward and reverse flow. In cold flow the total temperature for the flow in both directions is the same and thus also the exit velocity and densities are the same. The forward to reverse mass flow ratio equals then the forward flow to reverse flow exit area ratio which is $\bar{A}$.

For hot flow, the temperature ratio (T_r) between the hot combustion chamber temperature and that of the cold air intake plenum further increases the diodicity. Because the exit Mach number is the same with identical pressure ratio, the exit static temperature ratio will also be equal T_r, thus the exit density ratio is equals $1/T_r$ and the exit speed of sound ratio equals $T_r^{1/2}$ and the exit velocity ratio as well. Consequently, the forward to reverse mass flow ratio equals $\bar{A}T_r^{1/2}$ (see **Figure 15**). The higher the operating temperature difference between the pulse combustion chamber and the air inlet plenum, the higher the diodicity and the wider the dynamic range. The diodicity, however, becomes lower and poses a problem for gas turbine and vitiated air pulse combustion modes of operation. Further development is therefore needed for superior performance in these cases.

Experiments were conducted in a cold flow test facility at room temperature. **Figure 16** is a plot of the mass flow through an aerovalve of both forward and reverse flow against ΔP as measured by the differential manometer. For a ΔP of 6 psi, one can see where both the forward and reverse flows choke. This condition restricts both flow cases to the same throat sonic velocity but the diffuser losses in forward flow actually reduces the density and thus the forward mass flow to less than the reverse mass flow value at the same pressure drop. This makes the diodicity slightly less than one. It is a condition that does not occur in actual operation but it gives a feel of how the diffuser losses can play a significant role in the aerovalve performance.

A quasi-steady flow analysis was also performed using a numerical code. Diodicity of the aerovalve was determined as a function of area ratio, temperature ratio, and pressure ratio. With an increase in pressure ratio, the forward flow was found to choke first and the reverse flow later. This tends to place a limit on the pulse combustor pressure rise/dynamic pressure/SPL that can be achieved. WVU and MTCI have formulated an advanced aerovalve concept to delay the onset of forward flow choking, achieve high diodicity, and permit ease of fabrication.

FUTURE WORK

MTCI has formulated an alternate advanced concept to meet the DOE mission-oriented criteria for performance, emissions and economics. Additional investigations are planned at MTCI, PSU and WVU to expand the combined control tests and further develop the MTCI advanced coal-fired gas turbine combustion technology.

REFERENCES

1. Mansour, M.N. and R.R. Chandran, "Sonic Enhanced Ash Agglomeration and Sulfur Capture, Proc. Tenth Annual International Pittsburgh Coal Conference, Pittsburgh, PA, Sept. 20-24, 1993, pp. 190-195.

2. Smolensky, L.A. and B.H. Easom, "Particulate Control for Coal-Fueled Diesel Engine Exhaust," Proc. of the Joint Contractors Meeting: FE/EE Advanced Turbine Systems Conference, FE Fuel Cells and Coal-Fired Heat Engines Conference, DOE/METC-93/6132 (NTIS/DE93011308), August 1993, pp. 327-333.

3. Diehl, R.C., P.J. Loftus, D.B. Stickler, and P.W. Pillsbury, "Emissions Control in a Coal-Fueled Gas Turbine Slagging Combustor for Utility Applications," Proc. Seventh Annual Coal-Fueled Heat Engines and Gas Stream Cleanup Systems Contractors Review Meeting, DOE/METC-90/6110 (NTIS/DE90000480), March 1990, pp. 113-122.

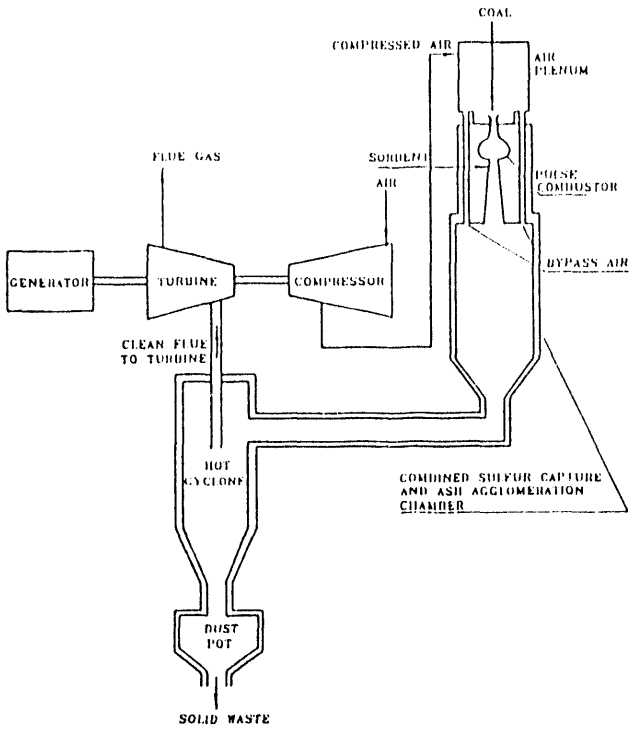

Figure 1. MTCI's Combustor Island for Direct Coal-Fired Gas Turbine Application

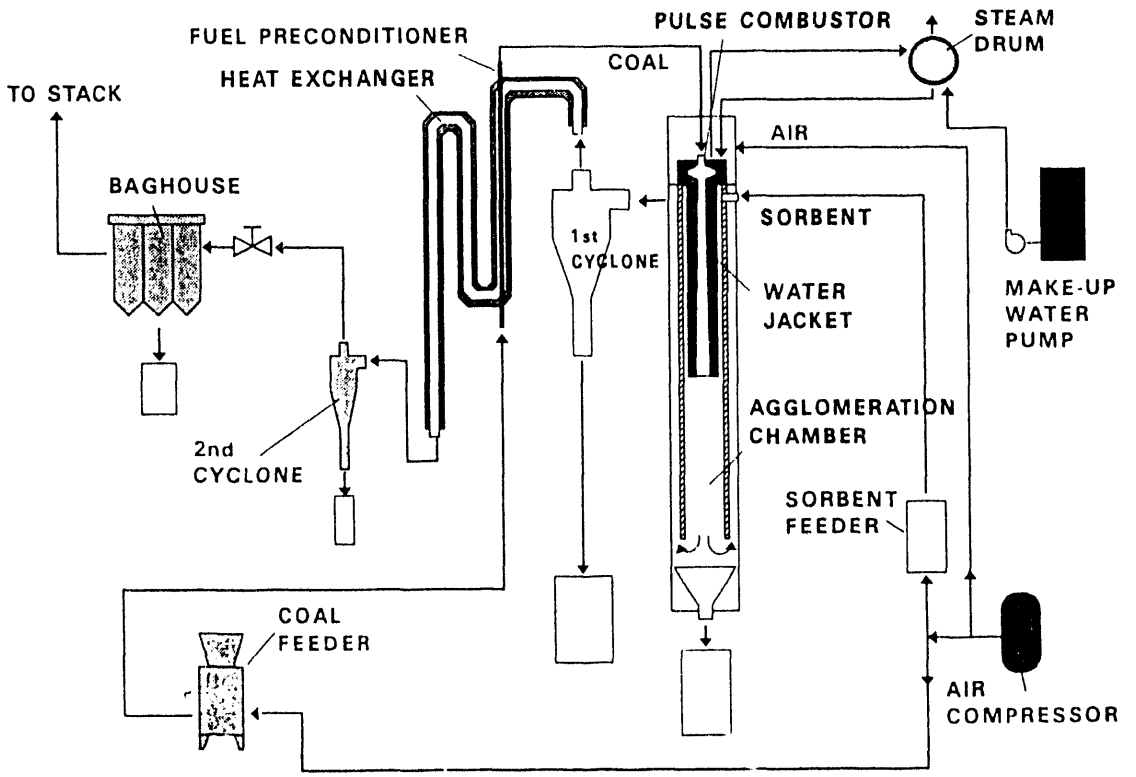

Figure 2. Schematic of the Test System

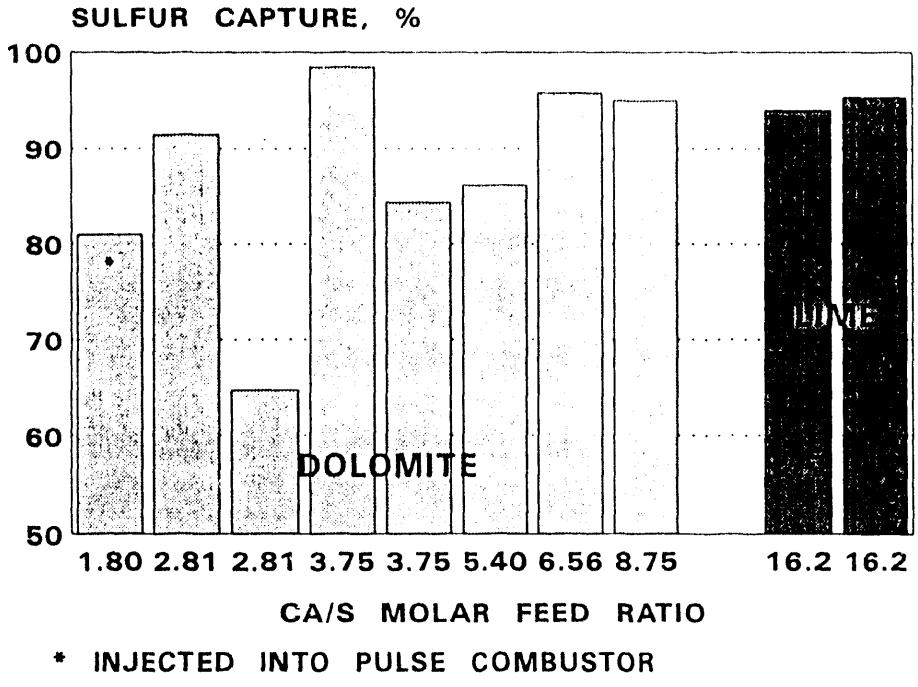

Figure 3. Sulfur Capture Efficiency

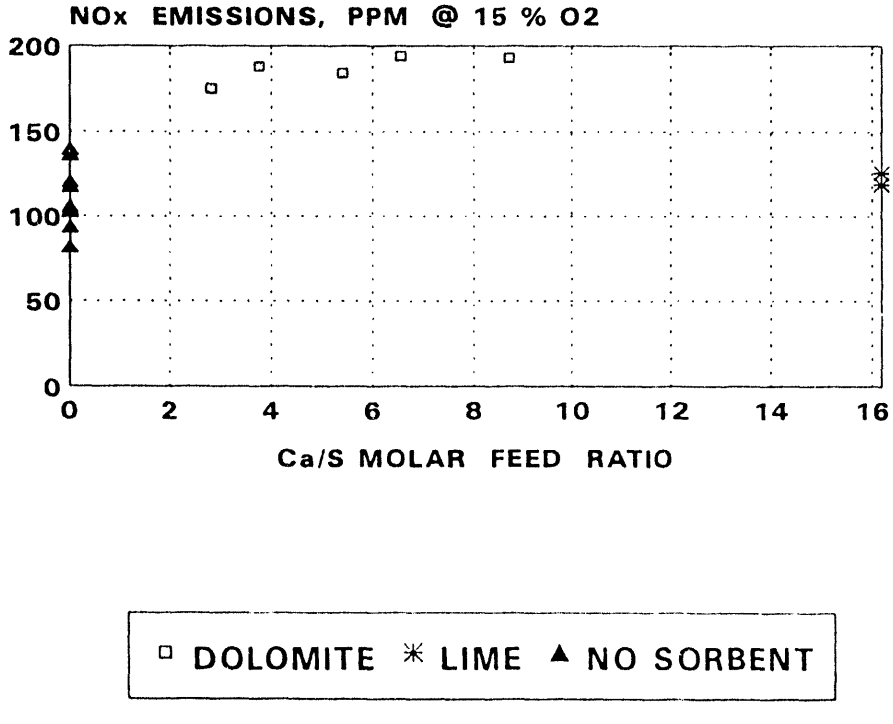

Figure 4. NO_x Emissions With Coal and Sorbent Feed

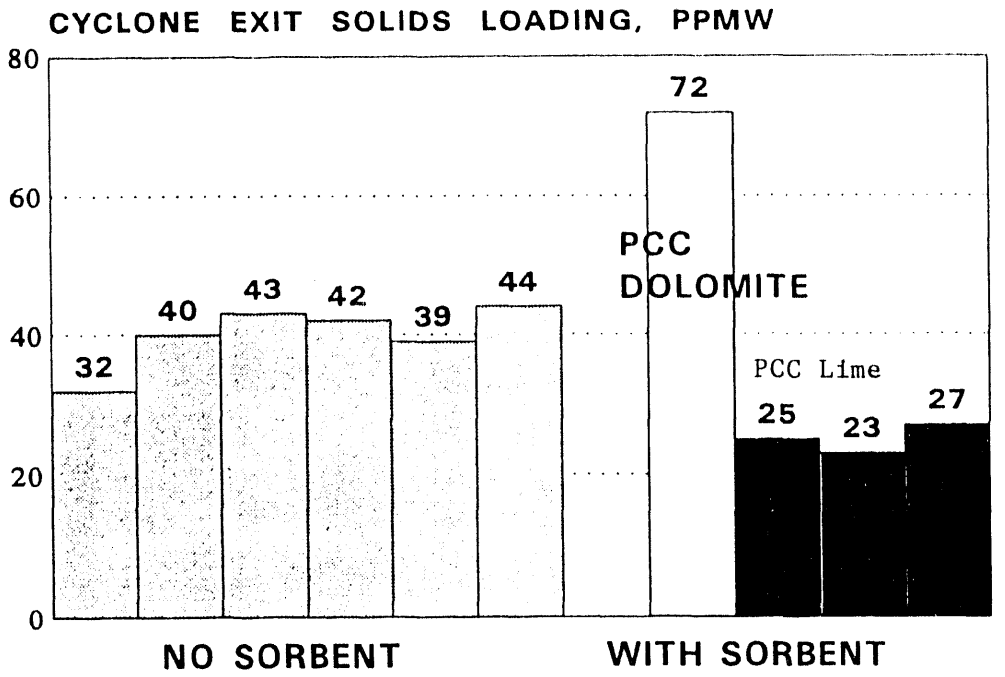

Figure 5. Cyclone Exit Solids Loading With and Without Sorbent Feed

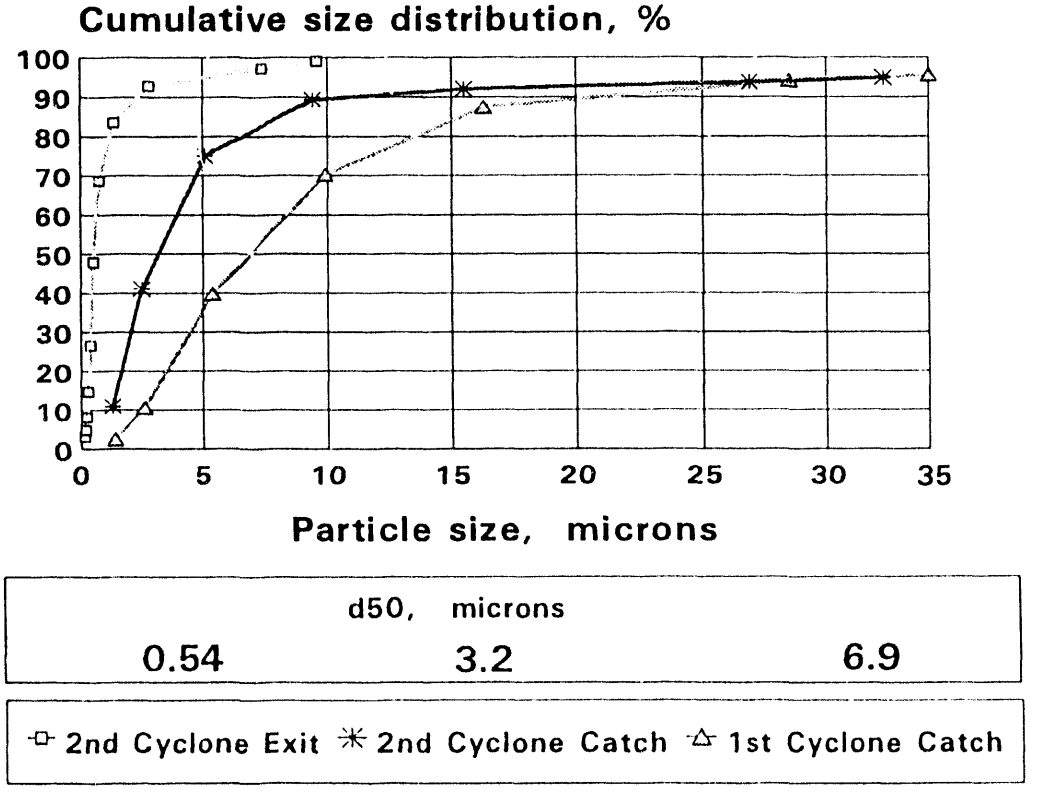

Figure 6. Particle Size Distributions of Different Streams

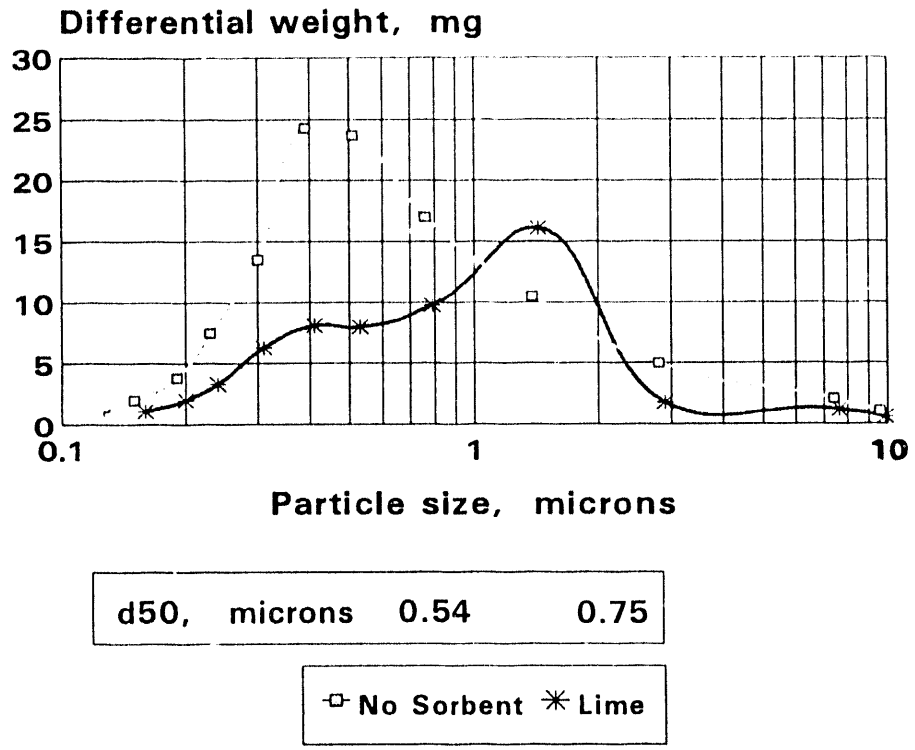

Figure 7. Comparison of Secondary Cyclone Exit Particle Size Distributions

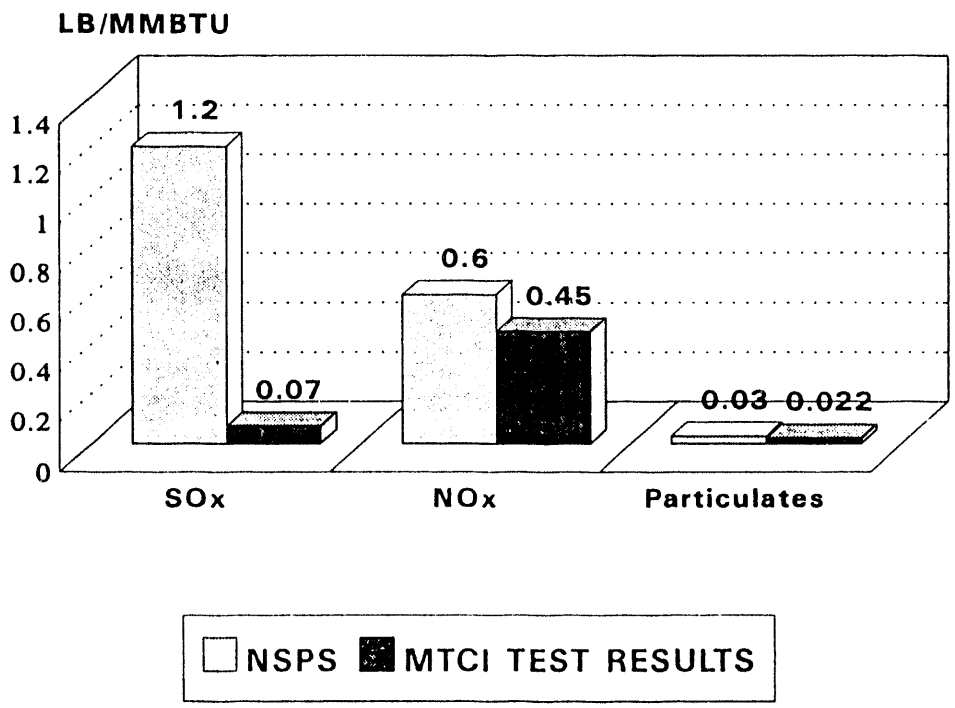

Figure 8. Comparison of Measured Emissions with NSPS

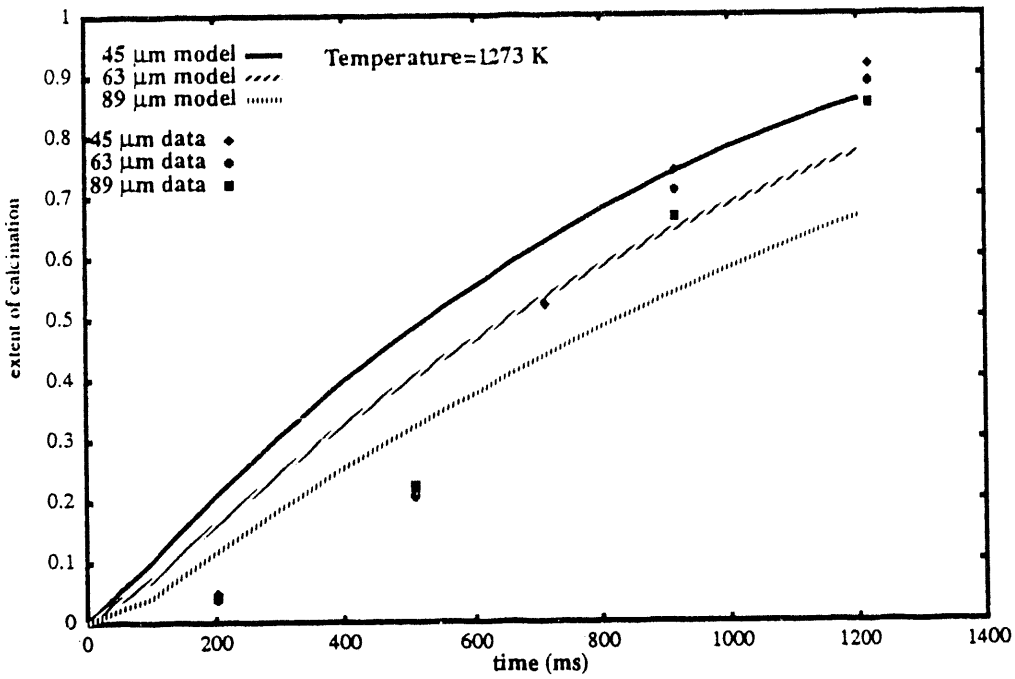

Figure 9. Relationship of Particle Size to the Extent of Calcination with Time

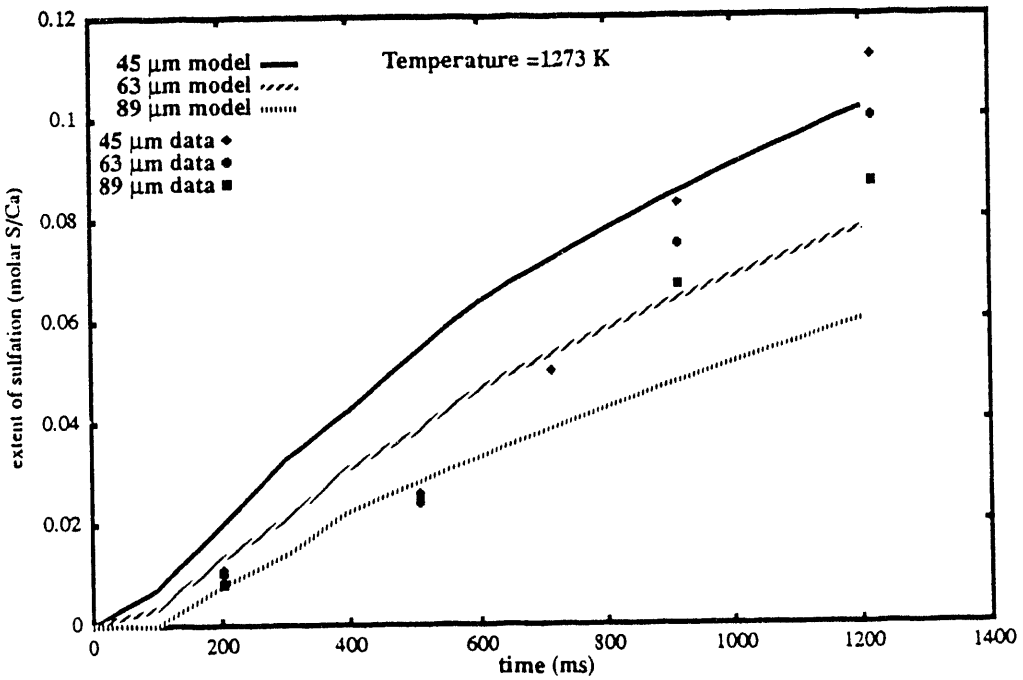

Figure 10. Relationship of Particle Size to the Extent of Sulfation with Time

Diameter = 100 μm

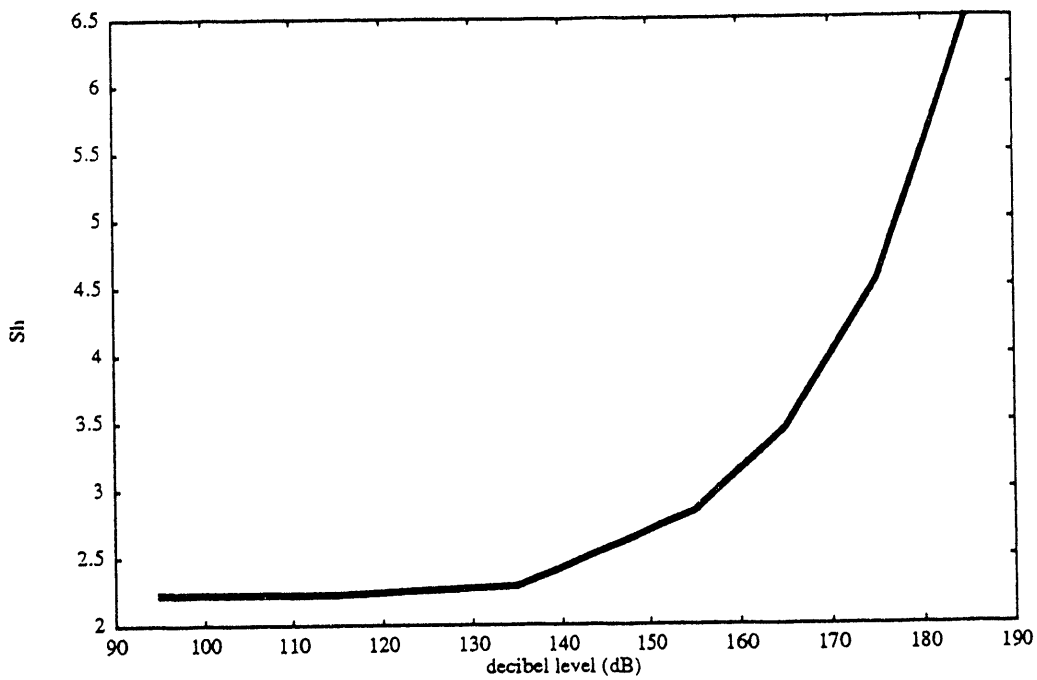

Figure 11. Relationship of Sherwood Number to Sound Pressure (dB)

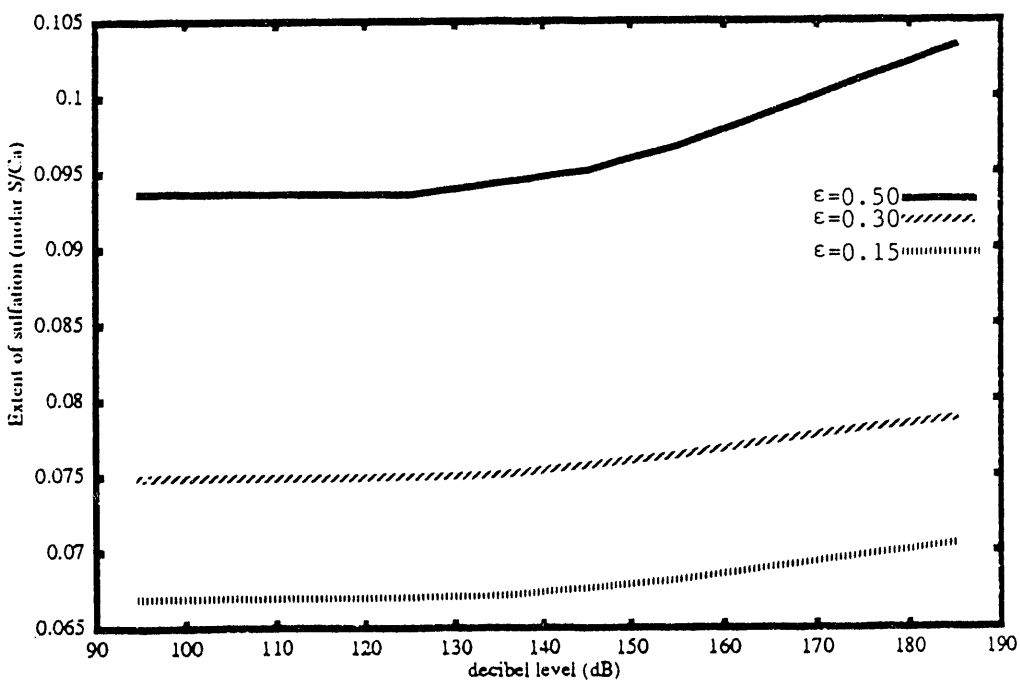

Diameter of sorbent particle = 100 μm

Figure 12. Relationship of the Extent of Sulfation to Sound Pressure (dB) as a Function of Porosity (ϵ)

❒ Acoustic Particle Interaction Phenomena

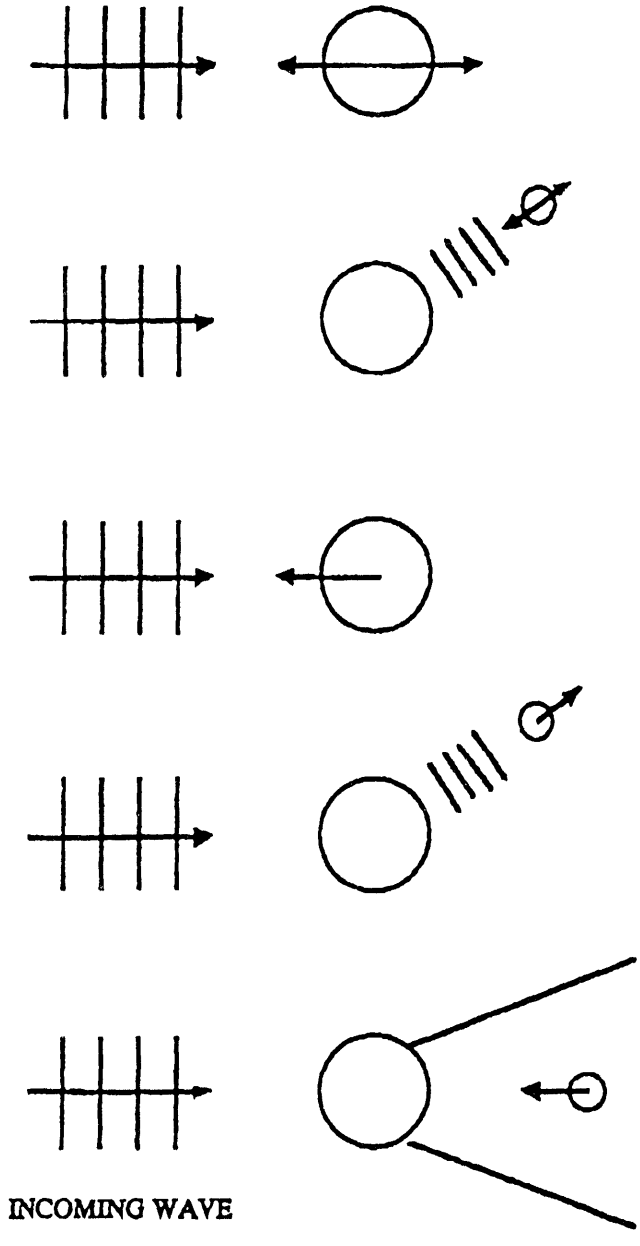

MEDNIKOV, 1965:
ACOUSTIC ENTRAINMENT
ORTHOKINETIC EFFECT
linear, single particle

SONG, 1990:
ACOUSTIC ENTRAINMENT
BY THE SCATTERED WAVE
linear, multiple particles

GORKOV, 1962:
ACOUSTIC RADIATION
PRESSURE
non-linear, single particle

DANILOV, MIRONOV, 1984:
MUTUAL ACOUSTIC
RADIATION PRESSURES BY
THE SCATTERED WAVES
non-linear, multiple particles

PSHENAI-SEVERIN, 1959:
ACOUSTIC WAKE EFFECT DUE
TO ASYMMETRIC FLOW FIELDS
non-linear, multiple particles

Figure 13. Theoretical Analysis

❒ Acoustic Wake Effect

- **Caused by Asymmetry of the Flow Field around Moving Particles:**
  Stokes flow conditions: for dissimilarly sized particles
  Oseen flow conditions: for all pairs of particles

- **The Trailing Particle Moves in the Wake of the Leading Particle:**
  drag reduction for the following particle leads to convergent velocity

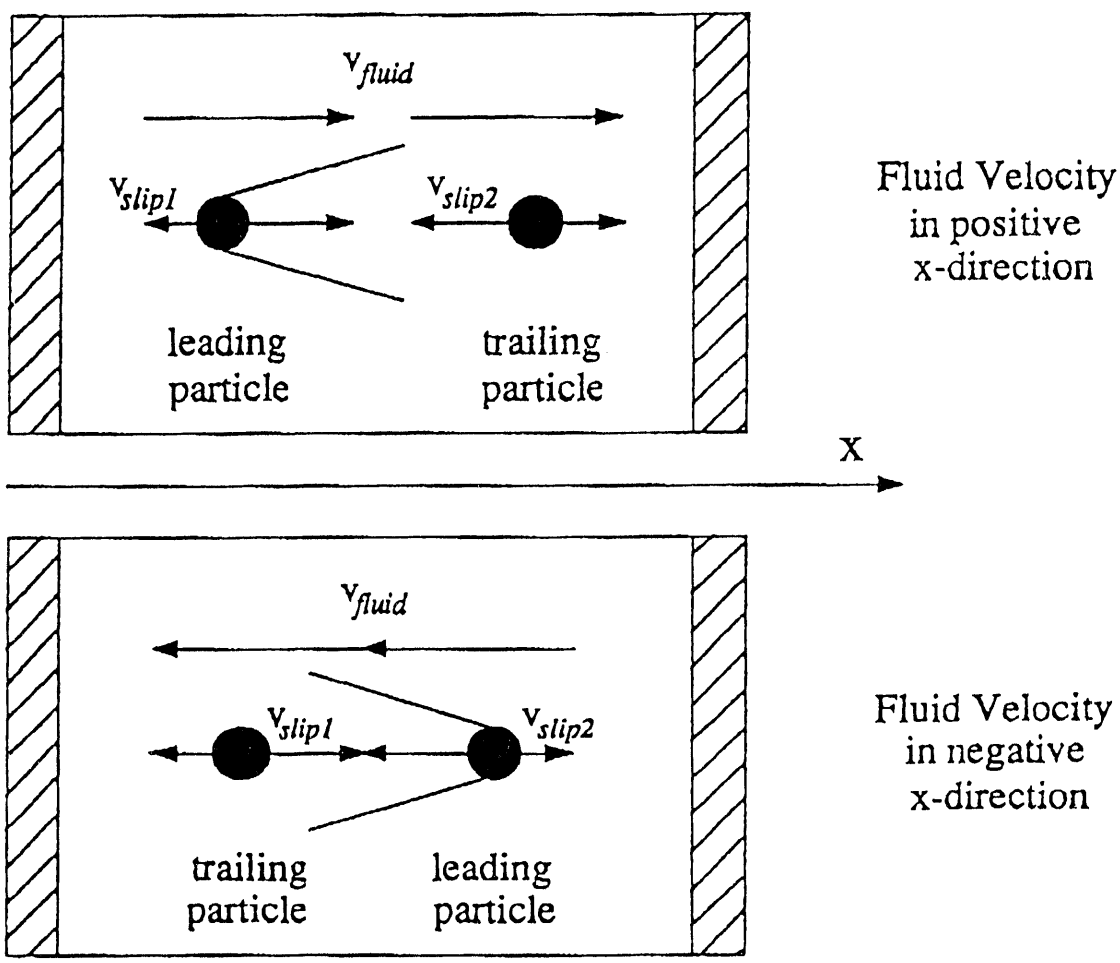

Figure 14.

Table 1: Summary of Conclusions Regarding Status of Proposed Acoustic Agglomeration Mechanisms

MECHANISM	CONCLUSION
Orthokinetic Agglomeration	Not Supported
Agglomeration Volume and Refill Mechanism	Not Supported
Gravitational Effects	- Important for dissimilar sized particles. - Disadvantageous for the agglomeration process.
Mutual Radiation Pressure Interaction	Captive force field generated by the interaction of mutual radiation pressure and acoustic wake effect explaining the effect of pair building.
Acoustic Wake Effect	Dominant interaction mechanism which accounts for the hydrodynamic agglomerations observed.
Tuning Fork Agglomerations	- The determining mechanism for acoustic agglomeration of similarly sized particles. - No agglomeration between dissimilarly sized particles. - Very high sound power leads to excessive dinetic energy of the particles; rebound is possible during collision.

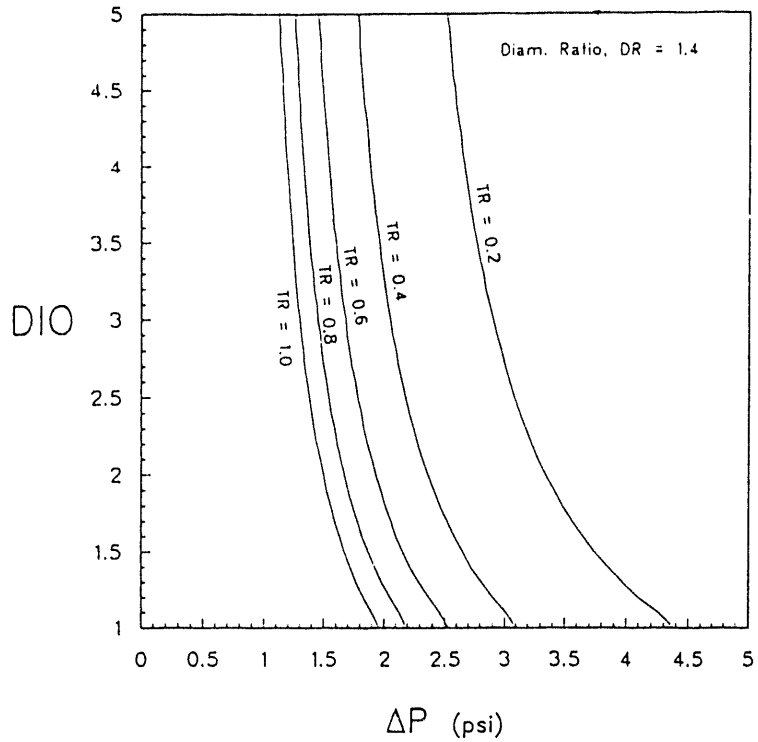

Figure 15. Computed Diodicity vs. ΔP for Various T_R

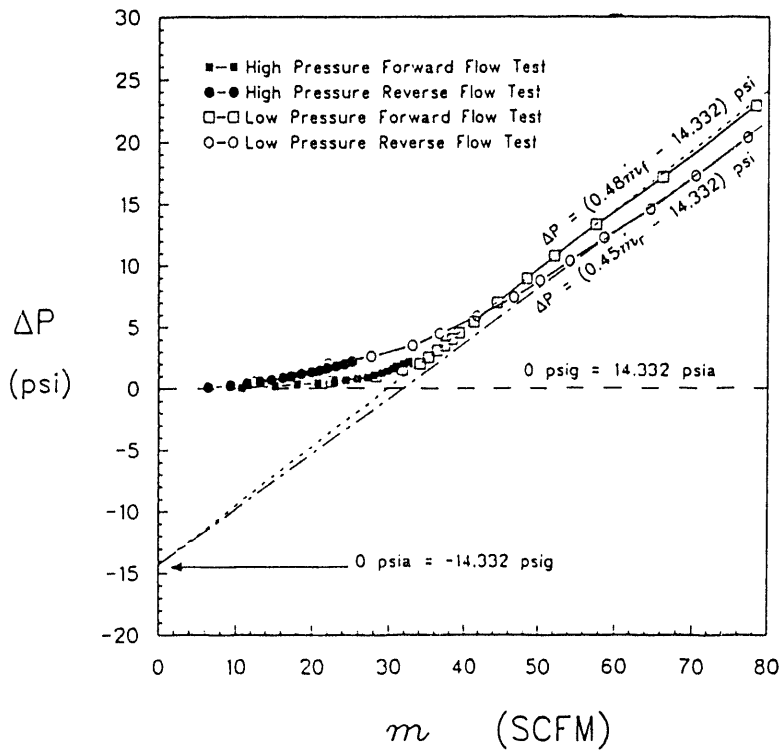

Figure 16. Aerovalve Inlet Pressure Drop vs. Mass Flow

Session 6

Desulfurization Systems

6.1 METC Hot Gas Desulfurization Program Overview

Daniel C. Cicero
Morgantown Energy Technology Center

This overview provides a frame of reference for the Morgantown Energy Technology Center's (METC's) on-going hot gas desulfurization research. Although there are several methods to separate contaminant gases from fuel gases, that method receiving primary development is absorption through the use of metal oxides. Having completed initial development using iron oxide in the 1970's, METC's research focus in sulfur control was and is set around certain requirements:

- Regenerability -- the primary goal
- Withstand highly reductive gas atmospheres
- Temperatures: 538 to 760°C (1000 to 1500°F)
- Pressures: 2 to 4 MPa (300 to 600 psi)
- Separate small volume percentage of H_2S from fuel gas (less than 0.5%)
- Regeneration temperatures: 580 to 780°C (1075 to 1450°F)
- Recover reactivity and resist attrition
- Long life at low costs

The temperature requirement for the clean-up subsystem was established to balance the integration between the gasifier and the gas turbine subsystems without the penalties associated with loss of valuable heat. The sorbent must also exhibit and consistently demonstrate less than 100 ppm by volume hydrogen sulfide (H_2S), with a goal of 10 ppm by volume in the outlet streams. Of course, all of this must be done without loss of absorption effectiveness and with little or no mechanical decrepitation. And most important, such sorbents must demonstrate a very long life and maintain low costs both in their production and disposal.

Research into high-temperature and high-pressure control of sulfur species includes primarily those sorbents made of mixed-metal oxides, which offer the advantages of regenerability. These are predominantly composed of zinc and are made into media that can be utilized in reactors of either fixed-bed, moving-bed, fluidized-bed, or transport configurations. Zinc Ferrite ($ZnO\text{-}Fe_2O_3$), Zinc Titanate ($ZnO\text{-}TiO_2$), Z-SORP®, and METC-2/METC-6 are the current mixed-metal sorbents being investigated. Z-SORP® is a proprietary sorbent developed by the Phillips Petroleum company originally for use in petro-chemical refining, and METC-2/6 are materials being developed by METC in-house researchers.

The METC desulfurization program is composed of three major components: bench-scale research, pilot-plant operation, and demonstration that is a portion of the Clean Coal Demonstration projects. Bench-scale research establishes the chemical and physical feasibility of newly conceived sorbents and accommodates quick turn-around testing of varied formulations. The chemical aspects normally investigated include reactivity, sorbent capacity (weight of H_2S captured per weight of sorbent), loss of active component (ZnO), recovery of absorptivity after regeneration, and attack of contaminant gases, e.g., hydrogen chloride (HCl). Of foremost concern is the mechanical integrity of the sorbent, which is dependent on the reactor configuration in which it is employed. The sorbent must be resistant to attrition, spalling, and the deleterious effects of steam content in the oxidative regeneration gases. The participants in bench-scale research include the GE

Corporate Research and Development Center, Research Triangle Institute (RTI), and METC.

Pilot-plant operation applies candidate sorbents from bench-scale research against real conditions and generates the initial evidence of desulfurization operability in a complete system. This level of investigation uses real gas streams produced by coal-fed gasifiers for removal of H_2S. It determines the sorbent's tolerance to contaminants at high pressures and extreme temperatures. The sorbent's reactivity and capacity are revealed as they relate to the system's through-put. The particular aspects, such as particle size and shape, and specific issues, such as vessel and valve plugging and sorbent transport velocities, as they relate to the different reactor configurations are uncovered. The players providing pilot-plant facilities are GE Environmental Services, Inc. in Schenectady, New York; EnviroPower, Inc. in Tampere, Finland; and in-house facilities at METC. The GE desulfurizer employs a moving-bed mode, while the EnviroPower unit is a fluidized-bed. The METC hot gas desulfurizer (HGD) is beginning construction and will have dual capability in examining both fluidized and transport reactor modes of operation.

Prior to becoming useful in pilot-plant and commercial operation, sorbents must be produced in larger amounts. Therefore, the technology of manufacture becomes very important in providing not only tonnage production but also constant quality at reasonable cost. The three methods of pelletizing, granulation, and spray drying are all under examination. Companies that are assisting in optimizing manufacturing techniques are United Catalysts of Louisville, Kentucky, Contract Materials Processing of Baltimore, Maryland, and Phillips Petroleum of Bartlesville, Oklahoma. Other catalysts manufacturers have shown interest and possess additional capabilities.

Figure 1 shows the relationship between the research work, the pilot plant tests, and the Clean Coal demonstration plants. The desulfurization modules of the Tampa Electric and Toms Creek projects have been and are being supported by the laboratory studies done by GE, RTI, and METC. GE's fixed-bed gasifier pilot plant has been in operation for many years, but has only recently tested zinc titanates and Z-SORP® in a moving-bed desulfurizer. The EnviroPower integrated fluidized-bed gasifier and fluidized-bed desulfurizer plant have likewise begun testing different formulations of zinc titanate, albeit for fluidized applications. METC has supported the Piñon Pine fixed-bed zinc-based cleanup system for many years, although the METC-HGD will now be exploring the fluidized and transport configurations.

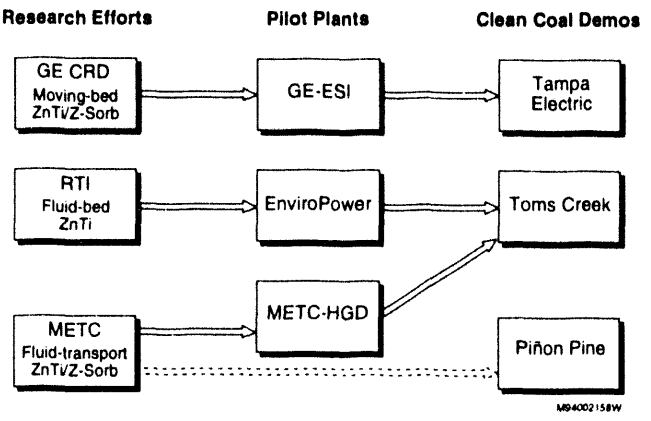

Figure 1. Desulfurization Research with Reference to Clean Coal Demonstration Projects

Future METC-sponsored research in desulfurization will involve projects in Advanced Sulfur Control Concepts and Advanced Sorbent Development. The goal of the sulfur control project is to develop simpler and economically superior processing concepts of regenerable sorbents and to produce by-product elemental

sulfur. A recent award has been made to Louisiana State University and is to be guided by Professor Douglas Harrison. A second award was made to RTI, where Dr. Santosh Gangwal is serving as principal investigator. Recent system studies have shown that pushing the upper temperature envelope above 760°C (1400°F) will not improve overall system efficiency. Since this is the case, the inherent increase in capital and operating costs associated with higher and higher temperatures may be avoided. Thus, METC has decided to explore a milder range of temperature operation, i.e., from 343°C to 538°C (650 to 1000°F) for what may promise to be more practical design and operating considerations and to yield more economical systems. Initial indications are that the existing slate of zinc-based sorbents can effectively absorb H_2S at these lower temperatures, although possibly somewhat less than optimally. Other metal oxides, such as iron oxide, could also achieve equilibrium concentrations down to below 100 ppm by volume. This advanced sorbent development project should see its beginning in late 1994.

DCICER\1:940781

6.2 Integrated Operation of a Pressurized Gasifier, Hot Gas Desulfurization System and Turbine Simulator

CONTRACT INFORMATION

Contract Number DE-AC21-87MC23170

Contractor GE Environmental Services, Inc.
200 N. Seventh St.
Lebanon, PA 17042
(717-274-2400)

Contractor Project Manager Steve Bevan - GEESI, David Najewicz - GE-CRD

Principal Investigators Eli Gal
David Najewicz
Anthony H. Furman
Raul Ayala
Alan Feitelberg

METC Project Manager Justin Beeson

Period of Performance September 30, 1987 to September 30, 1994

Schedule and Milestones

Project Schedule

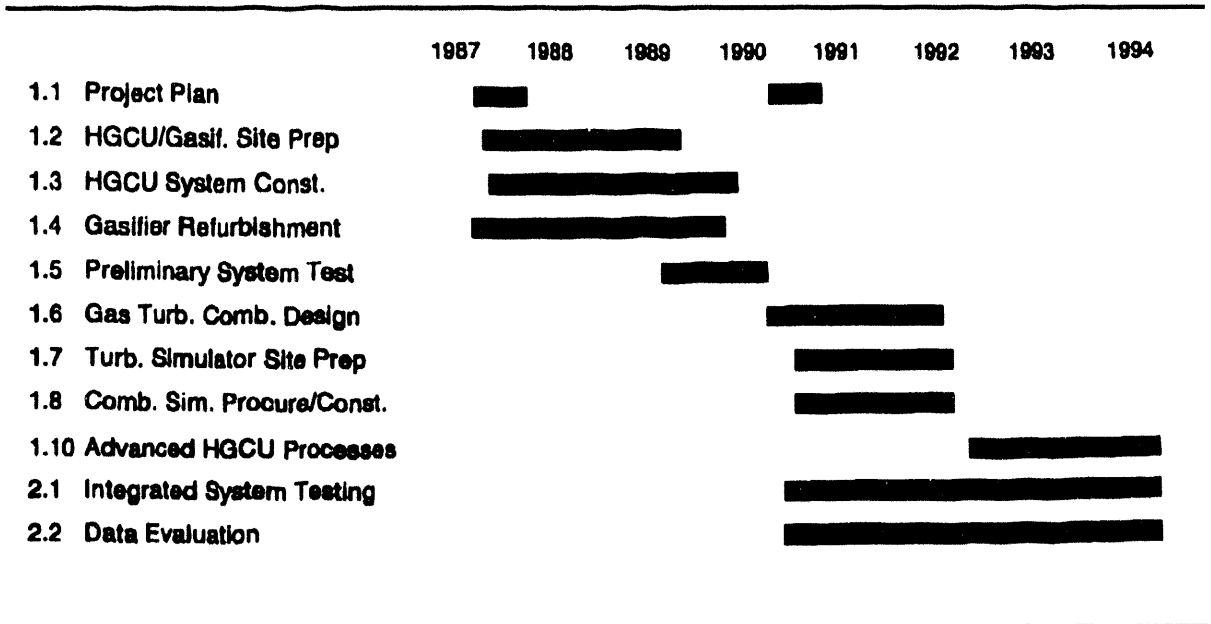

OBJECTIVES

The overall objective of the General Electric Hot Gas Cleanup (HGCU) Program is to develop a commercially viable technology to remove sulfur, particulates, and halogens from a high-temperature fuel gas stream using a moving bed, regenerable mixed metal oxide sorbent based process. This technology will ultimately be incorporated into advanced Integrated Gasification Combined Cycle (IGCC) power generation systems. In IGCC applications, HGCU will improve overall power generation cycle efficiencies by 1 to 2% compared with conventional low-temperature cleanup technologies, and will also offer the potential for reducing plant capital and operating costs.

The HGCU Program is based on the design and demonstration of the HGCU system in a test facility made up of a pilot-scale fixed bed gasifier, a HGCU system, and a turbine simulator in Schenectady, NY, at the General Electric Research and Development Center (GE-CRD). A modified GE MS6000 gas turbine combustor and a film-cooled, first-stage LM6000 nozzle assembly are incorporated into the turbine simulator.

The objectives of the turbine simulator testing are (1) to demonstrate the suitability of fuel gas processed by the HGCU system for use in state-of-the-art gas turbines firing at "F" conditions (2350°F rotor inlet temperature) and (2) to quantify the combustion characteristics and emissions of such a combustor. The turbine simulator program also includes the development of experimental combustors based on the rich-quench-lean concept to minimize the conversion of ammonia and other fuel-bound nitrogen species to NO_x during combustion.

The HGCU system and turbine simulator have been designed to process approximately 8000 lb/hr of low heating value fuel gas produced by the GE fixed bed gasifier. The raw fuel gas is provided to the HGCU and turbine simulator systems at 280 psig and 1000°F. The HGCU system has utilized several mixed metal oxide sorbents— including zinc ferrite, zinc titanate, and Z-Sorb (a proprietary zinc-based sorbent developed by Phillips Petroleum Company)— with the objective of demonstrating good sulfur removal and mechanical attrition resistance as well as economic cost characteristics. Demonstration of halogen removal and the characterization of alkali and trace metal concentrations in the fuel gas are subordinate objectives of the overall program.

BACKGROUND

As a result of the availability of advanced gas turbine combined cycles that fire at temperatures of over 2350°F and the advent of integrated gasification/oxygen separation technology, IGCC plants now offer overall plant efficiencies of 42–44% with extremely low emissions of SOx, Nox, and particulate.

Although the capital cost of IGCC technology is higher than conventional coal-fired steam turbine plants, it is rapidly dropping and is approaching competitive levels. As IGCC power generation technology reaches the early stage of demonstration and commercialization, the first plants built will use conventional low-temperature gas-cleaning technology. However, the goal of HGCU is that when fully developed, it will represent a "second generation" clean-up technology offering further improvements in IGCC power generation efficiency and operation flexibility, as well as reduced capital and operating costs.

Fuel gas derived from coal by gasification processes contains sulfur in the form of H_2S and COS at concentrations of up to several thousand parts per million (ppm). In order to comply with increasingly stringent environmental regulations and to meet the conditions required for the long life of gas turbine components, it is necessary to reduce both the sulfur and particulate in coal-derived fuel gas to low levels. In the temperature range of approximately 800–1200°F, mixed metal oxides, such as zinc oxide, react with these gaseous sulfur species, forming metal sulfides under reducing conditions. These metal sulfides can then be regenerated to their original oxide state, producing a sulfur-dioxide-rich off-gas suitable for conversion either to sulfuric acid or to elemental sulfur. GE Environmental Systems, Inc. (GEESI) has patented a moving bed process to utilize mixed metal oxide sorbents to remove sulfur from a high-temperature fuel gas stream and regenerate the sorbent for reuse while producing a byproduct stream suitable for the recovery of sulfur. The history of this project and the concurrent development of high-temperature particulate removal systems based on cyclones has been documented by Smith et al. (1987) and Cook et al. (1988,1989, 1990, 1991, and 1992). In addition, the previous development of the mixed metal oxide sorbents and turbine simulator have been documented by Ayala et al. (1992, 1993) and Feitelberg et al. (1993).

PROJECT DESCRIPTION

The HGCU Program is based on the design and demonstration of gas cleaning technologies at GE-CRD's Process Evaluation Facility (PEF). This work is being carried out under a current DOE contract, with the most recent schedule shown in the Schedule and Milestones section at the beginning of this paper. Construction of the basic facility was completed in late 1990, with continuing modifications and test operation taking place since that time. A summary of the test runs performed to date is shown in Table 1. These tests include 9 long dura-

Table 1. Gasifier/HGCU/Turbine Simulator Test Operation – 20 atm, 1000°F

Run	Date	Run Hours	Coal Type	System Configuration
1-2B	12/90-4/92	230	I6	Gasifier/HGCU/GT Valve
3	8/30/92	88	I6	Gasifier/HGCU/GT Valve/MS6000 Simulator
3A	2/7/93	120	Anthracite	Gasifier/HGCU/GT Value/MS6000 Simulator
4	6/13/93	100	I6, Crown II	Gasifier/HGCU/GT Valve/Simulator/Halogen
5	11/1/93	103	I6, Crown II	Gasifier/HGCU/GT Valve/Halogen/"F" Simulator 2300°F
6	5/1/94	85	I6	Gasifier/Guard Bed/HGCU/GT Valve/Halogen/ "F" Simulator 2500°F
4A	4Q94	24	I6	Gasifier/HGCU/GT Valve/R-Q-L Sub-Scale
7A	3Q94	100	I6, Crown II	Gasifier/HGCU/GT Valve/Halogen/"F" Simulator 2500°F
7B	3Q93	100	I6, Crown II	Gasifier/HGCU/GT Valve/CFB Halogen/R-Q-L Full Scale
8	4Q94	100-200	I6, Crown II	Gasifier/HGCU/GT Valve/CFB Halogen/R-Q-L Full Scale

tion runs (approximately 100 hours each), incorporating a variety of new hardware features and sorbents. Tests 4A, 7A, 7B, and 8 are scheduled for later in 1994.

A schematic of the PEF facility, as configured at the conclusion of Test 6, is shown in Figure 1. The GE-CRD fixed bed, pressurized air-/steam-blown gasifier is shown on the left. The gasifier includes a water-cooled bed stirrer, alternating pressurized coal feed lock-hoppers, and a rotating grate for ash removal. The PEF also includes a primary cyclone immediately downstream of the gasifier, the HGCU system consisting of the absorber and associated upper and lower lock-hoppers, regenerator with recycle gas system, fines screen, and elevator. A secondary cyclone is located downstream of the HGCU system, and the cleaned fuel can be directed either to the MS6000 turbine simulator or to the system flare. Using analytical instrumentation in "real time" to allow process control, both the process fuel gas and the recycle gas are sampled extensively during the run. Solid flow is sampled hourly for later chemical analysis and to support the preparation of overall heat and mass balances.

RESULTS

Testing of the GE HGCU system has been underway since December 1990. During this period, a variety of sorbents and system configurations have been tested, including zinc ferrite and zinc titanate sorbents, single/double stage open cylindrical regenerators, and alternate recycle blower configurations. The two most recent tests, Test 5 (completed in November 1993) and Test 6 (completed in May 1994), represent the latest advancements in regenerator configuration, type of sorbent, and chloride control systems. Test 5 was based on the use of zinc titanate sorbent and included a revised regenerator configuration and a

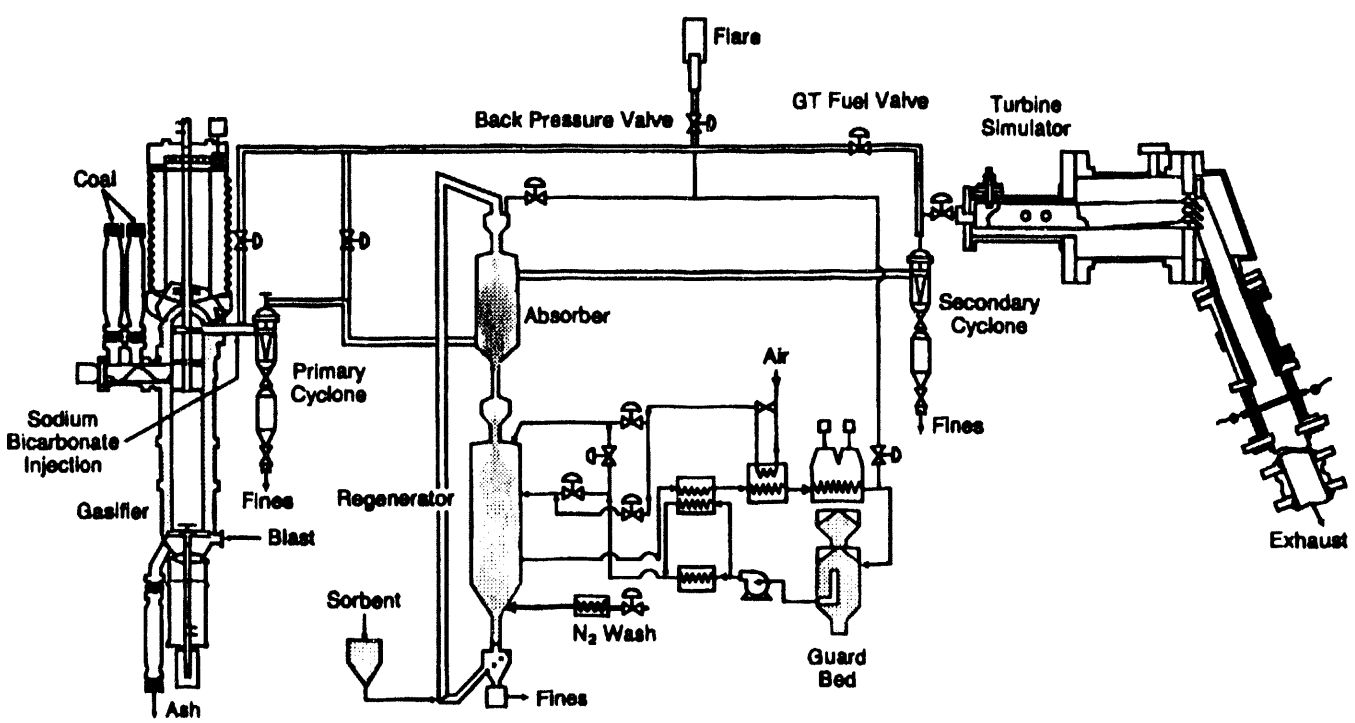

Figure 1. GE Gasifier/Hot Gas Cleanup Process Flow Diagram

sodium bicarbonate injection system for chloride control. Test 6 incorporated the use of Z-Sorb, a chloride guard in the regenerator recycle loop, and further modifications to the regenerator internal configuration. The following sections describe the test conditions in detail and discuss the test results.

Test 5 Conditions and System Modifications

Long Duration Test 5 was performed in early November 1993 at GE-CRD's PEF using zinc titanate (L2535M) sorbent. This sorbent had been used in previous tests and had been subjected to periodic high-temperature regeneration conditions during those tests. A blend of Illinois #6 (1.9% sulfur) and Crown II (3.7% sulfur) coals were used, resulting in effective sulfur levels in the range of 2.5–3.0%.

The regenerator, previously modified in Test 4 to include a single-stage annular configuration, was further modified for Test 5 to include a two-stage annular configuration. These modifications are shown in Figure 2.

The regenerator modifications were made to improve control of sorbent temperature in the regenerator, which was found to be a problem in Test 4. Freshly sulfided sorbent, which also includes tar (associated with the GE fixed bed gasifier) entering the top of the regenerator is very reactive. For that reason, the oxygen content of the recycle gas must be reduced in order to control the sorbent temperature rise caused by the exothermic regeneration and tar oxidation reactions at the top of the regenerator bed. To complete the regeneration of sorbent in the middle and bottom of the regenerator, however, additional oxygen is required. In a single-stage configuration it was difficult to satisfy both criteria.

To solve this problem, a two-stage regeneration approach was reinstituted in the regenerator. In the

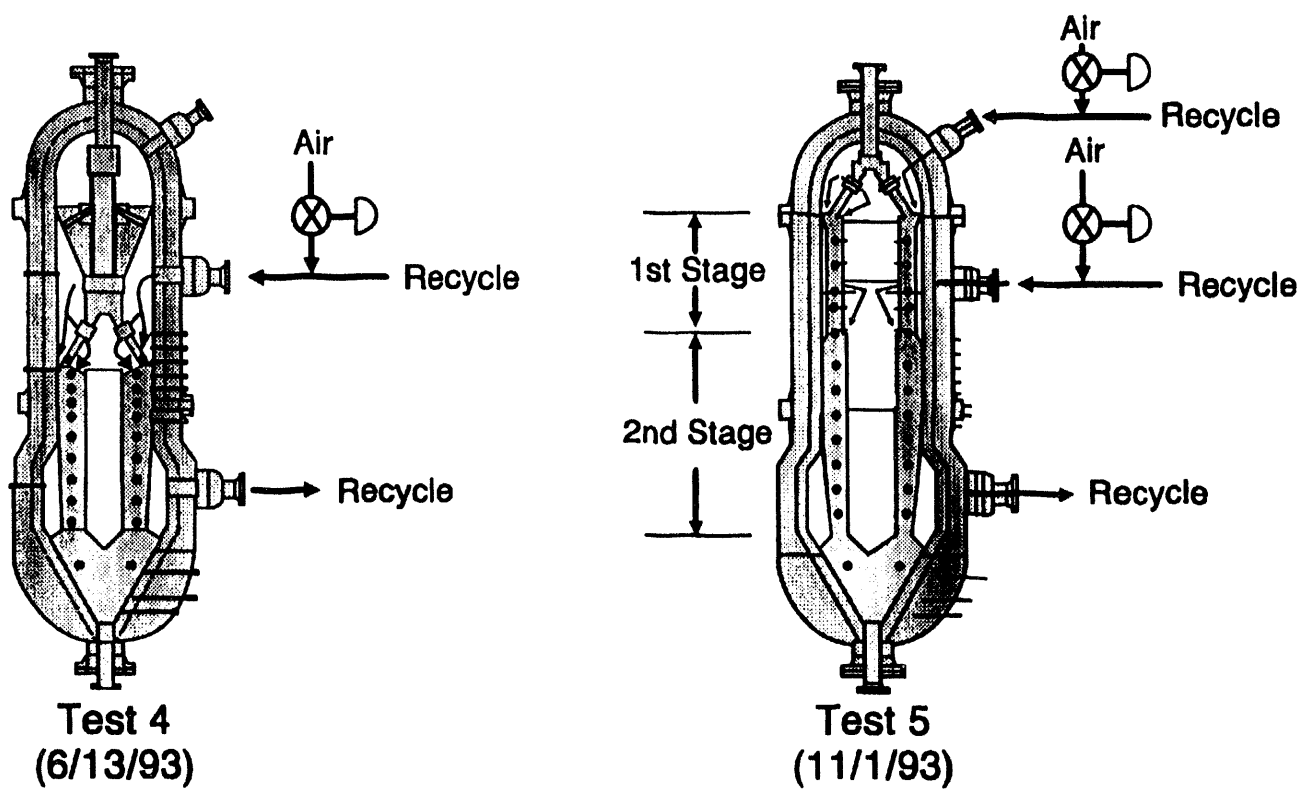

Figure 2. Hot Gas Cleanup Regenerator Modifications – Test 5

modified regenerator configuration, the sorbent passes through two regeneration stages, each with an independent air (oxygen) control, allowing control of the oxygen content and temperature of the sorbent in each stage. In addition, larger valving and piping were installed in the air feed and off-gas bleed lines to increase the flow capacity of these systems.

As previously reported, chlorides in the coal gas cause problems to the HGCU system by adsorbing onto the sorbent in the absorber and being transported to the regenerator, where they are released in the recycle gas. In the recycle gas, the chlorides react with both the sorbent and the SO_2 in the recycle gas to form zinc sulfate and zinc chloride deposits in the recycle loop heat exchangers. This condition causes blockage of the heat exchangers after several days of operation. To prevent this problem, a fuel gas chloride removal system was designed and installed for demonstration in Test 5. The chloride removal system consists of a pressurized sodium bicarbonate powder injection system located upstream of the primary cyclone. The sodium bicarbonate powder flow is metered through a feeder and transported to the coal gas piping using a dilute phase nitrogen transport system. Sodium bicarbonate powder injected into the hot fuel gas stream at 1000°F rapidly calcines to sodium carbonate, forming highly porous particles. The sodium carbonate reacts with the hydrogen chloride in the coal gas to form solid sodium chloride within the particles. The particles, consisting of unreacted sodium carbonate and sodium chloride, are captured by the primary cyclone. The location of the sodium bicarbonate injection system is shown on the system schematic (Figure 1).

The MS6000 turbine simulator configuration was not modified significantly from the previous test. Improvements were made to the nozzle cascade cooling circuits to improve cooling flows to the leading and trailing edges of the vanes. In addition, an automatic temperature control system was incorporated to maintain a constant firing temperature despite variations in the fuel gas heating value caused by the movement of the gasifier stirrer.

Test 5 Results

The results of Test 5 are summarized in Figure 3. The figure plots the inlet and outlet temperature of the absorber and the outlet H_2S levels of the gas leaving the absorber. The data is shown for the entire week's operation; periods when the absorber was off line are indicated by decreases in the absorber temperatures. The turbine simulator was operational for 41 hours. Most of the turbine simulator operation was at 2100°F combustor exit temperature, with two hours of operation at 2300°F.

The gasifier was operated for 103 hours in Test 5, with 65 hours of integrated operation of the HGCU system. The input sulfur loading ranged from 4000 ppm H_2S on Monday to nearly 6000 ppm H_2S on Tuesday and was lowered to approximately 4000 ppm Wednesday through Friday. As shown in Figure 3, the H_2S levels in the fuel gas downstream of the absorber ranged from 50–500 ppm during the test. This corresponds to a sulfur removal range of 90–97% overall.

The test was interrupted several times when the absorber was taken off line. The first two interruptions, on Tuesday evening and Wednesday morning, were caused by poor performance of the regenerator, as evidenced by outlet H_2S levels in the 300–400 ppm range. This degraded performance was caused by incomplete regeneration of the sorbent in the regenerator. As a result, the absorber was removed from the coal gas stream, allowing the regeneration process to continue without the addition of freshly sulfided material to the regenerator.

Post-test material analysis indicated that the sulfur levels in the sorbent leaving the regenerator during these periods were in the range of 2–3%, indicating that regeneration of the sorbent was incomplete. Although both periods of off-line regeneration were successful in improving the performance for several hours, the outlet H_2S levels again increased to the 300–400 ppm range.

The period the absorber was off line on Thursday morning was associated with plugging of the recycle loop heat exchanger. This condition required disassembly of the heat exchangers for cleaning to restore full recycle gas flow. Subsequent problems on Thursday evening associated with the sorbent elevator electrical system took approximately 12 hours to correct. The final operation on Friday demonstrated improved operational and regeneration conditions and the ability to reduce outlet H_2S levels to below 100 ppm under proper control conditions.

Overall, sulfur removal performance during Test 5 degraded in comparison with previous tests. We concluded that the performance was due to incomplete regeneration and higher sulfur input levels. Despite the incomplete regeneration, the regenerator recycle gas attained SO_2 levels of 10% for over 36 hours of operation. During shut-downs and restart periods, the regenerator loop was able to recover to high SO_2 levels quickly. These SO_2 levels are much higher than the 7–8% required by the input stream of the sulfuric acid conversion process.

Other results from Test 5 included the demonstration of greatly improved temperature control of the sorbent. The first stage of the regenerator was operated in an automatic control mode, which controlled the input oxygen level based on the peak temperature measured in the first stage. This control approach allowed the maximum temperature in the first stage to be maintained at less than 1500°F throughout the test. The second

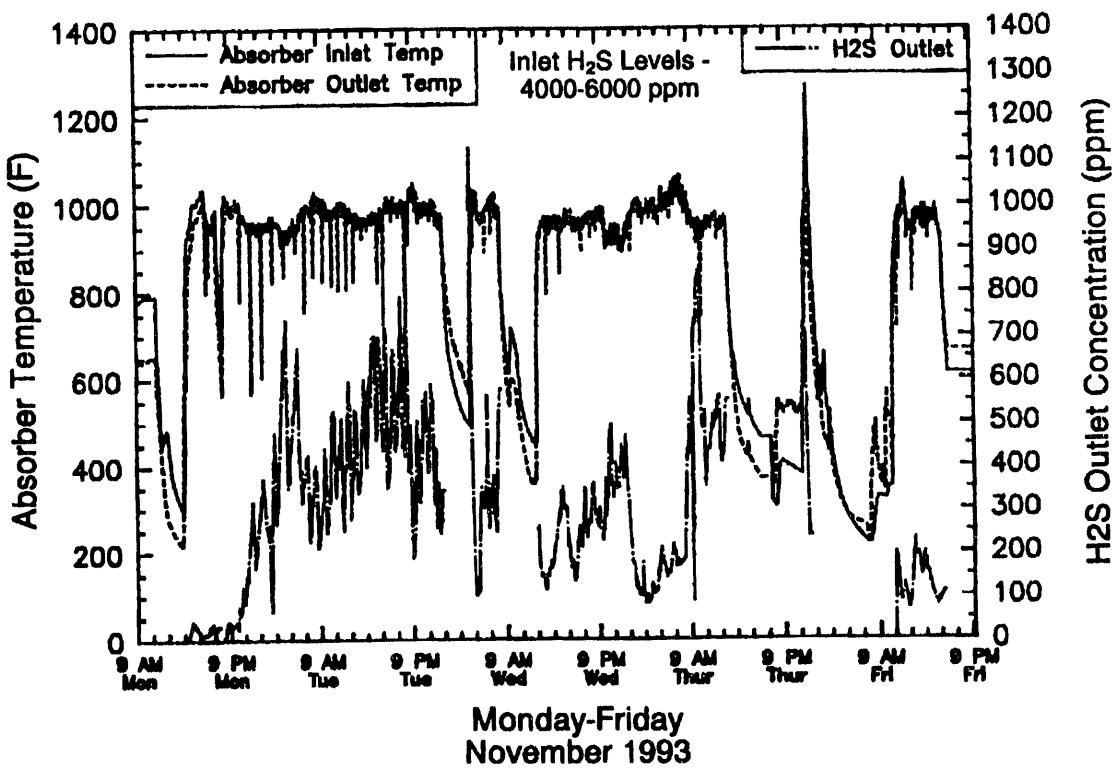

Figure 3. Absorber Performance – Test 5

stage was manually controlled to maintain desired sorbent temperatures.

The pressurized sodium bicarbonate injection system functionally performed as designed. Approximately 20–23 lb/hr of sodium bicarbonate were injected into the coal gas stream using a nitrogen carrier gas upstream of the first-stage cyclone. The sodium bicarbonate had a residence time of approximately 1.5 seconds prior to being removed by the cyclone. The mean particle size was relatively coarse, 85% greater than approximately 75 microns and 98% less than 150 microns, and the stoichiometry was approximately 2.5:1. However, based on measurements in the fuel gas stream and a post-test solids analysis, the chloride mass balance around the system indicated that only 35% of the chloride was removed from the gas.

The mass balances for chloride and sodium are shown in Figure 4. Measurements of the chloride in the recycle loop gas were also performed periodically throughout the test. Chloride levels in the recycle gas were found to range from 1000 to 2000 ppm, as measured in previous tests. Since the plugging of the recycle loop heat exchangers sharply limited test operation of the PEF and represented a significant problem, it was decided to add a chloride "guard bed" to remove chlorides directly from the recycle loop.

To improve our understanding of the kinetics of sodium bicarbonate reactions with HCl in hot fuel gas streams, testing was performed at the University of North Dakota Energy and Environmental Research Center's pressurized drop tube furnace (PDTF). The tests used various powder sizes, residence times, and stoichiometry of sodium bicarbonate in simulated coal gas containing HCl. The results demonstrated that removal rates of over 90% were possible using longer gas/solids residence times, finer powder, or increased stoichiometry. The conclusion of the PDTF testing was that the PEF residence time was too short and that an improved configuration to increase both the residence time

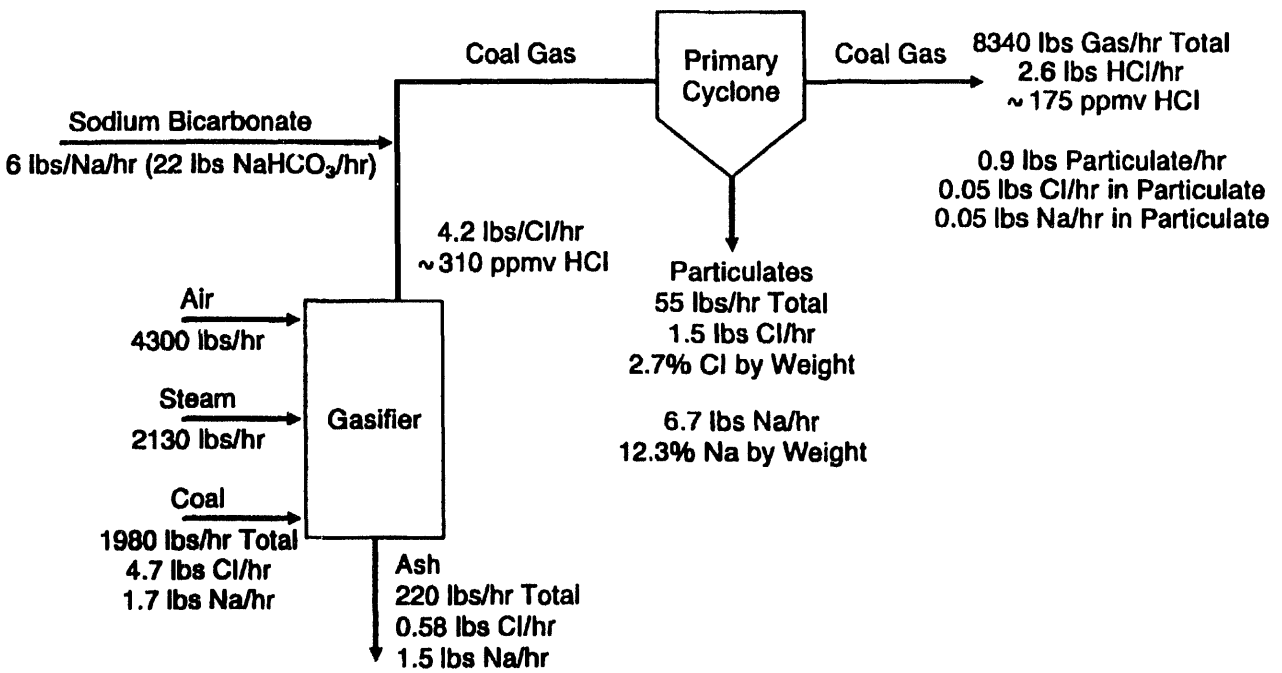

Figure 4. Gasifier Sodium and Chloride Balance for Run 5

and stoichiometry by use of a recycle cyclone should be incorporated into the facility. However, because of the time required to revise the plant high-temperature fuel piping, this modification has been postponed until after Test 6.

During Test 5, it was observed that the sorbent pellets leaving the regenerator were not uniform in color, indicating that some pellets were not fully regenerated. This observation led to the hypothesis that the pellets were not moving through the regenerator in a uniform plug flow condition. It appears that some sorbent pellets were moving through the regenerator more quickly and did not have enough residence time to be fully regenerated, while other pellets were moving very slowly and were fully regenerated at the exit. This hypothesis was tested by constructing scale models of the regenerator geometry and flowing sand through the model to observe the behavior of a colored tracer layer of sand. From tests on a modified regenerator model, it was determined that a diverter located in the discharge of the regenerator would greatly improve the uniformity of the solids flow in the annular section of the regenerator. The data from this testing is shown in Figure 5, indicating the ideal flow characteristics and the modified and non-modified flow characteristics. On the basis of these results, modifications to the regenerator exit were designed and incorporated into the PEF regenerator.

Disassembly of the turbine simulator after Test 5 indicated that although the simulator operated without apparent problems, the cap/cowl louvers in the head end of the combustor had been damaged. Several of the cooling louvers were damaged. The appearance of the combustor suggested that the flame structure was located very close to the head end of the combustor and was the cause of the overheating of the cap/cowl assembly. This condition was reviewed with GE Power Generation

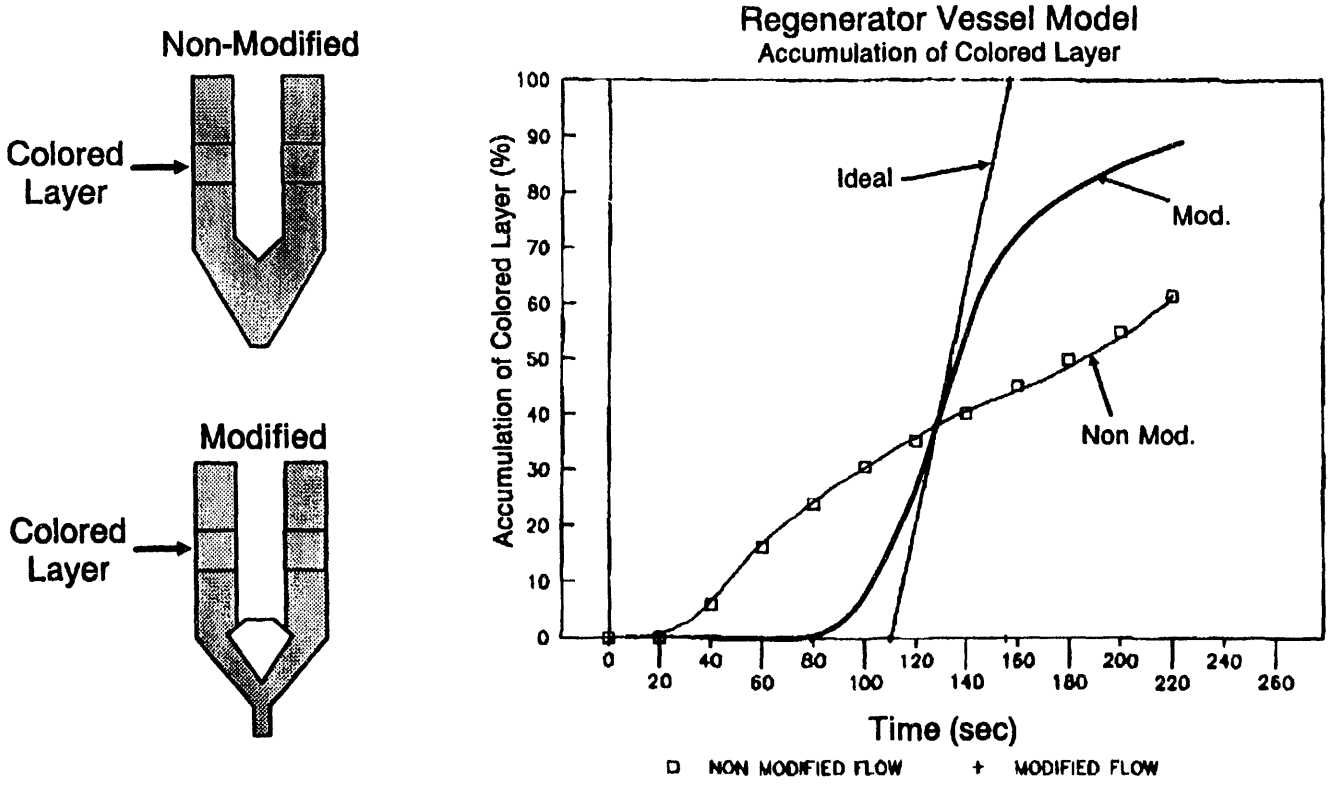

Figure 5. Solids Flow Test – Regenerator Discharge

Engineering, and minor modifications to the axial location of the air and fuel swirler were made. In addition, the swirl angles of the air and fuel swirlers were reduced, thus modifying the location of the flame within the combustor.

Test 6 Conditions and System Modifications

Long Duration Test 6 was performed during the period of May 1 to May 5, 1994. Several significant modifications and changes were made to the HGCU and turbine simulator systems in preparation for Test 6. The most significant change from previous tests was the use of Z-Sorb sorbent.. Characteristics of Z-Sorb are detailed in a paper presented in the sorbent development session of this conference (Ayala et al., 1994).

Modifications to the lower section of the regenerator internal configuration, as shown in Figure 6, were fabricated and installed with the objective of improving the uniformity of sorbent solids flow. The annular, two-stage regenerator configuration was retained from Test 5.

A "guard bed" was added to the recycle loop to continuously remove chlorides from the recycle gas. The guard bed is a small fixed bed contains an active volume of approximately 300 pounds of sodium bicarbonate pellets (3–4 mm). Since sodium bicarbonate will react with SO_2 as well as chlorides, the guard bed was located in the lowest temperature position in the loop, upstream of the recycle compressor. Bench-scale testing of sodium bicarbonate pellets in simulated recycle gas demonstrated that at temperatures of 500 to 550°F, reactions with SO_2 are minimized and chloride reactions will proceed rapidly.

In addition to the modifications made for Test 5, minor modifications were made to the primary cyclone to improve performance of particulate

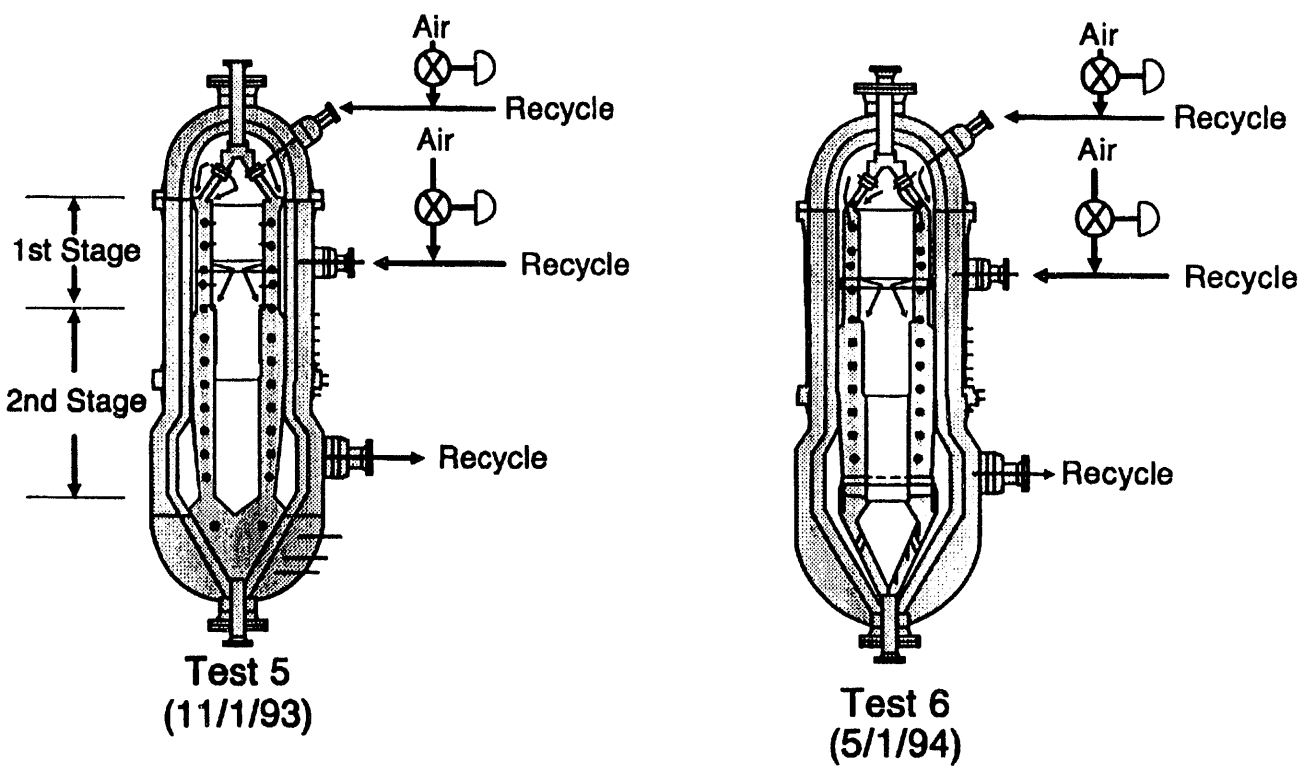

Figure 6. Hot Gas Cleanup Regenerator Modifications – Test 6

collections during lock-hopper operation. Sorbent transfer valves manufactured by two vendors were installed in the HGCU system to evaluate alternate valve designs in high-temperature, high-solids loading applications.

Test 6 utilized Illinois #6 (1.9% sulfur) as the gasifier input fuel, producing approximately 3500–4000 ppm H_2S in the coal gas. Sodium bicarbonate injection into the coal gas was also retained during Test 6. The system was tested with finer grades of sodium bicarbonate. Because the finer grades caused bridging of the feeder, the original grade of sodium bicarbonate was used for Test 6 and no improvement in this system's performance was expected.

Modifications to the turbine simulator, as previously noted, included relocation of the air swirler/fuel nozzle, changes to the swirl angle, and blocking of dilution holes in the liner. An improved cooling scheme for the nozzle cascade mounting flange area was also incorporated to prevent problems caused by thermal growth of the cascade relative to the mounting flange.

Test 6 Results

Test 6 resulted in approximately 80 hours of integrated gasifier/HGCU system operation and represents the longest integrated test operation to date in the program. The only hardware problem encountered during Test 6 was the failure of the sorbent elevator cable on Wednesday evening. This failure resulted in severe damage to the elevator bucket; however, repairs to the bucket and elevator were made in a very short time, and the system was returned to operation on Thursday morning.

The overall results of Test 6 are shown in Figure 7. The performance of Z-Sorb was very encouraging. Removal of H_2S from the gas stream was very good, with long periods of testing with

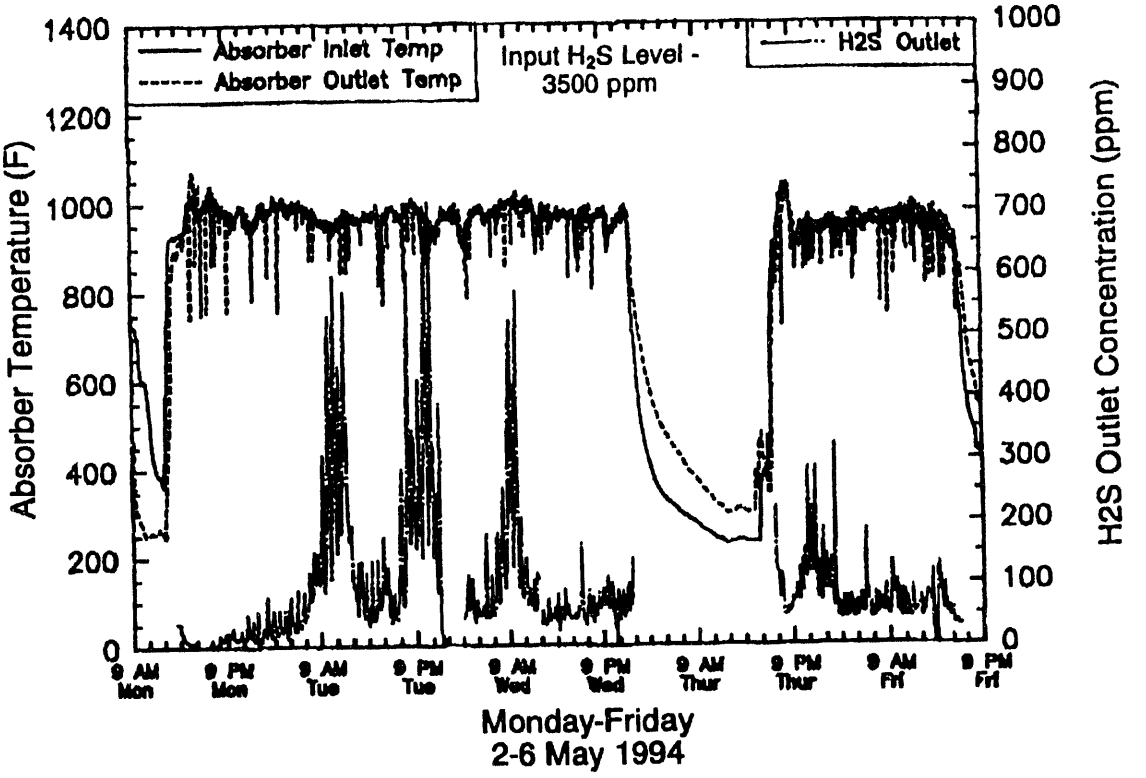

Figure 7. Absorber Performance – Test 6

less than 50 ppm H_2S in the absorber outlet stream. No problems were encountered with the use of Z-Sorb in a moving bed system. The sorbent flowed well and no significant water gas shift in the absorber was observed. Although an exothermic methanation reaction was predicted during the first sulfidation cycle of the material, that reaction was not observed. Post-test inspection did not reveal any agglomeration of sorbent or other signs of physical degradation.

As shown in Figure 7, the performance of the HGCU system fell off slightly during three periods on Tuesday and Wednesday. This decrease in absorber performance was associated with adjusting the regeneration control conditions to determine the best regeneration strategy for Z-Sorb. Once the proper regeneration conditions were met, the performance of the Z-Sorb returned to predicted H_2S performance levels.

One difference between Z-Sorb and the zinc titanate previously tested was the limitation on the upper temperature of the sorbent. Phillips Petroleum Company recommended that the peak regeneration temperature of Z-Sorb be limited to approximately 1350°F, significantly lower than the 1500°F peak temperature used for zinc titanate. This operational limitation required that close control be maintained over the regeneration process.

Due to the different regeneration characteristics of Z-Sorb compared to zinc titanate, several operational changes (e.g., lowering the temperature of the inlet recycle gas) were necessary to maintain the proper temperatures. For most of the test, a nitrogen purge through the regenerator exit area was maintained to decompose any sulfate that might have formed during regeneration. Post-test analysis indicates that sulfate levels in the sorbent leaving the regenerator were very low, generally less than 0.5%. Total residual sulfur in the sorbent leaving the regenerator was approximately 1% for those periods of good regeneration. These levels are significantly lower than the regenerator sorbent sulfur levels observed in Test 5. Although the use of Z-Sorb improved performance of the HGCU system, the test results continued to indicate that improved control of sorbent temperature (i.e., sufficient heat rejections), while maintaining sufficient oxygen content in the recycle gas to complete regeneration is the key to HGCU performance.

Fines were collected under the vibrating sorbent screen at the bottom of the regenerator in order to measure the attrition loss of Z-Sorb. The attrition resulting from movement of fresh sorbent through the HGCU system at ambient temperature was approximately 0.2% of the total material circulated through the system. The overall attrition loss over 8 cycles of absorption/regeneration in Test 6 was approximately 0.4% of the total sorbent moved. This attrition rate is considered to be very low at the scale of the PEF and is significantly better than the attrition rate of zinc titanite in Test 5.

A major achievement of Test 6 was the demonstration of effective chloride removal by the regenerator recycle guard bed. Chloride levels downstream of the guard bed averaged 308 ppm compared to 1000–2000 ppm in previous tests. This reduction enabled us to maintain full recycle gas flow throughout the test. The heat exchanger pressure drop was constant throughout the test.

Test 6 was the first test that did not require cleaning of the recycle loop heat exchangers during a long duration test. The sodium bicarbonate material in the guard bed did react with chlorides as expected; however, SO_2 in the recycle loop also reacted with the sodium bicarbonate and reduced the SO_2 levels to 6–7% during the test. The use of

sodium bicarbonate in the recycle loop guard bed was effective in removing chlorides; although an improved guard bed material, demonstrating lower reactivity to SO_2 while maintaining reactivity towards chlorides, is under investigation.

The performance of the sodium bicarbonate injection system for removal of chlorides in the fuel gas was found to be of the same level as demonstrated in Test 5. The system removed 25–35% of the chlorides from the fuel gas, and an improved sodium bicarbonate/recycle design is in progress.

Turbine simulator testing totaled 67 hours of fired operation. The simulator operated for over 24 hours at 2300°F combustor exit temperature and at 2500°F for three hours. The modifications to the turbine simulator were successful, resulting in low metal temperatures both in the cap/cowl area and in the combustor liner. No deposits were observed on the turbine simulator nozzle or liner after the conclusion of the test. The NO_x emissions from the turbine simulator were approximately 200 ppm (@ 15% oxygen) due to the conversion of fuel-bound nitrogen species, such as ammonia, to NO_x. Ammonia in the fuel gas was measured at 4100 ppm. Carbon monoxide (CO) and unburned hydrocarbon emissions were also found to be very low.

Vapor phase alkali measurements in the hot fuel gas (850°F) were performed by the research staff of Ames Laboratory during Test 6. This testing was performed using an on-line atomic absorption spectrometer to measure alkali directly in the vapor phase of the fuel gas. Preliminary results of this testing indicated that the alkalis in the fuel gas were present at levels well below 10 ppb. This level is well below the turbine alkali tolerance specification required by GE. Details of the turbine simulator testing and alkali testing are discussed in a concurrent paper presented by Feitelberg et al. (1994) in these proceedings.

Overall, Test 6 was the most successful test of the HGCU program to date. Sulfur removal efficiency of 98 to 99% was demonstrated, and sorbent attrition was very low. The guard bed prevented plugging of the recycle heat exchanger during the test period and all HGCU mechanical systems (with the exception of the elevator) performed well. The turbine simulator reached "F" class turbine firing conditions with no damage to the hardware.

FUTURE WORK

Several additional tests are planned for the gasifier/HGCU/turbine simulator in calendar year 1994. Two 100-hour tests are planned for August and October to demonstrate an improved internal sorbent flow configuration for the absorber and the addition of the recirculating sodium bicarbonate chloride removal system to the fuel gas stream. The test year will culminate with a longer term test (100 to 200 hours) in December 1994. A 24-hour test of an experimental rich-quench-lean combustor will also be performed during the fourth quarter of 1994. All remaining testing in 1994 is based on the use of Z-Sorb and will be focused on demonstrating long-term durability of the HGCU system and the sorbent.

REFERENCES

Ayala, R., September 1992. "Enhanced Durability of High Temperature Desulfurization Sorbents for Moving-Bed Applications," Twelfth Annual Gasification and Gas Stream Cleanup Systems Contractors Review Meeting, Report DE/AC21-88C25003.

Ayala, R.E., E. Gal, and R.P. Gupta, 1993. "Testing of Zinc Titanate Sorbents for Moving Bed Applications." In Proceedings of the Coal Fired Power Systems 93- Advances in IGCC and PFBC Review Meeting, pp. 136-145. DOE/METC-93/6131.

R. E. Ayala, T. Chuck. E. Gal, and R.P. Gupta, 1994. "Testing of Zinc Titanate Desulfurization Sorbents for Moving-Bed Applications. Included in the present volume.

Cook, C.S., E. Gal, A.H. Furman, R. Ayala, and R.M. Tucker, May 1988. "Integrated Operation of a Pressurized Fixed Bed Gasifier and Hot Gas Desulfurization System," Eighth Annual Gasification and Gas Stream Cleanup Systems Contractors Review Meeting, Report DOE/METC/88/6092.

Cook, C.S., E. Gal, A.H. Furman, R.M. Tucker, and B. Parekh, June 1989. "Integrated Operation of a Pressurized Fixed Bed Gasifier and Hot Gas Desulfurization System," Ninth Annual Gasification and Gas Stream Cleanup Systems Contractors Review Meeting, Report DOE/METC/89/6107, Vol. I.

Cook, C.S., E. Gal, A.H. Furman, R.M. Tucker, and B. Parekh, August 1990. "Integrated Operation of a Pressurized Fixed Bed Gasifier and Hot Gas Desulfurization System," Tenth Annual Gasification and Gas Stream Cleanup Systems Contractors Review Meeting, Report DOE/METC/90/6115, Vol. I.

Cook, C.S., E. Gal, A.H. Furman, and R. Ayala, August 1991. "Integrated Operation of a Pressurized Fixed Bed Gasifier and Hot Gas Desulfurization System," Tenth Annual Gasification and Gas Stream Cleanup Systems Contractors Review Meeting, Report DOE/METC/91/6123, Vol. I.

Cook, C.S., E. Gal, A.H. Furman, and R. Ayala, September 1992. "Integrated Operation of a Pressurized Fixed Bed Gasifier and Hot Gas Desulfurization System," Twelfth Annual Gasification and Gas Stream Cleanup Systems Contractors Review Meeting, Report DOE/METC-92/6128, Vol. I.

Feitelberg, A.S., C.S. Cook, N. Abuaf, S.L. Hung, M.S. Samuels, and D.J. Najewicz, 1993. "Combustion Tests of a Turbine Simulator Burning Low Btu Fuel and a Ruch-Quench-Lean Combustor. In Proceedings of the Coal Fired Power Systems 93- Advances in IGCC and PFBC Review Meeting, pp. 169-178. DOE/METC-93/6131.

Smith, D.P., E. Gal, C.S. Cook, and A.H. Furman, June 1987. "Design Studies for Hot Gas Cleanup System in a Load Following Mode," Seventh Annual Gasification and Gas Stream Cleanup Systems Contractors Review Meeting, Report DOE/METC/87/6079.

6.3

Enviropower Hot Gas Desulfurization Pilot

CONTRACT INFORMATION

Cooperative Research and Development Agreement Number: 93-016

Contractor:
Enviropower Inc.
P.O. Box 35
33701 Tampere
Finland
+358-31-2413511

Contractor Administrative Contact: Kari Salo

Contractor Technical Contact:
Reza Ghazanfari
Gabor Feher

Principal Investigators:
Jukka Konttinen
Reza Ghazanfari
Arto Lehtovaara
Wahab Mojtahedi

METC Project Manager: Thomas P. Dorchak

Period of Performance: September 8, 1993 to December 31, 1995

Schedule and Milestones:

1993-95 Program Schedule

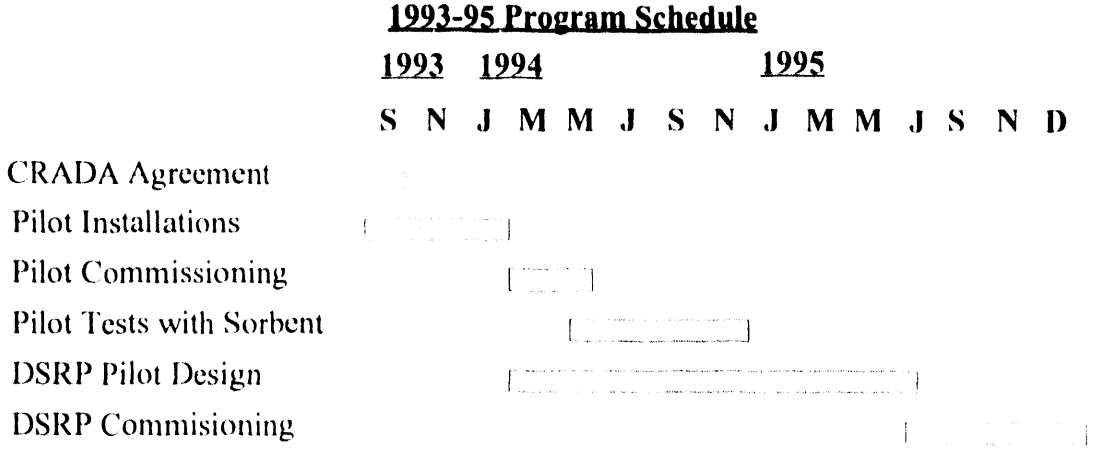

OBJECTIVES

In September 1993 Enviropower Inc. entered into a Cooperative Research and Development Agreement (CRADA) with the Department of Energy in order to develop and demonstrate the major components of an IGCC process such as hot gas cleanup systems.

The objectives of the project are to develop and demonstrate 1) hydrogen sulfide removal using regenerable zinc titanate sorbent in pressurized fluidized bed reactors, 2) recovery of the elemental sulfur from the tail-gas of the sorbent regenerator and 3) hot gas particulate removal system using ceramic candle filters.

BACKGROUND INFORMATION

Enviropower Inc. is a subsidiary of Tampella Power Inc. which is the parent company of the Tampella Power Corporation in the U.S.A. Enviropower Inc. is actively involved in the development of IGCC process. Enviropower's IGCC concept incorporates pressurized fluidized bed gasification of different solid fuels, applying air-blown gasification and hot gas clean-up. The IGCC process diagram can be seen in Figure 1.

As part of the Clean Coal IV-program in 1992, Tampella's IGCC technology was chosen by the United States Department of Energy (DOE) to be demonstrated in the U.S.A. Currently, an IGCC demonstration plant to be built in Finland is being designed by Enviropower Inc. to utilize biomass and coal. The IGCC process and the demonstration projects have been described in detail elsewhere /1, 2/.

Enviropower's U-GAS-based gasification pilot plant is located in Tampere, Finland. The thermal input of the gasifier is 15 MW (or 35 tons of coal per day) and maximum operating pressure of 30 bar. The pilot plant has the capability of gasifying coal, biomass and different waste materials. It also includes the components for hot gas cleanup including hot gas desulfurization and fine particulate removal using ceramic candle filters. The components of the pilot-process are described in Figure 2.

In the Enviropower's present concept of IGCC, the bulk of fuel bound sulfur is removed in the gasifier by means of a calcium based sorbent such as limestone or dolomite and the rest is removed externally in a fluidized bed system using a regenerable sorbent such as zinc titanate. The sulfur removal options in Enviropower's IGCC process can be seen in Figure 3. Novel zinc titanate sorbents suitable for fluidized bed application has been tested and the plan is to use the regenerable sulfur removal system as the sole method of sulfur removal in the future. This will reduce the bulk of solid waste from the gasifier and improve the system performance and economy.

Cyclic sulfidation and regeneration tests with zinc titanate have been carried out in a 3-inch I.D. batch fluidized bed reactor which is located at the Institute of Gas Technology in Chicago. The reactor is capable of operating at temperatures up to 1000°C and pressures up to 30 bar with synthetic gas mixtures containing all the gaseous components for sulfidation and regeneration reactions. The 3-inch pressurized fluidized bed reactor assembly has been described in detail elsewhere /5/ and a schematic diagram can be seen in Figure 4. A typical H_2S breakthrough curve in cyclic tests for one of the sorbents is shown in Figure 5. Figure 6 shows the corresponding regeneration curve. The laboratory- and bench-scale test results have been reported in more detail elsewhere /3, 4, 5/.

PROJECT DESCRIPTION

The CRADA-project consists of the following subtasks:

· Laboratory-scale tests will be conducted on selected sorbents for removal of hydrogen sulfide. These tests will be performed in a 3 inch pressurized fluidized bed under conditions simulating the real situation with respect to temperature, pressure, gas composition and contaminants. Sorbents will be fully analyzed for their physical, chemical and mechanical durability characterization.

· Full-scale pilot-plant testing of the sorbents will be carried out in Finland, using a pressurized fluidized-bed absorber and regenerator. The sulfur removal efficiency and long term durability of the sorbent will be evaluated in these tests. Sorbent samples from the pilot-plant tests will be analyzed the same way as fresh sorbents by Enviropower, IGT and METC.

· The tail gas from the regeneration contains sulfur dioxide which can be converted to usable elemental sulfur. A technology called the Direct Sulfur Recovery Process (DSRP) has been developed at Research Triangle Institute (RTI) /6/ to achieve this objective. A skid-mounted DSRP unit will be designed and built in METC and will be shipped to the pilot plant in Finland for installation and testing with a slipstream of the U-gas process coal gas. Suitability of the DSRP process and sulfur conversion efficiency will be examined during testing. Design data will also be obtained for scale-up for commercial-sized systems.

· The collection efficiency and operability of ceramic candle filters for removing solid particles from the hot gas will be examined in full scale pilot plant tests in Finland. The filter ash, fuel and U-gas gasifier fly ash will be analyzed for their physical properties.

RESULTS AND FUTURE WORK

Pilot design and testing

The installation of the sulfur removal pilot was under way in September 1993 when CRADA was signed. The major part of the installation took place in 1993 and it was completed in January 1994. The pilot consists of HTHP fluidized-bed type sulfider and regenerator reactors and systems for fresh sorbent feeding, sorbent circulation between reactors and gas preheating/cooling for regenerator. In February 1994, the operational check-out of the pilot at actual process conditions was carried out with the objective of testing the mechanical integrity of the system as part of the pilot plant. Inert sand was used as bed material in sulfider and regenerator reactors. The tests showed that the sorbent feeding and circulation systems could be operated as designed, and the automation and control systems were working well. Bed material samples from both reactors could be taken without difficulty.

In March 1994, two tons of zinc titanate sorbent produced by the United Catalysts, Inc. was received from U.S.A. The average particle size of the sorbent batch is about 200 μm and particle density about 2 g/cm^3, which is in the region of well fluidizable particles according to Geldart classification /7/. Another batch of zinc titanate sorbent (ZT-4) with about the same fluidization properties has been ordered by DOE to be shipped to Finland by September 1994.

In May 1994, the commissioning of the pilot was accomplished with zinc titanate sorbent at actual process conditions with coal gas. Bituminous (Polish) coal was used as gasifier feedstock. The test run was successful and several operation test points was run. The data are presently being analyzed and some of the results are shown in Figures 7, 8 and 9.

The following preliminary conclusions from the pilot commissioning with zinc titanate sorbent can be drawn:

· several steady-state operation test points of the sulfider and regenerator fluidized bed reactors linked together near and at design pressures and temperatures was obtained

· the regeneration of the sorbent with steam+air mixture seemed to work without problems

· it was possible to keep the regenerator bed temperature in the range of 650-750°C and SO_2 outlet content between 0-4 vol-% (mainly 2 vol-%) by controlling the air flow into the reactor

· As can be seen in Figures 7, 8 and 9, the continuous transport of the sorbent between the fluidized bed-type reactors seemed not to interrupt regeneration or sulfidation much.

· Very high sulfur removal efficiencies in sulfider were obtained by adjusting the bed height and gas superficial velocity (Figure 7)

· more tests are needed to obtain larger steady-state runs to optimize the system. These will be undertaken in 1994.

The tests with the pilot will continue in fall 1994 by using the current and ZT-4 sorbent.

Laboratory-scale work

Bed samples taken from the pilot tests and fresh zinc titanate samples will be tested by the DOE and IGT according to the project plan.

Other subtasks

The performance of ceramic filters with coal gas was and will be tested during the same test runs with sulfur removal pilot unit.

The data from the test run in May 1994 are currently being analyzed. The preliminary results show however that the filtration efficiency is high enough to satisfy gas turbine requirements.

The design of the DSRP-pilot equipment is proceeding with the preliminary objective to test the unit in connection with the pilot-plant in Finland by mid-1995.

Modelling efforts

A steady-state kinetic model for hot gas desulfurization system has been developed based on laboratory- and bench-scale tests on zinc titanate sorbents. The model has been used in the preliminary dimensioning of the commercial-scale sulfur removal system. The results from the pilot test run in May show that the model predictions were in good agreement with the test results.

A dynamic model for the pilot and commercial-scale post-bed sulfur removal system is under development. The objective is to use it for predicting the effects of the changes in regenerator inlet gases, sorbent transport velocity, fluidization velocities etc. on the overall performance. This information can be used to adjust the control system of the process. After the verification of the dynamic model with pilot test results it will be added as a module into the Enviropower's existing IGCC-plant dynamic simulator for design and training purposes.

REFERENCES

1. PATEL J.G., *The simplified IGCC Process - Clean Coal Technology for Power Generation.* Paper presented at Comparative Economics of Emerging Clean Coal Technologies III: Advanced Power & Environmental Control. Washington, DC, USA, February 28 & March 1, 1994.

2. SALO K., *Using Biomass-Gasification Combined Cycle Technology in Power Generation.* In: Energy in Finland 1993, pp. 32 - 35

3. KONTTINEN J., MOJTAHEDI W.; *Gasifier gas desulfurization at high temperature and pressure.* Kemia-Kemi (Finnish Chemistry) (1993)11-12. (In English)

4. MOJTAHEDI W., SALO K., ABBASIAN J.; *Desulfurization of hot coal gas in fluidized bed with regenerable zinc titanate sorbents.* Fuel Processing Technology 37(1994) 53-65.

5. ABBASIAN J., BACHTA R.P., WANGEROW J. R., MOJTAHEDI W., SALO K.; *Advanced High-Pressure Bench-Scale Reactor for Testing with Hot Corrosive Gases.* Ind. Eng. Chem. Res. 33(1994)1.

6. GANGWAL S.K., MCMICHAEL W.J., AGARWAL S.K., CHEN D.H., HOPPER J.R.; *Bench-Scale Testing and Evaluation of the Direct Sulfur Recovery Process.* In: Proceedings of the Twelth Annual Gasification and Gas Stream Cleanup Systems Contractors Review Meeting. Sponsored by U.S. Department of Energy. WV USA, September 15-17, 1992.

7. KUNII D., LEVENSPIEL O.; *Fluidization Engineering, Second Edition.* Butterworth-Heinemann, USA 1991.

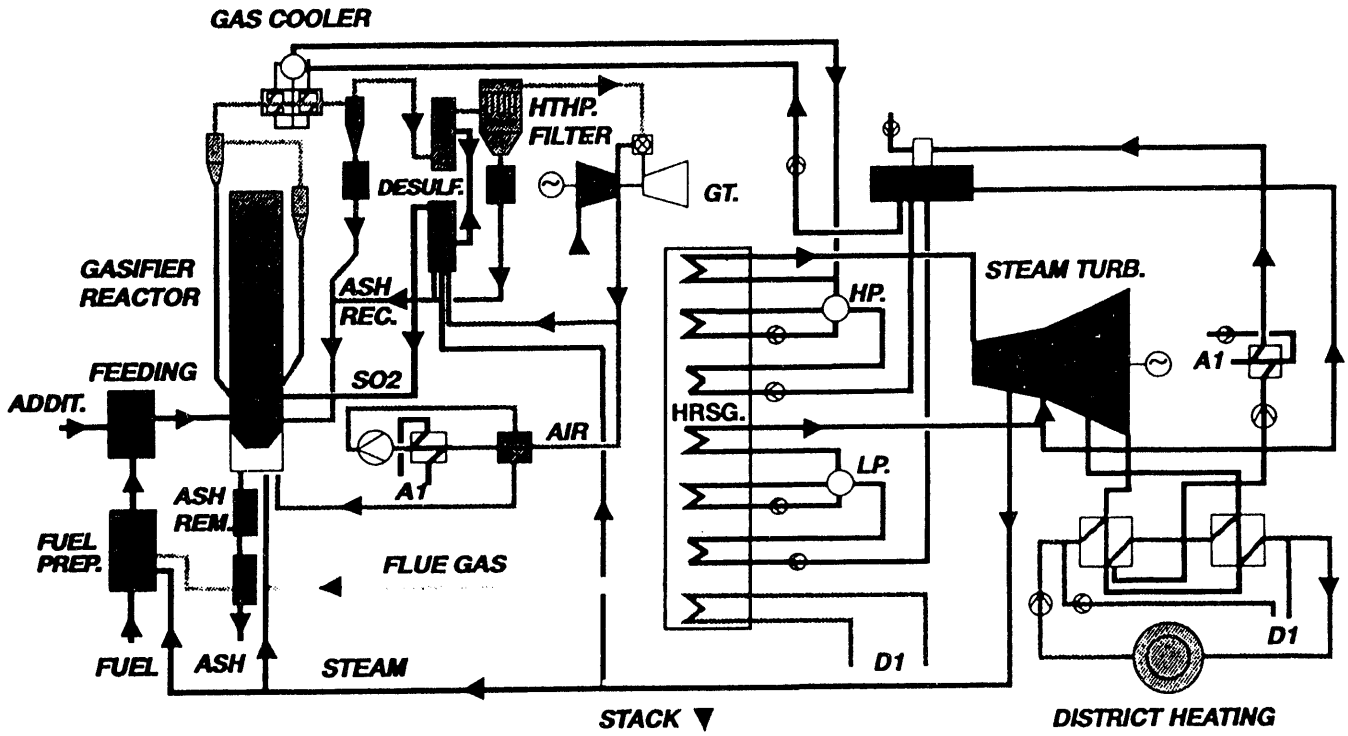

Figure 1. Tampella's IGCC process scheme.

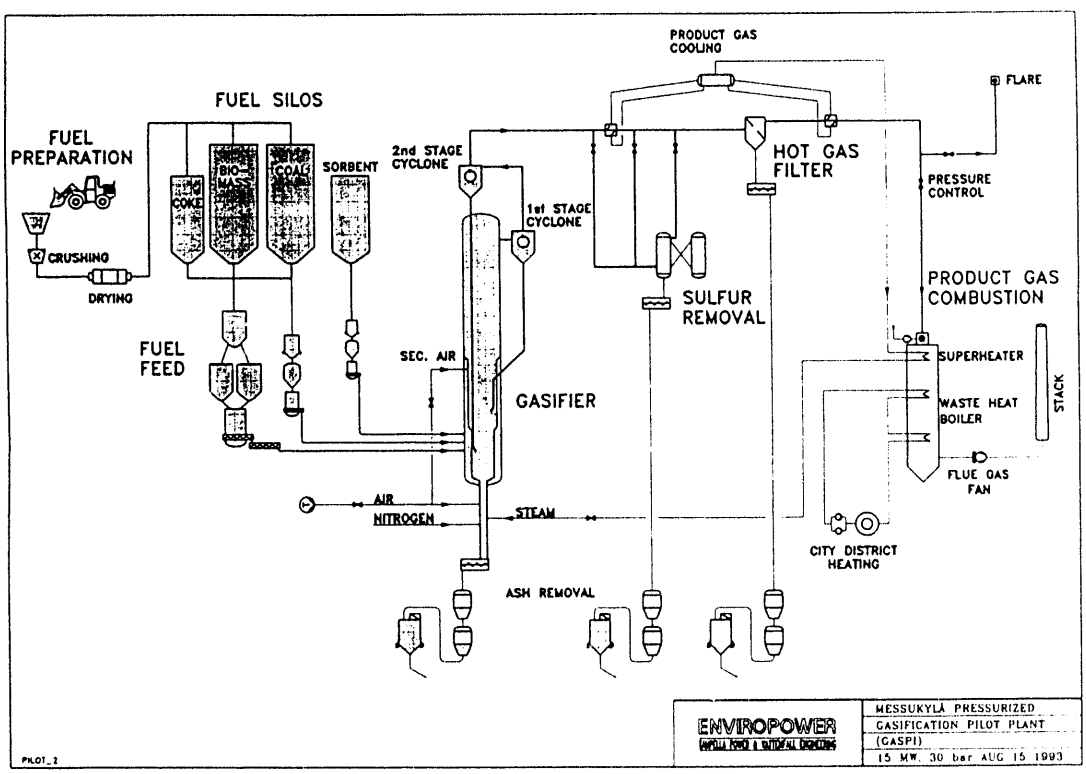

Figure 2. Scheme of the Enviropower's pressurized gasification pilot plant.

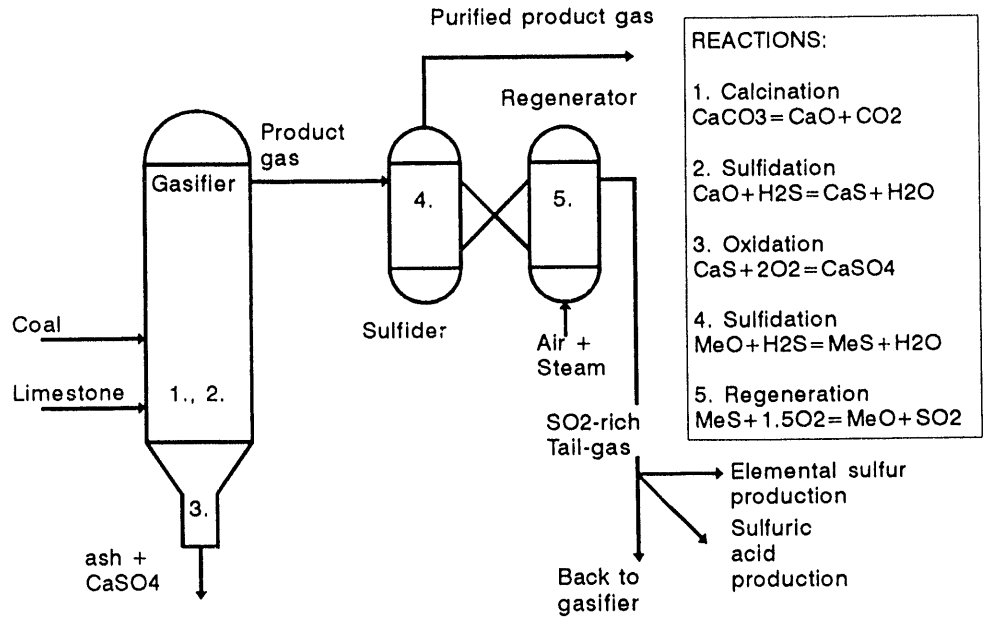

ENVIROPOWER

Figure 3. Different stages in Tampella's IGCC sulfur removal.

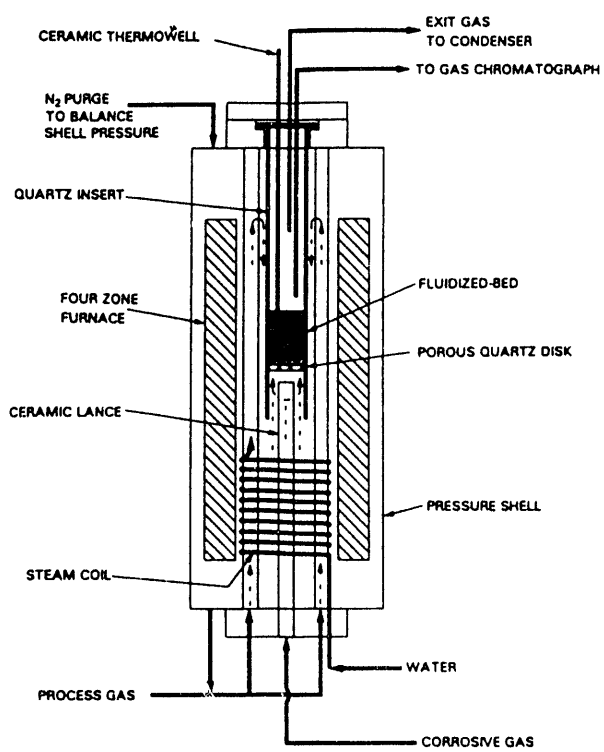

Figure 4. High-temperature/high pressure 3-inch batch fluidized bed reactor assembly.

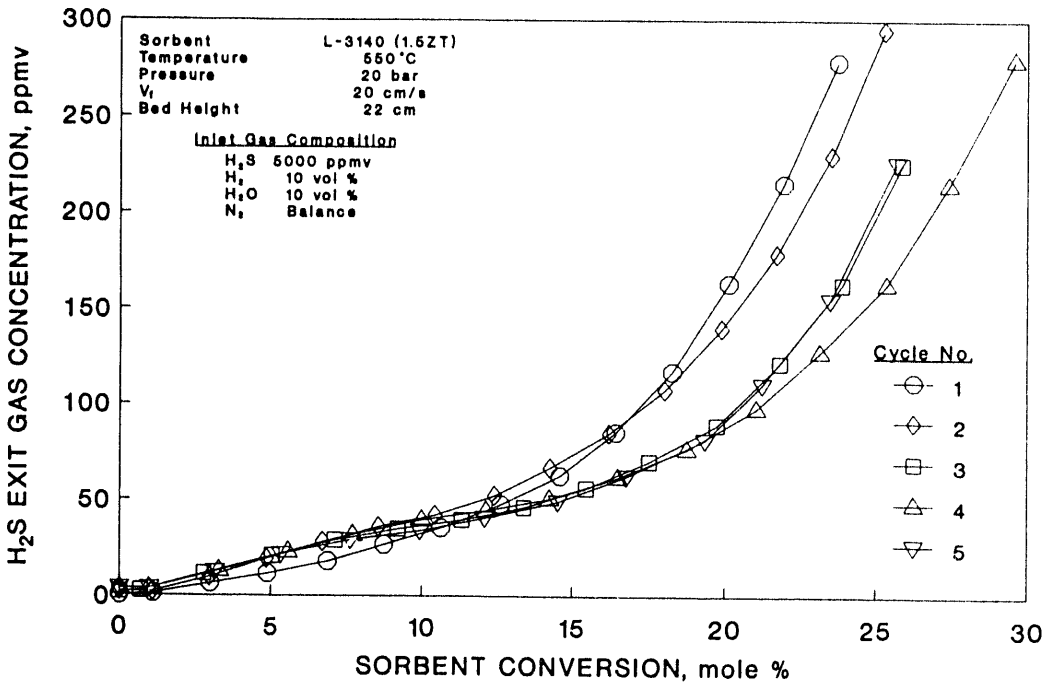

Figure 5. H_2S breakthrough curve for L-3140 zinc titanate sorbent in the 3-inch batch reactor.

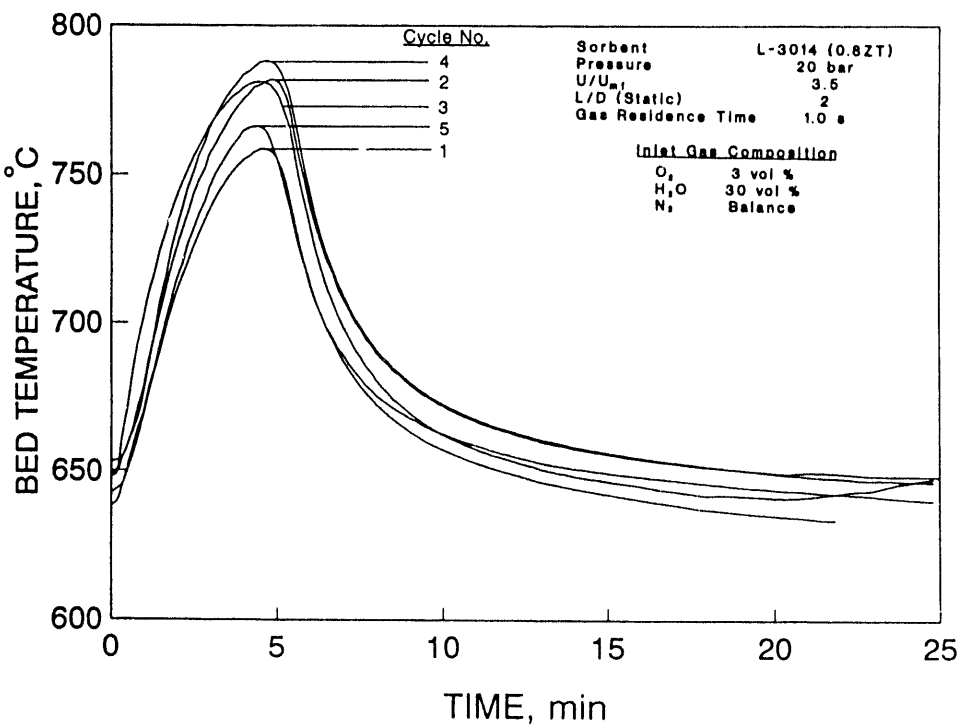

Figure 6. Bed temperature rise in 3-inch batch fluidized bed reactor due to exothermic regeneration reaction.

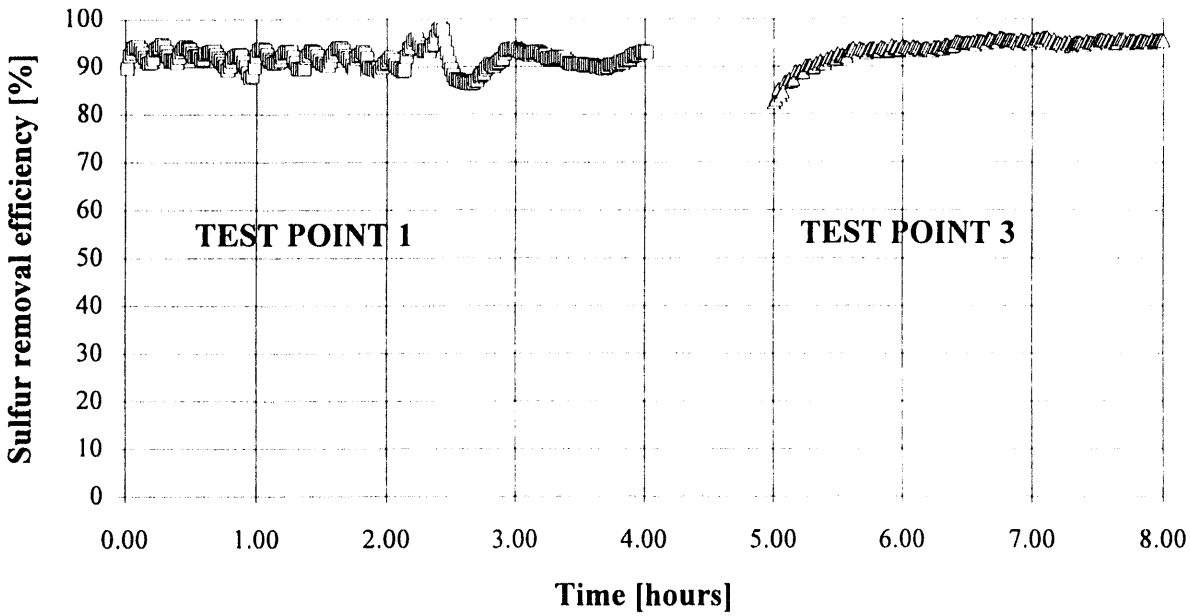

Figure 7. Hot gas desulfurization pilot test run in May 1994. Calculated sulfur removal efficiencies in sulfider during two test points.

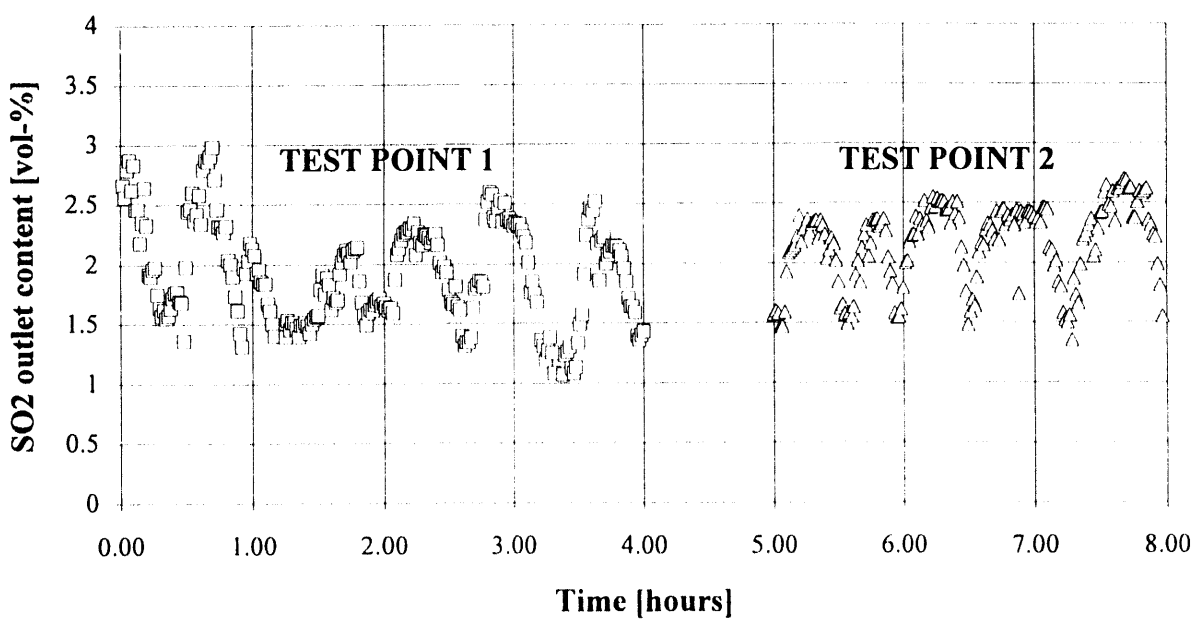

Figure 8. Hot gas desulfurization pilot test run. SO_2 outlet content [vol-%] in the regenerator off-gas during two test points (manual regenerator air inlet control).

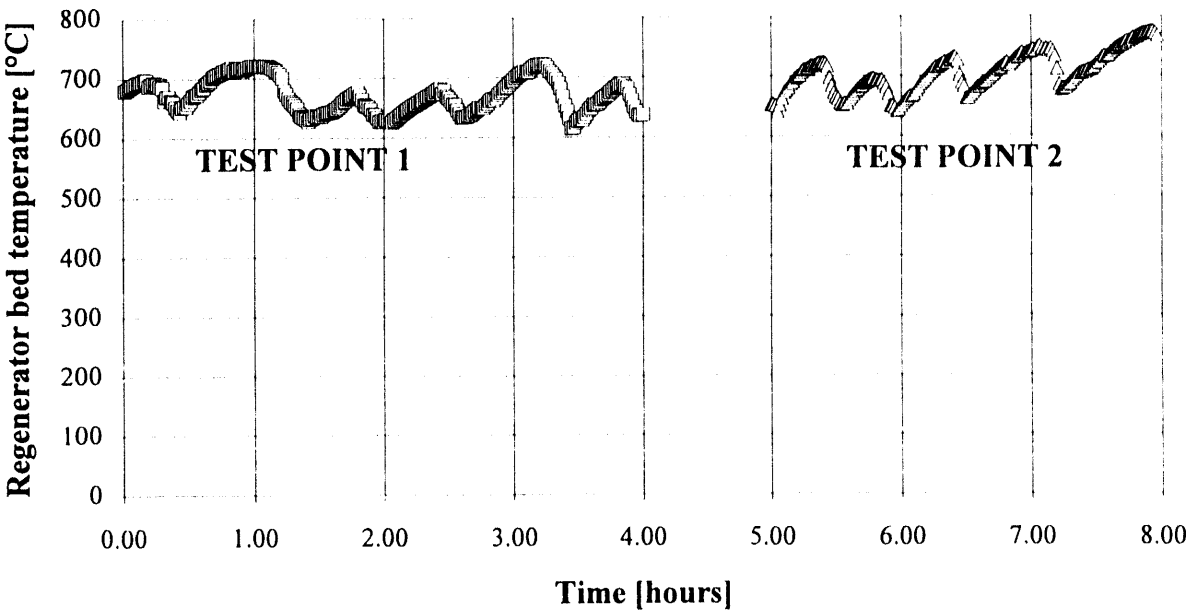

Figure 9. Hot gas desulfurization pilot test run. Regenerator bed temperature during two test points.

6.4 Slipstream Testing of the Direct Sulfur Recovery Process

CONTRACT INFORMATION

Contract Number	DE-AC21-93MC30010
Contractor	Research Triangle Institute P. O. Box 12194 Research Triangle Park, NC 27709-2194 (919) 541-8033
Contractor Project Manager	Santosh K. Gangwal
Principal Investigators	Jeffrey W. Portzer Gary B. Howe Daniel H. Chen (Lamar University) Michael H. McMillian (DOE/METC)
METC Project Manager	Thomas P. Dorchak
Period of Performance	July 1, 1993 to December 12, 1994

Schedule and Milestones

FY94-95 Program Schedule

	J	A	S	O	N	D	J	F	M	A	M	J	J	A	S	O	N	D
MET Field Test																		
Large-Scale System																		

OBJECTIVES

The objective of this work is to continue further development of the zinc titanate fluidized-bed desulfurization (ZTFBD) and the Direct Sulfur Recovery Process (DSRP) technologies for hot gas cleanup in integrated gasification combined cycle (IGCC) power generating systems. There are three main goals of this project:

- Development of an integrated, skid-mounted, bench-scale ZTFBD/DSRP reactor system;
- Testing the integrated system over an extended period with a slipstream of coal gas from an operating gasifier to quantify the degradation in performance, if any, caused by the trace contaminants present in coal gas (including heavy metals, chlorides, fluorides, and ammonia); and

- Design, fabrication, and commissioning of a larger, pilot-plant scale DSRP reactor system capable of operating on a six-fold volume of gas greater than the reactors used in the bench-scale field tests.

BACKGROUND INFORMATION

Hot gas desulfurization processes for IGCC and other advanced power applications utilize regenerable mixed metal-oxide sorbents to remove hydrogen sulfide (H_2S) from raw coal gas. Regeneration of these sorbents produces an off-gas typically containing 1 to 3 percent sulfur dioxide (SO_2). Reduction to elemental sulfur is a highly desirable option for the ultimate disposal of the SO_2 content of this off-gas. Elemental sulfur, an essential industrial commodity, is easily stored and transported. The DSRP is a simple and attractive process for production of elemental sulfur from the regeneration off-gases.

As shown in Figure 1, the DSRP consists of two catalytic reactors, each followed by a sulfur condenser. Hot regeneration off-gas is mixed with a hot coal gas slipstream (to act as the reducing gas) and is fed to the first DSRP reactor. Approximately 95 percent of the combined sulfur in the inlet stream of the first reactor is converted to elemental sulfur. The outlet gas of the first DSRP reactor is cooled, condensing out sulfur. The flow of reducing gas to Stage I is controlled so that there is a 2-to-1 H_2S-to-SO_2 ratio at this point. This cooled gas stream is then sent to the second DSRP reactor where 80 to 90 percent of the remaining sulfur compounds are converted to elemental sulfur via the modified Claus reaction at high pressure. The total efficiency of the two reactors for the conversion of sulfur compounds to elemental sulfur has been demonstrated to be 99 percent.

The development of the DSRP has proceeded from lab-scale experiments utilizing 25- to 50-cc

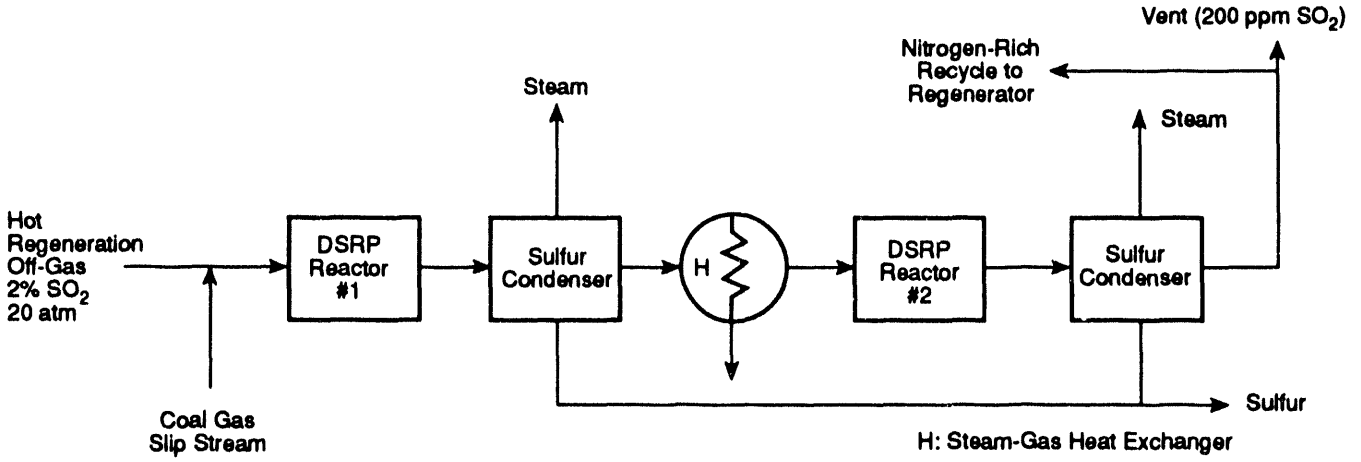

Figure 1. DSRP Process

fixed-bed reactors (McMichael and Gangwal, 1990) through bench-scale (Gangwal and McMichael, 1991; Gupta et al., 1992; Gangwal et al., 1992), and fluidized-bed testing (Gangwal et al., 1993). The composition of the regeneration off-gas has been varied to as high as 12.4 vol% SO_2; pressures have ranged from 1.7 to 24.8 atm. The results indicate the effectiveness in obtaining up to 96 percent conversion to sulfur in one stage of reaction and up to 99 percent in two stages with efficient interstage sulfur removal. Independent studies by Gilbert Commonwealth, Texaco, and the Research Triangle Institute (RTI) have shown the economic attractiveness of the DSRP (Robin et al., 1993; Buchanan et al., 1994; McMichael and Gangwal, 1990).

Through bench-scale development, both fluidized-bed zinc titanate and DSRP technologies have been shown to be technically and economically attractive. The demonstrations to date, however, have only been conducted using simulated (rather than actual) coal gas and simulated regeneration off-gas. Thus, the effect of trace contaminants in actual gases on the sorbent and DSRP catalyst is currently unknown. Also, ZTFBD and DSRP have not been demonstrated in an integrated manner. Finally, data from a larger reactor size are needed for realistic scaleup to commercial scale. Thus, this project continues further development of the zinc titanate desulfurization and DSRP technologies by testing with a slipstream of actual coal gas in bench-scale and larger equipment.

PROJECT DESCRIPTION

The slipstream testing activities that are the subject of the present project will be conducted in two distinct phases. The first will be at the Morgantown Energy Technology Center (METC), using a slipstream from the 10-in. experimental gasifier directed to the ZTFBD/DSRP system housed in a mobile unit. The second phase will be design and commissioning of a larger scale DSRP unit that is to be eventually tested at the Enviropower pilot plant employing a 10 MWe (thermal) U-gas gasifier coupled to a ZTFBD system. Enviropower, a subsidiary of Tampella Power Corporation, is commercializing IGCC systems in the United States.

METC operates an air-blown, fluidized-bed, 10-in. dia gasifier capable of providing approximately 300 lb/h—approximately 4,750 standard cubic feet per hour (scfm)—of low-Btu coal gas from a nominal charge rate of 80 lb/h of coal. A simplified vessel and piping layout showing the gasifier, modular gas cleanup rig (MGCR), and the location of the slipstream are provided in Figure 2. Table 1 shows the typical coal gas composition following gasification of a medium-sulfur coal. The raw coal gas is supplied at 538 °C (1,000 °F) and 425 pounds per square inch gage (psig) pressure to downstream cleanup devices. The system includes several particle removal stages that provide the capability to tailor the particle loading to the cleanup section. The cleanup test section consists of a closely coupled MGCR. To supply the ZTFBD and DSRP test apparatus, a coal gas slipstream of approximately 185 scfh (4.3 percent of the gasifier flow) at 538 °C (1,000 °F) and 350 to 400 psig is taken from the MGCR section between the filter vessel and the MGCR sorbent reactor, vessels F100 and V100, respectively. The particulate-free coal gas slipstream is transported through an insulated, heat-traced process line to the RTI ZTFBD/DSRP system.

All of the process equipment, control equipment, and sampling and analysis equipment for field testing at METC is housed in a specially modified office trailer (mobile laboratory). The experimental apparatus is being fabricated, assembled, installed, and commissioned in the lab trailer while it is conveniently located at an RTI site. Provision has been made for a full pressure, full-power checkout of all equipment before relocating the trailer at METC. The system will be pres-

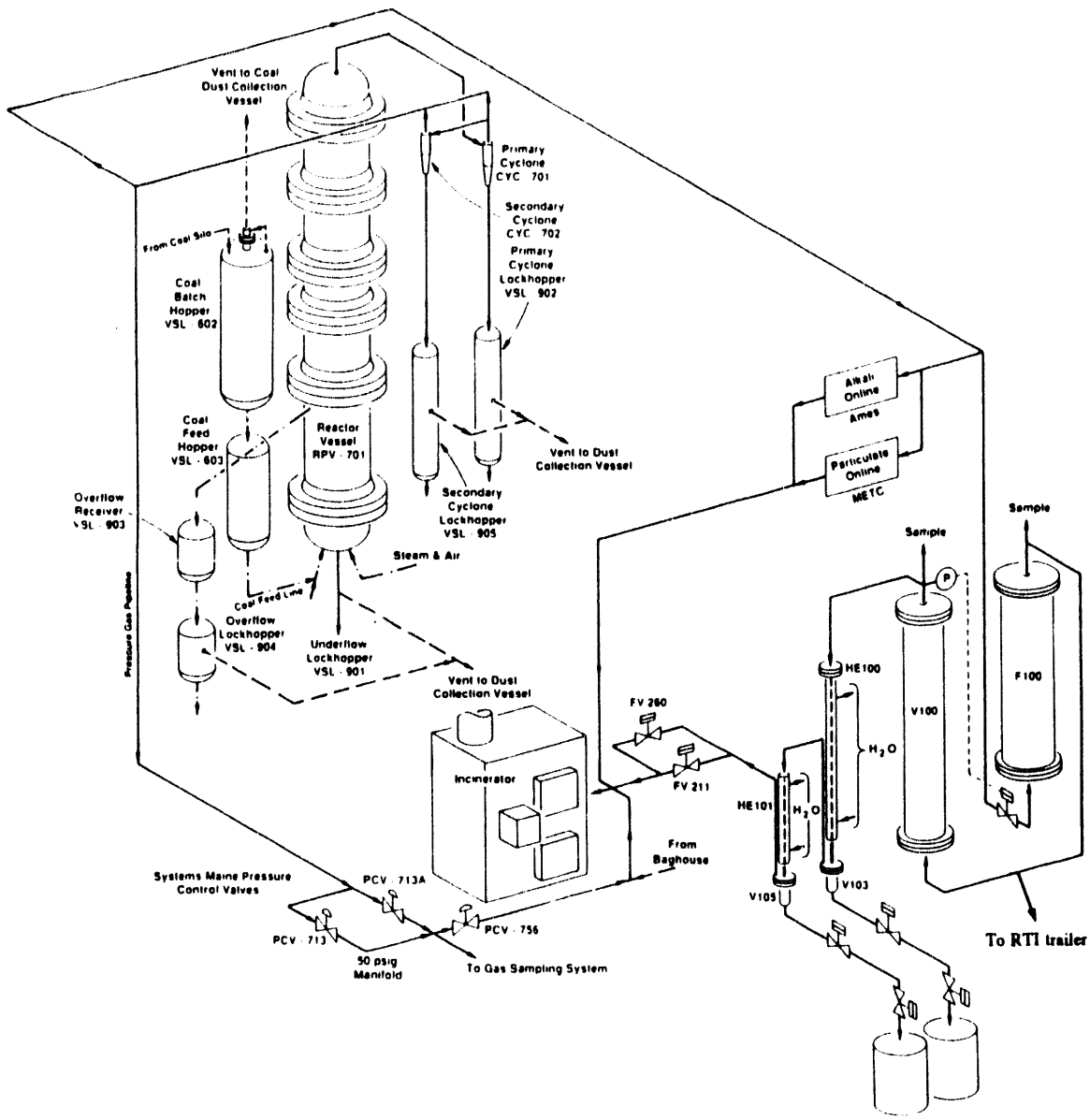

Figure 2. B-12 Fluidized-Bed Gasifier and Cleanup Rig Simplified Vessel and Piping Layout

sured up with inert gases, and the electrically heated furnaces, mass flow controllers (MFCs), computer data loggers, flow control valves, and automatic shutdown system can be operated and checked out. All equipment will be leak-tested prior to installing the insulation. In addition, the toxic gas sensors will be calibrated and the emergency shutdown procedures will be operated.

The fully configured relocatable laboratory will then be transported to the METC site. Only minimal construction on site will be required to

Table 1. Typical Coal Gas Composition (vol%)

N_2	46
H_2	16
CH_4	3.8
CO	10.4
CO_2	12
H_2O	11.5
H_2S	0.30

connect electric power, potable water, sewer, cooling water, and the process gases—a slipstream of coal gas, high-pressure nitrogen, high-pressure air, and instrument air. The systems will be checked out, and automatic safety shutdowns and other safety features verified. The continuous runs will be made in coordination with operating campaigns of the METC 10-in. gasifier. Following completion of the test runs, the process and utility lines will be disconnected. The mobile laboratory will then be returned to the RTI site. It can be reinstalled at RTI for additional test programs, or it could be relocated to another site for future additional slipstream testing.

The ZTFBD/DSRP system consists of a newly constructed bench-scale skid-mounted ZTFBD reactor system and a renovated and modified existing skid-mounted bench-scale DSRP reactor system. The bench-scale DSRP unit has been described previously (McMichael and Gangwal, 1990). It is configured for this project with two stages of reaction using a fixed bed of catalyst in each stage, with interstage sulfur condensation and removal. The reactor designs for both the ZTFBD and DSRP reactors are similar. A pipe cylinder, flanged at one end, is capped with a porous alumina plate to act as a gas distributor. This "cage" holds the fluidizable sorbent or fixed-bed catalyst, as appropriate. The cages are inserted vertically into reactor shells made from 4-in. (nominal) Schedule 160 stainless-steel pipe; the sorbent and catalyst cages are made from 3-in. (nominal) stainless-steel pipe. With the ZTFBD reactor utilizing a 3-in. diameter sorbent cage, the size is more than a two-fold scaleup from that used for much of the previous bench-scale sorbent testing.

The ZTFBD reactor system is integrated with the existing renovated DSRP reactor system, i.e., the regeneration off-gas from the ZTFBD becomes the feed to the DSRP reactor system. Additionally, the DSRP unit can be operated independently of the ZTFBD by using simulated regeneration off-gas—a mixture of nitrogen and (vaporized) liquid SO_2. In both DSRP modes of operation, the reducing gas required for the process is a slipstream of actual coal gas.

Figure 3 shows the layout of the mobile laboratory built into a 12 ft wide × 50 ft long × 8 ft high (open height inside) modified office trailer. The trailer is partitioned into two rooms, with one room housing the reactor systems and the other acting as the control and instrumentation room. A single door provides access between the rooms. A window in the door and another window in the partition provide visual access to the equipment from the control room. Each room has a separate personnel exit door. In addition, the reactor systems room is equipped with a roll-up door that provided access for installing the shop-fabricated, skid-mounted reactor system units. This door has subsequently been blocked off with a semipermanent closure.

Shelving along one wall of the control room holds the analytical instruments, computer data acquisition system, and toxic gas alarm monitors. On the opposite wall of the control room, a counter with base cabinets provides a sink, a hot water heater, and an eyewash fountain so that simple laboratory procedures can be undertaken. A control panel with automatic controls for the reactor systems is located on the partition wall.

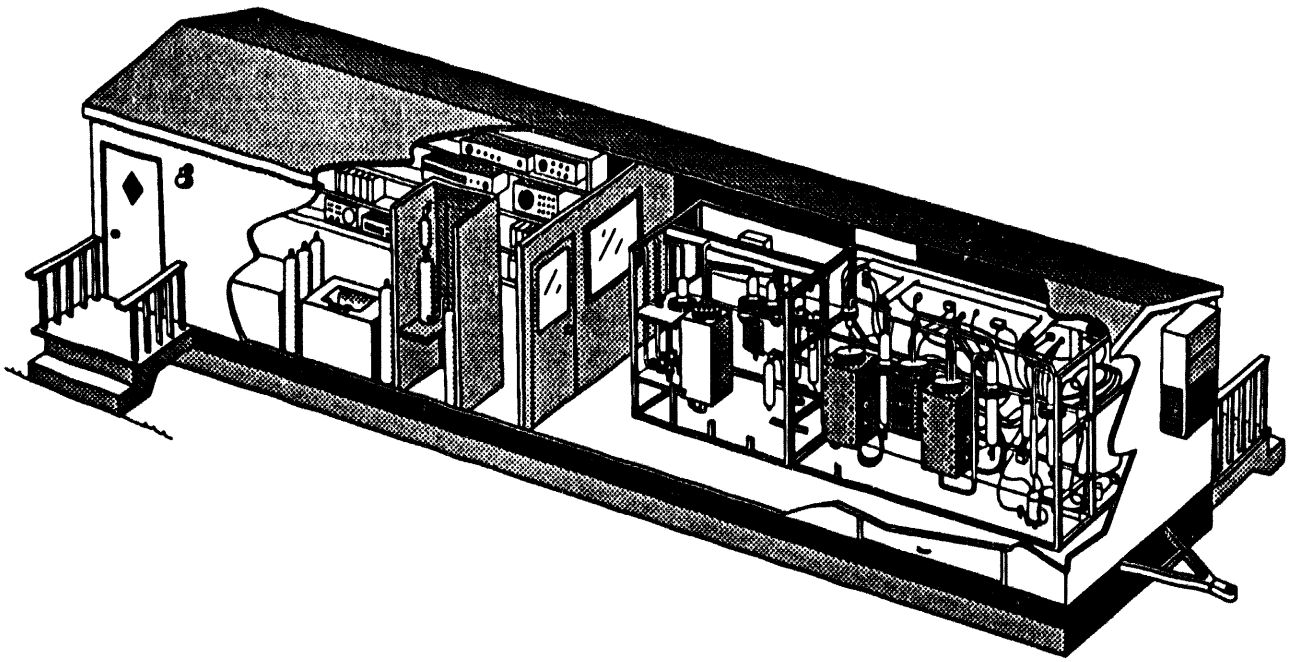

Figure 3. ZTFBD/DSRP Mobile Laboratory

Also in the control room section of the trailer is a 3-ft x 3-ft vented closet to house a liquid SO_2 supply system.

Special provisions have been made to protect the operating personnel from hazards associated with elevated pressure and temperature, and the use of toxic gases in enclosed spaces. A sophisticated toxic gas monitoring and alarm system has been installed. The design philosophy is that the high-temperature, high-pressure (HTHP) reactor systems will be operated semi-remotely. The equipment is isolated in the equipment room, and operating personnel will normally stay in the control room when the system is operating at elevated temperature and pressure. The gas flow rates can be adjusted from the control room, the modes of operation can be switched, using the remotely actuated valves, and data can be logged from the control room. Only occasional hands-on action is required to turn a valve or to draw liquid samples of condensate and molten sulfur. Special procedures will be followed on these occasions.

To operate the ZTFBD/DSRP reactor systems remotely, the process units have been equipped with 14 pneumatically operated control valves and shutoff valves. The coal gas feed line from METC is additionally controlled by two pneumatically operated shutoff valves on the exterior of the trailer and interlocked with the RTI control system. The pneumatic valves in the process can be operated with operator intervention from the control panel, or they can be placed in automatic mode where their operation is controlled by a programmable logic controller (PLC). The PLC will shut down part or all of the reactor system process units in response to inputs from the process pressure sensors, oxygen analyzers, flow meters, or emergency. For instance, a drop in system pressure, indicating a significant leak, or a rise in differential pressure across the coal gas

filter, indicating pluggage, will trigger a shutdown and purging of process gases from the system.

The ZTFBD/DSRP system can be operated in four modes of operation shown in Table 2. Actual coal gas is flowing to the trailer at all times during testing. Modes A and B could be considered to be "startup" modes in which only one reactor system is operating, each independent of the other. The fully integrated operation is shown as Mode C and could be considered to be "normal operation," in which the regeneration off-gas from the ZTFBD is used as the feed to the DSRP. Mode D would normally alternate with Mode C so that the DSRP can be operated continuously while the ZTFBD is being sulfided.

Table 2. Operating Plan

	ZTFBD		DSRP	
Mode	Sulfidation	Regeneration	Actual Regeneration Off-gas	Simulated Regeneration Off-gas
A	X			
B				X
C		X	X	
D	X			X

The basic plan for the field test is that the DSRP will be operated continuously, 24 hours per day, through a 7-day campaign of the METC gasifier, with additional startup and shutdown periods. Table 3 summarizes the operating conditions that will be used in the continuous field test. The DSRP will be operated with both simulated and actual regeneration off-gas each day. The cycle times for the various modes will be on the order of 1.5 to 3 hours. With this frequent changing of modes, a fair amount of operator attention will be required. It is envisioned that two teams of two operators each will split coverage of each 24-h period.

Table 3. Field Testing — Range of Operating Conditions

Desulfurization Reactor	
Pressure:	250 to 350 psig
Sulfidation temperature:	600 °C (1,112 °F)
Regeneration:	Inlet gas temperature = 650 to 725 °C (1,202 to 1,337 °F) Inlet gas O_2 = 1% to 3%
ZT-4 sorbent loading:	1,000 g (50 to 150 μm)
Gas flow rate:	40 to 80
DSRP Reactors	
Pressure:	250 to 350 psig
Stage I:	Temperature = 550 to 650 °C (1,022 to 1,202 °F) Fixed-bed operation Inlet gaseous sulfur = 1 to 3 vol% 600 g catalyst
Stage II:	Temperature = 280 to 320 °C (536 to 608 °F) Fixed-bed operation 600 g catalyst
Flow rate:	40 to 80 slpm

The process control strategy (independent of the remote operator control and automatic shutdown systems) incorporates significant use of automatic controls. In both reactor systems, the pressure is maintained by a pair of self-regulating back-pressure regulators. The hot coal gas flow to the ZTFBD unit during the sulfidation half cycle is regulated by a lab-scale pneumatically operated flow control valve operating at HTHP conditions. In the regeneration mode, the ZTFBD requires a hot nitrogen stream containing 2 percent oxygen as a feed gas. This is accomplished by blending air from compressed gas cylinders with high pressure nitrogen supplied by METC. MFCs are used to meter the flows and the gas is preheated prior to delivery to the reactor.

When the ZTFBD and DSRP are operating in the integrated mode, the DSRP is receiving actual regeneration gas (100 percent of the ZTFBD gas flow) as the feed gas. The flow through the system is controlled by the MFCs supplying the regeneration nitrogen/air mixture. When the DSRP is operating independently of the ZTFBD, using simulated regeneration off-gas, the flow through the DSRP is controlled by the MFC supplying nitrogen to the simulated regeneration off-gas system. In this system, the nitrogen that makes up the bulk of the regeneration off-gas (the "SO_2 carrier" nitrogen) is preheated and a small quantity of liquid SO_2 is mixed with it prior to the first-stage reactor. The liquid SO_2 is pressure-transferred from a reservoir equipped with a dip tube by using a metered quantity of nitrogen flowing into the head space (the "motive" nitrogen).

An innovative scheme has been designed for controlling the flow of coal gas to the DSRP. As with the ZTFBD, the flow is adjusted by a lab-scale control valve operating at HTHP conditions. The valve position is set by a flow ratio controller receiving feedback signals from a continuous analysis of the composition of the exit gas. The goal is to maintain the ratio of H_2S to SO_2 at 2:1 throughout the DSRP reactor system. Increasing the flow of reducing gas will tend to increase the conversion of SO_2 to elemental sulfur and H_2S, thus raising the H_2S:SO_2 ratio. Similarly, decreasing the flow of reducing gas will decrease the conversion, lowering the H_2S:SO_2 ratio. The ratio controller will adjust the flow of coal gas, in response to changing operation, so that composition ratio is maintained at the set point.

In order to operate this control scheme, continuous analysis of the DSRP exit gas is required. Separate analyzers have been installed in the control room to measure the H_2S and SO_2 concentrations in the DSRP exit gas. A small sample stream is continuously bled off the process and feeds these instruments. Their electrical output signals go to the flow controller. To monitor the progress of the zinc titanate sorbent regeneration, and for safety reasons, a trace oxygen analyzer has been installed. Finally, to provide a more detailed understanding of the process operation, additional gas analyses, will be by gas chromatograph (GC). One objective will be a complete sulfur balance around the system so that the conversion efficiency can be tracked during optimum operation.

As the test runs in this project will use actual coal gas, trace contaminants are expected to be present. A scheme has been incorporated in the design of the process equipment and the layout of the mobile laboratory to permit sampling of the process streams for heavy metals, fluoride, chlorides, and ammonia. There are several sampling points located throughout the process to identify the input levels and potentially to identify any sequestering or removal of the trace compounds by the sorbent, the catalyst, or the filters. The heavy metal compounds, As, Be, Cd, Co, Hg, Se, Sb, V, Zn, will be analyzed using a modification of the U.S. Environmental Protection Agency (EPA) Reference Method 29. The chloride and fluoride species will be analyzed from 0.1 N NaOH solution through which the sample has been passed. The ammonia (NH_3) will be captured in a 1.0 N H_2SO_4 solution.

RESULTS/STATUS OF FABRICATION AND CONSTRUCTION

The results so far on the first phase of this project are limited to design and construction of the test apparatus. The period July through December 1993 was occupied with experiment design, process design, equipment design, and procurement issues. The construction permit application for a project at METC was drafted, and the site safety review was held.

Starting in January 1994, the fabrication of the apparatus proceeded in earnest. A new aluminum frame was built for the ZTFBD unit, and the exist-

ing frame for the DSRP was modified so that it could mate with the ZTFBD and be mounted in the trailer. The pressure vessels and the electric furnaces required to heat them were mounted on the frame. The pneumatic valves were located, and process tubing between them was installed. The sample points and connections for analyzer sample tubing were installed.

The trailer was received at RTI's facility in early April. RTI Facilities and Maintenance personnel completed outfitting the unit with shelves, electric service, steps, emergency lighting, and framework to support additional small apparatus. In late April the two equipment skids were moved into the trailer through the large roll-up door provided in the side.

In May, with the two skids installed together, the system process piping was integrated. In addition, all the control and analysis systems were installed in the control room, and tubing and cables routed between the two halves of the trailer. The toxic gas alarm system was installed, as well as the smoke detectors, fire extinguishers, and eyewash fountain. The two vent headers intended to be connected to the METC incinerator and stack were installed, and the exhaust fan was mounted temporarily on the roof of the trailer. May was a period of intense activity with several technicians and construction tradesmen working in the mobile laboratory simultaneously.

In June, the systems are being checked out for mechanical integrity (pressure- and leak-testing) and for operability. The analyzers and GCs are being calibrated and the sample system operation verified. The control panel is being checked out for remote operation of the valves, automatic shutdown features, proper operation of the flow controllers, and correct display of digital data. The heat-trace lines are being tested to verify that proper temperatures can be maintained, and the furnaces are being exercised to verify that the reactors can be held at the desired operating temperatures. The computer-based data logger is being set up to record key flows, pressures, and temperatures.

FUTURE PLANS

Mobile Laboratory Testing at METC

In the remainder of June 1994, it is anticipated that checkout of the process and control systems at RTI will be completed, and the mobile laboratory can be prepared for transport to METC. An operating permit application will be prepared and submitted to METC for review. Shutdown and pack-up will entail a fair amount of disassembly of sensitive equipment and special packing procedures.

In early July 1994, the packed-up mobile laboratory will be transported to METC. At approximately 20,000 lb gross weight, it is relatively heavy compared to a typical mobile home or office trailer of this size, 12 ft × 50 ft. It will be installed at METC at a spot behind building B-12. METC support personnel will temporarily block it in position, and reconnect the utility lines—electricity, instrument air, potable water, and sewer. In addition, the process lines—hot coal gas, high pressure nitrogen, and process water—will be connected. This is all scheduled to be completed by the end of July, so that the laboratory and experimental apparatus will be available for use in time for the scheduled August 1 gasifier run.

During the August 1994 gasifier campaign, the process apparatus will be checked out with coal gas. Although no specific problems are foreseen, it is not unrealistic to expect that some equipment may need to be modified, or operating strategy modified, in order to achieve a successful extended period continuous run. The time period

of late August to early September is available for repairs and modification.

The extended run of slipstream testing is scheduled to coincide with the mid-September gasifier campaign. When the run is complete, the reactors will be opened and the sorbent and catalyst removed for final analysis. The equipment in the trailer will then be secured for transit. The process and utility lines at METC will be disconnected, and the trailer will be transported back to RTI's facility. In the October to December 1994 time frame, the data analysis will be completed and a topical report will be written.

Larger Scale DSRP Unit

Work has already begun on the preliminary process design and equipment sizing for the larger scale DSRP unit. The specifics of utility availability, control system interface, and equipment layout are being coordinated with Enviropower. The DSRP sliptream testing by Enviropower is tentatively scheduled for August through December 1995.

REFERENCES

Buchanan, T.L., H.T. Chen, M.G. Klett, M.D. Rutkowski, and R. Zaharchuk. 1994. "Optimization of Gas Stream Cleanup in Three IGCC Systems." Final Report. DOE/METC Contract No. DE-AC01-88FE61660. March. Reading, PA. Gilbert/Commonwealth, Inc.

Gangwal, S.K., et al. 1993. "DSRP, Direct Sulfur Production." In *Proceedings of the Coal-Fired Power Systems 93—Advances in IGCC and PFBC Review Meeting.* DOE/METC-93/6131. (DE93000289). June.

Gangwal, S.K., and W.J. McMichael. 1990. "Bench-scale Testing of Sulfur Recovery Process." In *Proceedings of the Tenth Annual Gasification and Gas Stream Cleanup Systems Contractors' Review Meeting.* DOE/METC-90/6115. Vol. 1. (DE90009689). August.

Gangwal, S.K., and W.J. McMichael. 1991. Bench-scale Testing of Sulfur Recovery Process. In *Proceedings of the Eleventh Annual Gasification and Gas Stream Cleanup Systems Contractors' Review Meeting.* DOE/METC-91/6123. Vol. 2. (DE92001102). August.

Gangwal, S.K., W.J. McMichael, S.K. Agarwal, D.H. Chen, and J.R. Hopper. 1992. "Bench-scale Testing and Evaluation of the Direct Sulfur Recovery Process." In *Proceedings of the Twelfth Annual Gasification and Gas Stream Cleanup Systems Contractors' Review Meeting.* DOE/METC-92/6128. Vol. 1. (DE93000228). September.

Gupta, R., W.J. McMichael, S.K. Gangwal, S.C. Jain, and T.P. Dorchak. 1992. "Development of a Hot-Gas Desulfurization System for IGCC Applications." AIChE Annual Meeting. Miami Beach, FL. Paper No. 244f. November 1-6.

McMichael, W.J., and S.K. Gangwal. 1990. "Recovery of Sulfur from Hot Gas Desulfurization Processes." Final Technical Report. Department of Energy/Morgantwon Energy Technology Center. Contract No. DE-AC21-86MC23260. May.

Robin, A.M., T.F. Leininger, L.A. Davis, D.Y. Jung, J.S. Kassman, W.L. Lafferty, J.S. Stevenson, J.K. Wofenbarger, M.M. Wu, and P.P. Yang. 1993. "Integration and Testing of Hot Desulfurization and Entrained-Flow Gasification for Power Generation Systems." Final Report Department of Energy/Morgantown Energy Technology Center. Contract No. DE-FC21-87MC23277. Vol. 1. October. Montebello, CA. Texaco, Inc.

6.5 METC Fluid-Bed Hot-Gas Desulfurization PDU

Larry A. Bissett
Morgantown Energy Technology Center

OBJECTIVE

METC is constructing an on-site, hot-gas desulfurization (HGD) process development unit (PDU) to support the U.S. Department of Energy's (DOE's) Integrated Gasification Combined Cycle (IGCC) power systems program. With industrial participation, this PDU will be used for the further development of fluid-bed and transport reactor HGD configurations.

BACKGROUND INFORMATION

Fluid-beds and transport reactors, either alone or in combination, are conceptually attractive for HGD processes because they offer continuous steady-state operation, superior temperature control, and a wide range of achievable regeneration gas sulfur dioxide (SO_2) concentrations. These attributes potentially simplify system control strategies, prolong sorbent activity, and add process flexibility with respect to sulfur recovery options.

During the early conceptualization phase of this project, an economic study failed to show any notable cost and performance differences between IGCC systems with fluid-bed HGD and the same systems with moving-bed HGD (1). Based on testing activities ongoing at that time, relatively low velocity HGD fluid beds were used in this study. A sensitivity analysis showed that costs could be improved by employing higher fluidizing velocities. The study also revealed economic advantages for a system that uses a minimal amount of undiluted air to produce a concentrated SO_2 stream during sorbent regeneration.

These considerations provided the incentive to look at progressively higher velocity regimes and alternative contacting modes during PDU conceptualization (2,3). As a result, the fluid-bed absorber and regenerator in the PDU were designed to operate in a turbulent as well as a bubbling regime. In addition, when encouraging results from a small-scale transport reactor unit became known, the decision was made to incorporate transport reactor provisions on both the sulfidation and regeneration sides of the PDU. Little additional expenditure was required to gain these extra capabilities.

With completion of National Environmental Policy Act (NEPA) documentation requirements, the preliminary process and equipment design, and the April groundbreaking to prepare the project site, the project is now proceeding at a faster, more visible pace. Equipment installation should be completed in about 2 years.

PROJECT DESCRIPTION

As shown by Figure 1, the project is being centrally located in the METC experimental facilities. A nearby natural gas-fired synthesis gas (syngas) generator, which will share the PDU control room, will supply the PDU with up to 4,000 Nm^3/hr (150,000 scfh) of simulated coal gasification fuel gas (4). The PDU equipment will be housed in an open-steel structure with dimensions (excluding stairs) of about 6 by 15 by 24 m in height (20 by 48 by 80 feet).

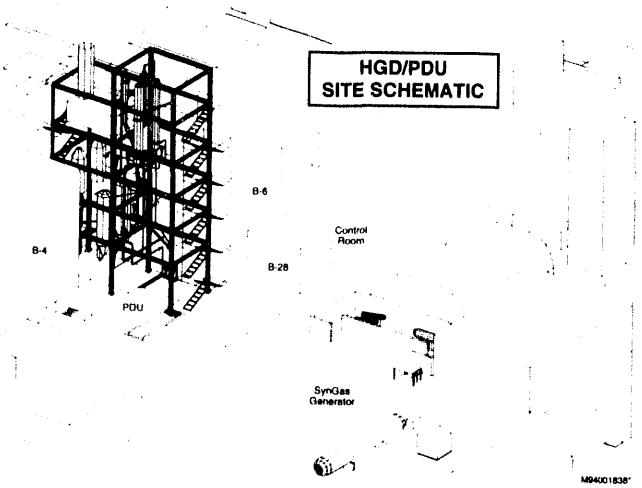

Figure 1. Isometric View of PDU Site

The adjacent fluid-bed vessels will be about 9 m (30 feet) in length, have a top elevation of about 23 m (76 feet) above grade, and have closely coupled external cyclones and diplegs. The vessels will be carbon steel with refractory linings with constant inside diameters throughout the vessel length. Maximum bed depths for the absorber and regenerator will be 3 m (10 feet) and 4 m (12 feet), respectively. A second absorber stage can be added if needed, in which case the vessel will accommodate two 1.5-m (5-foot) beds. The design also has provisions for testing with submerged or freeboard risers and with underflow or overflow standpipes. Standpipe diameters vary from 5 to 15 cm (2 to 6 inch) in diameter. All standpipes and sorbent transfer lines will be unlined, externally insulated alloy pipes.

The PDU will have operating pressure capabilities of 2.8 MPa (400 psia) and operating temperature capabilities of 650°C (1,200°F) on the sulfidation side and 760°C (1,400°F) on the regeneration side. Sulfidation temperatures down to about 425°C (800°F) can be accommodated. As shown by Figure 2, fuel gas can be fed to either the 46-cm-i.d. (18-inch) fluid-bed absorber or to the 15-cm diameter (6-inch) absorber transport reactor. During fluid-bed sulfidation testing, the absorber transport reactor will not be used, and sorbent will be circulated with steam or nitrogen from the regenerator to the absorber through the 5-cm diameter (2-inch) absorber riser. Preheated regeneration gas (air, steam, nitrogen) can be fed to either the 25-cm i.d. (10-inch) fluid-bed regenerator or to the 5-cm diameter (2-inch) regenerator transport reactor, which serves as the regenerator riser during fluid-bed regeneration testing.

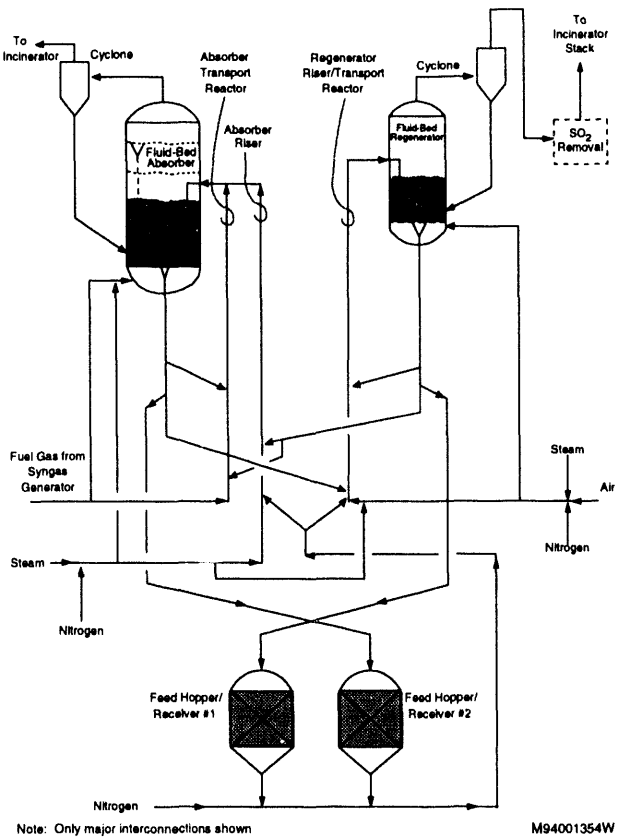

Figure 2. Simplified Flow Diagram of PDU

During transport reactor mode testing and unlike in a commercial configuration, the associated fluid beds will serve as disengagers and remove excess regeneration heat by adjusting the flow rate and temperature of the fluidizing gas. The preheated steam and

nitrogen shown entering on the left side of the diagram provide this service and also serve as aeration/stripping gas and transport gas during fluid-bed mode testing.

Y-bend transfer lines will be used to circulate sorbent between the sulfidation and regeneration sides, and for recirculation to the 15-m long (50-feet) transport reactors. Control valves in the standpipes will be used to control sorbent flow rates. If the circulation control valves in the standpipes prove troublesome at this scale, the Y-bends can be converted to U-bends, which do not require control valves.

Sorbent circulation rates will be in the range of about 900 to 2,300 kg/hr (2,000 to 5,000 lb/hr). Sorbent recirculation rates will range up to about 23,000 kg/hr (50,000 lb/hr) through the absorber transport reactor and about 2,300 kg/hr (5,000 lb/hr) through the regenerator transport reactor. Recirculation is needed on the sulfidation side to improve contacting and to increase sorbent sulfur loading, and on the regeneration side to control temperature. Solids loadings in the absorber and regenerator transport reactors are expected to be respectively about 140 to 190 kg/m^3 (9 to 12 lb/ft^3) and 30 to 190 kg/m^3 (2 to 12 lb/ft^3). The absorber and regenerator transport reactors are respectively sized for superficial velocities of about 8 m/s (25 ft/s) and 5 m/s (15 ft/s). The design is based upon 70 to 250 micrometer-sized zinc titanate and Z-Sorb, the latter being a proprietary material developed by Phillips Petroleum Company.

Figure 2 also shows two vessels that can alternately serve as feed hoppers or receivers. These were included in the design so that the sulfidation and regeneration sides can be operated separately (decoupled). This provision was included to aid process development but may not get constructed for budgetary reasons.

RESULTS

The following figures illustrate certain aspects of transport reactor HGD. These are presented to indicate trends that might be observed when PDU operations commence. All of these figures are based on the use of Z-Sorb to desulfurize fuel gas containing 5,000 ppmv of hydrogen sulfide (H_2S) at 650°C (1,200 °F) and 2.1 MPa (300 psia). Comparable figures could have been prepared for zinc titanate sorbent or for other process conditions.

A transport reactor HGD system has numerous possible operating points depending upon factors such as sorbent characteristics, processing conditions, regeneration scheme, and system performance targets. Sorbent circulation/recirculation rates and utilization levels/swings are interrelated. Figure 3 depicts one possible operating point and is presented here to introduce and illustrate certain concepts. Utilization, expressed here as a fraction, is a measure of the amount of sulfur in a sorbent relative to its completely sulfided state. The sulfur content of the sorbent used for this illustration varies by about 15 weight % as the utilization goes from 0 to 1.0. System utilization swing is the change in utilization as the sorbent circulates between the sulfidation and regeneration sides. Thus, for the example in the figure, the sulfur content of the sorbent circulated to the regenerator is about 2.3 weight % higher (0.15 times 15 weight %) in sulfur content than the sorbent returned to the absorber.

Figure 3 shows that for each time sorbent is circulated from the absorber to the regenerator and back (i.e., one sulfidation-regeneration cycle), it has been recirculated on average about 50 times through the transport absorber, and about 2 times through the transport regenerator. Correspondingly, the sulfur content of the sorbent flowing through the transport absorber

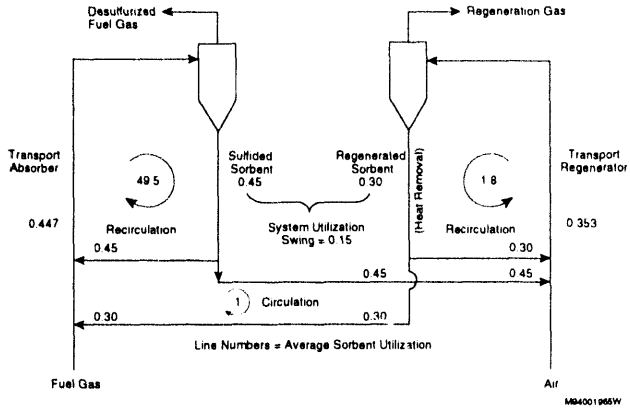

Figure 3. Illustrative Schematic of Transport Desulfurization

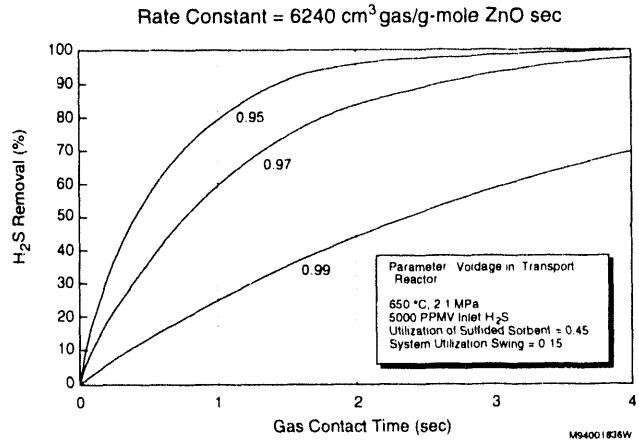

Figure 4. Illustrative Predicted Performance of Transport Absorber

increases by only about 0.04 to 0.05 weight % per pass, and decreases by about 0.8 weight % per pass through the transport regenerator. Since flow splits for circulation and recirculation are purely random, these utilization and sulfur levels are mass-averaged values for a potentially wide distribution. Also, the recirculation levels for this and subsequent figures assume no slip velocity between the sorbent and gas. To the extent that slip occurs, recirculation-circulation ratios will decrease.

During the PDU conceptualization phase, a small-scale transport reactor proof-of-concept test was conducted by the M.W. Kellogg Company using Z-Sorb. Excellent desulfurization performance with little sorbent attrition was reported. From the results, a first approximation of the sulfidation rate constant for the transport mode was made assuming pseudo first-order kinetics and plug flow. Figure 4 shows the resulting predicted removal of H_2S as a function of gas residence time and void fraction in a transport reactor. These illustrative trends, which encouragingly indicate that greater than 99 % sulfur removal may be possible in about 3 seconds gas contact time, solidified the decision to have transport reactor provisions in the PDU.

For a given process condition and gas contact time, the extent of desulfurization increases as the initial molar ratio of ZnO-to-H_2S (i.e., reactants) increases. Thus, higher sorbent loadings in a transport reactor (i.e., lower voidages, higher reactor density), and higher zinc oxide contents in a sorbent (i.e., lower utilization levels), increase the probability of achieving a target level of sulfur capture. This analysis assumes that all of the zinc oxide in the sorbent is equally accessible to H_2S. Testing is required to determine to what extent this assumption is valid.

These general trends are illustrated by Figure 5, which shows that as utilization of the sulfided sorbent increases, the transport reactor must be run at a higher density (i.e., lower voidage) to maintain desulfurization performance (in this case, 99 % sulfur removal). Because the sorbent undergoes only fairly small density increases as utilization increases, circulation remains nearly constant for a given system utilization swing. Therefore, higher reactor densities are achieved primarily with higher recirculation

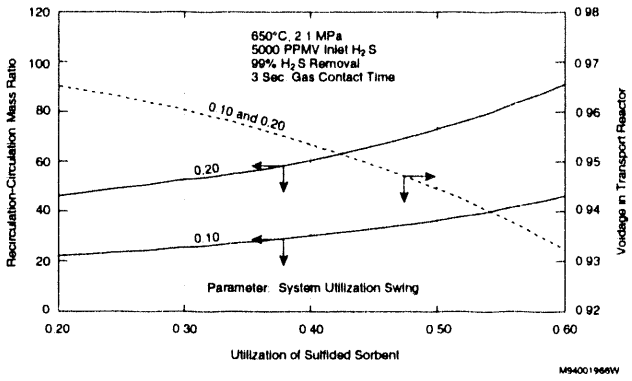

Figure 5. Illustrative Predicted Trends for Transport Absorber

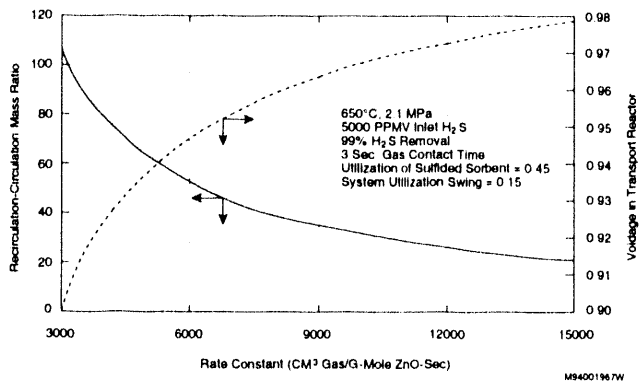

Figure 6. Illustrative Predicted Trends Showing Importance of Sulfidation Rate Constant

rates. The figure also shows that the recirculation ratio increases at higher system utilization swings (due to decreased circulation), and that the needed voidage becomes essentially independent of system utilization swing since, as discussed earlier, the utilization change per pass through the transport absorber is very small.

The ability to achieve a certain level of desulfurization improves as sorbent activity increases. As shown by Figure 6, this lowers the required reactor densities and recirculation rates, which should beneficially translate into lower sorbent attrition tendencies due to reduced sorbent movement. This is also important in the sense that as a sorbent potentially deactivates with use, a higher initial activity provides more operating flexibility to adjust system parameters to maintain performance before limiting factors such as choking are encountered.

In the absence of relevant kinetic information, comparable illustrations of transport regeneration can not be prepared. Given the likely high rate of reaction, obtaining sufficient regeneration in a transport reactor of reasonable length should not be a problem. However, the possibility of particle overheating may be encountered if the reaction rate is too rapid and outpaces heat transfer. This could prove to be especially troublesome for a process that uses a minimal amount of undiluted air (i.e., 21 percent oxygen) for regeneration. Depending upon temperature regimes and kinetics, sulfate formation may also be encountered since oxygen and SO_2 will both be present in considerable concentrations. In addition to being potentially detrimental to a sorbent, this would increase the regeneration air requirement and generally lower efficiency.

A simple heat balance can illustrate some transport regeneration trends and may ultimately prove to be more relevant than kinetic considerations for establishing sorbent flow rates. During regeneration, sorbent serves as a heat sink and limits overall temperature rise. As shown by Figure 7, the amount of sorbent circulated per unit of sulfur regenerated decreases as system utilization swing increases. Consequently, more heat is released per unit of circulated sorbent, which translates into the need for more sorbent recirculation to limit the higher potential temperature rise. With temperatures used for this figure, the total amount of circulated and

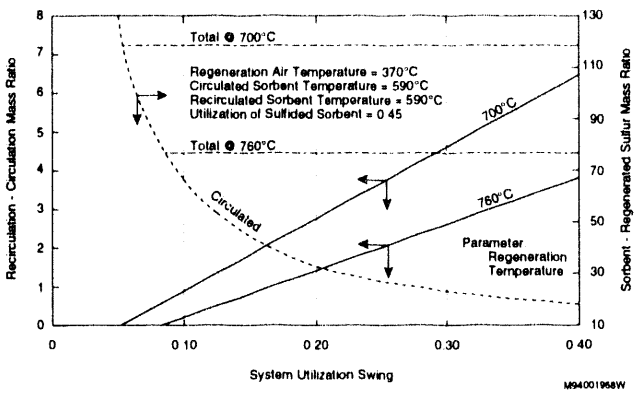

Figure 7. Illustrative Trends for Transport Regenerator

recirculated sorbent necessary for any given regeneration temperature is constant (horizontal lines) throughout the range of system utilization swings. Higher total amounts are needed for lower regeneration temperatures. The difference between total and circulated is the amount of sorbent that must be recirculated. The resulting recirculation ratio is graphically shown as constant-temperature operating lines for two regeneration temperatures.

Where the operating lines meet the horizontal axis, or where the total and circulated sorbent trends intersect, the recirculation requirement becomes zero. For the conditions used, this occurs for the two regeneration temperatures plotted when about 0.8 and 1.3 weight % sulfur is regenerated from the sorbent. These regeneration amounts would change for different assumed regenerant and sorbent temperatures. From a systems viewpoint, this becomes a tradeoff between having a large circulation rate and a once-through regenerator without heat removal versus a smaller circulation rate and a regenerator with recirculation and heat removal. The once-through system is simple, and has the additional potential benefit of maximizing the transfer of regeneration heat to the absorber. On the other hand, the more complex system with recirculation appears to offer better process flexibility. The PDU, which is configured to test both systems, should begin to sort out the operational problems and capabilities associated with each.

WRAP-UP

DOE is making a sizeable investment in this facility and believes it can accelerate HGD development and commercialization. With its ability to demonstrate fully coupled sulfidation-regeneration operations at a meaningful scale, the PDU represents an essential step beyond the small-scale batch reactors used to date. Since a number of technologies can likely emerge as winners in the HGD market due to site-specific factors, the PDU can provide the opportunity to explore candidates and serve as an initial proving ground.

Industrial participation is considered essential for maximizing the effectiveness and outcome of the project. Both sorbent and process developers are encouraged to participate, preferably through the Cooperative Research And Development Agreement (CRADA) program.

REFERENCES

1. Rutkowski, M.D., H.T. Chen, and M.G. Klett. 1992. Sensitivity of Hot Gas Desulfurization on IGCC Cost of Electricity. In *Proceedings of the Twelfth Annual Gasification and Gas Stream Cleanup Systems Contractors Review Meeting*, 263-279. DOE/METC-92/6128, Vol. 1. NTIS/DE93000228. Springfield, Va.: National Technical Information Service.

2. Bissett, L.A., J.M.Rockey, and S.C.Walczak. 1991. Preliminary Conceptualization of METC's Fluid-Bed, Hot-Gas Desulfurization PDU. In *Proceedings of the Eleventh Annual Gasification and Gas Stream Cleanup Systems Contractors Review Meeting*, 556-565. DOE/METC-91/6123, Vol. 2. NTIS/DE92001102. Springfield, Va.: National Technical Information Service.

3. Bissett, L.A. 1993. Fluid-Bed HGD PDU. In *Proceedings of the Coal-Fired Power Systems 93 -- Advances in IGCC and PFBC Review Meeting*, 302-306. DOE/METC-93/6131. NTIS/DE93000289. Springfield, Va.: National Technical Information Service.

4. Monahan, M.J. 1991. METC's Synthetic Gas Generator Project. In *Proceedings of the Eleventh Annual Gasification and Gas Stream Cleanup Systems Contractors Review Meeting*, 533-540. DOE/METC-91/6123, Vol. 2. NTIS/DE92001102. Springfield, Va.: National Technical Information Service.

LBISSE\2:940761b

Session 7

Turbine Systems

7.1 Development of Topping Combustor for Advanced Concept Pressurized Fluidized Bed Combustion

CONTRACT INFORMATION

Contract Number	DE-AC21-86MC21023
Contractor	Westinghouse Electric Corporation 4400 Alafaya Trail Orlando, Florida 32826-2399 (407) 281-2000
Contract Project Manager	William F. Domeracki
Principal Investigators	Thomas E. Dowdy Dennis Bachovchin
METC Project Manager	Donald L. Bonk
Period of Performance	June 1, 1988 to December 31, 1994 (Phase II)
Schedule and Milestones	

FY94 Program Schedule

OBJECTIVES

The objective of this program is to develop a topping combustor to operate in a Second-Generation Pressurized Fluidized Bed (PFBC) Combined Cycle power generation system. The combustor must be able to:

- Lightoff with a high heating value fuel and compressor discharge air to heat the fluidized bed(s) and provide power for PFBC and carbonizer off-line.
- Operate with 1600°F (870°C) oxygen depleted air from the PFBC and high heating value fuel to handle carbonizer off-line conditions.
- Ramp up to 100% carbonizer syngas firing (normal operation) by firing a blend of decreasing high heating value fuel and increasing low heating value syngas.
- Utilize the vitiated air, at temperatures up to 1600°F (870°C) for as much cooling of the metal combustor as possible, thus minimizing

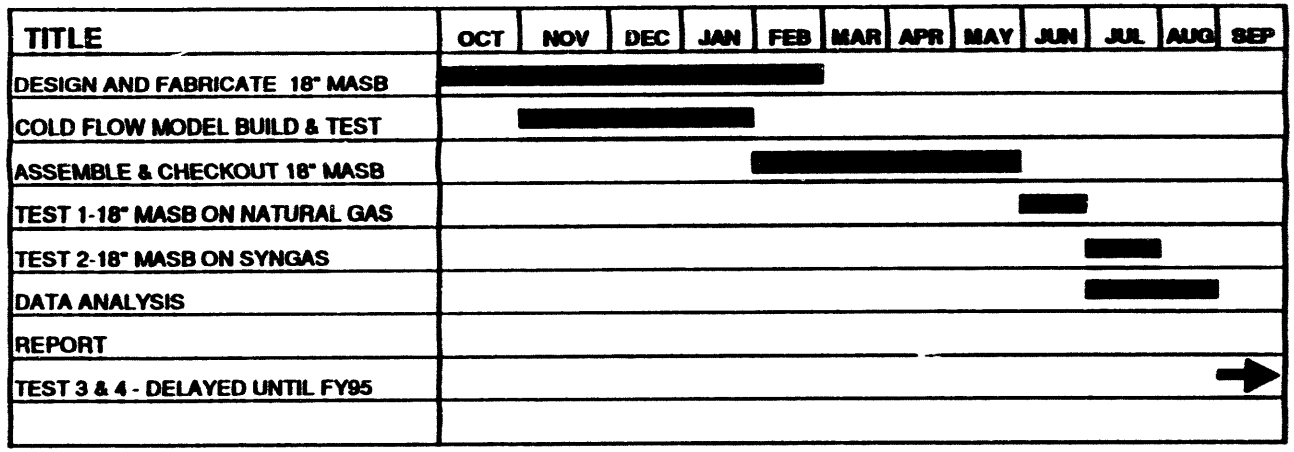

FY94 Program Schedule

the compressor bypass air needed for combustor cooling.

- Provide an acceptable exit temperature pattern at the desired burner outlet temperature (BOT).

- Minimize the conversion of fuel bound nitrogen (FBN) present in the syngas to NO_x.

- Have acceptably high combustion efficiency, and low emissions of carbon monoxide, UHC, etc.

BACKGROUND INFORMATION

A project team consisting of Foster Wheeler Development Corporation, Westinghouse Electric Corporation, Gilbert/Commonwealth, and the Institute of Gas Technology, are developing a Second Generation Pressurized Fluidized Bed System. Foster Wheeler is developing a carbonizer (a partial gasifier) and a pressurized fluidized bed combustor. Both of these units operate at a nominal 1600°F (870°C) for optimal sulfur retention.

Since this temperature is well below the current combustion turbine burner outlet temperature (BOT) operation of 2350°F (1290° C), to reach commercialization, a topping combustor and hot gas cleanup (HGCU) equipment must be developed. Westinghouse is participating in the development of the HGCU equipment (reported elsewhere at this conference) and the topping combustor. Work performed on the topping combustor since the last contractor's review meeting (Domeracki, et al. 1993) is presented in this paper.

This paper updates only one part of a multi-phase program. This test program is part of Phase II of a three-phase ongoing DOE/METC program. Phase I involved the conceptual and economic study (Robertson et al., 1988); Phase II addresses subscale testing of components; Phase III will cover pilot plant testing of components integrated into one combustion system.

PROJECT DESCRIPTION

The topping combustor in this cycle must utilize a low heating value syngas produced from the carbonizer at approximately 1600°F (870°C) and 150 to 210 psi (1.0 to 1.4 MPa).

The syngas entering the topping combustor has been previously cleaned of particulates and alkali by the HGCU equipment. In addition to the combustible materials (primarily CO, H_2 and CH_4) it also contains significant fuel bound nitrogen (FBN) from the coal present as ammonia (NH_3) and other compounds. This FBN is significant because it will selectively convert to NO_x in the highly oxidizing conditions of standard combustion turbine combustors.

The hot syngas must be burned with the vitiated (partially burned) air from the pressurized fluidized bed combustor (PFBC). This air is at 1600°F (870°C) and still contains sufficient oxygen for combustion and has been cleaned of particulates and alkali in a separate HGCU system. To obtain optimum efficiency, the 1600°F air must also be utilized to cool the metal combustor surfaces to as great an extent as possible, though a small amount of compressor discharge air at a lower temperature, 700°F (370°C) will also be needed for combustor rich zone cooling.

These application requirements indicate that a specially designed rich-quench-lean (RQL) combustor be used and Westinghouse has selected the Multi-Annular Swirl Burner (MASB, Beér, 1965& to 1969&) for further development for this application.

In selecting a combustor design that will withstand the conditions expected in the topping application, the effective utilization of the 1600°F (870°C) air could satisfy the wall cooling challenge by maintaining a cooling air layer of substantial thickness. Thick layers of cooling air at the leading edge of each inlet section are easily achieved if the combustor is made up of concentric annular passages. In addition to wall cooling considerations, the burner must inhibit the formation of NO_x from syngas that contains FBN, have high combustion efficiency, produce an acceptable exhaust temperature pattern, exhibit good stability, and be able to light off at cold plant conditions. The MASB has demonstrated that it can meet all of these requirements.

This paper reports the results of tests of a 14" diameter topping combustor with a modified fuel-rich zone conducted in June 1993, design of an 18" diameter topping combustor to be tested in June 1994 and afterwards, and results of a 50% scale cold flow model which has been built and tested.

RESULTS

June 1993 14" Diameter Test Results

In June 1993 a test was performed at the University of Tennessee Space Institute (UTSI) with a modified 14" diameter MASB. This test was considered to be very successful, as will be shown in the following data and text.

The "old" MASB, which had been utilized in pre-1993 tests (Figure 1) was modified, as shown in Figure 2. This design was described in the 1993 contractors review, (Domeracki, 1993). Essentially the new design increased the residence time in the fuel-rich zone, obtained backmixing and a controlled reaction temperature in the fuel rich zone, and tested the most recent "Wilsonville" paste feed composition. If sufficient fuel remained (which it did) we were to also test the "Wilsonville" dry feed compositions. These compositions, as predicted and as tested, are shown in Tables 1 & 2.

Table 1. Wilsonville Paste Syngas Composition

	Volume Predicted	Percent as Tested
CO	14.31	14.31
H_2O	11.44	11.44
CO_2	9.44	0
H_2	15.48	15.48
CH_4	2.15	2.15
N_2	46.45	56.45
NH_3	.17	.17

Table 2. Wilsonville Dry Syngas Composition

	Volume Predicted	Percent as Tested
CO	17.22	17.22
H_2O	9.17	9.17
CO_2	7.82	0
H_2	18.01	18.01
CH_4	2.62	2.62
N_2	44.42	52.76
NH_3	.23	.23

The main interest was to confirm the predicted NH_3 to NO_x conversion. The new 14" nozzle (Figure 2) was designed to improve recirculation and to have the rich zone operate within a temperature range of 2900°F +/- 100°F. Due to higher than anticipated leakage around the MASB (i.e., lower than measured oxidizer flow through the MASB), most calculated (allowing for

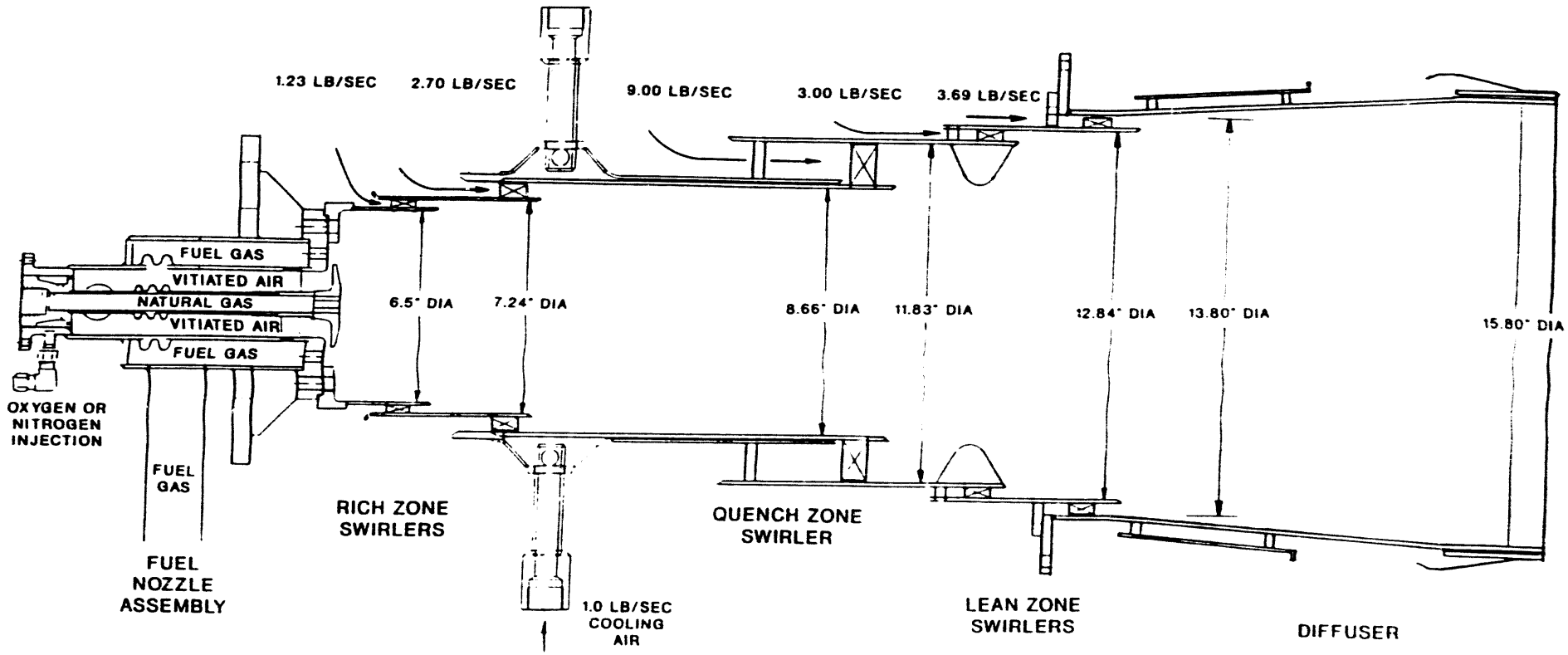

Figure 1. Old 14" MASB Design

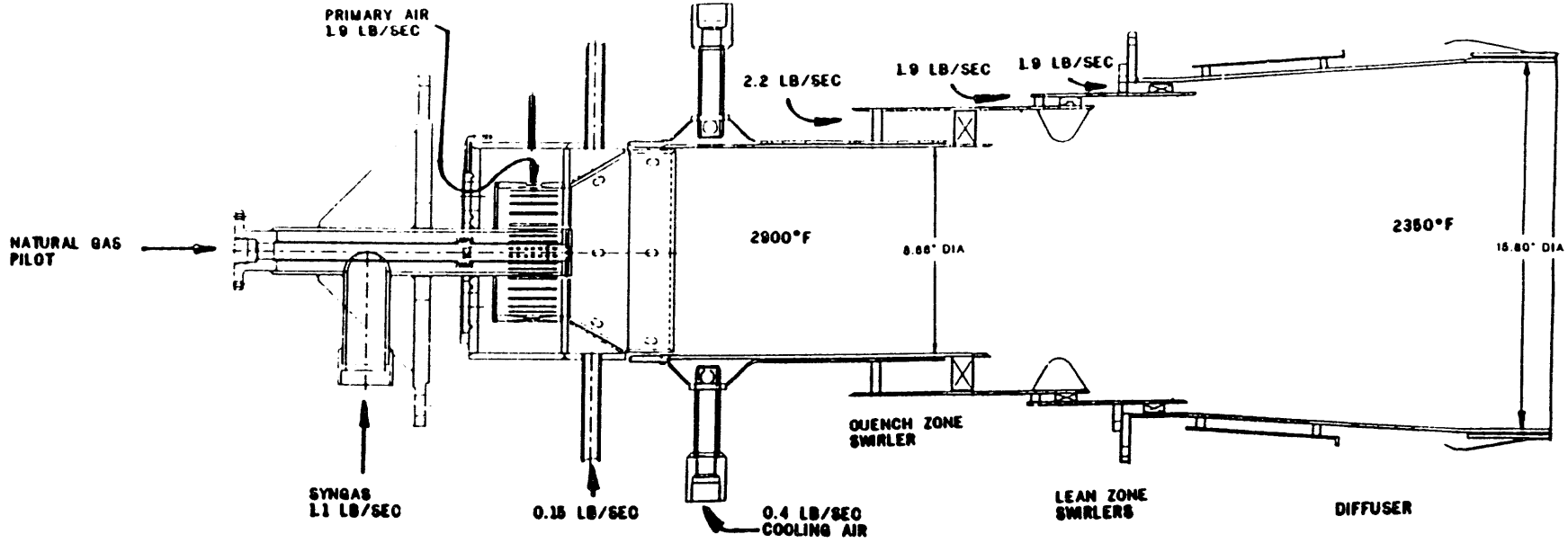

Figure 2. New 14" MASB Design

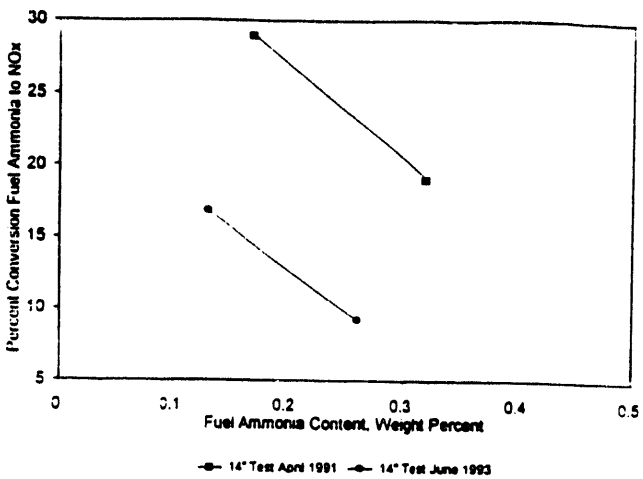

Figure 3. Comparison of 1991 and 1993 14" MASB Ammonia Conversion

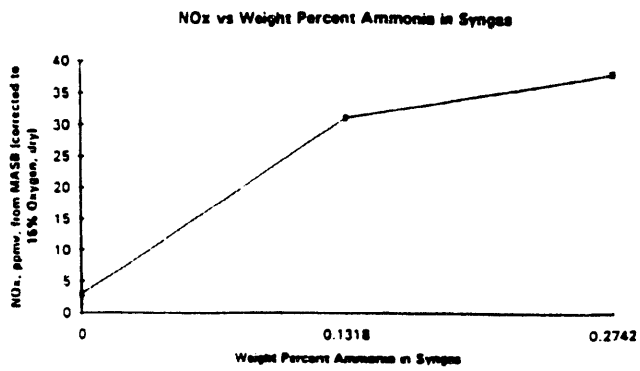

Figure 4. NOx vs Weight Percent Ammonia in Syngas

leakage) rich zone temperatures were between 3000°F and 3300°F. Thus, in spite of running at this off design condition, the bulk of the NH_3 conversions to NO_X were about 10 to 20 percent (Figure 3). Figure 3 shows that this was significantly better than previous test results at similar conditions. This was within our target range of expected results and thus demonstrated that our objective of demonstrating that our methodology for the redesign of the rich zone was acceptable and on the conservative side.

Carbon monoxide emissions were near zero at all points of the test with syngas firing. Even though the oil-fired direct heated preheater generated some carbonmonoxide, it was usually below detection limits of the gas analyzers at the MASB exit.

Modifications for 14" Test

A fuel blending station was added at UTSI, so that the cost of syngas (which had been bought premixed) could be lowered, the run time extended, and any desired composition of syngas could be produced by on-line adjustment. Prior computational fluid dynamics (CFD) and chemical kinetic computations had indicated that the previously utilized syngas entrance temperature of 800°F (425°C) at UTSI was not sufficiently high to rapidly initiate the desired reactions (Domeracki, 1993). Therefore, the syngas heater at UTSI was modified to provide 1200°F (650°C) syngas to the MASB.

Most of the results presented in this section represent percent conversion of ammonia to NO_X. However, Figure 4 shows three data points taken over a few minutes of time. All conditions were held constant except for the weight percent ammonia in the syngas. Two things should be noted from this plot:

First, with no ammonia in the syngas, very little NO_X was formed. The 3ppm plotted cannot be assumed to be an absolute value, since the preheater was generating approximately one order

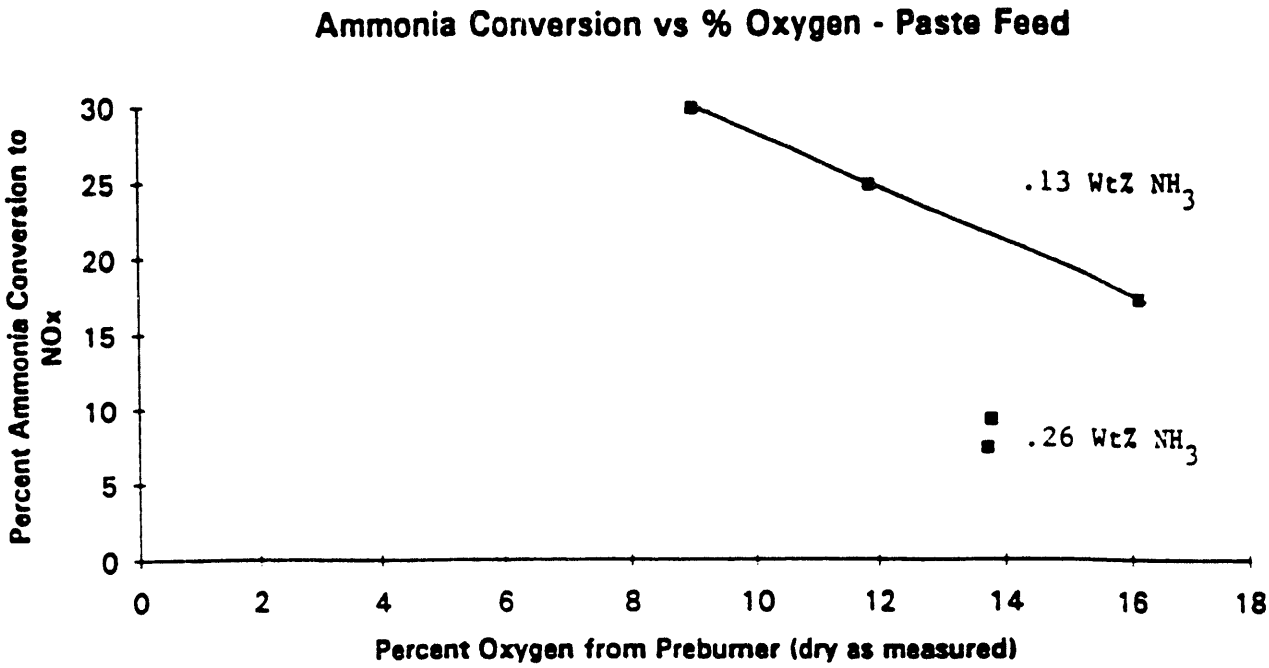

Figure 5. Ammonia Conversion vs % Oxygen - Paste Feed

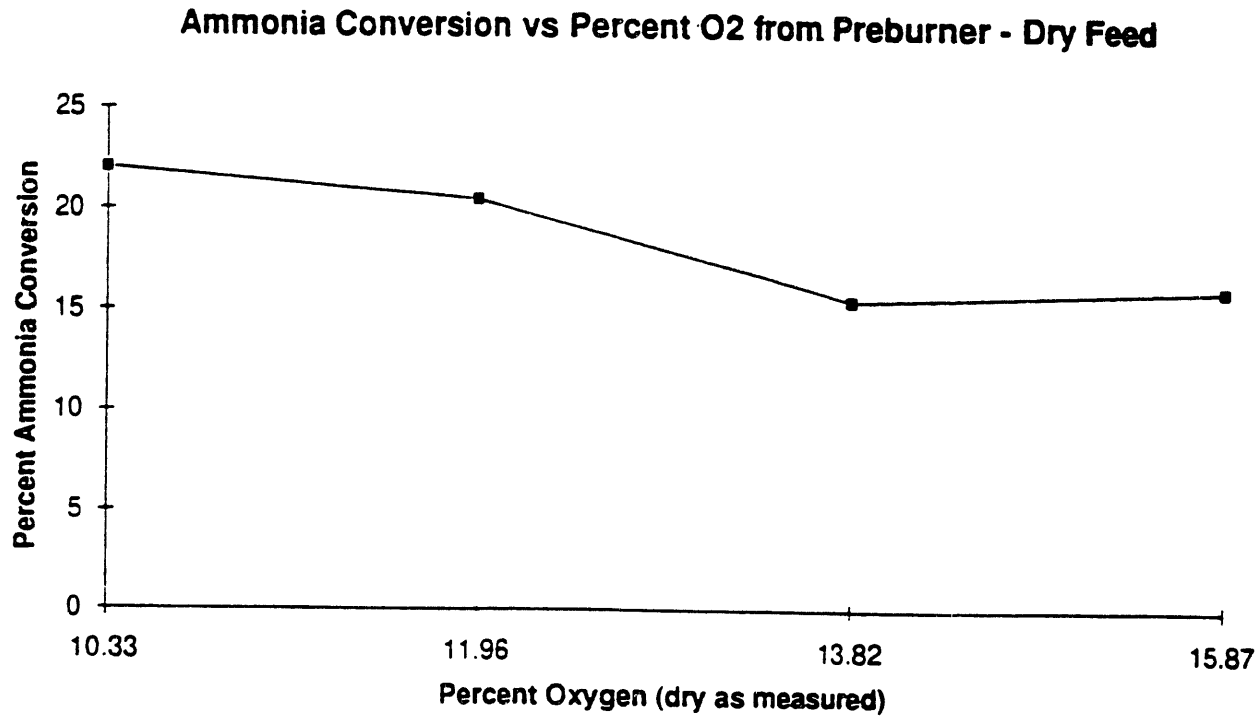

Figure 6. Ammonia Conversion vs % Oxygen - Dry Feed

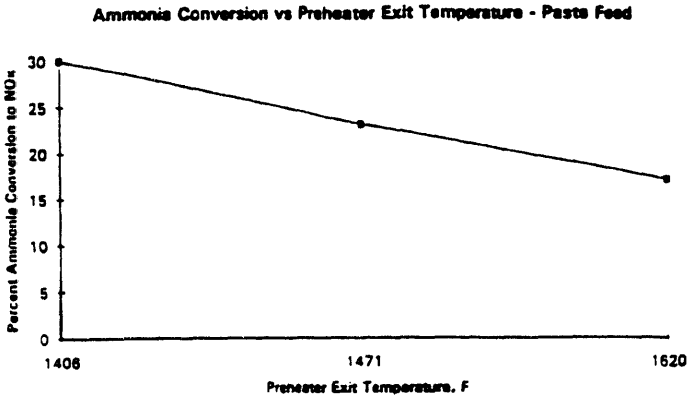

Figure 7. Ammonia Conversion vs Preheat Temperature - Dry Feed

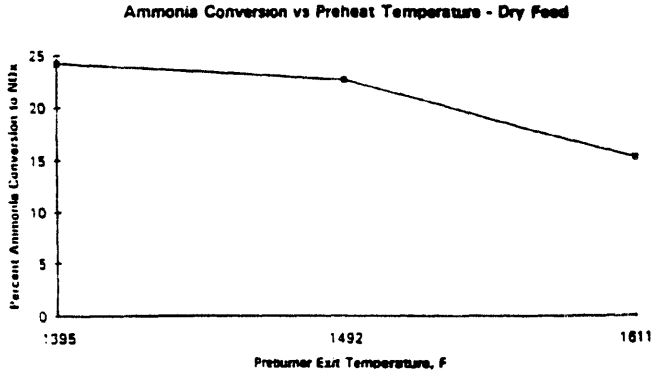

Figure 8. Ammonia Conversion vs Preheat Temperature - Dry Feed

of magnitude more NO_X, and this value is calculated by difference between two much larger numbers, (i.e. NO_X - NO_X in). Still, the combined thermal and prompt NO_X formed is extremely low.

Second, between 0.13 weight percent NH_3 and 0.27 weight percent, the slope is relatively flat. Thus the absolute NO_X emissions from the MASB is relatively insensitive to ammonia content, as our analysis predicts.

Figures 5 and 6 show that the percent ammonia conversion is an inverse function of oxygen content from the preburner. Figures 7 and 8 show that the percent ammonia conversion decreases with increasing preburner exit temperature. Both of these can be explained by the higher inlet oxygen or higher inlet vitiated air temperature which will initiate the NH_3 to N_2 conversion in a shorter period of time. With corrections made for higher than expected leakage of the oxidizer, corresponding with higher than expected rich zone temperature, the calculated flame temperature in the rich zone was higher than desired in most tests. However, even with the hotter than desired temperatures, the NH_3 conversion was equal to or below our design predictions. Thus we conclude that our design simulation technique is acceptable, though conservative.

Cold Flow Model Pattern Verification

A half scale cold flow model with similar Reynolds number and velocity profiles as the hot 18 inch MASB at full pressure was tested to verify the flow characteristics required and expected. Table 3 compares the hot 18 inch and the cold model MASBs.

Extensive mapping of the flow pattern in the MASB was performed using a two-dimensional flow probe (United Sensor model W-187), which measures yaw angle, static pressure, and dynamic pressure, giving the direction (in the tangential/axial plane) and magnitude of flow velocity as a function of axial and radial positions.

Figure 9 is a map of the resulting axial velocities. The results verified CFD modeling projections and the existence of desired flow patterns. The following significant features are apparent:

1. A strong donut-shaped recirculation region was confirmed in the wake of the bluff body end of the fuel swirler. This extends about one third of the way down the rich zone cylinder. The existence of this recirculation is essential for backmixing of free radicals to initiate combustion early so the whole rich zone residence time is available for the relatively slow conversion of NH_3 to N_2.

2. There is an absolute boundary (location C to C_2) between the rich and quench zones through which no reverse flow occurs, thereby guaranteeing the existence of fuel rich combustion.

3. Swirl was very strong (100 to 200 ft/sec tangential velocity), for good stabilization.

4. Axial velocities are also high near the wall for necessary effective wall cooling.

Design of the 18-Inch MASB

The 18-inch MASB (Figure 10) is intended to be a full-scale prototype of a single basket, incorporating all commercially required features. Therefore, the 18-inch MASB has been designed to accomplish the following four major technology advancements with respect to the 14 inch MASB.

1. Scale up from half-scale (in terms of mass flow) to full-scale.

   The 18-inch MASB is the same scale as planned for the Wilsonville Pilot Facility. Future applications to commercial combustion turbines would feature a multiple number of cans of this design. Table 4 shows the typical achieved conditions in the 14 inch MASB test, the planned operating conditions for the 18-inch MASB, and the conditions expected for the Wilsonville MASB.

   The rich zone diameter for the 14-inch MASB was 8.5 inches, whereas for the 18-inch MASB, this diameter is 14 inches. All fuel nozzle end dimensions are a direct geometric scale up.

2. Optimize combustor rich zone performance for better conversion of NH_3 to N_2.

   Although very good NO_x performance was achieved in the 14-inch testing, analysis indicates that better performance is possible. Table 5 shows the effects of rich zone equivalence ratio and residence time on NO_x generation in the MASB. The first line represents 14-inch achieved performance. These calculations were made using a Westinghouse combustion chemical kinetic data base with the Sandia Chemkin-II chemical kinetics modeling program.

   Table 5 shows that if the rich zone stoichiometry is too lean substantial NO_x is generated in the rich zone itself. If too rich, then NH_3 survives the rich zone to be converted to NO_x in the downstream lean regions. An optimum occurs in the 1.4 to 1.5 equivalence ratio range, as shown in Table 5. Also, performance is better with increased residence time.

   Consequently, an increase in residence time to 40 msec from 25 msec, by increasing length, and an increase in fuel equivalence ratio to 1.4 from 1.2 are goals of the 18-inch design and test plan.

18 Inch MASB Design
Cold Model Results

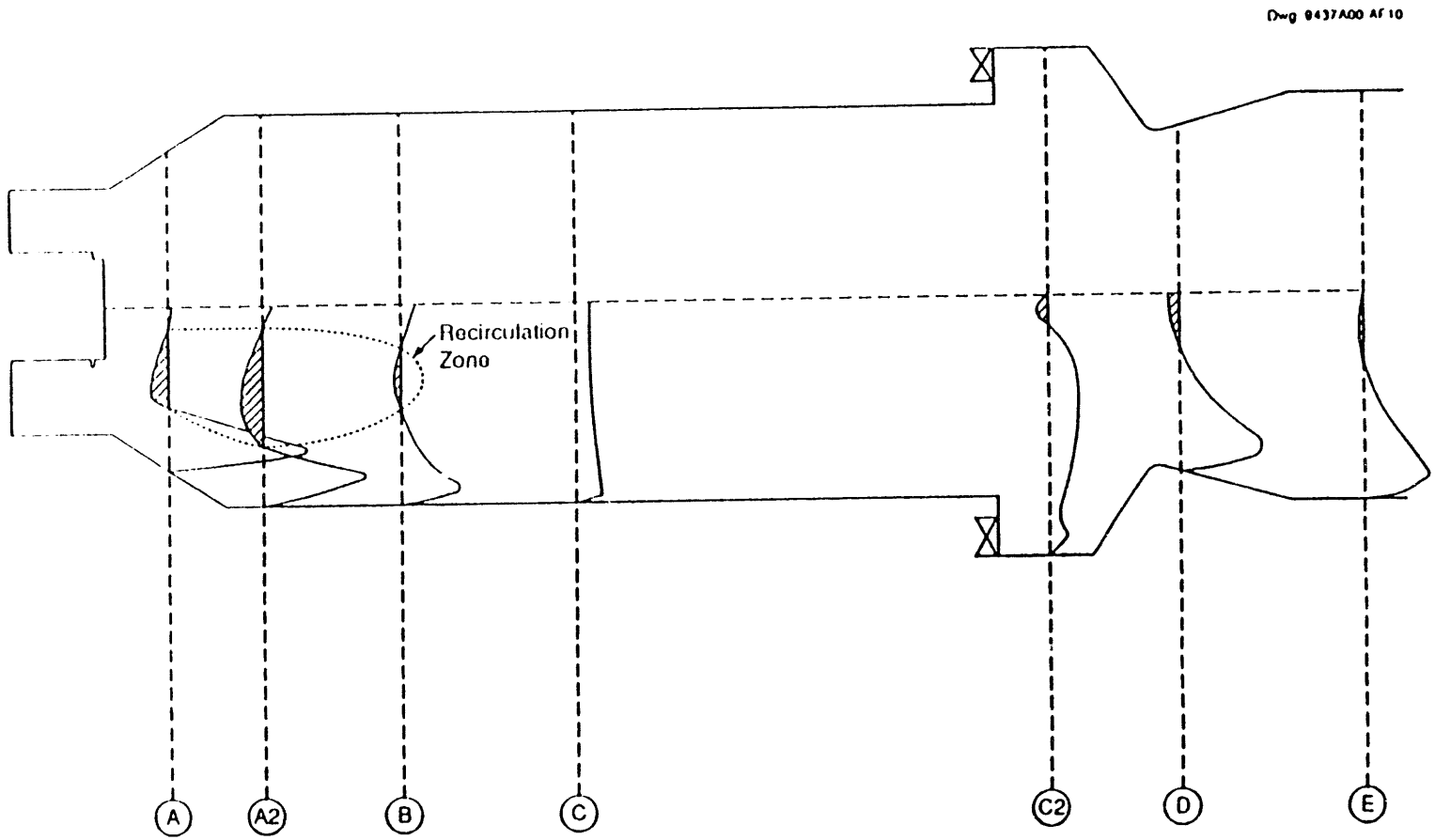

Figure 9. 18 Inch MASB Design Cold Model Results

Table 3. Similarity of Hot 18-Inch MASB and Cold Model

	18-Inch Hot MASB	Cold Model
Rich zone:		
Diameter, in.	14.5	7.0
Length, in.	27.9	13.5
Temperature, F	2900	70
Pressure, psia	160	16.2
Gas density, lbm/ft3	0.124	0.082
Gas velocity, ft/sec	55	52
Gas viscosity, lbm/ft-sec	0.00004	0.000012
Reynolds No.	206,000	206,000
Quench zone:		
Diameter, in.	12.0	5.8
Length, in.	6.9	3.6
Temperature, F	2850	70
Pressure, atm	160	16.2
Gas density, lbm/ft3	0.126	0.082
Gas velocity, ft/sec	120	114
Gas viscosity, lbm/ft-sec	0.00004	0.000012
Reynolds No.	380,000	380,000

3. Incorporate and demonstrate natural gas firing capability in both vitiated air and compressor air.

   The design features the capability for natural gas firing via a central dual fuel burner as shown in Figure 10 and magnified in Figure 11. A modified Pabst burner is utilized for natural gas combustion. Design natural gas consumption rates are 0.2 lb/sec for vitiated air firing and 0.4 lb/sec for compressor air firing. When doing so, steam (1 lb per lb natural gas) is injected through the syngas swirlers, both to keep it purged and to moderate rich zone temperature. Since this is a rich/lean combustor, the steam is not needed for NO_x reduction. A specially designed axial ignitor rod is used. These technologies are now to be demonstrated.

4. Incorporate improved mechanical designs.

   A number of hardware mechanical improvements have been incorporated.

   - The convergent-divergent flow deflector in the quench zone (see Figure 2) is now directly cooled by the incoming dilution section vitiated air in contract to the uncooled 14 inch flow vitiated air, in contrast to the uncooled 14-inch deflector where some thermal distress occurred. Also, a thermal barrier coating is now applied to all internal surfaces.

18 Inch MASB Design

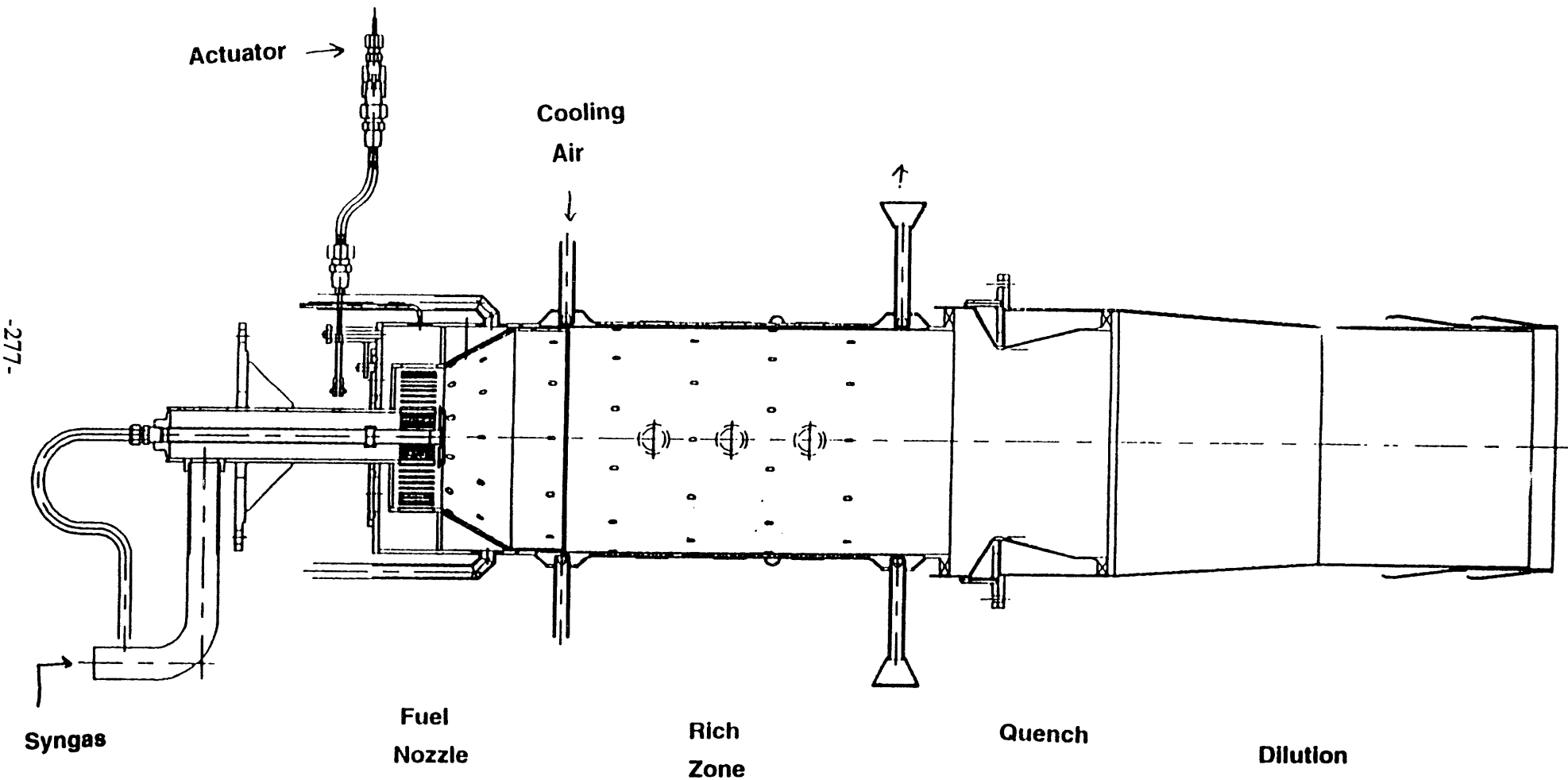

Figure 10. 18 Inch MASB Design

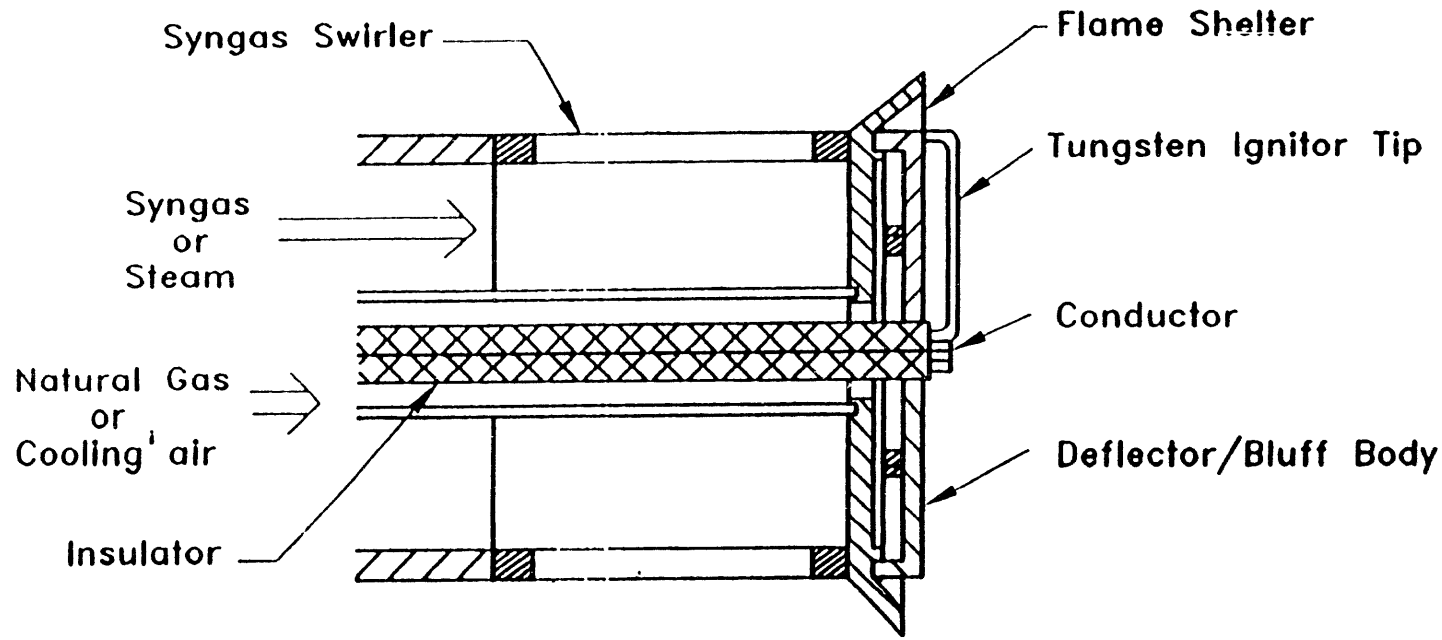
Syngas Swirler
Flame Shelter
Tungsten Ignitor Tip
Syngas
or
Steam
Conductor
Natural Gas
or
Cooling air
Deflector/Bluff Body
Insulator

Figure 11.

Table 4. Scale up of the MASB

	UTSI 14"	UTSI 18"	Wilsonville 18"
Syngas			
Temperature, xF	1200	1200	1600
Vitiated air			
Temperature, xF	1600	1600	1470
Pressure, atm (abs)	10	7.3	10
Rich zone velocity, ft/sec	45	55	55
Rich zone res. time, msec	28	45	43
Pressure drop, psid	2.8	2.8	2.5
Temperatures, xF			
Rich zone	3100	2750	2800
Quench zone	2650	2850	2850
Exit	2250	2350	2100
Turbine inlet			1977
Flows, lb/sec			
Syngas	0.7	2.6	3.3
Primary vit. air	0.9	2.0	4.3
Quench vit. air	0.4	3.2	6.8
Dilution vit. air	2.2	6.4	9.0
Cooling air	0.9	0.8	5.0

Table 5. Theoretical Fuel NO_x Formation vs. Rich Zone Parameters

Case	Equivalence ratio	Res. time,	NH_3 from rich zone, ppmv	NO_x from rich zone, ppmv	Fuel NO_x from MASB, ppmv
1	1.2	25	15	150	36
1	1.2	45	14	132	32
2	1.5	25	61	17	18
2	1.5	45	33	14	12
3	1.7	25	317	12	57
3	1.7	45	199	12	38
4	2.0	25	725	10	109
4	2.0	45	514	10	78

7.2 Development and Testing of Low Btu Fuel Gas Turbine Combustors

CONTRACT INFORMATION

Contract Number DE-AC21-87MC23170

Contractor
GE Environmental Services, Inc.
200 N. Seventh St.
Lebanon, PA. 17042
(717) 274-7000

Contractor Project Manager Stephen Bevan

Principal Investigators
Nesim Abuaf, GE Corporate Research and Development
Alan S. Feitelberg
Stephen L. Hung
Martin S. Samuels
Anil K. Tolpadi

METC Project Manager Justin L. Beeson

Period of Performance September 30, 1987 to September 30, 1994

Schedule and Milestones

Program Schedule

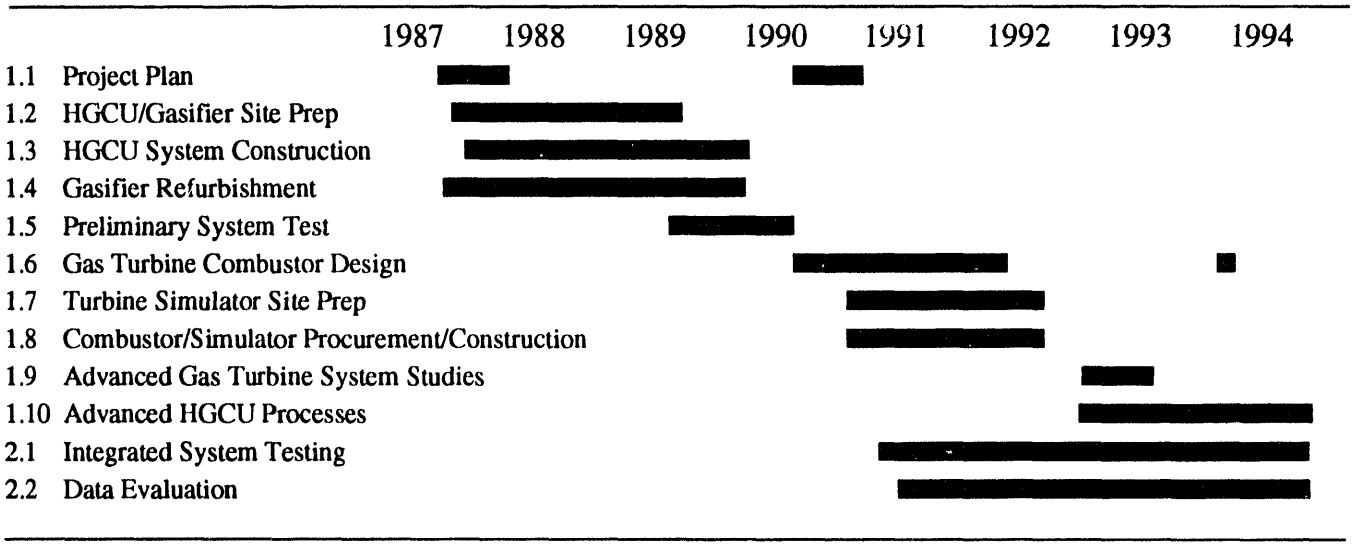

OBJECTIVES

The integrated gasification combined cycle (IGCC) concept represents a highly efficient and environmentally compatible advanced coal fueled power generation technology. When IGCC is coupled with high temperature desulfurization, or hot gas cleanup (HGCU), the efficiency and cost advantage of IGCC is further improved with respect to systems based on conventional low temperature gas cleanup.

Commercialization of the IGCC/HGCU concept requires successful development of combustion systems for high temperature low Btu fuel in gas turbines. Toward this goal, a turbine combustion system simulator has been designed, constructed, and fired with high temperature low Btu fuel. Fuel is supplied by a pilot scale fixed bed gasifier and hot gas desulfurization system. The primary objectives of this project are: (1) demonstration of long term operability of the turbine simulator with high temperature low Btu fuel; (2) characterization of particulates and other contaminants in the fuel as well as deposits in the fuel nozzle, combustor, and first stage nozzle; and (3) measurement of NO_x, CO, unburned hydrocarbons, trace element, and particulate emissions.

In a related project, a reduced scale rich-quench-lean (RQL) gas turbine combustor has been designed, constructed, and fired with simulated low Btu fuel. The overall objective of this work is to develop an RQL combustor with lower conversion of fuel bound nitrogen (FBN) to NO_x than a conventional combustor.

BACKGROUND INFORMATION

Combustion of the high temperature (~1000°F) low Btu fuel produced from an IGCC/HGCU system is significantly different from the combustion of typical gas turbine fuels, such as natural gas and fuel oils. Differences in the air/fuel ratio, fuel composition, and fuel temperature affect many of the combustor operating parameters including the lean blowout limit, flame stability, and emissions. These differences require modification of the fuel nozzle and combustor liner. In addition, gas turbines used in IGCC/HGCU applications will require fuel control valves that are capable of operating with high temperature low Btu fuel. Other concerns include the possibility that particles and vapor phase contaminants in the fuel may form deposits on and/or cause the corrosion of the fuel nozzle, combustor liner, and turbine blades.

PROJECT DESCRIPTION

Turbine Simulator

Figure 1 shows the low Btu gas turbine simulator that has been constructed and integrated with the coal gasification/hot gas cleanup facility at GE Corporate Research and Development in Schenectady NY. The pilot scale gasification/hot gas cleanup system consists of a fixed bed gasifier, a sodium bicarbonate based halogen removal system, a moving bed high temperature desulfurization system, and a polishing cyclone. The turbine simulator is designed to operate at the full capacity of the gasifier, 8000 lb./hr of fuel gas from the gasification of 1800 lb./hr of coal. The low Btu fuel is supplied at a pressure of 20 atm and a nominal temperature of 1000°F. Details of the gasifier and the hot gas cleanup system can be found in Cook *et al.* [1,2].

The turbine simulator includes: a low Btu gas fuel nozzle; a modified GE MS6000 combustor liner; a film cooled, first stage LM6000 nozzle assembly, and an impingement cooled transition piece. A GE MS6000 combustor liner was chosen because its fuel requirements are close to the capacity of the gasifier/HGCU system. The liner was modified to meet the air requirements of low Btu fuel combustion, while the reverse flow sleeve is standard hardware. The fuel nozzle wa

designed specifically for low Btu gas combustion [3]. A film cooled LM6000 first stage nozzle was chosen to simulate the film cooled nozzles found in advanced gas turbines with high firing temperatures.

Design of the turbine simulator was initiated in April 1991. Fabrication and assembly were completed in August 1992. The current test plan includes seven fired tests with coal gas from the pilot scale gasifier/HGCU system, designated as Runs 3, 3A, 4, 5, 6, 7, and 8. This paper focuses on the results from Runs 5 and 6, which were completed in November 1993 and May 1994, respectively. The results from previous tests have been discussed by Cook *et al.* [4,5].

A recent addition to the turbine simulator is the optional ability to augment the low Btu fuel with natural gas. Because the fuel requirements of the turbine simulator slightly exceed the capacity of the gasifier/HGCU system, the heating value of the low Btu fuel must be enhanced with natural gas to reach sustained combustion exit temperatures in excess of 2100°F. The natural gas is added to the low Btu fuel far upstream of the combustor so that the blended fuel entering the turbine simulator is completely mixed. This capability was first exercised during selected time periods of Run 6. The blended fuel was less than 10% (by volume) added natural gas.

RQL Combustor

A new reduced scale RQL combustor design is nearly complete. Nominal design conditions are 0.75 lbs./sec total flow and combustor exit temperatures up to 2500°F. The RQL combustor has a modular construction, which allows for

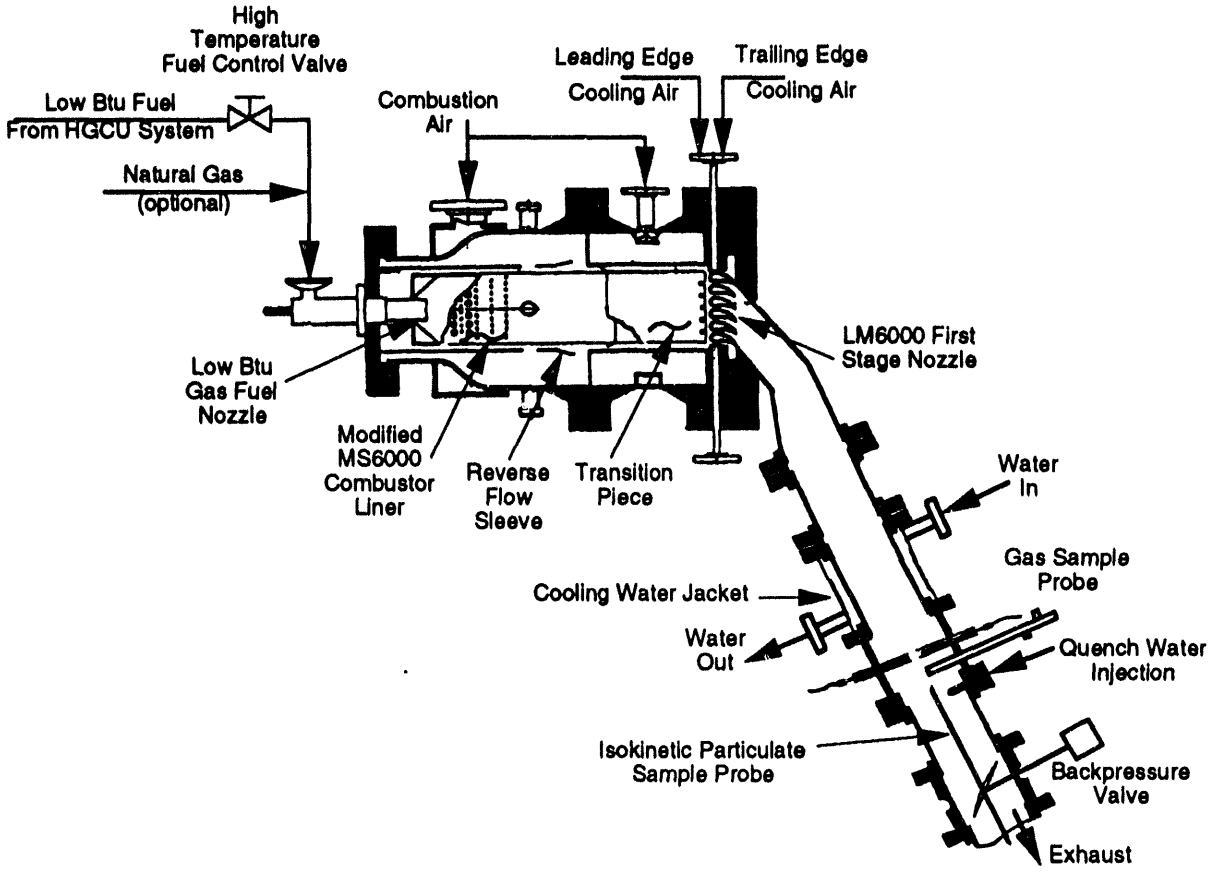

Figure 1. The Turbine Simulator Test Stand

rapid evaluation of different hardware configurations. The rich and lean stages are separate components, and the air flow to each stage can be independently varied.

Insights gathered from previous reduced scale RQL combustion tests [5], cold flow visualization tests, and computational fluid dynamics (CFD) studies have been incorporated into the new design. The new design includes a converging rich stage to separate the fuel rich and fuel lean combustion zones, and a backward facing step at the inlet to the lean stage for flame stabilization. The converging cone has been added to the tail end of the rich stage to close the rich stage recirculation zone. The reduction in diameter also accelerates the flow and helps prevent upstream flow of quench air into the rich stage.

RESULTS

The turbine simulator was fired with coal gas for 41 hours during Run 5 and 67 hours during Run 6, for a total of 179 hours of fired operation over 5 tests. The gasifier was fueled with Illinois #6 coal for both Runs 5 and 6. A typical fuel composition (after H_2S removal) is given in Table 1. During Run 5, the turbine simulator was operated at a combustor exit temperature of 2300°F for the first time. In addition, the low Btu fuel and burned gas were sampled for trace elements in both the solid phase and the vapor phase. Radian Corporation assembled and operated the trace element sample trains, and also performed all trace element sample analyses. Deposits were collected from several locations within the turbine simulator at the conclusion of Run 5 and were also analyzed for trace elements.

The turbine simulator reached a combustor exit temperature of 2500°F, representative of GE "F" class gas turbines, for the first time during Run 6. An on-line atomic emission spectrometer, developed at Ames Laboratory, was also used to measure vapor phase alkali species concentrations in the hot low Btu fuel.

Wall Temperatures

Except for the head end of the combustor, metal wall temperatures throughout the turbine simulator (including the transition piece and film-cooled cascade) have been within design specifications for all of the long duration tests. However, metal wall temperatures at the head end of the combustor frequently have exceeded design limits. As a result, sections of the cap/cowl were damaged during three of the first four long duration tests. An improper fuel/air ratio at the head end of the combustor was probably the largest single factor which contributed to the high wall temperatures.

After Run 5, during which the cap/cowl was again damaged by high metal wall temperatures, several modifications were made to the fuel nozzle and combustor liner. First, a small step between the fuel nozzle assembly and the cap/cowl was eliminated by bringing the fuel nozzle forward. Second, the swirl angle on the fuel side of the fuel nozzle was reduced from 40 degrees to 15 degrees. Finally, the first two rows of mixing holes in the combustor liner were

Table 1. Typical Pilot Plant Low Btu Fuel Composition

Species	Mole Percent
CO	8.6
H_2	17.3
CH_4	2.7
N_2	30.1
CO_2	12.6
H_2O	28.0
Ar	0.3
NH_3	0.4
TOTAL	100.0

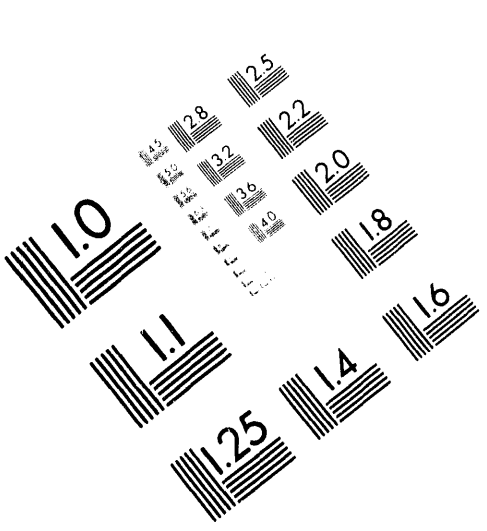

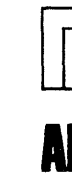

Association for Information and Image Management

1100 Wayne Avenue, Suite 1100
Silver Spring, Maryland 20910

301/587-8202

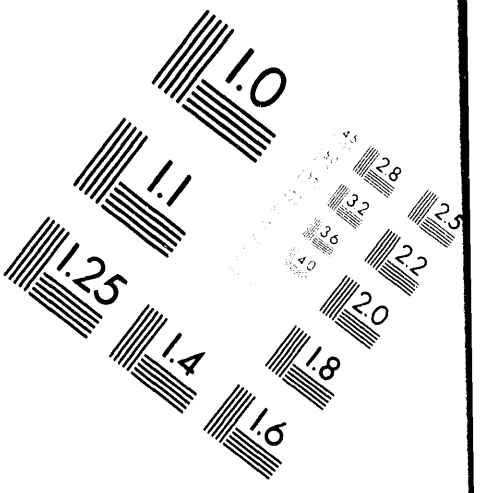

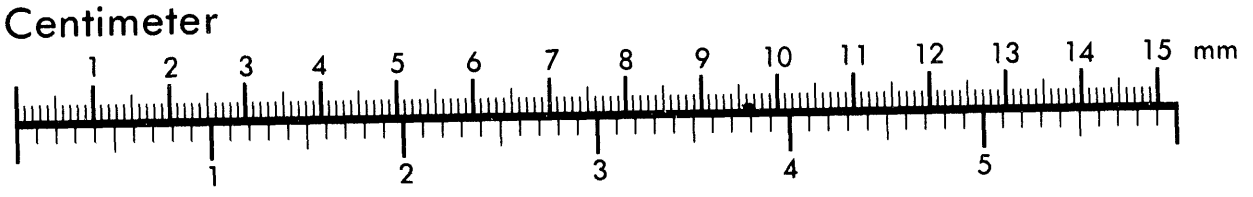

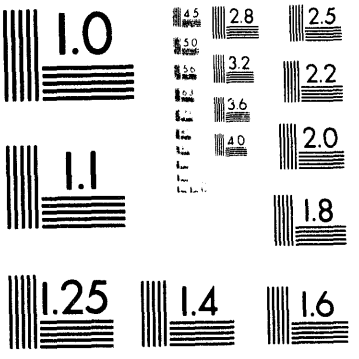

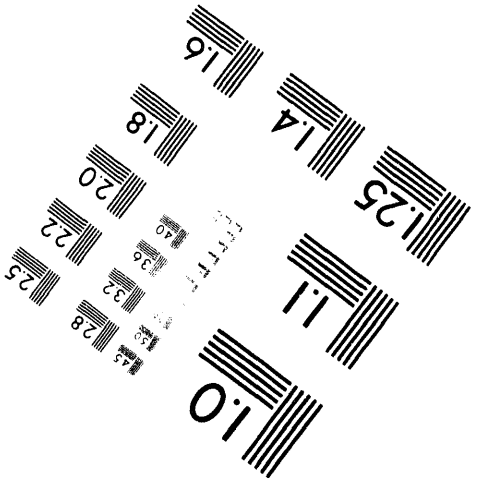

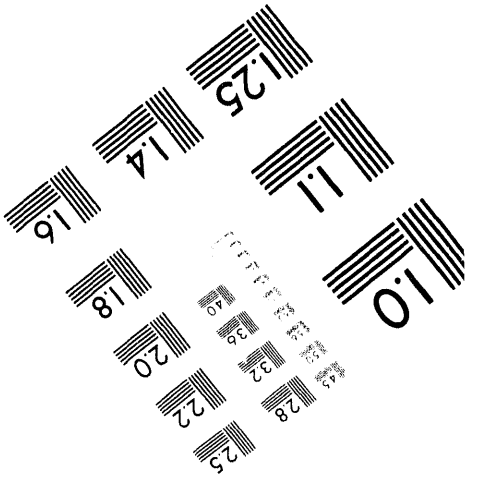

MANUFACTURED TO AIIM STANDARDS
BY APPLIED IMAGE, INC.

4 of 6

closed to increase the fuel/air ratio at the head end of the combustor. These changes were designed to reduce recirculation of hot burned gas towards the cap/cowl and to move the combustion zone downstream, away from the cap/cowl.

The effectiveness of these hardware changes was demonstrated during Run 6. Cap/cowl temperatures never exceeded 1000°F, even at combustor exit temperatures as high as 2500°F. The hardware modifications also resulted in significantly lower combustor liner temperatures.

Emissions

The fuel nozzle and combustor liner modifications had little effect on NO_x emissions (see Figure 2). The slightly higher NO_x emissions seen in Run 6 can be attributed to a slightly higher NH_3 content in the fuel. The average NH_3 concentration in the low Btu fuel was 4100 ppmv during Run 5, while the average NH_3 concentration was 4400 ppmv during Run 6. The emissions measurements shown in Figure 2 (and all of the emissions measurements reported in this paper) were taken when the turbine simulator was fueled solely with low Btu gas.

Figure 2 shows NO_x emissions tend to decrease as the combustor exit temperature increases. At 2300°F, NO_x emissions averaged 180 ppmv (on a dry, 15% O_2 basis) during Run 5, representing a conversion of NH_3 to NO_x of about 20%. At a combustor exit temperature of 1600°F, NO_x emissions averaged 300 ppmv (on a dry, 15% O_2 basis) during Run 6, representing a conversion of NH_3 to NO_x of about 30%. The decrease in NO_x as exit temperature increases is primarily due to the increasing equivalence ratio at the head end of the combustor.

The combustor liner and fuel nozzle modifications made to decrease cap/cowl temperatures were expected to cause an increase in CO emissions. Figure 3 shows the increase was relatively small. CO emissions were below the detection limit of about 1 ppmv (on a dry, 15% O_2 basis) at combustor exit temperatures above 2100°F. CO emissions increased as the combustor exit temperature decreased, and CO emissions increased more rapidly with the modified hardware. UHC emissions also increased as the combustor exit temperature decreased (see Figure 4).

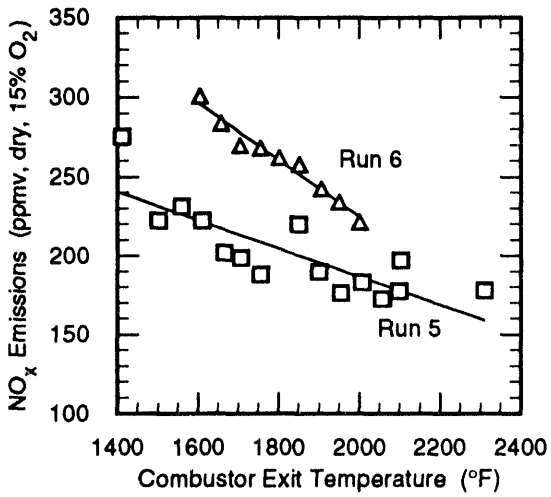

Figure 2. Turbine Simulator NO_x Emissions

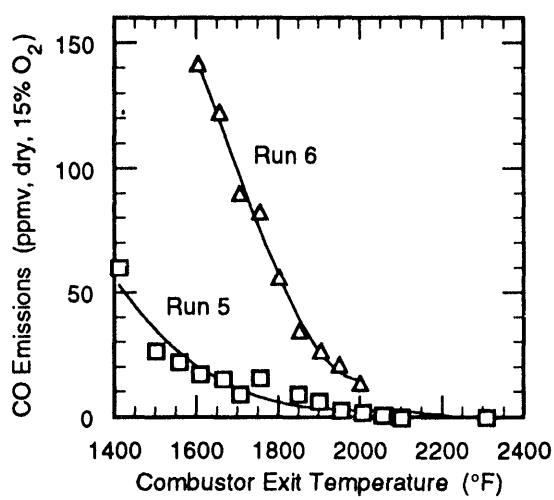

Figure 3. Turbine Simulator CO Emissions

Fuel Alkali Levels

During Run 6, vapor phase alkali concentrations were measured with the Ames Alkali Monitor, an on-line atomic emission spectrometer developed by Ames Laboratory [6]. Low Btu fuel was sampled isokinetically just upstream of the turbine simulator and then filtered before being sent to the alkali monitor. Although the low Btu fuel exited the HGCU system at about 1000°F, the fuel cooled to about 860°F at the alkali sample location. The sample line and filter were maintained at a temperature of about 950°F.

The results of the vapor-phase alkali measurements are shown in Table 2. The alkali monitor was unable to observe any vapor phase potassium above the detection limit of about 1 ppb by weight as K. Vapor phase sodium concentrations averaged about 3 ppb, with a maximum of approximately 5 ppb by weight as Na.

Also shown in Table 2 are chemical equilibrium calculations of expected vapor-phase alkali species concentrations at two coal gas temperatures. The calculations were performed with a modified version of CET89, the NASA chemical equilibrium code [7]. The coal gas composition listed in Table 1 was used for the calculations, with the addition of 200 ppmv HCl, 2500 ppmv H_2S, and sufficient amounts of sodium and potassium to insure the existence of condensed sodium and potassium species in the equilibrium mix.

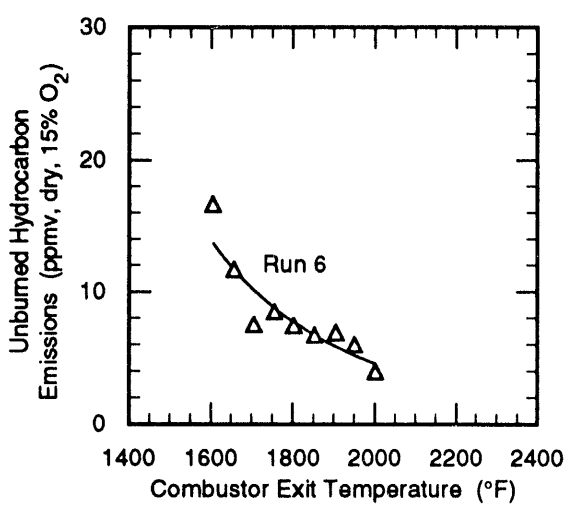

Figure 4. Turbine Simulator UHC Emissions

The two principal sources of thermodynamic data were the JANAF tables [8] and the extensive compilation of Barin [9]. Approximately 60 solid, liquid, and vapor sodium and potassium species were considered. Only the most abundant alkali species are listed in Table 2; all other alkali species were present in the vapor phase at concentrations below 0.01 ppb by weight as Na or K. Solid carbon (coke) was deliberately excluded from the equilibrium composition, based on kinetic constraints. Sodium and potassium silicates and aluminates were also excluded for similar reasons.

Table 2 shows the measured total vapor phase sodium concentration is within the range of the equilibrium calculations, assuming a coal gas temperature of between 850°F and 1000°F. Alkali species concentrations were calculated at two temperatures because of the uncertainty in the fuel temperature. As the low Btu gas in the main fuel line cooled from 1000°F to 860°F, some of the vapor phase alkali may have condensed on the surface of entrained particles. This condensed material may have been partially (or fully) volatilized when the sample gas was heated in the sample line and/or when the particles came to rest on the heated particulate filter.

At these temperatures, both the measured and calculated vapor phase alkali levels are well within gas turbine limits (20 ppb by weight total alkali in the products of combustion). The bulk of the sodium is expected to exist in the solid phase as sodium carbonate (Na_2CO_3) and sodium chloride (NaCl), and the bulk of the potassium is predicted to exist in the solid phase as potassium chloride (KCl). The predicted vapor phase potas-

sium concentrations shown in Table 2 are slightly higher than previously reported [5] because of refinements to the thermodynamic database and computational procedures.

The chemical equilibrium calculations were performed assuming a large excess of solid sodium and potassium compounds in the equilibrium mix. This is a good assumption for sodium, because sodium bicarbonate is injected into the low Btu fuel upstream of the HGCU system. However, this is a very conservative assumption for potassium. For this reason, the calculated equilibrium vapor phase concentration of sodium is in better agreement with the measurements than the calculated equilibrium vapor phase concentration of potassium.

Trace Elements

The turbine simulator burned gas was sampled isokinetically for vapor phase trace elements during Run 5. The burned gas was diluted 1:1 with nitrogen and then cooled to approximately 250°F before being filtered according to EPA Method 5. A portion of the sample gas was then passed through the impinger train specified in EPA Method 29. Three vapor phase trace element samples were collected using this technique. Two blank samples, collected during a period when low Btu fuel was not available, were obtained by establishing normal air flows through the simulator and sampling according to the above procedure.

Table 3 shows the average concentration of each element detected in the vapor phase burned gas samples. Element concentrations were determined by GFAAS (Graphite Furnace Atomic Absorption Spectrophotometry), ICPES (Inductively Coupled Plasma Emission Spectroscopy), or CVAAS (Cold Vapor Atomic Absorption Spectrophotometry). Ten other elements (aluminum, antimony, beryllium, cobalt, copper, magnesium, molybdenum, phosphorus, potas-

Table 2. Comparison of Measured and Equilibrium-Modeled Vapor Phase Alkali Concentrations in Low Btu Fuel

	Gas Phase Concentration (ppb by weight as Na or K)		
	Equilibrium Model Calculations		Measurements
Gas Phase Species	T = 850°F	T = 1000°F	T = 860°F
Na	<0.01	<0.01	
NaCl	0.1	4.3	
NaOH	<0.01	<0.01	
$(NaCl)_2$	0.03	1.9	
Total Na	0.13	6.2	3
K	<0.01	<0.01	
KCl	0.5	19.6	
KOH	<0.01	0.01	
$(KCl)_2$	0.1	7.6	
Total K	0.6	27.2	<1

sium, and vanadium) were below the detection limit in all the burned gas samples.

The presence of relatively volatile elements (such as arsenic, mercury, and selenium) in the vapor phase samples is not surprising. Even at an exhaust gas temperature as low as 250°F, these elements might be expected to remain in the vapor phase. The detection of relatively non-volatile elements (such as iron and and manganese) suggests the vapor phase samples were contaminated with a small amount of particulate matter. In particular, the concentration of sodium in the vapor phase samples is greater than expected, based on the measured amount of condensed-phase and vapor-phase sodium in the fuel. The relatively large amount of sodium in the blank samples indicates the blank samples were also contaminated with some sodium containing condensed matter.

RQL Combustor

Figure 5 shows the velocity vectors calculated by a two-dimensional CFD analysis of the new RQL combustor rich stage. The strong swirl generated by the fuel nozzle creates a central recirculation zone and a corner recirculation zone at the head end of the rich stage. There is also another weak recirculation zone, near the wall of the converging section, which extends most of the length of the rich stage. Without a converging section the rich stage recirculation zone would extend to the point of quench air injection, and quench air would be drawn into the rich stage.

Table 3. Vapor Phase Emissions of Trace Elements

	Concentration in Turbine Simulator Exhaust ($\mu g/Nm^3$)	
Element	Burned Gas	Blank Sample
Arsenic	16	BDL
Barium	6.0	1.4
Cadmium	0.4	BDL
Calcium	70	44
Chromium	40	2.0
Iron	1440	13
Lead	3.2	1.1
Manganese	280	24
Mercury	4.0	0.6
Nickel	52	7.9
Selenium	1.2	0.8
Sodium	120	61
Titanium	2.0	BDL
Zinc	32	6.6

BDL = below detection limit

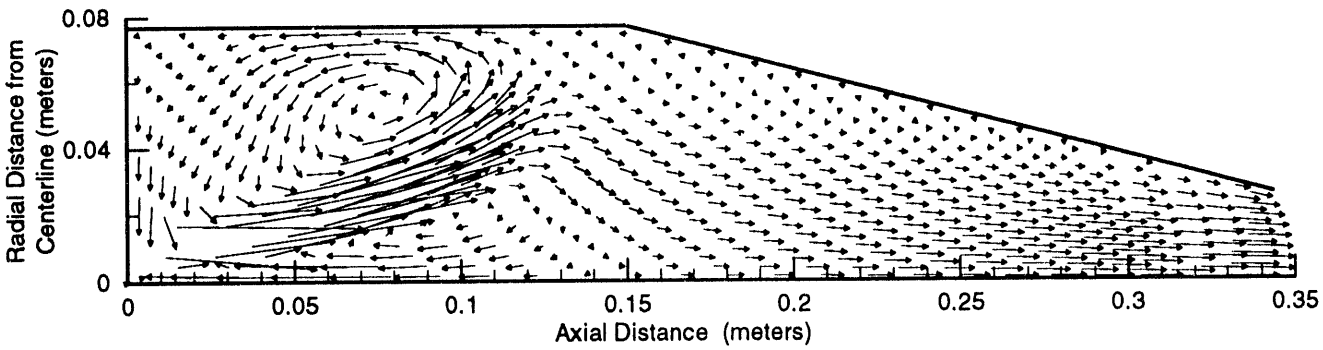

Figure 5. Computed Velocity Vectors in Rich Stage of RQL Combustor

FUTURE WORK

One additional long duration test of the turbine simulator is scheduled for 1994. A new low Btu fuel nozzle design, incorporating a radial air swirler, will be used in this test. The cap/cowl will have to be modified to accept the new fuel nozzle, since the new nozzle has a significantly smaller overall diameter than the current nozzle. Fuel nozzle performance will be evaluated by measuring NO_x, CO, and UHC emissions, as well as combustor liner and cap/cowl temperatures. After the test, the nozzle will be examined for deposits and signs of erosion.

Design of the new reduced scale RQL combustor is nearly complete. Initial tests will be conducted using natural gas/nitrogen/ammonia blends for fuel. A reduced scale RQL combustion test with a slip stream of low Btu fuel from the pilot plant gasifier/HGCU system is also scheduled for 1994. The information gathered from these tests will be used to design a larger scale (turbine simulator scale) RQL combustor.

REFERENCES

1. Cook, C. S., E. Gal, A. H. Furman, and R. Ayala. 1992. Integrated Operation of a Pressurized Fixed Bed Gasifier and Hot Gas Desulfurization System. In *Proceedings of the Twelfth Annual Gasification and Gas Stream Cleanup Systems Contractors Review Meeting*, 84-94. DOE/METC-92/6128. NTIS/DE93000228. Springfield, VA: National Technical Information Service.

2. Cook, C. S., E. Gal, A. H. Furman, and R. Ayala. 1991. Integrated Operation of a Pressurized Fixed Bed Gasifier and Hot Gas Desulfurization System. In *Proceedings of the Eleventh Annual Gasification and Gas Stream Cleanup Systems Contractors Review Meeting*, 45-55. DOE/METC-91/6123. NTIS/DE92001101. Springfield, VA: National Technical Information Service.

3. Lawson, C. C. *Water-Cooled Components Test Program, Final Report.* 1985. DOE/MC/20192-1953. Contract DE-AC21-83MC20192.

4. Cook, C. S., N. Abuaf, A. S. Feitelberg, S. L. Hung, D. J. Najewicz, and M. S. Samuels. 1993. Combustion Tests of a Turbine Simulator Burning Low Btu Fuel and a Rich-Quench-Lean Combustor. In *Proceedings of the Coal-Fired Power Systems 93 — Advances in IGCC and PFBC Review Meeting*, 169-178. DOE/METC-93/6131. NTIS/DE93000289. Springfield, VA: National Technical Information Service.

5. Cook, C. S., N. Abuaf, A. S. Feitelberg, S. L. Hung, D. J. Najewicz, and M. S. Samuels. 1993. Combustion Tests of a Turbine Simulator Burning Low Btu Fuel From a Fixed Bed Gasifier. In *Proceedings of the Joint Contractors Meeting: FE/EE Advanced Turbine Systems Conference FE Fuel Cells and Coal-Fired Heat Engines Conference*, 199-208. DOE/METC-93/6132. NTIS/DE93011308. Springfield, VA: National Technical Information Service.

6. Haas, W. J., Jr., D. E. Eckels, S. H. D. Lee, W. M. Swift, L. H. Cowell, M. D. Stephenson, and R. T. LeCren. 1991. Alkali Monitoring for Direct Coal-Fired Turbine Combustors. In *Proceedings of the Eight Annual Coal-Fueled Heat Engines and Gas Stream Cleanup Systems Contractors Review Meeting*, 360-371. DOE/METC-91/6122. NTIS/DE91002091. Springfield, VA: National Technical Information Service.

7. McBride, B. J. 1989. *CET89 – Chemical Equilibrium with Transport Properties.* University of Georgia: Computer Software Management and Information Center.

8. Barin, I. 1989. *Thermochemical Data of Pure Substances.* New York: VCH.

9. Chase, M. W., C. A. Davies, J. R. Downey, Jr., D. J. Frurip, R. A. McDonald, and A. N. Syverud. 1985. *JANAF Thermochemical Tables, Third Edition.* Journal of Physical and Chemical Reference Data, 14, Supplement 1.

7.3 Advanced Turbine Systems Program Overview

Holmes A. Webb
Morgantown Energy Technology Center

ABSTRACT

The U.S. Department of Energy's (DOE) Office of Fossil Energy and Office of Energy Efficiency & Renewable Energy are jointly supporting a program to develop Advanced Turbine Systems (ATS). Demonstrations of commercial prototypes will be completed by the year 2000 for both utility- and industrial-scale applications. The systems will exhibit the following characteristics:

- **Ultra-high efficiency** (Utility systems: greater than 60 percent [lower heating value basis]/industrial systems: greater than 15 percent improvement over today's best technology),
- **Environmental superiority** (single digit NOx and reduced carbon dioxide, carbon monoxide, and unburned hydrocarbons),
- **Cost competitiveness** (10 percent lower cost of electricity),
- **Reliability, Availability, and Maintainability (RAM)** equivalent to today's best systems.

The program is primarily directed toward natural gas utilization, but eventual application of the technology to coal-fired systems is not overlooked. In major procurements, contractors are required to address (in paper studies though not in testing) the eventual adaptation of their systems to coal firing. Another program element targets the transfer of ATS technology to coal-fired turbine systems being funded by DOE, such as integrated gasification combined cycle, pressurized fluidized bed combustion, and externally fired combined cycle.

Implementation of the program is proceeding well. Phase I systems studies have been completed, and Phase II concept development has been underway for about a year. Release of solicitation for Phase III proposals has been announced for July, 1994. This phase of the program will see teams led by turbine manufacturers move into full scale testing of critical components. Generic research and development has been proceeding in parallel with the major development effort. METC has started testing in their Advanced Turbine Combustion test facility, and Oak Ridge National Laboratory has initiated a materials test program. The industry/university consortium established by the South Carolina Energy Research and Development Center has completed their second round of university awards, with 23 university projects now underway.

Support for this $700 million program has been strong, and budgets have been consistent with those outlined in a Report to Congress on the program. Funding was about $28 million in FY 94, and the President's budget for FY 95 includes $65 million for ATS.

Poster Session

P1 High Temperature Electrochemical Separation of H_2S from Coal Gasification Streams

CONTRACTOR INFORMATION

Contract Number	DE-FG22-91PC91288
Contractor	Georgia Institute of Technology School of Chemical Engineering Atlanta, Georgia 30332-0100 (404) 894-2839
Contractor Project Manager	E. Faith Gleason
Principle Investigator	Jack Winnick
METC Project Manager	Kamalendu Das
Period of Performance	October 1, 1991 - November 30, 1994

OBJECTIVE

A method of polishing coal synthesis gas by an electrochemical membrane operation is being perfected. The operation takes advantage of an electrochemical potential gradient rather than conventional techniques, separating the H_2S from the coal gas stream, leaving only H_2 to enrich the exiting fuel gases. Sulfur is the by-product that is carried away by a separate inert sweep gas and condensed downstream. The technology is attractive due to simplicity as well as economics when compared to alternatives.

An analytical model describing the preferred reduction of H_2S, the transport of S^{2-}, and the competing transport of CO_3^{2-} through the removal cell has continued[11]. The main objective is the relation between cell polarization and current efficiency. This has been realized.

Recent experiments have focused on removing 100 ppm inlet H_2S, utilizing laboratory fabricated cobalt cathodes.

INTRODUCTION

A schematic of the mechanism used for electrochemical separation is presented in Figure 1. The process gas, cleansed of particulates, passes over the cathode. Here the best Lewis acid, electron acceptor, will be reduced. In this case H_2S is favored, resulting in the following:

$$H_2S + 2e^- \rightarrow S^{2-} + H_2 \qquad (1)$$

The sulfide ions are transported, by migration and diffusion, across the membrane. Once the sulfide ion reaches the anode side, oxidation to elemental sulfur occurs by the following:

$$S^{2-} \rightarrow 1/2\, S_2 + 2e^- \qquad (2)$$

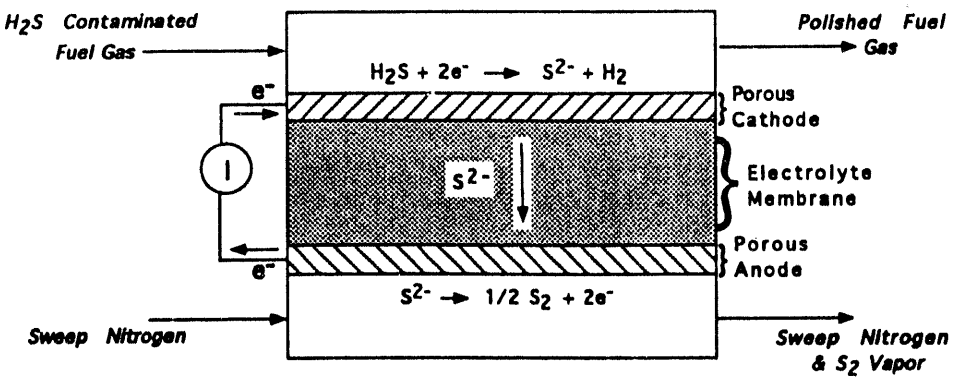

Figure 1. Schematic of Electrochemical Cell

The vaporous sulfur is condensed downstream.

Processes to remove H_2S typically rely on low-to-ambient temperature adsorption, followed by sorbent regeneration and Claus plant treatment for conversion of H_2S to a salable by-product, sulfur. Although effective, this type of removal is very process-intensive as well as energy-inefficient due to low temperature operation. Gasification streams generally range from 500°C - 1000°C, requiring cooling before and reheating after process gas sweetening. Although these technologies have proven capable of meeting H_2S levels required by MCFC, there are several disadvantages inherent to these processes[7,8].

Alternative high temperature methods are presently available, but process drawbacks including morphological changes in catalytic beds[9] or inefficient molten salt sorbent processes[10] negate savings incurred through energy efficient removal temperatures.

An electrochemical membrane separation system for removing H_2S from coal gasification product streams is the subject of this investigation. The high operating temperature, flow-through design, and capability of selective H_2S removal and direct production of elemental sulfur offered by this process provide several advantages over existing and developmental H_2S removal technologies. The remaining factor is a thorough economic evaluation asserting the viability of the process.

An initial economic evaluation[11] showed the process noteworthy. Further analysis will require developing an analytical model describing 1) the preferred reduction of H_2S among competing reactants in the gasification stream, 2) the transport of S^{2-} through the electrolyte filled membrane, and 3) competing transport of CO_2 through the removal cell. The model can give the maximum current efficiency for H_2S removal, depending on variables such as flow rate, temperature, current application, and total cell potential. Extended application of the model will predict cell performance under varying cell currents, gas compositions and flow rates. It will also permit economic projection in various applications.

Analytical Model

A theoretical model based on applied current, flow rate, and electrochemical effects has been investigated, relating anode CO_2 production with % H_2S removal. Although the model is not completed, adequate power estimates for percentage removals of H_2S can be computed.

Preferential Reduction of H_2S.

H_2S has been shown to be readily reduced in hot gas mixtures, even at low ppm levels. The situation is complicated when coal gas mixtures are processed. Carbon dioxide and water vapor compete in the reduction reaction at the cathode by:

$$CO_2 + H_2O + 2e^- \Rightarrow CO_3^{2-} + H_2 \quad (3)$$

The ionic flux through the membrane depends on the relative mobility of carbonate and sulfide ions as well as their concentrations.

Preventing the oxidation of carbonate at the anode is necessary for prohibiting its transport through the membrane, the desired anodic reaction being:

$$S^{2-} \Rightarrow 1/2\ S_2 + 2e^- \quad (2)$$

This occurs at a standard potential some 700 mV lower than the oxidation of carbonate:

$$CO_3^{2-} \Rightarrow CO_2 + 1/2\ O_2 + 2e^- \quad (4)$$

Summing the half-cell reactions (**1**) and (**2**) results in the following overall reaction at 923K:

$$H_2S \Leftrightarrow H_2 + 1/2\ S \quad (5)$$
$$E_a^o = -0.239\ V$$

and when the half-cell reactions (**3**) and (**4**) are summed:

$$H_2O \Leftrightarrow H_2 + 1/2\ O_2 \quad (6)$$
$$E_b^o = -1.030\ V$$

The relative extent of each of these reactions is determined by chemical equilibrium. Each will occur at the *same cell potential*; but as expressed by the Nernst relation, the concentration terms will be greatly affected by the large difference in the standard cell potentials, E^o, values.

$$E = E_a^o - \left(\frac{RT}{nF}\right) \ln \left\{ \frac{a_{S^{2-}_{cath}} P_{H_2\,cath} P^{\frac{1}{2}}_{S_2\,an}}{a_{S^{2-}_{an}} P_{H_2S_{cath}}} \right\} \quad (7)$$

$$E = E_b^o - \left(\frac{RT}{nF}\right) \ln \left\{ \frac{a_{CO_3^{2-}_{cath}} P_{H_2\,cath} P_{CO_2\,an} P^{\frac{1}{2}}_{O_2\,an}}{a_{CO_3^{2-}_{an}} P_{CO_2\,cath} P_{H_2O_{cath}}} \right\} \quad (8)$$

We here assume a process gas is supplied to the cathode with an H_2S level of 100 ppmv, a CO_2 level of 14.2%, and an H_2O level of 5.7%, and that 90% of the H_2S is to be removed via reaction (**1**). There exists an activity ratio of $\frac{a_{CO_3^{2-}}}{a_{S^{2-}}}$ on the order of 10^5 in the anolyte, assuming equivalent electrode kinetics[5,6] for the two reactions, before a significant amount (e.g. 1%) of the carbonate is oxidized. When compared to the activity ratio of $\frac{a_{CO_3^{2-}}}{a_{S^{2-}}}$ in the catholyte of 3000, this shows the huge thermodynamic preference for the oxidation of S^{2-} to elemental sulfur by equation (**2**).

The net effect, under these conditions, is continuous and selective removal of H_2S from the process gas accompanied by enrichment of the process gas with H_2 and direct generation of elemental sulfur at the anode.

Electrical Power Requirements.

The power to drive the electrochemical membrane separator is a direct function of the potential required to drive the removal cell multiplied by the current carried by the sulfide ions across the membrane.

Power=(CellPotential) *(Cell Current) (9a)

Estimation of the current carried by the removal cell is straight-forward since two faradays of charge are carried by each mole of sulfide transported (or each mole of H_2S removed). Calculation of the cell potential is outlined below.

Along with the Nernst relation, additional energy is required to operate the separation cell due to irreversible losses. These losses occur by internal resistance, concentration effects in the process gases, and the activation barrier for electron transfer. The result is the total cell potential increasing over the reversible potential[1].

Ohmic Polarization:

Ohmic losses occur due to resistance in ionic and electronic transfer of current through the separation system. The ohmic losses can be expressed by:

$$\eta_{ohm} = IR \qquad (9)$$

with **I** representing current and **R** the total cell resistance.

Concentration Polarization:

Concentration polarization originates from developing concentration gradients due to consumption of electro-active species at the electrode surface. Transport of these species is composed of four steps, occurring in series: 1) the H_2S must diffuse through the gas-phase boundary layer to the cathode interface, 2) it must diffuse through the pores of the electrode to the electrolyte film, 3) the sulfide ion must migrate to the anode, and 4) the oxidized species must diffuse out into the sweep gas at the anode. The effect of step 3 has been minimized due to proper membrane design and steps 2 and 4 have been found to be of no consequence[2]. The limiting process for removal is thus diffusion of electro-active species to the electrode pores from the bulk gas. Since the gas-phase concentration of H_2S changes along the length of the channels, a log-mean average is used in the calculation of limiting current density by:

$$i_L = nFk_m\rho\frac{(y_{inlet} - y_{exit})}{\ln\left(\frac{y_{inlet}}{y_{exit}}\right)} \qquad (10)$$

where **n** is the number of electrons transferred per mole of species removed, **F** is Faraday's constant, $\mathbf{k_m}$ is mass transfer coefficient, ρ is the molar density of the bulk gas, and $\mathbf{y_x}$ is the inlet and exit mole fraction of H_2S. The average mass transfer coefficient was derived from an estimated Sherwood number dependent on channel dimension and constant H_2S surface concentration[3] given by:

$$N_{Sh} = \frac{k_m D_{eq}}{D_{ab}} \qquad (11)$$

with $\mathbf{D_{eq}}$ defined as the equivalent channel diameter above the electrode surface:

$$D_{eq} = 4r_h = \frac{4(\text{cross-sectional area})}{(\text{wetted perimeter})} \qquad (12)$$

and $\mathbf{D_{ab}}$ the diffusion coefficient of H_2S through the predominant species by volume in the bulk according to[4]:

$$D_{ab} = \frac{0.0018583T^{\frac{3}{2}}}{P\sigma_{ab}\Omega_{D_{ab}}}\sqrt{\frac{1}{M_a} + \frac{1}{M_b}} \qquad (13)$$

therefore, concentration overpotential is expressed in terms of applied current by:

$$\eta_{conc} = \frac{RT}{nF}\ln\left(1 - \frac{i}{i_l}\right) \qquad (14)$$

Activation Polarization:

The activation polarization at both cathode and anode is related to the rates of electrochemical reactions occurring at these electrodes. The

expression relating the kinetics of these electrode reactions is the Butler-Volmer equation:

$$i = i_o\left[\exp\left(\frac{\alpha_a F\eta_{act,a}}{RT}\right) - \exp\left(\frac{-\alpha_c F\eta_{act,c}}{RT}\right)\right] \quad (15)$$

which holds for specified temperature, pressure, and concentration of reacting species. The transfer coefficients α_a and α_c sum to the number of electrons transferred in the reaction:

$$\alpha_a + \alpha_c = n \quad (16)$$

Cell Voltage:

Total cell voltage incorporating *ohmic*, *concentration*, and *activation* overpotentials along with the Nernstian effects (7) sums to:

$$V_{cell} = \Delta E_{c-a} - |\eta_{conc}| - |\eta_{act}| - \eta_{ohmic} \quad (17)$$

where ΔE_{c-a} is the total cathode-to-anode cell voltage.

The results exhibited in Figure 2, 3, and 4 were generated using this analytical approach. The run conditions assumed equal cathodic and anodic flow rates of (200 cc/min) (the calculated results are independent of anode sweep gas flow rate), atmospheric system pressure, a run temperature of 650 °C, and three order of magnitude changes in H_2S removal (1000 ppm to 1 ppm). The cathodic and anodic exchange current densities were estimated at 40 mA/cm^2 after the results of the free electrolyte studies[5,6]. The exchange coefficients, α_a and α_c, were assumed to be unity. Ohmic resistance across the cell was conservatively estimated to be 1 Ω, based on Molten Carbonate Fuel Cell (MCFC) results[1]

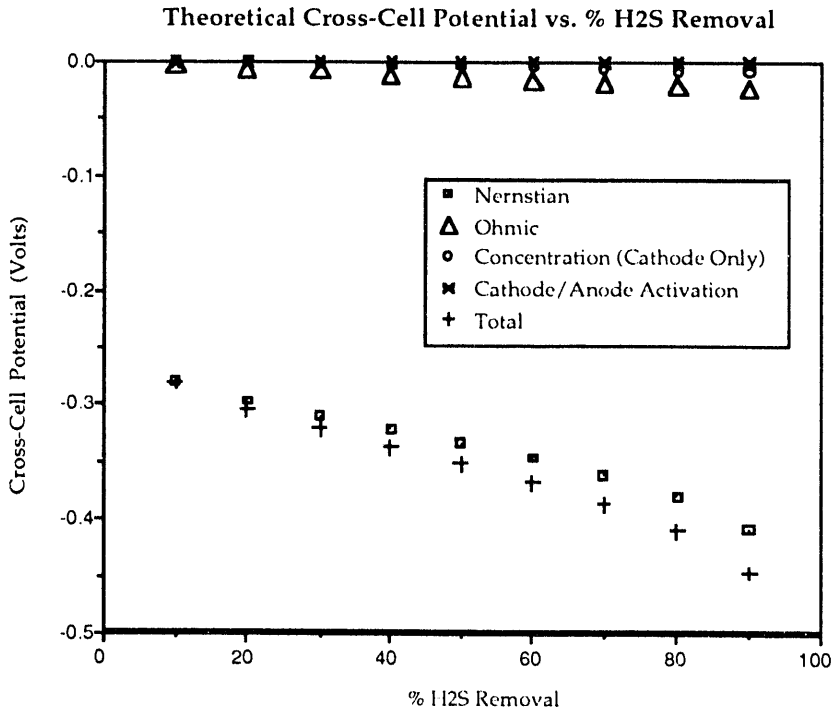

Figure 2. Theoretical Cross-Cell Potential vs. % H_2S Removal; 1000 ppm inlet

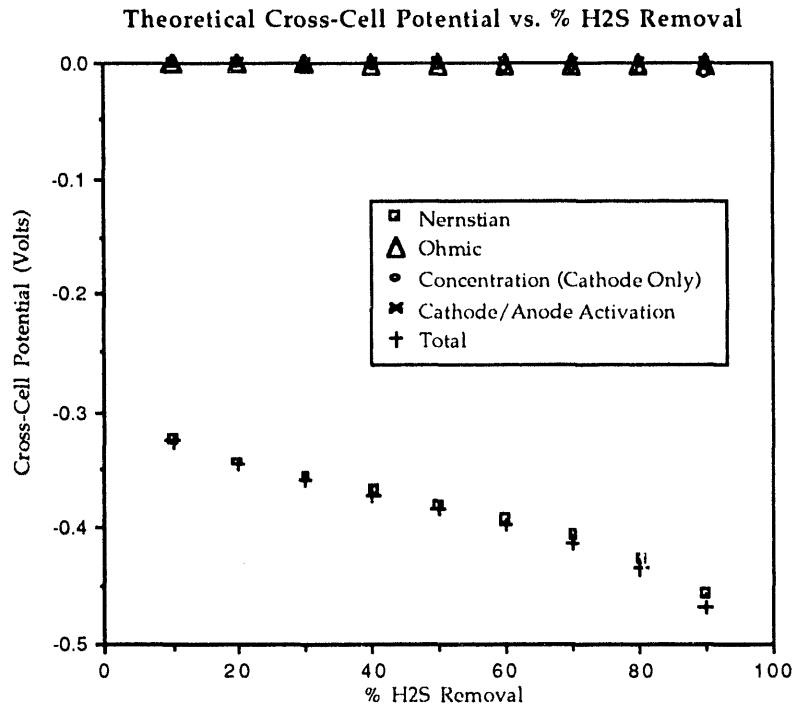

Figure 3. Theoretical Cross-Cell Potential vs. % H_2S Removal; 100 ppm inlet

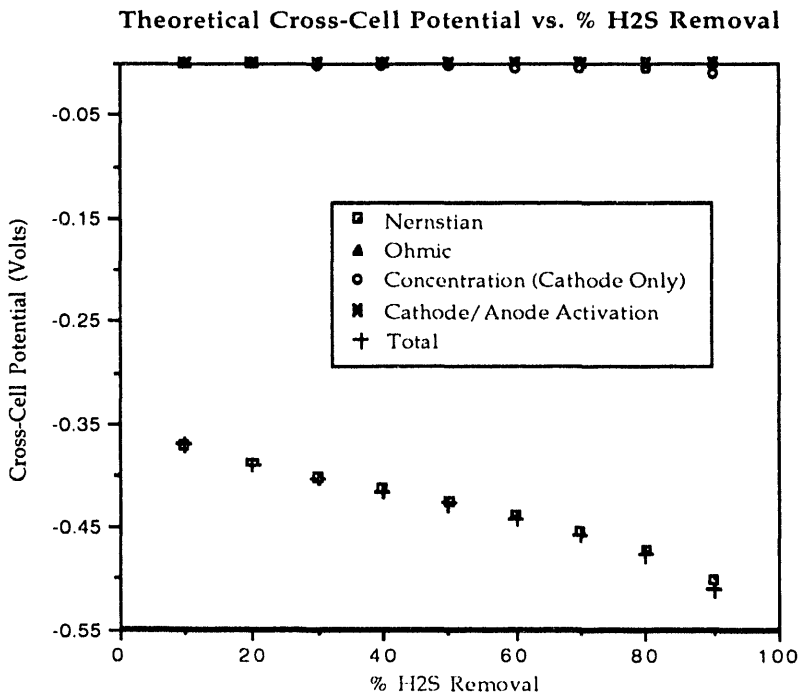

Figure 4. Theoretical Cross-Cell Potential vs. % H_2S Removal; 10 ppm inlet

These results show the activation overpotentials at both cathode and anode are negligible. This shows extremely rapid electrochemical kinetics as compared to diffusion effects from the bulk gas phase and through the electrolyte filled membrane. Cross-cell potentials are shown as the sum of the Nernstian, concentration, and ohmic polarization effects. Therefore, at 90% removal H_2S (1000 ppm - 100 ppm; 100 ppm - 10 ppm; 10 ppm to 1 ppm), the data of Figure 2, 3, and 4 show total cross-cell potentials of -0.4474 V, -0.4675 V, and -0.5107 V, which agree well with experimental cross-cell potentials. Total power requirements for these removals from (**9a**) are 10.5 W, 1.09 W, and 0.12 W (not considering current loss from anodic CO_2 production).

Parallel Sulfide, Carbonate Transport.

Since the carbonate transport of reaction (**6**) parallels the sulfide transport of reaction (**5**), the same current is available for transport of both species. Therefore, only a certain amount of current will act to transport either constituent giving a finite maximum current efficiency with respect to H_2S removal for any percentage of H_2S removed. This is dependent on gas composition and total cross-cell potential required for the desired separation of H_2S. Once the total cross-cell potential is calculated for the desired H_2S removal, the Nernst expression for transport of carbonate (**8**) can be equated to this value, since the relative extent of each occur at the same potential. The extent of parasitic CO_2 current from the removal cell associated with $\%H_2S$ removal is shown in Figure 5, 6, and 7.

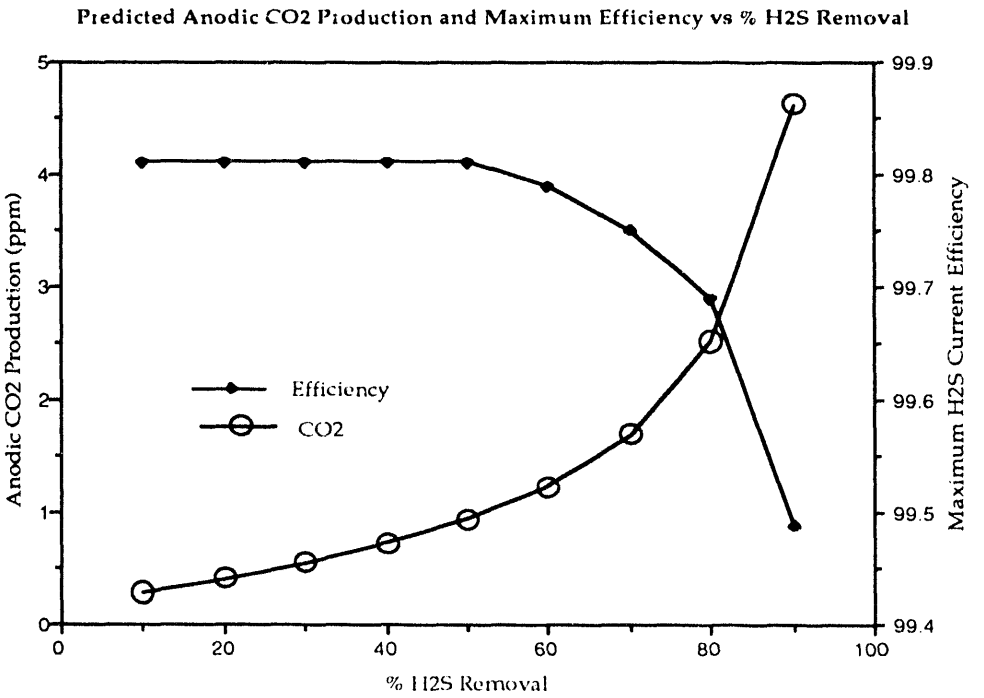

Figure 5. 1000 ppm inlet H_2S

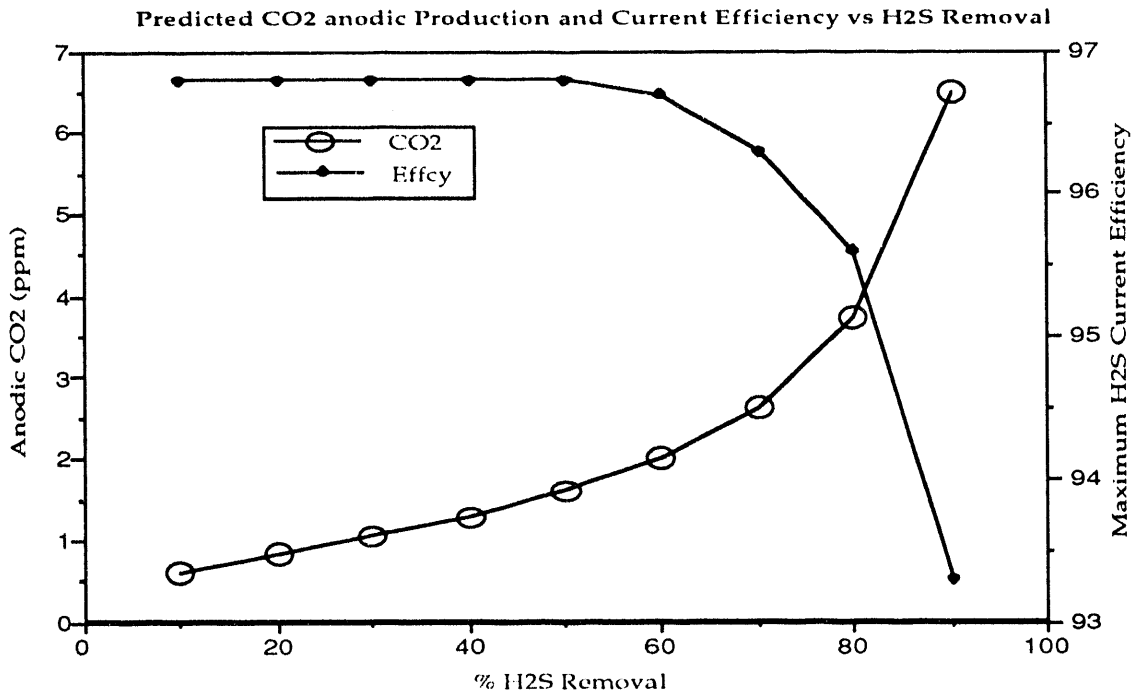

Figure 6. 100 ppm inlet H_2S

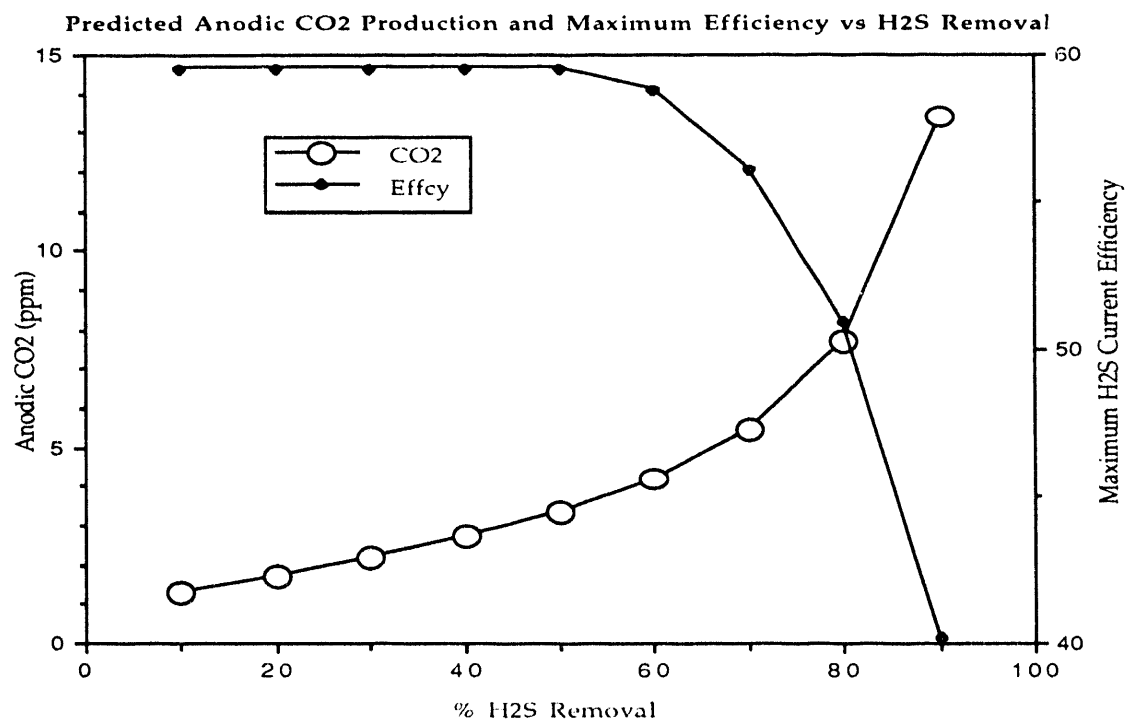

Figure 7. 10 ppm inlet H_2S

Examination of the results shows that H_2S current efficiency drops only to 99.5% at 90% H_2S removal (1000 ppm to 100 ppm H_2S), 93.2% at 90% H_2S removal (100 ppm to 10 ppm H_2S), and 40.2% at 90% H_2S removal (10 ppm to 1 ppm H_2S). The excess current goes to produce anodic CO2.

This is a favorable result considering the power requirement at higher inlet H_2S concentrations is considerably greater than at lower concentrations, Figure 8 (10.52 W at 1000 ppm inlet H_2S, 0.29 W at 10 ppm inlet H_2S); a high efficiency is a must in the higher H_2S concentrations if the process is to be economically viable. Energy requirements for the 10 ppm H_2S removal are negligible, shown in Figure 8, alleviating concern due to lower current efficiencies.

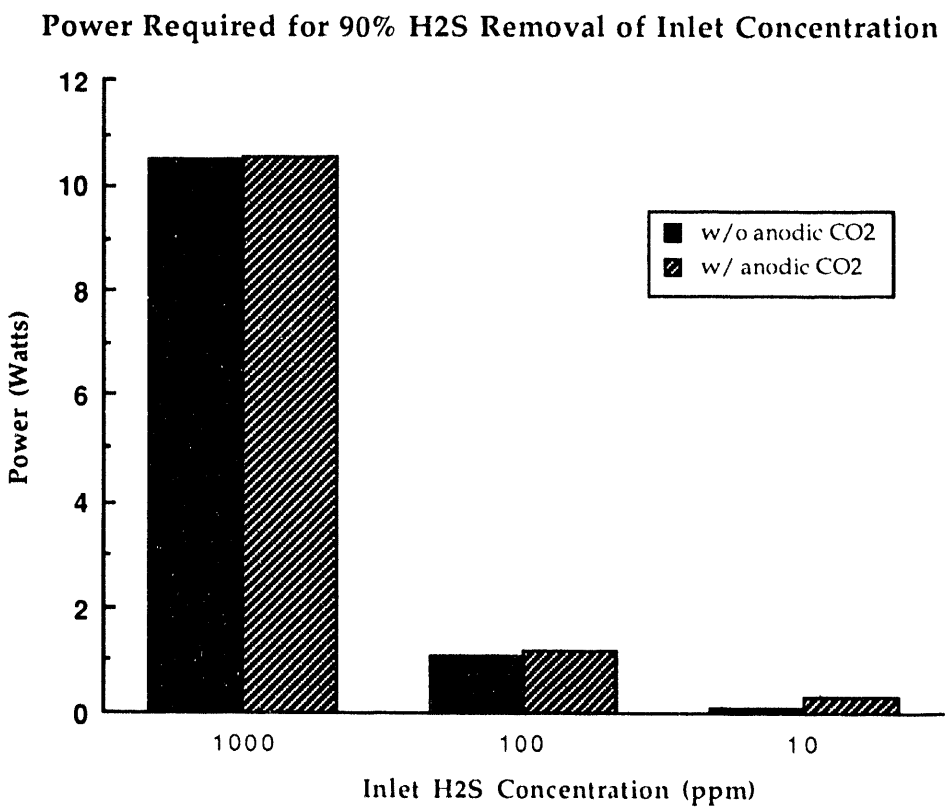

Figure 8. Power Estimates

Table I. Percentage Removal with Applied Current

I_{app} (mA)	% of Total H_2S Removed	% of Total CO_2 Removed
200	0	10
500	28	30
1000	50	50
1500	70	75

EXPERIMENTAL RESULTS

An experiment (Run#16) examining the removal capability of the EMS with cobalt cathode was recently performed The focus dealt with H_2S removal as well as containing hydrogen cross-over from the process gas side (cathode) of the membrane to the sweep gas side (anode).

Run #16

Cell materials consisted of a cobalt cathode (80% porous), the anode material remained Ni (85% porous), a stabilized zirconia membrane (66% porous), housings of MACOR (machineable ceramic), aluminum foil gasket seals, and a prepressed disk of $(Li/K)_2CO_3$ (8 grams) corresponding to the void volume in the zirconia membrane. Electrode materials were verified by x-ray diffraction, Figure 9.

Examination of the cobalt-cathode electrochemical membrane separator (EMS), produced stoichiometric CO_2 removal and addition at both cathode and anode, respectively, before addition of H_2S. After introducing H_2S to the EMS, system gases equilibrated to 10% CO_2, 18% CO, 10% H_2O, 36% H_2, 26% N_2 and 90 ppmv H_2S after the water-gas shift reaction. H_2S removal at varying currents was attempted, starting with stoichiometric current (2 mA for a flow of 158 cc/min), and increasing to 200 mA. H_2S removal did not appear significant (< 10 ppmv), with continued stoichiometric CO_2 removal at the cathode and production at the anode. Further application of current in steps from 200 mA to 1.5 A revealed percentage of total H_2S removal coincided with percentage of total CO_2 removal, shown in Table I. This trend was evidenced in past experiments with hydrogen cross-over present. Micro-cracks in the membrane that would enable hydrogen to cross from the process gas side (cathode side) to the sweep side (anode side) seem to be evident from Scanning Electron Microscopy (SEM) in pre-run analysis, Figure 11.

a)

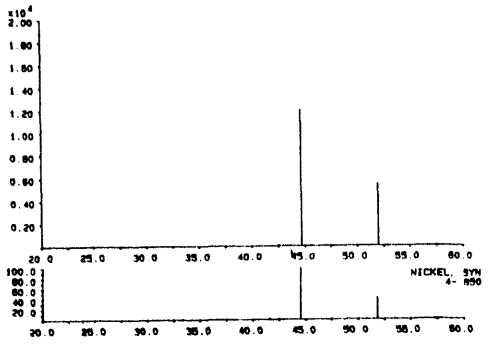

b)

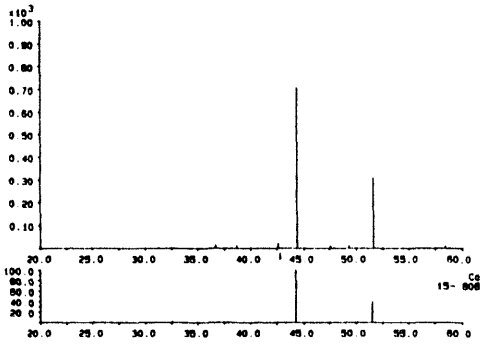

Figure 9. a) Pre-run Ni anode and b) Pre-run Co cathode

a)

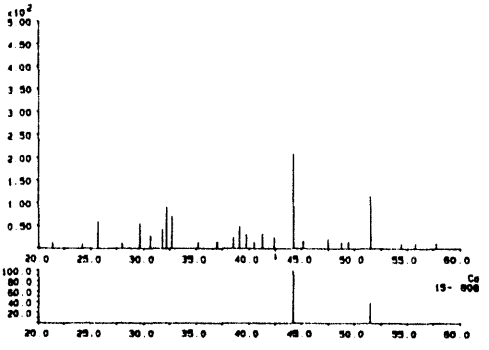

b)

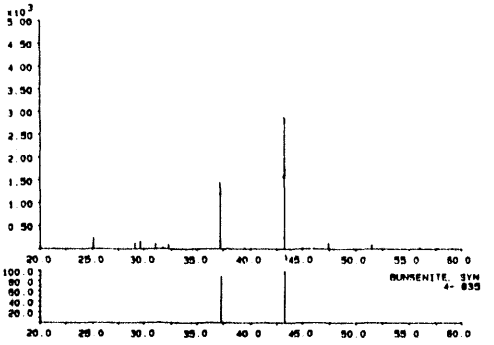

Figure 10. a.) Post-run Co cathode and b.) Post-run NiO anode

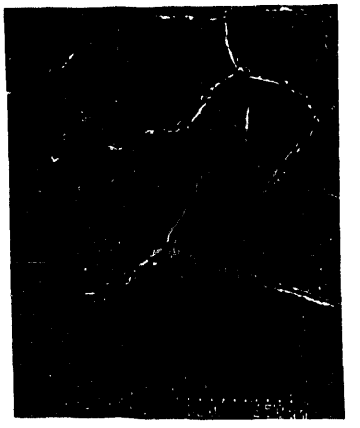

Figure 11. Scanning Electron Microscopic view of zirconia membrane.

If hydrogen cross-over occurs, two reactions are possible at the anode. One reaction is the oxidation of hydrogen and the sulfide ion to hydrogen sulfide.

$$H_2 + S^{2-} \rightarrow H_2S + 2e^-$$

Anode exit gases checked by gas chromatography showed no evidence of H_2S. The other possible reaction is the oxidation of hydrogen and carbonate to water and carbon dioxide.

$$H_2 + CO_3^{2-} \rightarrow H_2O + CO_2 + 2e^-$$

Gas chromatography did reveal minute amounts of water vapor on the anode side substantiating hydrogen cross-over. This creates loss of carbonate from the electrolyte, induces the favorability of carbonate reduction at the cathode over H_2S due in part to the higher pressure of CO_2 and H_2O available at the cathode (order of 10^5 higher than H_2S) promoting the parasitic reaction.

Favored:
$H_2S + 2e^- \rightarrow H_2 + S^{2-}$

Competing:
$H_2O + CO_2 + 2e^- \rightarrow CO_3^{2-} + H_2$

Internal resistance remained ~1 ohm.

Ineffective removal due to hydrogen cross-over forced shut-down of the cell after 76 hours of operation. Post-mortem X-ray diffraction of electrode materials revealed a conversion of the Ni cathode to NiO (bunsenite), with the cathode remaining Co, Figure 10.

SUMMARY

Initial results from the analytical model show favorable H_2S current efficiencies. Upper H_2S concentration removal resulted in a minuscule loss in current to the parasitic reaction (**6**) at 90% H_2S removal. Although the lower concentrations showed less efficiency, the amount of current needed for these removals are negligible.

The cobalt cathode used in the EMS proved stable and efficient. Removal of H_2S was deterred by the possibility of hydrogen cross-over from process gases creating alternate reactions unfavorable to the removal system. Application of back-pressure from the anode side of the cell was attempted to resolve H_2 cross-over, but proved ineffective. Examination of water vapor in the anode exit gases provided proof of the H_2 cross-over reactions parasitizing applied current.

FUTURE WORK

The main focus will be on H_2S current efficiency using a fabricated zirconia membrane with 100 ppmv H_2S fuel gas; hopefully, preventing alternate reactions due to hydrogen cross-over.

Work will continue with the analytical model; a complete economic analysis based on the completed model is the ultimate goal, if a match with real-time data exists.

REFERENCES

1. U.S. Dept. of Energy, Fuel Cell: A Handbook, DOE/METC-88/6090, Morgantown, West Virginia, 1988.

2. Kang, M. and Winnick, J., *J. Appl. Electrochem.*, **15**, 431-39 (1985).

3. Incropera, F.P., and DeWitt, D.P., Fundamentals of Heat and Mass Transfer, 2nd ed., John Wiley and Sons, New York, 1985.

4. Reid, R., Prausnitz, J., and Poling, B., The Properties of Gases and Liquids, 4th ed., McGraw-Hill, New York, 1987.

5. Banks, E., and Winnick, J., *J. Appl. Electrochem.*, **16**, 1986.

6. White, K.A., and Winnick, J., *Electrochem. Acta.*, **30**, 1985.

7. EPRIEM-1333, *Assessment of Sulfur Removal Processes for Advanced Fuel Cell Systems, Final Report,* C.F. Braun and Co., Alhambra, CA, Jan., 1980.

8. Vidt, E.J., DOE/METC DE-AC-21-81MC16220, DE82013942, Westinghouse, Dec., 1981.

9. Focht, G.D. et. al., DOE/MC/121166-2163, DE86016041, July, 1986.

10. Lyke, S.E., DOE/MC/19077-1803, DE8500961, Battelle Pacific Northwestern Laboratories, Jan. 1985.

11. Alexander, S., *PhD Thesis*, Georgia Institute of Technology, Atlanta, GA, 1992.

P2

Characterization and Fixed-Bed Testing of a Nickel-Based Hot Gas Desulfurization Sorbent

Lee D. Gasper-Galvin
Morgantown Energy Technology Center

James H. Swisher
Southern Illinois University at Carbondale

Kurt Hammerbeck
Oak Ridge Associated Universities

OBJECTIVES

The objective of this project was to (1) extend a preliminary investigation completed earlier on dispersed nickel sorbents[1] by developing new processing methods, characterizing sorbent materials more extensively, and evaluating the materials in fixed bed reactor tests, and (2) to determine the feasibility of using dispersed nickel sorbents with reductive regeneration for hot gas desulfurization.

BACKGROUND

There has been interest and active research on desulfurization of coal-derived gases since they were first produced by coal carbonization more than a century ago. A comprehensive review of the literature on metal and binary oxide sorbents was published by Swisher and Schwerdtfeger[2]. A later paper by the same authors[3] reviewed literature on mixed oxide sorbents and discussed the importance of thermodynamics in research on sulfur sorbents.

During the past 10 years, research in this field has focused on desulfurization at high temperatures because of the need for application of the technology to Integrated Gasification Combined Cycle (IGCC) systems. In the 1980's, the sorbent material receiving the most attention was zinc ferrite[4]. While it was very effective in reducing hydrogen sulfide (H_2S) concentrations in the product gas to the low ppmv level, it suffered from zinc loss due to vaporization and poor resistance to decrepitation and attrition.

More recently, zinc titanate sorbents have been shown to have comparable desulfurizing ability to zinc ferrite and to be better in durability[5-10]. There is now more research being done on zinc titanate than any other class of sorbents. However, there are still unanswered questions about its durability and reactivity over many sulfidation/regeneration cycles and its ability to serve applications in which the temperature of the gas to be desulfurized is 750°C or higher. Therefore, continuing research is justified on alternate sorbent materials.

There has been some, but not an extensive amount, of prior work on sorption of sulfur (S) by nickel (Ni) for hot gas desulfurization applications. One of the properties of nickel that is somewhat unique is that it forms a liquid sulfide at sufficiently high temperatures with high sulfur potentials or H_2S levels[11,12]. A eutectic exists in the Ni-S phase diagram at 637°C and a composition of 33.4 wt % or 21.5 wt % S[13]. Under controlled conditions, the formation of a liquid

phase can be used to advantage in hot gas desulfurization. The approach used by Steiner and Gutterman[14] was to use pellets of Ni and NiO in a fixed-bed reactor. When simulated coal gas was passed through the beds at 740°C, liquid sulfide formed and flowed away from the pellets. Thus, there was no solid sulfide present to serve as a diffusion barrier and curtail the reaction. Their concept included a provision for collecting the sulfide formed and regenerating it in a separate reactor.

Thermodynamic calculations show that the solid Ni-liquid Ni sulfide equilibrium will not reduce H_2S levels in coal gasification product gas to the low ppmv level. Fortunately, however, another mechanism can be used for sorption of S by Ni in the low concentration range. Patel, Rich, and Maru[15] showed that chemisorption of S on Ni occurs readily in the 500 to 700°C temperature range. They evaluated ten commercial catalysts containing dispersed Ni in a fixed-bed reactor, and success was achieved in reducing S species concentrations from 10 ppmv to 20 ppbv. The sulfur capacity varied from 2,000 to 10,000 ppmw or 0.2 to 1.0% by weight, depending on reactor conditions.

Initial work on sorbents containing dispersed Ni in an alumina (Al_2O_3) matrix was carried out by Swisher and Schwerdtfeger[16]. Two compositions were studied. One contained 26 wt % Ni in Al_2O_3, and the other contained 24 wt % Ni plus 7 wt % copper (Cu) in Al_2O_3. Copper was added because it is known to decrease the melting temperature and broaden the composition range of the liquid sulfide formed during sulfur sorption. There is a ternary eutectic reaction in the Ni-Cu-S system at 575°C. The eutectic composition in wt % is 69.8% Ni, 5.7% Cu, and 24.5% S[17,18]. The reactivity of individual pellets was studied in a Cahn thermogravimetric analyzer (TGA). Sulfidation was carried out in a mixture of 1 volume % H_2S in H_2, and regeneration was carried out in H_2. Results of the TGA experiments showed that the sorbents could be subjected to four sulfidation/regeneration cycles with no loss of reactivity. The temperature range for the experiments was 500° to 1000°C. It was found through visual observation and scanning electron microscopy that the liquid sulfide was retained in the Al_2O_3 structure during these TGA experiments.

PROJECT DESCRIPTION

Sorbent Preparation

The sorbent was prepared for evaluation using traditional powder processing methods. Reagent-grade NiO, CuO, and Al_2O_3 powders (all -325 mesh size) were blended in a 1 wt % solution of starch in water. Excess water was decanted, and the resulting paste was extruded through a metal tube to produce cylindrical pellets 9.3 mm in diameter and 10 to 12 mm long. The extrudates were dried in an oven at 120°C for 24 h. The dried extrudates were then placed in an electrically heated kiln; the temperature of the kiln was ramped up over a period of several hours, with a holding time of 2 h at the final sintering temperature of 1520°C. The extrudates were crushed and sieved to obtain samples in the -6, +16 mesh size range for fixed bed testing. The sorbent designation was 24Ni-7Cu-Al_2O_3, indicating a nominal composition of 24 wt % nickel and 7 wt % copper.

Description of Experimental Unit

The experimental studies were carried out in a bench-scale fixed bed reactor. A simplified schematic of the reactor system is shown in Figure 1. The reactor tube was alonized 316 stainless steel with an inside diameter of 2.21 cm (0.87 in) and a 0.165-cm (0.065-in) wall thickness. The sorbent bed was located in approximately the center of the 114.3-cm (45-in) long reactor tube, and the bed height was 5.08 cm

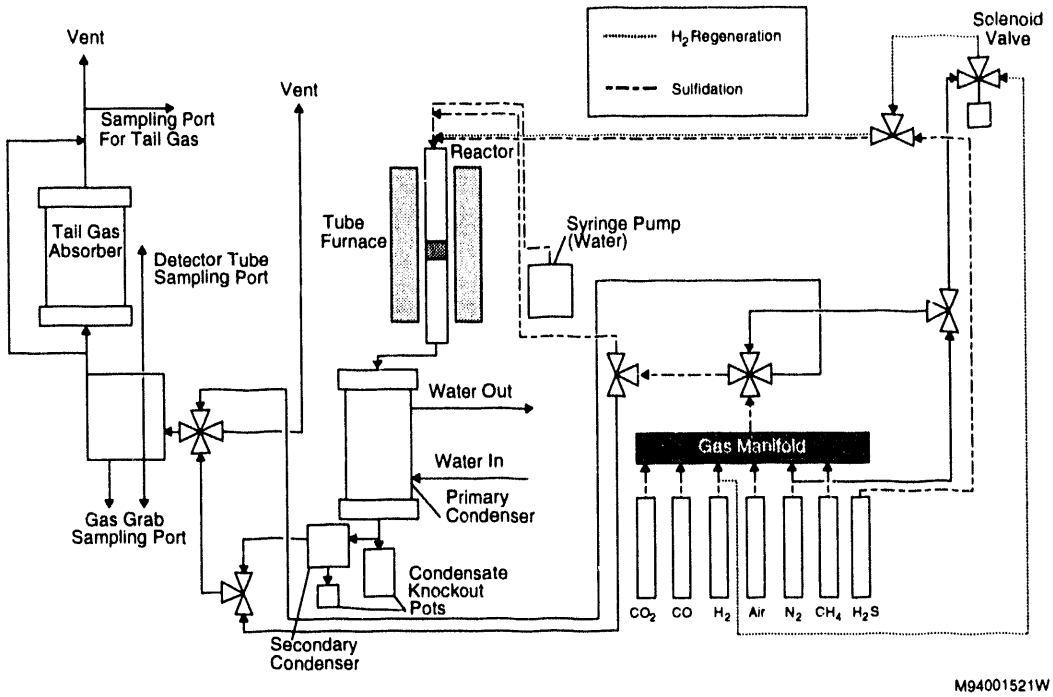

Figure 1. One-Inch Sorbent Screening Unit

(2 in). Gases were supplied from gas cylinders, and the flow rates were controlled through MKS mass flow controllers. All of the gases except hydrogen sulfide were first mixed together in a manifold prior to being fed into the reactor. Hydrogen sulfide gas was added to the other gases separately just upstream of the reactor inlet. Steam was provided by adding a predetermined amount of water into the preheated gas stream via an Isco model 100DM syringe pump. Both sulfidation and regeneration were conducted in the downflow mode. A heavy metal shield and a hydrogen flame detector with automatic reactive gas shutoff were installed for the protection of the operators from possible flames or explosions due to hydrogen leaks. The reactor temperature was maintained with a single-zone tubular electric furnace. The temperatures of the gases flowing into the bed and at the core of the bed (3.8 cm [1.5 in] from the bottom of the bed) were measured using type K thermocouples. The maximum allowable temperature of the reactor was 927°C (1700°F), which precluded doing the regeneration at higher and possibly kinetically more favorable temperatures. A preheat coil consisting of a 0.635-cm (0.25-in) outside diameter, 0.089-cm (0.035-in) wall thickness 316 stainless steel tube placed between the reactor and the furnace was used to preheat all inlet components, except for hydrogen sulfide and water, during the first two and a half cycles of sulfidation/regeneration. (A cycle is defined as one complete sulfidation followed by a complete regeneration of the sorbent.) This preheat coil was removed, and gases were heated to the required temperatures while passing through the top portion of the reactor tube during all subsequent experiments.

Experimental Procedure

Before the first sulfidation could be performed, the sorbent was pretreated to reduce the NiO to Ni metal. A 3-hour pretreatment with pure hydrogen was conducted at 871°C (1600°F) at the beginning of each series of cycles. A simulated Shell oxygen-blown entrained gasifier mixture was used as the sulfidation gas, and pure hydrogen was used as the regeneration gas. The Shell gas was chosen because it is the most likely to be applicable to this sorbent; clean fuel gas of this type could potentially be used instead of hydrogen for regeneration. The inlet gas compositions and other reaction conditions for sulfidation and regeneration are given in Table 1. Each sulfidation of the sorbent was stopped when the outlet concentration of H_2S reached 1000 ppmv. The regenerations were stopped when the outlet concentration of H_2S was less than or equal to 200 ppmv. The outlet stream was tested for hydrogen sulfide by the use of Sensidyne gas detector tubes of various ranges and gas grab samples, which were analyzed using gas chromatography.

A first series of six and a half cycles (designated JS1 experiments) were performed on the sorbent; afterward, the sorbent was removed from the reactor and sent for analysis. Blank runs on the empty reactor were conducted before and after the six and a half cycles of JS1 were performed; the blank runs consisted of two complete cycles of sulfidation/regeneration in each case. The reactor tube was replaced, and a second series of cycles were performed. The second series consisted of three and a half cycles (designated JS2 experiments). Two complete cycles of blank runs were conducted on the empty reactor just prior to performing the JS2 experiments.

The main difference between the JS1 and the JS2 series was that a preheat coil was located upstream of the reactor for the first two and a half cycles of the JS1 series. However, the preheat coil was removed after two and a half cycles and not replaced during the remaining experiments. The reason for removing it was that extensive carbon deposition in it caused a significant increase in pressure drop. It was thought that the carbon deposition occurred because, although the unalonized preheat coil had been passivated with nitric acid, it catalyzed the reaction in which carbon monoxide disproportionated to form carbon dioxide and carbon solids.

RESULTS

The H_2S breakthrough curves for the JS1 and JS2 series experiments are shown in Figures 2 and 3, respectively. It appears that the sorbent increased in capacity with each successive cycle, as evidenced by the longer times required for breakthrough. (Breakthrough is defined here as the point at which the concentration of H_2S in the outlet gas reaches 200 ppmv.) After the first three cycles of series JS1, and the first two cycles of JS2, the prebreakthrough concentration of H_2S in the outlet gas plateaued between 50 and 100 ppmv, with a gradual drift above these values as the sorbent approached breakthrough.

Since pure hydrogen was used as the regeneration gas, H_2S was released during regeneration. The regeneration curves showing H_2S outlet concentration as a function of time on-stream are shown in Figures 4 and 5 for the JS1 and JS2 series experiments, respectively. Note that the time required for regeneration increased during the first three cycles and then tended to stabilize. Regeneration took significantly more time than the corresponding sulfidation of the same cycle. Typically, the duration of each regeneration was more than six times that of the previous sulfidation.

Table 1. Reaction Conditions

Regeneration	Sulfidation
871°C (1600°F)	704°C (1300°F)
205 kPa (15 psig)	205 kPa (15 psig)
320 cc/min or 1000 1/hr	639 cc/min or 2000 1/hr
Regeneration Gas	Gas Mixture (Volume %)
Hydrogen 100.0%	Carbon Monoxide 64.1
End at 200 ppmv H_2S in Outlet	Hydrogen Sulfide 0.3
	Nitrogen 4.3
	Hydrogen 27.3
	Water 2.0
	Carbon Dioxide 2.0
	End at 1000 ppmv H_2S in Outlet

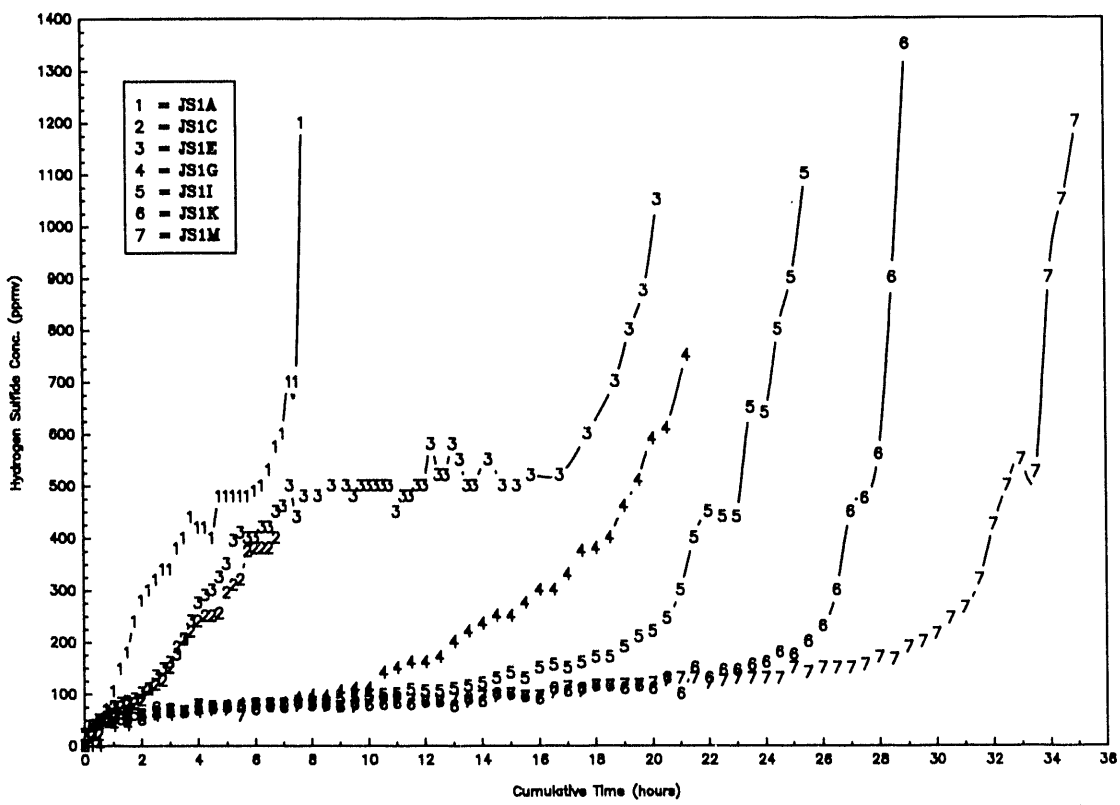

Figure 2. JS1 Sulfidation of 24Ni - 7Cu - Al_2O_3 at 704°C (1300°F)

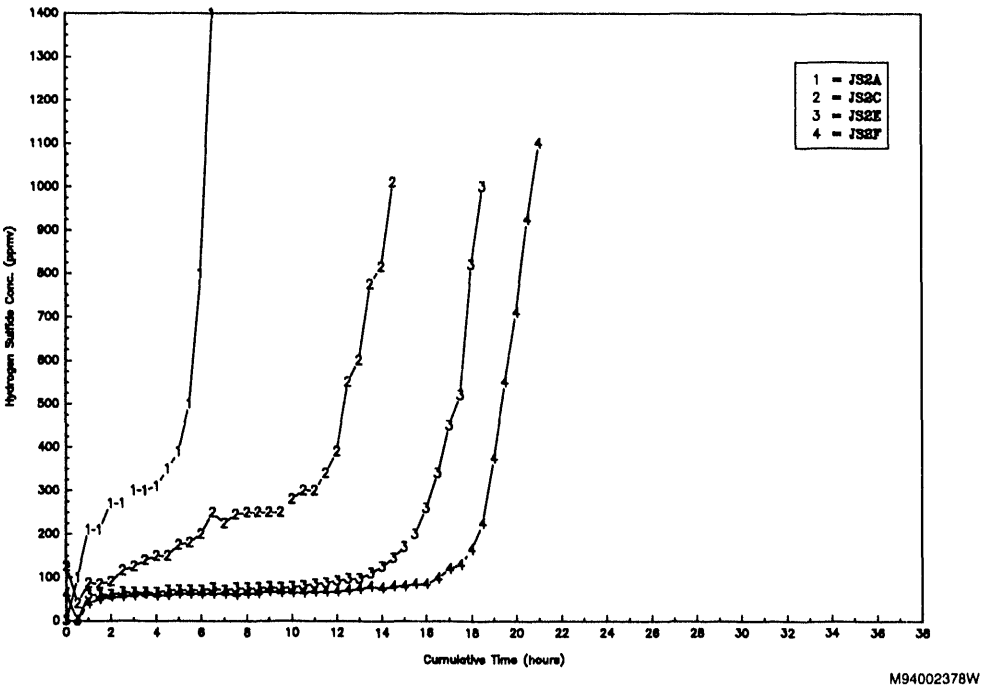

Figure 3. JS2 Sulfidation of 24Ni - 7Cu - Al_2O_3 at 704°C (1300°F)

Fig. 4 JS1 Regeneration of 24Ni - 7Cu - Al_2O_3 at 871°C (1600°F)

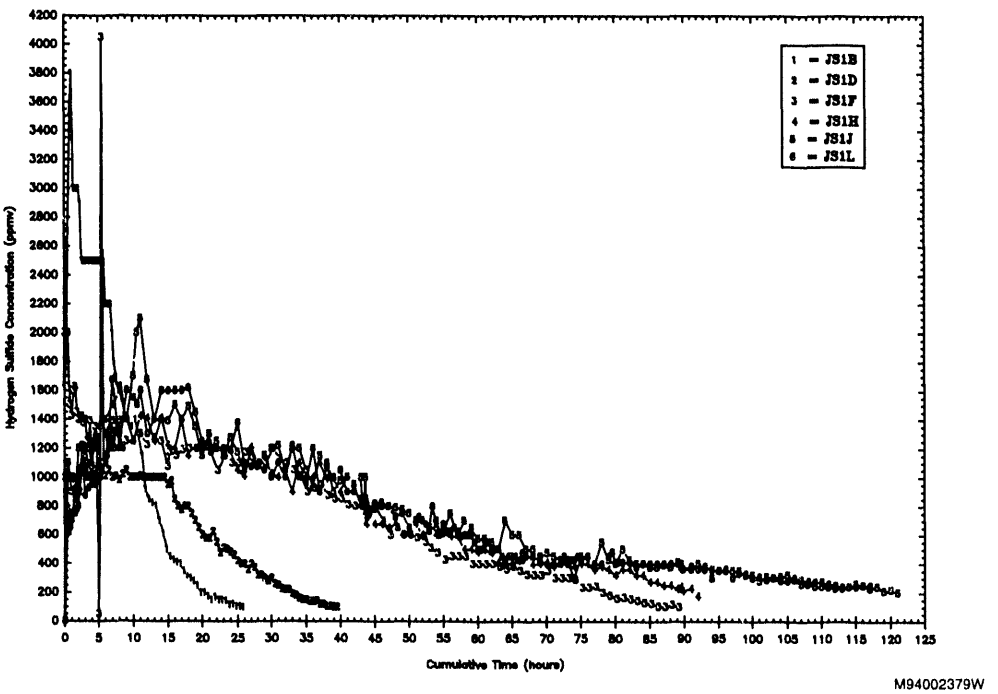

Figure 4. JS1 Regeneration of 24Ni - 7Cu - Al_2O_3 at 871°C (1600°F)

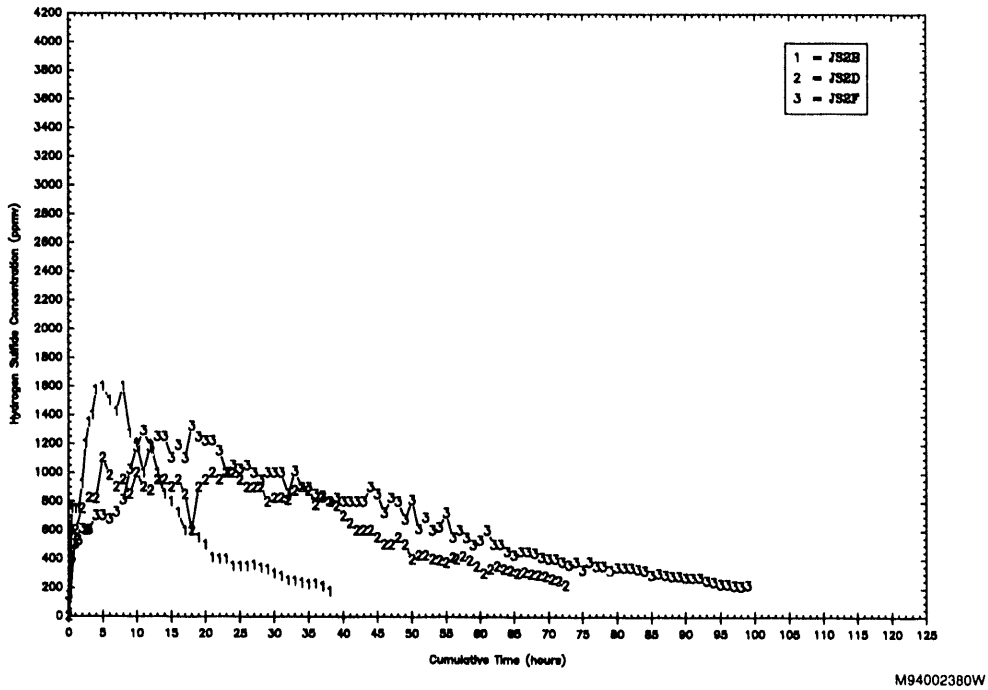

Figure 5. JS2 Regeneration of 24Ni - 7Cu - Al_2O_3 at 871°C (1600°F)

Figure 6 shows the H_2S breakthrough curves for the blank runs (empty reactor tests), which were conducted before and after the JS1 experiments and on the new reactor before the JS2 experiments. Breakthrough time on the empty reactor was significantly longer for runs conducted at the end of the test than those conducted at the beginning. However, the blank runs conducted at the end of the JS1 series had a much shorter breakthrough time than the 7th sulfidation, which was performed just prior to these, indicating that the sorbent had indeed increased remarkably in capacity.

Both the H_2S breakthrough curves and the regeneration curves shown in Figures 2 through 6 were determined using Sensidyne detector tubes. Gas chromatographic analysis of the reactor outlet gas, collected downstream from the condenser units during sulfidations, showed the dry basis volume concentrations of all the major gaseous components, in addition to H_2S, SO_2, and COS. Small amounts of methane (CH_4) were formed, resulting in a concentration that was always less than 0.8%. The SO_2 concentration usually stayed below 5 ppmv, with a few excursions to higher values during some of the sulfidations, after several hours on-stream. The concentrations of CO, CO_2, and H_2 indicated that little, if any, water-gas shift occurred. The COS concentration usually remained below 100 ppmv, and tended to increase during each experiment, as H_2S increased toward breakthrough.

The chemical compositions of the fresh sorbent and the sorbent reacted for six and a half cycles (JS1 series) are shown in Table 2. The atomic absorption analysis was run twice on both the fresh and spent sorbents to recheck the

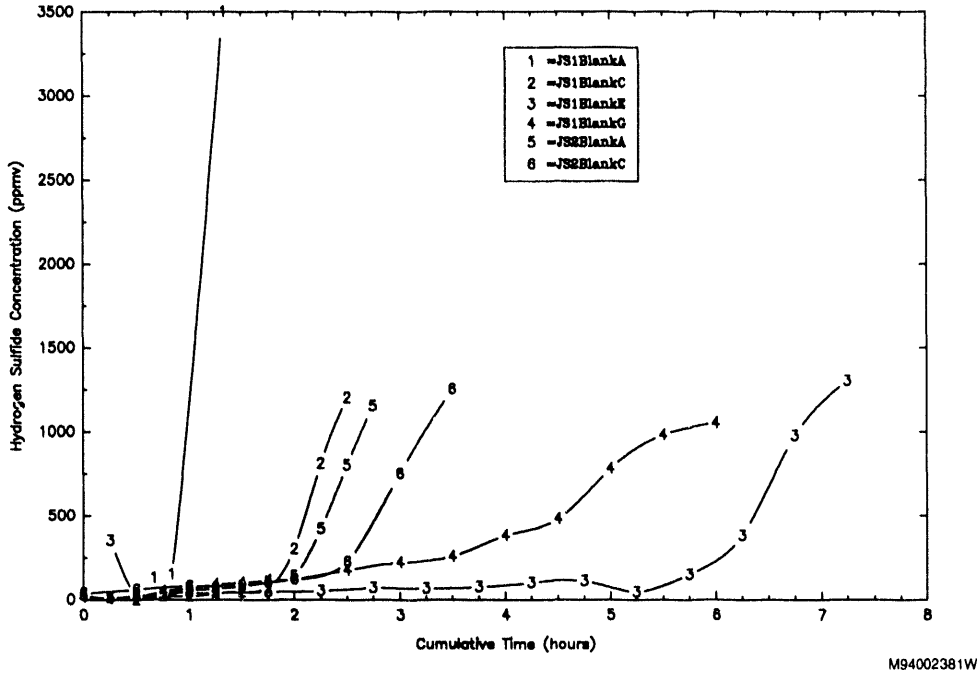

Figure 6. Blank Runs of 24Ni - 7Cu - Al_2O_3 at 704°C (1300°F)

Table 2. Chemical Compositions of Fresh and Reacted Sorbent

Element	Fresh (wt %)	Reacted (wt %)
Aluminum	28.10	28.60
Nickel	23.60	15.80
Copper	3.75	3.90
Total Sulfur	0.08	6.63

Ni content, resulting in exactly the same results for each. The analysis of Ni in the fresh sorbent also agreed quite well with the amount of Ni that was put into the sorbent during preparation (i.e., 24.0 wt % Ni was added during preparation, and the analysis showed 23.6 wt % Ni).

Calculations from the atomic absorption analysis of Al, Ni, and Cu were made assuming that the total amount of Al in the sorbent remained constant during the six and a half cycles. The calculations showed a 32% loss of Ni after the six and a half cycles; however, there was no loss of Cu. The sulfided sorbent contained 6.63 wt % sulfur. If it is assumed that each three Ni atoms can react with two S atoms to form Ni_3S_2 (although there are many different stoichiometric forms of Ni_xS_y possible[1]), and two Cu atoms react with one S atom to form Cu_2S, then the theoretical capacity of the sorbent is 9.54 g S/100 g fresh sorbent. Assuming the Al content of the sorbent to be constant, the actual sulfur content of the sorbent was 6.75 g S/100 g fresh sorbent, or 70.7% of theoretical capacity.

It should be noted that there is some question as to how the breakthrough time increased with each cycle, while there was simultaneously a loss of Ni from the sorbent. For example, fairly extensive redistribution of the remaining Ni would have to take place during hydrogen regeneration to compensate for this apparent volatilization loss of Ni.

Table 3 shows the physical characteristics of the fresh sorbent and the sorbent reacted for six and a half cycles (JS1 series). The mercury skeletal density, particle density, and cumulative pore volume remained essentially constant. However, the nitrogen pore volume increased seven-fold, and the BET nitrogen surface area increased 33-fold. The average pore diameter decreased to 28 percent of its original value. Porosity increased very little, if at all.

Electron micrographs of cross sections of the fresh and JS1 reacted sorbents are shown in Figure 7(a) and Figure 7(b), respectively. The sorbent appeared to be more uniform and more dispersed after reaction for six and a half cycles.

There was a concern about the possibility that some hydrogen embrittlement of the stainless steel reactor may have occurred, particularly during regeneration. Hydrogen embrittlement occurs when H_2 diffuses into the metal lattice and reacts with C in the metal to form CH_4. Cracks are formed as the CH_4 escapes. To determine whether this may have occurred, the reactor used during the JS1 series experiments was cut open length-wise, and electron micrographs were taken of the inner reactor wall. Microcracks and pitting were indeed observed on this inner surface of the reactor wall.

DISCUSSION

The 24Ni-7Cu-Al_2O_3 sorbent was unusual, compared to zinc-based and other sorbents, in that it increased in capacity with each successive cycle. The breakthrough curve performance of most sorbents tend to either stabilize after about three cycles, or gradually deteriorate with successive cycles. The physical characteristics of the fresh and reacted sorbent indicate that there was a large increase in surface area and in the number of small pores. This may have occurred through redistribution of the Ni and Cu to finer dispersions during each hydrogen regeneration.

The blank runs conducted on the empty reactor before and after the JS1 series experiments showed that there was increased sulfur sorption by the apparatus. Two possible explanations follow. Since there was an apparent large loss of Ni through volatilization from the sorbent, Ni may have been deposited on the walls of the reactor or downstream tubing, where it might have reacted with H_2S, resulting in a longer breakthrough time for the empty reactor. Electron micrographs suggested that hydrogen embrittlement of the reactor walls may also have occurred, resulting in microcracks which could penetrate the alonized surface, creating additional surface area for S sorption. However, it should be noted that the increase in breakthrough time on the empty reactor was small compared to the increase in breakthrough time between the first and seventh sulfidations. Therefore, the largest part of the increase in apparent sorbent capacity was due to changes in the sorbent itself. Corrective actions for the problem of hydrogen embrittlement could include the use of a reactor made of ceramic material, quartz, or an alloy with a very low C content.

Table 3. Physical Characteristics of Fresh and Reacted Sorbent

Item	Fresh	Reacted
N_2 Pore Volume (cc/g)	0.006354	0.04684
Hg Skeletal Density (g/ml)	4.16	4.20
Hg Bulk Density (g/ml)	2.38	2.37
Cum. Hg Pore Vol. (ml/g)	0.18	0.19
Surface Area (m^2/g)	0.0963	3.21
Avg. Pore Diameter (μm)	0.5858	0.1622
Porosity (%)	42.79	43.76

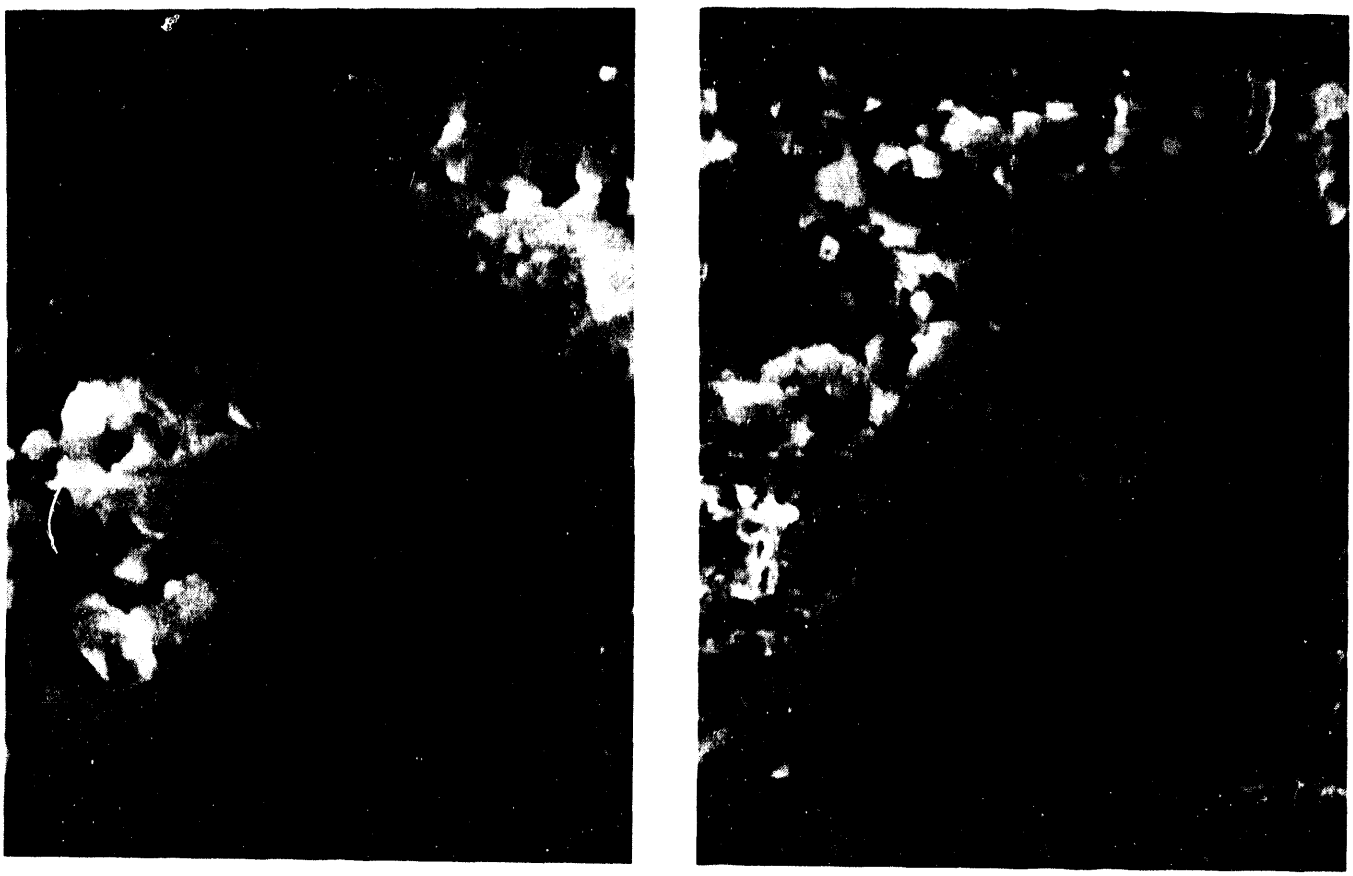

7a. Fresh **7b. After Six and a Half Cycles**

Figure 7. 24 Ni - 7Cu - Al_2O_3 Sorbent Magnified 3,000 Times

The prebreakthrough concentration of H_2S in the outlet gas was higher than expected. Patel, Rich, and Maru[15] had observed a reduction in S species concentration from 10 ppmv to 20 ppbv; in that case, a typical commercial Ni catalyst, 20 wt % Ni on Al_2O_3, was used for H_2S removal from a simulated coal gas. However, in the present study, the higher levels of inlet H_2S concentration apparently caused the reactive surface sites to become rapidly occupied by sulfur, after which bulk sulfidation took place.

Sulfides that form in commonly studied sorbents, such as zinc ferrite and zinc titanate, are solids at their hot gas desulfurization reaction temperatures. However, nickel sulfide became a liquid at the reaction conditions studied here. Since liquids tend to have higher vapor pressures than solids, it might be expected that the liquid nickel sulfide could give rise to vapors which could then be swept away by the simulated coal gas.

Long regeneration times were required by the sorbent (usually at least six times as long as the respective sulfidation breakthrough time, and as much as 22 times longer). If it is assumed that the species to be regenerated were Ni_3S_2 and Cu_2S, 70.7% of theoretical capacity of the sorbent had been reached (9.54 g sulfur/100 g fresh sorbent), and the shortest regeneration time observed is considered (i.e., from the first cycle of the JS1 series), then 310 gmoles of H_2 were required to remove each gmole of S from the sorbent. This makes the sorbent impractical for commercial use in a fixed-bed mode under these conditions, since at least as many reactors as the greatest number of times the length of regeneration was greater than its respective sulfidation would be required. Also, large volumes of reducing gas would be required for regeneration. However, it should be noted that Jhunjhunwala[1] showed in TGA experiments that when sulfidation was carried out at 700°C and regeneration at 950°C on the same type of sorbent, the regeneration time was slightly less than the time required for sulfidation. Unfortunately, the fixed-bed unit used in the present studies could not be operated at temperatures greater than 871°C.

FUTURE WORK

Since the presence of copper tends to reduce the temperature at which liquid nickel sulfides form, a Ni/Al_2O_3 without copper will be studied. Also, a lower reaction temperature will be used (593°C [1100°F] instead of 704°C [1300°F]); hopefully, this will help avoid nickel loss through volatilization. Since the time required for hydrogen regeneration was unacceptably long, oxidative regeneration will be attempted and directly compared with hydrogen regeneration.

ACKNOWLEDGMENTS

The authors would like to gratefully acknowledge the work performed by the METC operators of the bench-scale, fixed-bed reactor, which was used for these studies. Many 12-hour shifts were conducted by Lanny Golden, Todd Gardner, Ed Fisher, Grover Evans, Gary McDaniel, and Karl Warnick to make collection of this data possible.

This research was supported in part by an appointment to the U.S. Department of Energy Fossil Energy Postgraduate Research Training Program, administered by the Oak Ridge Institute for Science and Education.

REFERENCES

1. Jhunjhunwala, M., "Evaluation of Dispersed Nickel Sorbents for Hot Gas Desulfurization," Masters Thesis, Department of Mechanical Engineering and Energy Processes, Southern Illinois University at Carbondale, July, 1993.

2. Swisher, J. H., and Schwerdtfeger, K., "Review of Metals and Binary Oxides as Sorbents for Removing Sulfur from Coal-Derived Gases," *J. Mat. Eng. and Perf.*, *1*(3), 1992, 399-407.

3. Swisher, J. H., and Schwerdtfeger, K., "Thermodynamic Analysis of Sorption Reactions for the Removal of Sulfur from Hot Gases," *J. Mat. Eng. and Perf.*, *1*(4), 1992, 565-571.

4. Grindley, T. and Steinfeld, G., "Development and Testing of Regenerable Hot Coal-Gas Desulfurization Sorbent," Report No. DOE/METC-16545-1125, Morgantown Energy Technology Center, Morgantown, WV, 1981.

5. Mei, J. S., Gasper-Galvin, L. D., Everitt, C. E., and Katta, S., "Fixed-Bed Testing of a Molybdenum-Promoted Zinc Titanate Sorbent for Hot Gas Desulfurization," *Proceedings of the Coal-Fired Power Systems 93--Advances in IGCC and PFBC Review Mtg.*, D. L. Bonk, ed., DOE/METC-93/6131, Springfield, Va.: National Technical Information Service, 1993, 315-325.

6. Ayala, R. E., Gal, E., and Gupta, R. P., "Testing of Zinc Titanate Desulfurization Sorbents for Moving Bed Applications," Ibid., 136-145.

7. Gangwal, S. K., and Gupta, R. P., "Enhanced Durability of Desulfurization Sorbents for Fluidized-Bed Application," Ibid., 146-157.

8. Swisher, J. H., "An Attrition-Resistant Zinc Titanate Sorbent for Sulfur," Final Technical Report submitted to the Illinois Clean Coal Institute, Carterville, Illinois, Sept. 1993.

9. Swisher, J. H., O'Brien, W. S., and Gupta, R. P., "An Attrition-Resistant Zinc Titanate Sorbent for Sulfur," Quarterly Technical Reports submitted to the Illinois Clean Coal Institute, Carterville, IL, Dec. 1993 and Mar. 1994.

10. Gupta, R. P., Gangwal, S. K., and Jain, S. C., "Fluidizable Zinc Titanate Materials with High Chemical Reactivity and Attrition Resistance," U. S. Patent No. 5,254,516, Awarded to Research Triangle Institute, Research Triangle Park, NC, 1993.

11. Nagamori, M., and Ingram, T. R., "Thermodynamic Properties of Ni-S Melts Between 700° and 1100°C," *Met. Trans.*, *1*, 1970, pp. 1821-1825.

12. Rosenquist, T., "A Thermodynamic Study of the Iron, Cobalt, and Nickel Sulphides," *J. Iron and Steel Inst.*, *175*, 1954, 37-57.

13. Elliott, R. P., *Constitution of Binary Alloys, First Supplement*, McGraw-Hill, New York, 1965, 669.

14. Steiner, P. and Gutterman, C., "Nickel Sulfide Method for Separating Hydrogen Sulfide," Foster Wheeler Energy Corp., Clinton, NJ, German Patent No. DE 29 03 377 Al, 1979 (in German).

15. Patel, P. S., Rich, S. M., and Maru, H. C., "Trace Contaminant Removal from Hot Coal Gas for Molten Carbonate Fuel Cell Applications," *Proceedings of the Fifth Annual Contractors Meeting on Contaminant Control in Coal-Derived Gas Streams*, D. C. Cicero and K. E. Markel, eds., DOE/METC-85/6025, Springfield, Va.: National Technical Information Service, 1986, 419-424.

16. Swisher, J. H., and Schwerdtfeger, K., "The Behavior of Sulfur Sorbents Containing Dispersed Nickel," *Proc. 9th Annual Int. Pittsburgh Coal Conf.*, 1991, 646-653, Available from Conference Services, P.O. Box 270, Greensburg, Pennsylvania 15601.

17. Boldt, J. R., *The Winning of Nickel*, Methuen and Co., Ltd., London, UK, 1967, 275-280.

18. Sproule, K., Harcourt, G. A., and Renzoni, L. S., "Treatment of Nickel-Copper Matte," in *Extractive Metallurgy of Copper, Nickel, and Cobalt*, P. Queneau, ed., Interscience Publ., New York, New York, 1961, 33-52.

LGASPE\1:940851

P3 Pilot Gasification and Hot Gas Cleanup Operations

John M. Rockey, Edwin Galloway, and Teresa A. Thomson
Morgantown Energy Technology Center

Jay Rutten and Alain Lui
EG&G Technical Services of West Virginia

ABSTRACT

The Morgantown Energy Technology Center (METC) has an integrated gasification hot gas cleanup facility to develop gasification, hot particulate and desulfurization process performance data for IGCC systems.

The objective of our program is to develop fluidized-bed process performance data for hot gas desulfurization and to further test promising sorbents from lab-scale screening studies at high-pressure (300 psia), and temperatures (1,200°F) using coal-derived fuel gases from a fluid-bed gasifier.

The 10-inch inside diameter (ID), nominal 80 lb/hr, air blown gasifier is capable of providing about 300 lb/hr of low BTU gas at 1,000°F and 425 psig to downstream cleanup devices. The system includes several particle removal stages, which provide the capability to tailor the particle loading to the cleanup section.

The cleanup test section consists of a closely coupled modular gas cleanup rig (MGCR) which was acquired from The Institute of Gas Technology.

The MGCR receives coal-derived gas at 425 psig and 1,000°F from the METC Fluid-Bed Gasifier. The gas pressure is reduced to approximately 300 psia and filtered by a candle filter vessel containing up to four filter cartridges. For batch-mode desulfurization test operations, the filtered coal gas is fed to a 6-inch ID, fluid-bed reactor that is preloaded with desulfurization sorbent.

Over 400 hours of gasifier operation was logged in 1993 including 384 hours of integration with the cleanup rig. System baseline studies without desulfurization sorbent and repeatability checks with zinc ferrite sorbent were conducted before testing with the then most advanced zinc titanate sorbents, ZT-002 and ZR-005.

In addition to the desulfurization testing, candle filters were tested for the duration of the 384 hours of integrated operation. One filter was taken out of service after 254 hours of filtering while another was left in service. At the conclusion of testing this year it is expected that 3 candles, one each with 254, 530, and 784 hours of filtering will be available for analysis for effects of the exposure to the coal gas environment.

P4

Coal Ash Behavior in Reducing Environments

CONTRACT INFORMATION

Contract Number DE-FC21-86MC10637

Contractor

Energy & Environmental Research Center
University of North Dakota
PO Box 9018
Grand Forks, ND 58202-9018
(701) 777-5000

Contract Project Manager Steven A. Benson

Principal Investigators

Thomas A. Erickson
David W. Brekke
Bruce C. Folkedahl
James E. Tibbetts
Jan W. Nowok

METC Project Manager Venkat K. Venkatarman

Period of Performance November 1, 1990, to October 31, 1994

Schedule and Milestones

FY94 Program Schedule

	N	D	J	F	M	A	M	J	J	A	S	O
Task 1												
Task 2												
Task 3												

OBJECTIVES

The objective of the Coal Ash Behavior in Reducing Environments (CABRE) program is to advance the knowledge of ash behavior in coal gasification systems; this knowledge will help provide the understanding necessary to operate advanced coal utilization systems efficiently with a minimum of the operational problems associated with ash properties. The program approach is to use carefully controlled, laboratory-scale experiments coupled with detailed analysis of the materials involved to determine the critical fundamental mechanisms of ash behavior in coal gasification systems.

BACKGROUND INFORMATION

A key factor in the successful design and operation of coal gasification systems is the ability to control and mitigate ash-related problems. Some of the major ash-related problems are slag flow control, slag attack on the refractory, ash deposition on heat-transfer surfaces, corrosion and erosion of equipment and materials, and emissions control. Such problems are closely tied to the abundance and association of inorganic components in coal and gasification conditions.

In general, the inorganic components are associated in the coal as minerals or organic complexes (salts of carboxylic acid groups or organic coordination complexes). The minerals associated in coal vary widely in size, composition, and juxtaposition. Juxtaposition refers to the association of mineral grains with other mineral grains and coal particles. These associations directly influence the chemical and physical transformations that occur during the gasification process. Depending upon the type of gasification system, inorganic components are initially partitioned into intermediate species in the form of inorganic gases, liquids, and solids. The state of these species at any given stage or position in the gasifier directly influences their behavior at that stage. The transformations and partitioning of inorganic species directly influence slag behavior, extent and type of slag attack on the refractory, and corrosion and erosion of materials, as well as growth rate, quantity, and type of ash deposition on heat-transfer surfaces.

PROJECT DESCRIPTION

The CABRE project is a four-year program designed to investigate the transformations and properties of coal ash in reducing environment systems. This project is currently midway through its third year. The work to date has emphasized four areas of research: 1) the development of quantitative techniques to analyze reduced species, 2) the production of gasification-type samples under closely controlled conditions, 3) the systematic gasification of specific coals to produce information about their partitioning during gasification, and 4) the study of the physical properties of ashes and slags under reducing atmospheres.

The CABRE project is organized into three tasks which provide a strong foundation for the project. Task 1, Analytical Methods Development, has concentrated on the special needs of analyzing samples produced under a reducing atmosphere as opposed to the more often studied combustion systems. Task 2, Inorganic Partitioning and Ash Deposition, has focused on the production of gasification-type samples under closely controlled conditions for the study of inorganic partitioning that may lead to deposition. Task 3, Ash and Slag Physical Properties, has made large gains in the areas of sintering and strength development of coal ashes under reducing atmospheres for the evaluation of deposition problems.

RESULTS

Task 1 - Analytical Methods Development

The scanning electron microscope (SEM) technique most commonly used at the Energy & Environmental Research Center (EERC) to characterize deposits is the scanning electron microscopy point count (SEMPC) technique (Steadman and others, 1990), Figure 1. This technique was developed at the EERC to

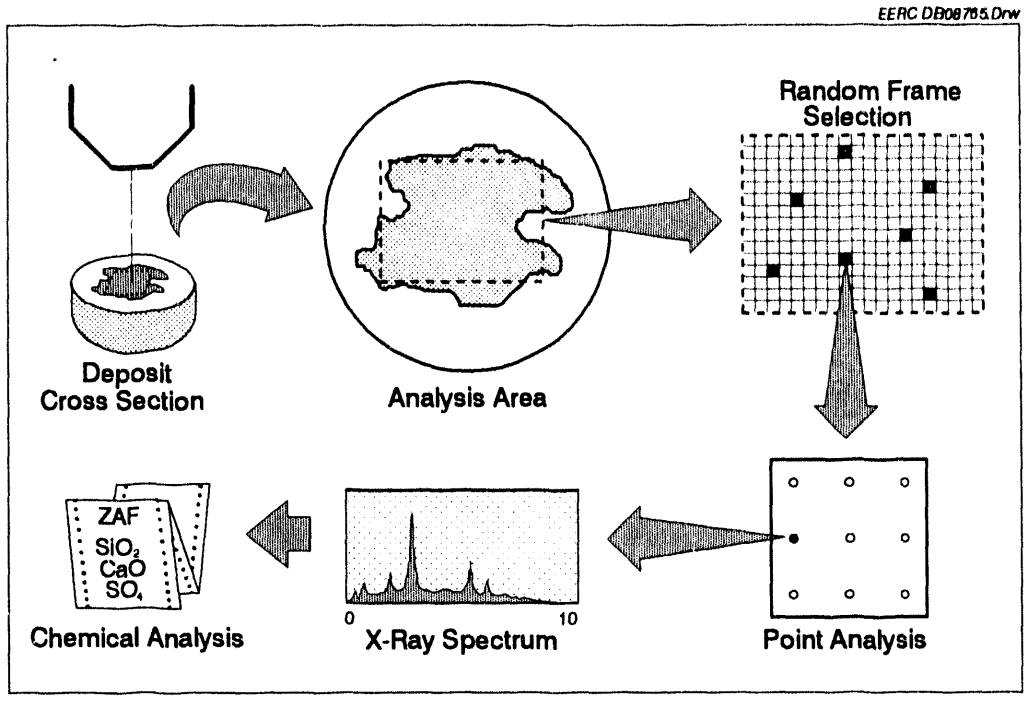

Figure 1. Scanning Electron Microscope Point Count Analysis Routine

quantitatively determine the relative amounts of the phases present in entrained ashes and deposits. The method involves microprobe analysis (for chemical compositions) of a large number of random points on a polished cross section of a sample. A data manipulation program then classifies each chemical composition into a phase category based on various weight and molar ratios. The criteria for the classification procedure have been developed from the stoichiometry of the various phases.

The most important addition to this technique from the CABRE project was the qualitative examination of carbon and oxygen during analysis. Carbon and oxygen are two of the more important chemical components in reducing environments. A rapid and accurate analysis of these elements concurrent with the analyses of other elements in an energy-dispersive x-ray spectrometer system is very advantageous. However, due to the complexity of the samples analyzed in this project, problems arise which hinder the quantification of carbon and oxygen. The samples vary widely in composition and, therefore, do not present a consistent background matrix to the correction routines. All samples must be carbon-coated to maintain conductivity under the electron beam. The best result that can be attained under these conditions is a qualitative/semiquantitative determination of carbon and oxygen. The advances made concerning carbon and oxygen determinations have been previously documented (Erickson and Others, 1993)

In conjunction with the SEMPC technique, three data manipulation programs were created to manipulate the data and present them in their best format: MINCLASS© for Microsoft® MS-DOS® (DOS), MINCLASS© for Microsoft® Windows™ (Windows), and VISCALC© for DOS. Each of these codes are discussed below.

MINCLASS©

The phase classification program, MINCLASS© 4.0, has been revised to incorporate advances in hardware and increased knowledge about the analytical demands of the CABRE project. Improvements include modifying the classification algorithms to incorporate quantified oxygen values, which allows any element to be included in the analysis, and tabulating the number of points that make up the various chemical composition summaries. These refinements make it easier to analyze SEMPC data from reducing environment samples where reduced phases are difficult to recognize.

A Windows version of MINCLASS© was also made available to those desiring to operate in that environment. This version of the program requires Windows 3.1 as the operating environment. The input file, classification routine, and output files are the same as the DOS version. Either program will produce the same results. Included in the MINCLASS© for Windows interface is the viscosity calculation program VISCALC©. An example of the output from MINCLASS© 4.0 is given in Table 1.

VISCALC©

A silicate liquid-phase viscosity calculation and viscosity distribution program named VISCALC© 4.0 is available to sponsors for the first time. VISCALC© has been used internally on CABRE samples since the beginning of the project. The program uses the chemistry and mineralogy of silicate and aluminosilicate phases determined by the SEMPC technique. Mineralogy is used to determine which phases to include in the viscosity calculations. Chemistry is used as input to a model developed by Kalmanovitch and Frank (1988) to calculate viscosity. The model is based on a modified version of a metallurgical slag viscosity model developed by Urbain and others (1981). Assumptions in the model include the chemistry expressed as oxides, iron expressed in the ferric state, and calculations performed only on silicate and aluminosilicate phases.

In addition to a file of calculated viscosities, the program includes an interactive graphics feature for comparing viscosities. The present version of VISCALC© allows the user to compare the viscosities of a single sample as three temperatures or up to three different samples at a single temperature. If certain silicate phases are known to be crystalline at the input temperatures, VISCALC© permits them to be excluded from the viscosity calculations. It is up to the user to decide which phases are to be excluded. An example of the output from VISCALC© is given in Table 2.

Task 2 - Inorganic Partitioning and Ash Deposition

The production of gasification-type samples under closely controlled conditions has been the primary goal of Task 2 for the duration of this project. A pressurized drop-tube furnace (PDTF) is used to produce the gasification samples. The PDTF can closely control the temperature profile, pressure, atmosphere, and residence time. The use of a small-scale gasifier such as this allows for the fundamental research of coal gasification without a large capital investment for equipment.

Table 1. Example Output from MINCLASS© Software

UND-EERC SEMPC Mineral Classification Version 3.1
Run Date: December 17, 1992, Using Definitions File rules. c

Mineral Name	Frequency Percent	Mineral Name	Frequency Percent
Oxide-Rich		Silicon-Rich	
Magnesium Oxide	0.0	Quartz	25.1
Aluminum Oxide	0.0	Albite	0.3
Calcium Oxide	0.0	Anorthite	0.0
Titanium Oxide	0.0	Potassium Feldspar	0.0
Chromium Oxide	0.0	Nepheline	0.0
Iron Oxide	0.3	Hauyne	0.0
Spinel	0.0	Leucite	0.0
Ca-Ti Oxide	0.0	Kaolinite	8.1
Ca-Al Oxide	0.0	Altered Kaolinite	2.7
Mixed Oxide-Rich	1.0	Illite	0.3
Total for Group	1.4	Montmorillonite	2.7
		Pyroxene	0.0
Sulfur-Rich		Wollastonite	0.0
Pyrite	0.0	Calcium Silicate	0.0
Pyrrhotite	0.0	Di Calcium Silicate	0.0
Iron Sulfate	0.0	$Na\text{-}Ca\text{-}SiO_3$	0.0
Sodium Sulfate	0.0	Gehlenite	0.0
Calcium Sulfate	0.7	Akermanite	0.0
Na-Ca Sulfate	0.0	Merwinite	0.0
Barite	0.3	Spurrite	0.0
Mixed Sulfur-Rich	0.0	Mullite	0.0
Total for Group	1.0	Mixed Silicon-Rich	0.2
		Total for Group	49.5
Phosphorous-Rich			
Apatite	0.0		
Mixed Phosphorous-Rich	0.0	User-Defined List	
Total for Group	0.0	Ettringite	0.3
		Calcium Aluminate	1.0
Carbon-Rich		Total for Group	1.4
Calcite	7.8		
Altered Calcite	0.0		
Dolomite	0.3		
Sulfated Dolomite	0.0	Other	9.5
Ankerite	0.0		
Sulfated Ankerite	0.0		
Mixed Carbon-Rich	8.8		
Total for Group	36.9		

Table 1 (continued)

Mineral Name	Frequency Percent	Mineral Name	Frequency Percent
Metal-Rich			
Aluminum	0.0		
Titanium	0.0		
Iron	0.0		
Nickel	0.0		
Copper	0.0		
Chromium	0.0		
Mixed Metal-Rich	0.3		
Total for Group	0.3		

Total Number of Points Analyzed = 295
Carbon Threshold for Analysis = 2000
Oxygen Threshold for Analysis = 300

Bulk Chemical Composition, oxide wt%

	A	B	C	D	E	F	G
SiO_2	4.9	1.6	62.2	1.5	48.2	55.5	56.0
Al_2O_3	19.5	26.8	20.1	37.4	15.0	17.4	17.9
Fe_2O_3	14.7	5.9	2.4	5.7	4.6	4.0	4.2
TiO_2	2.2	1.7	0.7	0.9	3.1	1.1	1.3
P_2O_5	0.1	0.0	0.2	0.0	0.1	0.1	0.1
CaO	41.5	30.9	5.1	48.7	17.2	12.7	13.4
MgO	13.2	3.9	2.6	5.0	4.2	3.5	3.6
Na_2O	1.9	0.5	4.2	0.4	5.9	3.2	3.3
K_2O	0.1	0.1	0.5	0.0	0.5	0.3	0.3
SO_3	0.5	3.6	0.4	0.3	0.2	0.8	0.0
Cl_2O_7	0.5	0.4	0.8	0.0	0.2	0.5	0.0
Cr_2O_3	0.1	0.0	0.1	0.0	0.1	0.1	0.0
BaO	0.7	24.6	0.6	0.0	0.7	0.9	0.0
Points	26	3	23	1	1	295	295

A Cumulative bulk composition of other.
B Cumulative bulk composition of mixed oxide-rich.
C Cumulative bulk composition of mixed carbon-rich.
D Cumulative bulk composition of mixed metal-rich.
E Cumulative bulk composition of mixed silicon-rich.
F Cumulative bulk composition of the entire sample.
G SO_3-, Cl_2O_7-, Cr_2O_3-, BaO-free composition of the entire sample.

Table 2. Example Output from VISCALC© Software

12345678 Test Sample
Viscosity Data

Index	1100.0	1300.0	1500.0	Temp. at 3.0 Critical Viscosity
1	4.065	2.868	1.948	1275.1
2	2.963	1.995	1.251	1093.6
3	3.606	2.505	1.658	1203.0
4	7.108	5.281	3.873	1652.1
5	3.810	2.666	1.786	1235.5
6	3.066	2.076	1.316	1111.6
7	3.118	2.117	1.349	1120.8
8	5.728	4.187	3.000	1500.1
9	5.578	4.068	2.905	1481.6
10	5.744	4.199	3.010	1501.8
11	3.670	2.555	1.698	1213.6
12	4.009	2.824	1.912	1266.7
13	4.015	2.828	1.916	1267.6
14	5.707	4.170	2.986	1497.4
15	5.839	4.275	3.070	1513.3
16	5.146	3.725	2.631	1427.1
17	5.530	4.030	2.875	1475.9
18	3.416	2.353	1.537	1171.8
19	3.710	2.587	1.723	1219.7
20	4.842	3.484	2.439	1386.7
21	6.153	4.524	3.269	1549.7
22	6.115	4.493	3.244	1545.3
23	10.084	7.640	5.755	1726.8
24	5.266	3.820	2.707	1442.5

Viscosity frequency distribution data:

0-1	1-2	2-3	3-4	4-5	5-6	6-7	7-8	8-9	9-10	10-11	11-12
1500											

Table 2 (continued)

Viscosity frequency distribution data:

0.0	45.8	25.0	25.0	0.0	4.2	0.0	0.0	0.0	0.0	0.0	0.0
1300											
0.0	4.2	41.7	12.5	33.3	4.2	0.0	4.2	0.0	0.0	0.0	0.0
1100											
0.0	0.0	4.2	29.2	16.7	33.3	8.3	4.2	0.0	0.0	4.2	0.0

T_{cv} cumulative % less than frequency data:

<70	80	90	100	110	120	130	140	150	160	170	180	190	>1900
0.0	0.0	0.0	0.0	4.2	16.7	45.8	50.0	70.8	91.7	95.8	100	100	100

The PDTF is a laboratory-scale, vertically oriented, downfired, entrained flow furnace able to perform gasification studies under closely controlled conditions. The PDTF furnace assembly, Figure 2, consists of an upper alumina tube (2.875-in. ID x 55 in. long) and a lower alumina tube (2.875-in. ID x 25 in. long) separated by a flow accelerator. The two vertically oriented tubes are held in position by a slightly larger concentric tube. The tube assembly is heated externally with three high-temperature tube furnaces (four heating zones) equipped with Kanthal Super 33 elements capable of heating the furnace to 1500°C. Each of the heating zones can be controlled separately for temperature profiling. The top two furnaces are used for the gasification zone, while the bottom furnace is used as a deposition and collection zone. The entire reactor, including the heating elements, is housed in a water-jacketed pressure vessel rated at 335 psi.

Fluidized coal, 80% −200 mesh, is introduced into the reactor with a carrier gas (primary gas) through a traversing, water-cooled injector positioned in the center of the tube. The feeding system allows close control of feed rates as low as 0.1 g/min. Optional (secondary) gas enters the reactor at the top of the tube and flows down through the tube around the injector assembly. The coal residue and process gases travel down the reactor tube in a laminar flow regime and pass through the accelerator where they are collected by a water-cooled, nitrogen-quenching ash collection probe or water-cooled deposition probe. Particle residence times can be controlled by inserting or retracting the coal injector into the furnace while the collection device remains fixed. Various collection devices can be attached to the outlet of the collection probe to collect the solids. Size segregation of the ash is facilitated by using a multicyclone or impactor in conjunction with a final filter. A bulk filter is used to collect ash for bulk

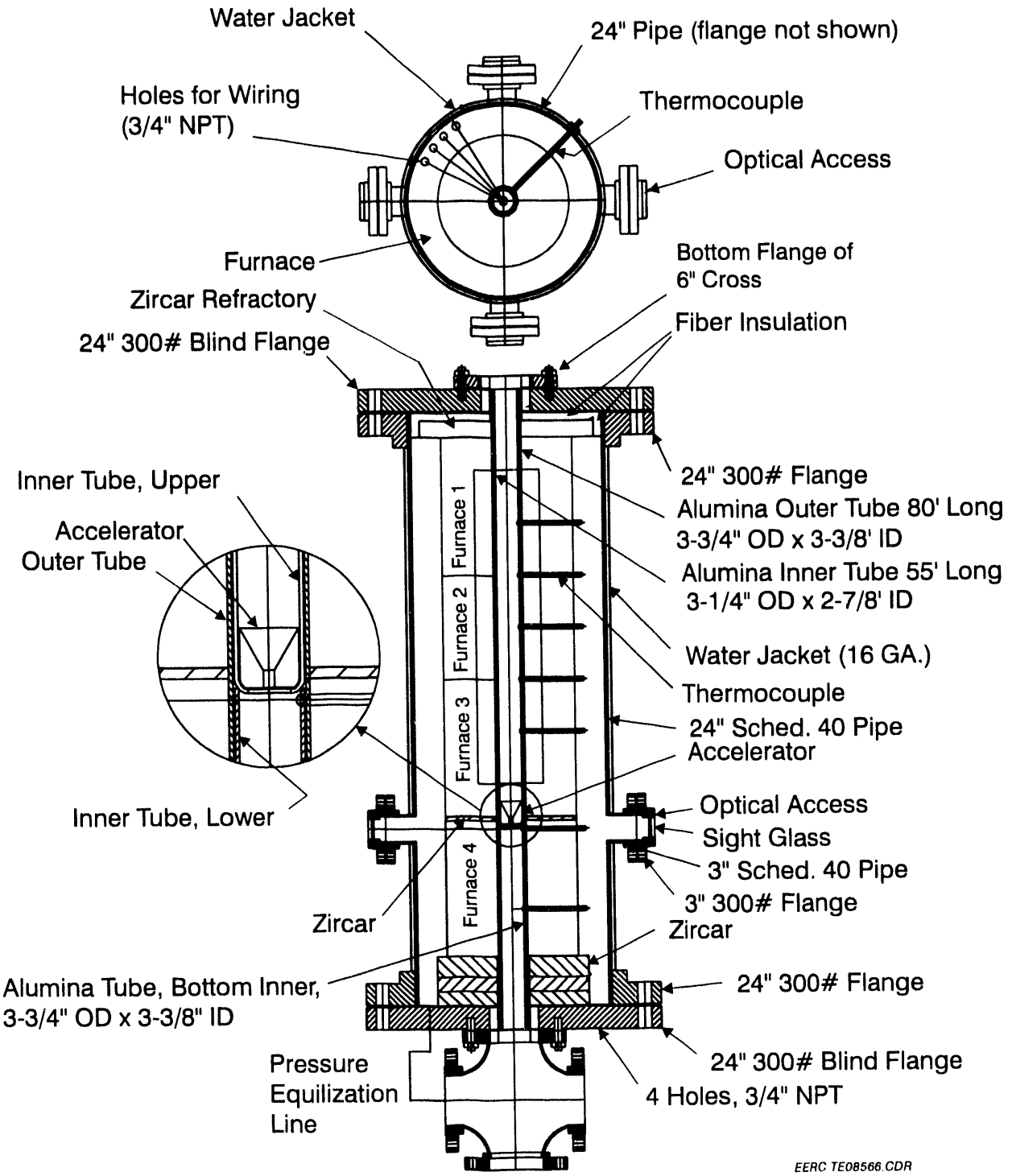

Figure 2. PDTF Assembly

chemistry. The process gases exiting the collection device are monitored on-line by O_2, CO, or CO_2 gas analyzers or off-line by a gas chromatograph (GC).

Deposition tests were conducted over the last twelve months on five coals: Sufco/Hiawatha, Illinois No. 6, Pittsburgh No. 8, Drayton, and Rochelle. These tests were conducted at a gasification temperature of 1500°C and deposition zone temperatures of 1000° and 800°C. The results from these tests are currently being investigated, and replicate runs are being performed for verification.

To enhance the work done in the PDTF, thermochemical equilibrium modeling was done to predict slag flow behavior. Thermochemical equilibrium modeling is an effective method to predict behavior in well-mixed equilibrium systems. Though slag in a gasifier is not an equilibrium mixture, it does approach equilibrium because of its high molten state. PHOEBE©, a thermochemical equilibrium code developed at the EERC, has been used extensively in the past to model high-temperature slags and deposits in combustion systems. With the latest enhancements to its database, it is now capable of modeling gasification systems as well. Three of the coals from the CABRE project have been run through the code at temperatures ranging from 1500° to 3000°F (815° to 1650°C). Both the viscosity and percent of ash as liquid phase were recorded for each temperature and coal.

The chemical compositions used in these predictions come from the original coal analysis (ultimate and x-ray flouresence). It should be noted that the composition of a slag in a real gasifier may be different because of the partitioning of specific species caused by the aerodynamic properties of the reactor. Figures 3-5 show the results of the modeling predictions. Each of the three graphs shows a temperature range at which there is no appreciable amount of liquid phase present, followed by an increase in the liquid phase amount and a decrease in its viscosity. The phases and their corresponding viscosities change as a function of temperature.

Task 3 - Ash and Slag Physical Properties

The third task of the CABRE project has concentrated on the various physical processes that take place in the formation of slags and deposits on various heat-exchange surfaces. The primary emphasis has been on the process of strength development under reducing conditions. The results of this project, along with literature on similar subjects, have pointed to the presence of three different strength development regimes (Figure 6) as defined by the dominant liquid phases: sulfides, sulfided silicates, and silicates. Figure 7 shows the thermal stability of various sulfides as determined under an atmosphere of $H_2S/CO_2/CO$.

Much of the work over the past year has focused on the effects of water vapor on the sintering potential of coal ashes. Three different sulfides were tested in a thermogravimetric analyzer (TGA) with and without the presence of water vapor. The results for $Fe_{1-x}S$, CaS, and Na_2S-1.7FeS are shown in Figures 8, 9, and 10, respectively. The iron sulfide appears to be relatively unaffected by the presence of the water vapor. The stability of the calcium sulfide is shifted to lower temperatures by the presence of water vapor. The Na_2S-1.7FeS system appears to undergo a more complex interaction with the water vapor which

involves the addition of weight to the system. It is possible that some of the sodium sulfide is being replaced with NaOH, which would involve a slight increase in weight.

FUTURE WORK

Over the final half year, the CABRE project will continue to study the transformations of inorganic species into ashes and deposits under reducing atmospheres. The following areas of research will be emphasized over the remainder of the project:

- The study of deposition and strength development mechanisms using the PDTF
- The continued evaluation of the physical properties affecting ashes and deposits which result in high-strength deposits

ACKNOWLEDGMENTS

The Energy & Environmental Research Center would like to thank the sponsors of this project for their desire to continue developing the future of the Fossil Energy Program. The six sponsors are Shell Oil Company, Texaco, DOW Chemical Company, Netherlands Energy Research Foundation the Electric Power Research Institute, and the U.S. Department of Energy.

REFERENCES

Erickson, T.A.; Brekke, D.W.; Folkedahl, B.C.; Tibbetts, J.E.; Nowok, J.W.; Benson, S.A. "Coal Ash Behavior in Reducing Environments," Presented at the Coal-Fired Power Systems 93 — Advances in IGCC and PFBC Contractors' Review Meeting, Morgantown, WV, June 28-30, 1993.

Kalmanovitch, D.P.; Frank, M. "An Effective Model of Viscosity for Ash Deposition Phenomena," Conference on Mineral Matter and Ash Deposition from Coal; The Engineering Foundation, Santa Barbara, CA, February 21-26, 1988.

Steadman, E.N.; Zygarlicke, C.J.; Benson, S.A.; Jones, M.J. "A Microanalytical Approach to the Characterization of Coal, Ash, and Deposits," In Seminar on Fireside Fouling Problems, ASME Research Communication on Corrosion and Deposits from Combustion Gases, Washington D.C., 1990.

Urbain, G.; Cambier, F.; Deletter, M.; Anseau, M.R. *Transitions of the Journal of the German Ceramic Society* **1981**, *80*, 139.

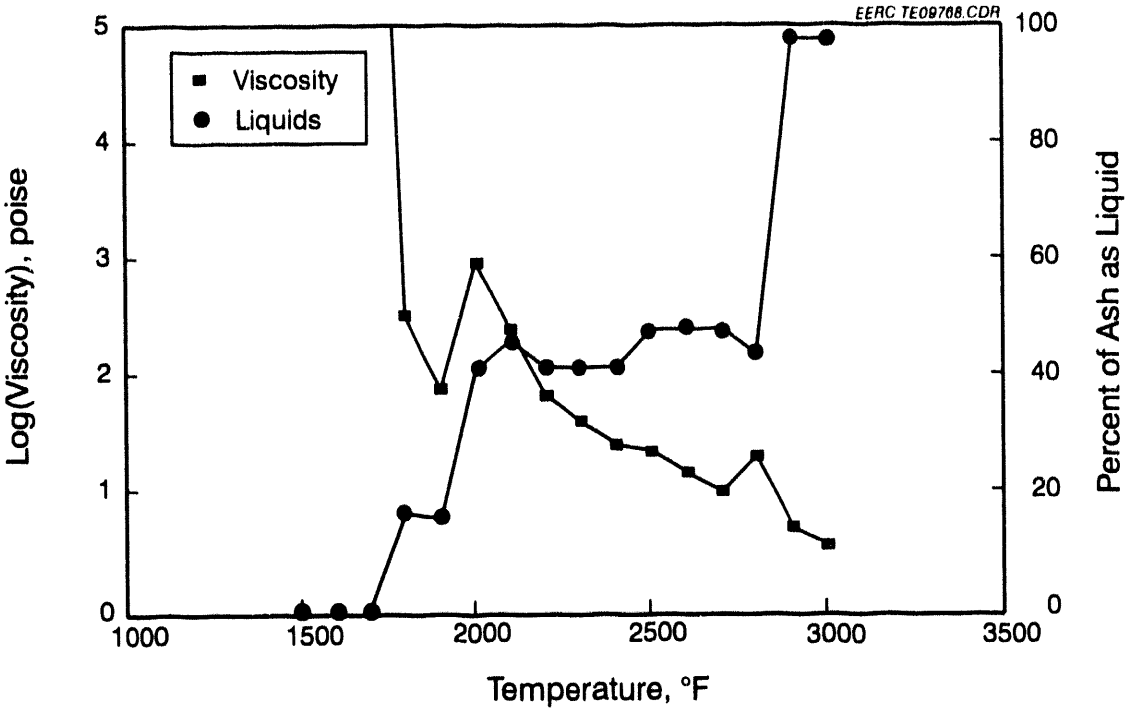

Figure 3. Thermochemical Equilibrium Modeling of a Slag Formed from the Gasification of Coal A

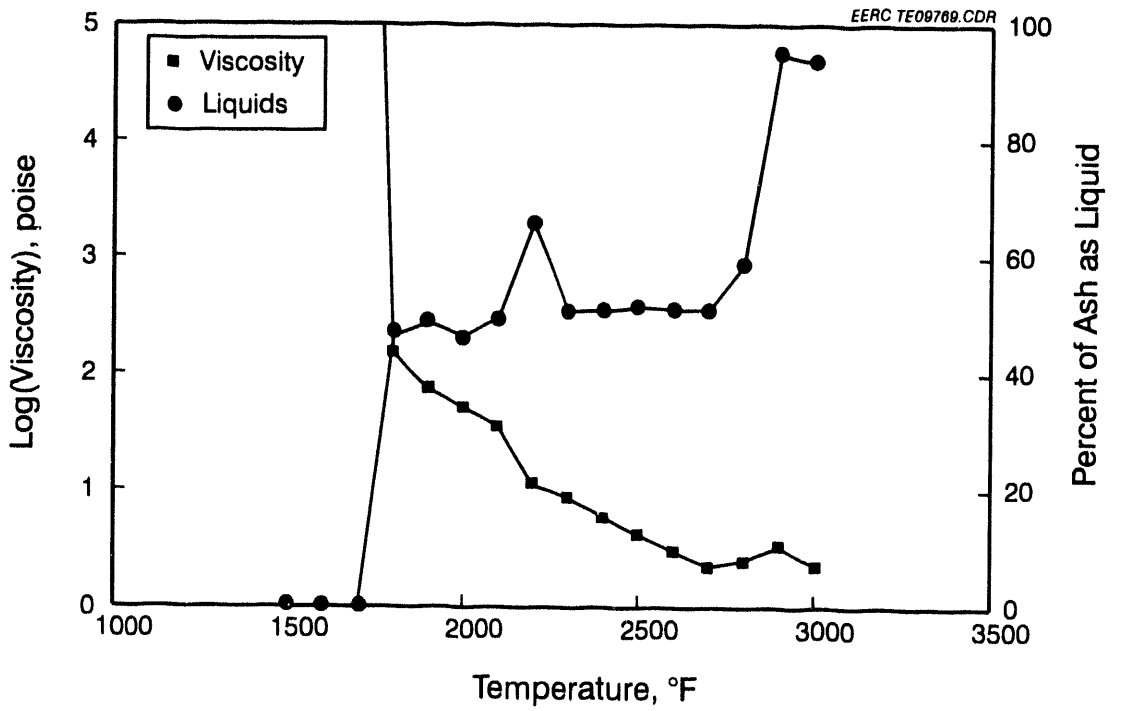

Figure 4. Thermochemical Equilibrium Modeling of a Slag Formed from the Gasification of Coal B

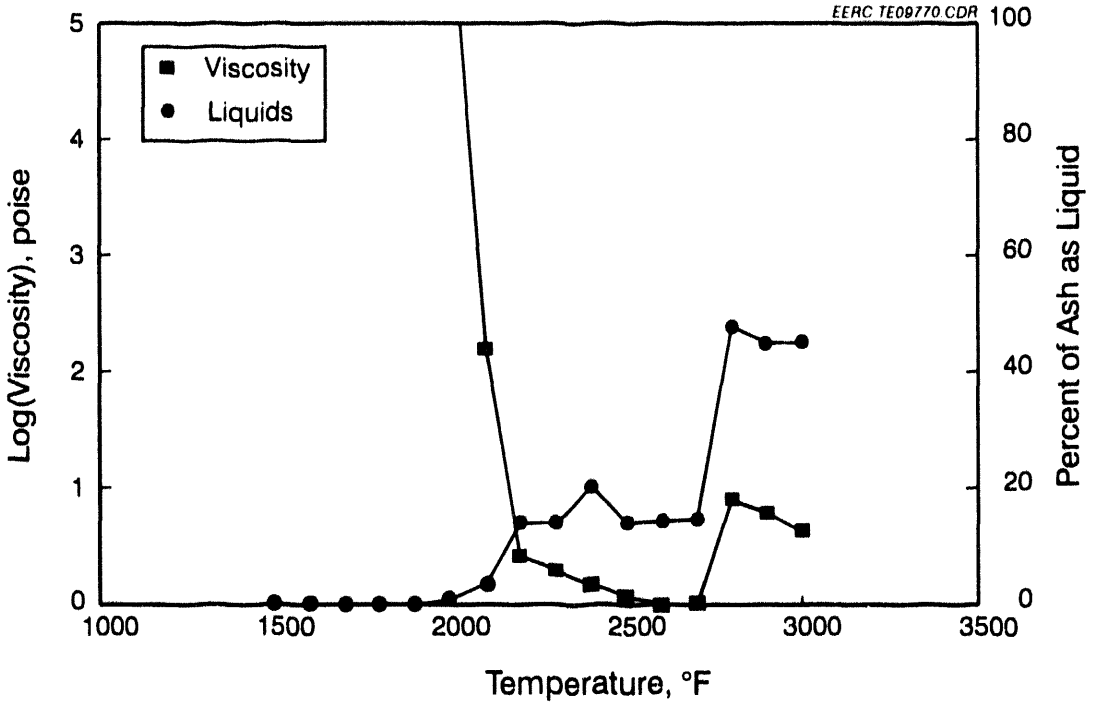

Figure 5. Thermochemical Equilibrium Modeling of a Slag Formed from the Gasification of Coal C

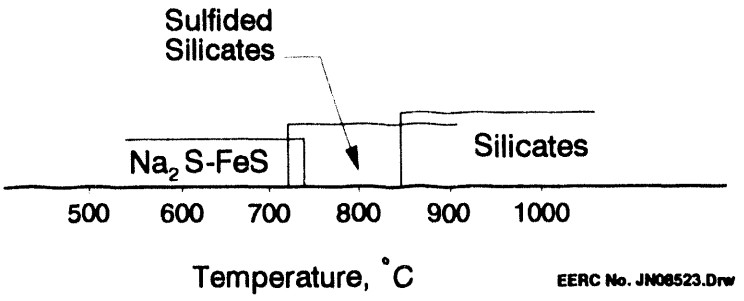

Figure 6. Diagram Showing a Sintering Model of Coal Ashes in Three Different Ranges of Temperatures and in the Presence of Three Possible Liquid Phases

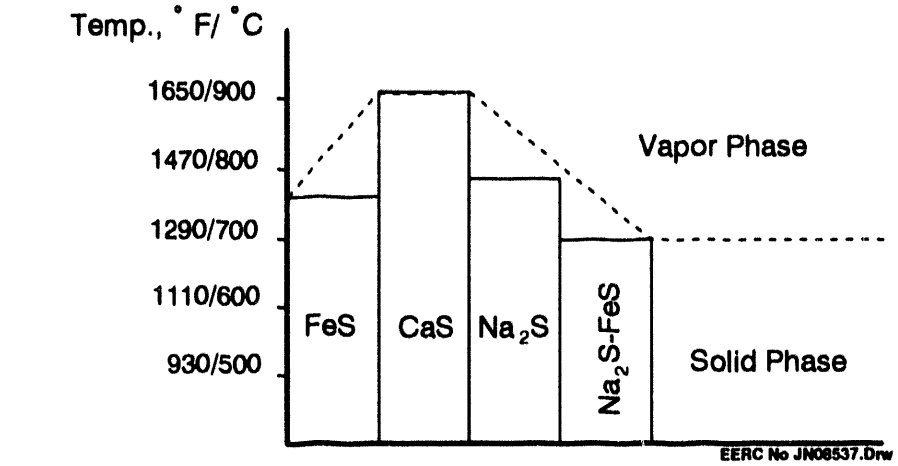

Figure 7. Thermal Stability of Major Sulfides Derived from Coal Ashes under Gasification Conditions

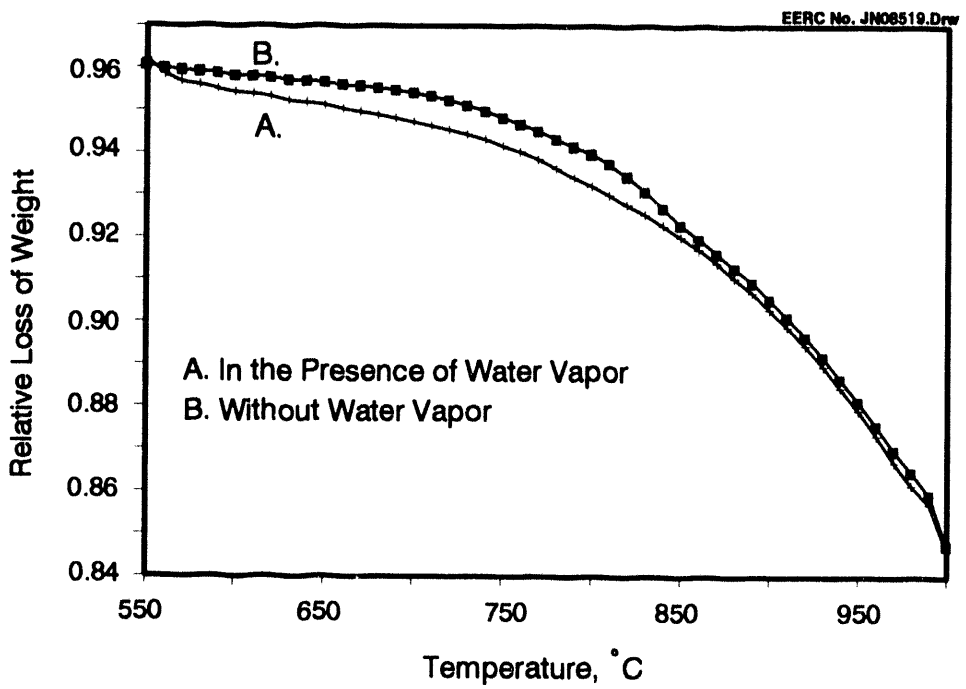

Figure 8. The Relative Loss of Weight of $Fe_{1-x}S$ in the Presence and Absence of Water Gas under Reducing Conditions

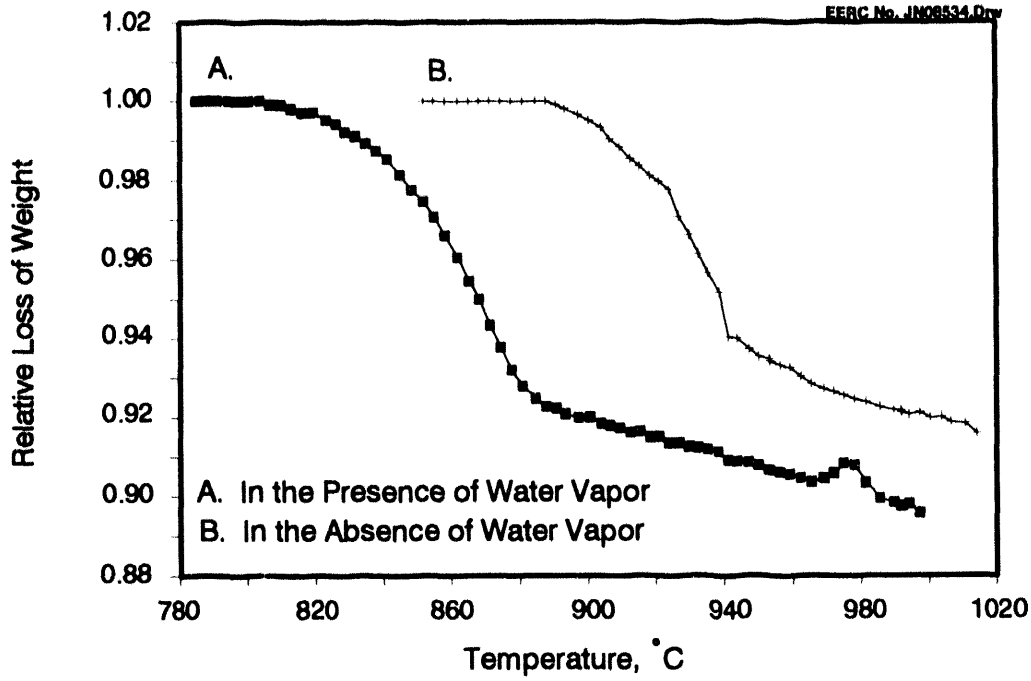

Figure 9. The Relative Loss of Weight of CaS in the Presence and Absence of Water Gas under Reducing Conditions

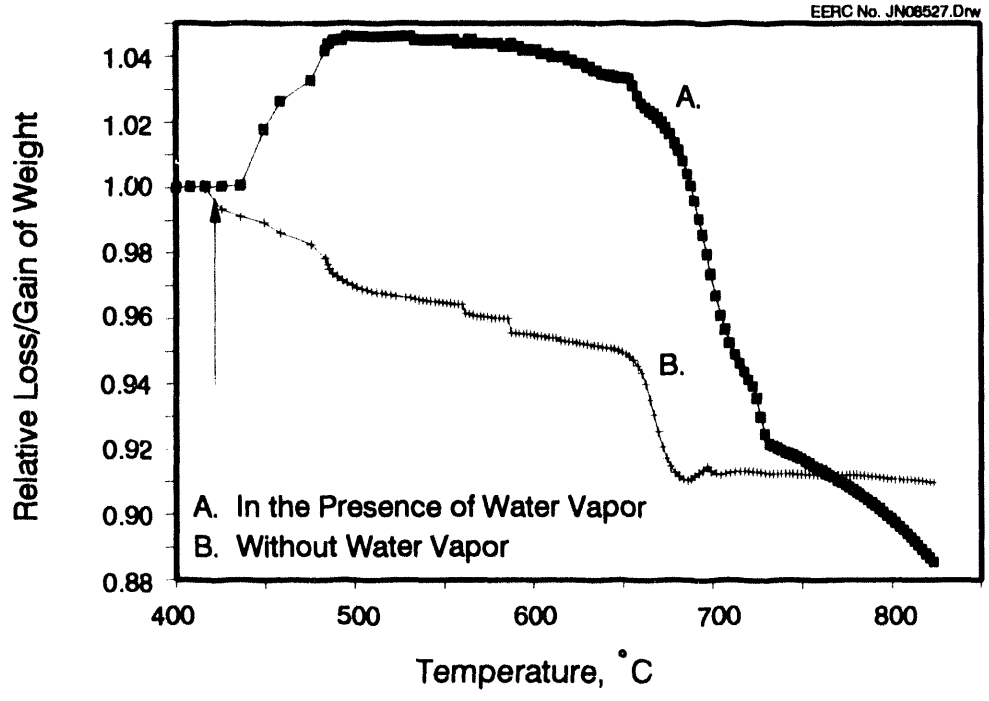

Figure 10. The Relative Loss of Weight of Na_2S-1.7 FeS in the Presence and Absence of Water Gas under Reducing Conditions

P5 Hot Coal Gas Desulfurization with Manganese-Based Sorbents

CONTRACT INFORMATION

Contract Number	DE-AC21-92MC29246
Contractor	University of Minnesota 500 Pillsbury Dr., S. E. Minneapolis, MN 55455-0220 (612) 625-6354
Contract Project Manager	Malcolm T. Hepworth
Principal Investigator	Malcolm T. Hepworth (P.I.) & Rachid Ben-Slimane (PhD Candidate)
METC Project Manager	Venkat K. Venkataraman
Period of Performance	9/18/92 - 9/17/94

ABSTRACT

In this paper, the physical and chemical behavior of several sorbent formulations fabricated from a manganese-containing compound, alundum (Al_2O_3), and a binder are addressed. The thermodynamic feasibility of hydrogen sulfide (H_2S)-removal from hot-simulated coal-gases using these sorbents and their subsequent regeneration with air are established. A formulation, FORM4-A, which consists of $MnCO_3$, alundum, and bentonite exhibits the best combination of capacity and reactivity; whereas, FORM1-A, which consists of Mn-ore, alundum, and dextrin exhibits the best combination of strength and reactivity. One important finding is that the capacity of the pellets for sulfur pickup from a H_2/H_2S mixture (at 950°C) and the kinetics of reduction, sulfidation and regeneration (at 1000°C) improve with recycling without compromising the strength.

The leading formulation, FORM4-A, was subjected to 20 consecutive cycles of sulfidation and regeneration at 900°C in a 2-inch fixed bed reactor. The sulfidation gas was a simulated Tampella U-gas with an increased hydrogen sulfide content of 3% by volume to accelerate the rate of breakthrough, arbitrarily taken as 500 ppmv. Consistent with thermo-gravimetric analysis (TGA) on individual pellets, the fixed bed tests show small improvement in capacity and kinetics with the sulfur-loading capacity being about 22% by weight of the original pellet, which corresponds to approximately 90% bed utilization!

OBJECTIVES

The objective of this study is to develop manganese-based sorbent pellets for the effective desulfurization of coal-derived fuel gases at high temperature (700-1200 °C). A number of formulations are prepared and screened first by testing in a thermogravimetric apparatus (TGA) in which individual pellets are weighed in mixtures of simulated coal-derived fuel gases at atmospheric pressure and high temperatures, and then in a bench-scale fixed bed-reactor. Sorbent screening criteria include measurement of sorbent (fresh, used, and regenerated) crush strength, chemical reactivity by thermogravimetric analysis, surface area, porosity, etc... The superior formulation is tested for long-term durability and chemical reactivity in the TGA apparatus and the bench-scale unit.

BACKGROUND INFORMATION

The Integrated Gasification Combined Cycle (IGCC) is one of the most promising proposed processes for advanced electric power generation that is likely to replace conventional coal combustion. This emerging technology not only will improve considerably the thermal efficiency but will also reduce or eliminate the environmentally adverse effects normally associated with coal combustion. The IGCC process gasifies coal under reducing conditions with essentially all the sulfur existing in the form of hydrogen sulfide (H_2S) in the product fuel gas. The need to remove H_2S from coal-derived fuel gases is a significant concern which stems from stringent government regulations and also, from a technical point of view, a need to protect turbines from corrosion. Westmoreland et al.[1] and Hepworth et al.[2] carried out comparative studies on several proposed sorbent systems which consisted almost entirely of metal oxides. Metal oxides have been proposed because they tend to be more reactive at high temperature where desulfurization is desirable to conserve the sensible heat in gasifier fuel gas. A sulfur concentration limitation of approximately 150 ppmv for IGCC systems has been established; therefore, a sorbent system capable of reducing H_2S concentration from about 5000 to 150 ppmv is sought.[3]

Zinc ferrite and zinc titanate have received much attention over the past twelve years because, from a theoretical point of view, they have desirable properties: high sulfur capacity, ability to remove H_2S from coal-derived fuel gas to levels of a few ppmv, and the feasibility of regeneration with air. Because it is economically necessary to recycle sulfur sorbents for at least 100 cycles, research has focused almost entirely on making the zinc-based sorbents durable. Unfortunately, extensive research carried out by the Morgantown Energy Technology Center (METC) of the Department of Energy (DOE) casts doubt that zinc ferrite or zinc titanate can be utilized even for fixed-bed operation. The desirable properties of Zn-based sorbents as well as their practical limitations will be discussed in detail in a later section of this paper.

Given the limited success of the zinc-based sorbents, METC has shown interest in formulating and testing manganese-based sorbent pellets.[4] There are a number of studies that led to the consideration of Mn-based sorbents.[1,2,5,6,7] This paper addresses the physical and chemical behavior of several sorbent formulations fabricated from manganese-containing compounds, alundum, and a binder and establishes the practical feasibility of H_2S removal from hot simulated coal gases using these sorbents and their subsequent regeneration with air. Experimental tests, utilizing the best formulation were carried out to study the kinetics of regeneration as a function of

temperature. Five repeated sulfidation and regeneration tests were then carried out to investigate the effect of pellet recycling on its chemical reactivity, physical durability, and capacity for sulfur pickup from fuel gases. Finally, the leading Mn-based formulation was subjected to 20 consecutive cycles of sulfidation, using a Tampella U-gas, and regeneration, with air, at 900°C in a 2-inch fixed-bed reactor.

PROJECT DESCRIPTION AND RESULTS

Sorbent Pellet Preparation For reasons which were previously explained,[4] the present investigation employed the following materials: Moanda manganese ore, regular manganese carbonate, alundum, bentonite, and dextrin. Four pellet formulations were prepared using combinations of a manganese-containing compound, an alumina-based matrix, and a binder, based on desired compositions determined on a dry weight-percent basis. After each blend is mixed, an appropriate amount of water is added prior to pelletizing. The composition of the initial make up of the formulations prepared using this procedure is reported in Table I.

Table I. Initial Make up of Formulations

Formulation No.	Raw Material Content in initial make-up, wt.%				
	Moanda Ore	Alundum	$MnCO_3$	Bentonite	Dextrin
1	68.18	22.73	-	-	9.09
2	73.53	24.51	-	1.96	-
3	-	15.51	75.4	-	9.09
4	-	16.73	81.31	1.96	-

Twenty-four induration campaigns were conducted. Preliminary tests indicated that Moanda ore-based pellets required a temperature of 1200 °C and manganese carbonate-based pellets required an induration temperature of 1250 °C, to produce a required strength of greater than 22 N per mm of pellet diameter (5 lbs/mm). In addition, two time periods for induration were explored, namely, 1 hour and 2 hours. The strongest formulations are bentonite-bonded as expected. At the conclusion of these tests, four formulations were selected for thermogravimetric analysis (TGA). They were given the following designations: FORM1-A, FORM2-A, FORM2-B, and FORM4-A. Letter "A" corresponds to induration for 2 hours at 1200 °C for the ore-based pellets, and 1250 °C for carbonate-based pellets; whereas, letter "B" corresponds to an induration time of 1 hour.

Table II summarizes the manganese assays and strengths of the formulations which were subjected to TGA analysis.

Table II. Manganese Assays and Strengths of Formulations Studied

Sample Designation	Weight % Mn	Strength, N/mm
FORM1-A	41.14	25.5
FORM2-A	37.48	64.7
FORM2-B	39.83	52.4
FORM4-A	44.22	23.8

Pellet Reactivity via Thermogravimetric Analysis (TGA) The TGA testing is divided into two campaigns; the first being only comparative loading for one cycle, and the second for regeneration studies and repeated cyclic loading and regeneration.

During the first campaign, emphasis was placed upon studying the kinetics of sulfidation using the above four sorbents. The reaction variables included temperature (700 to 1000 °C), fuel gas H_2S content (1%, 2%, and 3% in H_2/H_2S gas mixtures), and pellet diameter in the range 5-10 mm.

Figure 1 is a schematic diagram of the experimental equipment employed for TGA testing. The upper right-hand portion of the diagram shows the Cahn 1000-Series automatic recording balance assembly which holds up to twelve pellets in a nichrome wire-

mesh basket suspended with a nichrome chain from the left pan of the balance. The reactor consists of an alumina tube positioned in a high-temperature molybdenum-wound furnace. The reaction temperature was monitored by using a Pt/Rd thermocouple positioned directly below the sorbent pellets. The weighing unit was constantly blanketed with nitrogen during each test. The gas delivery and data acquisition systems are as depicted. Vent gases are scrubbed in a sodium hypochlorite solution prior to flaring and venting.

For each test, pellets were selected at random from a large batch of indurated pellets. The furnace pressure was 1 atm and the total flowrate was 500 cc/min. Before the heat was turned on, the reactor chamber was evacuated to 0.03 atm and then backfilled with nitrogen. The reactor was heated in a nitrogen atmosphere flowing at 1 l/min to the desired operating temperature before the balance platform was lowered to position the pellets in the center of the 10-cm-long hot zone. Five minutes after the sample was lowered into the hot zone, the nitrogen flow was shut off and the reactive gas mixture was started. Chemically pure (>99.9 %) hydrogen and hydrogen sulfide were metered into the TGA apparatus; flows were regulated by needle valves using calibrated rotameters. Finally, the nitrogen flow was turned on and the pellets were raised into the cold zone.

Figure 2 shows the results of TGA analysis at 1000 °C on the four selected sorbents which were described above. In all subsequent figures, W_o refers to the mass of the indurated pellet and W to the mass of the reacting pellet as a function of time. Initially, the ratio W/W_o for all pellets is unity; however, there is a decline in this value (reduction of Mn_3O_4 to MnO) when the pellets are exposed to hydrogen during the initial reduction period. Each reduction phase lasted 45 minutes although all pellets remained constant in weight for at least 20 minutes. Each of the sorbents appears to have lost the expected percentage of its original weight; FORM4-A pellets, which contain high manganese concentrations lost appreciably more weight than did the pellets containing lower proportions of manganese. Total percent loss at the conclusion of the reduction period ranged from 2% to 5% for FORM2-B and FORM4-A, repectively.

As indicated on the figures, hydrogen sulfide is added at 3% by volume to the gas which is flowing at a rate of 500 cc per minute. In the lower right-hand corner of the diagram are the theoretical maximum weight ratios which the pellets could exhibit based upon total conversion of the manganese in the pellet, as determined by chemical analysis, to the stoichiometry: MnS. Upon examining these calculated values, one should note that the formulation which resulted from manganese originating from purified carbonate (i. e., FORM4-A) has a greater capacity for sulfur than the formulations which originate from the ore because of the higher manganese content of the calcined carbonate. (see Tables I and II). Furthermore, dextrin-based formulations also yield higher sulfur capacities based upon the fact that dextrin volatilizes upon induration of the pellet; whereas, bentonite is a non-volatile impurity which effectively lowers the manganese content of the pellet.

The asymptote for time periods exceeding 90 minutes for formulation 4-A at 1000 °C actually exceeds the calculated value for sulfur capacity, which may indicate that the original sulfur assay is slightly on the low-side. The asymptotic value for formulation 1-A is very close to the calculated value; whereas, the asymptote for 2-A (Moanda ore plus bentonite) falls below the calculated value indicating that some of the manganese may be chemically combined with silicate compounds in the ore and therefore not

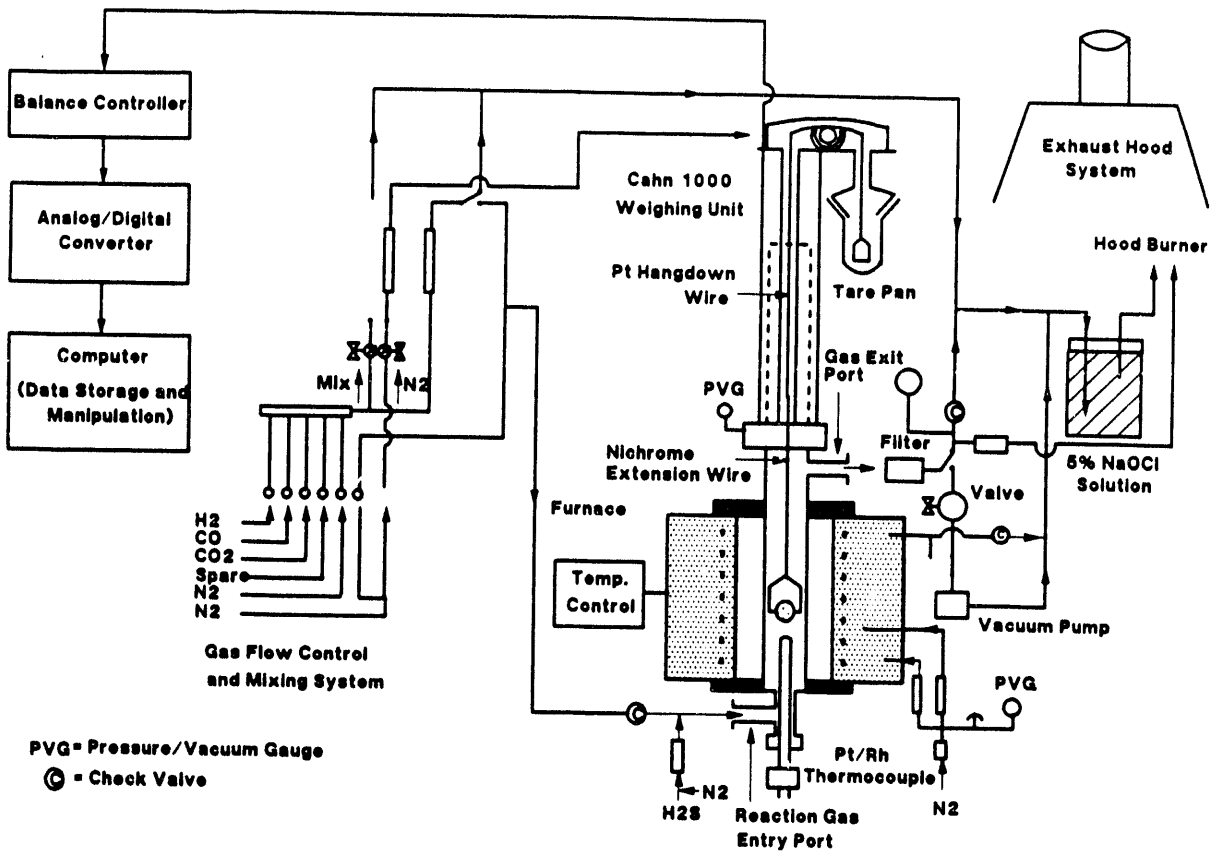

Figure 1. Schematic of the ASTRO Thermogravimetric (TGA) Apparatus.

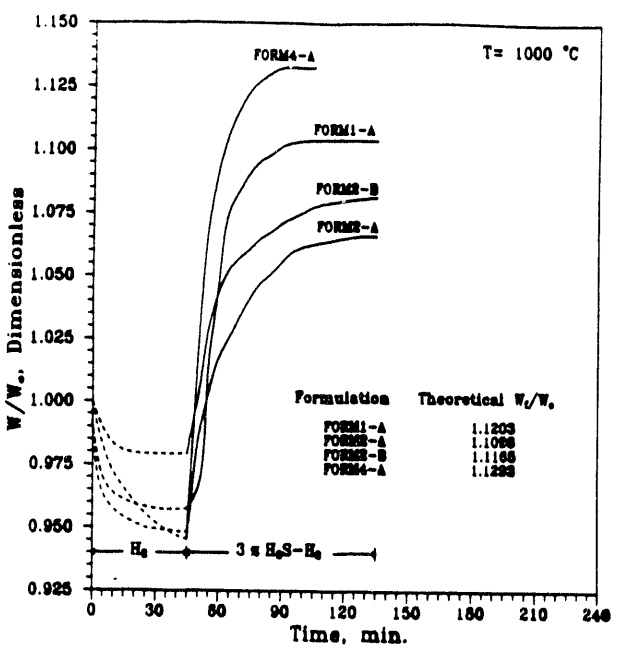

Figure 2. Normalized Weight vs. Time for Reduction and Sulfidation of Four Manganese-Based Formulations at 1000 °C in a 3% H_2S-H_2 Gas Mixture.

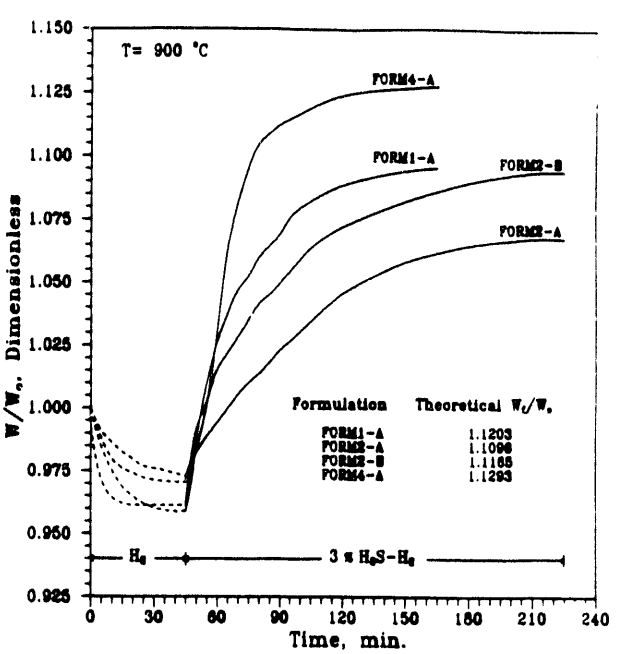

Figure 3. Normalized Weight vs. Time for Reduction and Sulfidation of Four Manganese-Based Formulations at 900 °C in a 3% H_2S-H_2 Gas Mixture.

available to react with hydrogen sulfide. In general, however, and at longer reaction times, each curve would approach its final weight corresponding to complete sulfidation.

In continuing the examination of Figure 2, one should note the rapid kinetics upon switching to the loading gas, which is most pronounced in formulation 4-A, i. e. manganese carbonate plus bentonite. Formulation 1-A (ore plus dextrin) has somewhat slower kinetics followed by formulation 2-A (ore plus bentonite). Figure 3 shows similar results for tests conducted at 900 °C. Again formulation 4-A shows the highest sulfur capacity and the most rapid kinetics of the four pellet groups. Tests conducted at 800 °C show somewhat slower kinetics again with the pellet groups showing similar trends in kinetics. Results from similar loading tests at 700 °C indicated that the kinetics are significantly slower so that only a fraction of the pellet capacity is utilized for all four formulations within the time-frame of the three-hour test regime.

Figure 4 is a composite of the data for formulation 4-A, the best of all the formulations studied, for the temperatures 760, 800, 900, and 1000 °C. The theoretical capacity for this formulation is shown as a dashed line on the plot with reactivity rates for all temperatures being rapid.

Regeneration Tests. The TGA tests focused on studying the effects of regeneration parameters (temperature and O_2 content) and on repeated loading and regeneration of the selected FORM4-A pellets. Since up to fifteen pellets may be used in each reduction/sulfidation test, various tests were needed to provide enough fully-loaded pellets for the various regeneration tests planned. This provided an opportunity to determine the reproducibility of the sulfidation tests. The reduction and sulfidation were carried out under standard conditions of 950 °C and 3%

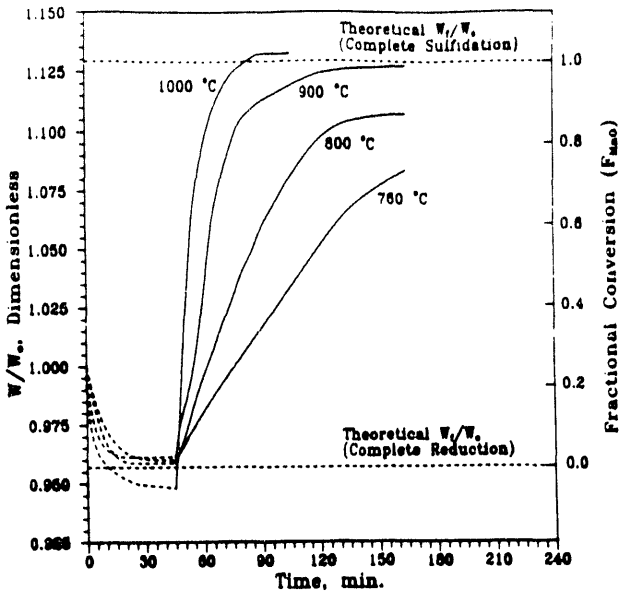

Figure 4. Effect of Temperature on Sulfidation Kinetics of FORM4-A Pellets

H_2S-H_2 gas mixtures at 500 cc/min delivery for a total of approximately 2 grams of pellets. Reduction was carried out with pure hydrogen for the first 45 minutes and then the hydrogen sulfide was added.

Figure 5 shows the reproducibility of loading tests resulting from five separate tests on fresh pellets (i.e., first loading cycle) at 950 °C with 3% by volume hydrogen sulfide in hydrogen. This figure gives the error bars on the data to indicate the range of the results. Although not shown for the reduction portion of the curve the reproducibility is particularly good, with reduction essentially completed in fifteen minutes. Figure 5 shows that deviations in extent of loading occur even though during each test the macroscopic properties (mass and size) of the pellets were kept as constant as possible. These deviations may be due to the difficulty associated with controlling temperature, flow rates, etc. However, the reproducibility of sulfidation is excellent beyond the first 30 minutes after the initial reduction period (total lapse time of 75

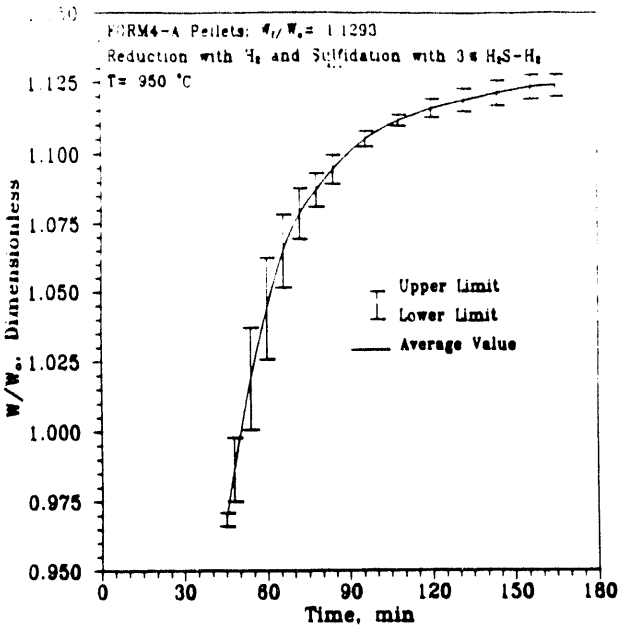

Figure 5. Reproducibility of Loading Tests at 950°C with 3% H_2S-H_2 Gas Mixtures Showing Average Value and Error Bars

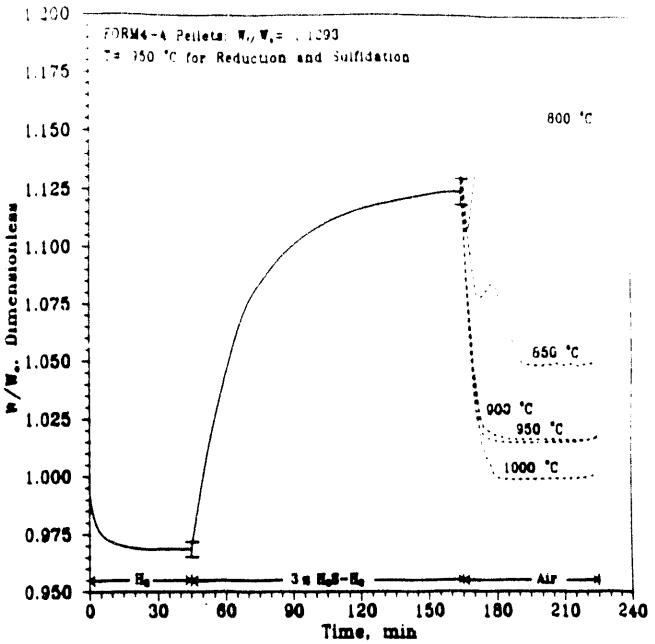

Figure 6. Effect of Temperature on Regeneration Kinetics of FORM4-A Mn-Based Pellets.

minutes). The solid line represents the average values and therefore serves as an indication for future test results.

A total of five regeneration tests were then carried out using five pellets during each test. The regeneration gas was air flowing at 500 cc per minute and regeneration temperature varied between 800 and 1000 °C in increments of 50 °C. The purpose was to determine the temperature at which loaded pellets could be fully regenerated in reasonable time. The results from these tests are reported in Figure 6. The loading curve corresponds to the solid line shown in Figure 5; however, the right-hand portion of this figure shows the regeneration portion after a total time lapse of 165 minutes. These results appear to be in strict accordance with thermodynamic predictions, viz.: at 800 °C the loaded pellets first oxidize (and hence lose weight) for about 3 minutes at which time sulfation with an concurrent weight gain becomes predominant. When approximately 60% of the MnS is converted to $MnSO_4$, sulfate decomposition starts and the pellets begin to show a weight loss. Continuing at higher temperatures, at 850 °C, the same trend is observed; however, the oxidation of the pellets appears to be faster than sulfation; this is reasonable since the driving force for the decomposition of sulfate is greater. Regeneration kinetics appear to be a weak function of temperature over the range 900 to 1000 °C. In this range regeneration is essentially complete in 10 to 15 minutes and sulfation does not occur, as concluded from the prior thermodynamic analysis of the Mn-S-O system. It must be noted, however, that full regeneration (i.e., $W/W_0=1$) apparently requires a temperature of 1000 °C or higher.

Multicycle Tests Over a five-day period, one loading and regeneration cycle was completed each day at 950 °C for reduction and sulfidation and 1000 °C for regeneration. The TGA data for these five tests are shown in

Figure 7. The arrows show the direction of increasing cycle sequence numbers, i. e. for loading, the capacity and reaction kinetics improve for each of the five cycles with the change between the first and second cycles being the most pronounced. For the tail of the curve terminating the regeneration step, the weight loss drop is steepest for the fifth

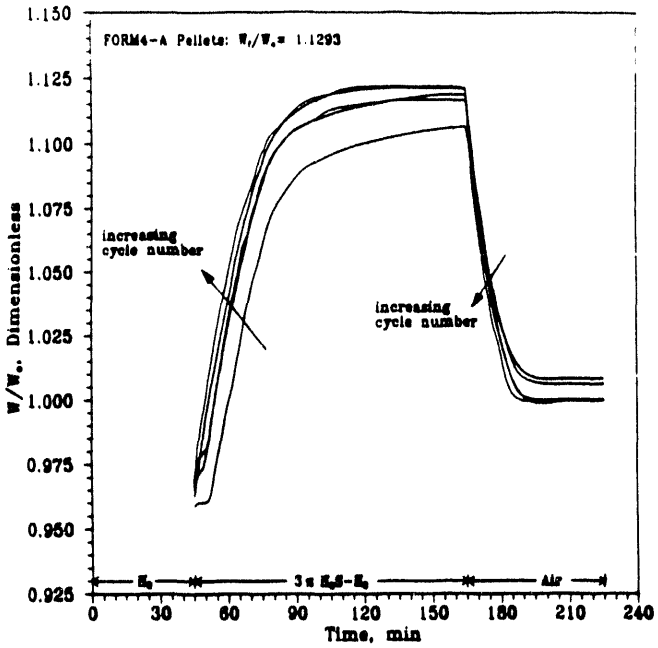

Figure 7. Effect of Repeated Cyclical Loading and Regeneration on the Reaction Kinetics and Capacity of FORM4-A Pellets.

cycle: again showing that the rate of regeneration increases with pellet re-use. An optical examination at 30 magnifications with a binocular microscope as well as petrographic thin sections examined at 100x showed the presence of radial cracks. The penetration distance of the sulfur as exhibited by the higher reflectivity of the manganese sulfide phase was densest adjacent to these cracks, indicating that the diffusion distance for permeation of sulfur (and counter-transport of oxygen) was decreased by the change in diffusion geometry occasioned by the cracking. Whereas the original pellet experiences diffusion for a gross pellet size of ≈2.5 mm in radius; upon cracking of the pellet, the solid-state diffusion distance is somewhat reduced. This permits gaesous species to be transported by the relatively faster mechanism of gaseous diffusion into the cracks compared with the slower process of solid state counter diffusion of oxygen out of the pellet to exchange for sulfur into the pellet.

This is a unique feature of manganese-based pellets, i. e. their retained strength upon micro-cracking and improved kinetics compared with competing sorbents, e. g., zinc titanate, in which the reaction kinetics and sorbent loading capacity and pellet strength decrease upon cyclic loading.

Bench-scale testing The overall schematic diagram of the experimental arrangement for fixed-bed tests is shown in Figure 8. The split or two-zone furnace is positioned with respect to the bed to accomplish gas preheating and careful control of the bed temperature. Gas combinations for flows can be produced via control of bottled gases through the valves and flowmeters shown in the diagram. The water content of the system is controlled by a metering pump acting on liquid water which is discharged into a heated stainless tube to vaporize the water and provide the gas composition required by the Tampella-U Gas composition, as reported earlier.[4]

The details of the reactor system are depicted in Figure 9. This figure shows the two-inch (I.D.) closed-end alumina reactor tube equipped with an alumina perforated-disc plate suspended over alumina chips. The coal-derived fuel gas simulating the Tampella-U Gas is passed through a small central tube (without contacting the reaction zone of manganese pellets) through the perforated disc and into a preheat zone of alumina chips which supports the disc. The gas is then discharged from the small central tube into

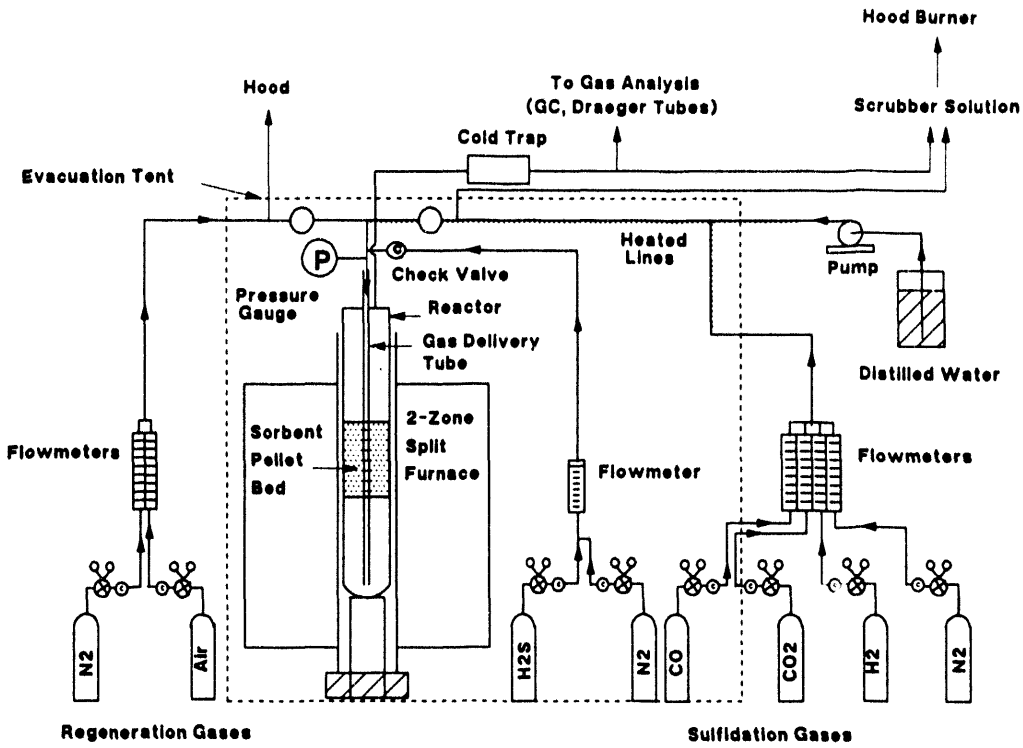

Figure 8. Schematic of Overall Experimental Arrangement for Fixed-Bed Tests.

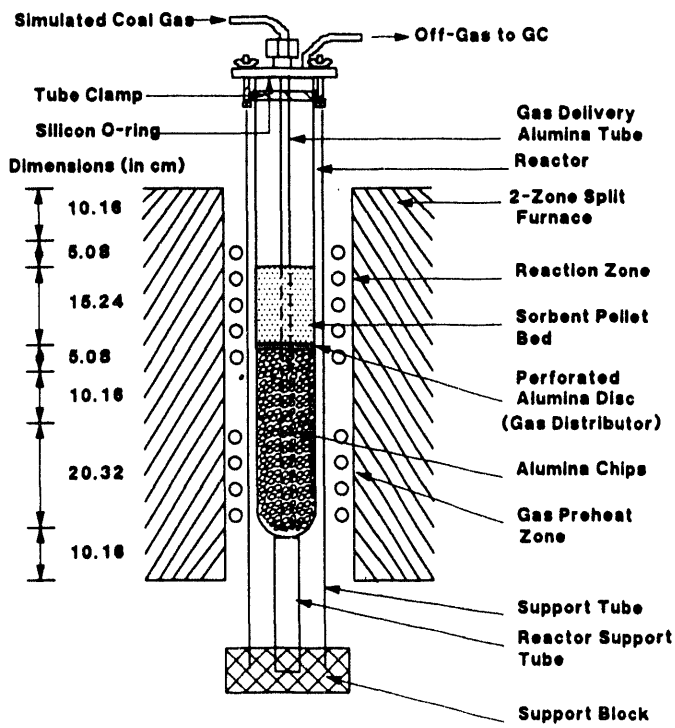

Figure 9. Schematic Diagram of Reactor Details.

the larger tube and moves upward, after reaching temperature, into gas preheat zone of a two-zone furnace. The gas, now at temperature, contacts the sorbent bed consisting of pellets ranging in size from 4 to 5 mm in diameter. The off-gas then is flared and discharged to a hood. A sample is taken via gas chromatograph (labelled in Figure 9 as GC).

A minor problem has arisen during the regeneration step in that sulfur tends to form and plug the exit tube during the early stages of regeneration (examination of the plug showed it to be elemental sulfur). This problem was overcome by reducing the air flow rate to limit the rate of heat release by the highly exothermic regeneration reaction and prevent the pellets from sintering. The addition of an after-burner on top of the pellet bed resulted in more oxidizing conditions and hence less tendency for sulfide sulfur ($S^{=}$) to oxidize to the intermediate elemental form (S^{0}) rather than to 4-valent (S^{+4}).

Loading proceeded at a rate of 3.5 liters per minute until breakthrough is observed. Breakthrough is defined as a sudden rise in the sulfur content of the gas as determined by gas chromatography. The bed is then flushed with nitrogen in order to expel remaining hydrogen and a regeneration gas consisting of air is initiated with the sulfur content of the gas being continuously analyzed for sulfur dioxide. The regeneration step is discontinued when the concentration of sulfur dioxide in the exit gas is measured below 500 ppmv. The loading and regeneration cycles are then repeated until twenty (20) cycles are completed.

Figure 10 shows the effect of cycling on the sulfur capacity of FORM4-A pellets at 900°C upon repeated loading and regeneration. The sulfur loading capacity (defined as grams sulfur per 100 grams of original pellet mass) shows a slight improvement with each cycle. The effect diminishes with each cycle since loadings approaching 23% S, (i. e., is ~90% of the maximum theoretical value) at 12 cycles. This sulfur capacity is calculated using mass balances, based upon gas analyses for H_2S entering and leaving the reactor. Before break-through the H_2S concentration in the cleaned gas approach more closely the equilibrium value, which is an indication of an improvement in pellet reaction kinetics with increasing cyclic loading. These results are consistent with the previous results from TGA tests on individual pellets.

Mn-Based Sorbents vs Zn-Based Sorbents

The theoretical capacity of manganese-based pellets for sulfur compares favorably with zinc ferrite and zinc titanate as shown in Table III. In generating this table, it is assumed that Fe_3O_4 is the stable form of Fe after reduction of $ZnFe_2O_4$, and that the optimized zinc titanate formulation is composed of 1.5 ZnO:1.0 TiO_2. Furthermore, the manganese ore-based formulation is based upon Moanda ore containing 51.2% Mn by weight.

Clearly, even the manganese ore-based sorbent pellet, which has a lower capacity than the Mn carbonate-based formulation, compares favorably with the optimized formulation of zinc titanate which was used extensively in pilot-scale and process development work.

Table III. Theoretical Sorbent Capacities

Sorbent	Theoretical Capacity, g S/100 g of sorbent
Zinc ferrite	39.8
Zinc titanate	23.8
Mn Ore-based	24.0
Mn carbonate-based	34.4

The ultimate degree of desulfurization of manganese-based pellets is less favorable than would be achieved with Zn-based

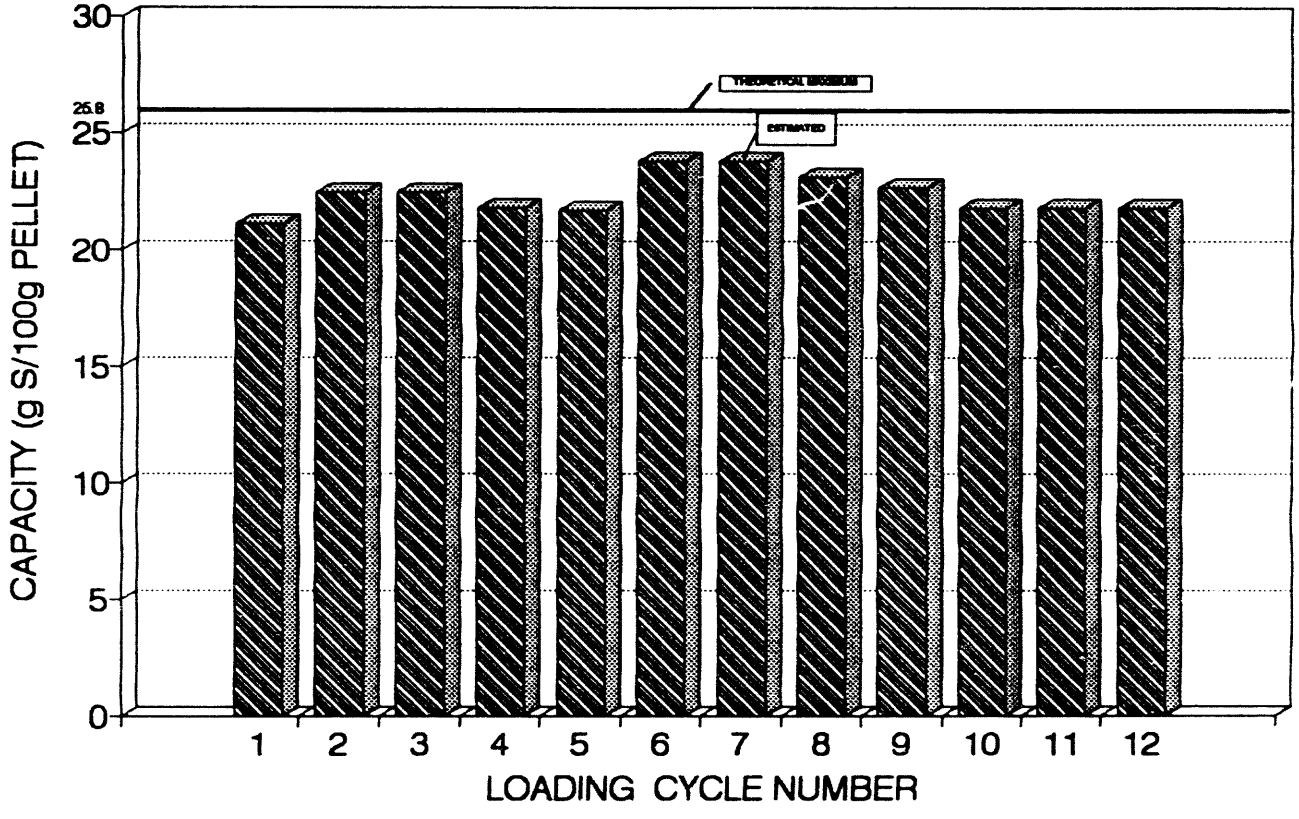

Figure 10. Effect of Cyclic Loading and Regeneration on Sulfur Capacity of FORM4-A Pellets at 900 °C.

sorbents. For example, for a fuel gas containing 5% H_2O and 1% H_2S, desulfurization at 1000 °K (727 °C) achieves 57 ppmv H_2S with MnO and 6 ppmv H_2S with ZnO, based on data compiled by Turkdogan.[8]

To compare the rate of sulfidation of Mn-based pellets with that of Zn-based sorbents, the results from sulfidation tests on L-3140 sorbent[3] at 760 and 870 °C are superimposed on the results reported above in Figure 4, as shown in Figure 11. The goal of exposing the Zn-based sorbent to the H_2S-free reducing gas is to quantify the weight loss which is solely due to ZnO depletion. At 760 °C this physical loss of reactive component is negligible; however, at 870 °C this phenomenon becomes noticibly more severe leading to lower sorbent capacity for sulfur. More importantly, the rate of sulfur pick-up from hot coal-derived fuel gases using Mn-based pellets compares favorably with that which is obtained using Zn-based sorbents.

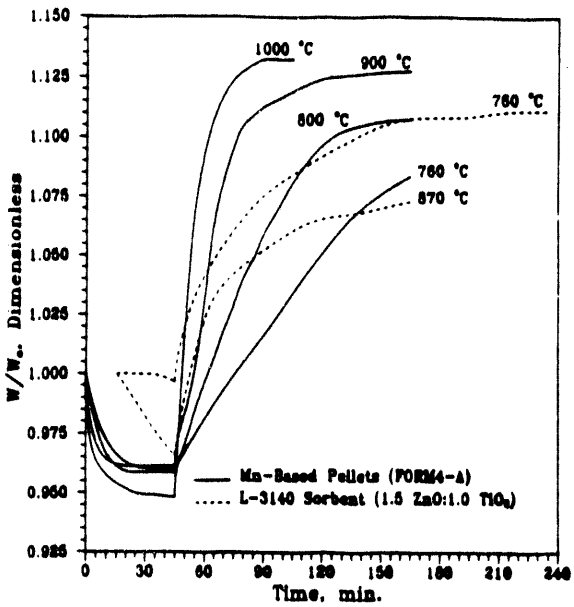

Figure 11. Comparison of Sulfidation Kinetics via Thermogravimetric Analysis of FORM4-A Mn-Based Pellets and L-3140 Zn-Based Sorbents.

One major problem associated with zinc-based sorbents is sulfate formation which is found to occur whenever SO_2 is present in the regeneration gas. Sulfation leads to volume expansion and swelling of sorbent pellets eventially causing them to spall and crack. For example: a 5 to 6-mm diameter loaded pellet expands to 9 mm after regeneration when sulfate was formed.[9] Certainly, in a fixed-bed operation some of the pellets will be saturated with sulfur and the regeneration gas will contain some SO_2. Therefore, sulfate formation is unavoidable along with accompanying spalling and cracking.

The role of chlorides in the gas system should be considered in any study because of the potential volatility of metal chlorides. The presence of HCl in the coal gas causes extensive volatilization of zinc in the form of $ZnCl_2$. All fuel gases contain some hydrochloric acid, under reducing conditions. Zinc chloride ($ZnCl_2$) has a boiling point of 1005 °K (732 °C); whereas, manganese chloride ($MnCl_2$) has a boiling point of 1504 °K[10] (1231 °C). The higher boiling point of manganese makes it much less susceptible to volatilization and losses from the sorbent than zinc. Losses of zinc as high as 5-10% by weight from the exit of a fixed-bed reactor have been reported,[9] even after one cycle of loading and regeneration. It follows that any gas system which is used as an environment for comparing the cyclic loading and regeneration behavior between manganese oxide and zinc-based sorbents should take into account the presence of chlorides in the fuel gases.

A fortuitous feature of the manganese-oxygen-sulfur system is its resistance to reduction to elemental manganese under the range of most of the fuel gas compositions for which it would be utilized as a sorbent. Furthermore the sulfidation and regeneration can be carried out at the same temperature, for example (800 °C) without the formation of sulfates. Another favorable feature of the

manganese-oxygen-sulfur system is its resistance to fusion as a result of temperature rises which may occur in the exothermic step of regeneration since the system is relatively refractory and non-volatile (i.e., lacks low melting-point phases) even in the presence of trace chloride impurities. For the case of zinc ferrite, it was found that temperature excursions as small as 50 °C could destroy the sorbent reactivity.[11] Exit gas temperatures from commercial gasifiers are likely to be in excess of 650 °C; in addition, operation of the desulfurization process at higher temperatures increases the overall IGCC plant efficiency. Manganese-based pellets appear to be capable of much higher temperatures of loading and regeneration than zinc without degradation; however, this question remains to be fully explored.

FUTURE WORK

Under the present contract a program was undertaken to optimize pellet formulations and evaluate them by multiple cyclic tests in a fixed-bed reactor; however, now that the FORM4-A pellets have been shown to be highly effective through repeated cycling, effort should be redirected toward exploring several parameters of fixed bed operation which may be more consonant with actual test conditions. For example after ten cyclic loadings of the pellets, a long cycle of loading at a lower H_2S content, more nearly representing the actual fuel gas compositions, should be undertaken. Upon completing this long cycle to break-through, the bed should be examined in vertical layers to explore the degree of sulfidation which has occurred on single pellets.

Also single-particle regenerations on selected pellets from the above long test should be explored by DTA as well as TGA analysis to determine the thermal effects which occur upon oxidation of the sulfides. The results on single pellet tests could then be compared with the thermal effects (e. g., local temperature rises) which would occur in fixed bed environments. The effect of space velocity, i. e. gas flow rates in fixed bed tests could also be explored.

Acknowledgements The authors express their appreciation to the Department of Energy, Morgantown Energy Technology Center, under Contract DE-AC21-92MC29246 and also the U.S. Bureau of Mines, Twin Cities Research Center, Grant USDI-BM/C0299002-Mod.3 for providing support for this study. They are also indebted to the Twin Cities Research Center for the use of their TGA apparatus which made this work possible.

REFERENCES

1. Westmoreland, P.R.; Harrison, D.P. Evaluation of Candidate Solids for High-Temperature Desulfurization for Low-Btu Gases. Environ. Sci. Technol. **1976,** 10, 659-661.

2. Hepworth, M.T.; Ben-Slimane, R.; Zhong, S. Thermodynamic Comparison of Several Sorbent Systems for Hot Coal-Derived Fuel-Gas Desulfurization. Energy Fuels **1993,** 7, 602-609.

3. Woods, M.C.; Gangwal, S.K.; Jothimurugesan, K.; Harrison, D.P. Reaction between H2S and Zinc Oxide-Titanium Oxide Sorbents. 1. Single-Pellet Kinetic Studies. Ind. Eng. Chem. Res. **1990,** 29, 7, 1160-1167.

4. Hepworth, M.T.; Ben-Slimane, R. Hot Coal Gas Desulfurization with Manganese-Based Regenerable Sorbents. Proceedings of the Coal-Fired Power Systems 93 -- Advances in IGCC and PFBC Review Meeting, 1993. David L. Bonk editor, DOE/METC - 93/6131, NTIS, Springfield, VA, pp. 432-444.

5. Westmoreland, P.R.; Gibson, J.B.; Harrison, D.P. Comparative Kinetics of High-Temperature Reaction Between H_2S and Selected Metal Oxides. Environ. Sci. Technol. **1977,** 11, 488-491.

6. Turkdogan, E.T.; Olsson, R.G. Desulfurization of Hot Reducing Gases with Manganese Oxide Pellets. Proceedings of the Third International Iron and Steel Congress ASM; ASM International: Materials Park, OH, **1979,** 277-288.

7. Jha, M.C.; Hepworth, M.T. Enhanced Sorbent Durability for Hot Gas Desulfurization; DOE Contract DE-AC21-84MC21168, Final Report, 1986.

8. Turkdogan, E.T. Physical Chemistry of High Temperature Technology, Academic Press: New York, 1980.

9. Venkataraman, V. K. Private Communication: Information on Workshop "Status and Direction of Research and Development for High Temperature Sulfur Removal Sorbents," Morgantown Energy Technology Center, January 28, 1993.

10. Handbook of Chemistry and Physics, 67th Edition, 1986-1987, CRC Press, Inc., Boca Raton, FL.

11. G.D. Focht; P.V. Ranade; D.P. Harrison. High-Temperature Desulfurization Using Zinc Ferrite: Reduction and Sulfidation Kinetics. Chemical Engineering Science, Vol. 43, No. 11, pp. 3005-3013, 1988.

P6 A Calcium Oxide Sorbent Process for Bulk Separation of Carbon Dioxide

CONTRACT INFORMATION

Contract Number	DE-AC21-89MC26366
Contractor	Louisiana State University Department of Chemical Engineering Baton Rouge, Louisiana 70803
Contract Project Manager	Douglas P. Harrison
Principal Investigators	D.P. Harrison C. Han
METC Project Manager	Venkat A. Venkataraman
Period of Performance	September 1989 to October 1994

OBJECTIVES

Initial phases of this project investigated the bulk separation of CO_2 from coal-derived gas at moderate to high temperature. The separation process was based upon the reversible noncatalytic reaction

$$CO_2(g) + CaO(s) \leftrightarrow CaCO_3(s). \quad (1)$$

We are presently studying the feasibility of combining CO_2 removal with the water gas shift reaction

$$CO(g) + H_2O(g) \leftrightarrow CO_2(g) + H_2(g). \quad (2)$$

The combined reactions, which are carried out in a single reaction vessel, provide an alternate and potentially simpler process for the production of H_2 from synthesis gas.

In this experimental investigation, a laboratory-scale fixed-bed reactor containing a calcium-based sorbent is being used to study the combined reactions as a function of calcination and carbonation temperature and pressure, synthesis gas composition, reactor space velocity, and sorbent composition and properties.

BACKGROUND INFORMATION

Hydrogen, one of the most important raw materials in both the chemical and petroleum industries, is produced primarily by the steam reforming or partial oxidation of gaseous or liquid hydrocarbons. In the future, coal gasification may become important as the supply of light hydrocarbons decreases. The initial product from all of these processes is a synthesis gas composed primarily of CO, CO_2, H_2, H_2O, and, in some cases, N_2. The water gas shift reaction is then used to produce additional H_2 by reacting the remaining CO.

Because the shift reaction is exothermic and reversible, multiple catalytic reaction steps are necessary to achieve complete CO conversion. Extensive gas-to-gas heat exchange

networks are required to adjust the temperatures at various stages in the process. The CO_2 product is normally removed using wet scrubbing or pressure swing adsorption. The alternate single-step process accomplishes the shift reaction and CO_2 removal in a single reaction vessel, and eliminates the need for expensive catalysts as well as the CO_2 absorber and stripper (or the PSA unit). Heat exchange requirements are minimized since the alternate process occurs at high temperature.

The potential advantages of the single-step process are illustrated by the following thermodynamic comparison. Consider a typical coal-derived synthesis gas containing 22% H_2, 30% CO, 8% CO_2, and 40% H_2O at a reaction temperature of 900K. Equilibrium calculations, using thermodynamic data of Barin et al. (1977), show that the shift reaction alone would result in only 56% conversion of CO. If the shift reaction is carried out in the presence of calcium-based sorbent, equilibrium at 1 atm corresponds to 99% conversion of CO, while effectively 100% conversion of CO will occur at 25 atm. In the later case, total carbon oxide concentration in the equilibrium product gas will be in the ppm level.

PROJECT DESCRIPTION

The laboratory-scale fixed-bed reactor has a capacity of 10 to 15 grams of sorbent. Gaseous feed components are obtained from high pressure cylinders with flow rate controlled by high pressure mass flow controllers. Liquid water is added using a high pressure syringe pump and is vaporized as it mixes with the permanent gases. The combined gas feed is preheated prior to contacting the sorbent.

Reactor product is sampled periodically and analyzed by gas chromatography. Argon is used as the carrier gas and the chromatograph system is equipped with multiple columns, automatic sampling and switching valves, and both thermal conductivity (TCD) and flame ionization (FID) detectors. The TCD is used for analysis of N_2, H_2, and high concentrations of CO and CO_2 ($\geq$ 0.5%). When CO and CO_2 concentrations are below the TCD detection limit, the reactor products pass through a ruthenium-catalyzed methanator which converts CO and CO_2 to CH_4, and analysis is completed using the more sensitive FID. More complete descriptions of the reactor and analytical system, including drawings have been published (Harrison et al., 1993).

A typical reactor response curve showing component concentrations as a function of time is presented in Figure 1. Results from both the TCD and FID are included as indicated. Early in the reaction CO and CO_2 concentrations were effectively constant at about 80 and 300 ppm, respectively, while H_2 concentration was constant at 1.5 x 10^5 ppm (15%). We refer to this stage as the prebreakthrough period, during which the total fractional removal of carbon oxides was 0.998. After much of the CaO was converted to $CaCO_3$, CO and CO_2 concentrations increased rapidly while H_2 concentration decreased. The slope of the concentration-time curves during this breakthrough period provides a measure of the global rate of the combined reactions. After essentially all of the CaO was converted to $CaCO_3$, a second steady-state, postbreakthrough period, was reached. Only the shift reaction occurred during this stage.

The prebreakthrough period is of primary interest since it is during this period that the true capability of the single-step process for carbon oxide removal and hydrogen production can be evaluated.

RESULTS

The parameters which have been (and are being) investigated include calcination and carbonation temperature and pressure, feed gas composition, reactor space velocity, and the composition and structural properties of the sorbent. Multicycle runs are being carried out because, for the process to be economically attractive, the sorbent must maintain its activity

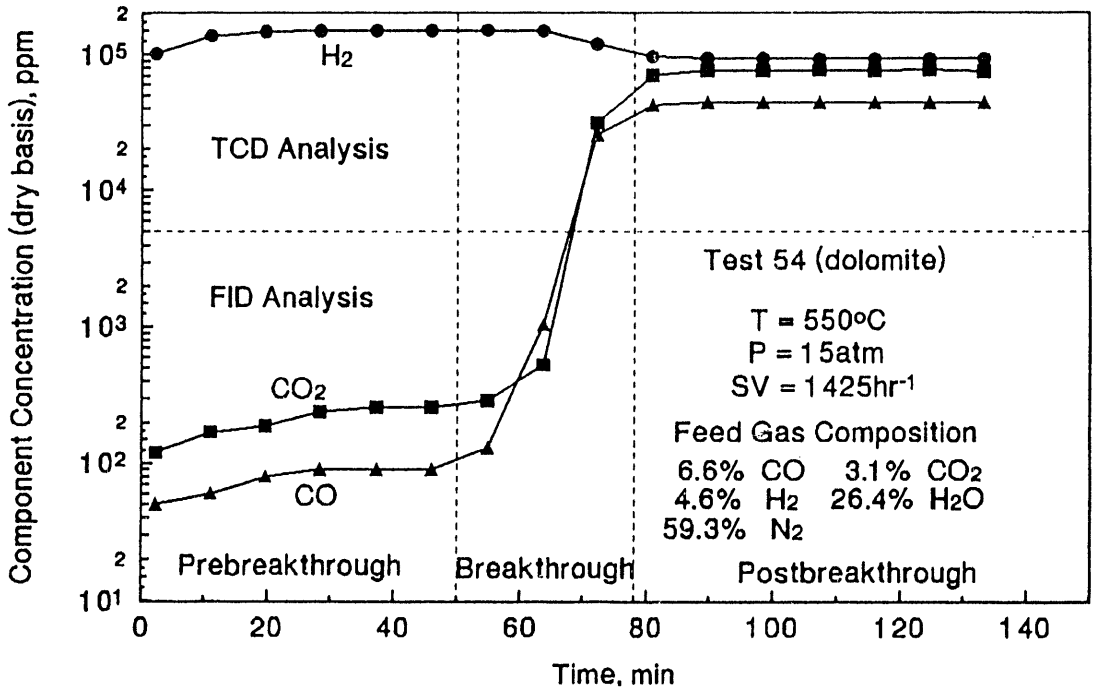

Figure 1. Typical Fixed-Bed Reactor Response Curve

through numerous calcination-carbonation cycles.

Comparison of Sorbents

Dolomite was found to be superior to limestone during the initial phase of this project, and the superiority has subsequently been confirmed in the fixed-bed studies. Figure 2 compares the performance of dolomite and limestone sorbents in a plot of fractional removal of total carbon oxides as a function of time. The product gas analysis in this example is based on the TCD only, so that, early in the reaction, the fractional carbon oxide removal approaches 1.0 with both sorbents. The actual CO and CO_2 concentrations during this period were approximately 80 and 215 ppm, respectively, during the test with limestone, and 22 and 250 ppm for the test with dolomite. These concentrations correspond to fractional removal of total carbon oxides during the prebreakthrough period of 0.996 in both tests.

In addition to the delayed initial breakthrough, the larger slope of the breakthrough curve for dolomite is indicative of larger global reaction rates. Finally, additional data (not shown) indicates that the multicycle durability of dolomite is significantly better.

The favorable properties of dolomite are attributed, to a large degree, on differences between the structural properties of calcined dolomite and calcined limestone. Complete decomposition occurs during the initial calcination phase so that dolomite is converted to (CaO + MgO) while limestone is converted to CaO. Carbonation conditions are such that CaO, but not MgO, reacts with CO_2. Therefore, after initial decomposition, dolomite cycles between fully calcined (CaO + MgO) and half-calcined ($CaCO_3$ + MgO) forms while limestone cycles between CaO and $CaCO_3$. The "excess" pore volume created by $MgCO_3$ decomposition during initial calcination is believed to be responsible for the favorable reaction properties.

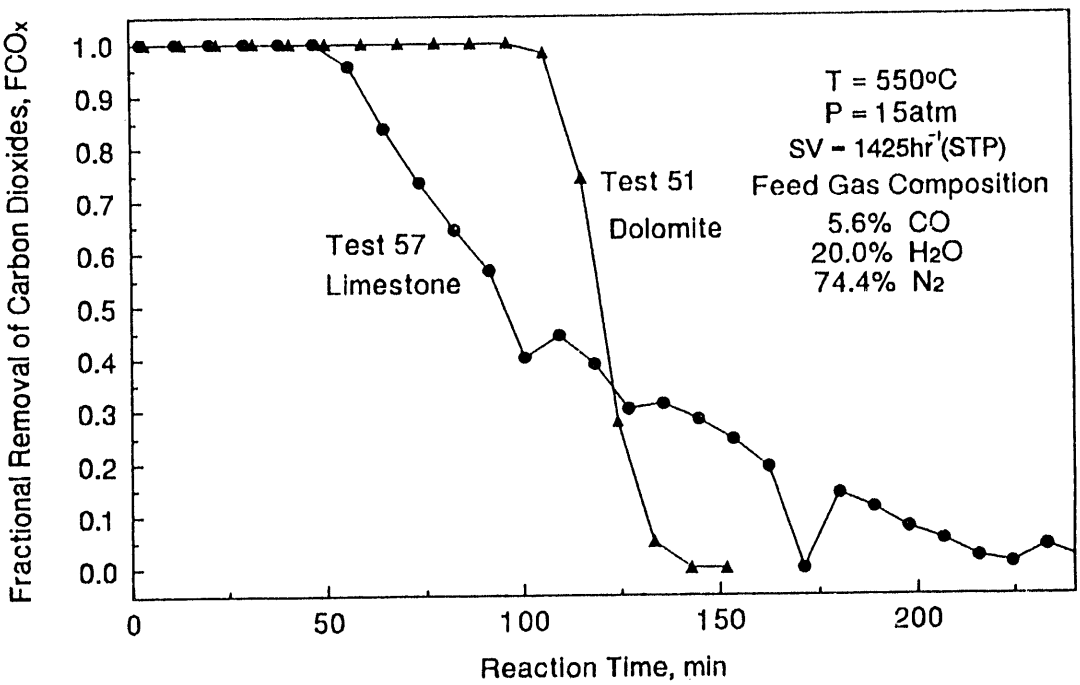

Figure 2. Comparison of the Performance of Dolomite and Limestone Sorbent Precursors

In a similar manner, a gradual change in structural properties caused by sintering is the suspected cause of the gradual deterioration in sorbent performance observed in multicycle tests (see subsequent discussion).

Calcination

Calcination at the mildest possible conditions is important if sintering is to be minimized and sorbent durability increased. All of the calcination experiments discussed in this paper were carried out at 750°C and 3.3 atm of N_2. At lower temperatures, the calcination rate is too small to be of interest while presently available data indicates more rapid sorbent deterioration at higher calcination temperature. Process analysis, however, suggests that, in order to reduce the required flow rate of calcination sweep gas, it is desirable to operate at more severe calcination conditions. Therefore, the final choice of calcination conditions must balance the conflicting considerations of sorbent durability and sweep gas flow rate.

Shift/Carbonation Temperature and Pressure

Choice of the optimum temperature for the shift and carbonation reactions also represents a balance between equilibrium and kinetic factors, and the desired extent of carbon oxide removal. Since both the shift and carbonation reactions are exothermic, higher temperature has an adverse effect on both equilibrium CO conversion and CO_2 removal. Experimental results shown in Figure 3 indicate that the kinetics during the prebreakthrough period are sufficiently rapid that equilibrium is closely approached at temperatures equal to or greater than 500°C. Minimum prebreakthrough CO and CO_2 concentrations of 3 and 35 ppm, respectively, at 500°C correspond, as shown in the upper portion of Figure 3, to 0.999 fractional carbon oxide removal. This figure also shows that greater

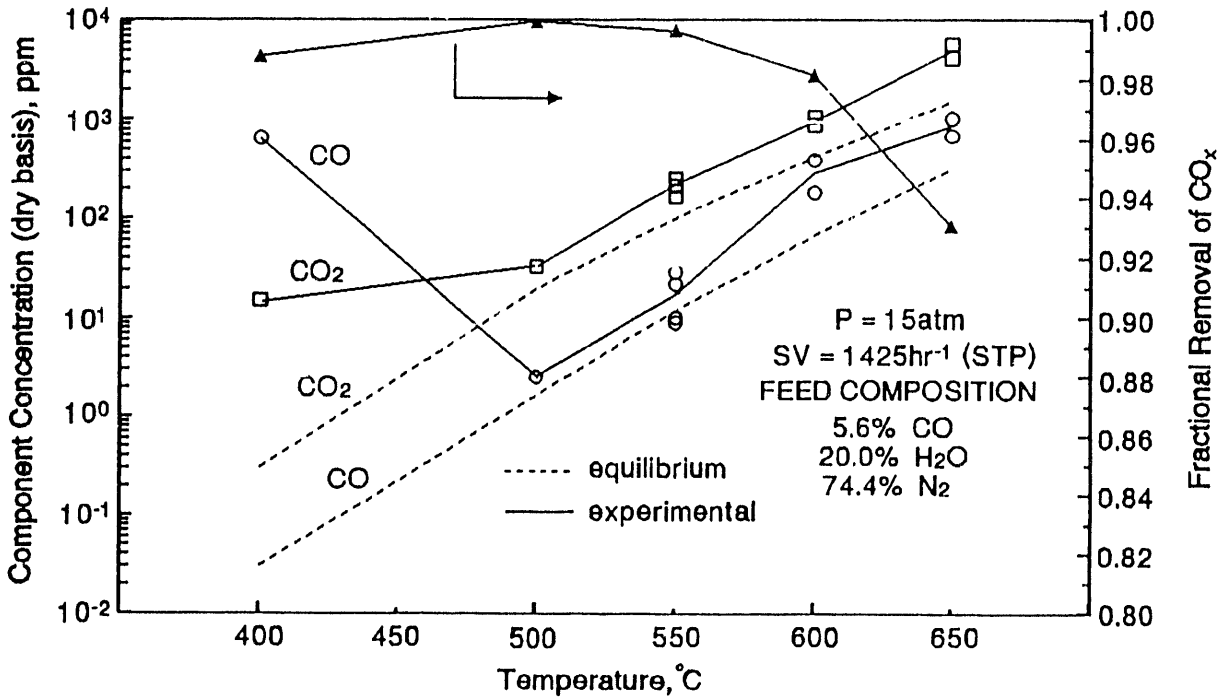

Figure 3. Prebreakthrough CO and CO_2 Concentrations as a Function of Temperature

than 0.995 fractional carbon oxide removal can be achieved throughout the temperature range of 450 to 550°C at these reaction conditions.

Data from multiple runs at the same reaction conditions are included in Figure 3 to provide evidence of the level of reproducibility which can be achieved. Some variation in the CO and CO_2 concentrations is evident, but there is no difference in the fractional removal of total carbon oxides between any of the duplicate tests.

Although the data at this time is limited, it does not appear that the shift-carbonation temperature has an important effect on multicycle durability. This is not surprising, as one would expect sintering to occur primarily during the calcination phase which operates at higher temperature.

While none of the experimental tests have exceeded 15 atm pressure, we expect the single-step process to be even more favorable at higher pressure. Equilibrium CO and CO_2 concentrations decrease with increasing pressure, and experimental results at 15 atm were significantly better than those at 5 atm. The prebreakthrough CO and CO_2 concentrations were both 4 to 5 times greater at the lower pressure.

Feed Gas Composition

In several tests, including those illustrated in Figures 2 and 3, the reactor feed contained only CO, H_2O, and N_2 diluent. This feed gas simplified the operation of the reactor system, and the presence of CO_2 in the reactor product provided conclusive evidence of the occurrence of the shift reaction. In other tests, such as illustrated in Figure 1, the feed gas contained all the major components of synthesis gas -- CO, CO_2, H_2, and H_2O. It is difficult to make a direct comparison of results from the two different feed types because both the total carbon oxide feed rate and the H_2O to CO ratio in the feed gas were different. However, the fractional carbon oxide removal from the

complex gas was generally comparable to that achieved when using the simple gas mixture.

The H_2O to CO ratio is the feed gas is an important parameter. The addition of excess steam promotes the shift reaction, but is also a significant cost item. Figure 4 shows prebreakthrough CO and CO_2 concentrations from a series of tests in which the feed gas contained all major components of a synthesis gas. The ratios of CO, CO_2, and H_2 for the Figure 4 tests are representative of a Texaco gas, with the quantity of steam determined by the desired H_2O to CO ratio. The large concentration of diluent N_2, which, of course, is not representative of a Texaco gas, is simply a requirement of the laboratory reactor.

The prebreakthrough CO_2 concentrations shown in Figure 4 are in the 200 to 250 ppm range, and are comparable to the CO_2 concentrations obtained using the simpler feed gas at equivalent reaction conditions. However, the minimum CO concentration of 90 ppm is significantly larger than the approximately 20 ppm achieved with the simpler feed gas. Nevertheless, the total fractional removal of carbon oxides increased from 0.993 to 0.997 to 0.998 as the H_2O to CO ratio increased from 2.0 to 3.0 to 4.0. The total fractional removal of carbon oxides using the simpler feed gas having a H_2O to CO ratio of 3.57 and otherwise equivalent reaction conditions was 0.997.

Space Velocity

All tests described to this point utilized a space velocity of 1425 hr^{-1} (STP). Because space velocity is such an important parameter in determining reactor size, and therefore cost, a series of tests using the simpler gas composition was carried out in which the space velocity was varied from 885 to 3400 hr^{-1} (STP). Prebreakthrough CO and CO_2 concentrations, as well as fractional removal of total carbon oxides are shown in Figure 5. The concentrations of CO and CO_2 change only marginally with space velocity, which indicates that the global reaction rates are sufficiently large to permit equilibrium

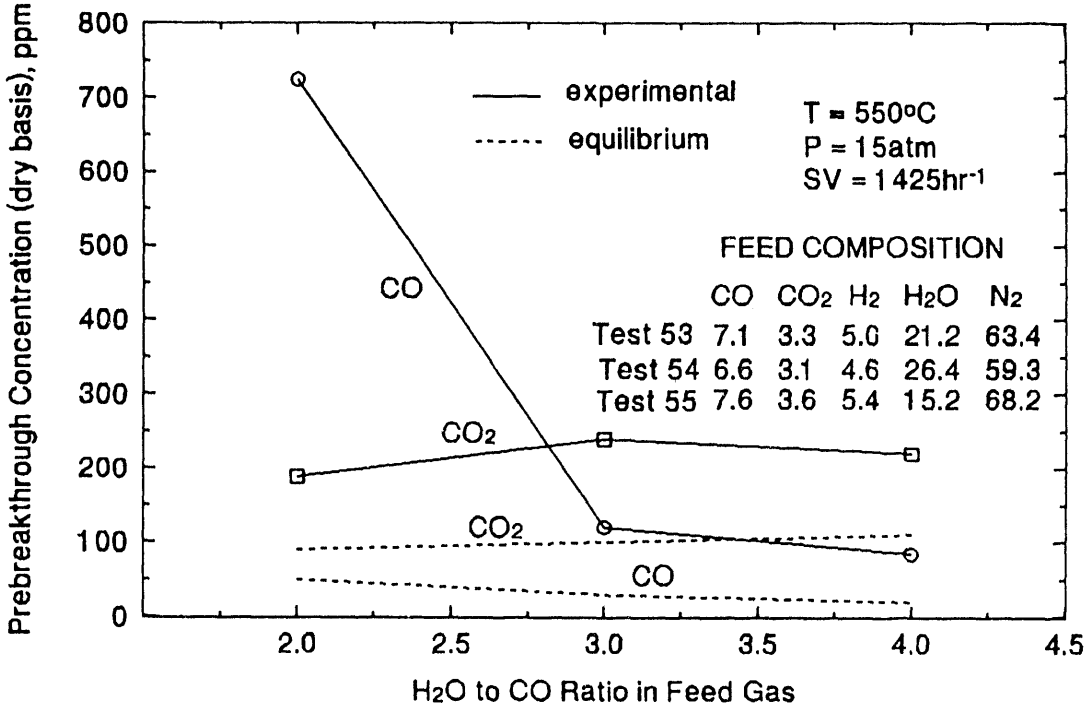

Figure 4. Prebreakthrough CO and CO_2 Concentration as a Function of H_2O to CO Ratio

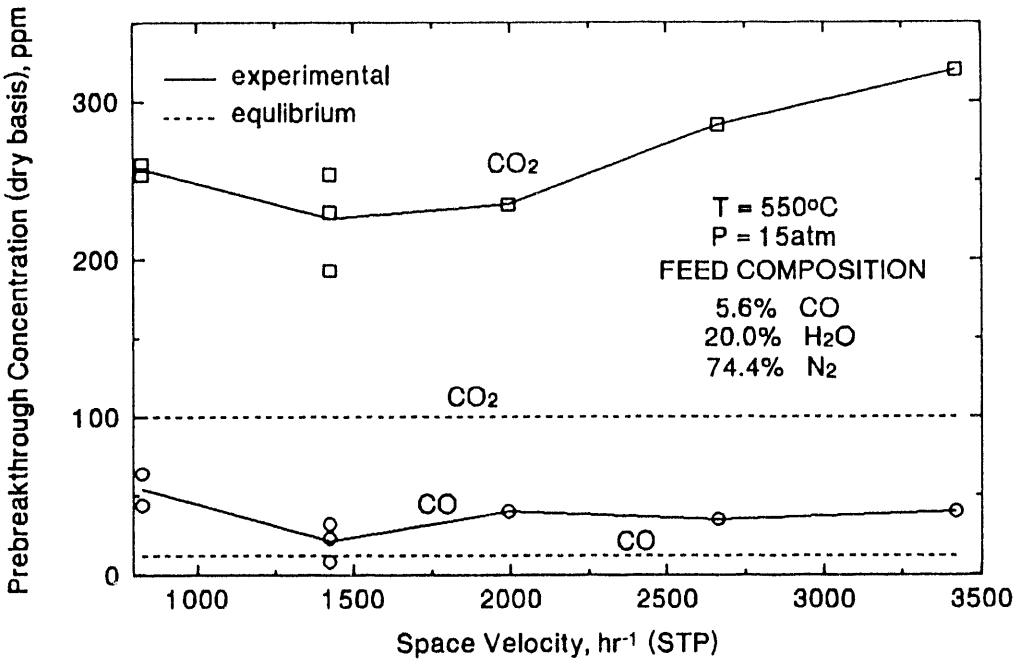

Figure 5. The Effect of Space Velocity of Prebreakthrough CO and CO_2 Concentrations

to be closely approached at all conditions. All concentrations shown in Figure 5 correspond to fractional carbon oxide removals of 0.995 or greater.

The Nature of the Shift Reaction

The driving force which causes the shift reaction is not clear. In commercial operation, where the temperature is from 150 to 200°C lower than the temperature of primary interest for the single-step process, a heterogeneous catalyst is required. The literature contains little information on the shift reaction at 500°C or above. Does the shift reaction at higher temperature occur homogeneously in the gas phase, or is a heterogeneous catalyst necessary? If a catalyst is required, what material in our system serves as the catalyst? In an attempt to learn more about the nature of the high temperature shift reaction, a number of special tests were carried out. These tests ranged from the use of an empty reactor to packing the reactor with a commercial iron-cobalt shift catalyst obtained from United Catalysts, Inc.

Fractional conversions of CO via the shift reaction at conditions where no carbonation could occur are shown in Figure 6. The results are surprising and, at this time, we are unable to explain the variation. Compared to the equilibrium fractional CO conversion of 0.91, the experimental fractional conversion ranged from 0.26 using the empty reactor to 0.87 when the reactor was packed with Al_2O_3. The low conversion using the empty reactor suggests that a catalyst is required if the shift conversion is to approach equilibrium, and that the stainless steel reactor surfaces do not serve as the primary catalyst. The fact that shift conversion in the test using Al_2O_3 exceeded the conversion with the shift catalyst is particularly surprising, since we have not found any references in the literature which claim Al_2O_3 to be a shift catalyst. The performance of the shift catalyst is likely far from optimum because of the higher

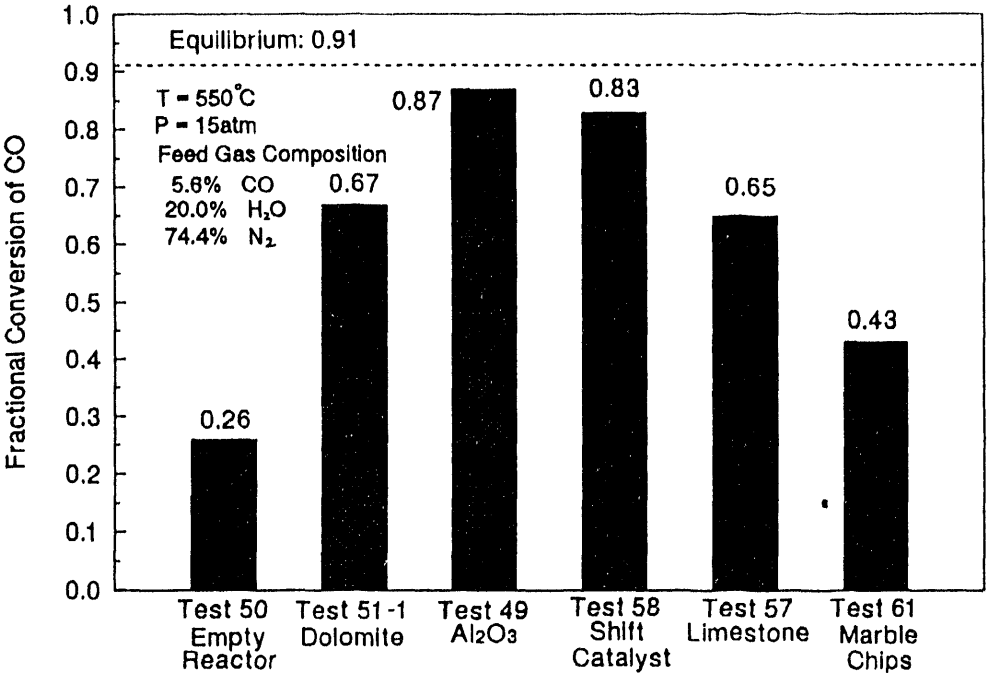

Figure 6. Fractional CO Conversion Via the Shift Reaction Without CO_2 Removal

reaction temperature. The experimental evidence suggests that H_2 formed by the shift reaction reduces the iron in the catalyst to a lower oxidation state.

Fractional shift conversion during the three tests (51-1, 57, and 61) in which the reactor contained a CO_2 sorbent is based on reactor product composition during the postbreakthrough period when the rate of carbonation is effectively zero. These results are also confusing in that MgO has been reported by a number of authors including Rofer-De Porter (1984) to be a shift catalyst. Yet the fractional shift conversion using limestone, which contains MgO only as an impurity, and dolomite, where MgO is a major component, were effectively equal.

However, in spite of the lack of a clear understanding of the nature of the shift reaction, it is clear that the reaction does occur at a rate sufficiently fast for equilibrium to be closely approached during the prebreakthrough period.

Multicycle Tests

One key to ultimate commercial interest in the single-step process is sorbent durability. Although dolomite is readily available and inexpensive, it must retain activity through a large number of calcination-carbonation cycles. Current experimental effort is concentrating upon multicycle runs under a variety of reaction conditions. At this time, a number of five cycle tests and one test lasting for 11 cycles have been completed.

Figure 7 compares the prebreakthrough CO and CO_2 concentrations and fractional removal of carbon oxides during the prebreakthrough period as a function of cycle number for two multicycle tests at equivalent reaction conditions. CO concentrations were consistently in the 20 to 30 ppm range for all cycles of both tests while CO_2 concentrations were generally in the 180 to 250 ppm range. These concentrations correspond to fractional removal of total carbon oxides of either 0.996 or 0.997 in each of the 16

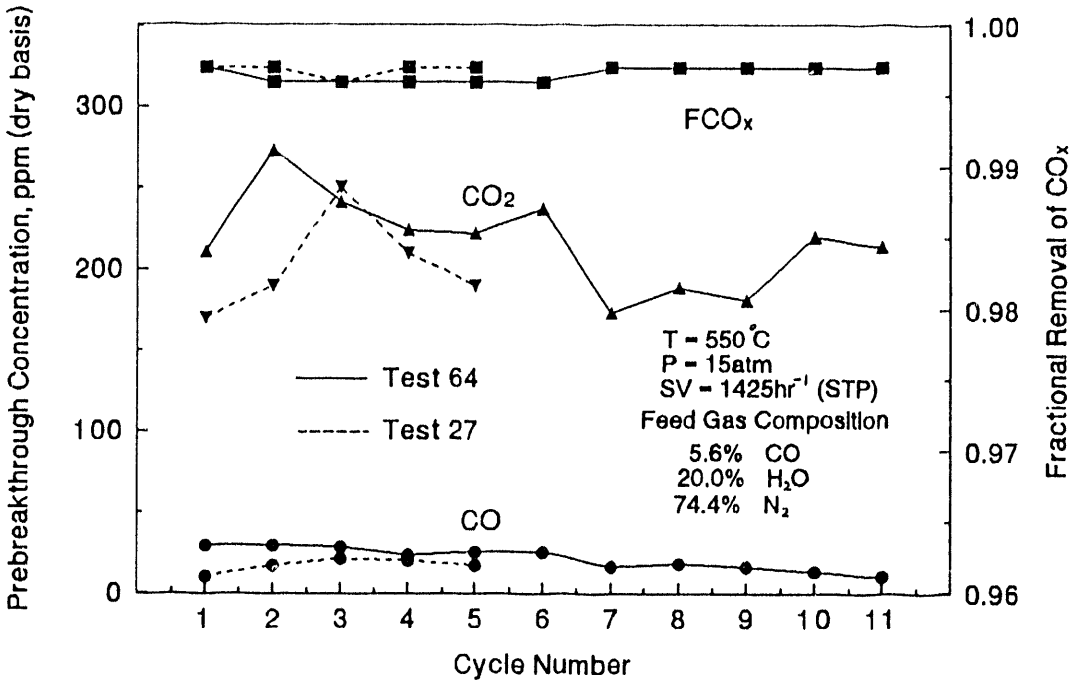

Figure 7. Prebreakthrough CO and CO_2 Concentrations in Multicycle Tests

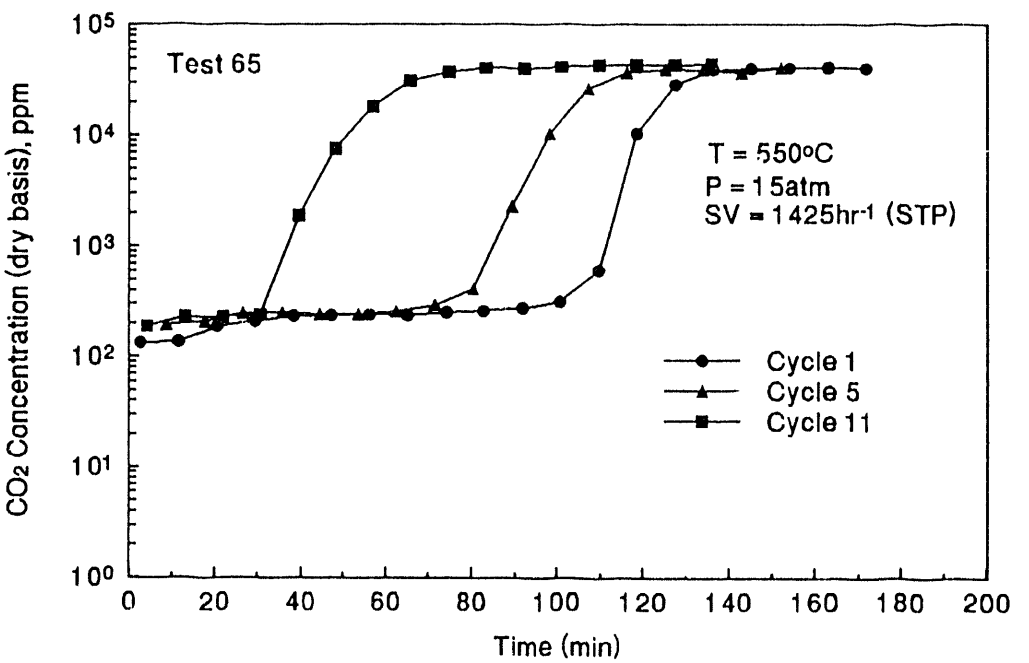

Figure 8. CO_2 Breakthrough Curves in the First, Fifth, and Eleventh Cycles

cycles. Concentration differences between the first five cycles of the two runs are attributed to random experimental variation. The appearance of decreasing CO concentration toward the end of the 11 cycle run is attributed to increasing difficulty in measuring a prebreakthrough steady-state as the number of cycles increased.

In spite of the fact that prebreakthrough concentrations did not increase in multicycle runs, sorbent deterioration must be considered when evaluating the single-step process. Deterioration manifests itself in a continuing decrease in the duration of the prebreakthrough steady-state and a decrease in the slope of the breakthrough curve. The problem is illustrated in Figure 8 where CO_2 breakthrough curves for the first, fifth, and eleventh cycles are compared.

FUTURE WORK

The project is scheduled to end in October 1994, and we are in the process of finishing the planned sequence of multicycle tests. METC has initiated an internal process analysis study of the single-step process under the direction of Dr. George Lee. This study uses Aspen simulation to construct a process flow sheet, to perform material and energy balance calculations, and to carry out a preliminary economic evaluation.

REFERENCES

Barin, I., Knacke, O., and Kubaschewski, O., 1977, Thermochemical Properties of Inorganic Substances, Springer-Verlag, Berlin.

Harrison, D.P., Han, C., and Silaban, A., 1993, A Calcium Oxide Sorbent Process for Bulk Separation of Carbon Dioxide. IV, Proceedings of the Symposium on Coal Fired Power Systems '93, Morgantown, W.V., DOE/METC-93/6131, p. 335.

Rofer-DePoorter, C., 1984, Untangling the Water Gas Shift from Fischer-Tropsch, in Catalytic Conversions of Synthesis Gas and Alcohols to Chemicals, R.G. Herman, ed., Plenum Press, p. 97.

P7 COMPCOAL™: A Profitable Process for Production of a Stable High-Btu Fuel from Powder River Basin Coal

CONTRACT INFORMATION

Cooperative Agreement	DE-FC21-93MC30126
Contractor	Western Research Institute P. O. Box 3395 Laramie, Wyoming 82071-3395 307-721-2011
Contractor Project Manager	Verne E. Smith
Principal Investigator	Norm W. Merriam
METC Project Manager	Dr. Madhav R. Ghate
Period of Performance	February 2, 1993 through February 1, 1994

BACKGROUND INFORMATION

Western Research Institute (WRI) is developing a process to produce a stable, clean-burning, premium fuel from Powder River Basin (PRB) coal and other low-rank coals. This process is designed to overcome the problems of spontaneous combustion, dust formation, and readsorption of moisture that are experienced with PRB coal and with processed PRB coal. This process, called COMPCOAL™, results in a high-Btu product that is intended for burning in boilers designed for midwestern coals or for blending with other coals.

PRB coal is relatively dusty and subject to self-ignition compared to bituminous coals. Dried (or processed) PRB coal is even more susceptible to spontaneous combustion than the raw coal. Also, PRB coal dried at low temperature typically readsorbs about two-thirds of the moisture removed by drying. This readsorption of moisture releases the heat of adsorption of the water which is a major cause of self-heating of low-rank coals at low temperature. PRB coal, and other low-rank coals, tend to be highly reactive. These reactive coals must be mixed regularly (every week or two) when fresh. However, they become somewhat more stable after they have aged for several weeks.

Low-temperature oxidation reduces the heating value of the coal, makes the coal less able to repel moisture (hydrophobicity), and is known to increase the unburned carbon remaining in the ash. Ingram and Rimstidt (1984) attribute increased moisture in naturally oxidized coals to increase in surface area caused by the physical effects of weathering and an increase in hydrophilic functional groups able to chemisorb water (organic acids are known to attract water to coal particles). Water molecules are generally thought to attach to polar oxygen sites in coal (this varies greatly with different types of coal).

Many efforts have been made to overcome these problems of dust formation and self-heating while keeping the cost of processing within the very competitive limits of the markets for coal. The University of North Dakota Energy Research Center has explored the use of various drying techniques to upgrade low-rank coals (Willson et al. 1987). They found that coals dried at low temperature readsorb moisture after cooling and return to essentially the original equilibrium moisture level. In contrast, they found that the processes using temperatures high enough to alter the structure of the coal particles resulted in reduced readsorption of moisture. They also concluded that the lowered equilibrium moisture levels resulted from the rejection of carbon dioxide by the decarboxylation reactions which occur during high- temperature drying. (The readsorption of moisture by coals dried at temperatures lower than a few hundred degrees Fahrenheit and reduction of equilibrium moisture in coals dried to about 500 to 700°F (260 to 316°C) is consistent with WRI experience, (Boysen et al. 1990).

A drying process was developed for PRB coal during the early 1980s. Initial work was done by Anaconda Minerals Co., later joined by Atlantic Richfield Co., using a 4 ton/hr pilot plant at Tucson, Arizona. The process has been licensed to Kaiser Engineers. The process uses fluidized-bed drying in conventional equipment with a proprietary product treatment step (Skinner et al. 1984). The developers conducted laboratory research to determine methods to avoid low-temperature oxidation of the product. They developed methods using cooling, controlled preoxidation, treatment with carbon dioxide, and spray application of oil or chemical solution.

Koppelman was awarded patents (U.S. Patents 4,728,339 and 5,071,477) for use of "temperatures from 200 to about 1200°F, pressures from 300 up about 3000 psig, and residence times of 1 minute to 1 hour to process organic carbonaceous materials to effect a desired physical and chemical modification thereof...whereby a substantial reduction in the residual moisture content...to improve physical properties including an increased heating value." The second patent describes the use of steam at high pressure to effect a controlled thermal restructuring, with the upgraded product possessing increased heating values. These patents are the basis for the K-Fuel® process.

Lien (1991) discusses the problems and progress AMAX has experienced with a McNally Pittsburgh dryer at the AMAX Belle Ayr mine. In this process, coal is dried by contact with a hot stream of fluidizing gas. The gas is comprised partly of flue gas from combustion of coal dust with air and partly from recycled gas. The hot drying gas contains less than 5% oxygen. The dried coal, which contains 12 to 13 wt % moisture, enters the cooler at a temperature of 180 to 190°F (82 to 88°C) where it is cooled to about 100°F (38°C) by contact with air. The cooled product is mixed with 2 to 4 gallons of number 6 fuel oil per ton to control product dustiness and help inhibit readsorption of moisture. Lien (1991) discusses the problems of upsets in the process caused by loss of feed and the experience with degradation of particles in the dryer. He also states that a major concern has been the stability of the product.

The Syncoal process is used at a Clean Coal I demonstration plant located at Western Energy Company's Rosebud mine near Colstrip, Montana. In the process, coal is passed through two vibrating fluidized-bed reactors where it is contacted by hot gas to dry the coal and remove carboxyl groups and volatile sulfur compounds. The dried coal is further desulfurized by pneumatically stratifying the product to separate pyrite-rich ash (Western Energy Company 1992).

The Carbondry process (Simmons and Simmons 1992) has been tested at the pilot-plant scale at Carbontec's facility at Bismarck, North

Dakota. The process involves a hot oil first stage drying unit and a flue gas drying unit. The process uses a coating of oil on the surface of particles to protect against readsorption of moisture and spontaneous heating. Published data indicate that the product made from PRB coal using the process contains about 6 to 10 wt % moisture and has a heating value ranging from 11,200 to about 11,700 Btu/lb.

The ENCOAL LFC process is used at a commercial demonstration facility located at Triton Coal Company's Buckskin mine north of Gillette, Wyoming (McPherson 1992). In the process, coal is roasted to drive off moisture, coal liquids, and sulfur compounds. The plant, which was built using an award from Clean Coal III, produces a crude coal liquid and solid process derived fuel.

Numerous mechanical treatments are available for stabilizing coal products by reducing the surface contact with air.These include briquetting, pelletizing, and extruding with or without an added binder. An excellent list of references describing the use of a binder in pelletizing is given in U.S. Patent 4,615,712 (Wen), which describes the production of humic acid from oxidation of coals or leonardite and the use of the humic acid as a binder.

It is relatively easy to develop a process to drive the moisture from PRB coal. It is considerably more challenging to develop a process which can remove the moisture from the coal, alter the coal structure to minimize readsorption of moisture, and prevent oxidation and spontaneous combustion of the finished product. We have dried coal and done partial decarboxylation in our past work (Merriam et al. 1990). Drying minus 8 mesh PRB coal in a fluidized-bed reactor at atmospheric pressure results in all of the moisture being removed when the temperature of the coal in the bed reaches 350°F (177°C) (Figure 1).

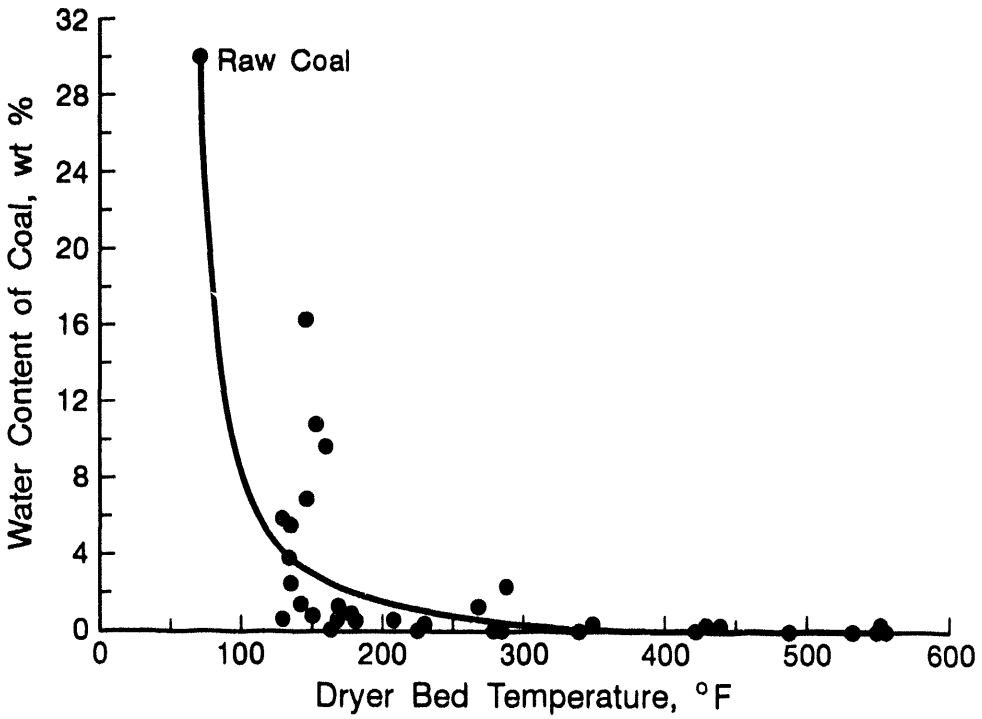

Figure 1. Drying Curve for Minus 8 Mesh PRB Coal Using Various Flow Rates of Fluidizing Gas

Continued heating of the coal as it moves along the cross-flow bed results in the partial decarboxylation, which removes oxygen from the coal in the form of carbon dioxide and carbon monoxide along with some methane (Figure 2). This removal of oxygen increases the heating value of the product and it has been reported to reduce the susceptibility of the coal to spontaneous heating (Tomuro et al. 1985). However, our experience with PRB coal treated in this manner is that the coal is highly reactive and is frequently observed to ignite spontaneously. The coal is most susceptible to self-ignition when it has been freshly processed. Dried coal which has been aged for several weeks (and which has contacted air) is less likely to self-ignite.

Early attempts at WRI to stabilize dried coal (Boysen et al. 1990) were focused upon heating the coal to a slightly higher temperature to reduce the tendency to readsorb moisture (Figure 3). This work, which was done using minus 28 mesh PRB and Usibelli coals in a fluidized-bed reactor, indicates that the equilibrium moisture can be reduced to about 13 wt % by heating the coal to about 700°F (371°C) (Thomas, K.P., personal communication, memorandum dated December 16, 1991). However, it is necessary to heat the coal to about 1100°F (593°C) to reduce the equilibrium moisture to about 10 wt %. The coal tars become mobile in PRB coal at temperatures just above 600°F (316°C). So much loss of liquids would occur if the coal is heated to 1100°F (543°C) in the presence of fluidizing gas.

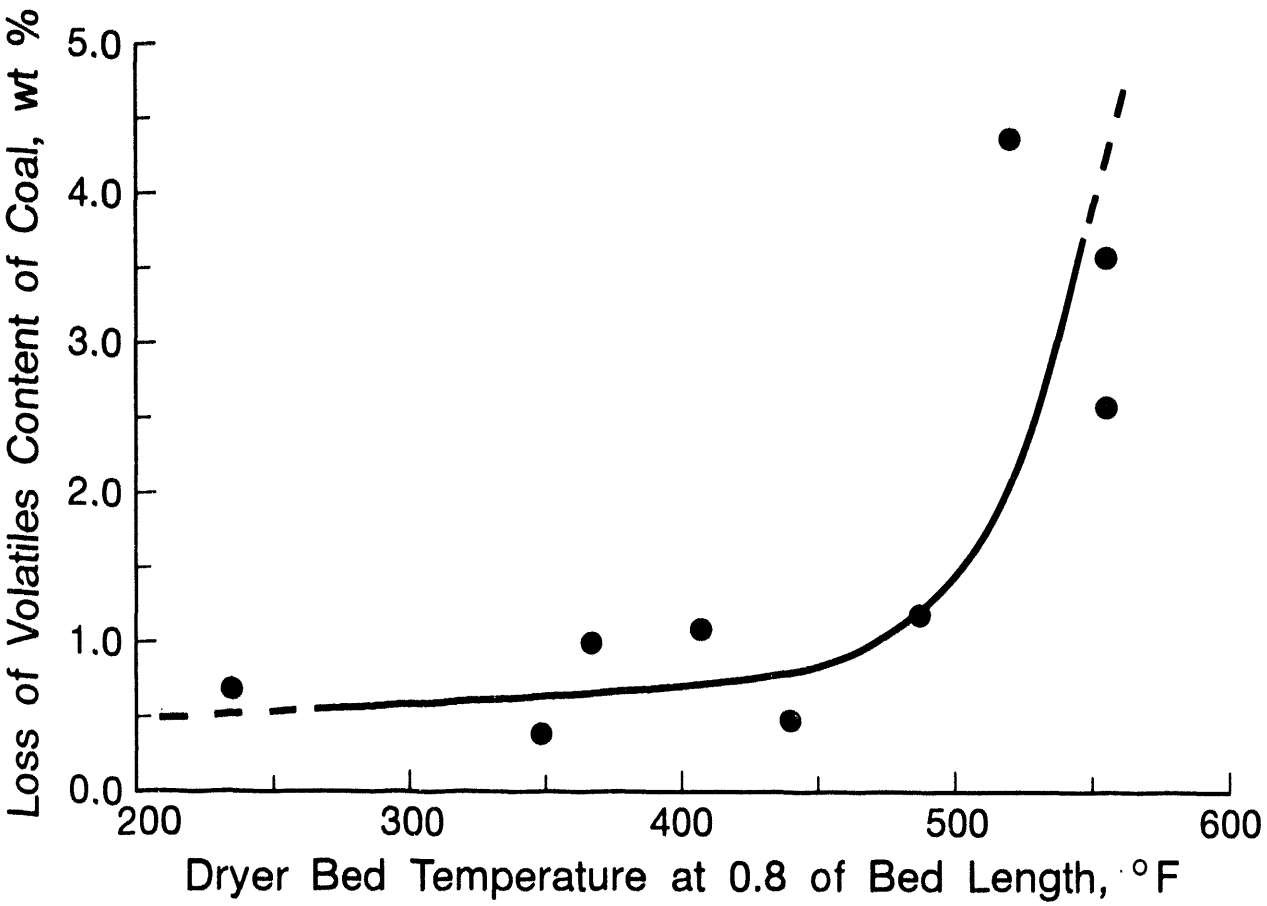

Figure 2. Partial Decarboxylation of Minus 8 Mesh PRB Coal in a Fluidized-Bed Dryer

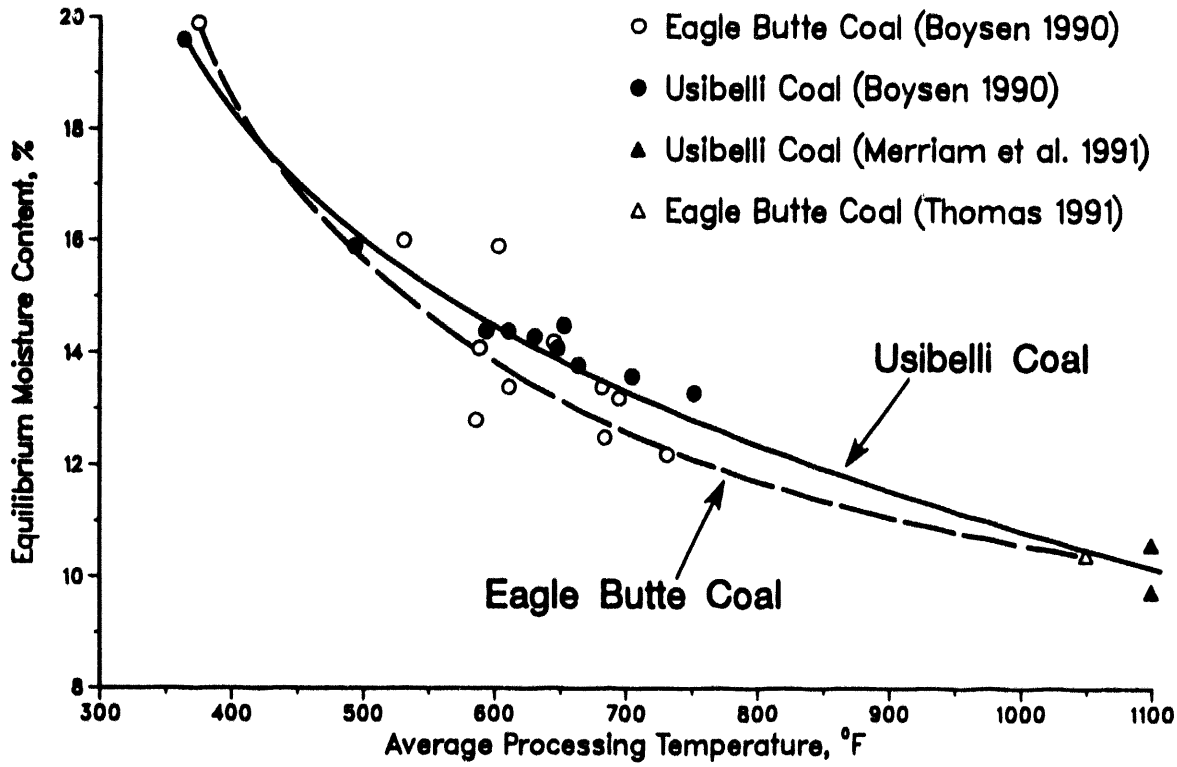

Figure 3. Equilibrium Moisture Content of Coals Subjected to Mild Pyrolysis

We later added a stabilization reactor to the pyrolysis reactor to coat char with the high-boiling fraction of the coal liquids driven from the coal in the pyrolysis reactor (Merriam and Sethi 1992). This work showed that we could further depress the equilibrium moisture to about 8 wt %. (Most of the increase in temperature that starts low-temperature oxidation is caused by the heat of adsorption of water upon the coal particles.)

PROJECT DESCRIPTION

In the COMPCOAL process, sized coal is dried to zero moisture content and additional oxygen is removed from the coal by partial decarboxylation as the coal is contacted by a stream of hot fluidizing gas in the dryer (Figure 4). The hot, dried coal particles flow into the pyrolyzer where they are contacted by a very small flow of air. The oxygen in the air reacts with active sites on the surface of the coal particles causing the temperature of the coal to be raised to about 700°F (371°C) and oxidizing the most reactive sites on the particles. This "instant aging" contributes to the stability of the product while only reducing the heating value of the product by about 50 Btu/lb. Less than 1 scf of air per pound of dried coal is used to avoid removing any of the condensible liquid or vapors from the coal particles. The pyrolyzed coal particles are mixed with fines from the dryer cyclone and dust filter and the resulting mixture at about 600°F (316°C) is fed into a briquettor. Briquettes are cooled to about 250°F (121°C) by contact with a mist of water in a gas-tight mixing conveyor. The cooled briquettes are transferred to a storage bin where they are accumulated for shipment.

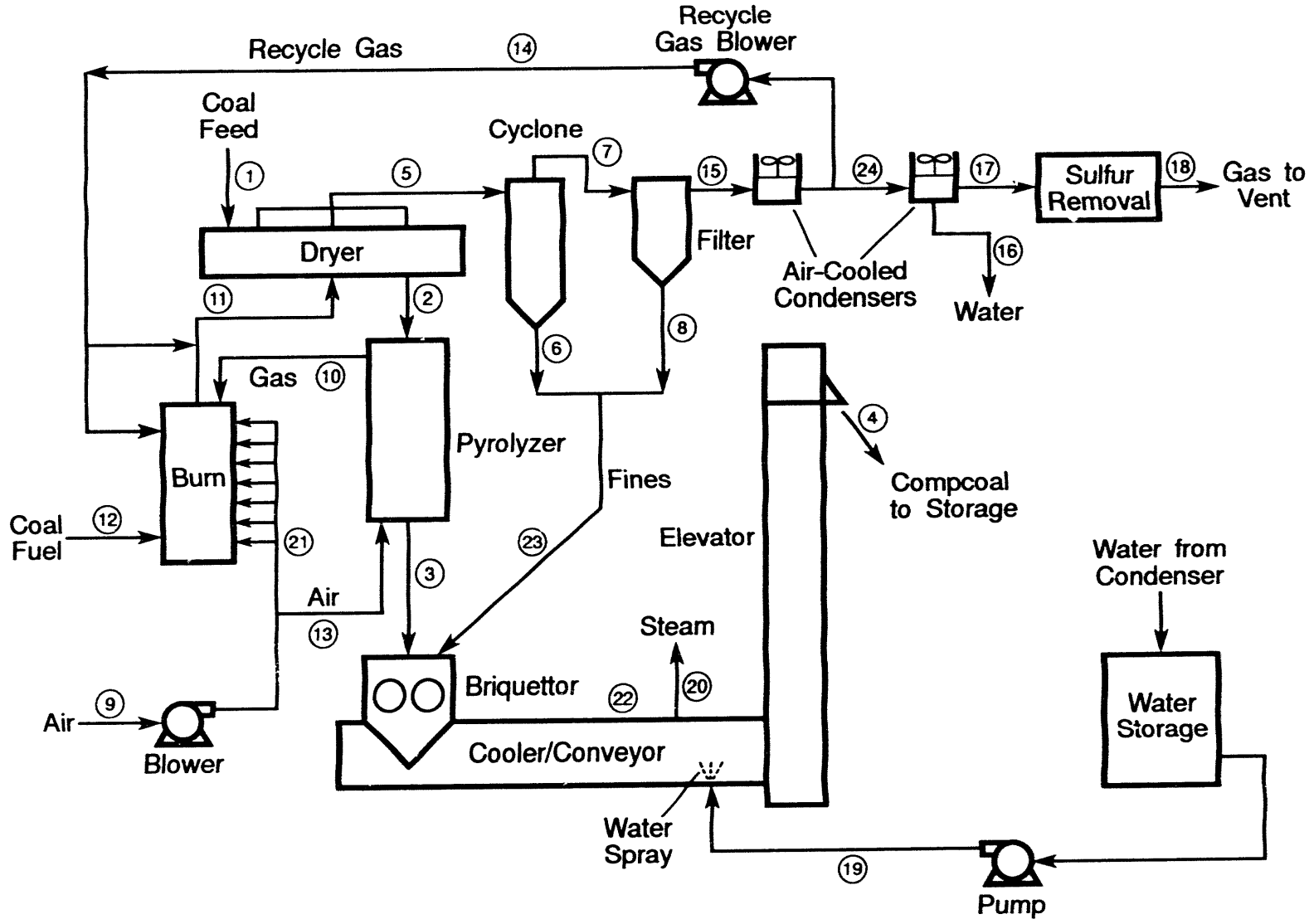

Figure 4. Identification of Stream Flows and Conditions Used to Size Equipment for the COMPCOAL Process

An important feature of the process is the avoidance of pyrolysis in the dryer and use of the onset of pyrolysis in the pyrolyzer to stabilize the particles. In the dryer, where the gas flow rate is high, the coal remains below the temperature at which liquids and vapors are formed. In the pyrolyzer, the temperature is raised to form liquids in the coal particles, but the gas flow is kept low to avoid stripping liquids out of the coal. In this manner, a high flow rate of gas can be used to carry heat into the dryer and subsequently, in the pyrolyzer, the tars in the coal may be melted and refrozen without producing a substantial loss of liquid or vapors from the coal.

A recycle gas stream is used to carry heat into the dryer while limiting the temperature at which fluidizing gas enters the dryer. Heat for drying is produced by burning coal using a low NO_x burner. Vapors from the pyrolyzer are incinerated in the burner. The flue gas is mixed with recycled gas to lower the temperature at which the fluidizing gas enters the dryer. The water is removed from the dryer effluent gas by condensation in air-cooled condensers supplying a nearly dry stream for sulfur removal. The water from the condensers is sprayed onto the hot COMPCOAL briquettes in the cooling conveyor where the water is converted into steam.

The process we describe herein is not yet optimized. For example, if we can tolerate a wet gas stream into the sulfur removal unit, then one of the air-cooled condensers is not needed and only the recycle portion of the dryer effluent gas needs to be cooled.

WRI has experience with the drying portion of the process using minus 8 mesh PRB coal at feed rates of 90 to 150 lb/hr in tests lasting from 24 to 120 hours (Merriam et al. 1990). The pyrolysis (stabilization) portion of the process is presently being developed using a batch, laboratory-scale reactor. We plan next to conduct tests using a continuous-flow, bench-scale reactor.

RESULTS

This section describes work conducted during the early part of 1993 by WRI to develop an effective method to stabilize dried coal.

Self-Heating and Oxidation

We conducted numerous tests to determine how much various treatments affect the self-heating and low-temperature oxidation tendencies of raw and processed PRB coal. Samples were evaluated by contacting the coal or processed coal with oxygen saturated with water vapor at a temperature of 122°F (50°C) in an adiabatic chamber (Figure 5). The test results are evaluated graphically by plotting the temperatures in the samples versus time. The intersection of the slope of the initial heating curve and the slope of the curve after the temperature has started to rise is used as the time to ignition. Tests are continued until the inflection point in the heating curve is defined or until the test has continued for 24 hours. Our experience has shown that an inflection point in the heating curve rarely develops after 24 hours of heating using this method. The results of the self-heating tests (Table 1) are used to compare the effectiveness of different processing conditions.

The tests to study the effects of temperature and oxygen on the self-heating of dried PRB coal were conducted using a small, stirred autoclave which is heated by immersion in a heated bed of fluidized sand (Figure 6). Samples of coal, which had been dried in a fluidized bed to 550°F (288°C) were split into 50-gram aliquots inside a nitrogen filled glove box to avoid contact with air. The aliquots were transferred into the reactor inside the glove box. The autoclave was then assembled and the gas pressure was cycled from 0 to 60 psig three times to flush unwanted gas from the reactor. The autoclave was then lowered into the heated sand for 35 minutes, including about 10 minutes at the desired maximum temperature.

Upon completion of the test the autoclave was removed from the sand bath and immersed in water to rapidly cool the treated coal. Gas samples were obtained for analysis by transfer into evacuated containers. The treated coal was removed from the autoclave in the nitrogen filled glove box and samples were placed in containers under a nitrogen blanket for further analyses.

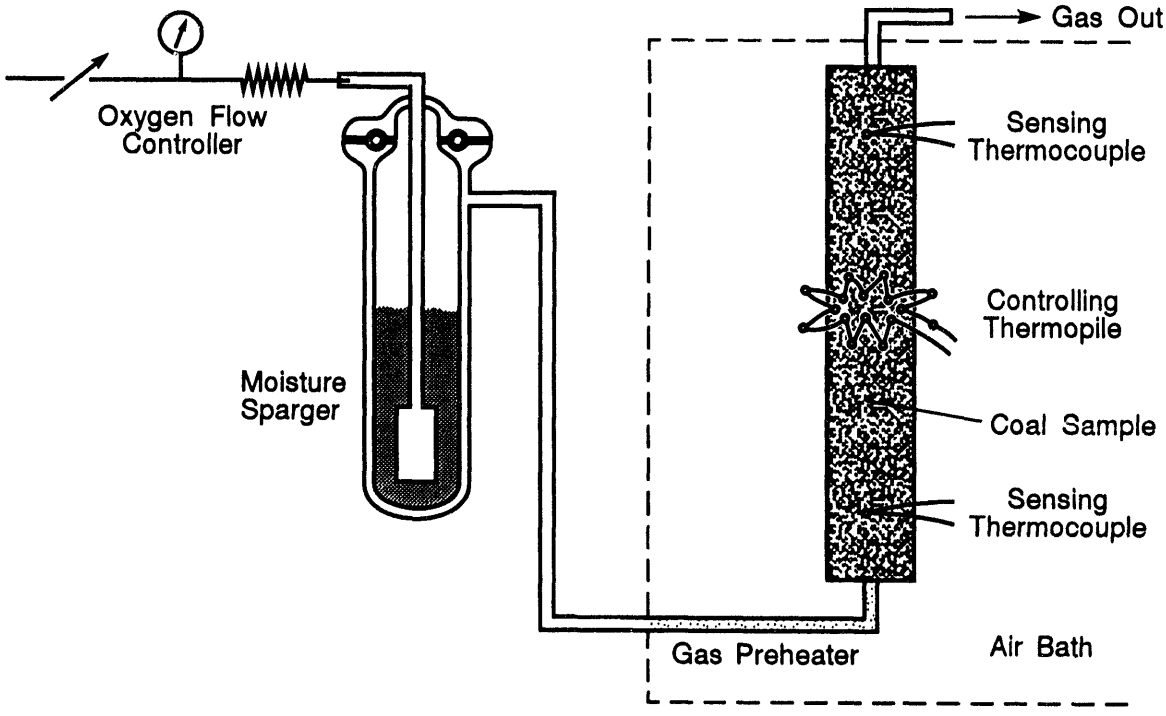

Figure 5. Apparatus Used to Determine the Susceptibility of Coal to Self-Heating and Oxidation

The data in Table 1 show several characteristics and trends which we have used to guide our development of the COMPCOAL process. The section of Table 1 showing "coal dried at various conditions" indicates that coal moved into and out of the drying oven five times (which was incidentally exposed to air) and the sample dried in air both show relatively long ignition times. This pattern of data is an indication that exposure of dried coal to air at 220°F (104°C) results in some resistance to self-heating relative to the coal samples dried in nitrogen.

The samples dried in nitrogen and carbon dioxide show reduced ignition times with increasing temperature over the range of temperatures from 220, 550, 565, and 658°F (104, 288, 296, and 348°C). We therefore conclude that heating the dried coal in inert gas increases the susceptibility to self-heating as the temperature is increased in the range studied. The dried coal which is heated in a small amount of air (at a starting pressure of 0.8 atmospheres at our laboratory) indicates a trend opposite to that shown by heating in nitrogen. The dried coal which is heated in air shows increased resistance to self-heating (longer ignition times) as the temperature is increased from 585 to 703°F (307 to 373°C). The trend when heating in air using a starting pressure of 0.8 atmospheres is not strong, but appears to be real.

Table 1. Time to Ignition for Minus 16 Mesh Raw, Dried, and Processed Coal, hr

	Temperature °F	Duplicate Tests	
Raw Eagle Butte Coal		>24	>24
Coal Dried at Various Conditions			
N_2, 5 times @ 1 hr each	220	17	>24
N_2, 1 time for 5 hr	220	6	8
Air, 1 time for 6 hr	220	24	24
Fluid Bed, CO_2, 5 min (A)	550	4	5
Dried Coal from (A) Heated in N_2			
Batch in Stirred Reactor	565	4	4
Batch in Stirred Reactor	658	2	3
Dried Coal from (A) Heated in 0.8 Atm Air			
Batch in Stirred Reactor	586	4	5
Batch in Stirred Reactor	675	6	5
Batch in Stirred Reactor	692	10	>24
Batch in Stirred Reactor	723	7	8
Dried Coal from (A) Heated in 3.4 Atm Air			
Batch in Stirred Reactor	565	4	6
Batch in Stirred Reactor	675	4	5
Batch in Stirred Reactor	691	14	9
Batch in Stirred Reactor	697	7	8
Batch in Stirred Reactor	708	>24	>24
Batch in Stirred Reactor	732	>24	>24

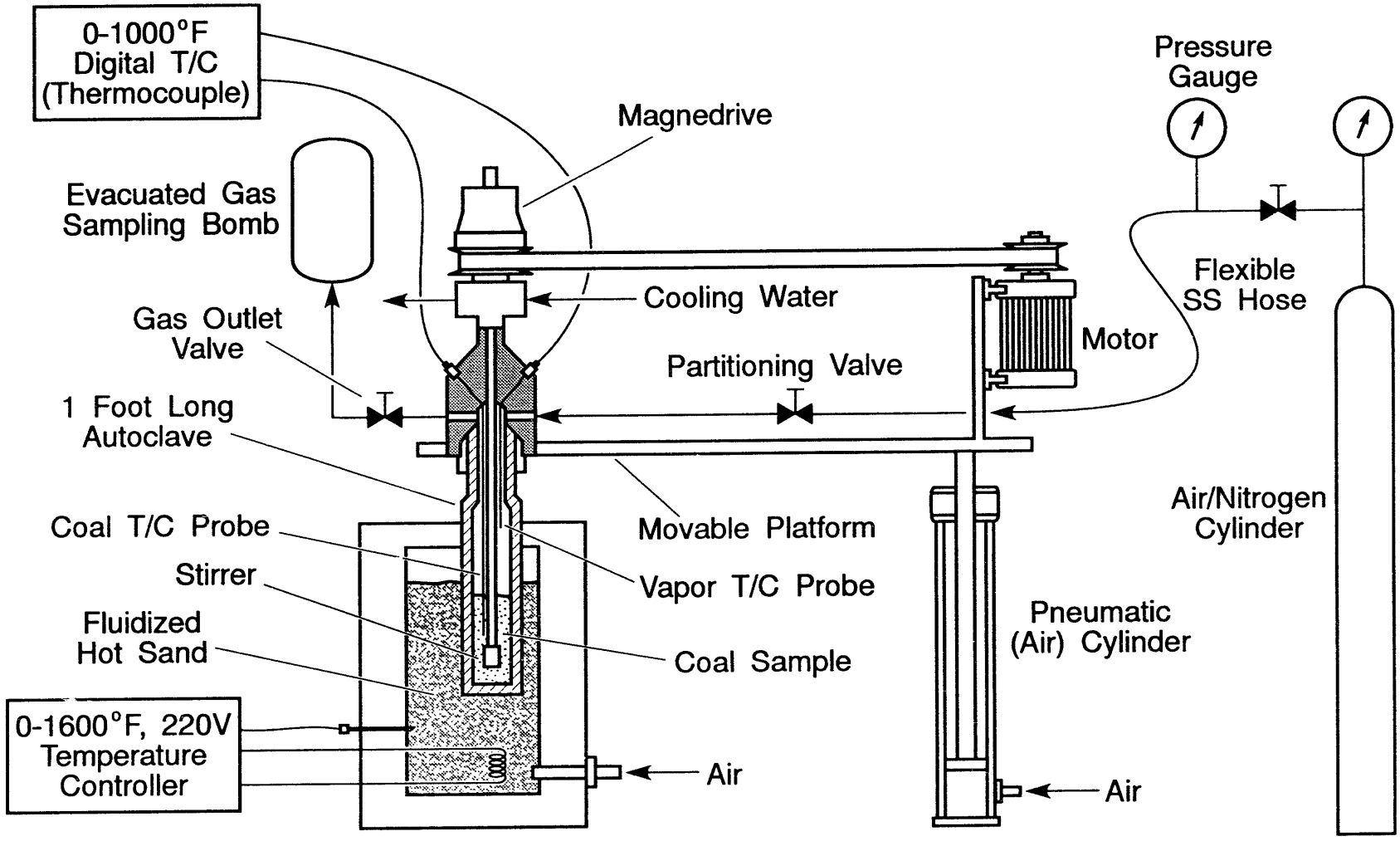

Figure 6. Stirred-Batch Reactor Used to Perform the "Accelerated Aging" Stabilization of Dried PRB Coal

The dried coal which is heated using more air available to react with the coal (a starting air pressure of 3.4 atmospheres) shows a strong and definite trend of increasing resistance to self-heating and oxidation. This last trend is also very sensitive to the temperature of the coal in the stirred bed when the oxygen is reacting with the dried coal (Figure 7). The pattern between the groups (heating in inert gas, heating in 0.8 atmospheres of air, and heating in 3.4 atmospheres of air) also shows a consistent trend of increasing resistance to self-heating and oxidation as the quantity of oxygen available to react with the dried coal is increased.

Tests with air in the stirred, batch reactor with an initial pressure of 3.4 atmospheres show a change in the quantity and composition of gas produced (Figure 8) in the temperature range of the tests. At the lower temperatures a small amount of gas composed of predominantly carbon dioxide, with lesser amounts of carbon monoxide and traces of methane is produced. The volatiles removed at the higher temperatures are mostly noncondensible gases. In the upper part of the temperature range the volume of gas produced is increased greatly and the concentration of the methane and the ethane in the gas increases.

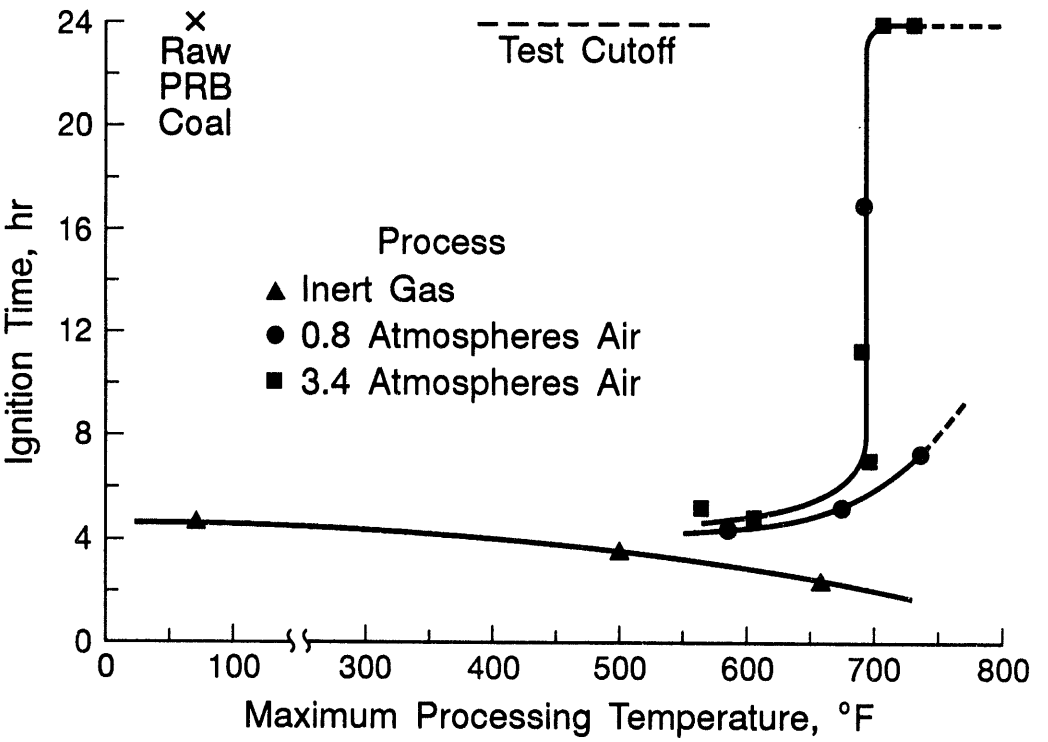

Figure 7. The Effects of Temperature and Oxidation on the Self-Heating Characteristics of Dried PRB Coal

Significantly, no oxygen is detected in the effluent gas, indicating that the oxygen in the air at the start of the tests is completely reacted with the coal. However, the consumption of the oxygen from the air by the coal is more than offset by the oxygen that is removed from the coal by the processing (Figure 9). The carbon dioxide and carbon monoxide emitted from the coal contain many times as much oxygen as is consumed from the air in the reactor.

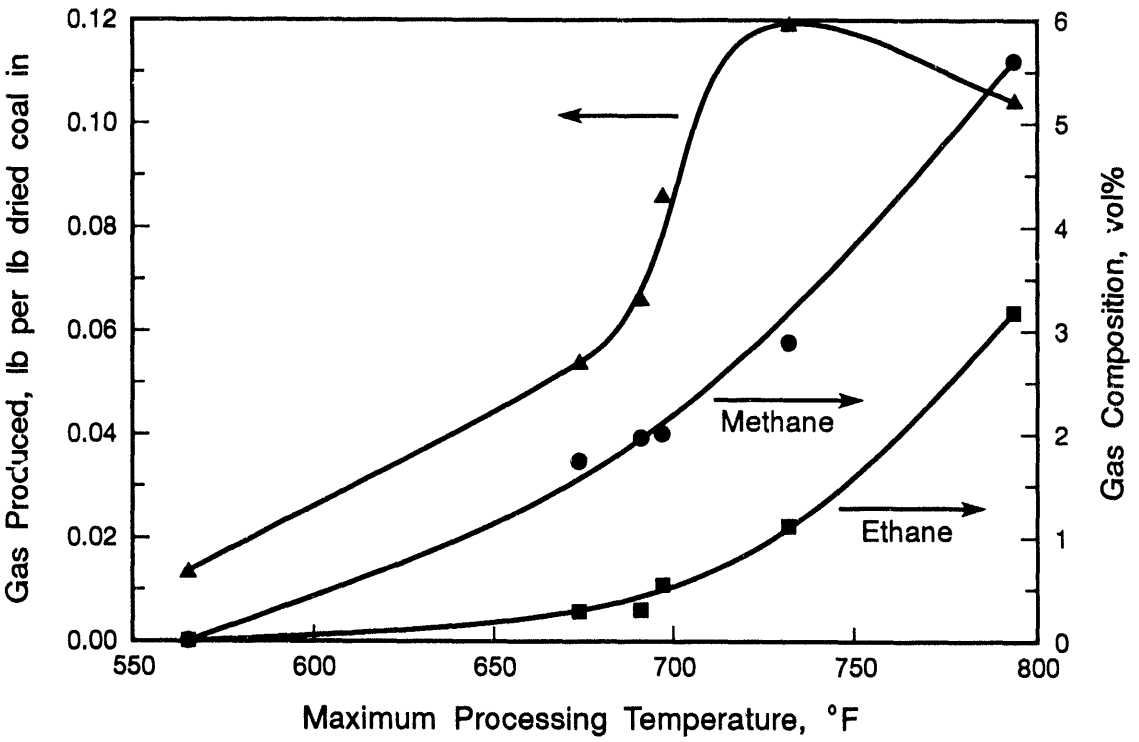

Figure 8. The Change in Composition of Gas Produced at Temperatures Below and Above the Onset of Stabilization

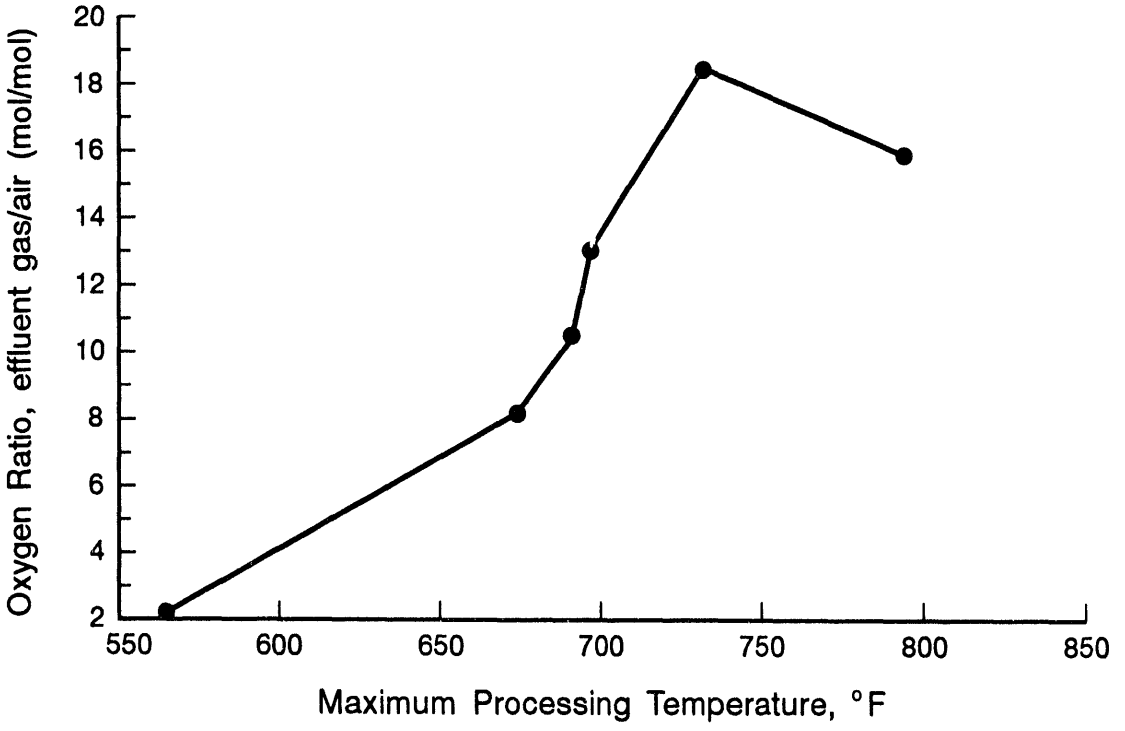

Figure 9. The Oxygen Released from the Coal is Many Times the Oxygen Taken Up by the Accelerated Aging

Readsorption of Moisture

The tendency of processed coal to readsorb moisture is an important characteristic which must be considered as a determinant of the quality of any dried or pyrolyzed coal. We have used the test for equilibrium moisture (ASTM D1412) as a measure of the maximum quantity of water which coal and processed coal can adsorb. The test is actually intended to measure the water content which a coal seam can contain. In the test, coal is crushed to minus 28 mesh and soaked in deionized water for 3 hours. The excess water is then removed from the coal by filtration and the coal is held in a sealed container at 98% relative humidity for 48 hours. The water content of the coal is then determined. We think this test may represent conditions which are somewhat more severe than processed coal may typically be exposed to, but we use it because it is an accepted ASTM procedure, and the test does not appear to overstate the readsorption characteristics of the coal by a large amount.

We use equilibrium moisture as an indication of the stability of the products from the various processing conditions we have tested. Low equilibrium moisture is indicative of a stable processed coal.

The results of our tests (Table 2) show that coal dried to 550°F (288°C) is less susceptible to readsorption of moisture than the raw coal. (However, dried coal, when untreated, is more susceptible to oxidation than raw coal.) Forming the dried coal into briquettes reduces the tendency to readsorb moisture even further, while the accelerated aging at 793°F (423°C) reduces the equilibrium moisture still more.

We have not yet tested the obvious combination of briquettes made from coal treated in the "accelerated aging" process. The beads and sand are included to show that materials having no porosity and nonpolar surfaces have an equilibrium moisture content of about zero.

Table 2. Equilibrium Moisture Content of Eagle Butte Coal, Dried Coal, Briquettes, and Treated Coal, wt %

	Duplicate Tests	
Eagle Butte Feed Coal	25	26
Dried in Air, 6 hr, 220°F	22	22
Fluid Bed Dried in CO_2 to 550°F	17	17
Briquettes Made from Dried Coal	13	9
Briquettes-Dried Coal-10% Fines	14	14
Dried Coal Heated in 3.4 Atm Air and 793°F	10	11
One Millimeter Glass Beads	1	1
Ottawa Sand	0	0

Characteristics of Stabilized Coal

The stabilized coal produced by reacting dried PRB coal with air using the stirred batch reactor contains 35 to 40 wt % volatiles and has heating values of 12,000 to 12,700 Btu/lb (Table 3 and Figure 10).

Table 3. Characteristics of the COMPCOAL Product

Test	11	10	12	6
Temperature, °F	565	691	697	708
Volatiles, wt %	40.2	36.7	35.4	34.5
Heating Value, Btu/lb	12,009	12,439	12,600	12,725

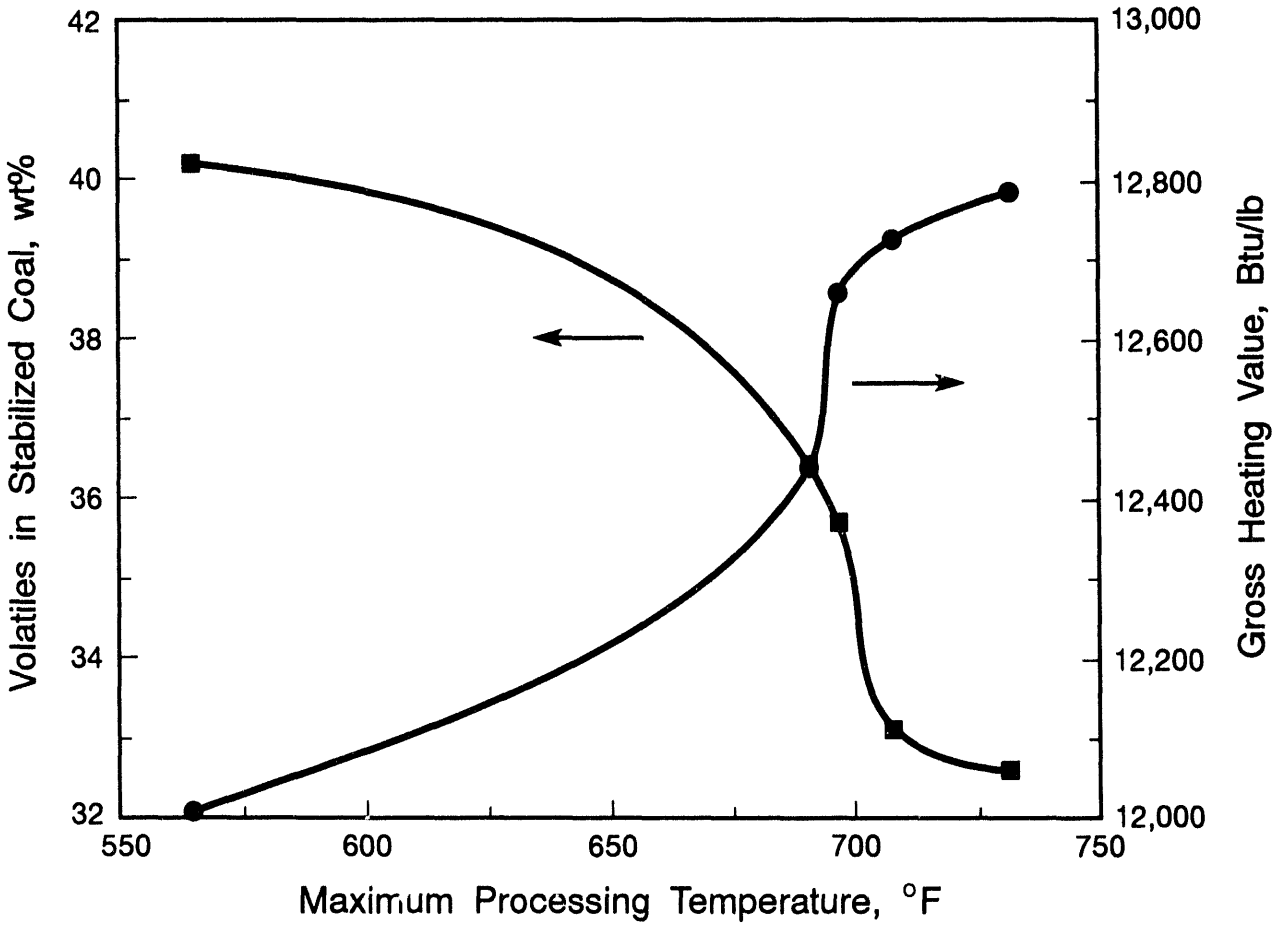

Figure 10. Volatile Content and Heating Value of the COMPCOAL Product

FUTURE WORK

Our report, "COMPCOAL™: A PROFITABLE PROCESS FOR PRODUCTION OF A STABLE HIGH-BTU FUEL FROM POWDER RIVER BASIN COAL" (WRI-93-R008) describes the bench-scale tests which we conducted to prove the process concept. We are presently seeking support to continue development of the process.

REFERENCES

Boysen, J.E., C.Y. Cha, F.A. Barbour, T.F. Turner, T.W. Kang, M.H. Breggren, R.F. Hogsett, and M.C. Jha, 1990, Development of an Advanced Process for Drying Fine Coal in an Inclined Fluidized Bed, Final Report. Laramie, WY, WRI Report to DOE, DOE/PC/88886-T5.

Ingram, G.R., and J.D. Rimstidt, 1984, Natural Weathering of Coal. Fuel; 63 (3): 292-296 (Mar 1984).

Lien, T.J., 1991, AMAX Advances Low-Rank Coal Drying. Coal, December, pp. 49-51.

McPherson, R., 1992, The Next Generation of Power Generation. Coal Market Strategies Tenth Annual Conference, Western Coal Council, Wheat Ridge, CO.

Merriam, N.W., C.Y. Cha, T.W. Kang, and M.B. Vaillancourt, 1990, Development of an Advanced, Continuous Mild-Gasification Process for the Production of Coproducts, Topical Report for Task 4, Mild Gasification Tests-System Integration Studies. Laramie, WY, WRI Report to DOE, DOE/MC/24268-3075.

Merriam, N.W., and V.K. Sethi, 1992, Status of Development of a Process to Produce a Premium Solid Fuel From Powder River Basin Coal. Laramie, WY, WRI Report to DOE, WRI-92-RO56.

Simmons, J., and J.J. Simmons, 1992, The Carbondry™ Process, An Innovative Approach to Drying Low Rank Coals. Proceedings of Coal Prep '92, McLean Hunter Presentations, Aurora, CO.

Skinner, J.L., L.B. Rothfield, B.F. Bonnecaze, S.W. Johnson, and Y.H. Li, 1984, Drying of Powder River Subbituminous Coal-Overview of a New Process. Coal Technology '84, 7th International Coal and Lignite Exhibition and Conference, Houston, TX.

Tomuro, J., S. Nogita, and Y. NaKamur, 1985, Reduction of Oxidation Rate of Coal by Coal-Derived Tar Coating. Proceedings 1985 International Conference on Coal Science, Pergamon Press, New York.

Western Energy Company, February 1992 Technical Progress Report. Submitted to U. S. DOE Pittsburgh Energy Technology Center.

Willson, W.G., S.A. Farnum, G.G. Baker, and G.H. Quentin, 1987, Low-Rank Coal Slurries for Gasification. Fuel Processing Technology, 15: 157-172.

P8 Development of Biological Coal Gasification (MicGAS Process)

CONTRACT INFORMATION

Contract Number DE-AC21-90MC27226

Contractor ARCTECH, Inc.
14100 Park Meadow Drive
Chantilly, VA 22021
(703) 222-0280

Contract Project Manager Dr. Daman S. Walia

Principal Investigator Dr. Kailash C. Srivastava

METC Project Manager Mr. Wu K. Lan

Period of Performance May 25, 1990 to March 26, 1996

Schedule and Milestones

FY 93-94 Program Schedule

Tasks/ Subtasks	FY 93	Months in FY 1994											
		O	N	D	J	F	M	A	M	J	J	A	S
1.1 NEPA Compliance	done												
1.2 Work Plan	done												
2. Enhancement of Methane Production													
2.1 Strain Improvement													
2.2 Effect of Co-substrates													
2.3 Nutrient Amendment													
3. Effect of Substrates on Microbes													

OBJECTIVES

The overall goal of the project is to develop an advanced, clean coal biogasification (MicGAS) Process. The objectives of the research during FY 1993-94 were to: (1) enhance kinetics of methane production (biogasification, biomethanation) from Texas lignite (TxL) by the Mic-1 consortium isolated and developed at ARCTECH, (2) increase coal solids loading, (3) optimize medium composition, and (4) reduce retention time.

BACKGROUND INFORMATION

State-of-the-art thermal coal gasification technologies, utilizing the abundant U.S. resource of low-rank coals, operate at high temperatures and pressures and require extensive synthesis gas clean-up for power generation. These technologies require not only high capital and operating costs, but also have to comply with increasingly stringent environmental regulations to control air, water and land pollution. Advanced coal conversion technologies, such as coal gasification are being developed to enhance the conversion efficiency as well as be economical for the abatement of emissions.

Low rank coals are more amenable to microbial conversions at near ambient conditions and thus a biological conversion technology could provide a comparatively economical system for utilizing low rank coals. Consequently, ARCTECH is developing the MicGAS Process as an integrated systems approach. This Process is being developed within ARCTECH's broad vision of the "Coal Biorefinery Concept" to enhance the economic value of coal and to develop additional markets for the usage of low-rank coals . Illustrated in Figure 1, the coal refinery concept involves the biological conversion of low-rank coals to value added products with minimal disposable waste (Figure 1). This concept envisions that all the three types of matter; namely, gas, liquid and residual solids will generate value added chemicals as co-products. These include:

1. clean burning fuel (biogas), as a gaseous product that will be used for advanced power generation, in fuel cell and in industrial applications,

2. the liquids will provide value added products, such as biopesticides and oxygenated chemicals (short-chain fatty acids and higher alcohols),

3. the residual coal mixed with process liquids will be converted into an organic soil amendment product - ACTOSOL™, that ARCTECH is currently marketing in domestic and international markets.

The Coal Biorefinery Concept is based on anaerobic microbial conversion of a variety of organic substrates to methane according to the schemes presented in Figure 2. Biomethanation can be hydrogenotrophic or aceticlastic depending upon the substrate (Figure 2A and B). In the case of a complex organic substrate, such as coal, the aceticlastic biomethanation is preceded by either acetogenesis only (Figure 2C), acedo-, and acetogenesis (Figure 2D), or a series of reactions involving hydrolysis, fermentation, acedo- and acetogenesis (Figure 2E), or any combination thereof. Initial studies conducted at ARCTECH[1-4] have established that despite the complexity of coal structure and variability among types of coals, low rank coals can be bioconverted to coproducts and methane under near ambient gasification conditions of temperature and pressure by a variety of unique anaerobic microbial consortia (eg. Mic-1, Mic-2, Mic-3, Mic-4)[1]. This

bioconversion has been confirmed by other scientists[cf.5,6-7]. The work at ARCTECH has demonstrated the specificity of a certain anaerobic microbial consortium to a given lignite[1]. For example, while Mic-1 consortium worked more efficiently with TxL, Mic-4 was more effective on Neyveli lignite. ARCTECH's strategy for the direct anaerobic bioconversion of low rank coals is based on the higher availability of coal carbon for the production of CH_4 and volatile fatty acids (VFAs) rather than the formation of CO_2.

An independent economic study[8], based on the laboratory scale reactor data on biomethanation of TxL and conceptual process design, demonstrated the process to be commercially attractive. The study recommended, however, that a cheaper organic nitrogen source, reduced retention time, and higher solids loading were essential to make the process profitable. In subsequent studies[2], a low-cost nutrient amendment, Sheftone-T™, was substituted for the originally used yeast extract + trypsoy mixture. This substitution brought about a ten fold reduction in the cost of the culture medium. In addition, three fold reduction in residence time was achieved and the solids loading were increased at least 10 fold. Despite these achievements, however, it became apparent that in order to successfully achieve the goals recommended by the Fluor Daniel study[8] further enhancement of methane production and reduction in residence time was necessary for the process to become commercially viable. Thus, a better understanding of the mechanism of coal biomethanation became imperative to the enhancement of the biomethanation of TxL.

It is generally agreed that coal consists of two fractions, a macromolecular and a lower molecular weight fraction. Based on the general empirical formula of a German lignite (brown coal)[9], it is also recognized that the micromolecular fraction of coal is more amenable to microbial attack than the macromolecular one. Furthermore, if the micromolecular fraction can be removed, upon long term incubation of micro-organisms with the macromolecular fraction, the latter fraction will also be bioconverted to added value products. Recent results[4] on the biomethanation studies of chemically and biologically pretreated TxL indicate that microbially pretreated TxL gave higher methane production even at higher solids loadings of 5%. Nevertheless, it also was apparent that at 10% solids loading, the pH of the culture medium dropped drastically which lead to inhibited methane production compared with that observed at lower solids loading of 0.1 and 1.0%.

A close examination of the schematics in Figure 2E indicates that the mechanism of coal biomethanation is similar to the one observed during biomethanation of lignocellulosic substrates. Similar to the constituents (cellulose and hemicellulose) of lignocellulose, TxL is also a water insoluble substrate. Literature indicates that microbial attachment to complex insoluble substrates[10] and biofilm formation[11] play an important role in efficient microbial utilization of such substrates. Consequently, the hypothesis that higher biomethanation of TxL is directly related to better attachment of Mic-1 consortium to TxL particles was tested. In a recent study, Srivastava and Manolov[12] demonstrated that a number of factors, such as sequestrants, solids loading, H^+-donors etc., that enhanced methane production, were also the ones that demonstrated higher attachment of microbial cells to TxL particles. The knowledge thus gained has been used to further address the recommendations of the Fluor Daniel Study[8] for the enhancement of methane production in the MicGAS Process. This is a report of recent laboratory findings to further enhance the MicGAS Process.

PROJECT DESCRIPTION

Biomethanation of coal (MicGAS Process) is a phenomenon carried out by the synergistic metabolism of at least four groups of anaerobic microorganisms that constitute a mixed population or consortium. In this respect, the process can be considered analogous to that of anaerobic digestion of municipal waste. The exception is that unlike municipal waste, coal is a much more complex and difficult substrate to degrade. This project was focussed on studying the factors that can result in consistent enhancement of methane production at higher than hitherto used solids loading (0.1-1.0%) and reduction of retention time in the regime (7-10 days) closer to that of anaerobic municipal digestion.

RESULTS

Biomethanation of coal is a multi-step process requiring distinct simultaneous metabolic activities of different groups of anaerobic bacteria. These steps explained in Figure 2E occur in syntrophy, rather than in a stepwise fashion. A closer analysis of the results described here indicate that biomethanation of TxL at >5% solids loading is feasible through appropriate development of nutrient medium and further adaptation of the microorganisms involved in this process. Further understanding of the inhibitory factors and some biochemical manipulations to overcome those inhibitions will hasten the process considerably.

Products of Biomethanation

Biomethanation of TxL resulted in gaseous, liquid, and solid products. While the major gaseous products were methane and CO_2 the liquid product was composed of a number of volatile fatty acids and some other compounds. The solid phase was composed of residual coal mixed with minimal biomass. A preliminary analysis of the residual solids indicated about 23% ash content in contrast to 16% ash content in the untreated TxL. Furthermore, preliminary results indicate that the carbon in the residue could be converted to humic acids. Humic acids are the major components of ARCTECH's ACTOSOL^R product which is being sold in the domestic and international markets for agricultural applications.

Enhancement of Methane Production

Several parameters were studied to enhance the production of methane from TxL.

Bacterial adaptation. Bacterial enrichment, a technique to manipulate growth and specific substrate conversion was applied to develop the Mic-1 consortium to utilize TxL as the sole source of carbon. The adapted Mic-1 consortium showed an increase in methane production from 10 to 50 mole% reaching up to 71-78 mole % - a 7.5 fold increase during the adaptation period (Table 1). Furthermore, as a result of this adaptation, the methane production from 5% TxL (as compared to 0.01% and 1% initial concentration) started at day 3 and reached a maximum of up to 230 cc/g coal, a 5 fold increase within 11-15 days compared to approximately 2 months time in initial experiments (Task 2). The maximum rate of methane production was observed to occur between 11-14 days (Table 1). These results indicate that the culture has the ability to adapt to the coal carbon and has improved significantly during the adaptation period. This is a positive indication for further improvement in the process research.

Effect of nutrient amendment substitutes. A variety of commercially

available nutrient amendments as the sources of organic nitrogen were tested to replace the expensive yeast extract(YE)/Tryptic soy broth (TSB) mixture used in the original culture medium. Results indicated that Sheftone-T™ enhanced methane production by 15.3% (Figure 3).

Effect of Solids Loading. The Fluor Daniel Study[8] also recommended that TxL solids loading should be increased in order to make the process economical. Consequently, biomethanation of TxL was studied at solids loading of 0.1, 1, 5 and 10 (% w/v). An inverse relationship was observed between increased solids loading and methane production (Figure 4). Furthermore, with the increase in solids loading (from 0.1 to 5%), the methane production was inhibited but remained more or less the same at 5% and 10% solids loading. Nevertheless, significantly higher methane production was observed at 5% solids loading than at 10% when upflow fluidized bed reactors (UFBR) were used (Figure 5).

Effect of initial pH of the culture medium. The relationship between the initial pH of the medium and biomethanation of TxL by the Mic-1 consortium is presented in Figure 6. Data from another study[12] clearly indicate that the reason for the inhibition of methane production at 10% TxL is poor microbial attachment to TxL particles at pHs lower than 7.8 (Figure 6). The data from Figure 6 also demonstrate that the optimum initial pH of the culture medium for biomethanation of TxL at 10% solids loading is 7.8.

Effect of Hydrogen (Proton, H^+) Donors. Having determined the pH that provided better microbial attachment and greater biomethanation of TxL, the next step was to further enhance the kinetics of methane production at the higher solids loading of >5%. Literature data[13-15] on biomethanogenesis indicate that hydrogen (H) plays an important role. However, lignites typically contain 6-7.5% hydrogen[16] and studies conducted with ^3H demonstrated that the additional H^+ required for the biomethanation of TxL is derived from the water in the culture medium[17].

Nevertheless, further supplementation of H^+ was critical to the enhancement of MicGAS Process. Therefore, the SNTM was supplemented with citrate, formate, lactate, methanol and succinate as potential H^+-donors. Among these, citrate, lactate and succinate enhanced the methane production with the highest effect being that from citrate addition (Figure 7). Analysis of VFAs demonstrated that acetate is in highest concentration until day 7, but sharply drops thereafter (Figure 8). This is the period when the methane production increases (Figure 7). Higher methane production was also observed at 5% solids loading in the presence of 0.5% (v/v) methanol (Figure 9). The biomethanation of TxL in serum vial cultures remained approximately the same despite the addition of 10 mM citrate (Figure 10). Nevertheless, in bench scale upflow fluidized bed bioreactors (UFBR) at 5% TxL solids loading, the methane production was drastically enhanced (Figure 11) reaching up to 78 mol% by day 8 (arrow, Figure 11). VFAs analysis indicated that the methane production is directly related to the amount of acetate produced during the metabolism of Mic-1 consortium (Figure 12) on TxL. These data also indicate that perhaps the accumulation of propionic acid in the culture medium, and the inability of members of Mic-1 consortium to metabolize this VFA into acetate may be one of the limiting steps in the continued bioconversion of TxL to methane. The results presented in Figure 13, however, demonstrate that the reduction in the retention time and higher methane production even at 5% solids loading are

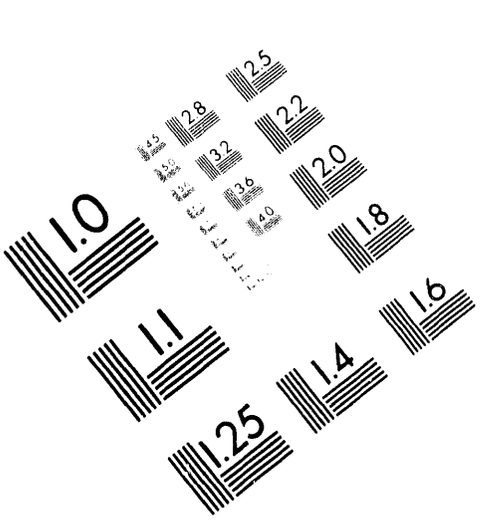

Association for Information and Image Management

1100 Wayne Avenue, Suite 1100
Silver Spring, Maryland 20910

301/587-8202

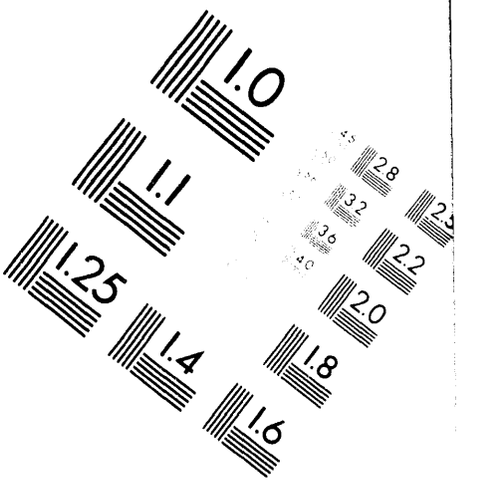

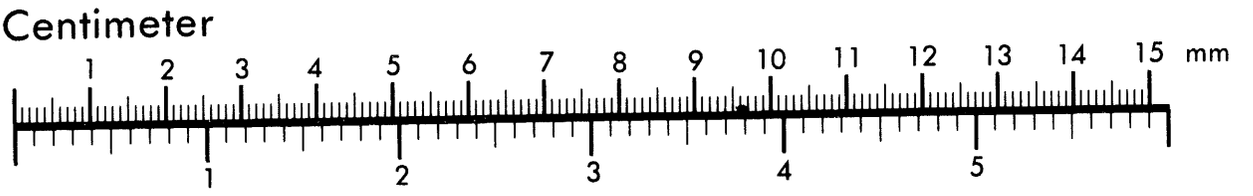

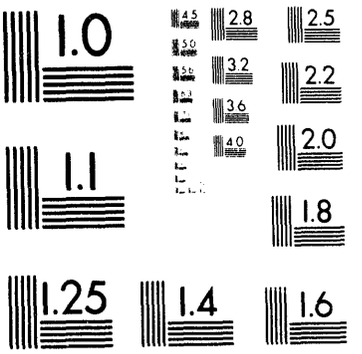

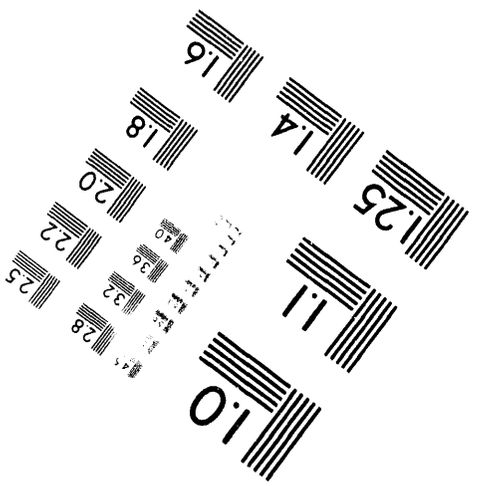

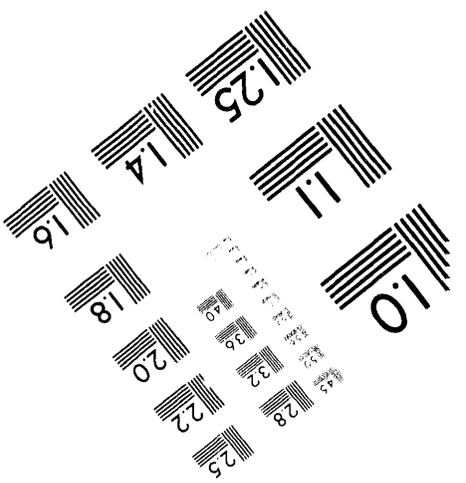

MANUFACTURED TO AIIM STANDARDS
BY APPLIED IMAGE, INC.

5 of 6

reproducible in another independent experiment using 3 separate bioreactors.

Carbon Balance

An analysis of the carbon in the untreated TxL and the resulting residue, together with the carbon coming from medium components (such as Sheftone-T™) and the analysis of carbon in the products shows a process efficiency (for methane) of 20% at 5% solids loading (Table 2) and a 91% carbon recovery.

FUTURE WORK

Significant advancements were made in enhancing the biomethanation of low rank coals, especially TxL by the Mic-1 consortium. However, for this process to be viable at a larger scale more research is needed. The programmed research plan includes: (A) further development of a culture medium with reduced cost, (B) identification of inhibitors, such as phenols, that might be produced from TxL as a result of microbial metabolism and in turn inhibit further microbial metabolism, (C) biochemical manipulations to modify the physiological characteristics of the microorganisms, and (D) evaluation of known and novel reactor designs. These tasks shall be accomplished through: (1) metabolic characterization of microorganisms, (2) further biochemical manipulation of the Mic-1 consortium for higher methane yields at (a) increased coal solids loadings, (b) reduced retention times, and (c) studying the effects of medium component on methane production.

ACKNOWLEDGEMENTS

ARCTECH is developing the MicGAS technology jointly with Houston Lighting and Power. This research was supported by the Department of Energy-METC.

REFERENCES

1. Barik, S., Tiemens, K., Harding, RE., Hawley, B., and Isbister, J.D. 1990. Biological Conversions of Coals to Methane. In *Proceedings: 1990 First International Symposium on the Biological Processing of Coal* Yunker, S. and Rhee, K., eds, Electric Power Research Institute, Palo Alto, CA, p. **5**: 19-32.

2. Walia, D.S., Srivastava, K.C., and Barik, S. 1992. Development of Biological Coal Gasification (MicGAS Process). In *Proceedings of the Twelfth Annual Gasification and Gas Stream Cleanup Systems Contractors Review Meeting*, METC, **2**, 535-549.

3. Srivastava, K.C., and Manolov, R.J. 1993. Development of the "MicGAS Process" : Enhancement of Biomethanation of Texas lignite. In *Abstracts, 4th International Symposium Biological Process Fossil Fuels, Alghero, Italy*, Yunker, S. and Rossi, G., eds, EPRI, Palo Alto, Ca. 5-12.

4. Srivastava, K.C. and Manolov, R.J. 1993. Studies on Coal Biomethanation. *In Joint Annual Meeting of Society for Industrial Microbiology and Canadian Society for Microbiology, Toronto, Canada,* August 1-6.

5. Isbister, J.D. and Barik, S. 1992. *In Microbial Transformations of Low Rank Coals*, Crawford, D.L. (Ed.), CRC Press, Boca Raton, FL.

6. Crawford, D.C., Gupta, R.K., Deobald, L.A. and Roberts, D.J. 1990. Biotransformation of Coal and Coal Substructure Model Compounds by Bacteria under Aerobic and Anaerobic Conditions. In *Proceedings: 1990 First International Symposium on the Biological Processing of Coal*, Yunker, S. and Rhee, K., eds, Electric Power Research Institute, Palo Alto, CA, p. **4:** 27-43.

7. Volkwein, J.C. 1993. Biological Production of Methane from Bituminous Coal. In *Abstracts, 4th International Symposium Biological Process Fossil Fuels, Alghero, Italy*, Yunker, S. and Rossi, G. eds., Electric Power Research Institute, Palo Alto, CA, **5**:14.

8. Fluor Daniel. An Economic Analysis of the ARCTECH,s MicGAS Process.

9. Polman, J.K., Breckenridge, C.R., Dugan, P.R. and Quigley, D.R. 1990. Growth Response of Microorganisms to Different Molecular Fractions of Lignite. In *Proceedings: 1990 First International Symposium on the Biological Processing of Coal*, Electric Power Research Institute, Palo Alto, CA, **4**: 61-72.

10. Costerton, J.W. 1992. Pivotal Roles of Biofilms in the Focused Attack of Bacteria on Insoluble Substrates. *International Biodeterioration & Biodegradation*, **30**: 123-133.

11. Marshall, K.C. 1992. Biofilms: An Overview of Bacterial Adhesion, Activity, and Control at Surfaces. *ASM News*, **58:** 202-207.

12. Srivastava, K.C. and Manolov, R.J. 1994. Biogasification of Texas Lignite-Factors Affecting Attachment of Microorganisms to the Coal Surface. In *Abstracts for Sixteenth Symposium on Biotechnology for Fuels and Chemicals, Gatlinburg, TN*, May 9-13,p.95.

13. Deckena, S. and Blotevogel, K.-H. 1990. Growth of Methanogenic and Sulfate-Reducing Bacteria with Cathodic Hydrogen. *Biotechnology Letters*, **12**: 615-620.

14. Winfrey, M.R., Nelson, D.R., Klevickis, S.C. and Zeikus, J.G. 1977. Association of Hydrogen Metabolism with Methanogenesis in Lake Mendota Sediments. *Applied and Environmental Microbiology*, **33**: 312-318.

15. Zehnder, A.J.B. 1978. Ecology of Methane Formation. In *Water Pollution Microbiology*, Mitchell, R. (ed)., New York, John Wiley and Sons, Inc. **2**: 349-375.

16. Hessley, R.K., Reasoner, J.N. and Riley, J.T. 1986. Coal Science, New York, John Wiley and Sons, 238 pgs.

17. Barik, S., Isbister, J. D., Harding, R., and Berrill, P. 1991. In *Proceedings: 1991 Second International Symposium on the Biological Processing of Coal*, Yunker, S. (Ed.). Electric Power Research Institute, Palo Alto, CA, **6**: 23-38.

CONCEPT OF COAL BIOREFINERY

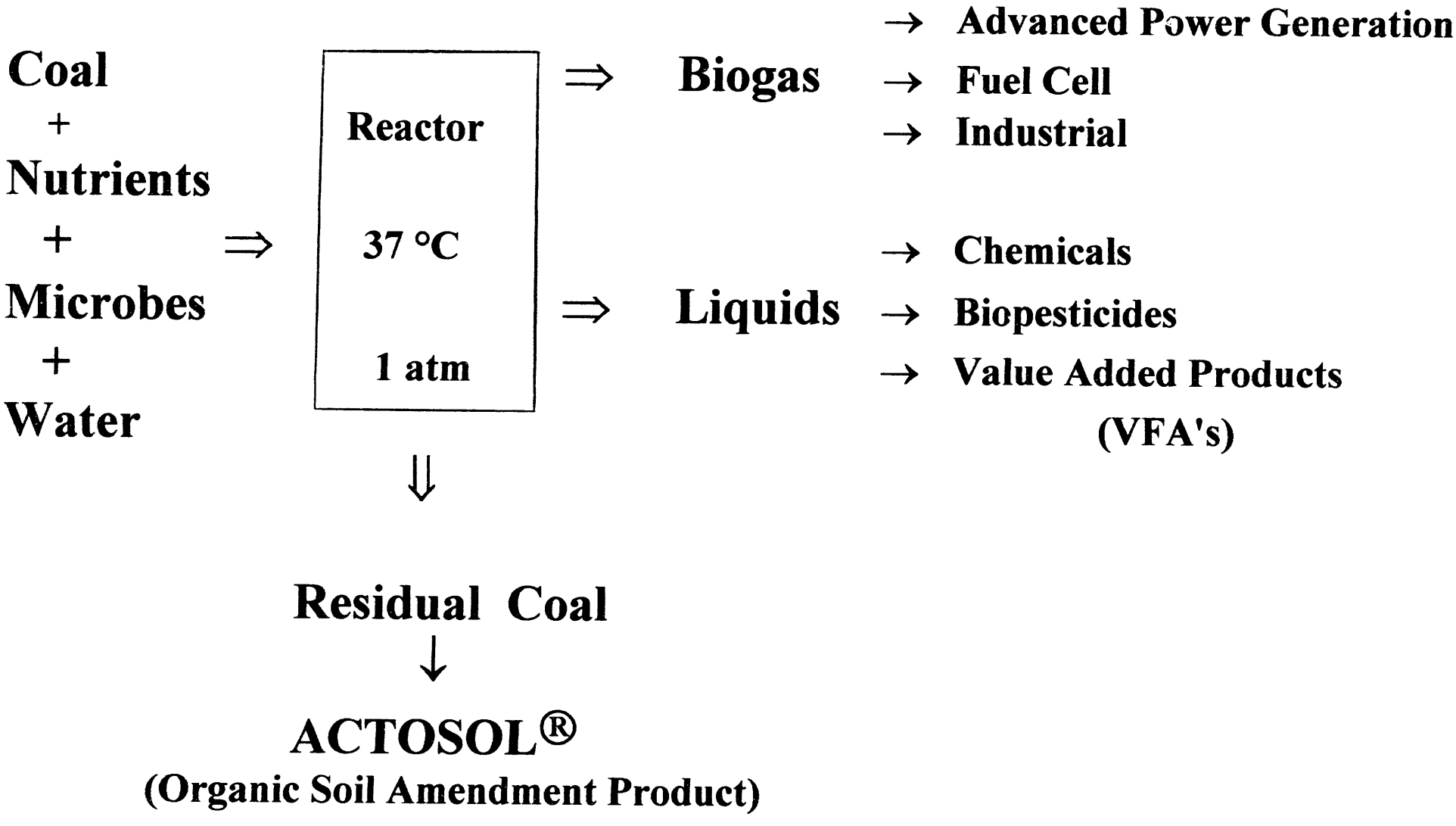

Figure 1

CONVERSION OF ORGANIC FEEDSTOCKS TO CH_4 IS A MULTISTEP PROCESS

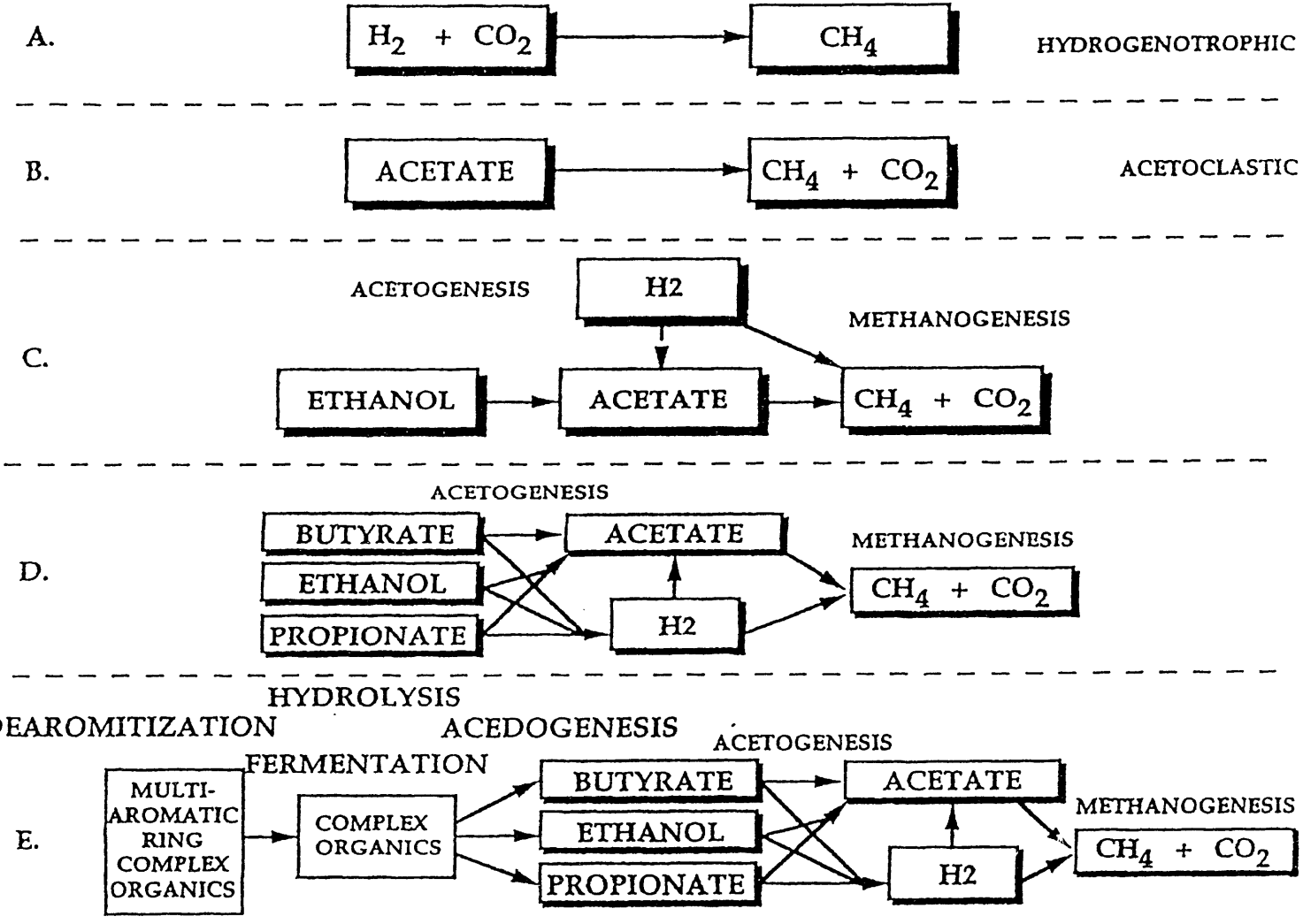

Figure 2

EFFECT OF NITROGEN SOURCE ON BIOMETHANATION OF TEXAS LIGNITE (1% w/v) BY Mic-1 CONSORTIUM

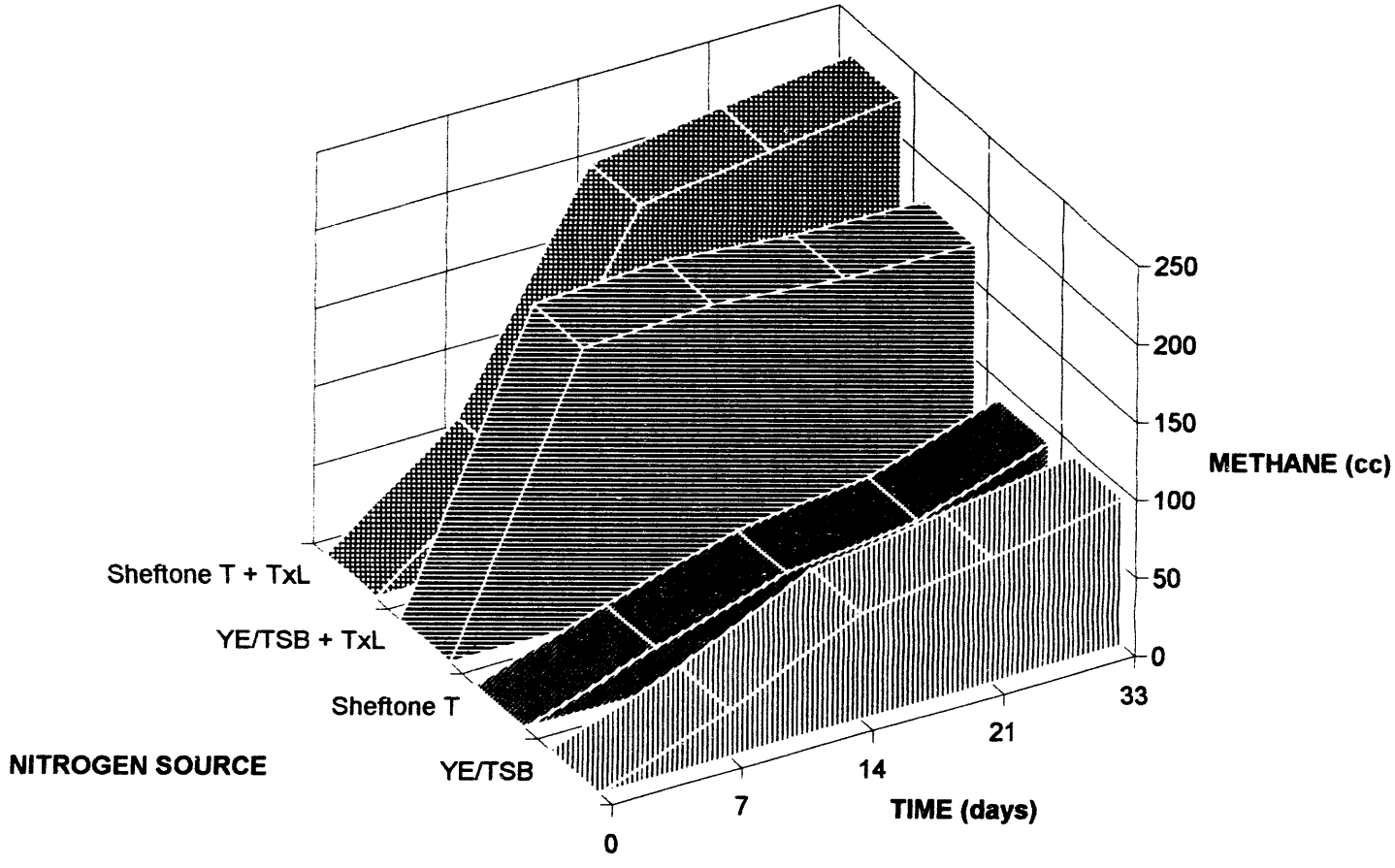

Figure 3

EFFECT OF DIFFERENT SOLIDS LOADING ON BIOMETHANATION OF TEXAS LIGNITE BY Mic-1 CONSORTIUM

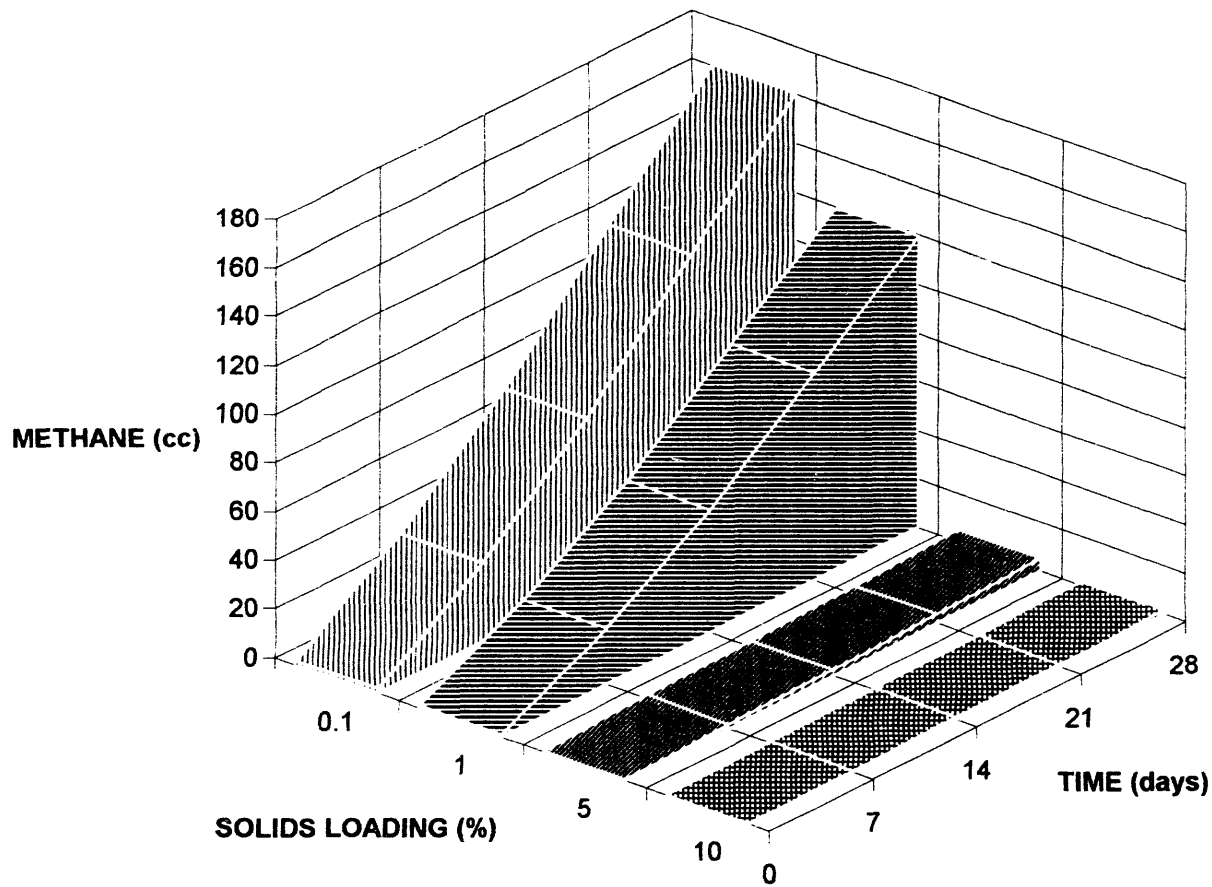

Figure 4

Bench Scale Bioreactors

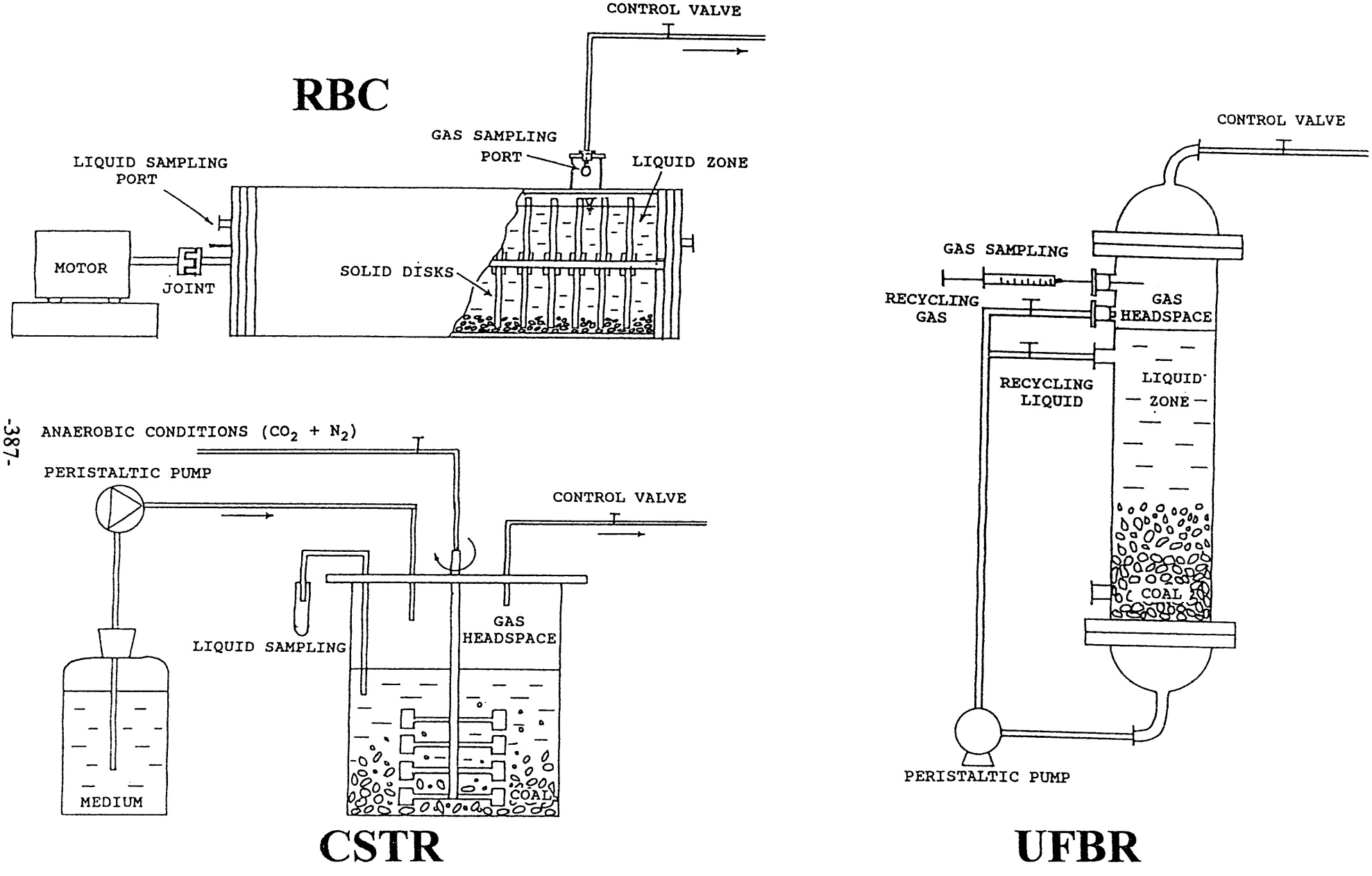

Figure 5

EFFECT OF DIFFERENT INITIAL pH OF THE MEDIUM ON BIOMETHANATION OF TEXAS LIGNITE (10% w/v) BY Mic-1 CONSORTIUM

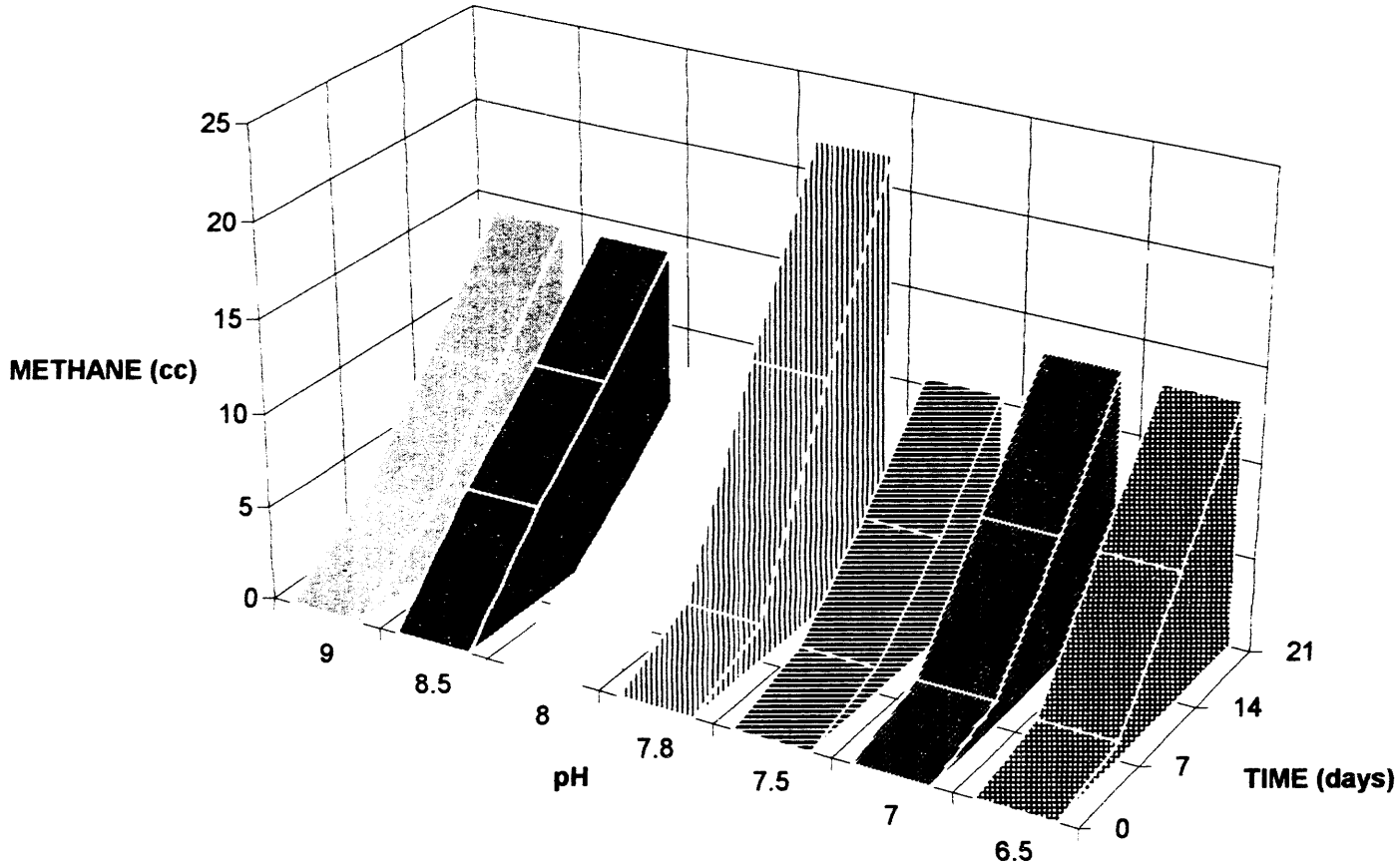

Figure 6

EFFECT OF HYDROGEN DONORS (10 mM) ON BIOMETHANATION OF TEXAS LIGNITE (1% w/v) BY Mic-1 CONSORTIUM

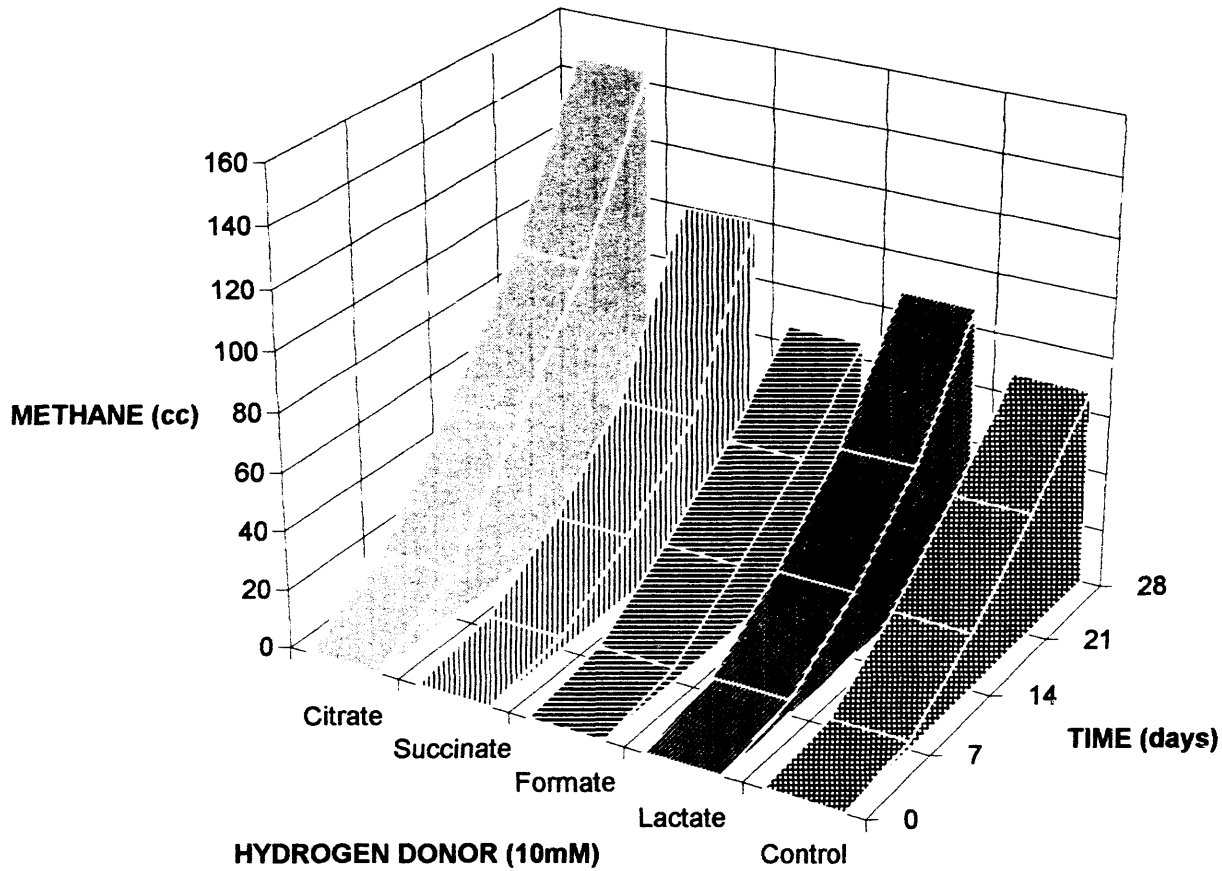

Figure 7

EFFECT OF HYDROGEN DONORS (CITRATE, 10 mM) ON BIOMETHANATION OF TEXAS LIGNITE (1% w/v) BY Mic-1 CONSORTIUM - VFA's CONCENTRATION

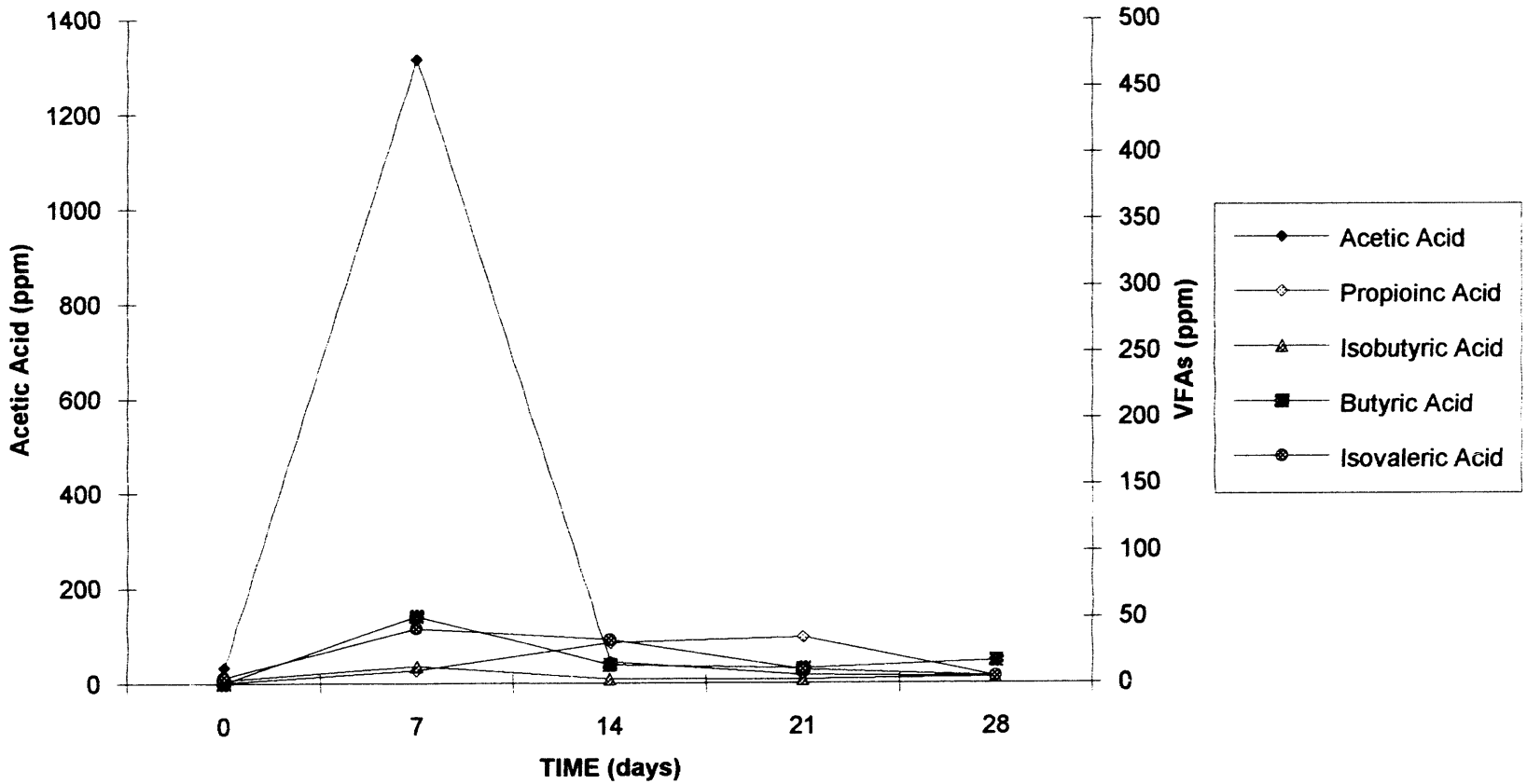

Figure 8

EFFECT OF HYDROGEN DONORS ON BIOMETHANATION OF TEXAS LIGNITE (5% w/v) BY Mic-1 CONSORTIUM

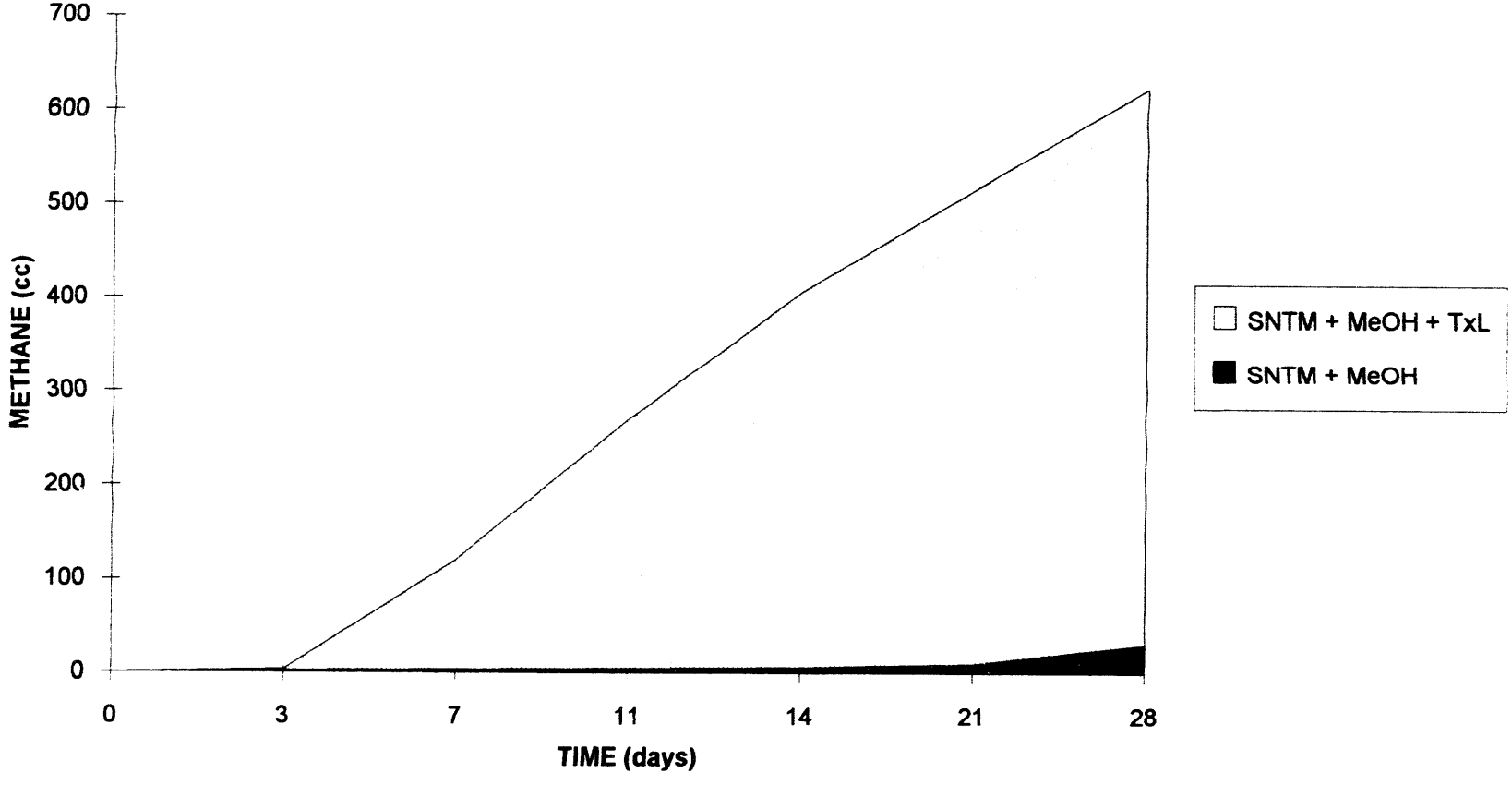

Figure 9

EFFECT OF HYDROGEN DONORS ON BIOMETHANATION OF TEXAS LIGNITE (5% w/v)

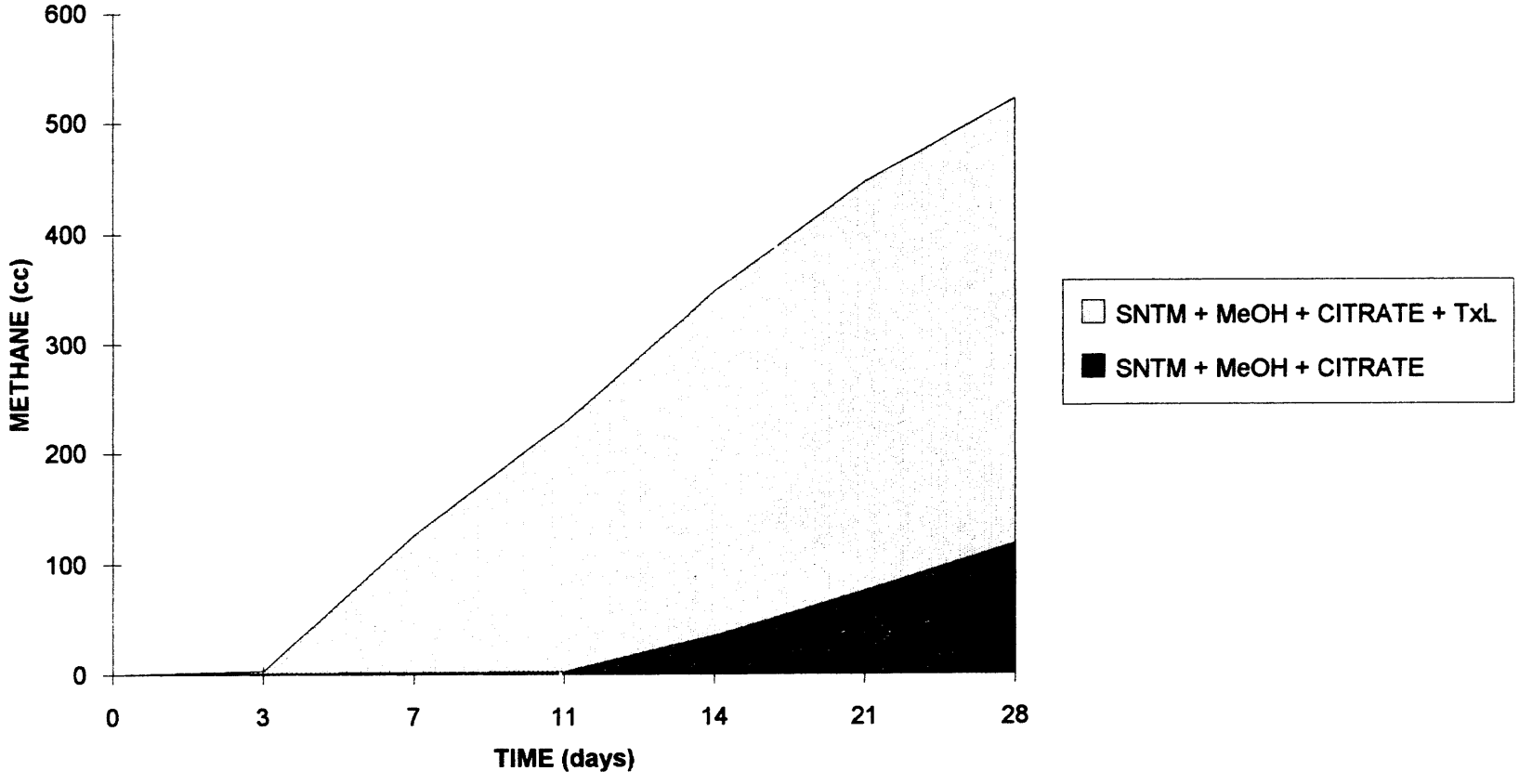

Figure 10

BIOMETHANATION OF TEXAS LIGNITE IS SIGNIFICANTLY ENHANCED IN AN UPFLOW BIOREACTOR

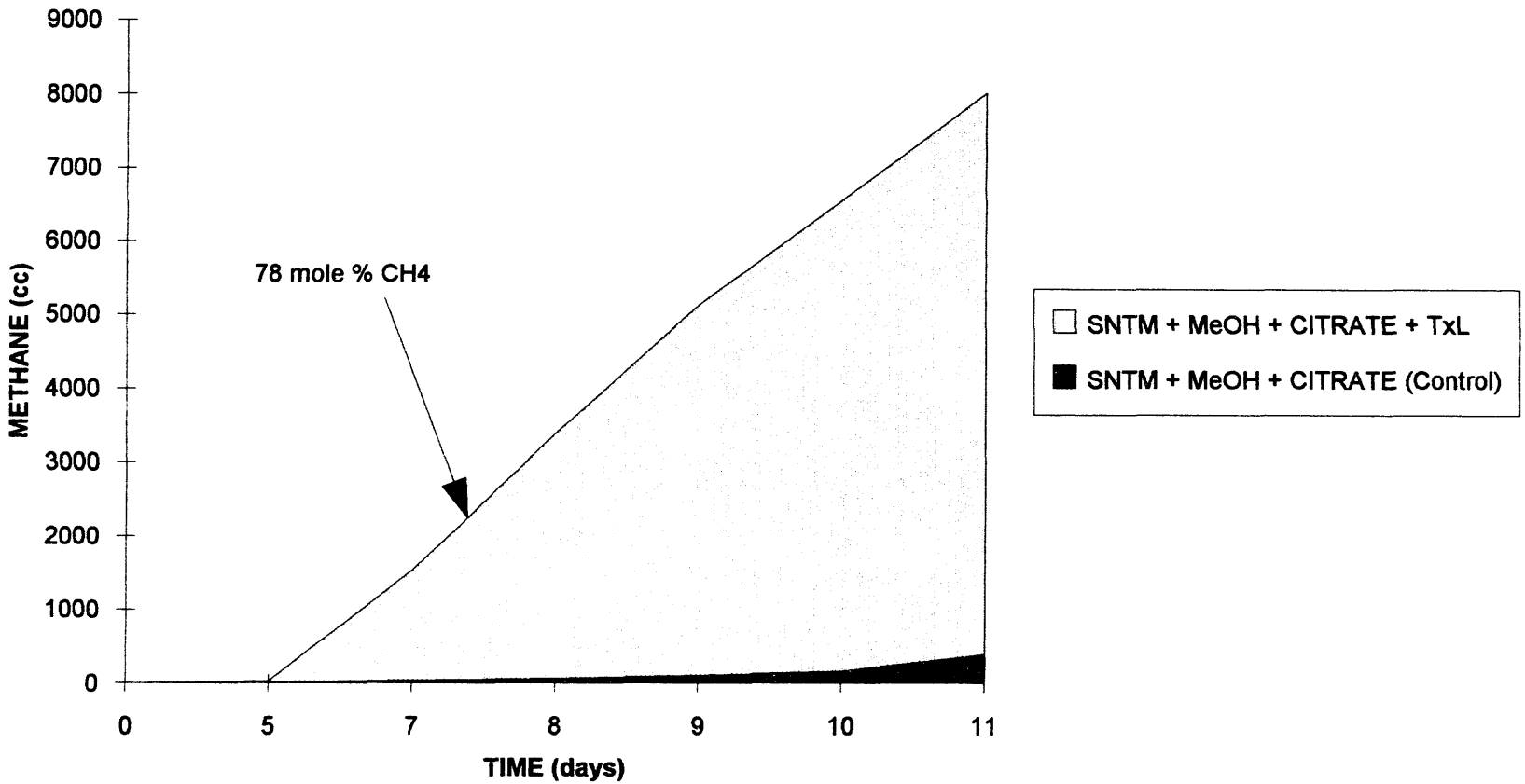

Figure 11

BIOGASIFICATION OF TEXAS LIGNITE IS DIRECTLY RELATED TO ACETATE CONCENTRATION

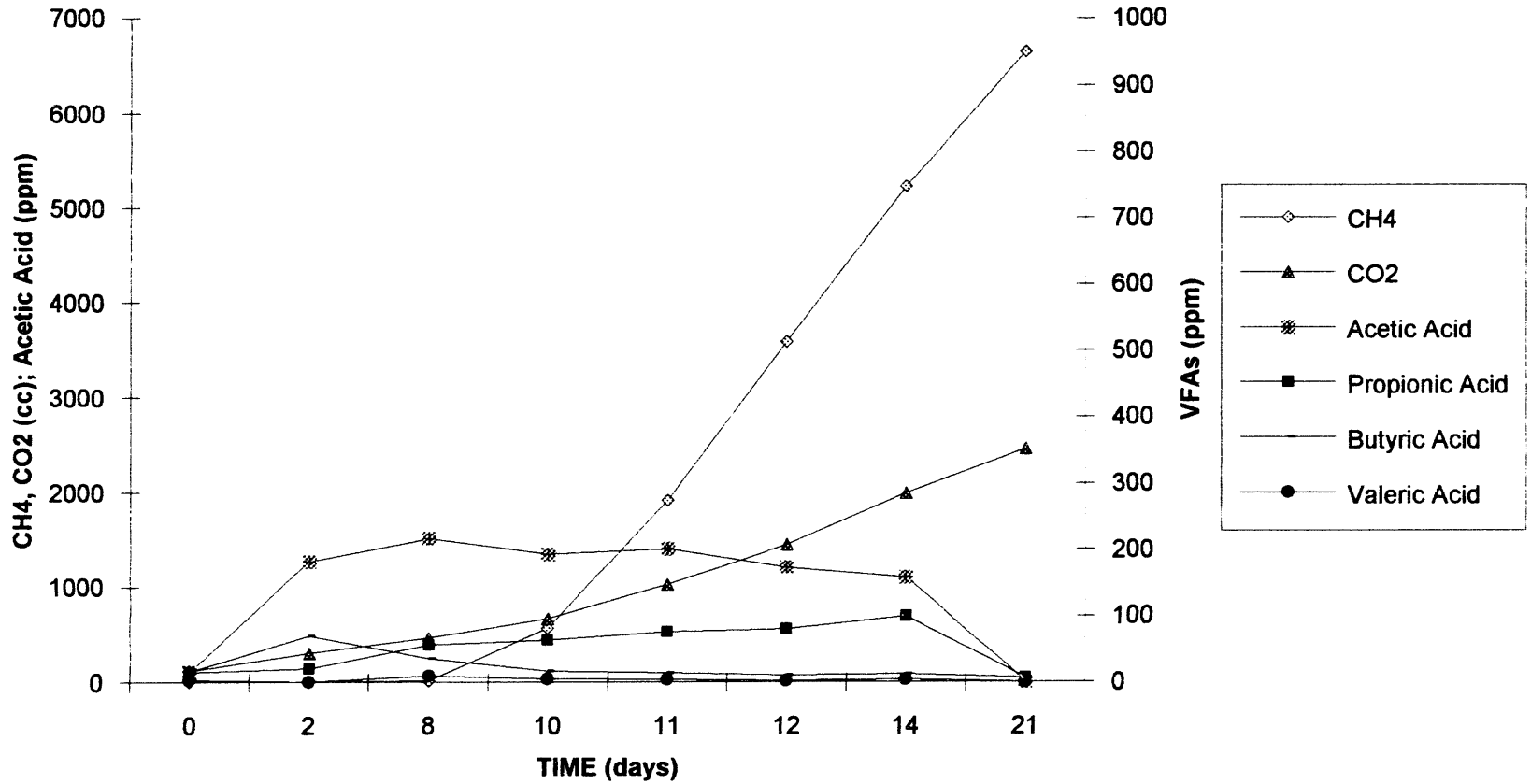

Figure 12

BIOMETHANATION OF TEXAS LIGNITE IS REPRODUCIBLE

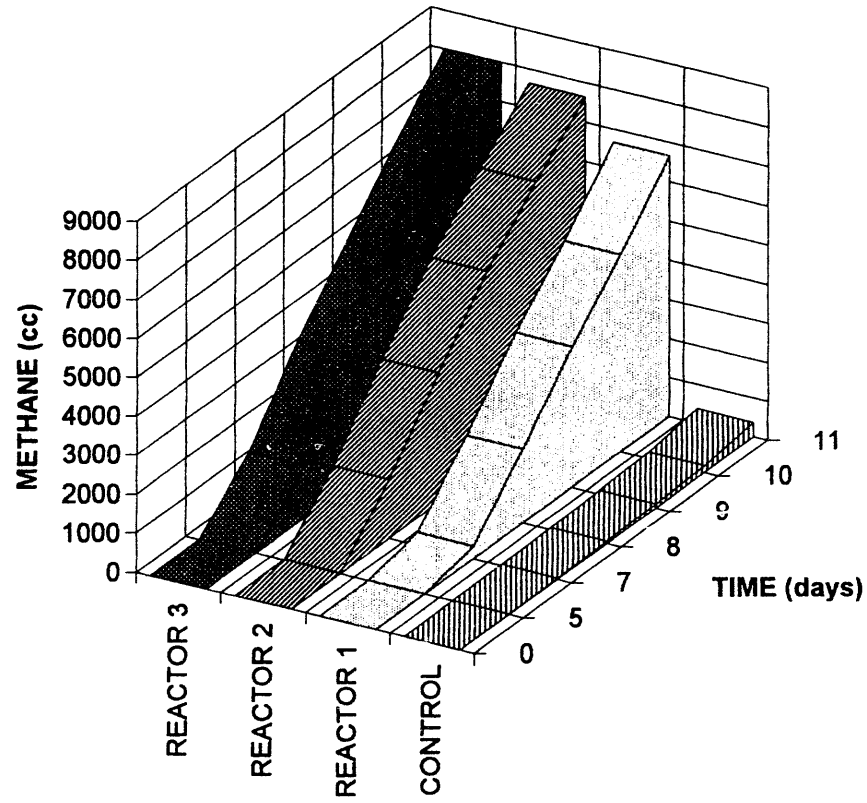

Figure 13

Table 1

Methane Production by Mic-1 Consortium Before and After Adaptation to Higher Coal Solids Loadings					
Parameters	Adaptation				Fold Increase
	Before	After			
Coal Solids (%)	0.01	0.1 - 1	5	5*	500
CH_4 (mole %)	10	40 - 50	48 - 52	71 - 78	7.5
CH_4 (cc/g coal)	40	96 - 193	134 -198	200 - 230	5
Time (days)	60	21 - 28	7 - 14	7 - 8	8**

* Bioreactor Studies

** Reduction in Residence Time

Table 2

CARBON BALANCE

CARBON IN	(%)	CARBON OUT	(%)
COAL	90	Biogas CH_4 - 20 CO_2 - 4	24
Media Components	10	Chemicals (VFAs)	2
		Humic Acid (ACTOSOL®)	74
TOTAL	100		100

P9 Simultaneous Removal of H_2S and NH_3 in Coal Gasification Processes

CONTRACT INFORMATION

Contact Number	DE-FG22-93MT93005
Contractor	Hampton University Department of engineering Hampton, VA 23668 (804) 727-5288
Contractor Project Manager	K. Jothimurugesan
Principal Investigators	K. Jothimurugesan Adeyinka A. Adeyiga Santosh K. Gangwal (RTI)
DOE Project Officer	Kamalendu Das
Period of Performance	September 2, 1993 to September 1, 1996

Schedule and Milestones

FY 1993 Program Schedule

	S	O	N	D	J	F	M	A	M	J	J	A
Test Plan	———											
Fabrication		———	———	———	———	———	———	———				
Sorbent-Catalyst Preparation					———	———	———	———	———	———	———	———
Sorbent-Catalyst Screening									———	———	———	———

OBJECTIVES

The objective of this study is to develop advanced high-temperature coal gas desulfurization mixed-metal oxide sorbents with stable ammonia decomposition materials at 550-800° C (1022-1472° F). The specific objectives of the project are to: (i) Develop a combined sorbent-catalyst materials shall be capable of removing hydrogen sulfide to less than 20 ppmv and ammonia by at least 90 percent. (ii) Carry out comparative fixed-bed studies of absorption and regeneration with various formulations of sorbent-catalyst systems and select most promising sorbent-catalyst type. (iii) Conduct long-term (at least 30 cycles) durability and chemical reactivity in the fixed-bed with the superior sorbent-catalyst.

BACKGROUND INFORMATION

Nitrogen (N_2) occurs in coal in the form of tightly bound organic ring compounds, typically at levels of 1 to 2 wt% on a dry-ash-free basis. During, coal gasification, this fuel-bound nitrogen is released principally as ammonia and nitrogen, with smaller levels of HCN. The formation of NH_3 in a coal gasification processes is a function of the fuel gas composition and the gasifier operating conditions. During the use of coal gas to generate electricity in gas-fired turbines, fuel bound (N_2) is converted to nitrogen oxides (NO_x), which are difficult to remove and are highly undesirable as atmospheric pollutants. Recent results indicate that while the efficiency of molten carbonate fuel cell (MCFC) anodes is not effected by exposure to NH_3, NO_X is generated during combustion of the anode exhaust gas. Thus, NH_3 must be removed from the coal gas before it is used in IGCC or MCFC applications.

The product stream from a high temperature, oxygen-blown gasifier, such as Texaco, contains about 2000 ppmv of NH_3, where higher concentrations (about 5000 ppmv) occur when the gasification is conducted at lower temperatures, such as in the Lurgi or GE air-blown gasifier. A range of 1500 to 3000 ppmv is considered for this study.

Removal of H_2S using zinc-based sorbents, particularly zinc titanate, to < 20 ppmv levels has been well established (Lew et al., 1989; Jothimurugesan and Harrison, 1990; Woods et al., 1990; Gupta and Gangwal, 1993). Previous literature study indicated that catalyst have high activities for NH_3 decomposition (Krishnan et al., 1988). If desulfurization sorbents such as zinc titanate could be used along with the NH_3 decomposition catalysts to decompose ammonia present in hot coal gas, then the number of unit processes necessary to clean hot coal gas could be reduced by one.

The objective of this project is to develop successful combination of an NH_3 decomposition catalyst with the mixed-metal oxide sorbent so that the sorbent-catalyst activity remains stable for NH_3 decomposition in addition to H_2S removal under cyclic sulfidation-regeneration conditions in the temperature range of 550-800° C (1022-1472° F) and pressures up to 20 atm.

PROJECT DESCRIPTION

Sorbent-Catalyst Preparation

The mixed metal-oxide sorbent (Zinc Titanate) was prepared by the coprecipitation method in order to generate as high a surface area as possible. In order to investigate the effect of calcination temperature, three zinc titanates were calcined at 600, 700 and 800°C. The surface area variations with temperature is shown in Figure 1. As the calcination temperature increases from 600 to 800° C , the surface area decreases from 89 to 19 m^2/g. The ammonia decomposition catalyst was added to zinc-titanium oxide by impregnation technique. After the impregnation, the material was dried at 110° C(230° F) , followed by calcination in air at 800° C (1472° F) for 1 hour.

Experimental Setup

The laboratory-scale fixed-bed reactor system constructed is shown schematically in Figure 2 to determine the activity of the sorbent-catalyst formulations for their ammonia decomposition activity and H_2S removal ability using a simulated coal gas. The simulated coal gas will be

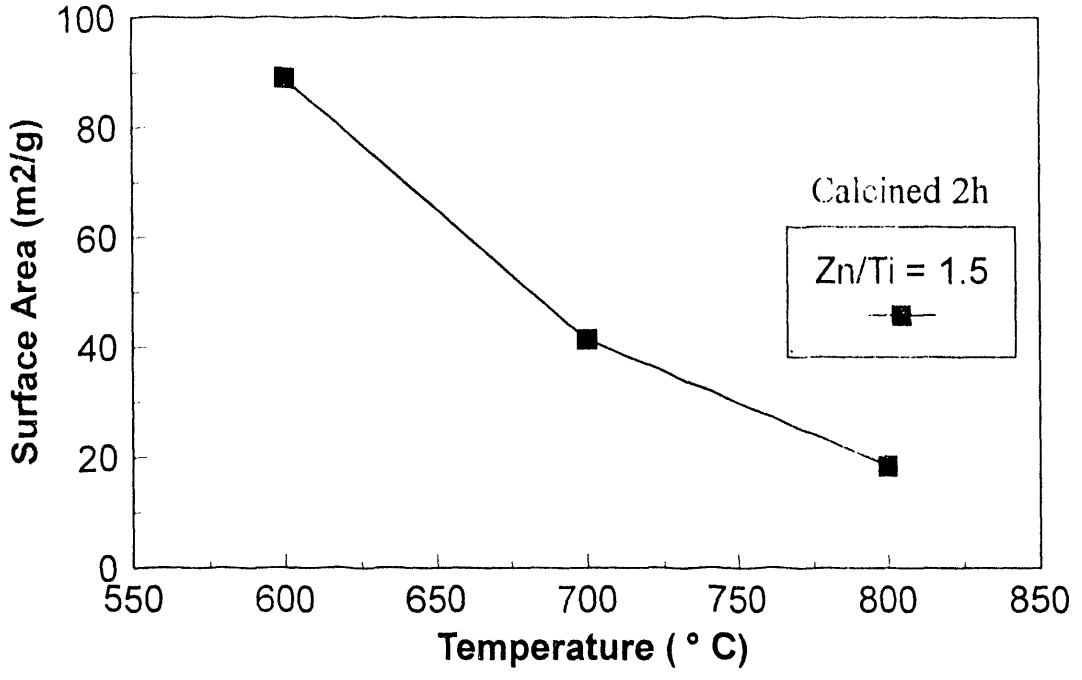

Figure 1. Effect of Calcination Temperature on the Zn-Ti-O Surface Area

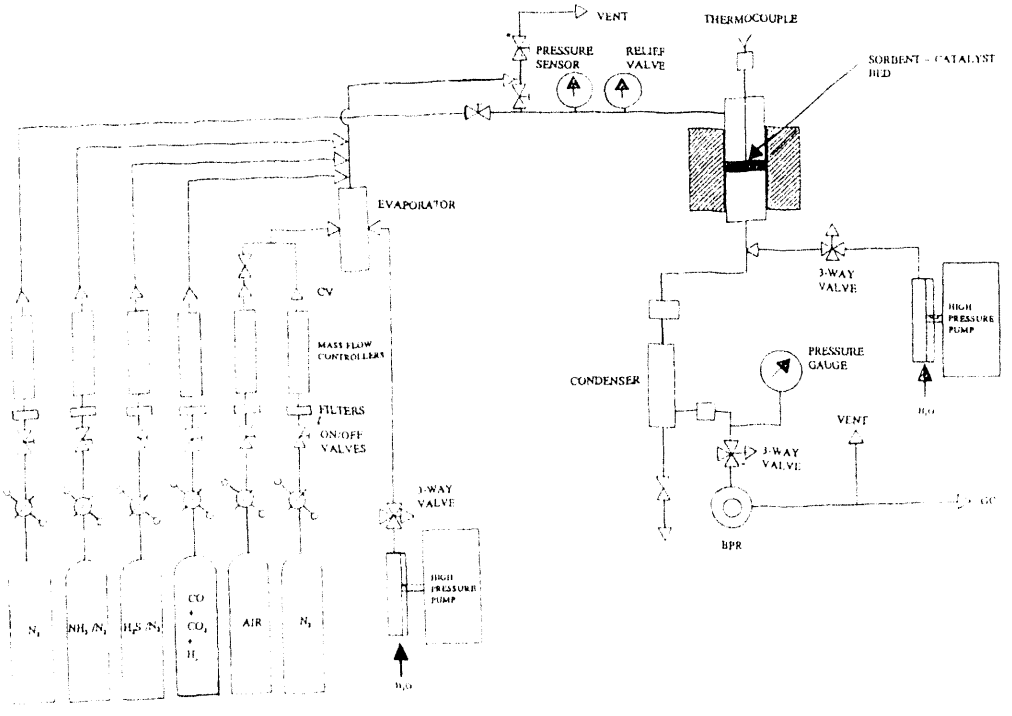

Figure 2. Schematic Diagram of Fixed-Bed Reactor System

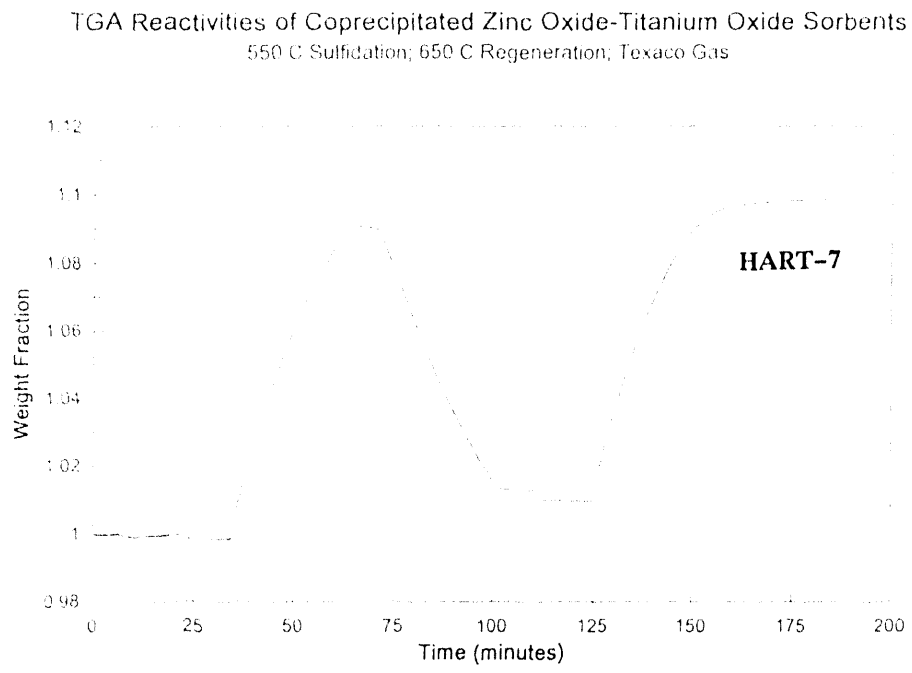

Figure 3. TGA Reactivities of Coprecipitated Zinc Oxide–Titanium Oxide Sorbents

prepared by blending the pure and pre-mixed gases. The flow rates of these gases will be controlled and monitored by high pressure mass flow controllers. Steam will be added to the mixed dry gas by vaporizing liquid water injected into the gas stream at a controlled rate by a high pressure syringe pump. The pressure inside the reactor will be controlled by a back pressure regulator and will be measured using an electronic pressure sensor. The thermocouples are positioned to measure the temperatures of the preheated feed gas, reactor bed temperature and the temperature of the product gas. The product gases will be analyzed for H_2S and NH_3 by using Detector Tubes and Ion-Selective Electrodes.

TEST RESULTS

The TGA reactivity of the sorbents was measured in simulated Texaco gas (with about 1% H_2S) at 550° C (Figure 3) using the RTI, TGA facilities. TGA runs consisted of a 550° C sulfidation, 650°C regeneration with 2% O_2, 18% H_2O, balance N_2, followed by a second sulfidation. As seen from Figure 3, the HART-7 sample showed excellent reactivity.

FUTURE WORK

Various formulations of sorbent-catalyst will be prepared and then it will be tested in the fixed bed reactor system.

REFERENCES

Gupta, R and Gangwal, S.K., "Fludizable Zinc Titanate Materials with High Chemical Reactivity and Attrition Resistance", U.S. Patent 5,254,516, 1993.

Jothimurugesan,K and Harrison, D.P., "The Reaction Between H_2S and Zinc Oxide–Titanium Oxide Sorbents: II. Single Pellet Sulfidation Modelling", Ind.Eng.Chem.Res, 29,1167(1990).

Krishnan, G.N., Wood, B.J., Tong, G.T., and McCarty, J.G., "Study of Ammonia Removal in Coal Gasification Processes", Final Report to U.S. DOE/METC. Contract Number DE-AC21-86MC23087, 1988.

Lew,S., Jothimurugesan, K and Flytzani-Stephanopoulos,M., "High-Temperature H_2S Removal from Fuel Gases by Regenerable Zinc Oxide - Titanium Dioxide Sorbents", Ind.Eng.Chem.Res., 28,535(1989).

Woods,M.C., Gangwal, S.K., Jothimurugesan,K and Harrison, D.P., "The Reaction Between H_2S and Zinc Oxide-Titanium Oxide Sorbents: I. Single Pellet Kinetic Studies", Ind.Eng.Chem.Res, 29,1160(1990).

P10 Granular Filtration in a Fluidized Bed

J.S. Mei, P.C. Yue, and J.S. Halow
Morgantown Energy Technology Center

ABSTRACT

Successful development of advanced coal-fired power conversion systems often require reliable and efficient cleanup devices which can remove particulate and gaseous pollutants from high-temperature high-pressure gas streams. A novel filtration concept for particulate cleanup has been developed at the Morgantown Energy Technology Center (METC) of the U. S. Department of Energy. The filtration system consists of a fine metal screen filter immersed in a fluidized bed of granular material. As the gas stream passes through the fluidized bed, a layer of the bed granular material is entrained and deposited at the screen surface. This material provides a natural granular filter to separate fine particles from the gas stream passing through the bed. Since the filtering media is the granular material supplied by the fluidized bed, the filter is not subjected to blinding like candle filters. Because only the in-flowing gas, not fine particle cohesive forces, maintains the granular layer at the screen surface, once the thickness and permeability of the granular layer is stabilized, it remains unchange as long as the in-flowing gas flow rate remains constant. The weight of the particles and the turbulent nature of the fluidized bed limits the thickness of the granular layer on the filter leading to a self-cleaning attribute of the filter. Batch mode filtration performance of the filter was first reported at the Ninth Annual Coal-Fueled Heat Engines, Advanced Pressurized Fluidized-Bed Combustion, and Gas Stream Cleanup Systems Contractors Review Meeting. This poster paper presents work since then on a continuous filtration system.

The continuous filtration testing system consisted of a filter, a two-dimensional fluidized-bed, a continuous powder feeder, a laser-based in-line particle counting, sizing, and velocimeter (PCSV), and a continuous solids feeding/bed material withdrawal system. The two dimensional, transparent fluidized-bed allowed clear observation of the general fluidized state of the granular material and the conditions under which fines are captured by the granular layer. A series of experiments were conducted over various ranges of operating conditions with two different bed materials: a 30x270 mesh acrylic powder with particle density of 1.1 gm/cc and a 40x270 mesh Millwood sand which has particle density of 2.5 gm/cc. During the experiments, fine sand (less than 100 micron) was fed continuously to the bed through the powder feeder at a constant rate of 3.8 gm/min (0.5 lb/hr). Bed material and captured fine particles were withdrawn continuously through an overflow tube. In order to maintain a constant bed level, makeup bed material was also fed continuously through an non-mechanical valve to the bottom of the fluidized bed. Performance of this granular filtration system was measured by the PCSV at downstream of the filter.

High filtration performance was measured when lower density powder was used as bed material. Collection efficiencies over 99 % were obtained with this bed material in a continuous flow mode. Low filtration performance was experienced with heavier bed material. The low filtration performance with this material may be attributed to the failure of maintaining a sufficiently thick granular layer at the screen filter surface. Filtration performance as a function of particle size distribution and the pressure drop across the granular filter will also be discussed in this poster paper.

P11

Dust Cake Behavior in Filters With High Surface Area to Volume Ratios

Douglas Straub
Ta-Kuan Chiang
Richard A. Dennis
Morgantown Energy Technology Center

INTRODUCTION

High-temperature particulate control devices are an integral part of advanced coal-fired power systems. By efficiently removing minute particles from high-temperature gas streams, environmentally clean and efficient power systems can be realized. In recent years, economic incentives have prompted developers of high-temperature and high-pressure (HTHP) particulate filtration systems to pursue filter element designs with more filter surface area for a given volume. Although higher surface-to-volume (SV) ratio filter designs are driven by economic incentives, physical constraints and the fundamental behavior of dust cake formation and removal will limit the maximum SV ratio.

In an attempt to improve the understanding of dust cake behavior in a well controlled environment, a two-dimensional cold flow filter module is being tested. This filter module can be used to investigate dust cake formation, removal, and re-entrainment over a range of operating conditions. Some of the operating conditions investigated include filter spacing (3.2 and 6.4 cm), filter length (51 and 102 cm), face velocity (160 to 460 cm/min), particle loading (10,000 to 40,000 ppm), and the physical properties of the particulate media.

Preliminary results suggest that the cohesive strength of the particulate media has a strong influence on how the dust cake is removed during reverse pulse cleaning. Furthermore, the properties of the particulate media play an important role in forming non-uniform dust cakes. In the following paragraphs, the experimental apparatus, preliminary results, and future plans will be discussed.

EXPERIMENTAL APPARATUS

In these tests, compressed air was used as a carrier gas for the particulate media studied. During the test, the air flow rate and pressure drop across the filter module were monitored by Rosemount (Model 3051) differential pressure transmitters. Flyash was injected using a K-Tron (Model #T20-90-048-F1) twin screw dust feeder. The filter surfaces were constructed from Grade 5 sintered stainless steel. This 1.6-mm thick filter slab had a pore size distribution in the 50 to 100 micrometer range. The air and particulate flow entered the filter plenum at the bottom of the filter module, and flowed upward into a rectangular channel formed by the two filter surfaces and two optically clear Lexan windows. (See Figure 1.)

In order to quantify dust cake thickness variations and determine dust cake permeabilities, an optical device was developed to measure the dust cake thickness in-situ. (See Figure 2.) This device monitored the cake thickness over the entire length of the filter.

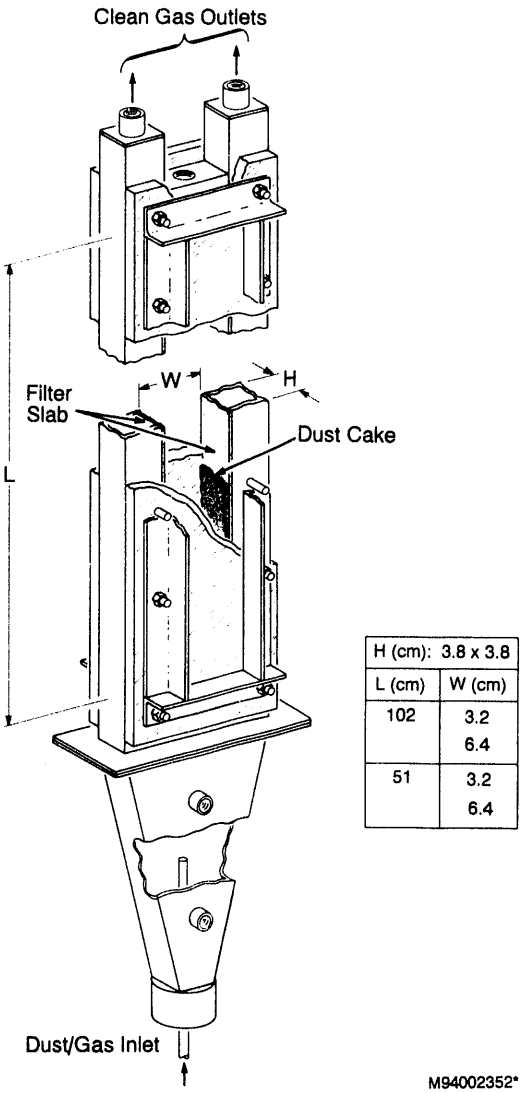

H (cm): 3.8 x 3.8	
L (cm)	W (cm)
102	3.2
	6.4
51	3.2
	6.4

Figure 1. Schematic of the Filter Test Module

The following three flyash materials have been proposed for study:

Sample 1: Pressurized Fluidized Bed Combustor (Tidd) flyash, sample taken December 1992

Sample 2: Pressurized Fluidized Bed Combustor (Tidd) flyash, sample taken February 1994

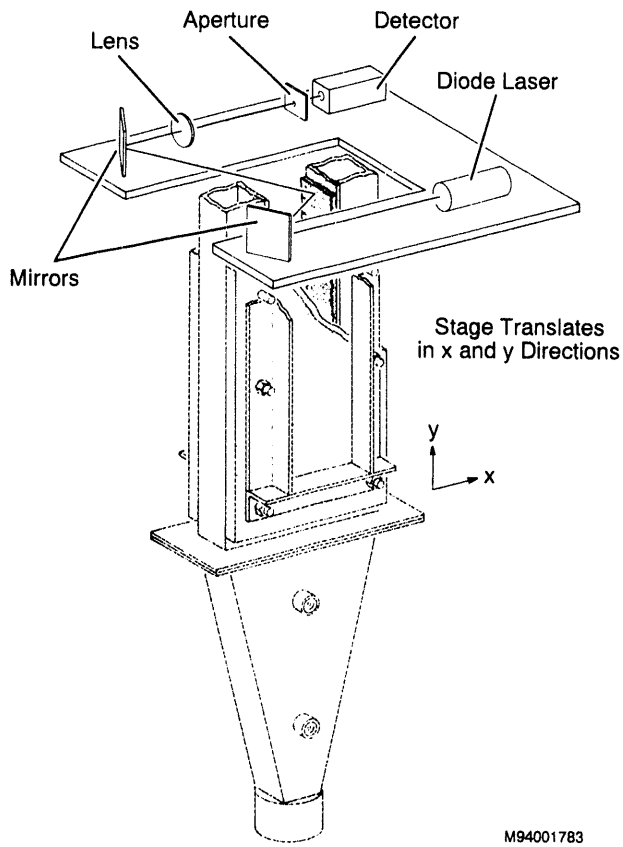

Figure 2. Schematic of the Dust Cake Measurement Device

Sample 3: Pulverized Coal Boiler (Ft. Martin) flyash

The major differences between Sample 1 and Sample 2 are a result of process modifications made at the Pressurized Fluidized-Bed Combustor (PFBC) plant facility. These modifications included spoiling the efficiency of a cyclone located upstream of the filter vessel, and injecting tempering air to lower the operating temperature in the filter vessel. The preliminary results presented in this paper will concentrate on Samples 1 and 3. Testing of Sample 2 will be completed in the future.

RESULTS AND DISCUSSION

The following discussion will address the particulate media characterization, dust cake formation, and dust cake removal data that have been collected at this time.

Particulate Media Characterization

Prior to testing, the particle size distributions were characterized by a Coulter Scientific Multi-sizer II. The mean particle diameters on a volume and population basis are shown in Table 1. The particle density was characterized by a Micromeritics Accu-Pic 1330 helium pycnometer. These results are also shown in Table 1.

In addition to the standard particle size and density analyses, Samples 1 and 2 were analyzed in greater detail. The bulk uncompacted fracture strengths were measured for Samples 1 and 2 as a function of temperature. (See Figure 3.) These samples were heated in a nitrogen environment, and the voidages of both samples were maintained at 86 percent. The theoretical relationship between fracture strength of bulk powders and the properties of its constituent particles can be expressed as follows (Molerus 1975):

$$\sigma_f = \frac{(1-\varepsilon)}{\pi} K \frac{H}{d^2} \quad , \qquad (1)$$

where

σ_f = Fracture strength, (Pa),
ε = Bulk powder porosity,
K = Co-ordination number (varies in the range of 6 to 16 for a uniform size distribution),
H = Isotropic contact force between particles, (N), and
d = Particle diameter, (m).

Although this expression has a strong dependence upon particle size, the Coulter Counter and the dry aerodynamic particle size analyses indicated that a factor of 30 difference in fracture strength could not be explained by differences in particle size alone. Thermogravimetric analyses were conducted to determine if these two samples exhibited significantly different chemical behavior. (See Figures 4 and 5.) Although these analyses showed similar trends, Sample 1 demonstrated a faster rate of weight loss around 900°C (1650°F). It is suspected that this weight loss is due to the decomposition of $CaMg_3(SO_4)_4$, and the faster rate observed for Sample 1 may be indicative of a higher concentration. At this time, it is not clear how $CaMg_3(SO_4)_4$ affects the fracture strength, but testing is planned to answer this question.

Table 1. Particulate Media Characteristics

Sample Number	Description	Mean Size Volume % (micrometer)	Mean Size Number % (micrometer)	Particle Density (g/cc)
1	PFBC Ash - Tidd (Sample taken 12/92)	4.63	2.50	2.84
2	PFBC Ash - Tidd (Sample taken 2/94)	5.63	2.55	2.78
3	PC Boiler Ash - Ft. Martin	67.53	20.81	2.74

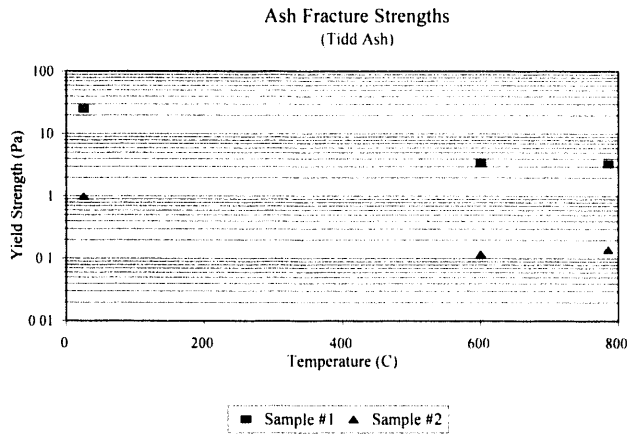

Figure 3. Fracture Strength of Two Pressurized Fluidized Bed Combustor Flyash Samples as a Function of Temperature

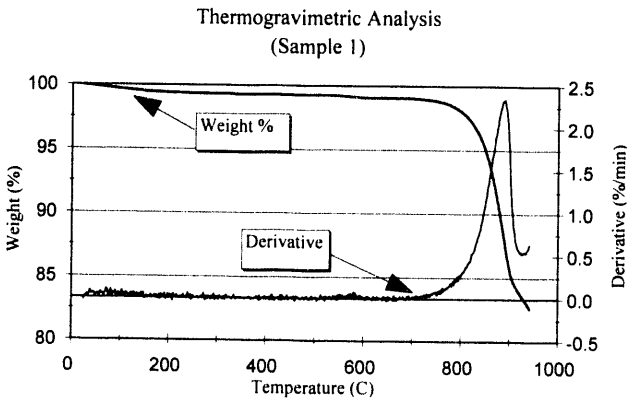

Figure 4. Thermogravimetric Analysis or Pressurized Fluidized Bed Combustor Flyash - Sample 1

Dust Cake Formation Behavior

The air and particulate were injected from the bottom of the plenum, upward toward the filter channel. The operating conditions investigated are shown in Table 2. It should be noted that the filter module with the 6.4-cm spacing was blinded at a face velocity of 458 cm/min. At this high face velocity, particles penetrated the surface of the porous metal surface and became trapped within the filter wall. As a result, the filter permeability decreased, and backflush cleaning was no longer effective. The filter module with the 6.4-cm spacing was blinded very early in the test plan, so the effect of filter aspect ratio has not been thoroughly investigated at this time.

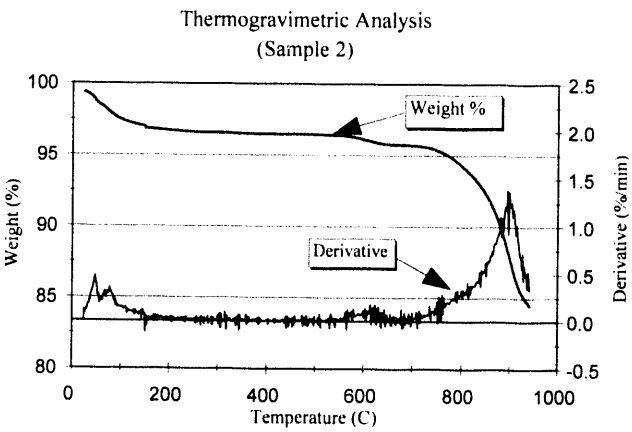

Figure 5. Thermogravimetric Analysis or Pressurized Fluidized Bed Combustor Flyash - Sample 2

For Sample 1, dust cake thicknesses were uniform for all of the operating conditions studied. However, when Sample 3 was investigated under the same operating conditions, distinct features formed along the top half of the filter surfaces. The length of these irregularly shaped mounds ranged from a few millimeters to roughly 50 mm. The thicknesses and the widths were in the 1 to 7 mm range. Along one filter surface, these features were periodically spaced every 35 to 40 mm. This filter surface had a small depression (roughly 25 to 40 mm in diameter and roughly 5 mm deep) located near the middle of the filter surface length. This depression was formed during assembly of the filter module, and may have been introducing turbulent effects into the flow. The mound-like features seemed to be more distinct at higher face velocities which also suggests that these features are dependent upon turbulent effects.

Table 2: Operating Conditions Investigated

Filter Aspect Ratio (length/filter spacing)	Face Velocity (cm/min)	Particle Loading (ppm)
32	168	10,000
32	168	40,000
32	229	10,000
32	229	40,000
16	229	10,000
8	458[1]	10,000

[1] This face velocity blinded the filter module with a 6.4 cm spacing.

These irregular formations were observed with Sample 3, and not with Sample 1. A potential explanation for this difference may be due to the significantly larger particle size distribution for Sample 3, and the fact that the gas momentum in the vertical direction is depleted along the length of the filter. Noting that the largest particles in Sample 3 are in the 100 to 200 micrometer range, at some point along the length of the filter, the velocity falls below the terminal velocity for these particles. Since the body forces on these large particles are more dominant than the drag forces pulling them to the filter surface, the particles fall toward the inlet of the filter module. At some point near the inlet, the vertical velocity component is large enough to re-entrain these particles. This behavior causes the particles to circulate, and is readily observed over an area of 35 to 50 cm of the filter length. This particle motion introduces more turbulence toward the top of the filter module, where the irregular dust cake features are observed. It is important to note that these features are easily removed during reverse pulse cleaning.

Dust Cake Removal Behavior

The behavior of Sample 1 and Sample 3 during pulse cleaning was significantly different. Under the same operating conditions, Sample 1 exhibited "patchy" or incomplete cleaning, whereas Sample 3 cleaned uniformly. The tensile strength of Sample 3 has not been measured, but Sample 1 seems significantly more cohesive.

When the dust cake removal is incomplete, it has been observed that subsequent cleaning pulse cycles do not remove the dust cake from the areas which were previously not cleaned. Although these "patches" have significantly lower permeabilities than the clean areas, the dust cake continues to form on these patches at a slow rate. Over time, these "patches" may lead to significant ash build-up and become nucleation sites for ash bridges. Qualitatively speaking, these "patches" seem to be more prominant near the top of the filter surface, but more data is necessary to substantiate this observation.

Although these results are preliminary, they emphasize the importance of dust cake properties on cleaning behavior, as well as behavior during dust cake formation. A thorough understanding of the relationship between particluate media properties and cleaning behavior of a particular media will lead to improved filter element designs and cleaning techniques.

FUTURE WORK

Plans for this project are as follows:

- Complete testing for Sample 2.
- Measure fracture strength of Sample 1 and Sample 3 at 925°C, to determine if the weight loss observed in the thermogravimetric analyses is responsible for increasing the ash cohesive strength. If these fracture strength measurements are significantly different than the measurements made at a slightly lower temperature, a thorough chemical analysis will be conducted.
- Utilize fast response instrumentation to characterize cleaning parameters.
- Improve existing module design to allow better quantification of incomplete cleaning.
- Investigate the feasibility of new filter designs and cleaning techniques.

ACKNOWLEDGEMENTS

We would like to gratefully acknowledge the diligent efforts of Mr. Rick Williams (EG&G) for his assistance in maintaining and operating this project. We would also like to thank Dr. Steven Woodruff (METC) for his expertise and efforts to develop our dust cake measurement device. Dr. H. O. Kono (West Virginia University) has played a key role in analyzing the fracture strengths of the particulate media used in these tests, and we would like to gratefully acknowledge his expertise and contributions.

REFERENCES

Molerus, O., "Theory of Yield of Cohesive Powders," *Powder Technology,* **12**, (1975), 259-275.

P12 Computer Simulations of IGCC/PFBC Components

Edward. J. Boyle, Thomas J. O'Brien, and Lawrence J. Shadle
Morgantown Energy Technology Center

Madhava Syamlal and Suresh Venkatesan
EG&G Technical Services of West Virginia

ABSTRACT

This modeling activity has provided numerical simulations and graphical visualizations of several IGCC and PFBC components. Specifically, the PyGas component of the Gasification Product Improvement Facility (GPIF) and the Industrial Filter and Pump (IFP), Tidd, and Karhula High Temperature, High Pressure (HTHP) filter unit were simulated. These calculations couple the complex physical phenomenon which affect the behavior of these units, such as, fluid dynamics, solid motion, heat transfer, and chemistry. Since all of these factors interact in a very nonlinear fashion, a complex computer code, based on multi-phase hydrodynamics is required in order to perform the simulations. The MFIX code, developed at METC, and the Fluent code, commercially available from Fluent Inc., were used for these simulations.

The GPIF contains is a novel coal gasification unit. It consists of a central "riser" in which caking coal is devolatilized, a free-board region, in which tar is combusted, and a concentric fixed-bed annular region, in which most of the gasification is completed. Air and coal is fed at the bottom of the riser. A shallow bed of coal and ash forms around the inlet jet. Solids strands of matter are lifted through the riser and overflow into the surrounding fixed-bed. Air is introduced from the top, with a radial divergence, to combust the tar produced during coal pyrolysis in the riser. A hot, annular recirculation region is predicted around this inlet, against the top dome of the vessel. The simulations predict that it will not be possible to sustain a co-flow gasification region. Gas flow from the riser section flows directly below the baffle and into the exit stream. This region shows large fluctuations in particle and gas velocity. Gas flow from below the grate supporting the fixed bed establishes a hot combustion front near the surface of the grate.

Several advanced power systems incorporate HTHP clean-up devices based on ceramic candle filter technology. The Fluent code was used to simulate gas/solid flow in the vessel housing these filters. The simulation of the Karhula design showed that the gas flow from the inlet was splitting on a baffle plate just inside the vessel, circulating down and around between the vessel and an inner shroud, and splashing over the inner shroud 180° from the inlet. This flow was so intense that it was entraining gas, up and out, over the shroud just behind the baffle.

The net effect was that the flow field on the candles themselves was very uneven. Various baffle designs were explored in order to distribute the flow more evenly. Because the inlet was located near the middle of the pressure vessel in the Tidd configuration, the flow pattern in that device was not nearly as complex. Both of these facilities were simulated using the 3-D capabilities of the Fluent code.

A series of simulations were performed in support of the IFP design. Because of the high degree of symmetry in this design, a series of simulations of different design options were performed in 2-D, cylindrical coordinates since this was less demanding computationally. The dimensions of the vessel were accurately represented, but the candles were idealized to a concentric filter ring with the same horizontal "footprint" as the actual array of 78 candles. In order to investigate the extent of flow between the candles, a 30° sector was simulated in 3-D using periodic boundary conditions. Since this calculation still used cylindrical coordinates, the individual candles were resolved so that their horizontal cross-sections were truncated pie shapes, rather than circular. However, their horizontal locations and cross-sections were preserved.

P13 Scaling of Pressurized Fluidized Beds

CONTRACT INFORMATION

Cooperative Agreement	DE-FC21-92MC29264
Contractor	Massachusetts Institute of Technology 77 Massachusetts Avenue Cambridge, MA 02139 (617) 253-2233
Contractor Project Manager	Susan Guralnik
Principal Investigator	Leon R. Glicksman
METC Project Manager	Peter Botros
Period of Performance	October 1, 1992 to September 31, 1995

FY 1994 Program Schedule

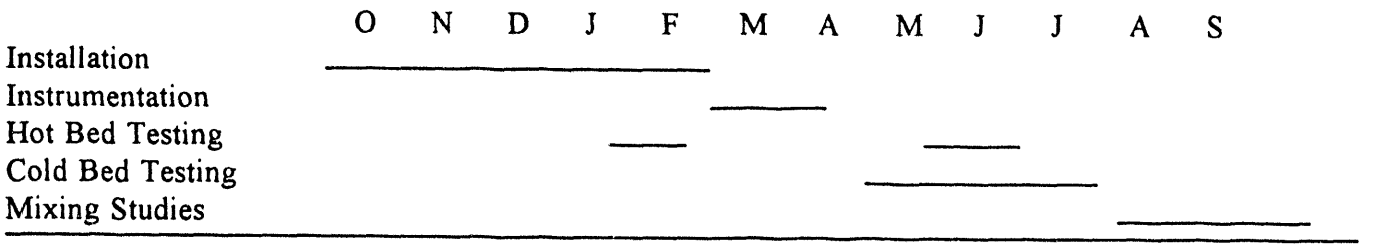

OBJECTIVES

This project has two primary objectives. The first is to verify a set of hydrodynamic scaling relationships for commercial pressurized fluidized bed combustors (PFBC). The second objective is to investigate solids mixing in pressurized bubbling fluidized beds.

American Electric Power's (AEP) Tidd combined-cycle demonstration plant will provide time-varying pressure drop data to serve as the basis for the scaling verification. The verification will involve demonstrating that a properly scaled cold model and the Tidd PFBC exhibit hydrodynamically similar behavior.

An important issue in PFBC design is the spacing of fuel feed ports. The feed spacing is dictated by the fuel distribution and the mixing characteristics within the bed. After completing the scaling verification, the cold model will be

used to study the mixing characteristics of PFBCs. A thermal tracer technique will be utilized to study mixing both near the fuel feed region and in the far field. The results will allow the coal feed and distributor to be designed for optimal mixing.

BACKGROUND INFORMATION

Hydrodynamic scaling

One of the most difficult problems facing a fluidized bed designer is to determine how bed size and operating parameters affect bed performance. This is particularly true when a large combustor is to be designed based on pilot plant experience. It is also critical in the operation or modification of an existing fluidized bed combustor. Research has been done to show that a cold model, designed using the proper hydrodynamic scaling parameters, closely simulates the hydrodynamic behavior of fluidized bed combustors. Accurate room temperature simulations of fluidized bed combustors allow rapid, inexpensive tests to determine the effects of varying operating parameters and bed design on the hydrodynamics of the combustor.

One of the first systematic developments of the dimensionless scaling parameters which control the modeling of a fluidized bed was presented by Glicksman (1984, 1988). The scaling parameters were developed by nondimensionalizing Anderson and Jackson's (1967) equations of motion. The resulting parameters, which we will refer to as the full set of scaling parameters, are as follows:

$$\frac{\rho_f}{\rho_s} \quad \frac{u_o^2}{gD} \quad \frac{\rho_f u_o D}{\mu} \quad \frac{L}{D} \quad \frac{D}{d_p} \quad \phi_s \quad PSD \qquad (1)$$

A great deal of experimental work has been done to verify that when these dimensionless groups are matched between two fluidized beds they exhibit hydrodynamically similar behavior (e.g. for bubbling beds: Nicastro and Glicksman, 1984; Newby and Keairns, 1986; Roy and Davidson, 1989; Almstedt and Zakkay, 1990; and for circulating beds: Glicksman et al., 1991; Chang and Louge, 1992, and Glicksman et al., 1993.)

When the full set of scaling parameters is used, once the scale model fluidizing gas is specified the size of the model is fixed. For example, if air at atmospheric temperature and pressure is used in a cold model of an atmospheric fluidized bed combustor, the model's linear dimensions will be roughly 1/4 those of the hot bed (scale down by factor of four). For the case of pressurized fluidized beds operating at 10-12 atm, a cold model fluidized using ambient air will have approximately the same linear dimensions as the combustor. This makes scaling large combustors using the full set of scaling parameters less tractable. Therefore, it is desirable to look for simplifications to the full set of scaling parameters which will make it possible to choose the scale factor.

Glicksman et al. (1993) proposed a simplification to the full set of scaling parameters which allows the scale factor to be independently specified. The simplification is based on the fact that the number of dimensionless groups can be reduced if the fluid-particle drag is dominated by either viscous or inertial effects. In both the viscous and inertial limits, the scaling parameters reduce to:

$$\frac{\rho_f}{\rho_s} \quad \frac{u_o^2}{gD} \quad \frac{u_o}{u_{mf}} \quad \frac{L}{D} \quad \phi_s \quad PSD \qquad (2)$$

where the bed Reynolds number and the ratio of the reference bed dimension (D) to the particle

diameter (d_p) in the full set [Eqtn. (1)] have been replaced by the ratio of the gas superficial (u_o) and minimum fluidization velocities (u_{mf}). Since this simplified set of parameters holds exactly at both high and low particle Reynolds numbers, it is reasonable to expect it to be approximately valid throughout the range of particle Reynolds numbers. Equation (2) will be referred to as the simplified set of scaling parameters. Glicksman et al. (1993) experimentally verified the simplified set of scaling parameters for atmospheric circulating fluidized beds (CFB) by making hydrodynamic comparisons between three fluidized beds. Hot-bed data was taken from the 2.5 MW_t Studsvik CFB prototype. Scaling comparisons were made between the hot-bed, a 1/4 scale model of the Studsvik CFB based on the full set of scaling parameters, and a 1/16 scale model of the hot-bed based on the simplified set of scaling parameters. The solid fraction profiles of the three beds were found to agree well.

Solids mixing

A properly scaled cold model provides similar hydrodynamics to that of a hot combustor. Solids mixing in bubbling beds is due primarily to bubble characteristics such as bubble size and frequency, which induce mixing in bubble wakes, and to bubble eruptions at the bed surface. A cold scale model with similar hydrodynamics makes it possible to investigate solids mixing for a hot bed combustor.

Lateral and vertical solids mixing is critical in fluidized bed combustors. Adequate mixing is required to ensure high combustion efficiency, sulphur capture, and heat transfer. Solid mixing is typically investigated using tracer techniques. These techniques involve the injection of tracer particles into a fluidized bed and the tracking of their movement in some way. The tracer should have the same density, diameter, and sphericity as the bed material so that its movement will accurately characterize particle motion within the bed. For an ambient air fluidized cold model of a pressurized fluidized bed combustor, the solid density must be approximately 900 kg /m^3. This rules out the use of magnetic tracers or other high density materials. Also, due to the seemingly random behavior of fluidized beds, numerous experiments need to be conducted to characterize the average solids mixing characteristics of the bed. Therefore the technique should not produce an elevated background of the tracer particles which would make it impossible to distinguish between tracers from current and previous experiments. A thermal tracer technique was developed (Valenzuela and Glicksman, 1984) which satisfies these criterion. It has also recently been used to study lateral solids mixing in circulating fluidized beds (Westphalen, 1993). The thermal tracer technique involves the injection of heated bed material particles into the fluidized bed. The motion of the particles is tracked using an array of thermistor probes. This technique has the advantage that the bed material is used as the tracer ensuring that the hydrodynamics will be similar. The heated tracers lose their distinctive signature after some residence time in the bed thus not disturbing the overall background level of subsequent experiments.

PROJECT DESCRIPTION

Hydrodynamic scaling

Experiments will be carried out on the Tidd PFBC and on a cold scale model at MIT. For bubbling beds, important bed characteristics such as gas and solids mixing and heat transfer are a direct function of the bubble characteristics. Thus the experimental verification will be based on a comparison of bubble characteristics.

Time-resolved pressure differences between two vertically spaced static pressure taps give a good indication of the bubble behavior; the amplitude is proportional to the bubble size while the frequency of the fluctuations gives the frequency of bubbles passing between the probes. Comparisons of these quantities can be made by evaluating the probability density function (PDF) and power spectral density (PSD) of the time-varying pressure signal. By placing probes at several locations within the bed, the spatial variation of bubble characteristics can be obtained. Verification of the scaled model with the combustor will be obtained by comparing the PDF and PSD results in nondimensional form.

Solids mixing

After the cold model is verified, it will be used to study solids mixing. The thermal tracer technique will be used.

There are two important sources of mixing which have an impact on the required coal feed spacing. Close to the feed point, mixing is determined by the interaction of the injected fuel and water flow with the bed dynamics. In this region, the momentum of the injected mass and the feed point design may be important. As the material moves away from the feed point into the far field, vertical and lateral mixing of the fuel and volatiles will be determined by the bed dynamics.

To simulate near field mixing in the vicinity of the feed point, preliminary experiments will be carried out using solid tracer and air injected with the same scaled flow rate and momentum as the fuel/water stream. It may also be necessary to simulate the dynamics of the phase change of the water injected with the coal. This may be modeled using chilled liquid refrigerant.

The thermal tracer technique in conjunction with the cold scale model will make it possible to evaluate the effect of varying operating parameters and bed geometry on the solids mixing.

RESULTS

Scaling calculations

Table 1 lists the geometric and operating parameters which are needed to calculate the values of the simplified scaling parameters for the Tidd PFBC. The particle density (ρ_s) was determined by measuring the displacement of a known mass of the Tidd bed material (dolomite). The particle sphericity (ϕ_s) was determined by evaluating a digitized picture of the Tidd bed material using computer software to estimate its average apparent circularity. Chang and Louge (1992) found that the square of the apparent circularity provided a good estimate of the particle sphericity. The particle diameter was determined through sieve analysis, and the minimum fluidization velocity was predicted using an expression proposed by Grace (1982).

Table 1 also lists the parameters for a 1/4 scale cold model of the Tidd PFBC based on the simplified set of scaling parameters. The values in the table are those required to exactly match the scaling parameters. The fluidizing gas properties are those of ambient air.

Cold scale model

A quarter scale cold scale model of a section of the Tidd PFBC has been constructed based on the simplified set of scaling laws. The Tidd boiler enclosure (Kinsinger, 1990) is illustrated in Figure 1. The dashed lines represent the section of the Tidd combustor

Table 1. Comparison of Tidd PFBC and required cold model parameters

	Tidd PFBC	Cold Model (1/4 Scale)
T (°K)	1116	322
p (N/m^2)	$1.013x10^6$	$1.013x10^5$
μ (kg/m-s)	$4.5x10^{-5}$	$2.0x10^{-5}$
ρ_f (kg/m^3)	3.2	1.1
ρ_s (kg/m^3)	2513	875
ϕ_s	0.82	0.82
u_{mf} (m/s)	0.27	0.13
u_o (m/s)	0.91	0.45
D (m)	3.4	0.85
d_p (μm)	920	670

which was scaled. The decision to scale only a section of the combustor was based on the observations of Glicksman and McAndrews (1985) and Glicksman et al. (1987). They found that the bubble distribution is nearly uniform throughout the bed cross-section for large-particle bubbling fluidized beds containing a large array of horizontal tubes.

Figure 2 is a sketch of the MIT cold model. Air from a main blower unit enters the inlet plenum of the model and then passes through a distributor plate fluidizing the bed material. The expanded bed height corresponds approximately with the top of the tube bank. The air leaving the bed passes through a cyclone to capture elutriated bed material. Finally the air exhausts into the room after passing through a filter box.

A granular linear low-density polyethylene manufactured by Union Carbide was chosen as the cold bed material. It has a solid density of

Figure 1. Tidd boiler enclosure with scaled section designated

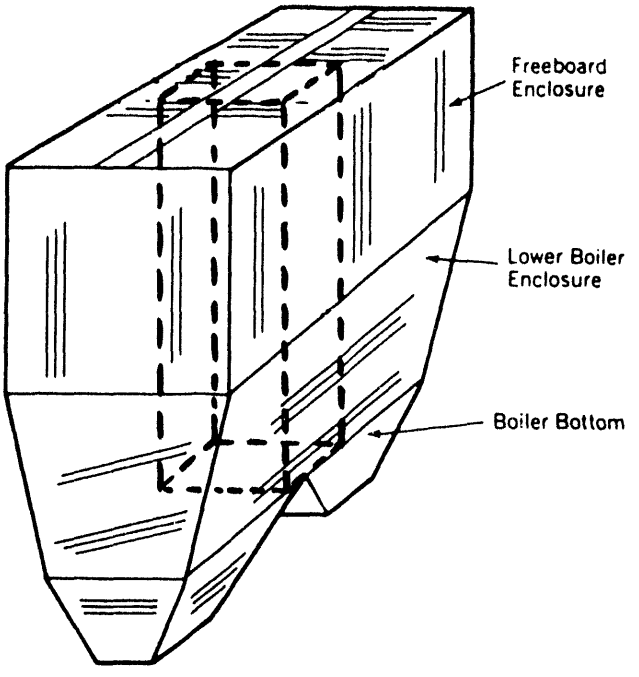

Figure 2. MIT cold model of Tidd PFBC

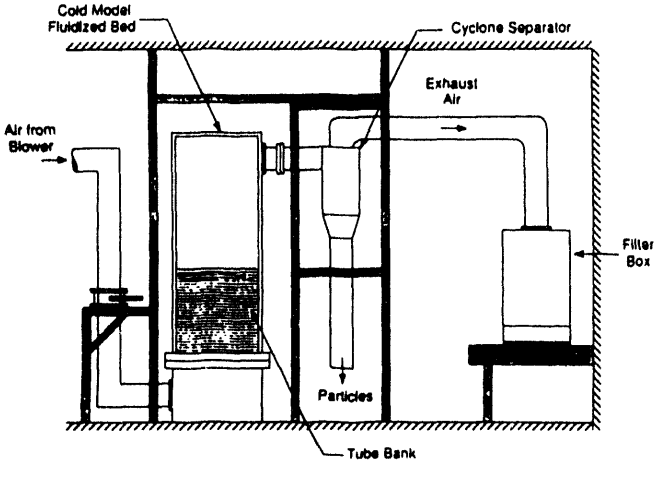

$918\ kg/m^3$ which allows the hot bed density ratio to be matched within 5%. The cold bed material particle sphericity is 0.85 which matches the hot bed value within 4%. Approximately 300 lbs of this material is required to achieve the full bed height.

Preliminary scaling comparisons

Some uncertainty exists in the mean particle diameter and particle size distribution of the Tidd bed material. It is not possible to obtain a particle sample from the center of the bed. Samples typically are taken from bed drains or sorbent reinjection vessels. These may or may not be representative of the material in the bed. The cold bed data presented here were taken with a mean particle diameter of approximately 420 μm which is smaller than the 670 μm particle diameter required to match all the scaling parameters. This was done to evaluate the sensitivity of the scaling to particle size. In the cold bed data u_o/u_{mf} and the particle size distribution were not matched between the hot and cold beds while u_o^2/gD, ρ_f/ρ_s, and L/D were matched. Table 2 summarizes the operating conditions for the hot bed and the cold model. Table 3 compares the values of the simplified scaling parameters for the two beds.

Figure 3 compares the Tidd bed and cold model solid fraction profiles. The solid fraction is the fraction of the bed between two pressure taps which is occupied by the bed material. In gas fluidized beds it is given approximately by

$$1 - \varepsilon \approx \frac{\Delta p}{\rho_s g \Delta h} \qquad (3)$$

Figure 3 shows that in the cold model, the solid fraction is lower (higher voidage) in the bottom of the bed and approximately constant in the upper part of the bed. The hot bed data appear to exhibit a similar trend. One possible explanation for the lower solid fraction in the bottom of the bed could be the presence of small slow moving bubbles causing a high voidage. As the bubbles coalesce they rise faster reducing the voidage. Throughout the tube bank the bubbles are prevented from growing any further producing a fairly flat solid fraction profile. The disagreement between the hot and cold bed solid fraction profiles in the bottom of the bed may be due to the mis-scaled particle size in the cold model. It is difficult to draw any definitive conclusions until data are taken from the cold model with all the scaling parameters matched. More hot bed data is needed to verify the preliminary data.

Table 2. Tidd PFBC and MIT cold model operating conditions

	Tidd PFBC	MIT Cold Model (1/4 Scale)
T (°K)	1116	322
p (N/m^2)	1.013×10^6	1.013×10^5
μ (kg/m-s)	4.5×10^{-5}	2.0×10^{-5}
ρ_f (kg/m^3)	3.2	1.1
ρ_s (kg/m^3)	2513	918
ϕ_s	0.82	0.85
u_{mf} (m/s)	0.27	0.06
u_o (m/s)	0.91	0.45
D (m)	3.4	0.85
d_p (μm)	920	420

Table 3. Comparison of Tidd PFBC and MIT cold model scaling parameters

	Tidd PFBC	MIT Cold Model (1/4 Scale)
ρ_s/ρ_f	795	834
u_o^2/gD	0.025	0.025
u_o/u_{mf}	3.37	7.5
ϕ_s	0.82	0.85

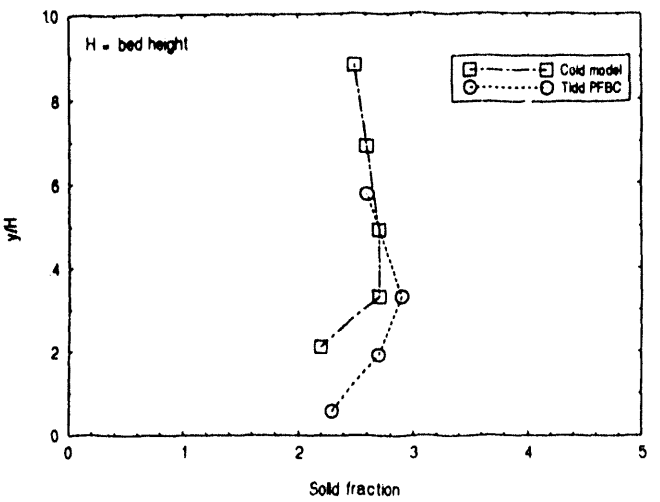

Figure 3. Comparison of Tidd and cold model solid fraction profiles

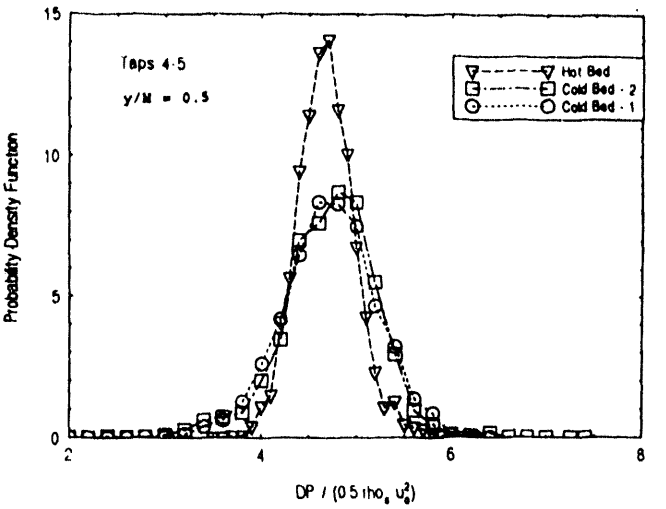

Figure 4. Comparison of probability density functions of Tidd and cold model pressure drop data

High speed time-varying pressure drop data have been taken by Babcock and Wilcox on the Tidd plant. As mentioned previously, the probability density function (PDF) and the power spectral density (PSD) are used to characterize the amplitude and the frequency of the time-varying pressure signal. The PDF measures the probability of the amplitude of the pressure fluctuations being in a certain interval. The PSD gives analogous information about the frequency of the fluctuations. Figure 4 compares the PDFs of the hot and cold bed pressure data as a function of the dimensionless pressure drop. Similarly, Figure 5 compares the PSD of the hot and cold bed pressure data as a function of the dimensionless frequency. These two figures correspond to a single differential pressure location in the bed, similar plots could be generated for the other locations in the bed. Again, due to the fact that all the scaling parameters have not been matched it is presently difficult to draw any conclusions. When data are taken on the cold model with all the scaling parameters matched, it will be possible to assess the level of agreement with the Tidd PFBC, and to evaluate the sensitivity of the scaling to the particle size.

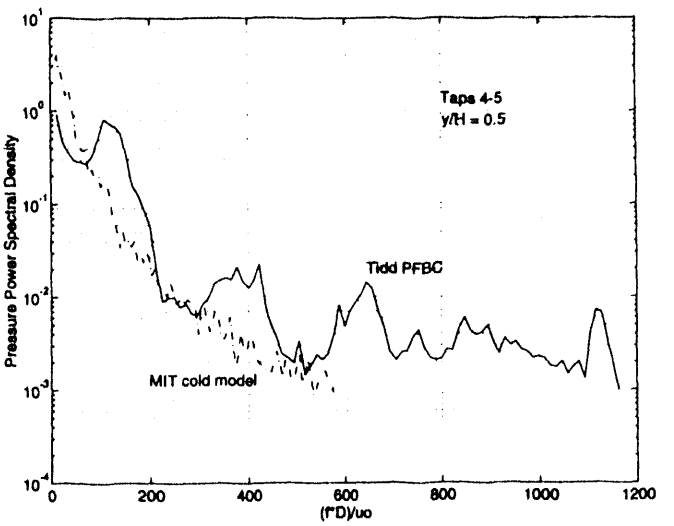

Figure 5. Comparison of power spectral densities of Tidd and cold model pressure drop data

FUTURE WORK

Hydrodynamic scaling

The properly scaled particle size and size

distribution must be attained in the cold model. This will permit direct scaling comparisons between the Tidd PFBC and the MIT cold scale model. Additional high speed hot bed data must also be obtained to corroborate the validity of the initial set of Tidd pressure data. Based on the results of the scaling comparison, the cold model tube bank details will be refined, if necessary, to obtain good agreement between the hot bed and the cold model. Current plans are to complete this work by August 1994.

Solids mixing

Once the cold scale model has been verified it will be possible to begin to investigate the solids mixing in the bed. The emphasis will be on obtaining information to help designers determine the necessary fuel feed spacing. Studies will also be done to evaluate the effects of varying bed operating and geometric parameters on solids mixing.

Tidd support

One of the advantages of having a cold scale model of an existing combustor is that it can be used as a diagnostic tool to evaluate problems related to the bed hydrodynamics. Tidd has experienced a number of problems related to solids mixing including: insufficient heat transfer surface area, poor fuel distribution, and sinter formation. It is often difficult to perform the detailed measurements necessary to solve a problem in the hostile environment of a combustor. AEP is currently interested in trying to obtain information from the cold model to give them guidance in addressing some of these problems.

NOMENCLATURE

D	Reference bed dimension
d_p	Surface-volume mean particle diameter
g	Acceleration due to gravity
L	Bed dimension
PSD	Dimensionless particle size distribution
u_{mf}	Minimum fluidization velocity
u_o	Gas superficial velocity
Δh	Distance between pressure taps
H	Expanded bed height
Δp	Incremental pressure drop
ε	Voidage
μ	Fluidizing gas dynamic viscosity
ϕ_s	Particle sphericity
ρ_f	Fluidizing gas density
ρ_s	Particle solid density

REFERENCES

Almstedt, A.E. and Zakkay, B., 1990, "An Investigation of Fluidized-Bed Scaling - Capacitance Probe Measurements in a Pressurized Fluidized-Bed Combustor and a Cold Model Bed," Chemical Engineering Science, 45, 4, pp. 1071-1078.

Anderson, T.B. and Jackson, R., 1967, "A Fluid Mechanical Description of Fluidized Beds - Equations of Motion," I&EC Fundamentals, 6, 4, pp. 527-539.

Chang, H. and Louge, M., 1992, "Fluid Dynamic Similarity of Circulating Fluidized Beds," Powder Technology, 70, pp. 259-270.

Glicksman, L.R., 1984, "Scaling Relationships for Fluidized Beds," Chemical Engineering Science, 39, 9, pp. 1373-1379.

Glicksman, L.R., 1988, "Scaling Relationships for Fluidized Beds," Chemical Engineering Science, 43, 6, pp. 1419-1421.

Glicksman, L.R., Westphalen, D., Brereton, C., and Grace, J., 1991, "Verification of Scaling Laws for Circulating Fluidized Beds," in Circulating Fluidized Bed Technology III, P. Basu, M. Horio, and M. Hasatani, eds., Pergamon Press, p. 119.

Glicksman, L.R., Hyre, M.R., and Woloshun, K., 1993, "Simplified Scaling Relationships for Fluidized Beds," Powder Technology, 77, pp. 177-199.

Glicksman, L.R., Lord, W.K., and Sakagami, M., 1987, "Bubble Properties in Large-Particle Fluidized Beds," Chemical Engineering Science, 42, 3, pp. 479-491.

Glicksman, L.R., and McAndrews, G., 1985, "Effect of Bed Width on the Hydrodynamics of Large Particle Fluidized Beds," Powder Technology, 42, pp. 159-167.

Grace, J.R., 1982, "Fluidized-Bed Hydrodynamics," Chapter 8.1, Handbook of Multiphase Systems, ed. G. Hestroni, Hemisphere, Washington, DC.

Kinsinger, F.L., 1990, "PFBC System Modularity," Babcock & Wilcox Technical Paper BR-1409, Presented to American Power Conference, Chicago, IL.

Newby, R.A. and Keairns, D.L., 1986, "Test of the Scaling Relationships for Fluid-Bed Dynamics, Fluidization V, Engineering Foundation, New York, pp. 31-38.

Nicastro, M.T. and Glicksman, L.R., 1984, "Experimental Verification of Scaling Relationships for Fluidized Bed," Chemical Engineering Science, 39, 9, pp. 1381-1391.

Roy, R. and Davidson, J.F., 1989, "Similarity Between Gas-Fluidized Beds at Elevated Temperature and Pressure," Fluidization VI, Engineering Foundation, New York, pp. 293-300.

Valenzuela, J.A. and Glicksman, L.R., 1984, "An Experimental Study of Solids Mixing in a Freely Bubbling Two-Dimensional Fluidized Bed," Powder Technology, 38, p. 63.

Westphalen, D., 1993, "Scaling and Lateral Solid Mixing in Circulating Fluidized Beds," Ph.D. Thesis, Department of Mechanical Engineering, Massachusetts Institute of Technology.

P14 Evaluation of Options for CO_2 Capture/Utilization/Disposal

CONTRACT INFORMATION

Contract Number	DE-92MC29220
Contractor	Argonne National Laboratory 9700 S. Cass Argonne, IL 60439 (708) 252-5913
Contractor Project Manager	David K. Schmalzer
Principal Investigators	Richard D. Doctor C. David Livengood
METC Project Manager	Richard A. Johnson
Period of Performance	June 1, 1993 to June 1, 1994

Schedule and Milestones

FY 94 Program Schedule

	S	O	N	D	J	F	M	A	M	J	J	A	S
IGCC/Commercial CO_2	———												
IGCC/Developmental CO_2		———											
IGCC/O_2/Commercial CO_2				———									
IGCC/O_2/Developmental CO_2								———					

OBJECTIVE

The project objective is to develop engineering evaluations of technologies for the capture, use, and disposal of carbon dioxide (CO_2). This project emphasizes CO_2-capture technologies combined with integrated gasification combined-cycle (IGCC) power systems. Complementary evaluations address CO_2 transportation, CO_2 use, and options for the long-term sequestration of unused CO_2. Commercially available CO_2-capture technology is providing a performance and economic baseline against which to compare innovative technologies. The intent is to provide the CO_2 budget, or an "equivalent CO_2" budget associated with each of the individual energy-cycle steps in addition to process design capital and operating costs. The value used for the "equivalent CO_2" budget is 1 kg CO_2/kWhe.

This study took the gasifier output from an IGCC plant through water-gas shift and then to either amine, low-pressure glycol, chilled methanol, or hot potassium carbonate CO_2

recovery prior to the combustion turbine. Carbon dioxide recovery from the main stack was set at 90%, and the combustion turbine now was fed a high hydrogen content fuel. From the IGCC plant, a 500-km pipeline took the CO_2 to geological sequestering. For these cases, the net electric power production was reduced by 73.6 - 185.1 MW with a 0.29 - 0.53 kg/kWhe CO_2 release rate (when make-up power was considered.) Life-cycle CO_2 sequestering costs ranged from 113 - 201 $/ton CO_2. Two additional life-cycle energy balances for emerging technologies were considered including: 1) high-temperature CO_2 separation with calcium- or magnesium-based sorbents, and 2) ambient-temperature polymer membranes for acid-gas removal.

BACKGROUND INFORMATION

The location of the IGCC plant is specified as the midwestern United States. We have set the location as 160 km. by rail from the Old Ben No. 26 coal mine in Seeser, IL, the source of Illinois #6 coal used in the study. Details of the IGCC portion of the system are taken from a previous report (Southern Company Services, 1990), which describes a plant utilizing an air-blown gasifier with in-bed sulfur removal. The base case is a 458-MW IGCC system using an air-blown Kellogg-Rust-Westinghouse (KRW) agglomerating fluidized bed gasifier, Illinois #6 bituminous coal feed and in-bed sulfur removal. Mining, feed preparation and conversion result in a net electric power production of 453 MW with a 0.835 kg/kWhe CO_2 release rate.

PROJECT DESCRIPTION

The gasifier output ran through water-gas shift and then to CO_2 recovery prior to the combustion turbine. Carbon dioxide recovery from the main stack was set at 90%, and the combustion turbine now was fed a high hydrogen content fuel. From the IGCC plant, a 500-km pipeline took the CO_2 to geological sequestering.

Coal and Limestone Mining

Old Ben No. 26 is an underground mine with an associated coal-preparation plant. The IGCC power plant is assumed to be 160 km from the mine, shipment of the coal being by rail using a unit train. In order to supply the 152,667 kg/h of coal required by the IGCC plant, the mine and preparation plant combination requires 2.42 MW of power and produces 2,418 kg/h of CO_2. Another 637 kg/h of CO_2 is produced by the diesel-powered rail transportation.

Limestone is used for in-bed sulfur capture in the gasifier. It is assumed that the limestone is extracted from a surface mine (quarry) about 160 km from the plant and transported by rail to the plant site. A total of 39,795 kg/h of limestone is used by the process, giving an energy consumption for extraction of 0.257 MW with an associated CO_2 production of 257 kg/h. Shipment of the limestone by diesel-powered train produces another 140 kg/h of CO_2.

Coal and Limestone Handling

The coal handling system at the plant includes equipment for unloading the coal from the unit train, passing it through preparation and crushing, and then conveying it to 14-h storage silos. The coal is crushed and dried in a series of three fluidized-bed roller mills where the heat for drying is provided by the hot (760 °C) flue gas from the IGCC sulfator process. This drying results in a significant CO_2 emission from the energy cycle that is not reclaimed, but presents a possible opportunity for further reductions. The CO_2 emissions from the sulfator are 13,099 kg/h.

Limestone is crushed in two pulverizers and then pneumatically conveyed to a 24-h storage silo and a 2-h storage bunker before being mixed with the coal in the gasifier surge bins. Energy consumption in this part of the plant is 3.58 MW.

Integrated Gasification Combined-Cycle Base Case

The base case for the comparisons uses air-blown KRW fluidized-bed gasifiers and in-bed sulfur removal. A simplified schematic for this process appears in Figure 1. The system includes two heavy-duty industrial gas turbines (1260 °C firing temperature) coupled with a reheat steam-turbine bottoming cycle. Spent limestone and ash from the gasifier are oxidized in an external sulfator prior to disposal. As noted previously, the sulfator flue gas is taken to the coal-preparation operation for drying coal and is not integrated into the later CO_2 recovery operation, nor is the small amount (158 kg/h) of CO_2 that is emitted from the gasifier lock hoppers.

The hot-gas cleanup system for particulate matter consists of a cyclone followed by a ceramic-candle-type filter. Solids collected are sent to the external sulfator prior to disposal. Gas temperatures are maintained at approximately 540 °C. Supplemental hot-gas desulfurization is accomplished in a fixed-bed zinc-ferrite system. Off-gas from the regeneration of this polishing step is recycled to the gasifier for capture.

The balance of the in-plant consumption of electricity is 33.0 MW, with a main stack CO_2 emission of 362,820 kg/h. The gross IGCC electric power output is 493.8 MW; the total in-plant consumption is subtracted to yield 457.2 MW at the busbar.

Integrated Gasification Combined-Cycle with CO_2 Recovery

Several changes were made to the base case IGCC plant in order to incorporate CO_2 recovery, as shown in Figure 2. These changes entailed processing the cleaned fuel gas through a "shift" reaction to convert the CO to CO_2, recovering the CO_2, and then combusting the low-CO_2 fuel gas in a modified turbine/steam cycle to produce electricity. Gas cleaning and sulfator performance were considered to be unaffected by these changes.

The fuel gas from the KRW process is high in CO. Conversion of the CO to CO_2 in the combustion process would result in considerable dilution of the resulting CO_2 with nitrogen from the combustion air and with water from the combustion reaction. If the CO_2 is removed prior to combustion, a substantial savings in the cost of the CO_2 recovery system is possible because of reduced vessel size and solvent flow rate. The CO in the fuel gas must first be converted to CO_2 by the shift reaction:

$$CO + H_2O \Longrightarrow CO_2 + H_2 .$$

The resulting CO_2 can then be recovered, leaving a hydrogen-rich fuel for use in the gas turbine.

The shift reaction is commonly accomplished in a catalyst-packed tubular reactor. A relatively low-cost iron-oxide catalyst is effective in the temperature range of 340 to 590 °C. Below that range, a more expensive copper-oxide catalyst is required. While the equilibrium concentrations of products are favorable at lower temperatures, this consideration must be balanced against the need for larger reactors. In view of these conflicting considerations, high CO_2 recovery is best achieved by staged reactors that allow for cooling between stages. A two-stage system was chosen for this study, configured to achieve 95% conversion of CO to CO_2.

A number of CO_2-removal technologies are commercially available for application to IGCC systems. However, all of these options involve cooling or refrigerating the gas stream, with an attendant loss of thermal efficiency. To minimize the loss, the heat removed during cooling must be recovered and integrated into the system. Several options for this integration were evaluated, including steam generation alone, fuel-gas

preheating with supplemental steam generation, and fuel-gas saturation and preheating. In the last case, which was the one chosen for this study, moisture condensed from the fuel gas prior to CO_2 recovery is injected into the clean fuel-gas stream as it is heated by recovered heat following CO_2 removal. This allows additional heat to be absorbed before combustion and increases the mass flow rate through the gas turbine. The balance of the thermal energy is used in the heat-recovery steam generator for feedwater heating and steam generation.

The commercial CO_2 recovery processes operate by absorption of the CO_2 in a liquid solvent and subsequent regeneration of the solvent to release the CO_2. The temperature of absorption is solvent-specific. In general, however, the solvents have low boiling points so that substantial cooling of the synthesis gas is required, as noted above. Furthermore, lower temperatures favor absorption, thereby reducing the necessary solvent flow rate. This implies a need for further cooling or refrigeration of the solvent, with additional energy losses. The regeneration of the solvent is also energy-intensive for most processes, since it is usually accomplished by flashing (pressure reduction) and/or heating. If flashing is employed, repressurization of the solvent is required. Heating is generally accomplished by the extraction of steam from the steam cycle.

Five alternative CO_2-recovery processes have been evaluated to date: (1) high-pressure (1000-psi) absorption by a glycol-type solvent with regeneration by flashing, (2) low-pressure (250-psi) absorption by a glycol-type solvent with regeneration by flashing, (3) absorption by monoethanolamine (MEA) with regeneration by throttling and heating via a reboiler, (4) absorption by hot potassium carbonate with regeneration by throttling and heating, primarily by a reboiler, and (5) absorption by low-temperature methanol with regeneration by thermal stripping and distillation.

From an energy perspective, the glycol options have the advantage. This is particularly true for the low-pressure system, which does not require compression of the synthesis gas prior to absorption. The low-pressure glycol system was the most favorable of any of the systems surveyed. The busbar rating of the plant dropped to 473 MW, from which 87.4 MW of internal plant use must be subtracted. Total CO_2 emissions from the preparation plant through compression to 2100 p.s.i. pipeline pressure were 47,267 kg/h.

Pipeline Transport of CO_2

Once the CO_2 has been recovered from the fuel-gas stream, its transportation, utilization, and/or disposal remain as significant issues. Carbon dioxide represents a large-volume, relatively low-value by-product that cannot be sequestered in the same way as most coal-utilization wastes (i.e., by landfilling). Large volumes of recovered CO_2 are likely to be moved by pipeline. In some cases, existing pipelines could be used, perhaps in a shared mode with other products. In other cases, new pipeline construction would be required. Costs for pipeline construction and use vary greatly on a regional basis within the United States.

The recovered CO_2 (328,810 kg/h) represents about four million normal cubic meters per day (4×10^6 Nm^3/d) of gas volume. A supercritical CO_2 pipeline was designed for the transport of this recovered gas. The booster compression for this system contributed an additional 2,066 kg/h of CO_2 emissions and 2.07 MW of power use.

CO_2 Sequestering

It has been proposed that CO_2 be disposed of in the ocean depths. However, many engineering and ecological concerns associated with such an option remain unanswered, and the earliest likely reservoir is a land-based geological

repository. A portion of the CO_2 can be utilized for enhanced oil recovery (EOR), which sequesters a portion of the CO_2, or it can be completely sequestered in depleted gas/oil reservoirs and nonpotable aquifers. Both the availability of these zones and the technical and economic limits to their use need to be better characterized. The energy required at the sequestering site was analyzed, recognizing that the power required for compression will rise throughout the life-cycle of these sequestering reservoirs. However, it was found that the first reservoirs that would be used will in fact be capable of accepting all IGCC CO_2 gas for a 30-yr period without requiring any additional compression costs for operation.

RESULTS

Energy Balance

Comparisons of the system CO_2 and energy balances are given in Fig. 3. The amounts of raw materials (coal and limestone) supplied to the plant are assumed to be constant for both the base and CO_2-recovery cases. However, gross power generation varies with changes in internal energy use (primarily affecting the steam turbine output). Energy use for plant auxiliaries and the CO_2 recovery process is subtracted from the gross generation to yield the net busbar output. This must be further reduced by the external power consumption to yield the net system energy output.

For the CO_2 recovery cases, the system efficiency is reduced from the base-case value of 39.6% to 34.5% with a reduction of about 74 MW in the net system output. If the energy used for compression of the CO_2 at the IGCC plant is combined with the booster-station requirements, nearly one-half of that reduction is seen to be due to transportation of the CO_2 to the disposal site. Nevertheless, the total CO_2 emissions are reduced to only 16% of those in the base case, and the emission rate is reduced from 0.835 kg/kWh to only 0.156 kg/kWh. It should be noted that replacement of the "lost" 74 MW would likely entail additional CO_2 emissions that are not accounted for here.

Economics

The incremental capital and operating costs associated with CO_2 recovery appear in Table 1. While the equipment installed in the base plant has not changed, the cost in terms of $/kW escalates because of the derating of the plant. The annual costs of operating the plant in terms of $/yr uses a 4th quarter 1993 base, and assumes that the shift, CO_2 recovery and booster sections of the plant will not impact overall plant availability.

The base case power cost of 49.5 mills/kWh is increased by nearly 74% in the most favorable case to 86.1 mills/kWh. Part of this cost is charged to the purchase of 74 MW of make-up power for this case at a cost of 60 mills/kWh.

FUTURE WORK

The project will continue to evaluate cases for advanced technologies in oxygen-blown IGCC systems during the remaineder of the fiscal year. The results presented in this study show the value of approaching the issue of IGCC power generation with CO_2 recovery from a full life-cycle analysis.

ACKNOWLEDGMENT

The authors gratefully acknowledge the support and guidance provided by Dr. Richard A. Johnson of the Morgantown Energy Technology Center, who is the project officer for this research.

REFERENCES

1. Southern Company Services, Inc., et al., 1990, *Assessment of Coal Gasification/Hot Gas Cleanup Based Advanced Gas Turbine Systems*, DOE/MC/26019.3004 (DE91002084), prepared by Southern Company Services, Inc., Birmingham, Ala., for the U.S. Department of Energy, Morgantown Energy Technology Center, Morgantown, W.Va.

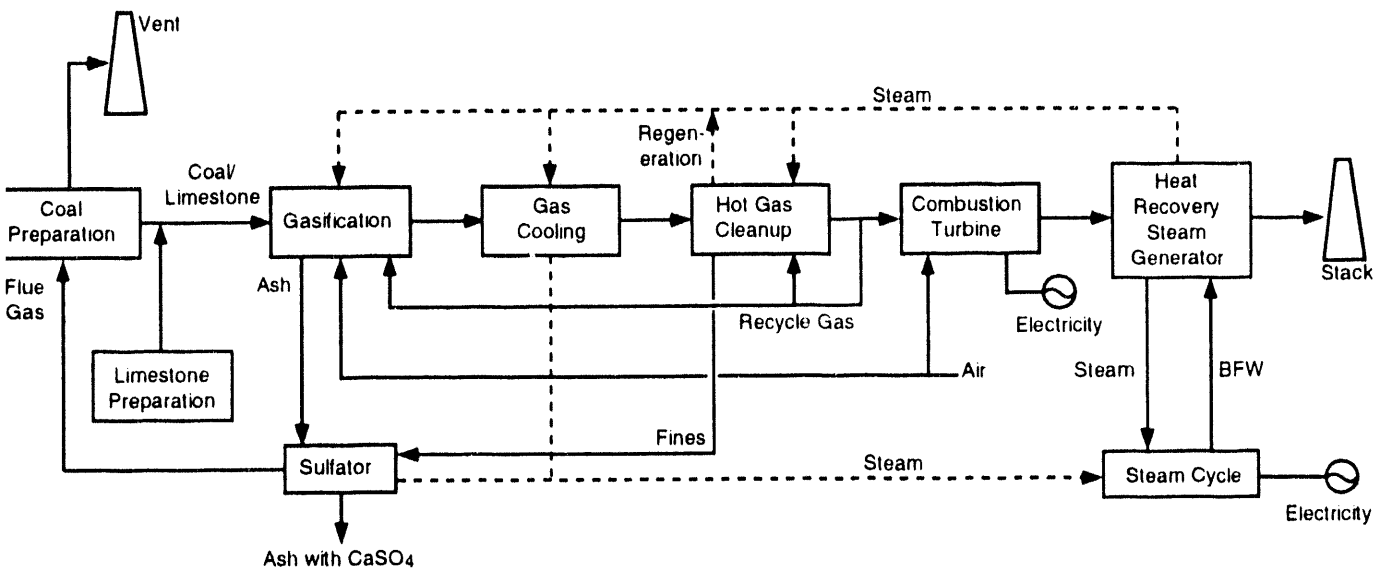

Figure 1. Block diagram of the base case IGCC system.

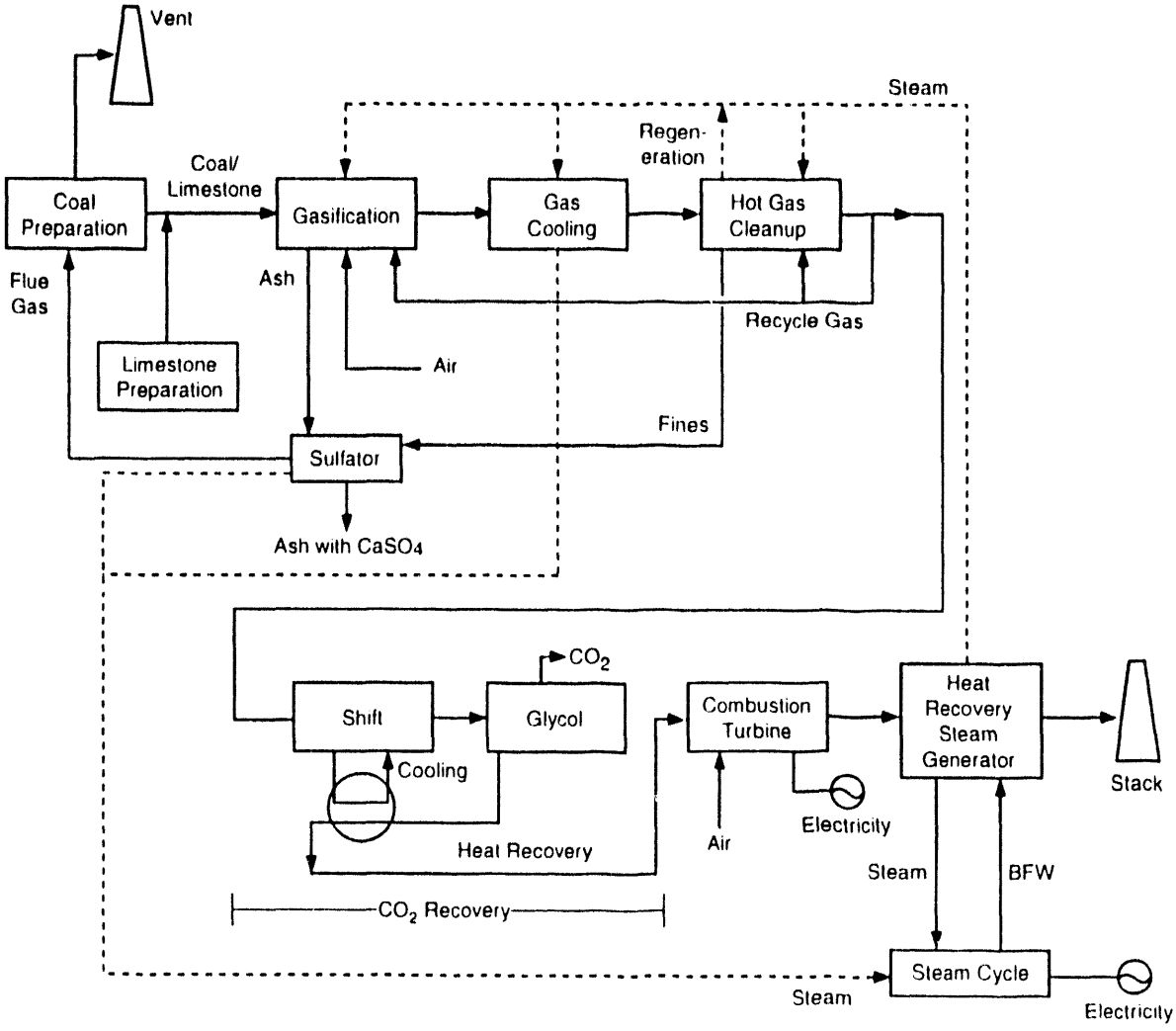

Figure 2. Block diagram of the IGCC system with CO_2 recovery

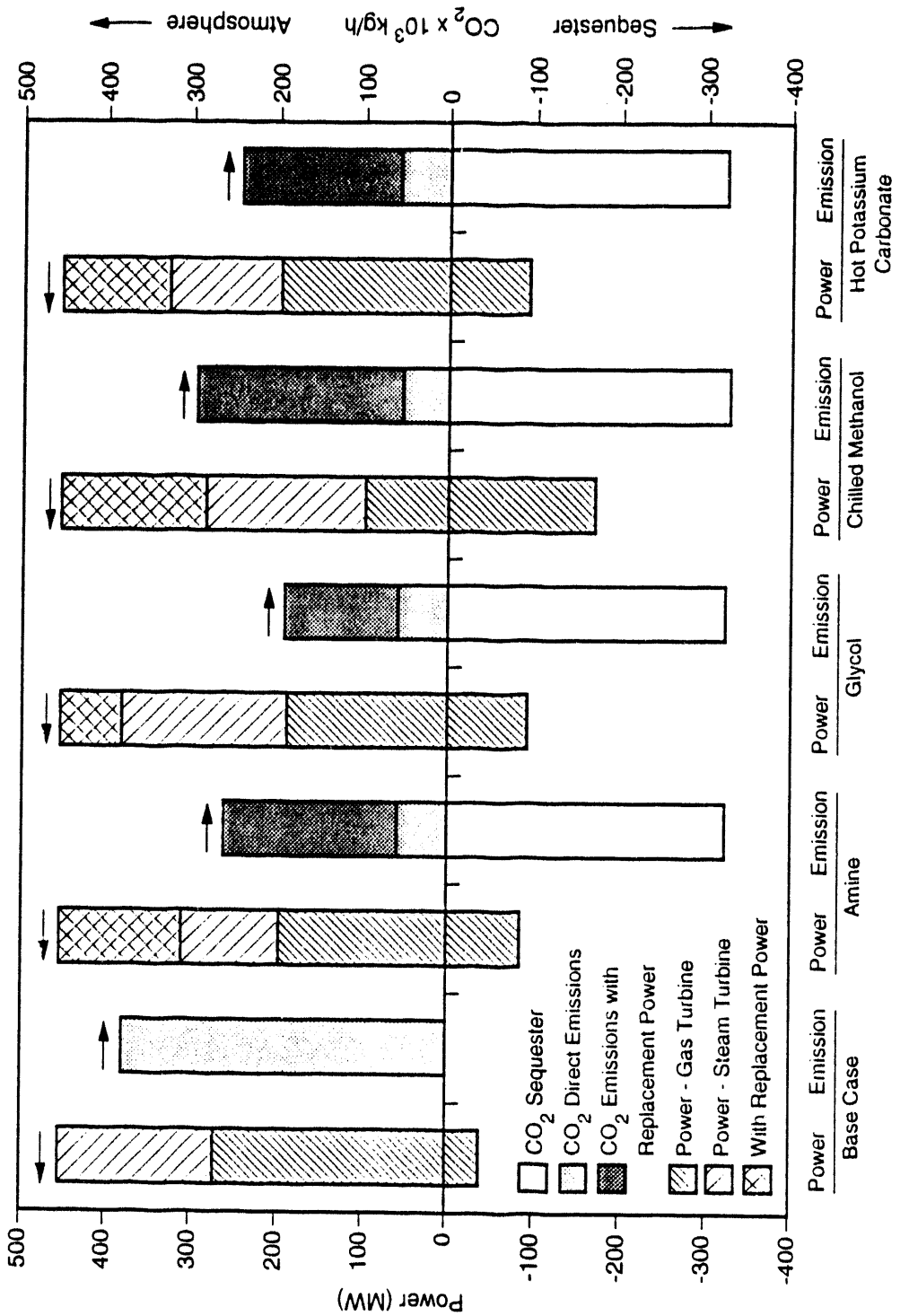

Figure 3. Net Power Generation and Associated Carbon Dioxide Inventory

Table 1. Comparitive Costs of IGCC with Shift/CO_2 Recovery/Pipeline

Component	Unit	KRW Base	MEA	Glycol	Methanol	K-Carbonate
Base Plant Capital	$/kW	1342	1945	1591	2238	1842
CO_2 Control Capital	$/kW	0	647	529	861	615
Power Plant Annual Cost	$/yr	$128,157,363	$148,835,848	$148,325,526	$160,519,522	$148,441,638
Base Plant Power Cost	mills/kWh	49.5	57.5	57.3	62.0	57.4
Pipeline (500 km)	mills/kWh	0.0	19.1	19.1	19.1	19.1
Replacement Power	mills/kWh	0.0	19.0	9.7	24.4	16.7
Net Power Cost*	**mills/kWh**	**49.5**	**95.6**	**86.1**	**105.6**	**93.1**
Coal Energy Input	10^6Btu/h	3940	3940	3940	3940	3940
Busbar Power Output	MW	493.80	395.50	473.00	439.10	420.30
In Plant Power Use	MW	36.63	80.13	87.35	164.98	87.19
Net Plant Output	**MW**	**457.17**	**315.37**	**385.65**	**274.12**	**333.11**
Net Heat Rate	Btu/kWh	8618	12493	10217	14373	11828
Thermal Efficiency - HHV	%	39.62	27.33	33.42	23.76	28.87
Out of Plant Power Use	MW	2.80	4.87	4.87	4.90	4.87
Net Energy Cycle Power	**MW**	**454.37**	**310.50**	**380.78**	**269.22**	**328.24**
Net Energy Cycle Heat Rate	Btu/kWh	8671	12689	10347	14635	12003
Thermal Efficiency - HHV	%	39.38	26.91	33.00	23.33	28.45
Net Energy Cycle Power	MW	454.37	310.50	380.78	269.22	328.24
Replacement Power	MW	0.00	143.87	73.59	185.15	126.13
Net Grid Power	**MW**	**454.37**	**454.37**	**454.37**	**454.37**	**454.37**

*All power costs on the basis of Net Grid Power

P15

Absorption of Hydrogen Sulfide by Zinc Ferrite in the Temperature Range 315 to 538°C (600 to 1,000°F)

Thomas Grindley
Morgantown Energy Technology Center

C. Elaine Everitt
EG&G Technical Services of West Virginia

BACKGROUND AND OBJECTIVE

The high-temperature, regenerable, desulfurization sorbents under development at METC for use in advanced power systems incorporating coal gasification have been designed to operate at temperatures upwards of about 538°C (1,000°F). This temperature has been thought to be optimal, taking into account such factors as higher sorbent reactivity, increased thermodynamic efficiency, and regeneration temperature.

Recent revision of total system considerations indicates that, in certain circumstances, it may be desirable to operate these sorbents at lower temperatures because of materials considerations. Therefore, a small laboratory investigation of the desulfurization performance of zinc ferrite, one of the sorbents under development, was conducted in the temperature range 315 to 538°C (600 to 1,000°). A previous study (Grindley 1982) had indicated a dramatic decline of zinc ferrite's desulfurization performance at 427°C (800°F) compared to that at 538°C (1,000°F).

A number of sulfidation tests were performed using a low-pressure, fixed-bed reactor and simulated gas containing hydrogen sulfide. Hydrogen sulfide breakthrough times were determined and sorbent properties, including sorbent sulfur loading, mineral properties, and porosity, were measured. An attempt was made to apply a fixed-bed simulation model to the data. These points are summarized:

Background

- Performance of regenerable hot-gas desulfurization sorbents below 538°C relatively neglected.
- Decline in rate of desulfurization known but not sufficiently quantified.

Objective

- Conduct sulfidation tests in a small fixed-bed reactor at 315 to 538°C.
- Determine hydrogen sulfide breakthrough times.
- Measure sorbent porosity by mercury porosimetry and nitrogen adsorption.
- Determine effect of sorbent reduction (i.e., $ZnFe_2O_4 \rightarrow ZnO + Fe_3O_4$) on reactivity.
- Estimate effect of sorbent pore size and crystallite size on reactivity.

PROJECT DESCRIPTION

Hot Gas Desulfurization Sorbents

The zinc ferrite sorbent studied was manufactured by United Catalysts, Inc., and designated L-2465. A zinc titanate sorbent, L-3024, also included in the study for comparison, was made by the same company. Details of the sorbents are given in Table 1.

Table 1. Fresh Sorbent Characteristics

	United Catalysts, Inc. L-2465 Zinc Ferrite	United Catalysts, Inc. L-3024 Zinc Titanate
Form	5 mm Extrudates	5 mm Extrudates
Composition	ZnO/Fe_2O_3	2 ZnO/TiO_2
Bentonite Binder (wt%)	2	3
Calcination Conditions (Hr @ °C)	2 @ 815°	2 @ 871°
Bulk Density (g/cm^3)	1.57	1.26
Crush Strength (N/mm)	24.0	35.8
B.E.T. Surface Area (m^2/g)	3.2	3.1
Median Pore Diameter, Volume (nm)	292.0	437.5
Mercury Porosity for Pores >12 nm (%)	54.5+	63.6#
Nitrogen Porosity for Pores <60 nm (%)	2.6*	2.3*
Helium Skeletal Density (g/cm^3)	5.3 g/cm^3*	5.2 g/cm^3*

+ Mercury porosity calculated using total pore volume reported by United Catalysts, Inc., and METC helium density.

Mercury porosity calculated using total pore volume reported by Coors Analytical Laboratory and METC helium density.

* Analysis performed at METC. All other data provided by United Catalyst, Inc.

Laboratory Test Unit

The test unit is the same as that used in previous studies (Grindley 1990, 1991). The process flow diagram is shown in Figure 1. The sorbent was placed in a 150-cm (60-in) long, 5-cm (2-in) diameter fused-silica reactor located within a 3-zone, clamshell, electric furnace. The reactor is shown in greater detail in Figure 2. The sorbent, in the form of extrudates, was supported by a perforated, fused-silica disc. Temperatures along the centerline of the reactor were measured by thermocouples, located inside a metal thermowell.

Gases and water are supplied through rotameters. The manifolded mixture was preheated before entering the reactor. Hot gases from the reactor were cooled by teflon condensers. The system was maintained at a positive pressure of 172 kPag (25 psig). In the sulfidation mode, gases were passed upwards through the reactor. Process conditions were recorded

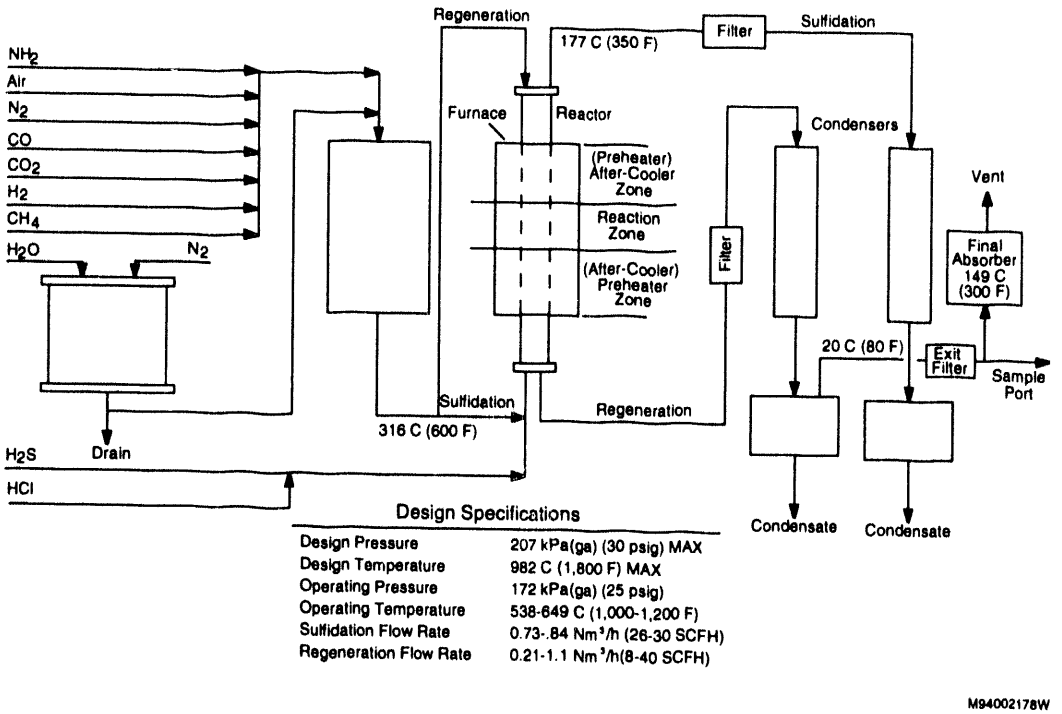

Figure 1. Hot Gas Desulfurization Lab-Scale Unit Process Flow Diagram Fixed Bed Operation

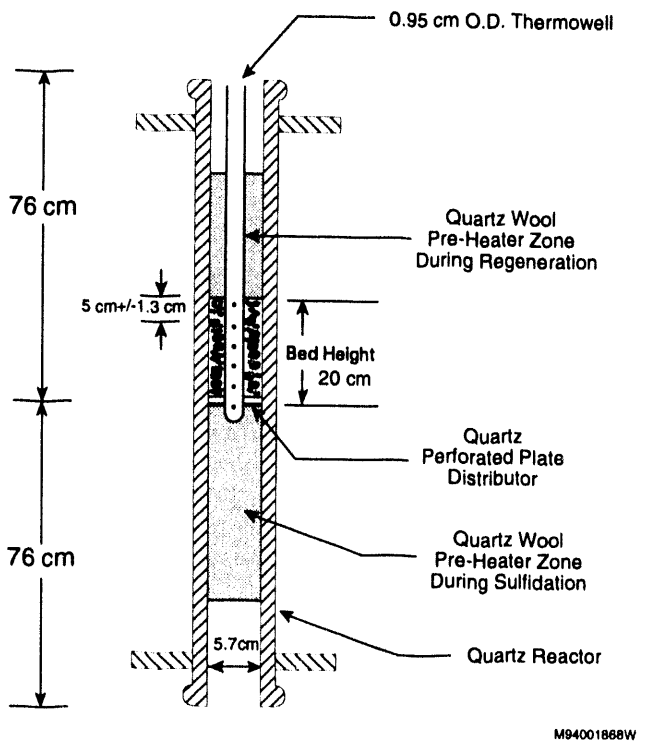

Figure 2. Reactor Details

by an automatic data acquisition and control system.

Test Unit Operation

Five sulfidation tests, 72A, 73, 74, 75, and 76, were performed on zinc ferrite and one test, 68, on zinc titanate. The tests were continued until a breakthrough point of 100 ppmv of hydrogen sulfide was reached. Nominal test conditions are detailed in Table 2. The sulfidation gas composition was typical of that from an air-blown, fluidized-bed gasifier, except for hydrogen sulfide, which was considerably higher, in order to produce an accelerated effect.

In Tests 74, 75, and 76, the sorbent was first reduced for 4 hours at 538°C (1,000°F) in the absence of hydrogen sulfide, followed by sulfidation at the prescribed test temperatures. The reduction converted the zinc ferrite into zinc oxide and magnetite ($ZnFe_2O_4 \rightarrow ZnO + Fe_3O_4$). At the end of each test, the sorbent was removed from the reactor, by vacuuming, in four sections for analysis.

EXPERIMENTAL RESULTS

Hydrogen Sulfide Breakthrough

Hydrogen sulfide breakthrough plots are shown in Figures 3 and 4. The hydrogen sulfide concentrations were measured by Gastec detector tubes, accurate to about 25 percent. Figure 3 illustrates the large effect of prereduction of zinc ferrite on the breakthrough plot at 427°C (800°F). Because sorbent reduction is rapid at 538°C (1,000°F), the breakthrough plot for Test 72A is the same as if the sorbent had been prereduced, and reduction accompanies sulfidation in this case. The plot for Test 73 at 427°C (800°F) shows a dramatic decline in breakthrough time to 1 hour from 7.5 hours in Test 72A. In Test 74, however, also at 427°C (800°F), but in which the sorbent has been prereduced at 538°C (1,000°F), the breakthrough time is somewhat greater than 5 hours, which represents a much more modest decline. The breakthrough time for zinc titanate in Test 68 at 538°C (1,000°F) is about 1.5 hours.

Figure 4 compares breakthrough times for prereduced zinc ferrite at 427°C (800°F), 371°C (700°F), and 315°C (600°F), which are contrasted with the breakthrough time for unreduced zinc ferrite at 427°C (800°F).

The decline of breakthrough time with temperature is faster than if linear. Whereas the decline for Test 72A to Test 74 (Figure 3) is from 7.5 to 5 hours, further decreases in temperature of 56°C (100°F) result in a breakthrough time of 1 hour in Test 76 and less than 0.5 hour in Test 75. The breakthrough plots are corroborated by the sorbent sulfur loadings given in Table 3. These were measured by LECO analyzer for samples at four levels in the sorbent bed. The sorbents from the various tests were analyzed by X-ray diffraction using a RIGAKU diffractometer at West Virginia University. The total integrated intensities, which are proportional to the concentrations of crystalline phases, are given in Table 4 for the predominant mineral constituents, franklinite, sphalerite, and zincite.

Of special interest is the small amount of zincite in the sorbent from Test 73, which was the only sorbent not to undergo prereduction at 538°C (1,000°F). This same phenomenon was observed in a previous investigation (Grindley 1988) in which reductive regeneration to eliminate residual sulfate was studied.

Crystallite sizes for the three mineral species were also obtained from the X-ray diffraction analyses. These are given in Table 5 where available, averaged over the sorbent bed. The crystallite size for franklinite in Test 73 is

Table 2. Nominal Test Conditions

Temperature, °C	315 - 538
Pressure, kPa(g)	172.3
Sulfidation Gas Composition, Volume %	
Nitrogen	45.6
Carbon Dioxide	5.1
Carbon Monoxide	18.3
Hydrogen	11.9
Hydrogen Sulfide	1.0
Steam	18.1
Space Velocity, hr^{-1}	2000
Bed Height, cm	20.3
Reduction Conditions when Applicable	4 Hours @ 538°C

Gas composition during reduction was sulfidation gas composition without hydrogen sulfide.

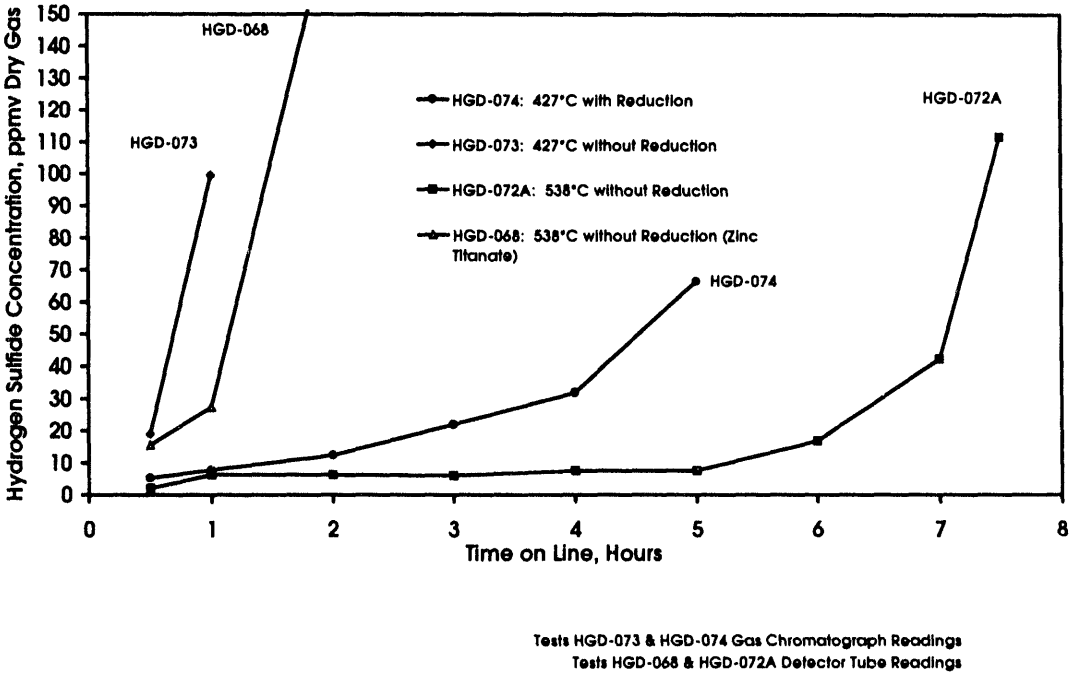

Figure 3. Hydrogen Sulfide Concentration in Exit Gas Stream Zinc Ferrite and Zinc Titanate

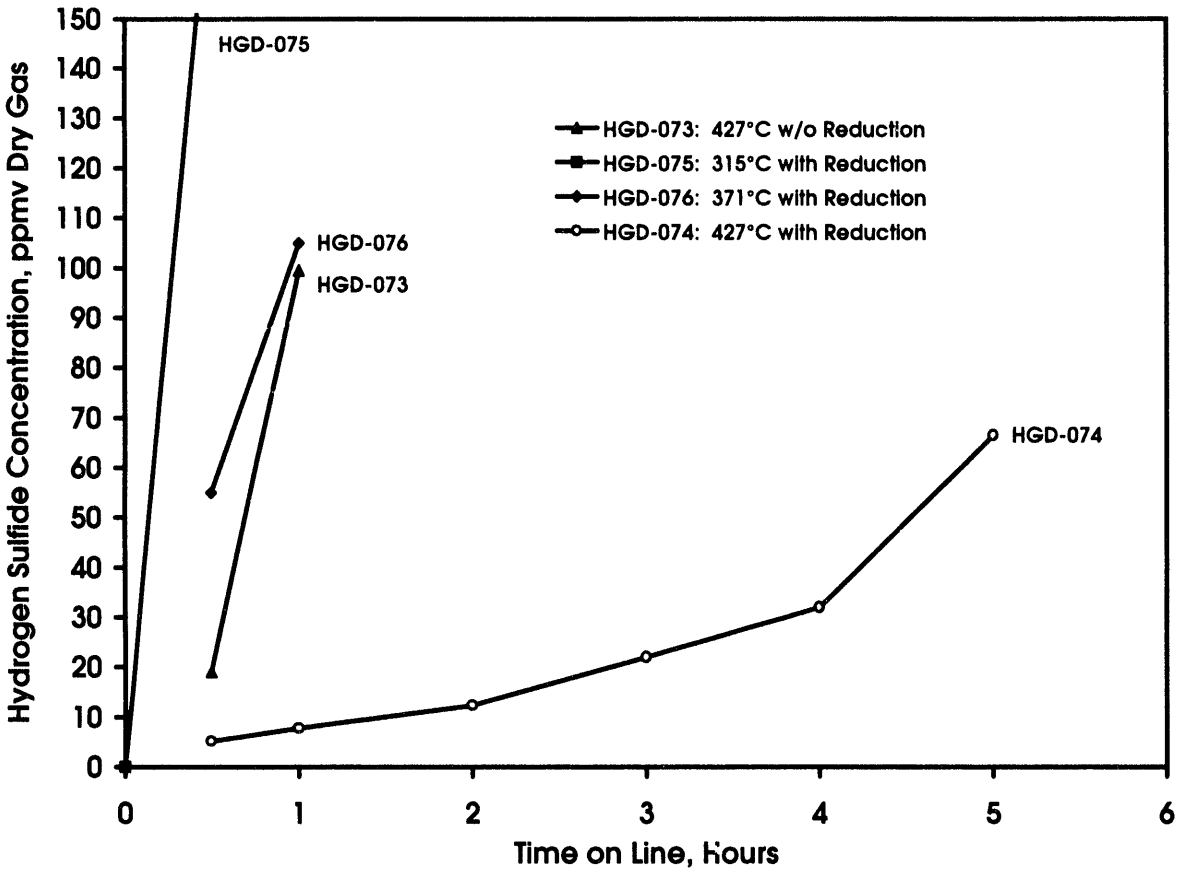

Figure 4. Hydrogen Sulfide Concentration in Exit Gas Stream: Zinc Ferrite

Table 3. Sorbent Sulfur Loading

Weight %
After Sulfidation

	Without Reduction			With Reduction		
TEST NUMBER	HGD-068			HGD-074		
Test Temperature	538°C	HGD-072A	HGD-073	427°C	HGD-075	HGD-076
Time on Stream	4 Hours	538°C	427°C	5 Hours	315°C	371°C
Sorbent	Zinc Titanate	7.5 Hours	1 Hour	Zinc Ferrite	0.5 Hour	1 Hour
Top	3.41	2.17	0.16	0.96	0.28	0.32
Top Middle	12.40	9.83	0.46	4.77	0.70	0.76
Bottom Middle	14.70	19.90	1.18	9.66	0.98	2.01
Bottom	19.20	28.50	3.80	18.30	1.37	4.55

Analysis by ASTM D4239-83 on LECO SC32 instrument.

Table 4. X-Ray Diffraction Analysis, % Total Integrated Intensity

United Catalysts, Inc., L-2465 Zinc Ferrite
After Sulfidation

	Without Reduction		With Reduction		
TEST NUMBER Test Temperature	HGD-072A 538°C	HGD-073 427°C	HGD-074 427°C	HGD-075 315°C	HGD-076 371°C
		TOP OF BED			
Franklinite $ZnFe_2O_4 + Fe_3O_4$	76.8	96.2	77.0	83.8	74.4
Sphalerite, βZnS + FeS	3.0	0.6	1.8	0.0	0.0
Zincite, ZnO	15.1	0.8	16.9	16.2	25.6
		BOTTOM OF BED			
Franklinite	34.9	92.7	63.0	85.3	82.4
Sphalerite	40.3	2.9	21.9	0.0	8.9
Zincite	5.0	1.2	4.0	14.7	8.7

% Total integrated intensity is proportional to the concentration of the crystalline phase.

much larger than that for Test 74, where prereduction occurred. This is probably a factor in explaining the lower sorbent reactivity in Test 73.

Sorbent Porosity

The sorbent porosity was measured using a Micromeritics Mercury Porosimeter and a Micromeritics Digisorb BET Surface Area Analyzer. The former is applicable to pore diameters greater than about 12 nm, whereas the latter applies to pore diameters less than about 60 nm, where it is considered to be more accurate. The porosity values for large pores together with average pore diameters are given in Table 6. Those for small pores are given in Table 7.

For the top of the sorbent bed in Table 6, there appears to be a slightly greater porosity in Tests 74, 75, and 76 where prereduction occurred, than in Test 73 where it did not. Also noticeable is a marked decrease in porosity and average pore diameter with sulfidation, which is greater at the bottom of the bed. Similar results can be seen in Table 7 for small pores. Selected sorbent porosities are plotted in Figures 5, 6, and 7.

Figure 5 illustrates the large impact of sulfidation on porosity in Test 72A. The bottom of the bed is much more heavily sulfided than the top. In Figure 6, porosities at the top of the bed for Tests 72A and 73 are compared. There is an outstandingly lower porosity for small pores in the case of Test 73 where sorbent prereduction

Table 5. X-Ray Diffraction Analysis

United Catalysts, Inc., L-2465 Zinc Ferrite After Sulfidation

	Without Reduction		With Reduction		
TEST NUMBER	HGD-072A	HGD-073	HGD-074	HGD-075	HGD-076
Test Temperature	538°C	427°C	427°C	315°C	371°C
	CRYSTALLINE SIZE, nm				
Franklinite $ZnFe_2O_4 + Fe_3O_4$	73.2	136.7	87.5	NA	NA
Sphalerite, βZnS + FeS	30.1	ND	14.8	NA	NA
Zincite, ZnO	28.5	ND	35.2	NA	NA
	TOTAL INTEGRATED INTENSITY, %				
Franklinite	59.9	94.9	73.4	80.0	79.7
Sphalerite	14.8	1.3	9.6	ND	3.4
Zincite	10.2	0.9	9.9	20.0	14.0

ND = None Detected. NA = Not Analyzed. Fresh zinc ferrite sorbent crystallite size as reported by United Catalysts: > 200 nm. All values are average for the entire bed. Total integrated intensity is proportional to the concentration of the crystalline phase.

did not occur. Figure 7 shows the smaller porosity of both large and small pores for Test 73 compared to Test 74, both at the same temperature but with sorbent prereduction only for Test 74.

Dynamic Simulation Model

The fixed-bed reactor model used to fit the experimental data was similar to that developed by Louisiana State University, assuming a shrinking unreacted core regime (Focht 1986; Wang 1988). In this case, the principal reaction resistances are diffusion within the sorbent pellets and mass transfer at the pellet exteriors. The rate of the intrinsic reaction between H_2S and the interior solid surfaces is assumed to be very rapid. These conditions appear to hold for Test 72A, as evidenced by the electron microscope, x-ray sulfur map for a pellet which is about three-quarters reacted (Figure 8). The sulfur map for Test 74 at a lower temperature (Figure 9) indicates a less sharp unreacted core. The x-ray maps were obtained by a JEOL-840A Scanning Electron Microscope interfaced to a Noran Instruments 8502 Switcher System equipped with a Noran Instruments Micro-Z Energy Dispersive Spectrometer. An attempt was made to fit the experimental hydrogen sulfide breakthrough plot by employing a $T^{1.8}$ temperature dependence of the effective diffusivity in the sorbent pores and an exp (-E/RT) dependence of

Table 6. Mercury Intrusion

United Catalysts, Inc., L-2465
Zinc Ferrite
After Sulfidation

	Without Reduction		With Reduction		
TEST NUMBER	HGD-072A	HGD-073	HGD-074	HGD-075	HGD-076
Test Temperature	538°C	427°C	427°C	315°C	371°C
	LARGE PORE POROSITY, %				
Top	52.5	52.6	54.3	54.8	52.9
Top Middle	52.5	53.5	49.9	54.5	53.2
Bottom Middle	38.4	52.2	46.3	53.5	49.4
Bottom	33.6	50.3	39.4	53.1	53.6
	MEDIAN PORE DIAMETER (Volume), nm				
Top	312.6	295.5	310.8	312.0	283.8
Top Middle	308.8	298.9	282.3	288.2	290.0
Bottom Middle	265.5	274.5	267.0	283.4	264.4
Bottom	255.0	261.0	244.1	268.7	272.7

Porosity for pores < 20 nm. Analyses performed at METC except for HGD-076 performed by Micrometrics. Fresh sorbent porosity 54.5%; median pore diameter 292 nm.

the intrinsic reaction rate constant. It was hoped that the latter would account for the departure from the unreacted core regime. As can be seen, the fit is fairly good (Figure 10). The principal parameters employed in the model are listed in Table 8, and comparison is made with a previous simulation done by Harrison for a similar test (Wang 1988).

CONCLUSIONS

Below about 538°C (1,000°F), there is a rapid fall in the rate of reduction of zinc ferrite (i.e., $ZnFe_2O_4 \rightarrow Fe_3O_4 + ZnO$) in coal-derived gas. This has a large effect on the rate of sulfidation, which also falls rapidly. Therefore, for operation at temperatures lower than 538°C (1,000°F), zinc ferrite should first be prereduced. This is easily accomplished at 538°C (1,000°F) by immersion for a short time in a flow of clean coal-derived gas. Such treatment would also eliminate any residual sulfate in the sorbent from a previous oxidative regeneration. These major findings are summarized below:

- Reduction of zinc ferrite (i.e., $ZnFe_2O_4 \rightarrow Fe_3O_4 + ZnO$) is necessary for good desulfurization.
- Reduction caused formation of zinc oxide and magnetite of smaller crystallite size than original zinc ferrite.
- Reduction of zinc ferrite caused a significant increase in small pore porosity.

Table 7. Nitrogen Adsorption Percent

United Catalysts, Inc., L-2465
Zinc Ferrite
After Sulfidation

	Without Reduction		With Reduction		
TEST NUMBER	HGD-072A	HGD-073	HGD-074	HGD-075	HGD-076
Test Temperature	538°C	427°C	427°C	315°C	371°C
Top	3.15	2.60	3.02	3.01	3.18
Top Middle	2.59	2.80	3.31	3.36	2.97
Bottom Middle	2.06	3.01	2.51	3.29	3.13
Bottom	1.98	2.94	2.21	3.31	2.91

Porosity for pores < 60 nm. Analyses performed at METC. Fresh sorbent porosity 2.6%.

- Zinc ferrite can be used below 538°C (1,000°F) if an initial reduction is carried out.

ACKNOWLEDGEMENT

We acknowledge with thanks the contributions of J. A. Poston, who provided the x-ray sorbent cross-sectional sulfur maps, and E. J. Boyle, who modeled the breakthrough plots.

Table 8. Model Parameters

HGD-072A:	
Bed Length (cm)	17.8
Bed Radius (cm)	2.85
Bed Mass (g)	629
Particle Diameter (cm)	0.476
Skeletal Particle Density (g/cc)	5.3
Bulk Density (g/cc)	1.39
Gas Velocity (cm/s)	12.8
Inlet Pressure (psig)	24
Temperature (K)	818
All Runs:	
De, effective diffusivity (cm^2/hr)	90 (Harrison: 400)
k, intrinsic reaction rate ($cm^2/mol\text{-}hr$)	3×10^7 (Harrison: 3×10^7)
ka, mass transfer (cm/hr)	55800 (Harrison: 22400)
E intrinsic/R (K)	17900
De temp dependence	$(T/884.26)^{1.78}$

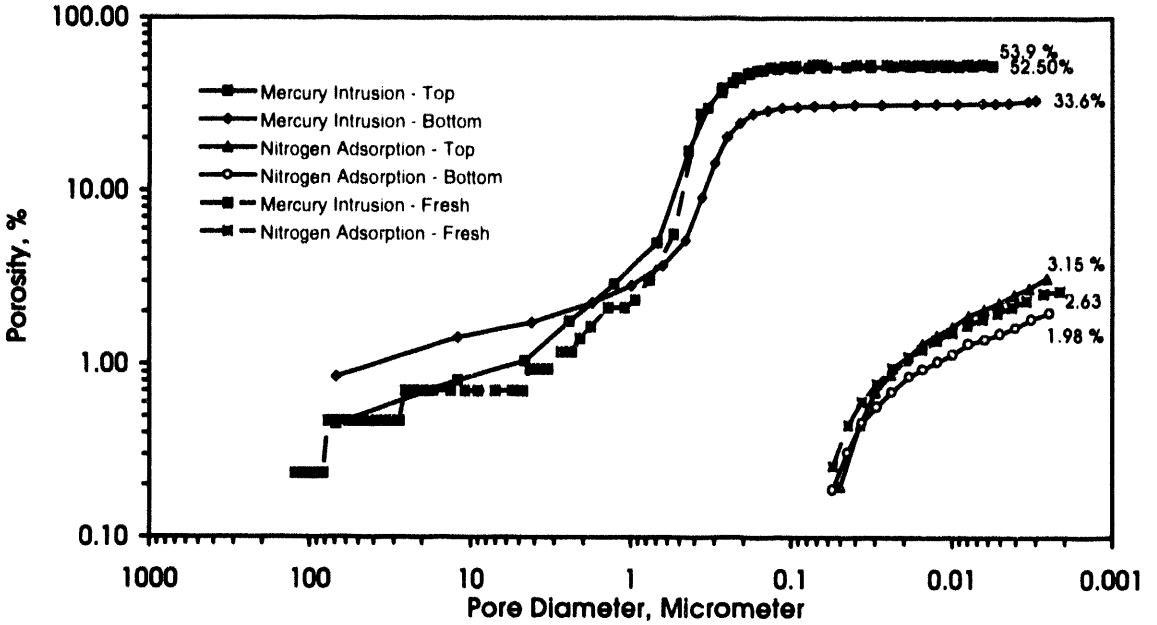

Figure 5. POROSITY vs. PORE DIAMETER
Sulfided L-2465 Zinc Ferrite Sorbent
Test No. HGD-072a 538°C

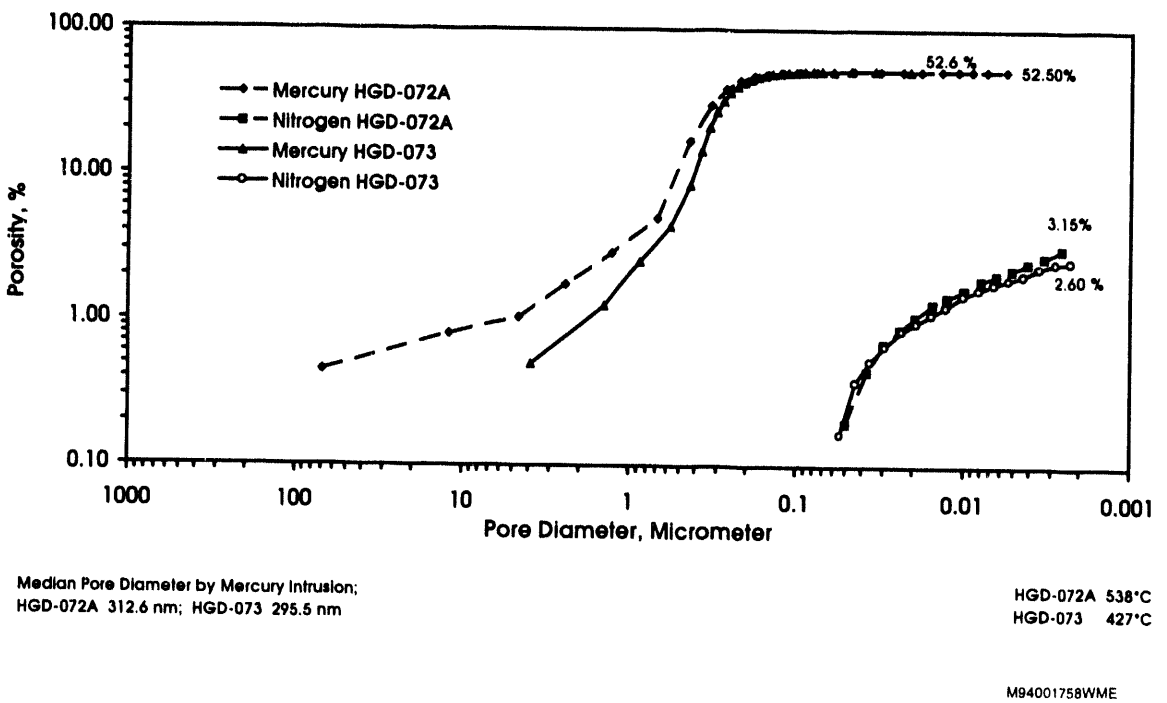

Figure 6. POROSITY vs. PORE DIAMETER
Sulfided L-2465 Zinc Ferrite Sorbent
Top of Bed

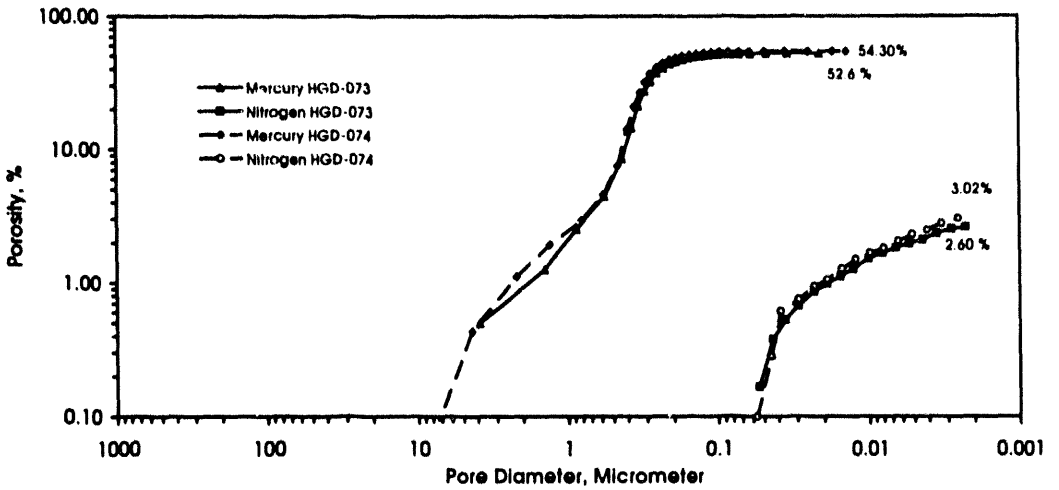

Median Pore Diameter by Mercury Intrusion;
HGD-073 295.5 nm; HGD-074 310.8 nm

HGD-073 Without Reduction
HGD-074 With Reduction

Figure 7. POROSITY vs. PORE DIAMETER
Sulfided L-2465 Zinc Ferrite Sorbent
Top of Bed

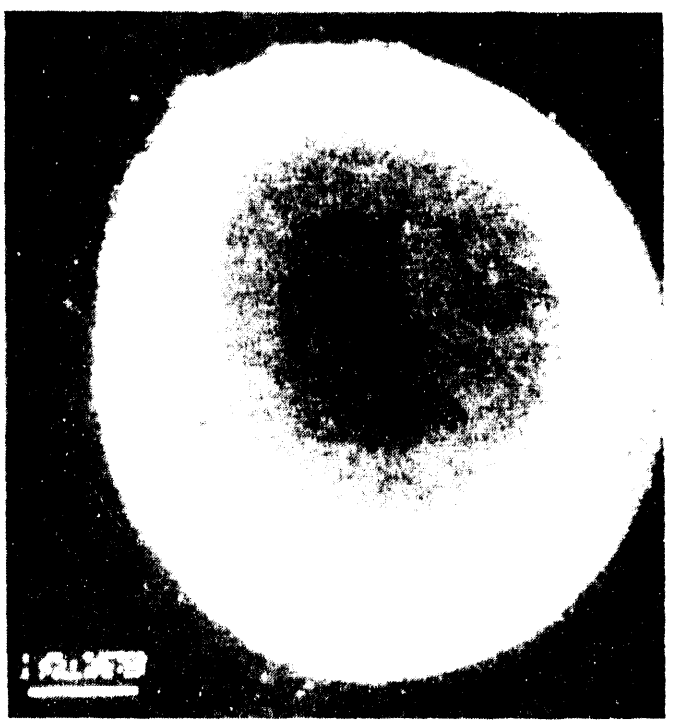

Figure 8. Zinc Ferrite Test 72A
Sulfur Map

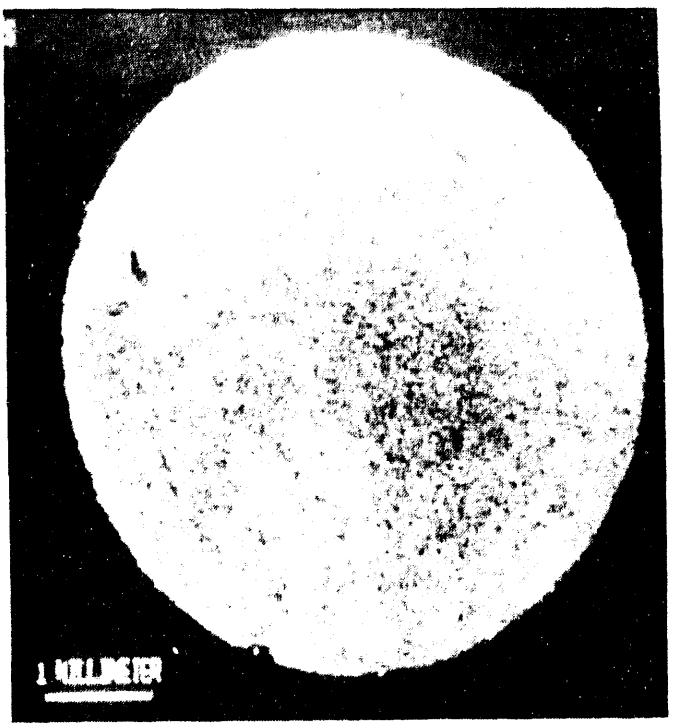

Figure 9. Zinc Ferrite Test 74
Sulfur Map

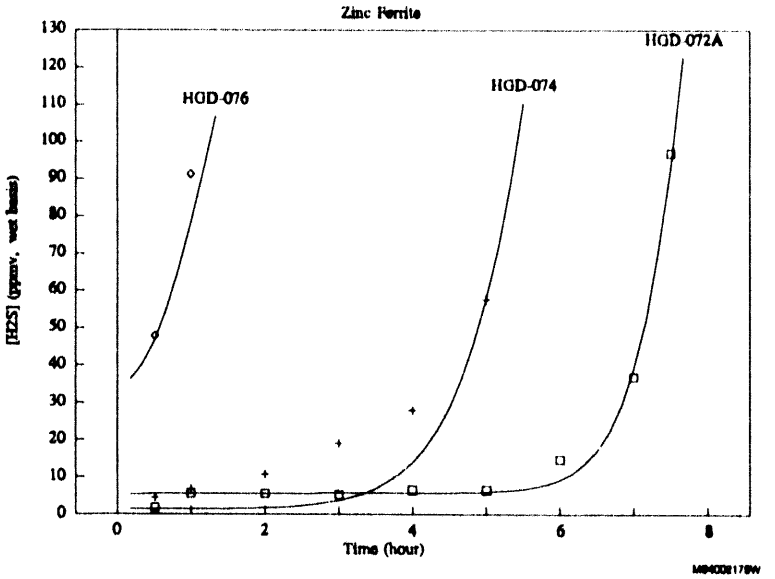

Figure 10. Breakthrough Curves

REFERENCES

Focht, et al., 1986, *Structural Property Changes in Metal Oxide Hot Coal Gas Desulfurization Sorbents*, Report No. DOE/MC/21166-2163, National Technical Information Service, Springfield, Virginia.

Grindley, T., 1982, Development and Testing of Regenerable Hot Coal Gas Desulfurization Sorbents, in *Proceedings of the Second Annual Contractors Meeting on Contaminant Control in Hot Coal Derived Gas Streams*, Report No. DOE/METC/82-47, National Technical Information Service, Springfield, Virginia.

Grindley, T., 1988, Sidestream Zinc Ferrite Regeneration Tests: Laboratory-Scale Study of Reductive Regeneration of Zinc Ferrite Sorbents, in *Proceedings of the Eighth Annual Gasification and Gas Stream Cleanup Systems Contractors Review Meeting*, Report No. DOE/METC-88/6092, National Technical Information Service, Springfield, Virginia.

Grindley, T., 1990, Effect of Chlorine on Hot Gas Desulfurization Sorbents, in *Proceedings of the Tenth Annual Gasification and Gas Stream Cleanup Systems Contractors Review Meeting*, Report No. DOE/METC-90/6115, National Technical Information Service, Springfield, Virginia.

Grindley, T., 1991, Lab-Scale Sorbent Development, in *Proceedings of the Eleventh Annual Gasification and Gas Stream Cleanup Systems Contractors Review Meeting*, Report No. DOE/METC/91-6123, National Technical Information Service, Springfield, Virginia.

Wang, et al., 1988, *Dynamic Simulation Models for High-Temperature Desulfurization Processes*, Report No. DOE/MC/23089-2601, National Technical Information Service, Springfield, Virginia.

TGRIND\7:940606

P16

High Temperature Hydrogen Sulfide Removal with Stannic Oxide

Contract Number	DE-FG03-90ER80998
Contractor	TDA Research, Inc. 12345 West 52nd Avenue Wheat Ridge, Colorado 80033 (303) 422-7830
Contractor Project Manager	Michael E. Karpuk
Principal Investigators	Robert J. Copeland (P.I.), D. Feinberg, D. Wickham, B. Windecker and J. Yu
METC Project Manager	Ron Staubly
Period of Performance	May 23, 1991 to July 31, 1994

FY94 Program Schedule

	S	O	N	D	J	F	M	A	M	J	J	A
Multiple Cycles on Single Sorbent	———											
Economic Analysis		———										
Integrated SnO_2/ZnO Experiment				—						———		

OBJECTIVES

This Phase II SBIR contract is developing a sorbent and process that removes H_2S from hot gasified coal and generates sulfur during regeneration of the sorbent. The process can be used with any type of reactor (*e.g.*, fixed or moving bed) and any gasifier (*e.g.*, KRW or Texaco) and shows lower costs than competing H_2S removal processes.

TDA Research's (TDA) process uses a regenerable stannic oxide-based (SnO_2) sorbent as the first sorbent and zinc ferrite (or zinc titanate) as a second sorbent to remove H_2S to very low concentrations. The process converts the sulfides from both sorbents to elemental sulfur, a commercial product that is easy to store and transport. The goal of this phase is to develop chemically active, high sulfur loadings, and durable stannic oxide sorbents and to demonstrate the process at the bench scale.

BACKGROUND INFORMATION

Low-cost and high-efficiency processes for the removal of sulfur compounds are required to economically apply Gasifier Combined Cycle (GCC) technology to the generation of electric power. Many commercial processes are available to remove sulfur from cold gas streams; however, cooling the gas stream reduces the overall plant efficiency. Hot gas cleanup is being developed to solve that problem; zinc oxide based sorbents effectively remove H_2S to low levels but require either land-filling or additional processing to convert the products of regeneration to a commercial item. TDA is evaluating a regenerable hot gas absorbent that will produce elemental sulfur directly during regeneration.

Elemental sulfur is the only product leaving the plant (*i.e.*, no landfill or sulfuric acid). Elemental sulfur is a dense solid that is not toxic or corrosive. Sulfur is easy to both store and transport long distances and requires less than one third of the weight and volume as the same sulfur in the form of sulfuric acid. Unless the end use of the sulfuric acid is nearby, elemental sulfur is clearly the most desirable commercial end product from the hot gas cleanup.

Process Reactions

The system is based on the absorption of hydrogen sulfide (H_2S) by stannic (tin) oxide. Two sorbents are required, the first sorbent is tin (stannic) oxide, which removes half of the sulfur. The second sorbent is a zinc oxide based material (*i.e.*, zinc ferrite or zinc titanate) that removes the other half of the sulfur from the gasified coal. The zinc oxide second sorbent reduces the sulfur of the coal gases to the low levels required by GCC. The second sorbent (*i.e.*, ZnO based) is regenerated by air producing SO_2.

TDA's process carries out a modified Claus reaction to reduce the SO_2 from the second sorbent generation to elemental sulfur. In this case the sulfided stannic oxide forms stannous sulfide (SnS), which reduces the SO_2. The reactions in the process are:

Absorption

$$SnO_2 + H_2 + H_2S \rightarrow SnS + 2\ H_2O$$
$$ZnO + H_2S \rightarrow ZnS + H_2O$$

Regeneration

$$ZnS + 1.5\ O_2 \rightarrow ZnO + SO_2$$
$$SnS + SO_2 \rightarrow SnO_2 + S_2$$

The absorption by SnO_2 could remove over 90% of the H_2S from typical coal gas streams, but we use zinc ferrite (or zinc titanate), a) to reduce H_2S to less than 20 ppm and b) as a source of SO_2 in regeneration. Due to stoichiometry of the regeneration reactions, we remove half of the H_2S by SnO_2 and the remainder by the second sorbent.

Figure 1 illustrates the process using fixed bed reactors. The H_2S containing coal gases leave the gasifier and flow first through the stannic oxide and then the zinc ferrite; both materials are contained in the same pressure vessel. During regeneration, the flow direction reverses. Air and steam flow first through the zinc ferrite, oxidizing the sulfide to SO_2. The sulfur dioxide produced by regenerating the second sorbent flows over the SnS regenerating SnO_2.

When there is both steam and SO_2 present, two regeneration reactions occur simultaneously:

$$SnS + SO_2 \rightarrow SnO_2 + S_2$$
$$SnS + 2\ H_2O \rightarrow SnO_2 + H_2 + H_2S$$

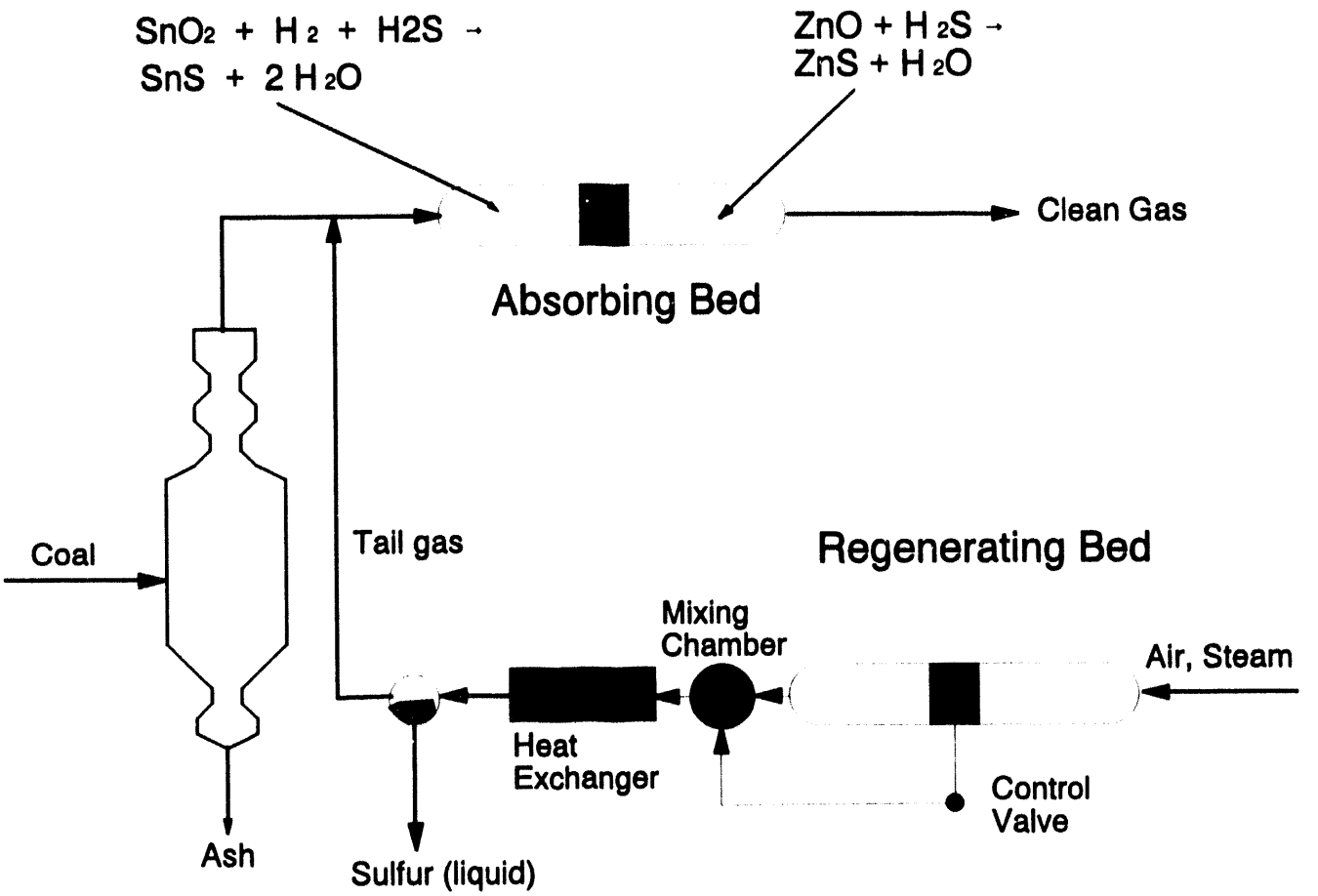

Figure 1. SnO_2 fixed bed system

One reaction produces sulfur and the second produces H_2S. We have measured the presence of both sulfur and H_2S when SnS is regenerated with a mixture of steam and SO_2. The proportion of each that is present depends on the time history of the regeneration half cycle. Early in the regeneration, H_2S is the primary product. Later in the regeneration of the fixed bed reactor, the quantity of SnS is reduced and some of the SO_2 passes through the bed. Near the end of regeneration, the H_2 and H_2S from the reaction of H_2O and SnS react with the SO_2 and sulfur is the primary product of regeneration.

The control valve shown in Figure 1 directs some of the SO_2 around the SnS portion bed. The quantity of flow diverted around the SnS varies with time. Thus, control valve maintains a stoichiometric mixture of 2 H_2S and 1 SO_2 to produce sulfur by the Claus reaction:

$$2\ H_2S + SO_2 \rightarrow 2\ H_2O + 1.5\ S_2$$

Since the gases exit the SnO_2 and ZnO beds at 700°C (1292°F), the Claus reaction in a small mixing chamber is very rapid. Cooling the mixed gases then condenses the sulfur. The sulfur condenses (but not the steam) and flows out of the system as a liquid. Un-reacted H_2O (steam), N_2, and H_2S (*i.e.*, tail gas) mixes with the gasifier outlet. The H_2S in the tail gas is then re-absorbed by the SnO_2 and/or ZnO and is ultimately removed as elemental sulfur.

The mixing of the tail gas with the gasifier outlet serves three functions simultaneously. First it cleans up the tail gas without the need for additional processing equipment. Second the cool tail gases reduce the temperature of the gasifier outlet, avoiding the need to add water to cool the gas stream down to the hot gas cleanup equipment (571°C, 1060°F). The third function is to change to composition of the gasifier outlet to one that will not reduce the stannic oxide to the metallic tin. Some gasifiers (*e.g.*, Lurgi) will not reduce stannic oxide; others (*e.g.*, KRW, Texaco) will reduce stannic oxide at high temperature. Using the steam required to control temperatures during the ZnO regeneration can also control the temperature and composition of the gas entering the hot gas cleanup system.

When this steam is already needed to control temperatures during the zinc titanate regeneration, there is no penalty in its use to control the temperature and pressure of the coal gases entering the hot gas cleanup. This dual use of steam (to cool the gasifier outlet using the steam from the ZnO sorbent regeneration) is unique to TDA's stannic oxide based process.

Regeneration Approaches

Different approaches can regenerate the stannic oxide based sorbent. We call these two approaches *high steam*, *low steam*, and *no air*. The *high steam* option is shown in Figure 1 for a fixed bed reactor but can be used with any type of reactor (*e.g.*, moving bed, fluidized bed). The *low steam* regeneration would be used with a moving, fluidized, or entrained bed. The third type using *no air* (*i.e.*, only steam) has been proposed by Nielsen *et al.* (1991) to regenerate stannic oxide from the sulfided material and reclaiming some hydrogen.

The *high steam* composition simulates a 6.5:1 steam to air ratio entering the sulfided zinc oxide based second sorbent. The regenerative gas contains 1.88% SO_2, 87.5% H_2O, and the balance N_2. This gas composition leaves the ZnO at 700°C (1292°F) due to the heat released by oxidation of the ZnS. This gas regenerates the stannous sulfide completely. Figure 1 illustrates the fixed bed system and the reactions that occur. As the SnS is regenerated initially the outlet is very high in H_2S. Some of the gases leaving the second sorbent regeneration (*i.e.*, high is SO_2) are by-passed around the SnS to the mixing chamber. The H_2S leaving the tin portion and the SO_2 leaving the zinc portion of the bed react producing elemental sulfur by the Claus reaction.

The *low steam* regeneration of the zinc oxide second sorbent is associated with a moving bed (see Figure 2) or fluidized bed reactor. This type of reactor recycles nitrogen and SO_2 to produce a high concentration of SO_2. Gal *et al.* (1992) produced SO_2 concentration as high as 10%. Our *low steam* regeneration is less demanding and requires only ≈ 3% SO_2 leaving the zinc oxide second sorbent regeneration.

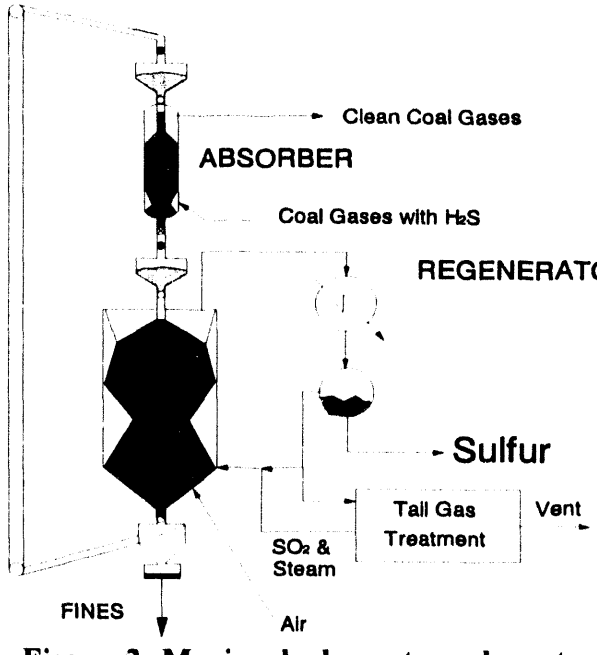

Figure 2. Moving bed reactors; low steam

In Figure 2 the sorbents are regenerated at low pressure. In that case the tail gases can not be returned to the high pressure gasified coal. The tail gases are treated (*e.g.*, SO_2 readily dissolves in water separating it from the N_2, which is then vented to the atmosphere). Heating the solution recovers SO_2 and reconditions the water. Some steam and the SO_2 steam are returned to the regeneration reactor that converts the SO_2 to sulfur.

If the regeneration is conducted at high pressure, the tail gases from the *low steam* reactors could be used to cool the gasifier outlet as in the *high steam* case. TDA's experiments utilize the *high steam* generation in most cases. We have conducted experiments with both *high steam* and *low steam* regeneration approaches and found complete regeneration of the sorbent with either approach.

The *no air* approach is described by Nielsen *et al.* (1991) using SnO_2 as the H_2S sorbent; they regenerate the SnO_2 by reversing the absorption reaction. That process uses super-heated steam [350 psia - 23.8 atm, 842°F - 450°C; 30 to 50 moles H_2O per mole of H_2S]. The steam is condensed and then a stripper solution separates the H_2 and returns it to the gasifier outlet. The concentrated H_2S is then converted to elemental sulfur in a conventional Claus plant. TDA has independently verified that the SnS can be regenerated by steam alone. However, the steam required by that process is substantially greater than both the high steam and low processes described above, thus the *no air* approach adversely affects power plant efficiency.

PROJECT DESCRIPTION

Phase II focuses on the demonstration of the process with fixed bed rectors. The fixed bed is readily scalable to small sizes, which minimizes the cost of the experiments. Sorbents suitable to moving beds could be produced by modifying the shape of the sorbent to rounded ends to improve attrition resistance. Smaller, rounded particles would be needed for fluidized or entrained bed reactors. TDA has also produced small sorbent particles suitable for fluidized and/or entrained bed reactors, but those sorbents have not been tested to date.

The key to the economic success of the proposed system is the development of a sorbent/support combination that retains its properties through multiple full absorption-regeneration cycles. These sorbents are screened for physical properties, chemical reactivity, and durability. Based on previous work in zinc ferrite and zinc titanate, TDA identified those properties that make a good hot gas cleanup sorbent.

TDA has produced >200 sorbents using different binders, different quantities of binders, firing temperatures, sources of stannic oxide, water content, forming pressure, forming technique (press, agglomerate, and extrude), and techniques for controlling pore size and porosity. Several methods of preparing the sorbent were investigated including mixed metal oxides, adding sorbent to a catalyst support.

The catalyst support method physically separates the structural and chemical requirements for the sorbent. An inert material (*e.g.*, alumina) forms the structure and the stannic oxide absorbs the H_2S. The support is first extruded and fired; then an aqueous solution of the chemical salt (*i.e.*, $SnSO_4$) is deposited on the support and decomposed. The supported catalyst approach produces a sorbent with high strength and long life but typically has low loadings and is expensive to produce.

TDA also developed a new method of producing hot gas cleanup sorbents. This new

method called a "geode" mimics the catalyst support approach, but the geode is made like a mixed metal oxide. The geode has the strength and durability of the supported catalyst but the high chemical content and low production costs of mixed metal oxides.

Geodes are naturally occurring rocks with a hollow interior; our approach was to make the geode with a porous, inert shell and to fill the interior with the chemically active stannic oxide]. We formed geodes by extrusion, pressing, and agglomeration. The best geodes were made by extrusion. We premix the inert binder material (*e.g.*, bentonite) and the stannic oxide. We then press or extrude the mixture only once and fire once to produce the geode. The geode is formed **without** decomposition of salt and **no** aqueous solution is needed anywhere in the process (*versus* a supported catalyst sorbent that requires an aqueous solution of a decomposable salt). The geode sorbent has high strength, high surface area, and high stannic oxide content (e.g. 67%, wt.).

RESULTS

Last year (Copeland *et al.* 1993) we reported on the screening of the sorbents. We identified several formulations that will meet all of our goals; and we selected one that had the best characteristics for a multiple cycle test of its properties. The selected sorbent was the geode, JY0121-1; a second batch was made after initial screening and is identified as BW0121-1. A third batch was extruded for TDA by AMAX and is identified as AX0121-1. Our most extensively tested geode is BW0121-1 and contains 67% SnO_2 by weight in the fired material; the inert is also a low cost material (bentonite). This paper describes the results of the multiple cycle testing on that geode.

Experimental Apparatus

TDA designed the experimental test apparatus to automatically cycle between absorption and regeneration while unattended. We use computer control 1) to sequence between absorption and regeneration, 2) to control all flow rates, 3) to automatically control the temperatures in the reactors, lines, boilers, and heaters and 4) to shut down the experiment in case of an emergency. The high degree of automation allows continuous operation, and we operate the system 24 hours per day.

The experimental apparatus delivers a controlled flow of mixed gases to a high pressure reactor to simulate either absorption or regeneration. The reactor is a 3.0" (O.D.) stainless steel tube that is designed for 300 psig and 1292°F (700°C). The isothermal zone of the reactor is 10" (254 mm) high with a 2.5" (6.4 mm) (I.D.). Without channelling in the bed we can tests pellets up to 0.25" (63.5 mm) in diameter with our current system.

Figure 3 illustrates the overall layout of the apparatus. A series of mass flow controllers meters the desired gas composition into the reactor. Cylinders of N_2, CO_2, CO, and H_2 are stored in the room. H_2S and SO_2 are stored in separate hoods and flow controllers supply the gases to the reactor that is inside a third hood. Water is stored in a drum and pumped into the vent hood where it is boiled and mixed with the bottle gas supply.

Two computers control and measure data for the experiments. The computer also monitors the alarms and high temperatures and shuts the experiment down if any factor (*e.g.*, high H_2S levels) exceeds preset limits. One computer controls the temperatures, flow rates, and sequences automatically between absorption and regeneration. The second computer controls the gas chromatograph and records the data from FPD and TCD detectors.

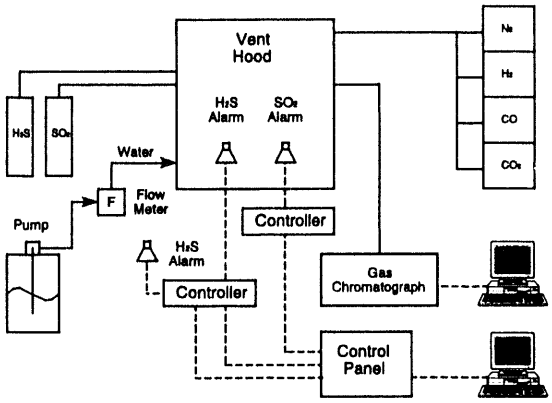

Figure 3. Schematic of experimental apparatus

We perform cycling tests simulating the inlet of a fixed bed. This location will have the highest loading of sulfur during absorption. Previous work on zinc titanate (Jung *et al.* 1992) has shown that high sulfur loadings reduce the strength of the pellets and cause failure of the sorbent. Thus, the crush strength on pellets tested under these conditions will be lowest and the most severe expected in service. The experiments are performed at high temperature. We sulfide at 1,060°F (571°C) with simulated KRW and Texaco gasifier coal gas streams and regenerate at 1,292°F (700°C) simulating both the temperature and composition of the ZnO based second sorbent outlet gas.

The experiments also evaluate the sorbent at conditions simulating the entire bed (*i.e.*, breakthrough curves). Hot gas cleanup reactors normally operate at space velocities in the range of 1500 to 2000 h^{-1}; but there are two sorbents in our bed (SnO_2 and ZnO). Since each sorbent must remove half of the H_2S, we operate the stannic oxide bed at a space velocity of 3000 to 4000 h^{-1} (ntp), which is about twice the total.

Sulfur Loading with Multiple Cycling

Two sulfur loadings are reported: the loading where the sorbent removed half of the H_2S from the inlet with a SV of 3400 h^{-1} (breakthrough) and the second loading after five hours of exposure to 1% H_2S in the inlet gas (full load).

We have measured the breakthrough sulfur loading at periodic intervals in an isothermal (1058°F) 570°C reactor. The loading has slowly declined with cycling from 4.5% sulfur at cycle 11, to 4.1% at cycle 37, and somewhat lower at cycle 64. During cycles 64 and 65 we had a boiler problem that allowed liquid water into the reactor (not steam as in previous runs) and caused the bed to be non-isothermal. Cycle 64 operated between 470 and 570°C and absorbed 3.0% sulfur. During cycle 65 the temperature was controlled to 573°C inside the reactor and the oven temperature was 727°C; under these conditions the BW0121-1 absorbed 8.4% sulfur and removed 78% of the H_2S. If the test had been continued to the point where 50% of the sulfur was removed by the stannic oxide, the sulfur loading would have been higher.

We also measured the sulfur loading after 5 hours of exposure to 1% H_2S with an isothermal 1058°F (570°C) reactor. The loading has slowly declined with cycling from 7.7% sulfur at cycle 11, to 5.7% at cycle 37, and noticeably lower at cycle 64. During cycle 64 and 65 we had a boiler problem and a non-isothermal reactor. Cycle 64 operated between 878°F and 1058°F (470 and 570°C) and absorbed 3.1% sulfur. During cycle 65 the temperature was 1063°F (573°C) inside the reactor and the oven temperature was 1341°F (727°C); under these conditions the BW0121-1 absorbed 8.4% sulfur.

Crush Strength & Mass Losses

Periodically, the pellets were removed from the reactor and the remaining mass of whole pellets was weighed. Some whole pellets were removed and analyzed for the properties of the sorbent (*i.e.*, crush strength). The remaining pellets were again weighed before returning them to the reactor. The properties of the BW0121-1 with cycling are given in Table I.

Table I. Cycling effects on crush strength and mass loss

Cycle Number	Crush Strength lb/mm	Mass Loss Rate %/cycle
initial	4.6	-
2 regenerated	-	0.33
10 regenerated	5.3	0.35
22 regenerated	6.2	0.35
36 regenerated	4.3[1]	0.92[1]
43 regenerated	_	0.008
63 sulfided	5.7	0.469

[1] At end of 36th cycle, cooling of the reactor caused all of the pellets in the reactor to be flooded with water; the rapid cooling associated with a water quench would not be experienced in practice. This quench may have weakened some pellets or caused fracturing with others.

The weight of the material that was removed from the reactor is subtracted from that which was added to calculate the loss of material. By dividing by the number of cycles, the average loss per cycle is then calculated (*i.e.*, the reciprocal of the cycle life) during each period.

We subtracted the mass of pellets that are used for sample taking and fitted a curve to the experimental data; Figure 4 illustrates the curve fit to the data. The average loss of material through 63 cycles is 0.476%/cycle implying a cycle life of 210 cycles.

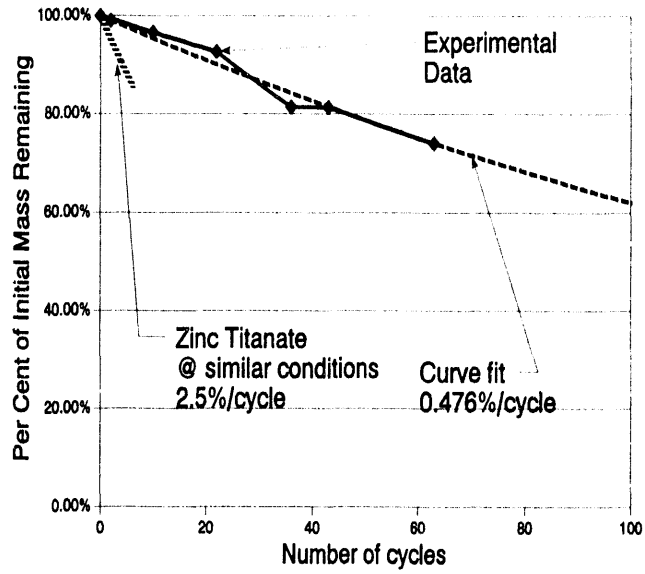

Figure 4. Effect of cycling on BW0121-1

The loss rates for a zinc titanate sorbent is also shown in Figure 4; the data are for TRZ-21 as reported by Jung *et al.* (1992). Both the stannic oxide and the zinc titanate sorbents were tested under simulated inlet conditions and the zinc titanate is rapidly destroyed under these conditions (2.5% mass loss per cycle). By comparison, the stannic oxide sorbent losses were very low (0.476%/cycle), which is a direct result of the way we make our sorbent and the properties of stannic oxide.

These experiments tested pellets that are at the inlet of a fixed bed reactor. At that condition the sulfur loading is the highest, creating the greatest changes in the chemical sorbent and the greatest stresses on the sorbent. However, the bed average sulfur loading would be smaller than these test conditions, the life of a whole pellet would be greater than the pellets that are at the

inlet (over 300 cycles for the bed average conditions is anticipated).

Surface Area

We measured the surface area of the materials regeneration sorbent with our BET apparatus. Table II presents the measured surface area of three batches of sorbents with the same formulation. The JY0121-1, BW0121-1, and AX0121-1 are chemically the same (but the AX0121-1 was extruded, the other two were different batches of pressed pellets). There is a loss of surface area with cycling and this roughly correlates with the loss of sulfur capacity with cycling.

Table II. Effect of cycling on surface area

Cycle Number	State	Surface Area: m^2/g
Initial Sorbent JY0121-1 AX0121-1	SnO_2	 3.9 4.5
Tenth JY0121-1 BW0121-1	SnO_2	 2.0 1.0
22nd BW0121-1	SnO_2	0.7
36th BW0121-1	SnO_2	0.6
63rd BW0121-1	SnS (SnO_2)	 1.7

The surface area for the BW0121-1 for cycle 63 was higher than all but the initial surface area for this sorbent. This sample was removed from the reactor in the sulfided state, and then regenerated in the oven at 1292°F (700°C). The high surface area may be due to the more rapid regeneration of the stannic oxide when oxidized by air *versus* SO_2-H_2O in the previous cycling. If that is true, surface area (and probably sulfur capacity) could be periodically recovered by air regenerating the sorbent.

Breakthrough Characteristics of SnO_2 Sorbent

Figure 5 presents the breakthrough characteristics of the SnO_2 sorbent. The bed contains BW0121-1 (same as JY0121-1, but a different batch) with a bed of 387 g occupying 256 cc. The simulated KRW gas stream flows at Space Velocity (SV) of 3400 h^{-1} and its pressure is 130 psia (8.85 atm). The inlet H_2S concentration was 9962 ppm (v) and set higher than a KRW gasifier's concentration to minimize the duration of the test. For a short time the concentration is around 800 ppm, indicating >90% removal of the H_2S. As the bed loads with sulfur the exit concentration rises rapidly at first, and then slowly.

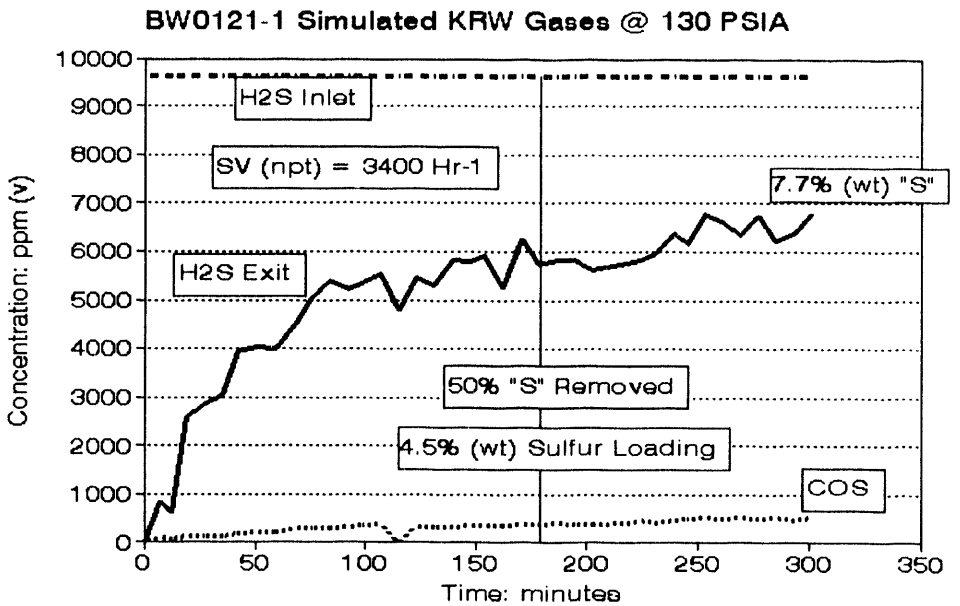

Figure 5. Breakthrough characteristics: 11th absorption cycle (570°C)

Figure 6 presents the breakthrough curve for absorption cycle number 37 on the BW0121-1 pellets. In comparison to the breakthrough curve for cycle number 11, the loading of the pellets decreased slightly to 4.1% from 4.5% (sulfur by weight). Breakthrough came at approximately the same time as in cycle number 11.

As shown in Figure 6 the pellets were not completely regenerated at the start. At time=0 minutes, we added H_2S and continued the flow for 5 hours. As in the previously data (Figure 5, cycle 11) the H_2S outlet increased rapidly and slowly with time.

The breakthrough characteristic for cycle 65 is shown in Figure 7 with simulated KRW gases. A very low H_2S concentration was sustained for a long period of time. The calculated sulfur loading was 8.4%. The data demonstrate that very high loadings can be achieved with this material in high temperature use, even after many previous cycles have been accumulated on the same batch of pellets. Following the 65th absorption we prepared to regenerated the sorbent. Unfortunately we experience a temperature excursion in our electrically heated tube furnace. The temperature exceeded 1832°F (1000°C) for a time. Since the melting point of SnS is 1918°F (881°C) and most of the tin was sulfided, the pellets melted and were destroyed. No addition cycling was possible with the BW0121-1 pellets.

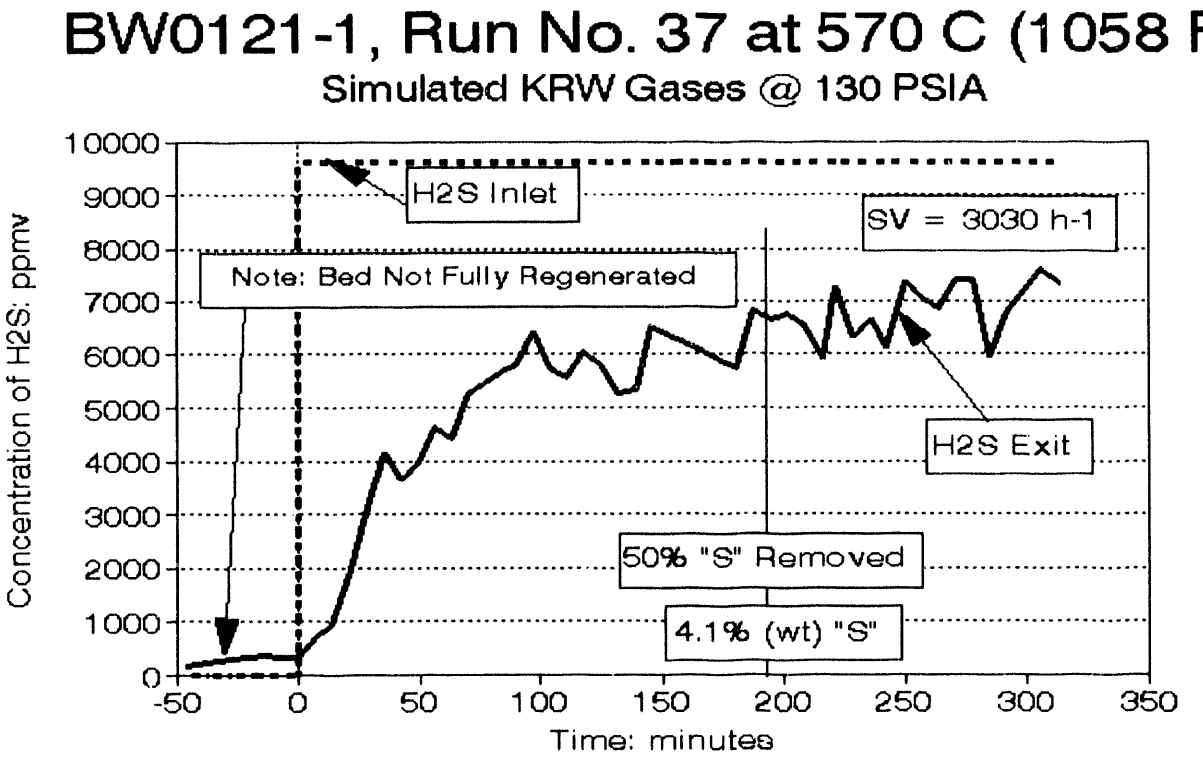

Figure 6. Breakthrough characteristics: 37th absorption cycle (570°C)

The high loading on cycle 65 was a direct result of the high temperature of the sorbent (570 to 727°C). We independently conducted experiments with another geode, BW0121-3 and measured its sulfur loading as a function of temperature. We found a very strong correlation with low temperatures absorbing low quantities of sulfur and high temperatures absorbing more.

Refabrication of Sorbent

An economical sorbent must have significant life at an affordable cost. The cost of SnO_2 is ≈ $5/lb; even with a life of 200 cycles the operating cost of the system would be high, if the stannic oxide were thrown away after a number of cycles. To avoid this problem TDA defined a tin recovery system to reclaim the tin from the spent sorbent. This system is illustrated in Figure 8 for a moving bed reactor. The recovery and reuse of the tin increases the effective cycle life (*e.g.*, > 4000 cycles with 95% recovery of the tin in each refabrication).

The moving bed reactors operate in the same manner as the reactors described by Cook *et al.* (1991). In this system the stannic oxide and zinc ferrite are mixed together (either as separately produced sorbents or combined in one sorbent). Both sorbents enter the top of the absorber, and the reaction with H_2S converts both the stannic oxide and zinc ferrite to sulfides. The same chemical reactions occur in the moving bed as in the fixed bed system. The tin recovery unit recovers the stannic oxide from sorbent fines.

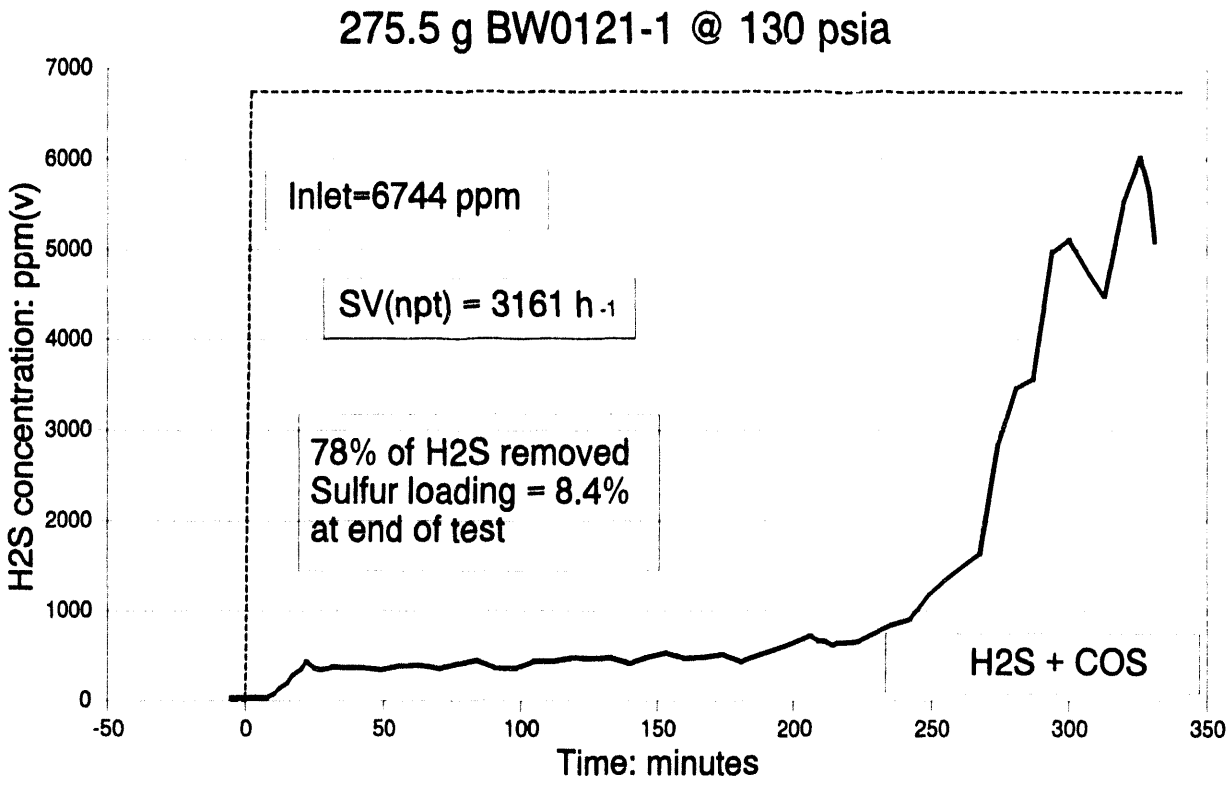

Figure 7. Breakthrough characteristics: 65th absorption cycle (570-727°C)

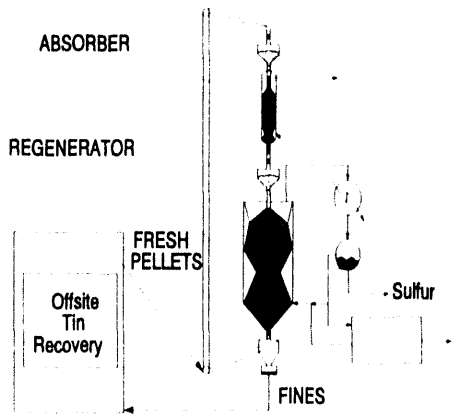

Figure 8. Tin recovery system

The recovered material is then made into fresh pellets that are returned to the moving bed reactors (or fixed bed or fluidized bed reactor).

TDA estimated the cost to produce stannic oxide pellets for IGCC power plants. We designed a conceptual pellet fabrication plant to service 500 MW_e power plants In this analysis we assume that SnO_2 removes half of the sulfur with a pellet sulfur loading of 4% by weight and a pellet life of 100 cycles. 5,778 tons/year of replacement pellets are required when operated on high sulfur coal (Illinois No. 6).

Each power plant will require an initial inventory of 2,889 tons of new BW0121-1 pellets (*i.e.*, 67% SnO_2 by weight). The quantity of pellets is large to provide a six month inventory of materials. This inventory is divided into several uses: 1) active material in the reactors absorbing H_2S, 2) spent sorbent awaiting shipment to the refabrication plant, 3) fresh pellets stored on site awaiting loading into the

to operate our system in that gasifier plant and operated it with high sulfur, Illinois No. 6 coal.

Figure 9 presents a comparison of the levelized electricity cost for four hot gas cleanup systems. Our stannic oxide process offers the lowest cost electricity when a nominal shipping cost is included. (Based on a price quote for shipping sulfur and sulfuric acid from Denver to Salt Lake City in Jumbo railway cars from a Union Pacific station to a Union Pacific station.) Shipping sulfur is much less expensive than sulfuric acid, since H_2SO_4 weighs about three times as much as an equivalent quantity of sulfur.

If users for the sulfuric acid are nearby and the operator wishes to market the sulfuric acid, then shipping would not be significant; in that case GE's process produces electricity at a cost slightly less than our process. Since the sulfuric acid process produces more usable heat (*i.e.*, the sulfur is burned to SO_2) and three times as much product at a similar selling price per ton, those factors generate more revenue for the sulfuric acid plant than selling sulfur. The higher revenues more than pay for its operating and capital cost (*i.e.*, producing sulfuric acid is a profitable business). Of course if the utility wanted to sell sulfuric acid, it could always burn the sulfur from our process to produce the acid in an on-site or off-site sulfuric acid plant. The two plant (power and acid) operations would be completely separated. That approach increases the reliability of the overall plant, since operation of the power plant is not tied to the operation of the acid plant.

RTI's Direct Sulfur Recovery Process (DSRP) produces the same product as our system. The primary difference between our stannic oxide system and the DSRP is the efficiency. We consume 0.5 moles of H_2 or CO per mole of H_2S removed from the gas. The DSRP consumes 4.0 moles of H_2 or CO per mole of H_2S. Thus, the DSRP removes a significant

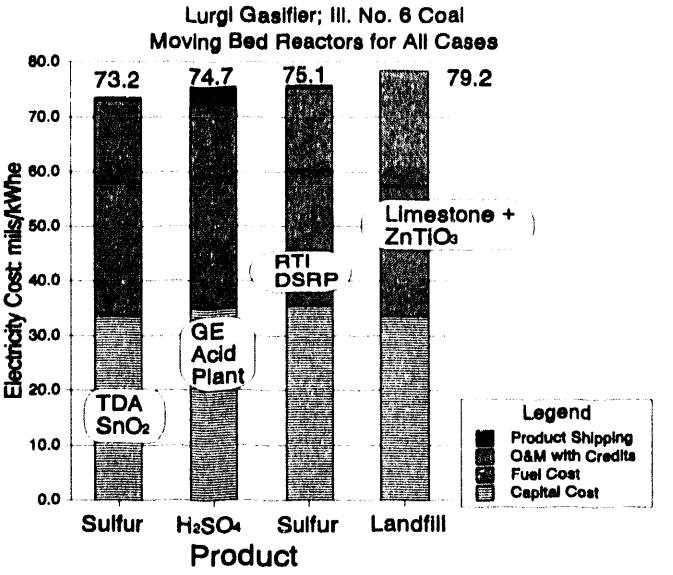

Figure 9. Comparison of electricity costs with the same gasifier and combined cycle

fraction of the heating value of the gasified coal and generates some steam for power generation with the heat that is generated. However, burning the fuel in the gas turbine is more efficient and that difference makes our process more efficient and lower cost.

The limestone + zinc titanate process has the lowest capital cost, the highest efficiency, and no product shipping cost (*i.e.*, we assumed a local landfill). However, the limestone incurs costs, landfilling adds more costs, and there is no product to sell. The operating costs are relatively high, making it the most expensive of the processes considered.

Closure

TDA has developed a new process and a long life sorbent for high temperate hydrogen sulfide removal. The economics of the process have been evaluated; the cost of electricity using the stannic oxide system is potentially the lowest cost hot gas cleanup system.

While stannic oxide is a relatively expensive material ($5/lb), spent sorbent can be refabrication into fresh sorbent. The price of the refabricated stannic oxide geode is <$2,000/ton, which is equal to or less than zinc oxide based sorbents.

REFERENCES

Chen, H.T., M.G. Klett, M.D. Rutkowski, and R. Zaharchuk (1993). "IGCC Database and Hot Gas Cleanup Systems Studies," *Proceedings of the Coal-Fired Power Systems 93 -- Advances in IGCC and PFBC Review Meeting*, sponsored by the U.S. Department of Energy, Morgantown Energy Technology Center: Morgantown, West Virginia, Report No. DOE/METC-93/6131 (CONF-9306148).

Chen, H.T., M.G. Klett, and M.D. Rutkowski (1992). "Sensitivity of Hot Gas Desulfurization on IGCC Cost of Electricity," in *Proceedings of the Twelfth Annual Gasification and Gas Stream Cleanup Systems Contractors Review Meeting*, Morgantown, WV: U.S. Department of Energy, Morgantown Energy Technology Center, Report Number DOE/METC-91/6128 (CONF-920951).

Cook, C.S., E. Gal, A.H. Furman, and R. Ayala. 1991. Integrated Operation of a Pressurized Fixed-Bed Gasifier and Hot Gas Desulfurization System. In *Proceedings of the Eleventh Annual Gasification and Gas Stream Cleanup Systems Contractors Review Meeting*, **1**, 45-55. DOE/METC-91/6123. Morgantown, WV: U.S. Department of Energy.

Copeland, R.J., D. Feinberg, B. Windecker, and J. Yu (1993) *Proceedings of the Coal-Fired Power Systems 93 -- Advances in IGCC and PFBC Review Meeting*, sponsored by the U.S. Department of Energy, Morgantown Energy Technology Center: Morgantown, West Virginia, Report No. DOE/METC-93/6131 (CONF-9306148).

Gal, E., A.H. Furman, and R. Ayala (1992). "Integrated Operation of a Pressurized Fixed Bed Gasifier and Hot Gas Desulfurization System, *Proceedings of the Twelfth Annual Gasification and Gas Stream Cleanup Systems Contractors Review Meeting*, editors R.A. Johnson and S.C. Jain, Morgantown, West Virginia: U.S. Department of Energy, Morgantown Energy Technology Center, Report No. DOE/METC-92/6128.

Heinemenn, H. and G.A. Somorjai (1992). "Catalytic Gasification Fundamentals," *Proceedings of the Twelfth Annual Gasification and Gas Stream Cleanup Systems Contractors Review Meeting*, editors R.A. Johnson and S.C. Jain, Morgantown, West Virginia: U.S. Department of Energy, Morgantown Energy Technology Center, Report No. DOE/METC-92/6128.

Jung, D.Y., J.S. Kassman, T.F. Leininger, J.K. Wolfenbarger, and P.P. Yang (1992). "Integration and Testing of Hot Desulfurization and Entrained Flow Gasification for Power Generation Systems," *Proceedings of the Twelfth Annual Gasification and Gas Stream Cleanup Systems Contractors Review Meeting*, editors R.A. Johnson and S.C. Jain, Morgantown, West Virginia: U.S. Department of Energy, Morgantown Energy Technology Center, Report No. DOE/METC-92/6128.

Nielsen, P.E.H., P. Rudbeck, and H. Christiansen (1991). "Steam Regenerable Sulfur Absorption Masses and Their Application in IGCC Plants," presented at the Tenth EPRI Conference of Coal Gasification Power Plants, San Francisco, California, October 16-18, 1991.

Ulrich, G.D. 1984. *A Guide to Chemical Engineering Process Design and Economics*. New York: John Wiley and Sons.

P17 Fossil Fuel Conversion - Measurement And Modeling

CONTRACT INFORMATION

Contract Number: DE-AC21-93MC30040

Contractor: Advanced Fuel Research, Inc.
87 Church Street
(203) 528-9806

Subcontractor:
Brigham Young University
(801) 378-4326

Contractor Program Manager: Peter R. Solomon — L. Douglas Smoot

Principal Investigators: Michael A. Serio, David G. Hamblen — B. Scott Brewster, Predrag T. Radulovic

METC Program Manager: Norman T. Holcombe

Period of Performance: September 14, 1993 to September 13, 1996

FY94 Program Schedule

		S	O	N	D	J	F	M	M	J	J	A
1.	Research Plan	———	———	———	———							
2.	Gasification Processes					———	———	———	———	———	———	———
3.	Gas Phase Combustion					———	———	———	———	———	———	———
4.	Fluidized-Bed Systems					———	———	———	———	———	———	———
5.	Applications					———	———	———	———	———	———	———

OBJECTIVES

The main objective of this program is to understand the chemical and physical mechanisms in coal conversion processes and incorporate this knowledge in computer-aided reactor engineering technology for the purposes of development, evaluation, design, scale up, simulation, control and feedstock evaluation in advanced coal conversion devices. To accomplish this objective, this program will: 1) provide critical data on the physical and chemical processes in fossil fuel gasifiers and combustors; 2) further develop a set of comprehensive codes; and 3) apply these codes to model various types of combustors and gasifiers (fixed-bed, transport reactor, and fluidized-bed for coal and gas turbines for natural gas).

BACKGROUND INFORMATION

To expand the utilization of coal, it is necessary to reduce the technical and economic

risks inherent in operating a feedstock which is highly variable and which sometimes exhibits unexpected and unwanted behavior. Reducing the risks can be achieved by establishing the technology to predict a coal's behavior in a process. This program is creating this predictive capability by merging technology developed at Advanced Fuel Research, Inc. (AFR) in predicting coal devolatilization behavior with technology developed at Brigham Young University (BYU) in comprehensive computer codes for modeling of entrained-bed and fixed-bed reactors and technology developed at the U.S. DOE-METC in comprehensive computer codes for fluidized-bed reactors. These advanced technologies will be further developed to provide: 1) a fixed-bed model capable of predicting combustion and gasification of large coal particles, 2) a transport reactor model, 3) a model for lean premixed combustion of natural gas, and 4) an improved fluidized-bed code with an advanced coal devolatilization chemistry submodel.

PROJECT DESCRIPTION

The program consists of five tasks: 1) Preparation of a Research Plan, 2) Modeling of Gasification Processes, 3) Modeling of Gas Phase Combustion, 4) Modeling of Fluidized Bed Systems, and 5) Applications. This paper describes the initial work performed during the first year of the contract.

RESULTS

Devolatilization of Large Coal Particles (AFR) - Large coal particles are typically used in fixed-bed combustion and gasification processes. The objective is to extend the Functional Group - Depolymerization, Vaporization, Crosslinking (FG-DVC) model that was developed for small coal particles to these centimeter size particles. Work is being carried out in three steps, 1) modeling heat transfer in a spherical coal particle, 2) development of a simplified coal devolatilization model based on FG-DVC, and 3) integration of the heat transfer model and the simplified coal devolatilization model.

Work started with the heat transfer model. Code development for the simplest situation with constant density, heat capacity and thermal conductivity and in the absence of pyrolysis was completed. The numerical solution is in good agreement with the analytical solution given by Jakob (1959). Future work will concentrate on integration of the FG-DVC pyrolysis model. Temperature dependent coal properties will be used in the code based on Merrick's thermal physical coal model (Merrick, 1983).

Reduced Version of Coal Devolatilization Model (AFR) - To model the devolatilization of large coal particles, it is necessary that the rate equations of coal devolatilization be appropriately expressed and solved along with the heat transfer equation. It is well known that coal devolatilization is a complicated process, and cannot easily be modeled with a single rate equation, especially when the elemental compositions of char, gas, and tar and the amounts of the individual gas species are desirable. The full FG-DVC model was implemented in the current version of the advanced fixed-bed code (FBED-1) in the previous contract, with the assumption that the particles are isothermal. Incorporating an intra-particle heat transfer model will require a substantial simplification of the FG-DVC model, in order to reduce the computational burden.

After a careful re-examination of the FG-DVC model, a number of model simplification options have been proposed. Option 1 is a single rate equation model which solves the total pyrolysis weight loss. Other time dependent variables, such as the yields of tar and gas species, are calculated by correlation with the weight loss. Option 2 has a single rate equation for total gas

yields and the DVC network submodel to predict the tar yield. Option 3 is Option 2 plus a submodel for nitrogen gas release, which cannot be evaluated accurately with the weight loss correlation due to its heating rate dependence. These options were constructed based on the following considerations:

1. Devolatilization of individual gas species occurs independently (except for NH_3, HCN) in the model.

2. Tar and gas evolution are coupled.

3. Tar evolution is influenced by pressure and heating rate. In order to model the pressure and heating rate dependence, the tar submodel in FG-DVC must be retained. However, this can be implemented in a pre-processing step so that the computational burden is not unduly increased.

It was therefore assumed that:

1. The total light gas evolution can be modeled using a single rate equation with a distributed activation energy accounting for multiple gas species contributions.

2. When the tar evolution amount is known from a pre-processing step, it can be treated as another "gas species" in addition to the light gas evolution, so the total volatile evolution can be modeled with a single rate equation.

3. Alternatively, the tar submodel can be solved along with the light gas species model, but it adds an additional computational burden.

4. The amounts of individual gas species can be recovered from correlation with the total volatile or total light gas amounts. This correlation is provided by the full FG-DVC model calculation which is run in a pre-processing step.

In summary, the light gas species can be modeled with a simplified model since these evolve independently, but the tar submodel cannot be easily simplified since the evolution depends on the process conditions (heating rate, pressure). With Option 1, the tar amount is estimated from the preprocessing step with FG-DVC based a nominal heating rate and bed pressure. Tar is then lumped into the total volatile equation and its contribution is modeled via its share in the activation energy distribution. In this case, the gas elemental composition is correlated with the total weight loss. The correlation is given by a standalone FG-DVC calculation and is an input to the one-equation model. The predictions of coal pyrolysis at a given heating rate by the one-equation model (Option 1) and by the full FG-DVC model are generally in good agreement.

Transport Reactor Modeling (AFR) - To model transport reactors, we plan to start with the entrained-bed coal gasification code developed at BYU, PCGC-2. Since transport reactors have particle loadings which are much higher than entrained-beds, dispersion of particles and their interactions with the gas phase become important. A stochastic turbulence particle dispersion model is being developed and is being verified with available data. It is also recognized that there exist fluctuations of particle number density everywhere in the reactor. A model accounting for this effect has been outlined and will be implemented into our particle model. Literature reviews for data on chemical and physical processes in transport reactors for model validation are underway.

The work during the first year was focused on developing and verifying a standalone turbulence particle dispersion model. Once it is verified, it will be implemented in PCGC-2, replacing the existing empirical particle dispersion model. The code then will be executed to convergence for transport reactor conditions which feature moderate particle loadings. This model uses the Ornstein-Uhlenbeck stochastic process to simulate the turbulent component of the gas velocity. It was demonstrated that the turbulence generated has the exact values of k and the time scale given by the k-ϵ model. This is the advantage of our model in comparison with those of Gosman and Ioannides (1981), and Shuen et al. (1983). Their models used a direct Monte Carlo method to alter the local gas velocity and these numerical schemes will not necessarily give the correct values of k and ε. There are in-depth discussions on the numerical solution of stochastic equations which use the Ornstein-Uhlenbeck process by Kloeden and Platen (1982). Truncated Fourier series with independent Guassian random coefficients were also used to simulate the gas turbulence (for example, Wang and Stock (1992)), but computing a truncated Fourier series consumes large amounts of computer time. Our model is much more efficient.

In order to verify our model, predictions of particle dispersion need to be compared with existing data. One such comparison has been made with data in grid generated turbulence by Snyder and Lumley (1971). It was found that our model under-predicts the data. Shuen et al. (1983) indicated that their model was calibrated with Snyder and Lumley's data (1971), but the nature of this calibration is not clear. We agree with Shuen et al. (1983) that it may be due to the arbitrary estimation of the time and length scales of the turbulence. It is true that, although the Eulerian integration time and length scales do present the scales in which the turbulence develops, they may not be quantitative enough to be used in the turbulence particle dispersion model. Our model is clearly limited by the state-of-the-art in understanding gas turbulence phenomenon. Although this is a fast advancing field, the k-ε description is still the most commonly accepted model. Using other turbulence models is beyond the scope of this contract and we will continue to rely on the k-ε description. In order to fit Snyder and Lumley's data (1971), the time scale given needs to be increased by a factor of 2.7. The validation of this approach needs to be proved by comparing with more data.

Work was also carried out to calculate the Eulerian particle properties, such as the mean velocity and the particle number density, from the stochastic particle model. Obtaining statistically meaningful values requires a large number of particle trajectories. The distributions of particle number density are plotted in Figures 1a and 1b with 500 and 5,000 particle trajectory calculations, respectively. The calculation was based on Snyder and Lumley's fluid data mentioned above and particles were injected from a point source up-stream. It is clear that, while the two calculations resulted in the same distributions, the distribution in Figure 1b is much smoother than that in Figure 1a. The insufficient number of trajectories which resulted in the noisy signals in Figure 1a, would cause severe convergence problem in the gas phase calculation, especially at high particle loadings. Since practical inlet pipes have finite diameters, model calculations have to inject particles from multiple positions throughout this diameter. Calculating 5,000 particle trajectories at each injection point imposes a heavy computational load on the code. We have to calculate only the number of trajectories, that is practically possible and look for ways to smooth the noisy distributions.

Fluidized-Bed Modeling (AFR) - The work on fluidized-bed modeling is directed toward developing a coal devolatilization submodel for an existing fluidized-bed code, MFIX. A simplified

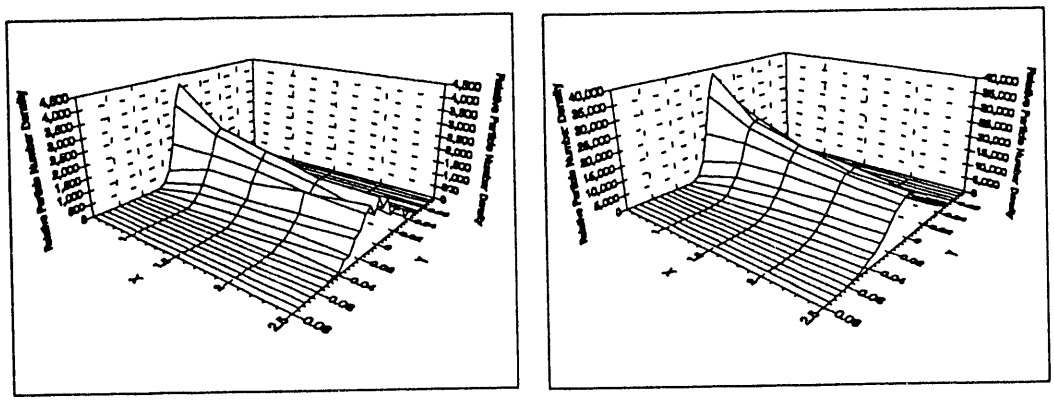

a. b.

Figure 1. Relative Particle Number Density Calculated From the Stochastic Particle Dispersion Model. Gas Fluid Data are From Snyder and Lumley (1971). a) 500 Particle Trajectories and b) 5000 Particle Trajectories.

version of FG-DVC will be tailored toward the needs of fluidized bed models. Currently, the same options for model simplification and submodel specifications that are being developed for the Fixed-Bed Reactor code are also being considered for the fluidized code.

Oxidation Rates for Large Coal particles at High Pressures (BYU) - Fixed-bed combustion and gasification processes are typically done with large coal particles at high pressures but the previously available fixed-bed codes use kinetic rates derived from small particle experiments at atmospheric pressure. Thus, work began to measure kinetic rates for large coal particles at high pressures.

A unique experimental facility was constructed to obtain oxidation rates of large particles at high temperatures and high pressures. It consists of a cantilever beam balance insert for the BYU High Pressure Controlled Profile (HPCP) reactor. The balance unit measures the mass loss of the particles as they oxidize in the HPCP reactor. It includes a force transducer, a ceramic cantilever beam, and a platinum wire-mesh sample basket. The basket is secured to the cantilever beam and extends into the reactor tube through one of the optical access ports of the HPCP reactor. This facility will permit measurements of the oxidation and gasification rates of char particles at pressures up to 17 atm and temperatures up to 1700 K. Bateman et. al., (1994a) successfully demonstrated the use of this experimental setup to study the effect of pressure on oxidation rates of mm-sized char particles. Bateman et. al., (1994b) conducted experiments with Utah bituminous and North Dakota lignite coals at 1, 5, and 7.5 atm total pressure. In these experiments, 5 and 8 mm diameter particles were used. The reactor temperature was varied between 900 and 1200 K and the bulk gas was air. Following the ignition and devolatilization stages, continuous char oxidation rates were measured to burnout. The oxidation rates were significantly increased with increased pressure but found to be independent of temperature. The effects of particle mass and pressure on the oxidation rates of a Utah bituminous char particle are shown in Figures 2 and 3, respectively. The effect of multiple particles on the oxidation rates was also studied. A pair of similarly sized individual particles of coal had similar oxidation times to a single particle having a mass equal to the sum of

the pair. The observed pressure effects could not be explained by a simple global model based on oxygen diffusion to the surface.

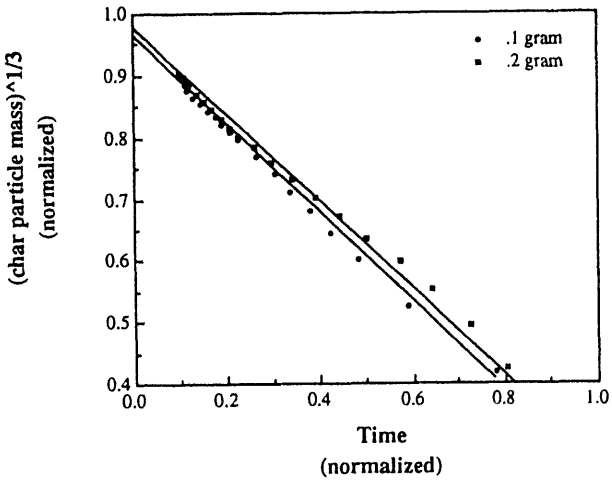

Figure 2. Normalization of the Oxidation Curve for Utah Coal, Sizes 0.1 Gram and 0.2 Gram, in the HPCP Reactor for a Gas Temperature of 900 K and an Air Flow Reynolds Number of 126 at Atmospheric Pressure.

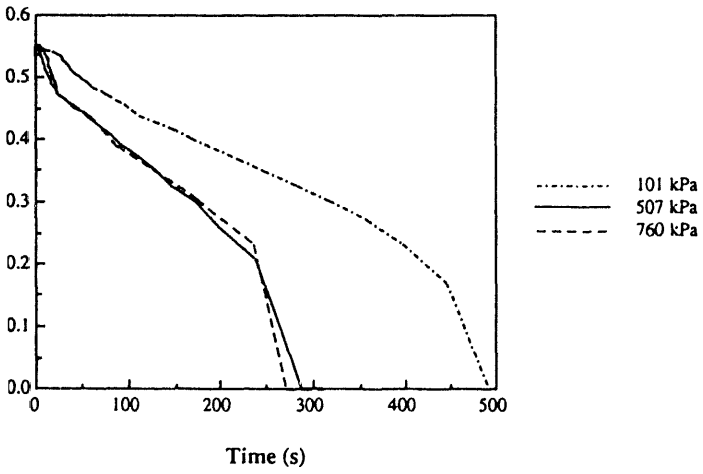

Figure 3. Comparison of Trends of 101 kPa, 507 kPa, and 760 kPa Tests for Utah Coal, Size 0.2 gram, in the HPCP Reactor for a Gas Temperature of 900 K and an Air Flow Re=126.

This study provided the first kinetic rate data for large coal particles at high pressures. The data gave significant new insights into the oxidation process regarding the temperature and pressure dependence and the role of the ash layer. The results also raised important questions: (1) What processes cause the significant effects of both temperature and pressure? (2) Why does the ash layer contract as it does during burning? (3) Why does a group of smaller particles burn like one large particle? (4) Why does the rate of burnout accelerate toward the very end of burnout? (5) Why do some low rank particles ignite before devolatilization? and (6) Why do some bituminous coal particles explode during devolatilization? Additional analysis and experiments will be conducted to answer these questions and develop a new large particle oxidation submodel.

Advanced Fixed-Bed Model Development and Evaluation (BYU) - The objectives of this task are to develop an advanced fixed-bed model incorporating the advanced submodels for large particle devolatilization and large particle oxidation and gasification, and to evaluate the model by comparing its predictions with the experimental data available from the literature. Advanced fixed-bed gasifiers are an integral part of the U.S. Clean Coal Technology (CCT) program and have been considered for integrated gasification combined cycle (IGCC) power generation systems and for mild gasification of lump coal. Recently, novel configurations have been proposed for gasification of caking coals and for mild gasification of lump coal. These configurations include the staged PyGas gasifier of the Gasification Product Improvement Facility (GPIF) project (Brown and Sadowski, 1991), and rotary kiln gasifier of the ENCOAL project (USDOE, 1993). Most of the available fixed-bed models can simulate only traditional fixed beds and there is a need to develop an advanced fixed-bed model capable of simulating both the traditional and emerging, novel gasifiers.

In a previous DOE-METC project, a one-dimensional model for fixed-bed combustion and gasification of coal, FBED-1, was developed (Radulovic et al., 1994). The FBED-1 model has achieved major advances in the treatment of various chemical and physical processes as well as in the solution procedure and has been extensively evaluated. There are still several important issues which must be resolved in the development of an advanced fixed-bed model capable of providing realistic simulations of the emerging configurations. These issues include treatment of large particle devolatilization processes, large particle gasification and oxidation processes, development of robust numerical solution methods, treatment of multiple additions and withdrawals of gases, handling of different flow patterns such as cocurrent, crosscurrent and countercurrent, and evaluation of the advanced model. The FBED-1 model provides a solid foundation for further developments which are continuing in this laboratory.

In order to simulate the combined-bed gasifiers, a preliminary integration of the cocurrent flow option was implemented in the FBED-1 model. The modified code was successfully used to simulate the PyGas gasifier of the GPIF project. The pyrolyzer section was simulated using the zero-dimensional submodel, FBED-0. The freeboard section was simulated by assuming full chemical and thermal equilibrium for the gas phase and no heat and mass transfer between the gas and solid phases. Both the upper and the lower fixed beds were simulated using the modified, fixed-bed model. The detailed profiles for the countercurrent and cocurrent sections of the gasifier are shown in Figure 4. The results predicted about 10% conversion of feed coal in the cocurrent section of the gasifier. Char consumption is due to gasification by CO_2 and H_2O. The gasification rates are higher at the top of the cocurrent section where temperature is relatively high. These rates decay as the solids cool down due to the endothermic gasification reactions. H_2O shows considerable depletion whereas the amounts of CO_2 remain almost constant. Only small amounts of CH_4 are produced in this section. The amounts of CH_4 produced in the countercurrent section are slightly larger. Large amounts of CO and H_2 are produced in the countercurrent section. The peak solid temperature is about 1500 K which is desirable for dry-ash gasifiers such as the PyGas staged gasifier. The product gas, which is the mixed stream from the cocurrent and countercurrent sections, is rich in CO and H_2, and has small amounts of CH_4.

Additional improvements will be made in the FBED-1 model to make it a design and analysis tool of significant industrial utility. These improvements will include incorporation of a large particle devolatilization submodel and a large particle oxidation submodel being developed under this project. A robust solution method suitable for stiff, non-linear problem of fixed-bed systems will be implemented. The model will be evaluated by comparison with the experimental data.

Submodel for Lean Premixed Combustion of Natural Gas in Industrial Gas Turbines (BYU) - A submodel for lean, premixed combustion (LPC) of natural gas in industrial gas turbines is being developed and implemented in a model being developed under independent funding for practical combustors. The submodel must incorporate finite-rate chemistry and predict NO_x and CO emissions at conditions approaching blowout (0.5 to 0.6 stoichiometric ratio in the primary zone). Proper accounting of the effects of chemistry/turbulence interactions is important. The Monte Carlo pdf method (Pope, 1985) is being considered as a basis for the submodel. A partially-stirred reactor (PaSR) model is being used to investigate the Monte Carlo pdf method. The PaSR (Chen, 1993) is similar to the perfectly stirred reactor (PSR) model, with no spatial variation of mean fluid properties. The difference

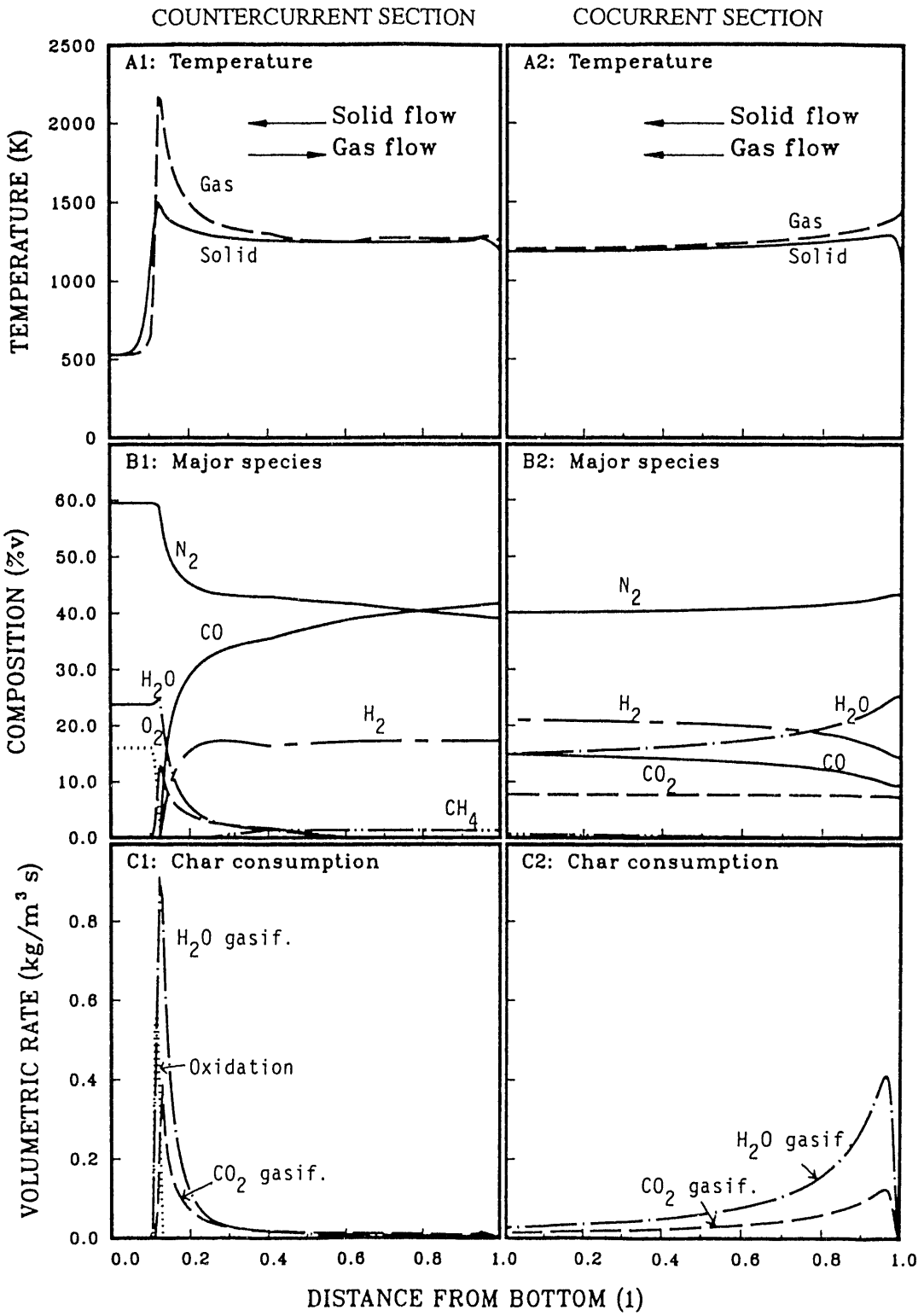

Figure 4. FBED-1 Predictions for the Countercurrent and Cocurrent Sections of the Staged PyGas Gasifier

is that molecular mixing is incomplete, so that the reactive fluids are not completely diffused into one another. Hence, there is a finite rate, given by a mixing frequency, at which the reactive fluids are mixed on a molecular level, as well as a finite rate at which they react after being mixed. Both the mixing and reaction time scales are important in the PaSR.

Calculations are being performed at conditions typical of LPC in stationary gas turbine combustors (premixed methane in air, 700 K inlet, 0.5~0.6 equivalence ratio, 15 atm, 10-20 ms residence time, and 100-5000 s^{-1} mixing frequency). The PaSR is being studied for several reasons. First, it provides an opportunity to understand the Monte Carlo pdf method in a simple model framework without the added complexities of fluid dynamics calculations. Second, many of the subroutines in the PaSR code may be applicable to a pdf submodel in PCGC-3 with little or no modification. Third, the PaSR model is a viable engineering model in its own right, with capability for including full chemistry (critical for predicting trace species). Fourth, the lessons learned from the PaSR are directly relevant to pdf methods for multi-dimensional flow, since the pdf equation for the PaSR is a degenerate case (integrated over reactor volume) of the pdf for the multi-dimensional case. Fifth, the PaSR provides an alternate test bed (to the more commonly used stirred-tank and plug-flow models) for evaluating reduced chemical schemes. And sixth, the PaSR provides a test bed for mixing models, a critical element of pdf models, in the context of full kinetics.

Results have been obtained using a reduced Miller-Bowman scheme (without C_2 chemistry and prompt NO) (Correa and Braaten, 1993). The effects of mixing rate, pressure, and mixing model were investigated. The effects of mixing rate at 15 atm and using the modified Curl's mixing model (Chen, 1993) are shown in Fig. 5. The importance of in-combustor mixing, even for premixed reactants, is clearly shown. Mixing of hot, partially-reacted particles in the combustor with the cold, incoming particles, is necessary to sustain combustion. Stable combustion was not achievable with a mixing frequency of 300 s^{-1} and lower. As shown in the figure, the PaSR converged to the non-reacting state at a mixing frequency of 300 s^{-1}. The higher the mixing frequency, the higher the temperature and the more complete the combustion, as the cold particles are quickly heated and brought to reaction temperature. The stochastic steady state is reached more rapidly with more rapid mixing. CO and the heat release chemistry (i.e. temperature) converge to the stochastic steady state at about the same rate, while NO converges considerably more slowly. This observation is in agreement with that of Correa and Braaten (1993). Scatter plots and pdf plots (not shown here) showed that the particles became more uniform in their properties as mixing frequency increased.

The above results were obtained with the modified Curl mixing model (Chen, 1993). The effect of the mixing model was investigated by repeating the calculations for a mixing frequency of 1000 s^{-1} with the Interaction-by-Exchange-with-the-Mean (IEM) model, but the solution converged to the non-reacting case. It was therefore decided to reproduce the results of Correa (1993) for CO/H_2/air combustion with a goal of determining whether the IEM model is implemented correctly in the PASR code. These calculations are in progress. If successful, calculations will then be performed with a full kinetic scheme for natural gas combustion, with a view toward obtaining a suitable reduced mechanism for use in a submodel to be implemented in a 3-D gaseous combustion code for application to lean, pre-mixed gas turbines.

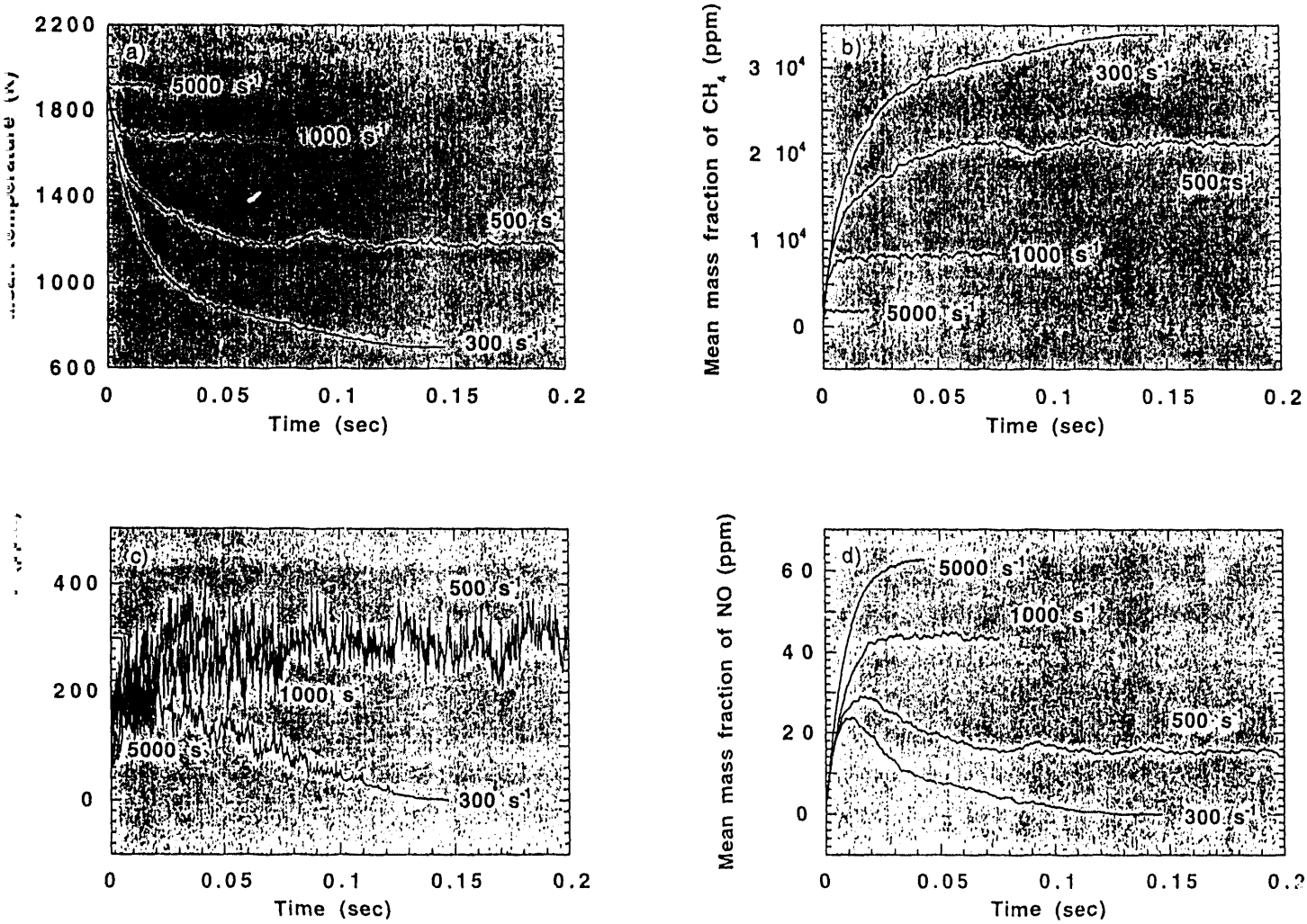

Figure 5. PaSR Predictions for Fuel-Lean, Premixed Methane Combustion in Air (0.6 Equivalence Ratio, 15 atm, 700 K Inlet, 10 ms Residence Time

FUTURE WORK

Work during the next year will include: 1) completion of simplified FG-DVC models for fixed-beds and fluidized-bed reactors; 2) integration of a particle heat transfer model with a simplified FG-DVC model; 3) complete stochastic particle dispersion model; 4) complete formulation of transport reactor code; 5) complete integration of simplified FG-DVC model into fluidized-bed code; 6) complete formulation of a large particle oxidation model; 7) complete integration of a large particle devolatilization submodel (based on FG-DVC) into FBED-1; 8) implement improved numerical solution method for FBED-1; 9) extend the PaSR pdf model to the case of natural gas combustion and use the model to develop/evaluate a suitably reduced kinetic mechanism for application in multi-dimensional flame codes.

REFERENCES

Bateman, K. J., Germane, G. J., Smoot, L. D., "A High Pressure Facility for Measurement of Oxidation Rates of Mm-Sized Chars," in preparation, Fuel (1994a).

Bateman, K. J., Germane, G. J., Smoot, L. D., and Blackham, A. U., "Effect of Pressure on Oxidation Rates of Mm-sized Char," in review, Fuel (1994b).

Brown, M.J., and Sadowski, R.S., "The PyGas Process, as Modeled by DOE-MGAS & KRW Kinetic Rate Equations," paper presented at the International Power Generation Conference, San Diego, CA, (October 1991).

Chen, J. -Y., "Stochastic Modeling of Partially Stirred Reactors," Fall Meeting of the Western States Sections/The Combustion Institute, Paper no. 93-071 (1993).

Correa, S. M., "Turbulence-Chemistry Interactions in the Intermediate Regime of Premixed Combustion," Comb. Flame, 93: 41-60 (1993).

Correa, S. M., and Braaten, M. E. "Parallel Simulations of Partially Stirred Methane Combustion," Comb. Flam, 94: 469-486 (1993).

Gosman, A.D., and Ioannides, E., AIAA Paper, No. 81-0323 (1981).

Jakob, M., Heat Transfer, John Wiley and Sons, New York (1959).

Kloeden, P.E., and Platen, E., Numerical Solutions of Stochastic Differential Equations, Springer-Verlag, (1992).

Merrick, D., Fuel, 63, 540 (1983).

Pope, S. B., "PDF Methods in Turbulent Reactive Flows," Prog. Energy Combust. Sci, 11: 119-192 (1985).

Radulovic, P.T., Ghani, M.U., and Smoot, L.D., "An Improved Model for Fixed-Bed Coal Combustion and Gasification," in press, Fuel, (1994).

Shuen, J-S., Chen, L-D., and Faeth, G.M., AIChE J., 29, 167 (1983).

Synder, W.H., and Lumley, J.L., J. Fluid Mech., 48, 41 (1971).

U.S. Department of Energy, "DOE, Clean Coal Technology Demonstration Program: Program Update 1992 (As of December 31, 1992)," U.S. Department of Energy Report, Washington, DC, DOE/FE-0272 (1993).

Wang, L.-P., Stock, D.E., J. Fluid Eng., Trans. ASME, 114, 101 (1992).

P18 CeraMem Filters for Removal of Particles from Hot Gas Streams

CONTRACT INFORMATION

Contract Number	DE-FG02-90ER80896
Contractor	CeraMem Corporation 12 Clematis Ave. Waltham, MA 02154 (617)-899-0467
Contract Project Manager	Bruce A. Bishop
Principal Investigator	Robert L. Goldsmith
METC Project Manager	Norman Holcombe
Period of Performance	May 19, 1991 - May 19, 1995

OBJECTIVES

The objective of this Phase II SBIR program is the development and demonstration of a novel ceramic filter for particulate removal from hot gas streams resulting from advanced coal conversion processes. This paper describes this novel filter, and provides information on a field testing conducted on a 10 MW pressurized circulating fluidized bed (PCFB) combustor.

BACKGROUND INFORMATION

The need for hot gas cleanup in the power, advanced coal conversion, process and incineration industries is well documented and extensive development is being undertaken to develop and demonstrate suitable filtration technologies. In general, process conditions include (a) oxidizing or reducing atmospheres, (b) temperatures to 1800°F, (c) pressures to 300 psi, and (d) potentially corrosive components in the gas stream. The most developed technologies entail the use of candle or tube filters, which suffer from fragility, lack of oxidation/corrosion resistance, and high cost. The ceramic membrane filter described below offers the potential to eliminate these limitations.

Ceramic Gas Filter Construction

The construction of the CeraMem ceramic filter is based on the use of porous honeycomb ceramic monoliths. These high surface area, low cost materials are widely used as catalyst supports for automotive catalytic converters. The monoliths have a multiplicity of "cells" (passageways) that extend from an inlet end face to an opposing outlet end face. The cell structure can be round, square, or triangular, and the cell "densities" can vary from 25 to 150 cells per

square inch. Porosity of the honeycomb material can be from below 30% to over 50%. The mean pore size can range from about 4 to 50 μm. The superior properties of commercially available honeycomb ceramic monolith materials make them ideally suited for applications requiring high thermal stability, mechanical strength, and corrosion resistance. These rigid ceramics have been used for years as automotive catalyst supports where conditions of high vibration and thermal cycling are encountered in a combustion gas environment. Other applications of these materials as catalyst supports include emission control systems such as catalytic incineration and NOx selective catalytic reduction (SCR).

The monolith structure used for catalyst support material is readily adapted to function as a filter to remove particulate matter from diesel engine exhaust. Unlike the catalytic convertor application in which automotive exhaust flows in a channel flow mode through the honeycomb cells, the diesel particulate filter (DPF) operates as a wall-flow filter. The carbonaceous soot in the exhaust gas is filtered on and within the cell walls of the monolith. This flow path is achieved by modifying the monolith structure by plugging every other cell at the upstream face of the device (Figure 1) with a high-temperature inorganic cement. Cells which are open at the upstream face of the monolith are plugged at the downstream face. Exhaust gas is thereby constrained to flow through the porous cell walls, and at appropriate intervals, the filter is cleaned by burning off the entrapped soot.

A variety of monolith sizes is available for DPF devices. Typical monolith characteristics are a square cell shape, a cell density of 100 cells/in^2, a cell wall side of 0.083 inch, and a cell wall thickness of 0.017 inch. DPF devices operate at least in part as depth filters. The pore size of the cell wall material is quite large (20-35μm), and fine particulates enter and plug the cell wall. Deposition inside the walls leads to pore plugging by particulates and makes regeneration by backpulsing difficult, if not impossible.

Ceramic Filter For Hot Gas Particulate Removal

To filter particulates from hot gas, CeraMem modifies the DPF device described above by applying a ceramic MF membrane to the cell wall surfaces. This technique creates a composite filter which can be operated as a backpulsable surface filter. The thin, membrane coating has a pore size approximately 100-fold finer than that of the monolith support (Figure 2). Thus, the retention efficiency of the filter for fine particles is determined by the membrane pore size. By keeping the membrane coating thin ($\approx$50 μm) the gas flow pressure drop is kept acceptably low. Yet, it is possible to use a large-pored, low-resistance support for the membrane. Because the support is coated by the membrane, the pore size of the support does not affect particle retention and the pore structure of the support does not become plugged by particulate matter.

In operation, particle-laden gas flows into the membrane- coated inlet cells. Particulate matter is collected in the inlet cells and the filtered gas exits the module via the downstream cells. As particulate material accumulates, pressure drop increases to a preselected level at which time the filter is cleaned by online backpulsing from the downstream end of the filter.

The compactness of the filter relative to other gas filters is evident from the data of Table 1. This compactness leads to small filter housings since the filters can be installed in a closely packed array in the vessel. Both the filters and total filter systems are expected to have costs much lower than those of traditional hot gas particulate filtration systems.

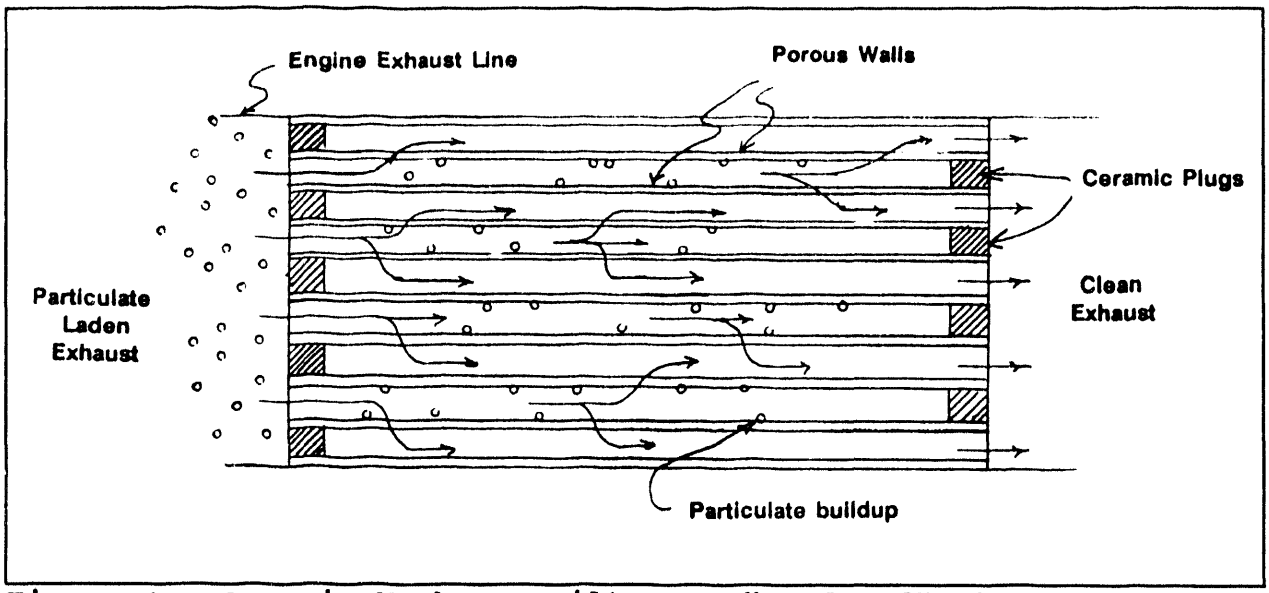

Figure 1. Ceramic Membrane Filter In "Dead-End" Flow Configuration

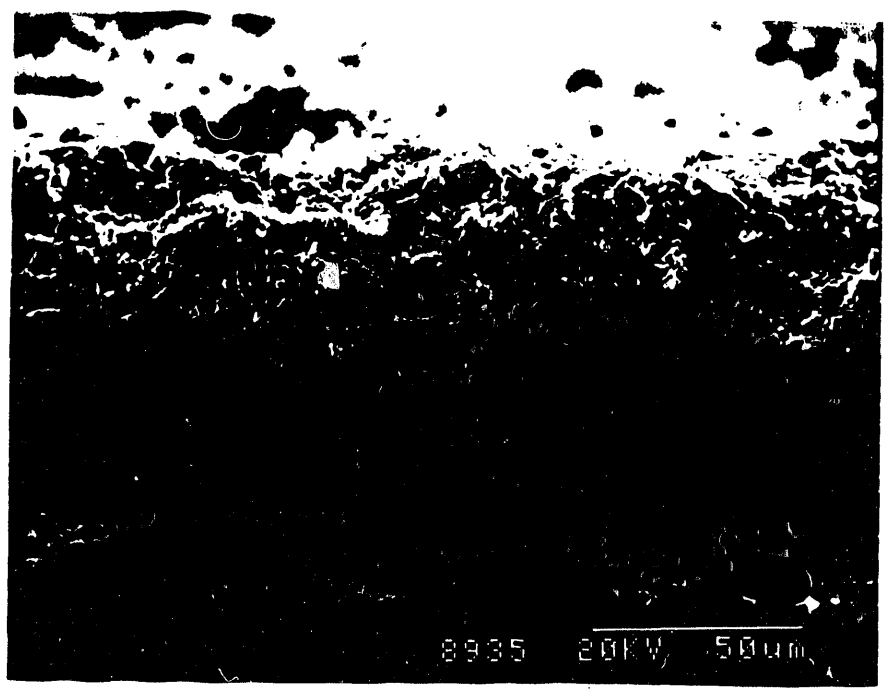

Figure 2. Scanning Electron Micrograph Of Membrane Coating

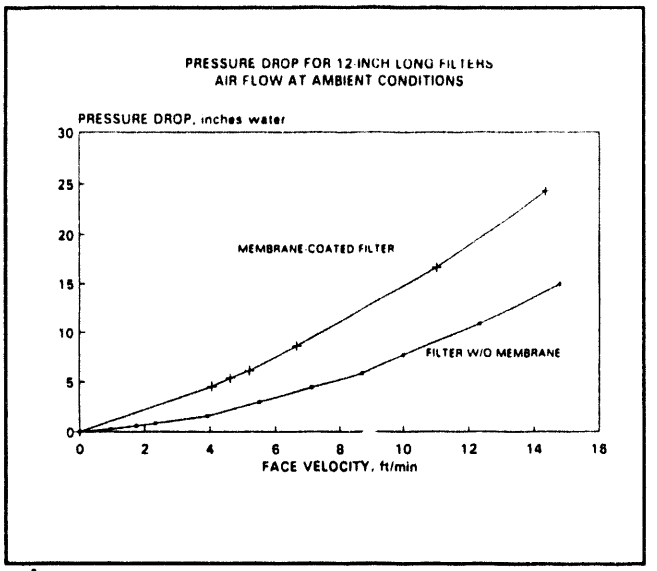

Figure 3. Pressure Drop vs. Flow For Ceramic Membrane Gas Filters

Table 1. Comparison Of Ceramic Membrane Filter With Other Filters

Filter Type	Filter Dimensions	Filter Area (ft^2)	Area/Volume ratio (ft^2/ft^3)
CeraMem	6" sq. x 12" long	37	155
Fabric Bag	6" ϕ x 20' long	31	8.5
Candle	2.5" ϕ x 59" long	2.8	20
Crossflow	11.8" x 11.8" x3.9"	8.3	26.5

Figure 3 shows flow versus pressure drop data for 12" long filters with and without the membrane coating. The membrane coating increases the resistance over that of an uncoated filter about two- to three-fold. For the uncoated filter, the increase in pressure drop with increasing filtration rate is caused by pressure drop in the filter passageways. For membrane coated filters the primary resistance to gas flow is that of the membrane coating itself.

PROJECT DESCRIPTION

The project involves three major tasks:

(1) Ceramic Membrane Filter Development

(2) Filter Demonstration in Field Trials

(3) Full-Size System Design and Costing

The first task has been completed, and the results have been reported in previous project progress reports to the DOE. The focus of this paper will be on task (2).

Filter Demonstration in Field Trials

Field testing of the CeraMem ceramic hot gas filter was conducted at A. Ahlstrom Corporation's 10 MWth PCFB test facility in Karhula, Finland between August 23 and September 8, 1993. During this period, 33 hours of filter operation while exposed to PCFB coal fired conditions were accumulated. The test filters were twelve EX-54 9" diameter x 12" long filters each with 70 square feet of filtration area in the 100 cell per square inch (cpsi) geometry. These filters had the ceramic membrane and cement cell plugs developed for this hot gas application.

Figure 4 shows how Ahlstrom installed and oriented the filters inside their filter pressure vessel. Each filter was wrapped with a ceramic fiber mat and mounted in a 10" ϕ x 13" long casing.

Figure 5 shows a schematic of the Ahlstrom designed backpulse air cleaning system. On-line cleaning of each 4 filter duct in a 1-2-3 sequence was initiated manually or automatically by an adjustable timing device. The pulse air reservoir was maintained between 215 psig and 235 psig

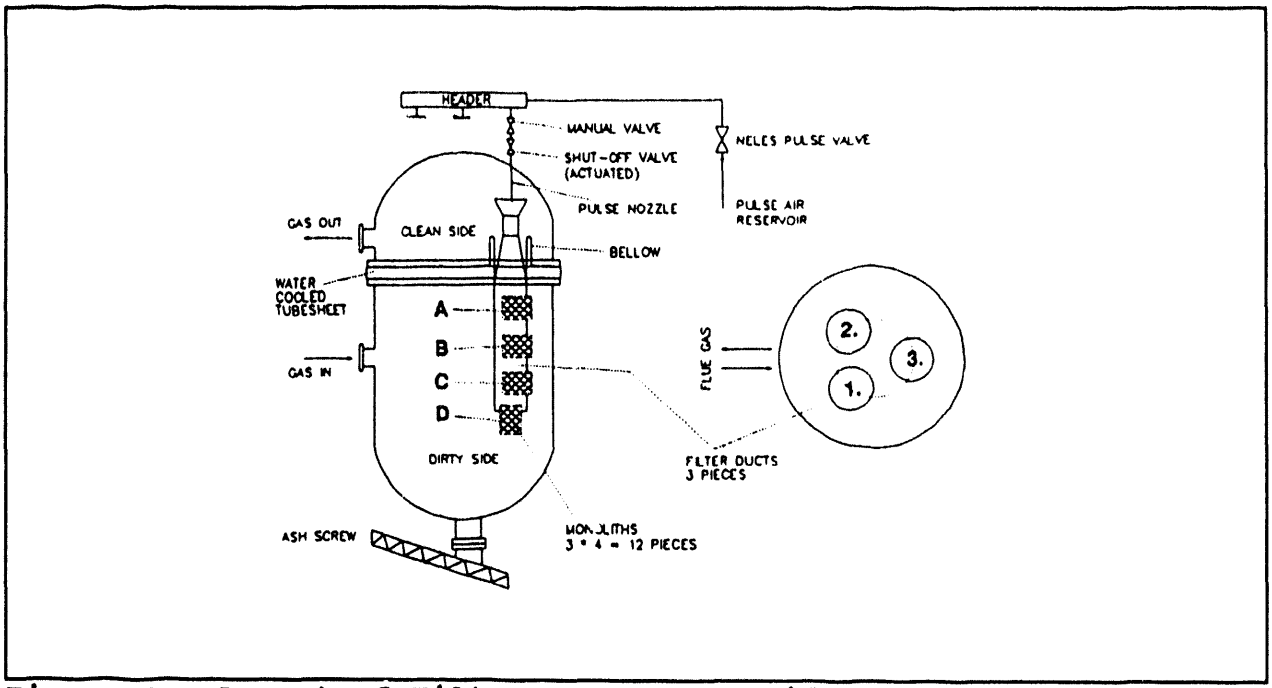

Figure 4. Layout of Filter Elements Inside the Pressure Vessel

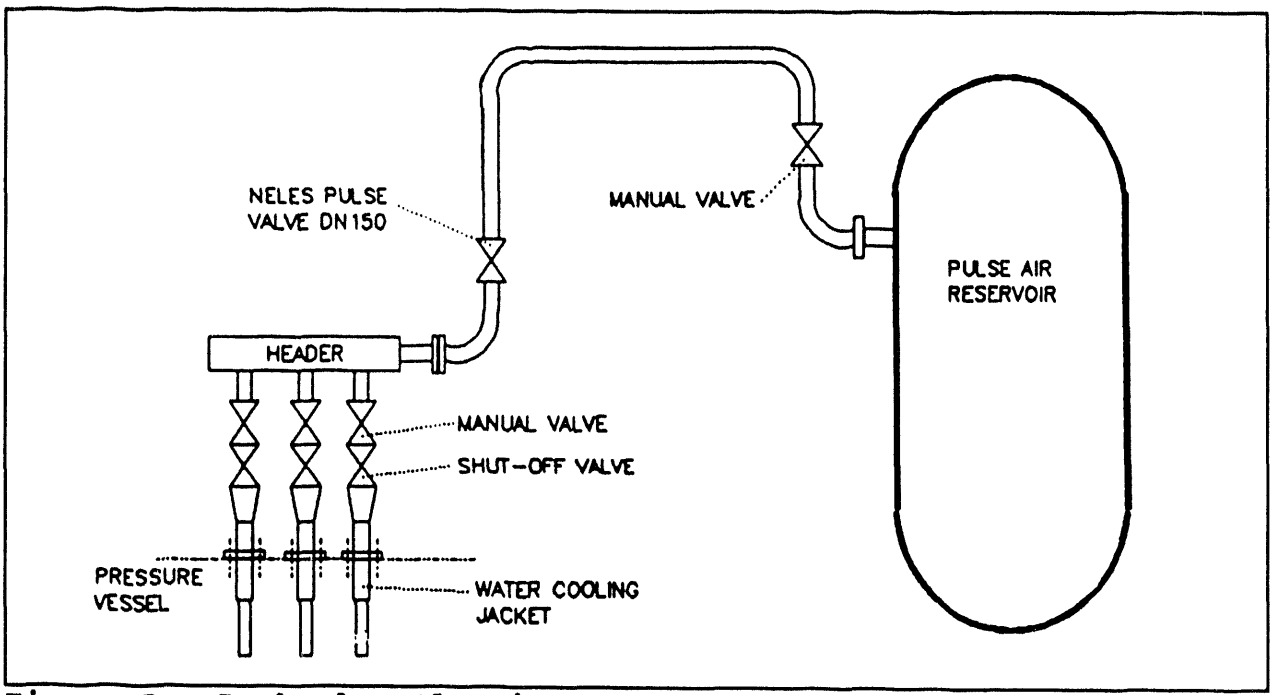

Figure 5. Backpulse Cleaning System

and followed ambient temperature.

RESULTS

Three test runs at coal fired conditions were accomplished before the testing was terminated. Each of these runs was preceded by a PCFB test facility heatup and checkout period using natural gas, light fuel oil and heavy fuel oil prior to conversion to firing with Illinois No. 6 coal and Iowa Industrial Limestone No. 1 in a coal-water slurry. Low dust loads present in the hot gas generated from gas and oil firing generally required manual pulsing to clean the filters and reduce pressure drop during these periods.

a. First Test Run (August 26, 1993) Summary

The first test run on coal generated hot gas lasted about four hours before an ash removal system problem caused a facility shutdown. This initial run achieved an initial baseline and subsequently stable post cleaning pressure drop level of 12" WC. The average operating conditions during the run were 132 psig, 1400°F, and a filter face velocity of 2.24 fpm. Pulse cleaning (at 217 psig) occurred 32 times at 7 minute intervals and maintained peak on-line filtration pressure drops around 32" WC with periodic spikes to between 40" WC and 56" WC in 37% of the cycles. Figure 6 contains the data for this 4 hour run.

b. Second Test Run (September 2-3, 1993) Summary

The longest of the test runs was the second. About 20 hours of operation were achieved at two sets of power level conditions. The PCFB combustor power level was 60% for the first 17 hours of the run, and 80% for the last 3 hours. The 17 hour "A" run average conditions were 129 psig, 1440°F, and 2.30 fpm filter face velocity. During this run, a new baseline and subsequently stable post cleaning pressure drop level of 16" WC was maintained. Pulse cleaning (at 232 psig) occurred 189 times at intervals of 6 minutes and maintained peak on-line filtration pressure drops around 36" WC with periodic peaks to between 40" WC and 60" WC in 15% of the cycles.

The 3 hour "B" run average conditions were 128 psig, 1520°F, and 3.18 fpm filter face velocity. During this run, the baseline shifted to 22" WC due to increased flow rate (face velocity) and higher temperature. Stable post cleaning pressure drop at the new level of 22" WC was again maintained. Pulse cleaning (at 232 psig) occurred 43 times at intervals of 6 minutes and maintained peak on-line filtration pressure drops around 44" with periodic peaks to between 52" WC and 80" WC in 26% of the cycles. Figures 7, 8, and 9 show the data for this 20 hour run.

Failure of the single pulse cleaning valve resulted in an on-line filtration pressure differential excursion of about 100 psi across the filters. The test run ceased and the facility was subsequently shutdown for repair.

c. Third Test Run (September 8, 1993) Summary

Following the pulse valve repair, the filters were pulse cleaned cold about 50 times. Visual inspection revealed substantial (50%) filter cell plugging and some dust evident in the clean gas duct. Following re-start, and in spite of a high filter pressure drop level of 44" WC, a third test run was initiated. This run lasted about 5 hours before being voluntarily shutdown. Upon inspection, the filters were found to be fractured within the holders. This failure was probably caused by the extreme differential pressure (100 psi) imposed across filter elements while being restrained by the holder's retaining ring. Since

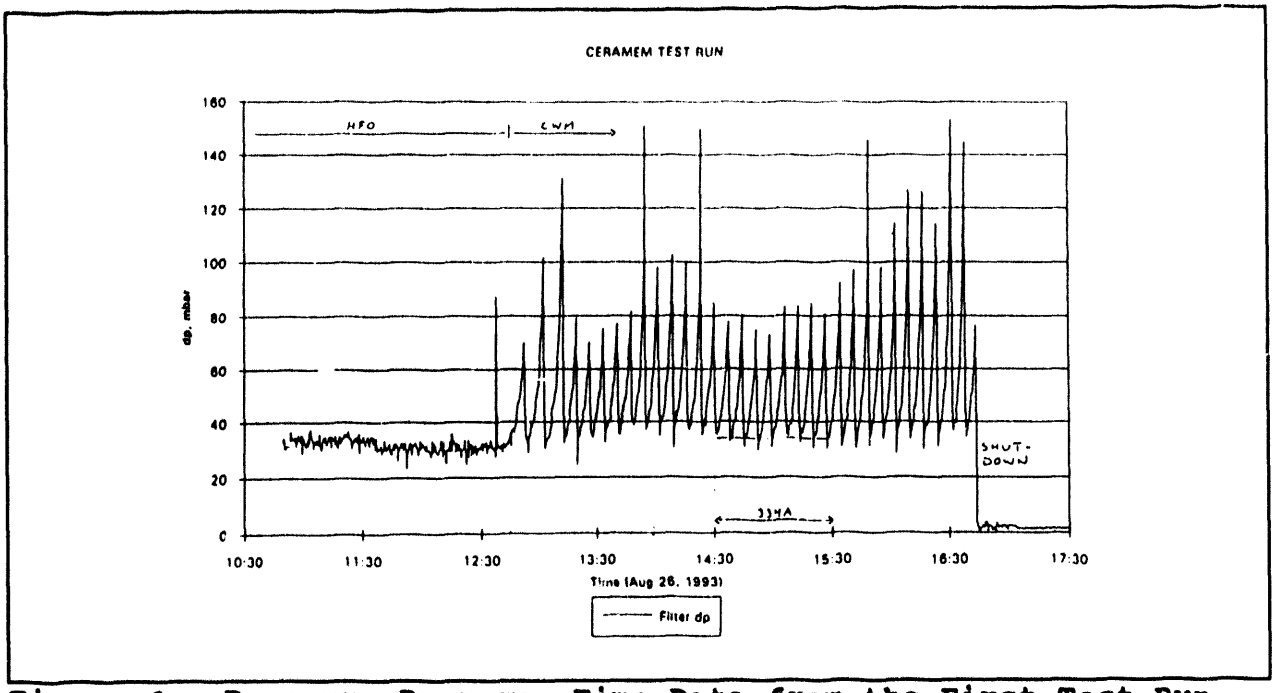

Figure 6. Pressure Drop vs. Time Data from the First Test Run

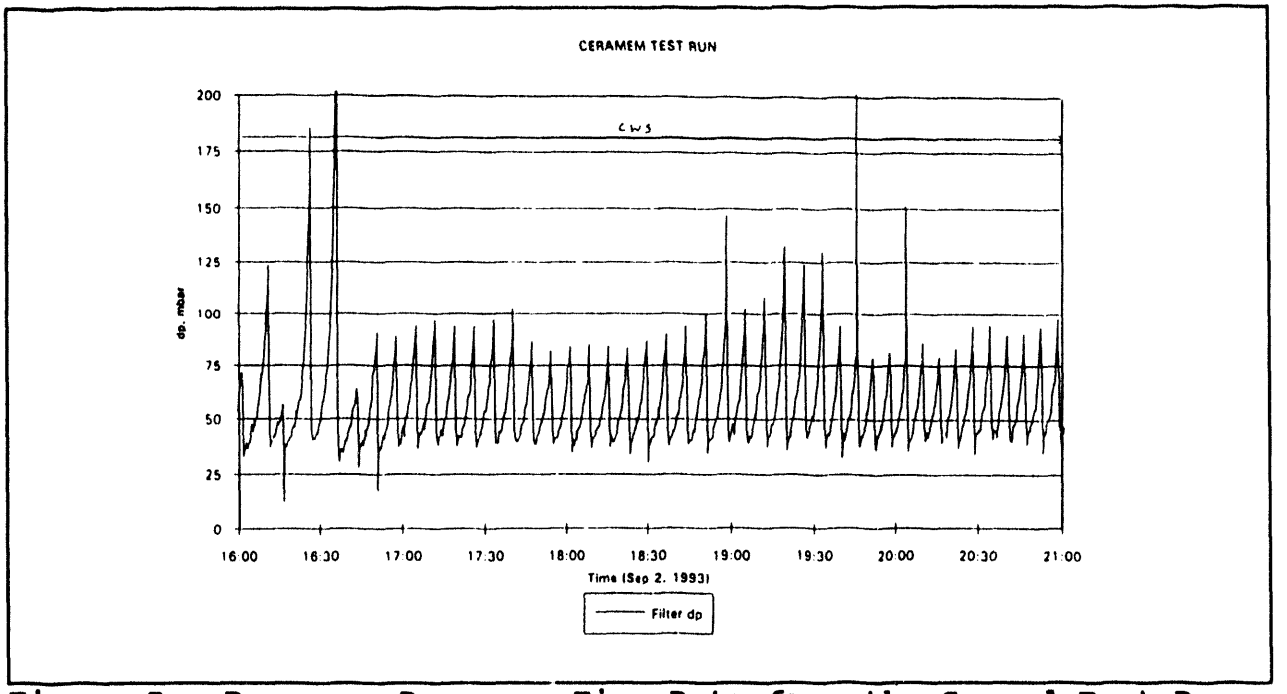

Figure 7. Pressure Drop vs. Time Data from the Second Test Run

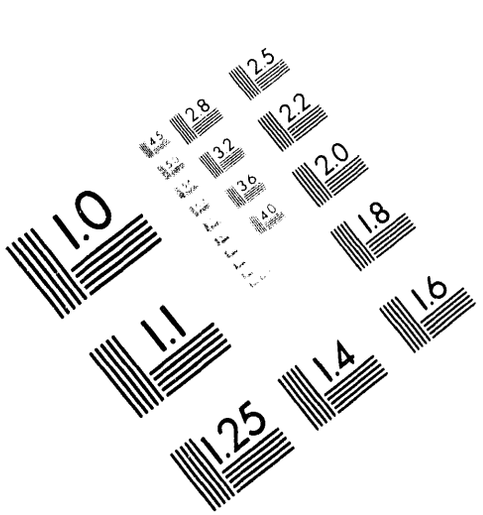

AIIM

Association for Information and Image Management

1100 Wayne Avenue, Suite 1100
Silver Spring, Maryland 20910

301/587-8202

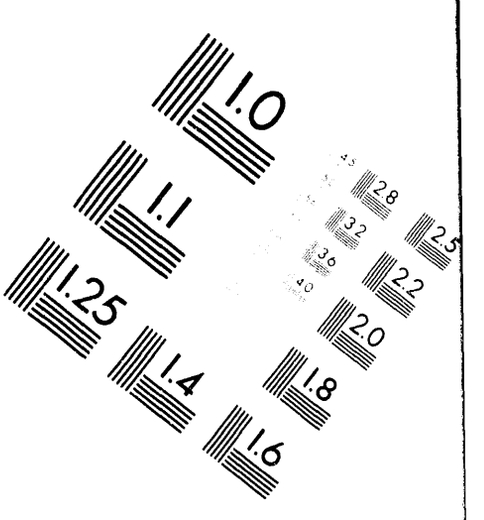

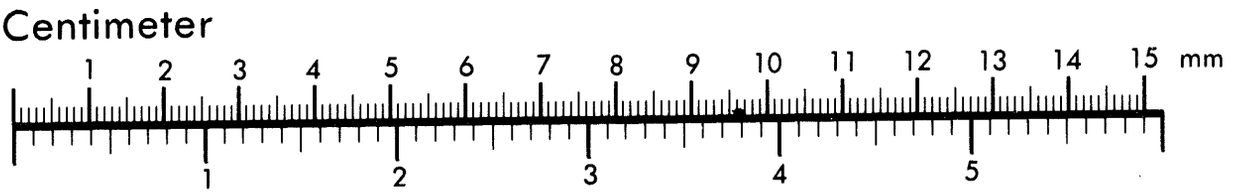

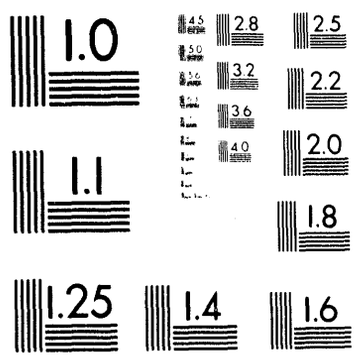

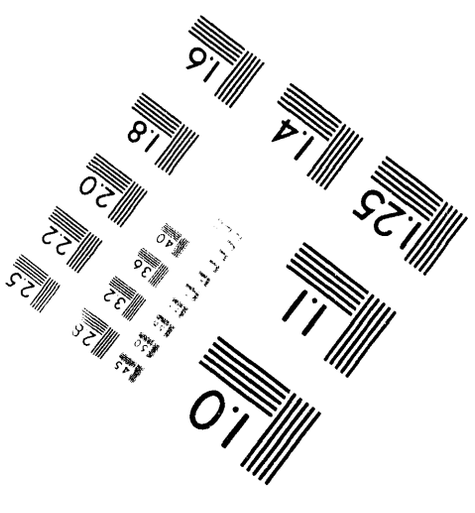

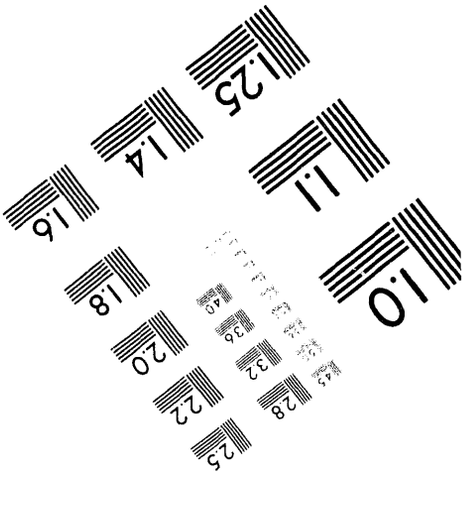

MANUFACTURED TO AIIM STANDARDS
BY APPLIED IMAGE, INC.

6 of 6

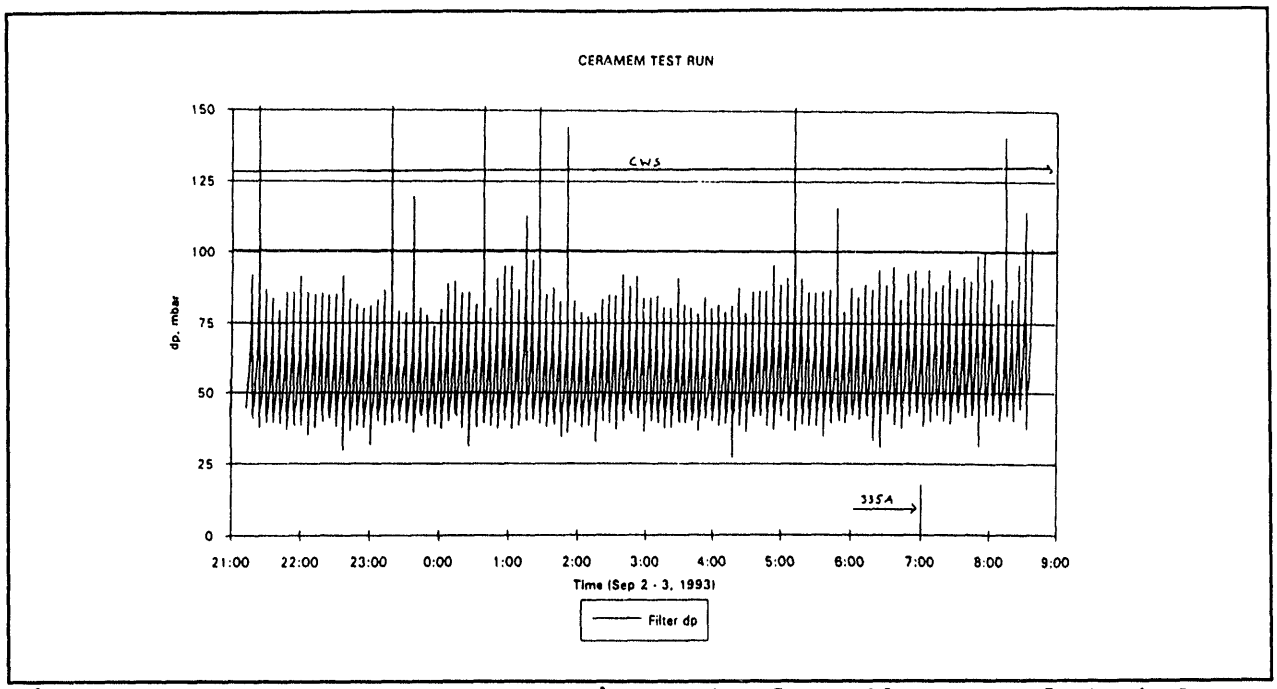

Figure 8. Pressure Drop vs. Time Data from the Second Test Run

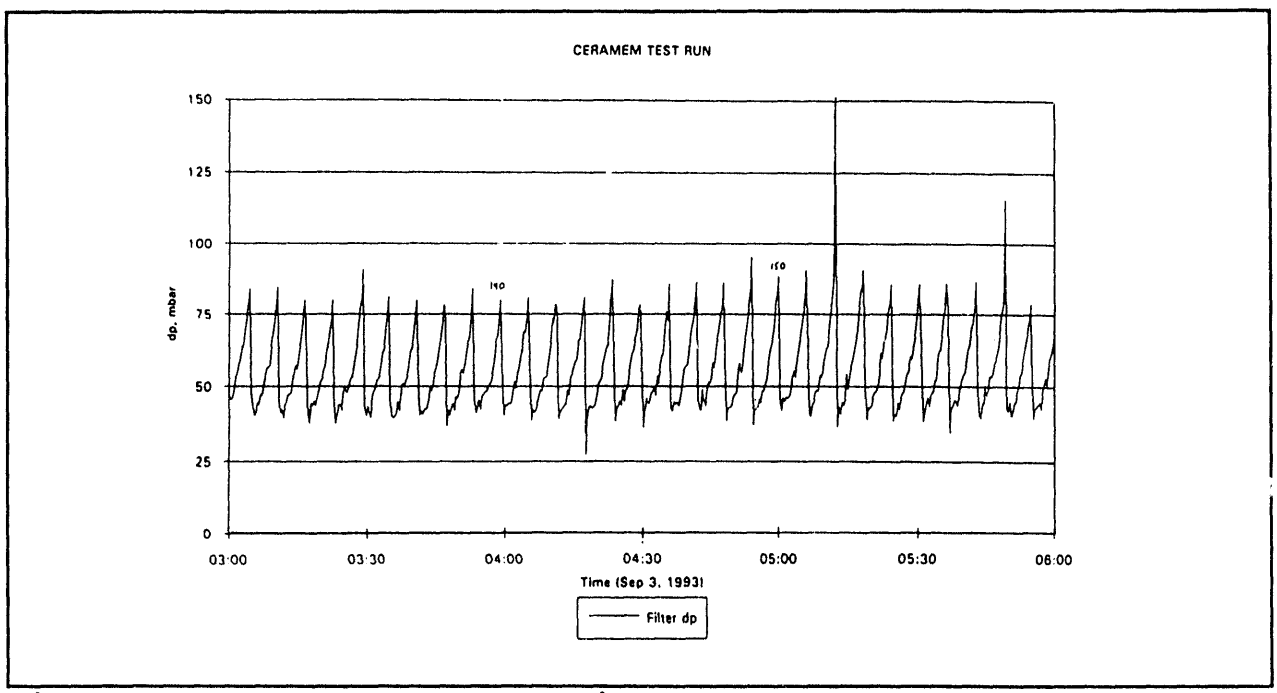

Figure 9. Pressure Drop vs. Time Data from the Second Test Run

the filter boundary had been breached by the fracture and substantial filtration area lost as a result of cell plugging, the data taken during this run was considered invalid and is not included here.

DISCUSSION

Although this test campaign was not of sufficient length to be considered a "demonstration" and fell considerably short of the 6 month objective, certain valuable information was learned from these short term test runs with multiple filters configured in a representative commercial PCFB filter vessel.

Cleanability

Multiple ceramic hot gas filters 9" diameter by 12" long (100 cpsi) were effectively regenerated on-line to initial baseline run pressure drop levels under PCFB conditions over short (up to 20 hours) periods of time. However, on subsequent runs following a previous shutdown, a new higher initial run pressure drop (16" WC from 12" WC) appears to be established while operating at the same conditions. Notwithstanding, the ability to recover back down to that new level was still accomplished. High dust loads (8000 ppmw) in the inlet gas and low volumetric dust holding capacity in the filter resulted in short cleaning cycle times between 4 and 7 minutes.

Clean Filter Pressure Drop

Determination of actual hot clean baseline pressure drop for 12" long 100 cpsi filters at desirable operating face velocities was performed in the early testing. Achieving operation at a level of 12" to 16" WC at 1400°F and 2.5 fpm face velocity was considered acceptable.

Filtration Cycle Behavior

Pressure drop was observed to increase at an accelerating rate during the filtration cycle. This phenomenon is characteristic of the filter's honeycomb goemetry and the filtration mechanism within the filter. A reduction of actual filtration area occurs as the filter cell fills with dust thus increasing actual face velocity (pressure drop); an increase in resistance (pressure drop) occurs through the membrane/wall as dust builds on the surface; and an increase in resistance (pressure drop) occurs to channel flow as the channel narrows with increasing dust buildup on the walls. It should be noted that the cleaning cycle was initiated on a timed basis, resulting in variability and instability of maximum pressure drop level reached before cleaning.

CONCLUSIONS

A novel ceramic membrane filter has been developed and tested for a short period on hot gas stream from a 10 MW PCFB . The filter has the attributes of ultra-high particulate removal efficiency, complete regenerability, compactness and low cost. Continued testing of the filter in hot gas environments, for long duration, and to determine its resistance to attack from potentially corrosive components of the gas streams is underway.

P19 Development of Disposable Sorbents for Chloride Removal from High-Temperature Coal-Derived Gases

CONTRACT INFORMATION

Contract Number DE-AC21-93MC30005

Contractor

SRI International
333 Ravenswood Avenue
Menlo Park, CA 94025
(415) 326-6200

Contract Project Manager Gopala N. Krishnan

Principal Investigators

G. N. Krishnan, B. J. Wood, and A. Canizales (SRI International)
R. Gupta and S. D. Sheluker (Research Triangle Institute)
R. Ayala (GE Corporate Reseach and Developement)

METC Project Manager Ronald K. Staubly

Period of Performance September 30, 1993 to September 29, 1995

Schedule and Milestones

FY94 Program Schedule

Task	S	O	N	D	J	F	M	A	M	J	J	A	S
Submission of NEPA Information													
Sorbent Preparation and Characterization													
Provision of a Bench-Scale Unit													
Bench Scale Testing													
Parametric Testing*													
Data Analysis													

* Scheduled to be initiated in January 1995.

OBJECTIVE

The objective of this program is to develop alkali-based disposable sorbents capable of reducing HCl vapor concentrations to less than 1 ppm in coal gas streams at temperatures in the range 480° to 750°C and pressures in the range 1 to 20 atm. The primary areas of focus of this

program are investigation of different processes for fabricating the sorbents, testing their suitability for different reactor configurations (fixed-, moving-, and fluidized-bed reactors), obtaining kinetic data for commercial reactor design, and updating the economics of the process.

BACKGROUND INFORMATION

Coal is a complex and heterogeneous substance that contains several impurities, including sulfur, chlorine, nitrogen, and metal compounds. The integrated coal gasification combined cycle approach is an efficient process for producing electric power from coal by gasification, followed by high-temperature removal of gaseous impurities, then electricity generation by gas turbines . Alternatively, molten carbonate fuel cells may be used instead of gas turbine generators. In either case, the coal gas must be treated to remove impurities such as hydrogen chloride (HCl), a reactive, corrosive, and toxic gas, which is produced during gasification from chloride species in the coal.

Concentrations of HCl in coal gas have not been determined precisely, but they are estimated to be in the range 1 to 500 ppm (TRW, 1981). Bakker and Perkins (1991) point out that concentrations of HCl in coal gas can be about five times higher than those in coal-fired boiler combustion gas streams because of the lower volume of the coal gas. The actual concentration of HCl vapor in a coal gas stream will depend on the chlorine content of the coal, the gasification temperature, and the type of gasifier. For example, an oxygen-blown gasifier that produces a medium-Btu coal gas will have a higher HCl concentration than an air-blown gasifier that produces a low-Btu fuel gas.

The high-temperature molten carbonate fuel cell (MCFC) is a promising device for future IGCC power generation plants because of its high efficiency. However, for sustained and efficient operation of the MCFC, the feedgas must be free of contaminants such as particulate matter, sulfur, and chloride species. Halogen compounds are deleterious to MCFCs because they can lead to severe corrosion of cathode hardware (Kinoshita et al., 1988). HCl also can react with the molten carbonate electrolyte to form corresponding halides such as LiCl and KCl. The high vapor pressures of these halides increase the loss of electrolyte. The allowable HCl concentration in the feedgas to such a fuel cell is estimated to be less than 1 ppm (Gillis, 1980).

The role of HCl as an impurity in coal gas used to fuel a gas turbine is not well defined and currently no concentration limit standards exist. In spite of the absence of specified limits, the removal of HCl vapor from the fuel can only be beneficial for IGCC systems, because the presence of HCl vapor is generally deleterious to the metal components of the IGCC systems. Perkins et al. (1990) report that the chloride deposits found on syngas coolers accelerate the corrosion of the heat exchanger material. HCl reacts with the deposited slags forming low-melting iron chlorides, and thereby accelerates the corrosion rate.

A number of processes are available for removing HCl vapor from industrial and incinerator waste gases. These processes scavenge HCl by adsorption onto activated carbon or alumina or by reaction with alkali or alkaline earth carbonates or oxides. In chemical plants where HCl must be removed from process feedstocks, commercial sorbents called chloride guards are marketed by catalyst manufacturers and these sorbents are relatively expensive. These sorbents reduce chloride contaminant levels to <l ppm, but they must operate at temperatures <450°C. Furthermore, none of them are economically regenerable. Hence, inexpensive and disposable sorbents are needed for the chloride removal in hot coal-derived gas streams.

Equilibrium thermodynamic calculations provide a theoretical limit to which chloride vapor level can be reduced by using sorbents. We calculated the equilibrium levels of both HCl and metal chloride vapor level as a function of temperature for various alkali and alkaline earth chlorides. Of the alkali salts considered, potassium yielded the lowest HCl vapor levels. However, at temperatures above 1000 K, NaCl(g) has a lower vapor pressure than KCl(g) (Table 1). In addition, the sodium minerals are more abundant than potassium minerals. Of the alkaline earth compounds considered, only barium compounds have both low equilibrium HCl level and chloride vapor pressure. But, the HCl vapor level in equilibrium with $BaCl_2$ exceeds that in equilibrium with NaCl.

Table 1. Equilibrium Vapor Pressures over Alkali and Alkaline Earth Chlorides

	Equilibrium Pressure (10^{-6}atm)	
System	HCl(g)	MCl(g)
800 K		
Na	0.5	<0.01
K	0.05	0.25
Ba	8.0	<0.01
Ca	560.0	<0.1
Sr	79.0	<0.01
1000 K		
Na	4.0	62.0
K	0.4	120.0
Ba	54.0	<0.1
Ca	1400.0	<0.1
Sr	260.0	<0.1

Previous bench-scale studies have shown that disposable sodium-based sorbents have sufficient chemical reactivity to reduce HCl vapor in simulated coal gas streams in the temperature range from 540° to 650°C. Early experimental studies at Physical Sciences, Inc. (PSI) focussed on shortite ($Na_2CO_3 \cdot 2CaCO_3$) and trona ($Na_2CO_3 \cdot NaHCO_3 \cdot 2H_2O$) as candidate sorbents (Ham et al., 1984). Trona exhibited a lower reactivity than shortite, a characteristic that was attributed to sintering of the mineral at the sorption temperature. Battelle Pacific Northwest Laboratories conducted both laboratory- and bench-scale studies to determine the feasibility of simultaneously removing H_2S and HCl in hot coal gas systems by using solid supported molten salts (Lyke, 1985). Using lithium, potassium, and calcium carbonates supported on lithium aluminate, they found that HCl vapor was reduced from about 200 ppm to less than 10 ppm at 800°C and 15 atm. The residual chloride in the gaseous effluent consisted mainly of alkali chloride vapor whose concentration increased with temperature. An operating cost of about $0.008/kWh was projected in a preliminary economic analysis.

Laboratory- and bench-scale experiments were performed by SRI International (Krishnan et al., 1986) to evaluate three natural carbonate minerals—nahcolite ($NaHCO_3$), shortite, and dawsonite ($NaAl(OH)_2CO_3$)—as HCl scavengers for simulated coal gas. A chloride guard (Katalco 59-3) and a commercial flue gas cleanup sorbent (NOXSO) were also examined in the project. All the tested sorbents reacted rapidly with HCl vapor and reduced the HCl vapor concentration from about 300 ppmv to about 1 ppmv. The performance of nahcolite was superior in its adsorption capacity; the spent sorbent contained up to 54 wt% chloride. Furthermore, the presence of H_2S and trace metal impurities in the coal gas did not significantly affect the performance of the bed for HCl sorption. An economic evaluation for HCl cleanup costs in a 100 MW_e plant indicated that the use of nahcolite to remove HCl vapor would add only about $0.002/kWh (2 mills/kWh) to the cost of the generated electric power.

Thus, alkali-based naturally occurring minerals and synthetic sorbents have been shown in bench-scale experiments to be capable of reducing HCl vapor levels to about 1 ppm in simulated coal gas streams.

PROJECT DESCRIPTION

The primary areas of focus in the current program are to investigate different processes for fabricating sorbents suitable for HCl vapor removal in hot, coal-derived fuel gas streams, test their suitability for different reactor configurations (fixed-, moving-, and fluidized-bed reactors), obtaining kinetic data for commercial reactor design, and update the economics of the process. This project is a colloborative effort between SRI, the prime contractor, and subcontractors Research Triangle Institute (RTI) and General Electric Coporate Research and Development (GE-CRD). RTI is developing and testing sorbents for fluidized-bed reactors, while GE-CRDC is preparing sorbents for moving-bed reactors. SRI is preparing and testing sorbents for fixed-bed reactors. The moving-bed sorbents prepared by GE-CRD will be also tested at SRI.

The program is divided into the following six tasks:

1. Information required for National Environmental Policy Act (NEPA)
2. Sorbent preparation and characterization
3. Provision of bench-scale test unit

4. Bench-scale testing
5. Parametric testing
6. Data analysis.

At the beginning of the project, information was provided to the U.S. Department of Energy (DOE) for a NEPA review. The review was completed and authorization was recieved to proceed with the program. Based on earlier studies, nahcolite, an abundant and available natural mineral, was the primary choice for the sorbent material. About 300 kg of nahcolite powder, obtained by solution mining from deposits near Rifle, Colorado, was supplied free-of-charge by NaTec Resources, Inc., Houston, Texas. For testing purposes, the powder was pelletized or granulated with binders and texturizing agents using pilot-scale equipment.

The HCl reactivity and chloride capacity of the granules and pellets are being determined using thermogravimetry and bench-scale reactors both at SRI and RTI using similar equipment. The reactors are typically 5-cm ID and 90-cm long and heated externally using electrical furnaces. Simulated gas mixtures representative of either Texaco oxygen-blown gasifier or METC's GPIF air-blown gasifier are blended using individual gases or binary gas mixtures. A higher than normal level of HCl vapor is used in these tests to reduce the reaction time. The HCl vapor in the product gas leaving the reactor is dissolved in water and the accumulated chloride in the solution is measured with an automated ion chromatograph. The concentration of HCl vapor in the gas stream is calculated by differentiating the cumulative chloride level with respect to time. The analytical system is capable of measuring sub-ppm levels of HCl vapor.

RESULTS

Sorbent samples for testing were prepared by pelletizing or granulating the powder with binders and texturizing agents. Pellets suitable for use in a fixed-bed reactor were extruded in sizes varying from 1.5 to 5 mm. They contained either bentonite (10wt%) or sodium silicate (2 and 5 wt%) as the binder (Table 2). In some cases, methyl cellulose was added as a texturizing agent. The pellets were calcined in air, and during calcination, when the temperature exceeded 150°C, the nahcolite mineral decomposed into sodium carbonate, releasing CO_2 and H_2O:

$$2NaHCO_3\ (s) = Na_2CO_3\ (s) + CO_2\ (g) + H_2O\ (g)$$

The evolution of these gases produced a porous sorbent, but at higher calcination temperatures, the surface area decreased due to sintering of the solid (Figure 1). However, neither the binder composition nor the presence of carboxy methyl cellulose affected the pellet surface area when they were calcined at temperatures higher than 400°C.

The physical properties of two types of pellets were comparable both after calcination and reaction with HCl (Table 3). The crush strengths of the extrudates, as determined by the ASTM method D4179, were similar for all pellets, irrespective of additive. The average crush strength of the pellets calcined at 300°C for 16 h was 450±70 kg/m and that of pellets calcined at 550°C was 700±100 kg/m.

Fixed-Bed Reactor Experiments

The reactivities of different pellet formulations were determined in a thin, fixed-bed reactor operating under near differential conditions. In these experiments, about 2 g of each sorbent was placed in a compartmented tray situated inside a quartz reactor. At 550°C, a simulated gas stream representative of Texaco oxygen-blown gasifier product containing 2000 ppm HCl was passed through the reactor at a rate of 5 SLM. The analysis of the chloride content of the pellets after exposure for 0.5, 8, 24, and 32 h (Table 4) indicated that the pellets made with 5 wt% sodium silicate binder (L-10) had the highest capacity for HCl uptake. The observed fractional chloride content of 0.61 corresponds to nearly 100% conversion of the sodium compounds in the pellets to NaCl. Decreasing the sodium silicate content from 5 to 2 wt% did not change the reactivity initially, but the ultimate chloride capacity decreased. No significant change in the HCl reactivity was observed between the pellets prepared with bentonite as a binder.

Table 2. Sorbent Preparation Paramters of Nahcolite Pellets

Pellet	Fabrication Date	Binder	Size of pellets
L-07	February 94	10% Bentonite+ methocel	3 mm extrudate
L-08	February 94	10% bentonite + methocel	1.5 mm extrudate
L-11	February 94	10% bentonite	3 mm extrudate
L-09	February 94	2% Sodium silicate + methocel	3 mm extrudate
L-10	February 94	5% Sodium silicate + methocel	3 mm extrudate
S-01	November 85	10% bentonite	4 mm extrudate

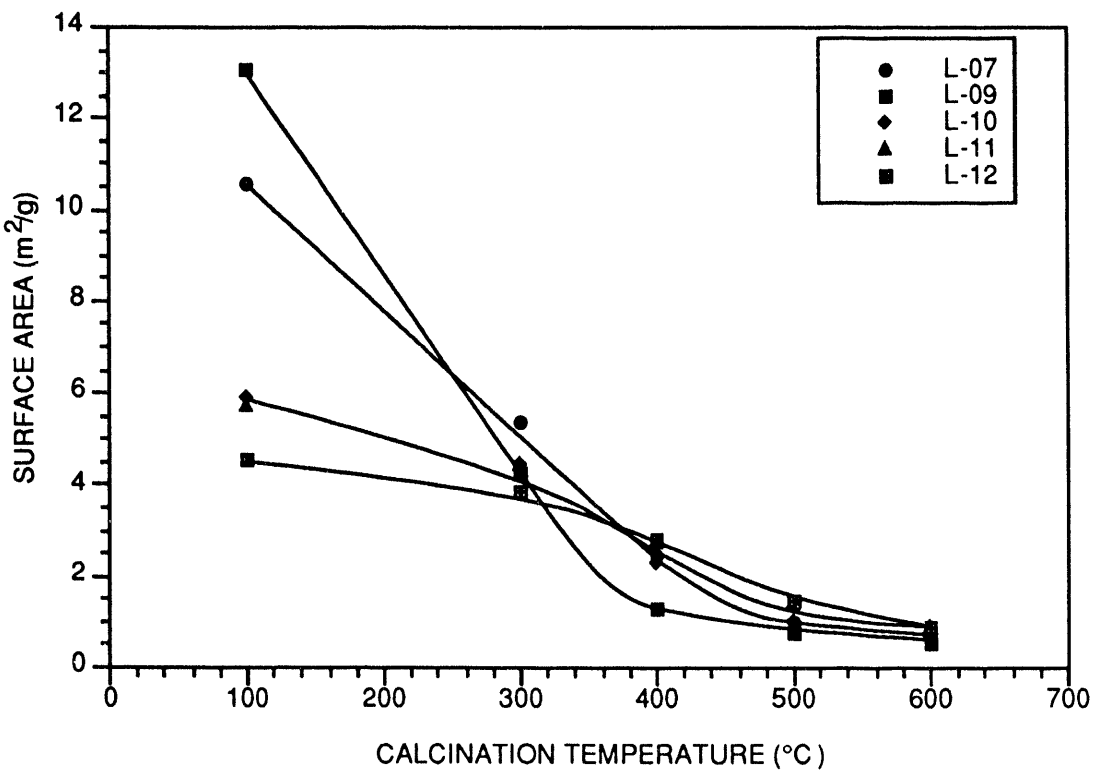

Figure 1. The Change in Surface Areas of Nahcolite Pellets as a Function of Calcination Temperature

Table 3. Physical Properties of Pelletized Sorbents

Parameter	L-10 Calcined	L-10 Spent*	L-07 Calcined	L-07 Spent*
Surface area (m^2/g)	1.0	0.4	1.0	1.8
Bulk density (g/cm^3)	1.1	1.3	1.0	1.2
Pore volume (cm^3/g)	0.29	0.30	0.52	0.27
Average Pore Dia. (μm)	1.0	0.24	0.56	0.36
Porosity (%)	54.9	38.2	54.0	33.4

* Exposed to 1500 ppm HCl at 550°C for 24 h.

Table 4. Chloride Uptake by Nahcolite Pellets as a Function of Exposure to 1500 ppm HCl Vapor at 550°C

	Chloride Content (wt% of the Pellets)				
Time (h)	L-07	L-08	L-11	L-09	L-10
0.5	1.40	1.10	0.00	1.00	0.92
8	15.00	12.00	14.00	22.00	23.00
24	29.00	17.00	39.00	29.00	44.00
32	32.00	40.00	34.00	37.00	61.00

Similar experiments were also carried out at a bed temperature of 450°C (Table 5). At this temperature, the pellets prepared with 5 wt% sodium silicate binder (L-10) had the highest chloride capacity followed by the pellets containing 10 wt% bentonite binder (L-07) with methocel added during preparation. However, the variations in reactivity and chloride capacity between the tested pellets were minor.

The crush strength of the nahcolite pellets did not change significantly after chloride uptake. The initial pellets had a strength of 661 kg/m. After exposure at 550°C for 36 h to an HCl containing gas stream in a deep bed, the pellets which had a chloride content of 25 wt% had a crush strength of 1475 kg/m and those that had 1 wt% had a strength of 830 kg/m. Thus, chloride uptake does not degrade the mechanical strength of the pellets.

Table 5. Chloride Uptake by Nahcolite Pellets as a Function of Exposure to 1500 ppm HCl Vapor at 450°C

	Chloride Content (wt% of the Pellets)				
Time (h)	L-07	S-01	L-11	L-09	L-10
1	1.48	0.30	4.39	5.31	1.79
8	5.90	8.24	9.92	10.1	7.60
24	18.9	–	32.5	26.9	37.0
32	51.1	46.4	45.6	44.8	63.6

Integral, fixed-bed reactor experiments were also conducted with L-10 pellets at 500°C. A deep bed of sorbent pellets (5-cm diameter by 15-cm long) was exposed to a simulated coal gas stream containing 1750 ppm of HCl at a space velocity of 3500 h^{-1}. The HCl level in the reactor exit remained at less than 1 ppm for a period of a 8 h (Figure 2). It required about 11 h to reach the breakthrough level of 10 ppm. When the HCl concentration reached 30 ppm, the experiment was stopped and the spent sorbent was removed from the bed in successive layers (about 1 cm deep) that were analyzed for chloride. The results (Figure 3) showed that the upstream end of the bed was nearly saturated with the chloride whereas the downstream end contained less than 2 wt%. A preliminary analysis of the data using a model for first-order reaction in an integral reactor, resulted in a rate constant of 4 ± 1 mole $HCl \cdot g^{-1}$ sorbent$\cdot h^{-1}$, a value similar to the one obtained in an earlier program at SRI (Krishnan et al., 1986).

Fluidized-Bed Reactor Experiments

Fluidized-bed, bench-scale reactor (2.6-cm ID) experiments were conducted at Research Triangle Institute with nahcolite powder and granules. Nahcolite powder (N-01) in the size range 90 to 300 μm was tested at 550°C in a simulated gas stream representative of Texaco oxygen-blown gasifier product containing 1750 ppm HCl. Experiments were also conducted with a nahcolite sorbent (N-23) granulated (90 to 300 μm in size) with 10 wt% bentonite as a binder. The physical properties of the fresh, calcined, and spent sorbents are shown in Tables 6 and 7.

These experiments also show that the granulated and powder sorbents can reduce the level of HCl vapor in hot coal gas to less than 1 ppm (Figure 4). The HCl breakthrough time at 1 ppm level was about 30 minutes at a space velocity of 4500 h^{-1} ($U/U_{mf} = 5$), but dramatically increased to 720 minutes when the space velocity was decreased to 3000 h^{-1} ($U/U_{mf} = 3.2$). It is believed that at the higher space velocity, the contact between the gas and the sorbent was poor due to the slugging of the bed. Because elutriation of granulated sorbent particles (N-23) occurred at a space velocity of 4500 h^{-1}, experiments were conducted only at a space velocity of 3000 h^{-1}. The granulated sorbent at the decreased gas flow rate was very effective and the 1-ppm breakthrough time was nearly 33 h. The chloride capacity of the granulated sorbent at 10-ppm breakthrough level was 27 wt% whereas only half that value was observed with the non-granulated sorbent (Table 8).

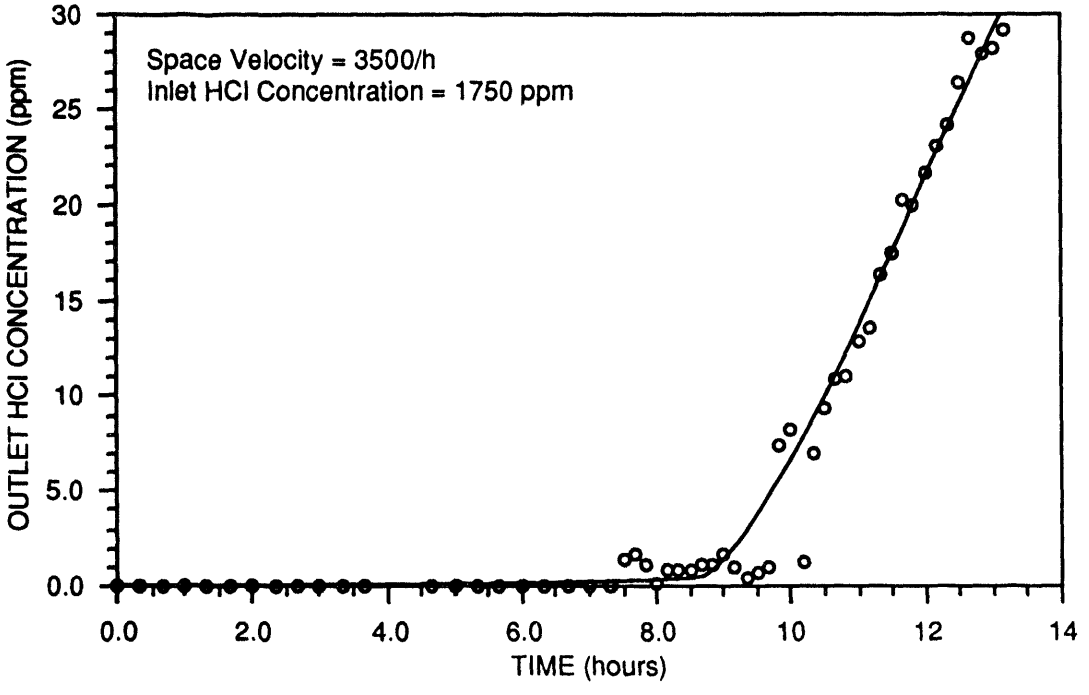

Figure 2. The HCl-Breakthrough Curve for L-10 Pellets in a Fixed-Bed Reactor at 500°C

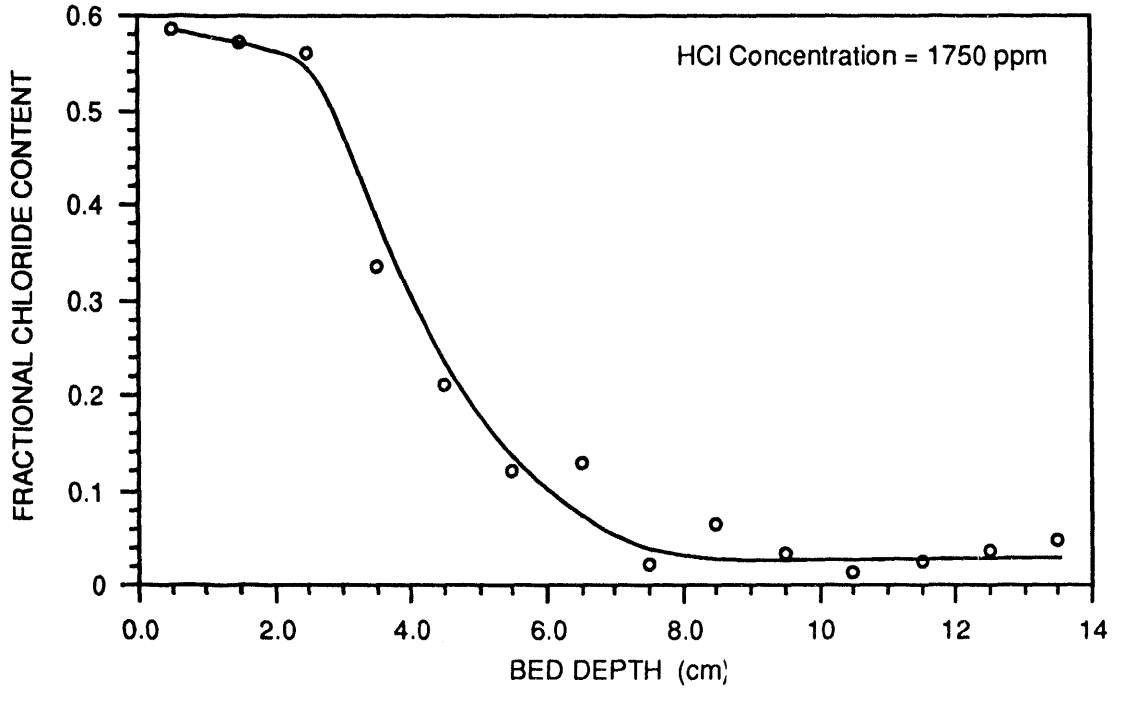

Figure 3. Distribution of Chloride in the Sorbent as a Function of Bed Depth

Table 6. Physical Properties of Granulated Nahcolite Sorbent (N-23)

Parameter	Fresh	Calcined	Spent
Surface area (m^2/g)	7.8	0.7	1.4
Bulk density (g/cm^3)	0.77	0.84	0.77
Pore volume (cm^3/g)	0.25	0.24	0.32
Median Pore Dia (μm)	0.41	1.6	1.8
Porosity (%)	36.5	36.5	39.4

Table 7. Physical Properties of Non-Granulated Nahcolite Sorbent (N-01)

Parameter	Fresh	Calcined	Spent
Surface area (m^2/g)	8.7	<0.5	<0.5
Bulk density (g/cm^3)	1.1	1.1	1.1
Pore volume (cm^3/g)	0.03	0.04	0.06
Median Pore Dia (μm)	2.9	2.0	1.9
Porosity (%)	7.2	8.2	11.5

Table 8. Results of Fluidized-Bed Experiments with Nahcolite Powder and Granules

Parameter	N-01 Sorbent at SV = 4500 h^{-1}	N-01 Sorbent at SV = 3000 h^{-1}	N-23 Sorbent at SV = 3000 h^{-1}
1-ppm breakthrough time (min)	30	720	1960
10-ppm breakthrough time (min)	40	900	2110
Chloride Capacity (wt%) at 1-ppm	0.6	9.8	25.2
Chloride Capacity (wt%) at 10-ppm	0.8	12.3	27.1

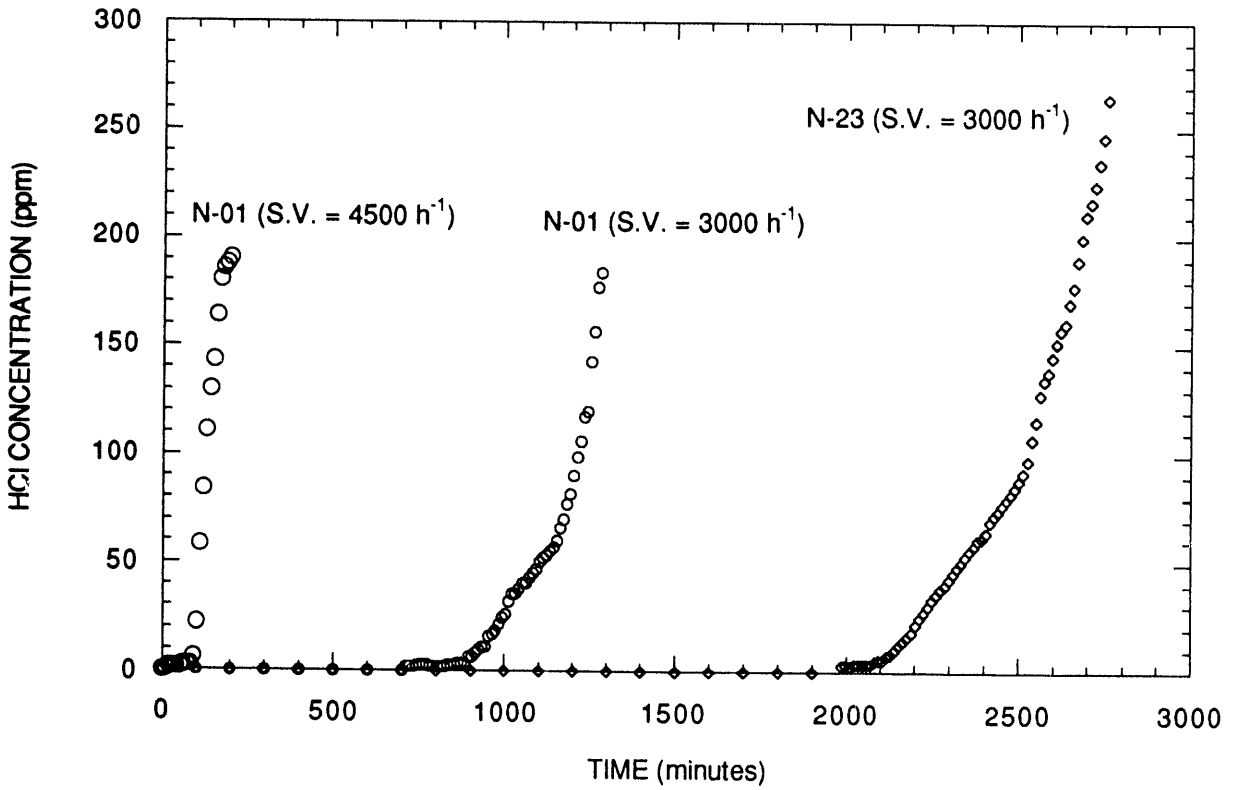

Figure 4. The HCl breakthrough curve for N-01 and N-23 sorbents in a fluidized-bed reactor at 550°C

The nahcolite sorbent particles in the size range of 45 to 90 μm were also tested for their chloride reactivity and capacity under conditions approaching an entrained-bed reactor. A gas mixture of 2.1% HCl in nitrogen was passed through the bed at a superficial gas velocity of at about 3 cm/s, slightly below the elutriation velocity of 5 cm/s for 45 μm particles. In this test, the 1 ppm HCl breakthrough time was nearly 36 h as shown in Figure 5. The experiment was continued until the HCl level reached 600 ppm. The chloride analysis of the sorbent at the end of the experiment indicated that the chloride level was 54.0 wt% at the upstream end and 37.3 wt% at the downstream end.

The above test was repeated with a simulated Texaco coal gas containing 2000 ppm HCl vapor. Under these conditions, the 1-ppm breakthrough time was nearly 435 h resulting in a chloride capacity of 51.6 wt%.

The fixed- and fluidized-bed experiments have established the following:

- The HCl vapor level was reduced consistently from about 1750 ppm to less than 1 ppm at 550°C indicating high reactivity of the sorbent for reaction with HCl.
- Chloride loading levels as high as 60 wt% were observed in the spent sorbent pellets. These results confirm the high chloride capacity of the sorbent.
- No significant loss in the crush strength was observed in pellets of spent sorbent.

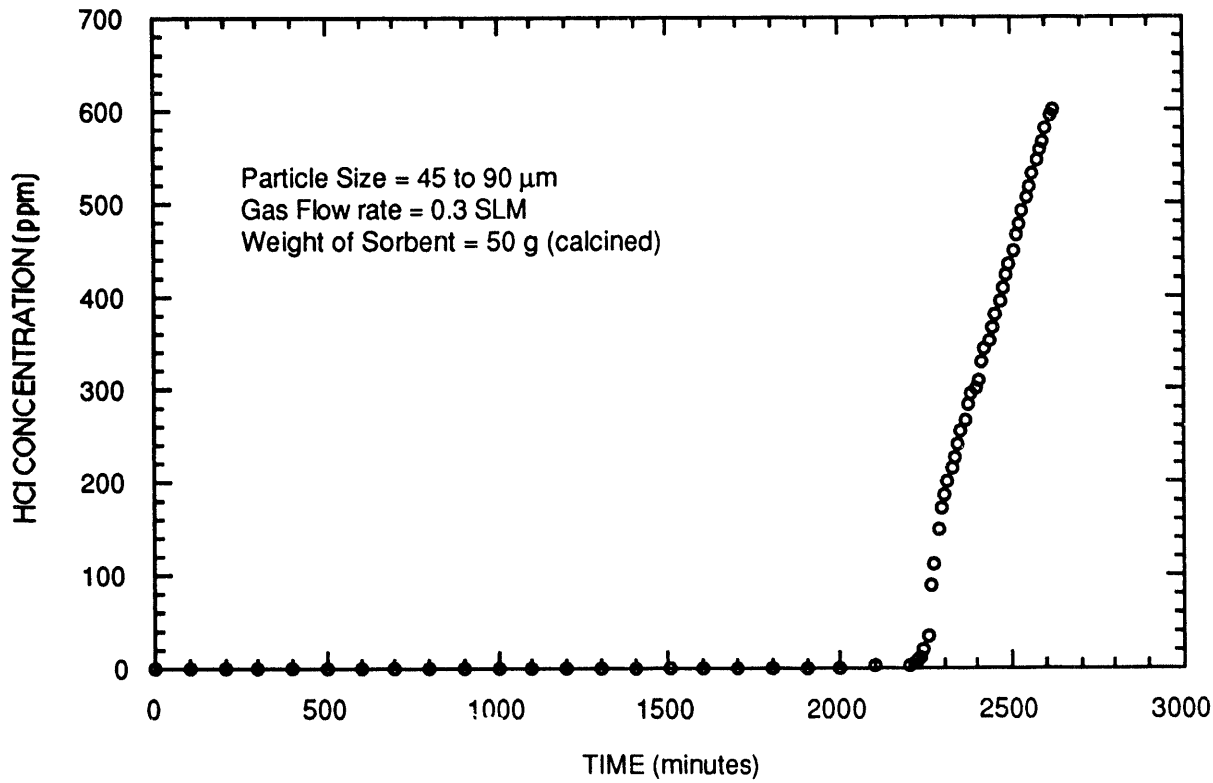

Figure 5. Removal of HCl Vapor by Non-Granulated Nahcolite at 550°C

FUTURE WORK

We will experimentally determine the suitability of other minerals such as trona and a few commercial sorbents. Additional experiments will be conducted with three suitable formulations in fixed- and fluidize-bed reactors at temperatures below 450°C and above 650°C using simulated coal-derived gas streams. Sorbent pellets suitable for moving-bed reactors will be prepared by GE-CRD and tested. A test plan will be submitted for parametric testing of one superior formulation.

Parametric tests (Task 5) will also be conducted with one superior sorbent identified in Task 4 for each type of reactor. The tests will be conducted at a minimum of three points within the ranges of interest of these critical parameters: space velocity (2,000 to 5,000 h^{-1}), temperature (480° to 750°C), and pressure (1 to 20 atm).

The experimental data will be analyzed to determine the effectiveness of the various sorbent formulations for removal of hydrogen chloride vapor in fixed-, moving-, and fluidized-bed reactors. A preliminary economic assessment is planned to determine the suitability of the sorbents for removing HCl vapor from hot coal-derived gas streams on an industrial scale.

REFERENCES

Bakker, W.T., and R.A. Perkins (1991). "The Effect of Coal Bound Chlorine on Corrosion of Coal Gasification Plant." In *Proceedings of International Conference on Chlorine in Coal*, J. Stringer and D.D. Banerjee, Eds., Elsevier.

Gillis, E. A. (1980). "Fuel Cells for Electric Utilities," Chem. Eng. Prog., **76**(10), 88.

Ham, D., A. Gelb, G. Lord, and G. Simmons (1984). "Hot-Gas Chloride Cleanup for Molten Carbonate Fuel Cells." Report No. DOE/MC/16242-1554, Morgantown Energy Technology Center, U.S. Department of Energy, Morgantown, WV.

K. Kinoshita, F. R. McLarnon and E. J. Cairns (1988). *Fuel Cells: A Handbook*, Report No. DOE/METC-88/6096, Morgantown Energy Technology Center, U.S. Department of Energy, Morgantown, WV.

Krishnan, G.N., G.T. Tong, B.J. Wood, and N. Korens (1986). "High-Temperature Coal-Gas Chloride Cleanup for MCFC Applications." Report No. DOE/MC/21167-2080, Morgantown Energy Technology Center, U.S. Department of Energy, Morgantown, WV.

Lyke, S.E., L.J. Sealock, Jr., and G. L. Roberts (1985). "Development of a Hot Gas Cleanup System for Integrated Coal Gasification/ Molten Carbonate Fuel Cell Power Plants," Report No. DOE/MC/19077-1830, Morgan-town Energy Technology Center, U.S. Department of Energy, Morgantown, WV.

Perkins, R.A., D.L. Marsh, and P.R. Clark (1990). "Corrosion in Syngas Coolers of Entrained Slagging Gasifiers." Report No. EPRI GS-6971, Electric Power Research Institute, Palo Alto, CA.

TRW (1981). "Monitoring Contaminants in Coal Derived Gas for Molten Carbonate Fuel Cells," Final Report to Argonne National Laboratory under contract No. 31-109-38-6108.

P20 PyGas Design Support

Lawrence J. Shadle, Abolghasem Shamsi,
Guo-Qing Zhang, and Edward J. Boyle
Morgantown Energy Technology Center

Yau-Hsin Wang, Madhava Syamlal, and Kalkunte Seshadri
EG&G Technical Services of West Virginia

ABSTRACT

METC is currently supporting CRS Sirrine Engineers Inc. in their development of a PyGas™ process as part of METC's implementation of the Gasification Product Facility (GPIF) project. Key issues in the gasifier have been identified and will be considered for each of the four principal sections in the gasifier: 1) the centrally located fluid bed pyrolyzer tube, 2) the top combustion and tar cracking zone, 3) the down flow co-current annular section, and 4) the counter-current fixed bed gasification zone.

The key design issues for the pyrolyzer include the desired fluidization, required conversion, size distribution of the product, the solids thru-put and residence time, and sufficient mixing in the jet to accomplish decaking of the coal. Char products from Foster Wheeler's carbonizer tests have been analyzed to evaluate the product size distribution and fluidization regime. This is compared with other fluidized bed pyrolyzers and gasifiers. A criteria for stabilizing the combustion zone and decaking the coal within the pyrolyzer jet is presented conceptually. In light of these concepts the flow patterns calculated using the MFIX code are interpreted. In addition, the characteristic times required for heating, devolatilization, and tar cracking were estimated and compared to the available residence timed to evaluate the potential for completing these processes in the pyrolyzer. Using a simple lumped analysis of this reactor some preliminary estimates for conversion in this reactor are discussed and unknowns identified.

The design issues in the top zone above the pyrolyzer include the mixing of air and steam with effluent from the pyrolyzer to achieve temperature control primarily for tar cracking. The extent of reaction of small char particles with air in this region depends on mixing and kinetics. This was evaluated using the Fluent code. Sensitivity studies were conducted assuming equilibrium predominates in this region. The results lead to the conclusion that increasing the temperature in this region has an adverse impact on gas quality.

The design issues in the co-flow section of the gasifier include the height of the bed, the rate of tar cracking and coal gasification which influence the pressure drops and exit gas temperatures. Preliminary cold flow tests suggest that small particle sizes, high gas velocities, and any compaction or tar deposition in the co-flow bed may lead to blowing out and losing the bed. These analyses have lead to the concept of flaring the inner shroud so that the cross-sectional area is larger at the exit thereby reducing gas velocities and forces leading to high

pressure drops. Tests on cracking of coal tars have been conducted using a laboratory fluid bed to evaluate the impact of char and dolomite on the rates of tar cracking. The co-flow bed was found to contribute in only a rather small portion of the total coal conversion when sensitivity studies were conducted using the MGAS code. But this impact and the final gasifier exit temperature will depend on the gasification reactivity of the char. Preliminary thermal gravimetric analysis (TGA) was used to evaluate the char reactivity and compare the observed expressions with those used for the simulations.

The counter-current fixed bed design is also based on the rate of char gasification, but the design approach assumes conservative expressions based on coke breeze and adjusted downward to account for the reduction in through-put in a conventional fixed beds when adding fines to the feed. With such fine feed materials as used in the PyGas™ fixed bed the thru-put is constrained by the gas velocity which will cause channeling or incipient fluidization. While cold flow modeling may help to define these operational limits, calculations of minimum fluidization velocity and gas flow rate as a function of conversion were used to define the useful operating regime. Gas velocities were determined from the sensitivity studies using MGAS by optimizing the air and steam to provide the highest quality gas while maintaining a peak temperature below 1260 C (2300 F) and keeping the residual carbon content in the ash below 5%.

P21 Chloride and Mercury Monitors for Air Toxics Measurements

CONTRACT INFORMATION

Contract Number	W-7405-Eng-82 (Ames) 93MC30024.000 (METC)
Contractor	Ames Laboratory Iowa State University Ames, Iowa 50011
Contractor Project Manager	William H. Buttermore
Principal Investigators	Glenn A. Norton Colin D. Chriswell
Contributing Authors	Dave E. Eckels Rachel E. Peters
METC Project Manager	Margaret A. Kotzalas
Period of Performance	October 1, 1993 - continuing
Schedule and Milestones	

FY94 Program Schedule

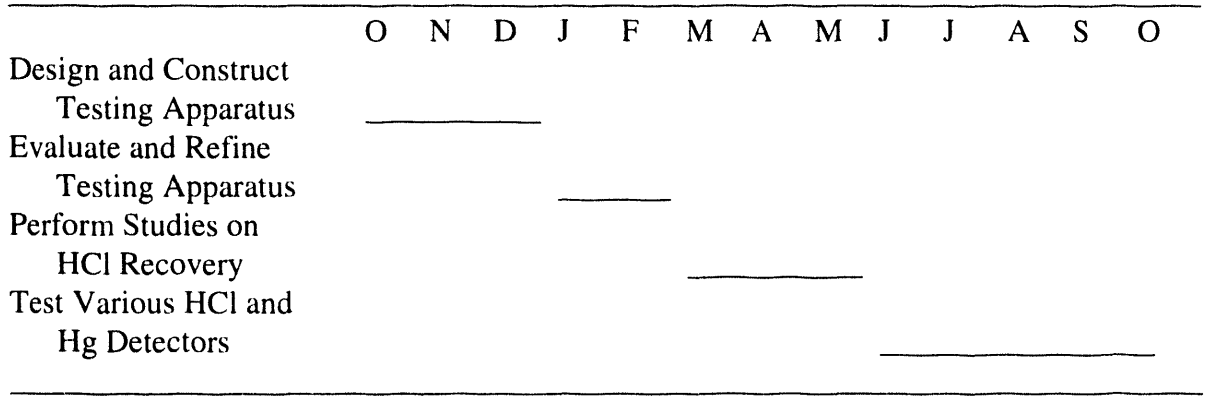

OBJECTIVES

Ames Laboratory will develop an integrated sampling and analysis system suitable for on-line monitoring of hydrogen chloride (HCl) and mercury (Hg) in advanced coal-based gasifiers. The objectives of this project are to 1) summarize current technology for monitoring HCl and Hg in gaseous effluents, 2) identify analytical techniques for such determinations in high-temperature, high-pressure gases from coal-based systems of interest to METC for producing electrical power, 3) evaluate promising analytical approaches, and 4) produce reliable on-line monitors which are adaptable to plant-scale diagnostics and process control.

BACKGROUND INFORMATION

The capability to continuously monitor and effectively control critical effluents must be developed in order to implement new clean coal technologies. Although HCl and Hg concentrations in hot, high-pressure gases from power producing systems are of environmental and technological concern, instruments suitable for determining HCl and Hg in those environments have not yet been sufficiently developed and tested. On-line analysis is more complex for such systems than for more conventional coal-based power producing systems because of the high temperatures (up to 500^{o}C) and pressures (up to 300 psi) involved. In addition, the different gas compositions involved can pose special analytical problems. Concentrations of HCl are anticipated to be in the range of 50 - 500 ppm in the raw gas and less than 1 ppm after the flue gas is treated (1-3). Concentrations of Hg are anticipated to be in the range of 0.2 - 20 ppb in the raw gas.

PROJECT DESCRIPTION

In previous work (4), commercially available instrumentation suitable for the monitoring applications of interest was reviewed and evaluated. Also, pertinent literature was assessed to obtain additional information on analytical methodologies which could potentially be used. Based on the results of that work and our continuing review of available instruments, analytical approaches which appear to have the most potential for our monitoring applications were identified.

For HCl, the techniques currently being considered are infrared absorption, colorimetry, and ion mobility spectroscopy. For Hg, atomic absorption and atomic fluorescence techniques have been selected for testing in the laboratory.

Subsequent laboratory work will determine which analytical systems show the most promise for on-line analysis of HCl and Hg. Promising analytical instruments (or components of instruments) will be assembled and/or modified for application to monitoring hot pressurized gases from coal gasifiers. Additional work will involve developing suitable gas conditioning and sample introduction systems. That work may be as important as the development of the analytical systems themselves. After the laboratory studies have been completed, prototype instruments will be tested and evaluated in the field.

RESULTS

Testing Apparatus

A laboratory apparatus was designed and constructed to blend, heat, and deliver gases to simulate gasifier streams. That apparatus will be used to study sample delivery and to evaluate various detectors. The basic design consists of a Teflon gas mixer for blending metered gases, a

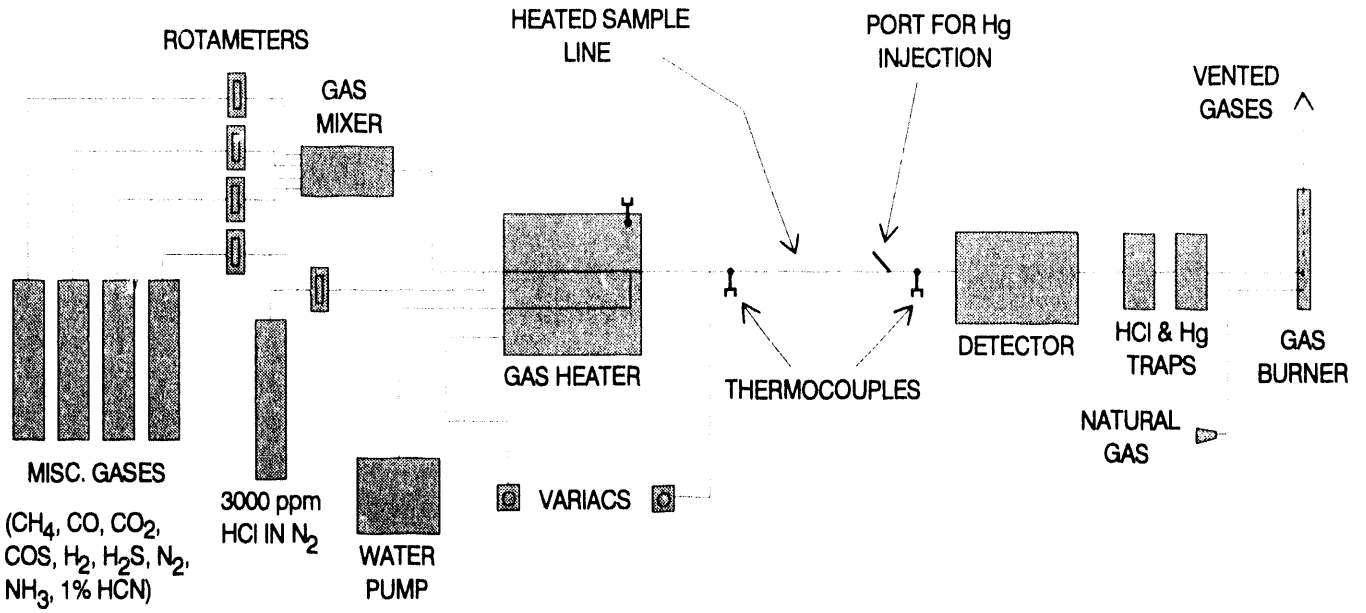

Figure 1. Testing Apparatus for Evaluating HCl and Hg Analyzers

gas heating system, a steam generator, toxic gas traps (to be used after the detector), and a gas burner for burning flammable gases and destroying toxic gases not collected by the traps. The tubing from the HCl gas cylinder is made of Teflon, while all the other gas lines are made of stainless steel. A schematic diagram of the current testing apparatus is shown in Figure 1.

After assessing the overall operation of the initial system, modifications or alternate approaches in the steam generation, gas heating, and gas burner components were made. Some of those changes included replacing a gas chromatography oven with a hot sand bath to heat the gases. The blended gases are heated by passing them into a stainless steel coil immersed in the sand bath. To achieve a gas temperature of about 200°C, the sand bath is maintained at 300-400°C. In addition, an external steam generation vessel was replaced with a pump from a liquid chromatograph (LC). The LC pump provides a precise, adjustable water flow in the proper range to give the desired moisture content in the sample gas mixtures. The water is pumped into a separate stainless steel coil in the hot sand bath. The water is vaporized in the steam coil and is introduced into the sample gas stream just before the sample gases exit the sand bath.

HCl Studies

Preliminary studies were initiated to determine whether a known amount of HCl can be reliably delivered to a detector. Initial tests involved recovering HCl directly from a cylinder containing a HCl gas mixture (3000 ppm_v in nitrogen). Recoveries were determined by bubbling the gas into an absorbing solution and then titrating the solution to determine the amount of chloride collected. Erratic results and low recoveries were obtained at relatively low gas flows (e.g., 10 cm^3/min), even when using Teflon lines directly from the gas cylinder. The erratic results do not appear to be caused by

analytical errors, problems in collection efficiency, gas metering errors, or losses in the Teflon line. Rather, there appears to be erratic adsorption/desorption processes occurring upstream from the regulator outlet, despite the precautions taken to select a regulator with nonreactive components. Good precision for HCl recoveries was obtained by increasing the gas flow rates to 100 cm^3/min or more.

Subsequent tests involved passing the HCl gas mixture through the entire testing apparatus. Those tests were performed both with heated (180-200°C) and unheated gases. In the former case, tests were also performed with and without about 50% water present in the gas stream. A total of about 25 tests were performed using HCl/N_2 gas flows of 100-550 cm^3/min. Overall, HCl recoveries averaged 86 ± 5%. The best precision and recoveries were observed for the tests where water vapor was present, in which case the HCl recovery averaged 92 ± 3%.

An alternate approach for delivering known amounts of HCl was investigated. In that approach, a dilute aqueous hydrochloric acid solution is pumped at a known rate into a stainless steel coil in a hot sand bath. The hot coil vaporizes the HCl and water, which are then introduced to the primary gas stream in a heated sample line. By varying the water flow rate and the HCl concentration in the water, it should be possible to obtain both the desired moisture and HCl gas concentrations in the delivered gases. Good recoveries and precision were obtained in some cases. However, pumping problems were encountered when attempting to use the low flows necessary to attain both the desired H_2O and HCl concentrations at the total gas flow rate (about 1 liter/min) being tested. Efforts in this area have been discontinued since the HCl gas mixture appears to be working satisfactorily.

We have begun contacting various companies in an attempt to borrow the detectors of interest. These include one colorimetric detector and two different gas filter correlation IR units. In addition, we are now performing our final screening of Fourier transform IR detectors and ion mobility spectrometers. One or two detectors from each of the latter analytical approaches will also be selected for study.

Hg Studies

In preparation for later tests involving Hg determinations, some preliminary studies were performed to study potential problems in analyzing Hg using conventional instruments and standard procedures. One potential calibration technique is to inject Hg vapors (using gas-tight syringes) into the sample gas stream. The validity of using that approach was experimentally confirmed.

Studies were also performed using liquid Hg standards. Minor procedural variations were found to significantly affect the amount of Hg detected in those standards. In particular, when and how the standards are acidified during preparation were found to be important variables. By carefully controlling those and other variables, full recoveries of 100-ng quantities of Hg in liquid standards can now be consistently obtained. That work will be important when verifying the operation of a Hg permeation tube calibration system which will be used to compare different Hg detectors.

A final review of potential instruments for use in an on-line monitor was made. Measurements based on resistance changes in a gold film originally appeared promising. However, after continued discussions with company representatives, it became evident that the gold film approach is probably not a method of choice at this time. This is largely due to the costs and logistics associated with the frequent off-line calibrations which would be required for continuous analyses of gas streams. Consequently, that approach is no longer being

considered for on-line monitoring of coal gasifier streams.

Two atomic absorption detectors and one atomic fluorescence detector have been selected for study in our laboratories. Contacts with the pertinent companies have been initiated in an attempt to acquire the detectors of interest as short-term cost-free loans. Brief acquisitions of those instruments will allow us to make valid, direct instrument comparisons. This will in turn help us select the best instrument for use in an on-line Hg analyzer.

FUTURE WORK

Studies on the delivery of known amounts of HCl from our testing apparatus will continue. In this regard, the effects of gas temperature, gas stream composition, and flow rate on HCl recovery will be studied in more detail. HCl recovery will be examined while the entire testing apparatus is in operation and while all of the gases selected to simulate coal gasifier streams are flowing through the system. After those tests, our laboratory evaluation of selected HCl detectors will begin.

For Hg, a permeation tube calibration system and manual injections of Hg vapor (using gas-tight syringes) will be used to evaluate various detectors. Testing will be performed both with and without the use of gold amalgamation for collecting and concentrating Hg prior to analysis. A double gold amalgamation approach may also be integrated into the analytical system and tested as a possible approach for improving accuracy and precision.

For both HCl and Hg, subsequent testing will include determining the effects of gas temperature, pressure, and composition (including moisture content) on detection limits, dynamic range, precision, and accuracy. The effects of sample line composition will also be studied. Modifications of existing instruments will be made, as needed, for application to gasifier streams.

The severity of interferences from compounds such as H_2S, CH_4, HF, and H_2O on HCl and Hg determinations will be investigated. In addition, suitable sample handling systems will be developed. Gas conditioning steps which may be required include temperature and pressure adjustments, filtering particulate matter, and removing moisture and interfering gases. The amount and type of gas conditioning will be largely dependent on the analytical methodology employed. Ultimately, prototype analytical systems which appear to be acceptable based on results of laboratory studies will be integrated with the gas handling system and then tested in the field.

ACKNOWLEDGEMENTS

This work was performed with funds provided by the U.S. Department of Energy through the Morgantown Energy Technology Center. Ames Laboratory is operated for the U.S. D.O.E. by Iowa State University under Contract No. W-7405-Eng-82.

REFERENCES

1. G. N. Krishnan, G. T. Tong, B. J. Wood, and N. Korens, "High Temperature Coal Gas Chloride Cleanup for Molten Carbonate Fuel Cell Applications," Final Report, DOE/MC/21167-2080 (DE87001041), November 1986, pp. 57-60.

2. G. L. Anderson, F. O. Berry, B. D. Harmon, R. M. Laurens, and R. Biljetina, "Development of a Hot Gas Cleanup System for Integrated Coal Gasification/Molten

Carbonate Fuel Cell Power Plants," Final Report, DOE/MC/19403-1816 (DE86001589), October 1985, p. A-4.

3. T. Grindley and T. H. Gardner, "Trace Contaminants in Fixed-Bed Gasifier Gas," in Proc. Twelfth Annual Gasification and Gas Stream Cleanup Systems Contractors Review Meeting, Volume II, DOE/METC-92/6128, Vol. 2 (DE93000229), September 1992, pp. 479-497.

4. G. A. Norton, C. D. Chriswell, D. E. Eckels, and W. H. Buttermore, "On-Line Monitoring of Mercury and Hydrogen Chloride in Hot Gases from Coal Gasifiers," in Proc. Coal-Fired Power Systems 93 -- Advances in IGCC and PFBC Review Meeting, DOE/METC-93/6131 (DE93000289), June 1993, pp. 276-283.

P22 Cooperative Research and Development Agreements at METC

J. Christopher Ludlow, Lisa A. Jarr, and William F. Lawson
Morgantown Energy Technology Center

ABSTRACT

With the passage of the Federal Technology Transfer Act of 1986, the Morgantown Energy Technology Center (METC) was empowered and encouraged to enter into joint research and development projects that would transfer fossil energy technologies into the private sector. Potential partners for these joint projects, formalized by a Cooperative Research and Development Agreement (CRADA), include private industry, educational institutions, and other research organizations. Development of CRADA with METC is a simple process. In a CRADA, both the Government and the participating partner(s) may contribute personnel, equipment, or facilities to the project but no funds may be supplied by the Government to the other party. Also facilitating working with the Government is the fact that METC's Director is able to negotiate directly with the partners on intellectual property issues including the exclusive licensing of METC inventions, protection of proprietary data, and allocation of patent rights developed under the agreement.

P23

Optimal Design and Synthesis of Advanced Power Systems under Uncertainty

Urmila M. Diwekar & Edward S. Rubin
Carnegie Mellon University
Pittsburgh, PA 15213

H. Christopher Frey
North Carolina State University
Raleigh, NC 27695

Abstract

Technical and economic uncertainties are not rigorously treated or characterized in most preliminary cost and performance estimates of advanced power system designs. Nor do current design methods rigorously address the issues of design under uncertainty. However, process costs and other important quality measures, such as controllability, safety, and environmental compliance, largely depend on the process synthesis stage. This conceptual design stage involves identifying the basic flowsheet structures from a typically large number of alternatives. This paper describes the status of on-going research at Carnegie Mellon University to develop and demonstrate advanced computer-based methods for dealing with uncertainties that are critical to the design of advanced coal-based power systems. Preliminary results are presented illustrating the use of these new modeling tools for the environmental control design of an advanced integrated gasification combined cycle (IGCC) system using hot gas cleanup. Additional applications to pressurized fluidized bed combustion (PFBC) and externally-fired combined cycle (EFCC) systems are in progress.

1 Introduction

Increasing environmental awareness and regulations have placed new requirements on process design for advanced power systems, and increased the need for sophisticated simulation and design tools for examining pollution prevention options. The conventional process models now in use are largely based on a deterministic framework used for simulation rather than process synthesis. An important shortcoming of these models is the ability to analyze uncertainties more rigorously. Such capability is especially important in the context of advanced energy systems, since available performance data typically are scant, accurate predictive models do not exist, and many technical as well as economic parameters are not well established.

Though design under uncertainty has received considerable attention in the chemical engineering literature during the past few years a generalized framework for analyzing uncertainty systematically has only recently been developed around a chemical process simulator (Diwekar and Rubin, 1991). This capability has been used successfully for the evaluation of different configurations of integrated gasification combined cycle (IGCC) systems, which represent a clean and efficient use of coal for electric power generation. In previous work we have applied probabilistic methods to evaluate the performance, cost, and emissions from IGCC systems, compare alternative systems with uncertainty, and the benefits from targeted R & D (Frey and Rubin 1992a, 1992b; Frey, et al., 1994).

In the present project, we enhance this framework through development of a generalized capabil-

ity to deal with process synthesis and optimization as well as with stochastic optimization and stochastic programming problems. Sequential-modular simulators like ASPEN and PRO/II have grown in sophistication over the years and are widely used in the chemical industries to solve complex problems with rigorous process modeling. Therefore, it is desirable to build the new process synthesis and stochastic optimization capability around such simulators. Such capabilities have been built around the public version of ASPEN simulator developed for DOE (MIT, 1982). First we describe the methodological basis for the new modeling capabilities. Then we present an illustrative case study of their application to power systems design.

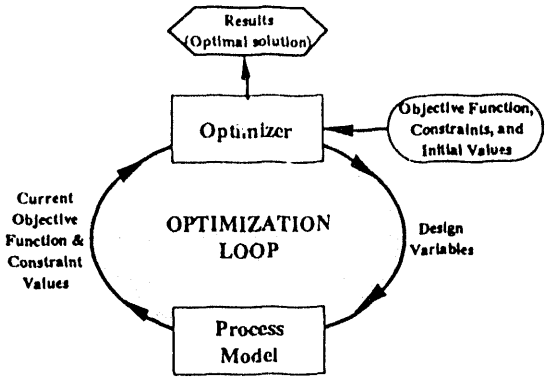

Figure 1: Pictorial Representation of the Optimization Framework

2 Methodology for Stochastic Optimization and Optimal Design under Uncertainty

The various problems reported in the literature on stochastic optimization/programming, and chemical process design under uncertainty are divided into two categories: 1) stochastic optimization, and 2) stochastic programming. The "here and now" problems involving expected value minimization, the chance constrained optimization problem, and the design for optimal flexibility problem all require that at each optimization iteration some probabilistic representation of the objective function and constraints is optimized. These problems are classified as stochastic optimization problems. On the other hand, the "wait and see," "flexibility index," and multiperiod optimization problems involve solution of a deterministic optimization problem for each scenario so that one gets a probabilistic representation of optimal solutions. These type of problems are considered under the category of stochastic programming, namely the effects of uncertainties on optimal design. This new division makes it easier to generalize the use of the new modeling capability for different kinds of optimization problems under uncertainty, and to design a uniform framework for solving large-scale problems.

2.1 The Optimizer

The goal of an optimization problem is to determine the decision variables x that maximize some aspect of the deterministic model represented by the objective function Z, while ensuring that the model operates within established limits enforced by the equality constraints h and inequality constraints g. A generalized statement of this problem is given by the following equation.

$$\underset{x}{\text{Optimize}} \quad Z = z(x) \tag{1}$$

subject to

$$h(x) = 0 \tag{2}$$

$$g(x) \leq 0 \tag{3}$$

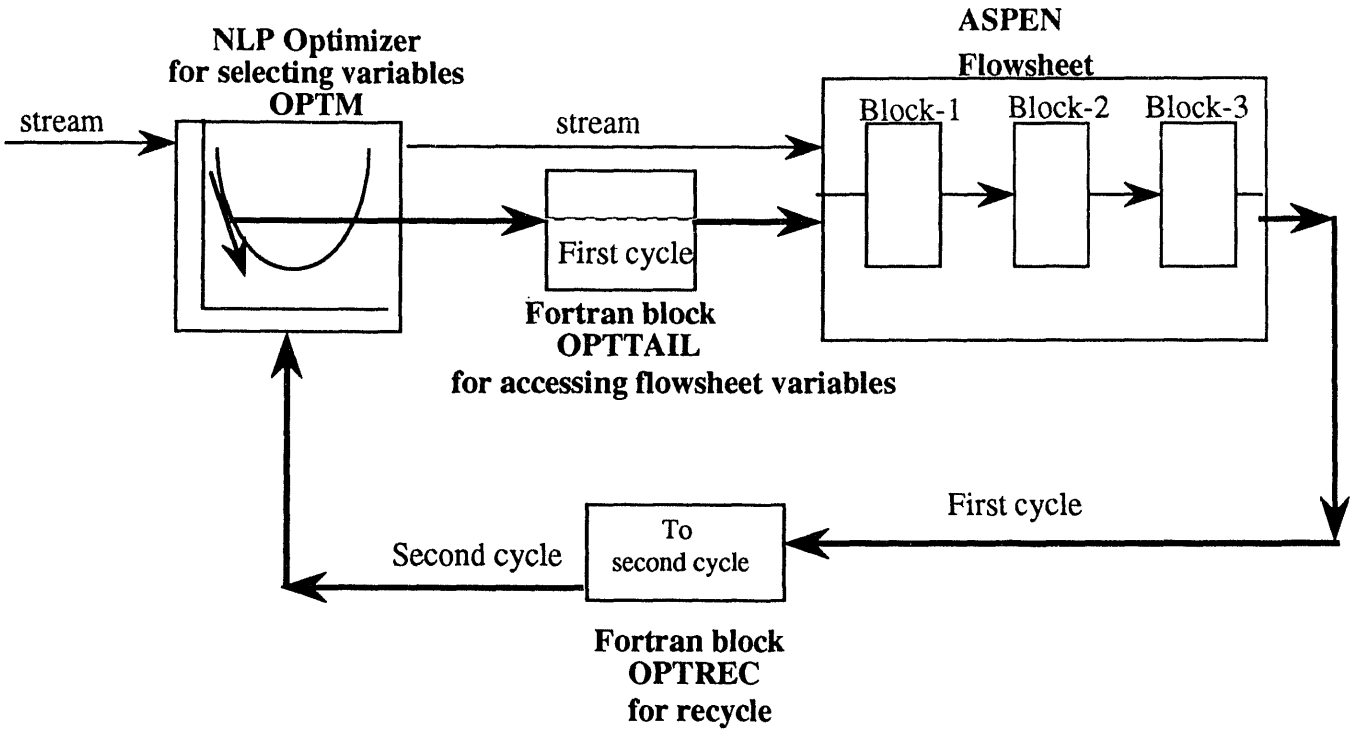

Figure 2: Basic Operation of the ASPEN Optimizer

where x is a decision variable vector. The above formulation represents the deterministic optimization problem, for which a generalized iterative solution procedure is illustrated schematically in Figure 1 and the ASPEN implementation in Figure 2. As seen in the figure, the optimizer invokes the model with a set of values of decision variables x. The model simulates the phenomena and calculates the objective function and constraints. This information is utilized by the optimizer to calculate a new set of decision variables. This iterative sequence is continued until the optimization criteria pertaining to the optimization algorithm are satisfied. In this case the model which is used is deterministic in nature.

The optimizer block, OPTM, in Figure 2 has been implemented in ASPEN as a unit operation block. The OPTM block is a flowsheet optimization block which solves the nonlinear optimization problem (NLP) described above.

Recent advances in constrained nonlinear optimization techniques provide better choices for solving large scale flowsheet problems. The most popular of these methods are generalized reduced gradient (GRG) and successive quadratic programming (SQP), and their variants. Among generalized reduced gradient methods, the most widely used algorithms are GRG2 and MINOS (Gill et al., 1981). Most literature on large scale optimization favors the SQP method because the GRG2 algorithm requires convergence of equality constraints at each iteration. Furthermore, historically the GRG strategy has been considered to be the less efficient mode of optimization (Biegler, 1983). Hence the GRG2 algorithm is not well suited for the large scale optimization problems we are proposing to address. On the other hand, MINOS does not require convergence of equality constraints, and is best suited for optimization problems with linear constraints.

SQP is the most widely used technique for large scale nonlinear optimization for chemical processes, which typically involve highly nonlinear models. In SQP, at each iteration the problem is approximated

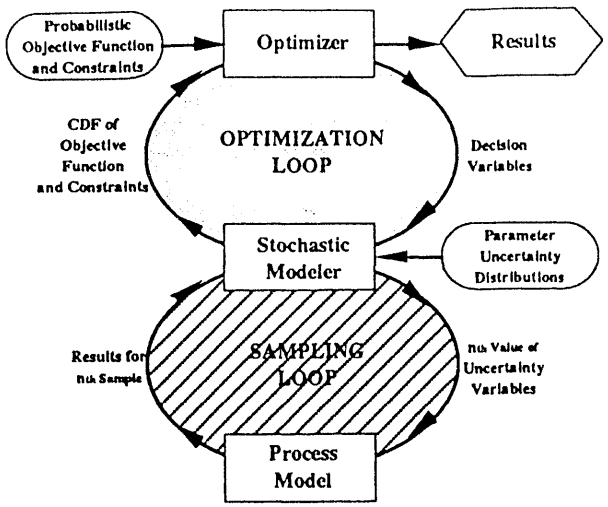

Figure 3: Pictorial Representation of the Stochastic Optimization Framework

as a quadratic program where the objective function is quadratic and the constraints are linear. Similar to linear programming, the special features of a quadratic objective function are exploited to solve the problem more efficiently. The quadratic programming subproblem is solved for each step to obtain the next trial point. This cycle is repeated until the optimum is reached.

In Figure 2, the NLP optimization block, OPTM, generates decision variable sets using the SQP method (Biegler and Cuthrell, 1985). This set is passed to the flowsheet using a Fortran OPTTAIL block. After the simulation run, the values of the objective function and constraints are calculated using the OPTREC block and passed to the OPTM block. The iterations stop when the best improvement to the process for the defined objective function and constraints is found. The modular nature of both the stochastic and optimization blocks allow one to solve different stochastic optimization and stochastic programming problems encountered in practice. The following subsection describes this functionality.

2.2 Stochastic Optimization

In many cases, including advanced energy conversion technologies, the model builder cannot ignore the uncertainties associated with some of the model input parameters. An uncertainty analysis thus becomes essential. As uncertainty is a broad concept, it is possible—and often useful—to approach it in several different ways. One rather general approach, which has been described earlier and successfully applied to a wide variety of problems, is to assign a probability distribution to the various uncertain or variable parameters (Diwekar and Rubin, 1991).

The generalized stochastic optimization problem, where the decision variables and uncertain parameters are separable, can then be viewed as:

$$\underset{x}{\text{Optimize}} \quad P1(Z) = P1(z(x,u)) \tag{4}$$

subject to

$$P2(h(x,u)) = 0 \tag{5}$$

$$P3(g(x,u) \leq 0 \tag{6}$$

where u is the vector of uncertain parameters and the P represents the probabilistic functional which for an expected value minimization reduces to:

$$E(F(u)) = \int_0^1 F(u)dp(u). \tag{7}$$

This function can be calculated by sampling the function and calculating the expected value of the samples.

$$E(F(u)) = \frac{\sum_1^{N_{samp}} F(u)}{N_{samp}} \tag{8}$$

On the other hand, in the case of chance constrained optimization the constraints are represented

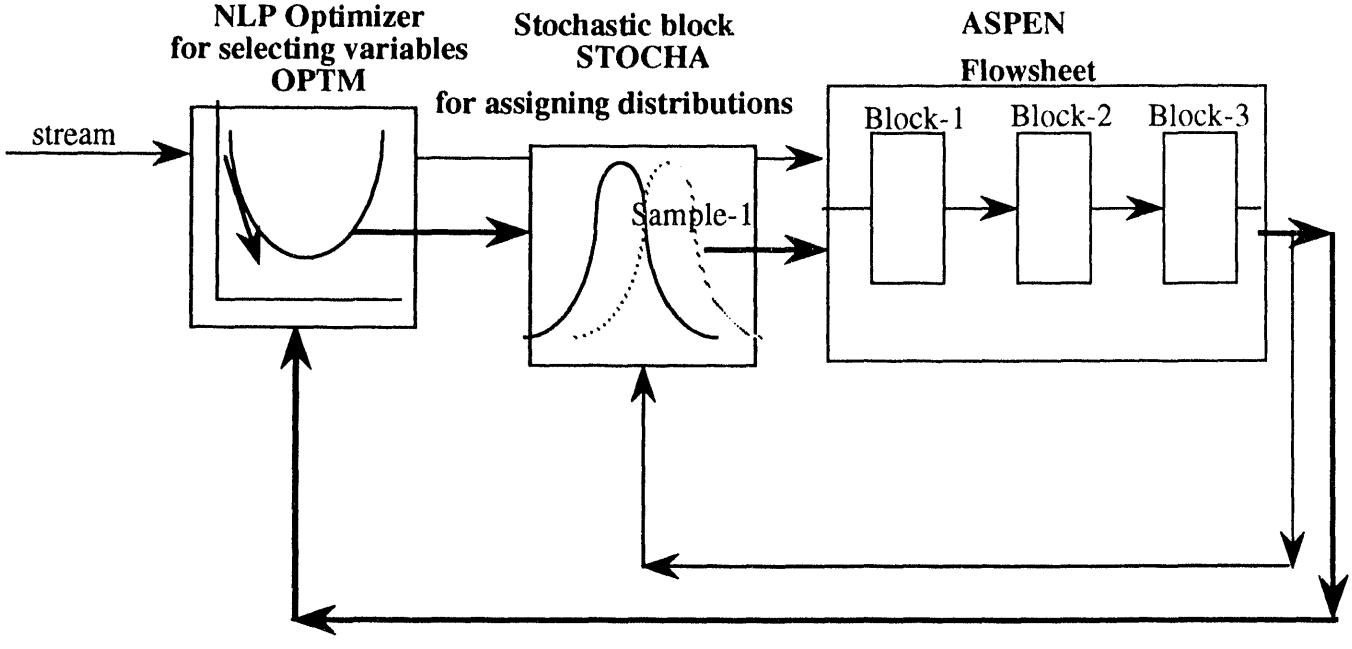

Figure 4: Schematic of the Stochastic Optimization Framework in ASPEN

in terms of a probability of exceeding certain value and is represented by:

$$\underset{x}{\text{Optimize}} \quad P1(z(x,u)) = E(F(u)) \qquad (9)$$

subject to

$$P(h(x,u) > \beta) \leq P_c \qquad (10)$$

where Equation 10 is the chance constraint.

It is apparent from the above discussion that unlike the deterministic optimization problem, in stochastic optimization one has to consider the probabilistic functional of the objective function and constraints. The generalized treatment of such problems is to use probabilistic or stochastic models instead of the deterministic model inside the optimization loop.

Figure 3 represents the generalized stochastic optimization problem solution procedure where the deterministic model in Figure 3 is replaced by an iterative stochastic model. Figure 4 illustrates the ASPEN implementation.

This stochastic optimization capability can also be used to achieve off-line quality control. In off-line quality control, the sensitivity of the design to the sources of variation is reduced at the design stage to make the controller design easier. One such approach based on the concept of Taguchi's parameter design method has been illustrated using the above-mentioned stochastic optimization capability (Diwekar and Rubin, 1994). This approach involves minimizing the variance of the objective function instead of the expected value.

2.3 Effect of Uncertainties on Optimal Design

In contrast to the stochastic optimization problems, which involve expected value minimization, and the chance constrained problems, the "wait and see,"

and multiperiod optimization problems are categorized as stochastic programming problems. The "wait and see" problem involves deterministic decisions at each random stage or random sample, which is the same as solving multiple deterministic optimization problems, and can be represented as:

$$\underset{x}{\text{Optimize}} \quad Z = z(x, u*)) \tag{11}$$

subject to

$$h(x, u*) = 0 \tag{12}$$

$$g(x, u*) \leq 0 \tag{13}$$

where $u*$ is the vector of values of uncertain variables corresponding to some sample. This optimization procedure is repeated for each sample of uncertain variables u and a probabilistic representation of outcome is obtained. Figure 5 represents the generalized solution procedure where the deterministic problem shown in Figure 3 forms the inner loop, whereas the stochastic sampling forms the outer loop. This procedure is implemented in the ASPEN simulator as shown in Figure 6. From the ASPEN representation, it is clear that by just interchanging the position of stochastic block, STOCHA, and the optimization block, OPTM, one can solve almost all the problems in the stochastic optimization/programming literature.

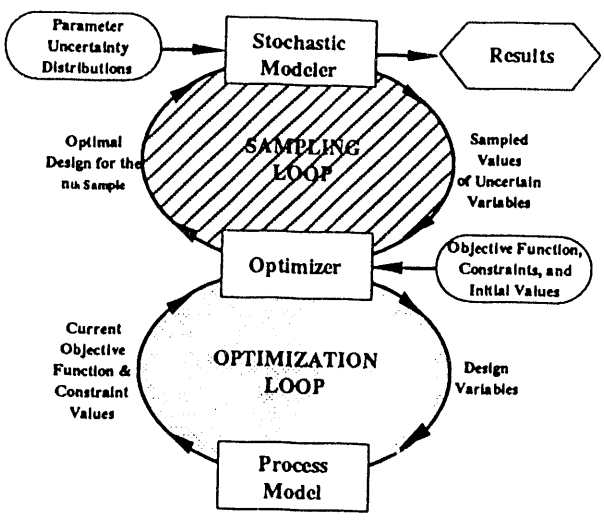

Figure 5: Pictorial Representation of the Stochastic Programming Framework

3 Methodology for the New Process Synthesis Capability

The alternatives for process design and environmental control often are numerous and involve a very large search space. Selection of the best alternatives can offer the potential for significantly reducing costs and/or improving performance. Therefore, there is a strong need for "systems" research to identify the best ways of configuring advanced energy systems. The current state of process synthesis techniques involves: (a) the heuristic approach which

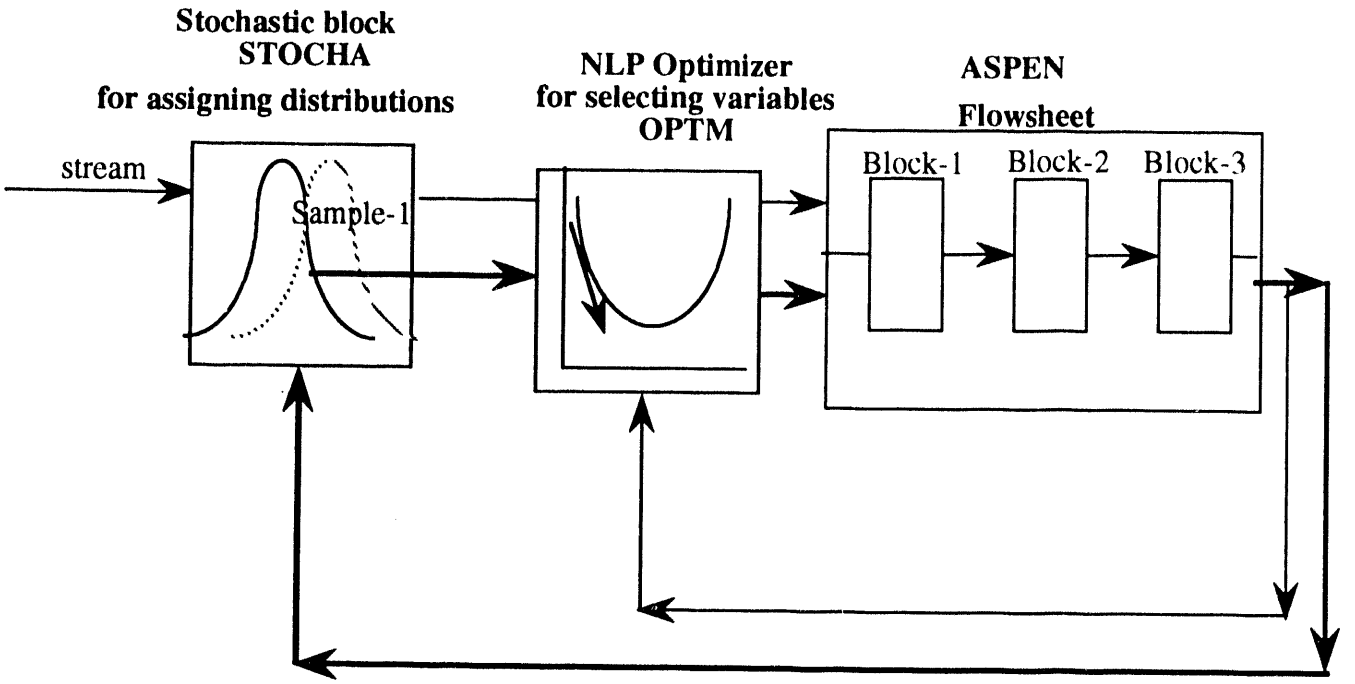

Figure 6: Schematic of the Stochastic Programming Framework in ASPEN

relies on intuition and engineering knowledge, (b) the physical insight approach which is based on exploiting basic physical principles, and (c) the optimization approach which uses the mathematical programming techniques. This section deals with a newly developed process synthesizer built around the public version of ASPEN, using the mathematical programming approach (Diwekar et al., 1991).

3.1 The Mathematical Programming Approach

The mathematical programming approach to process synthesis involves:

(a) Formulation of a flowsheet superstructure incorporating all the alternative process configurations.

(b) Modeling the superstructure as a mixed integer nonlinear programming (MINLP) problem of the form

MINLP:

$$Z = \min_{\overline{x}, \overline{v}, \overline{y}} \quad c^T\overline{y} + f(\overline{x}, \overline{v}) \tag{14}$$

subject to

$$\begin{aligned} h(\overline{x}, \overline{v}) &= 0 \\ h1(\overline{x}, \overline{v}) &= v - z(\overline{x}) = 0 \\ B^T\overline{y} + g(\overline{x}, \overline{v}) &\leq 0 \\ y \in Y;\ x &\in X \end{aligned} \tag{15}$$

where

$$Y = [y|Ay \leq a,\ y[0,1]^m]$$

$$X = [x|x^L \leq x\ le\ x^U]$$

The continuous variables x represent flows, operating conditions, and design variables. The variables v are the output variables which are

related to the input variables x by model equations. For equation oriented environments, these model equations are embedded in the equality constraints $h1(\bar{x}, \bar{v})$. The binary variables y denote the potential existence of process units.

(c) Identification of both the optimal configuration and operating process parameters by an algorithm based on alternating sequence of nonlinear programs (NLPs) and mixed integer linear programs (MILPs).

3.2 The ASPEN MINLP Process Synthesizer

The MINLP process synthesis capability in the public version of ASPEN is based on ZOOM (Marsten, 1986), the mixed integer linear programming (MILP) solver, and on SCOPT (Lang and Biegler, 1987), the nonlinear programming (NLP) solver. The method is based on an algorithm called GBD/OA/ER/AP presented by Diwekar et. al (1992) which involves solution of alternate sequence of MILP and NLP problem solving. The overall structure of the environment is shown in Figure 7. Optimization of the MINLP process synthesis problem is decomposed into continuous optimization of NLP problems at fixed choice of binary variables, and discrete optimization through the MILP master problem. The MILP solver (Master) and NLP optimizer have been implemented in ASPEN as unit operation blocks and can be executed easily with the ASPEN process unit blocks.

The process synthesis environment in ASPEN consists of the Master block, the NLP optimizer, and the entire superstructure. The initialization of the continuous and binary variables is done in the ASPEN input file. At this stage the scheme is translated into an initial flowsheet and subsystems using the decomposition strategy of Kravanja and Grossmann (1990). NLP optimization of the selected flowsheets is the first step in the inner loop, which results in the objective function and linearization information.

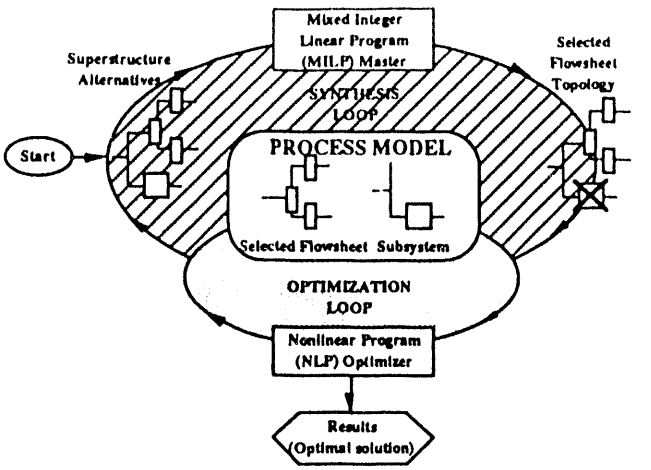

Figure 7: Schematic of the New ASPEN MINLP Synthesizer

This information is passed to the Master block which internally modifies the master problem to include the linearization information. The solution of the master problem results in a new flowsheet structure. The iteration stops when there is no improvement in the objective function value.

3.3 The Implicit Constraint Problem

The implementation of this new capability in a sequential modular simulator poses challenging problems which are not encountered in equation-oriented simulators; therefore, new strategies are necessary to solve these problems. One such problem associated with the MINLP sequential modular process synthesizer is that of *implicit constraints*.

The problem of implicit constraints is encountered because of the black box nature of the models in sequential modular simulators. The ASPEN MINLP environment is based on a two-level op-

timization algorithm consisting of an upper level MILP master problem and a lower level NLP problem. The MILP master problem predicts new binary variables, while the NLP problem provides new continuous variables. The MILP master problem represents the linearized NLP problem with non-fixed binary variables, since at each stage the MILP master problem obtains the linearization information from the NLP optimizer. Unlike equation oriented simulators, in sequential modular simulators most of the nonlinear constraints are not represented explicitly by equations. The linearization information on these constraints, which are essentially black box relations embedded in the simulator environment ($h1(\bar{x},\bar{v})$ in equation 2), therefore must be passed to the master problem.

In order to circumvent this problem of implicit constraints new decision variables are created. These are equated to the output variables from the flowsheet configurations. This procedure ensures that the original MINLP problem remains the same, while at each stage the MILP master problem receives increased information from the NLP optimizer. Although this procedure assures complete information transfer to the master problem, it also increases the computational load on the NLP optimizer, which is generally the rate-determining step in the MINLP process synthesis. Recently Diwekar and Rubin (1993) presented a partitioning strategy which reduces the computational load on the NLP problem crucial for the solution of large-scale synthesis problems.

4 Illustrative Examples of New Modeling Capabilities

The new capabilities for process synthesis and optimization under uncertainty provide powerful new tools for the design and analysis of advanced energy systems. An application of the new synthesis capability already has been described in a recent paper (Diwekar, et al., 1992), which focuses on choosing a least-cost approach to sulfur removal for an IGCC system with hot gas cleanup and a fluidized bed gasifier. In this paper we show new results that illustrate use of the stochastic optimization and stochastic programming capabilities for the design of a different IGCC system.

To illustrate these new capabilities, an air-blown dry ash Lurgi gasifier IGCC system flowsheet with a plant size of 650 MW and a high-sulfur Illinois No. 6 coal is analyzed. A schematic of this technology is shown in Figure 8. The hot gas cleanup system features high temperature (1100 degrees F) sulfur removal from the fuel gas with a zinc ferrite sorbent, and high efficiency cyclones and ceramic filters for particulate removal. Details of the performance and cost models are reported elsewhere (Frey and Rubin 1992a).

Two key design variables for the fixed bed zinc ferrite process are the sulfur absorption cycle time and the reactor vessel length-to-diameter ratio. The sulfur absorption cycle time is constrained to be at least as great as the time required to regenerate a bed of sulfated sorbent and return it to active service after a regeneration cycle. As the sulfur absorption time becomes longer, more sorbent is required to capture the syngas sulfur species over the increased time period. Larger absorption cycle times therefore require either larger reactor vessels and/or more reactor vessels. The length-to-diameter ratio of the reactor vessel also affects process economics.

Another key area of uncertainty for this technology is the NO_x emission rate. Thermal NO_x emissions are expected to be quite low for IGCC systems due to the low heating value of the fuel gas and the presence of thermal diluents such as H_2O, CO_2, and N_2 (Holt et al., 1989). However, the hot gas cleanup system employed by the air-blown Lurgi system does not remove fuel-bound nitrogen (in the form of ammonia) from the fuel gas, and a substantial portion of the ammonia is converted to NO_x upon combustion. Thus, NO_x emissions pose a critical concern for systems with hot gas cleanup. For example, using conventional com-

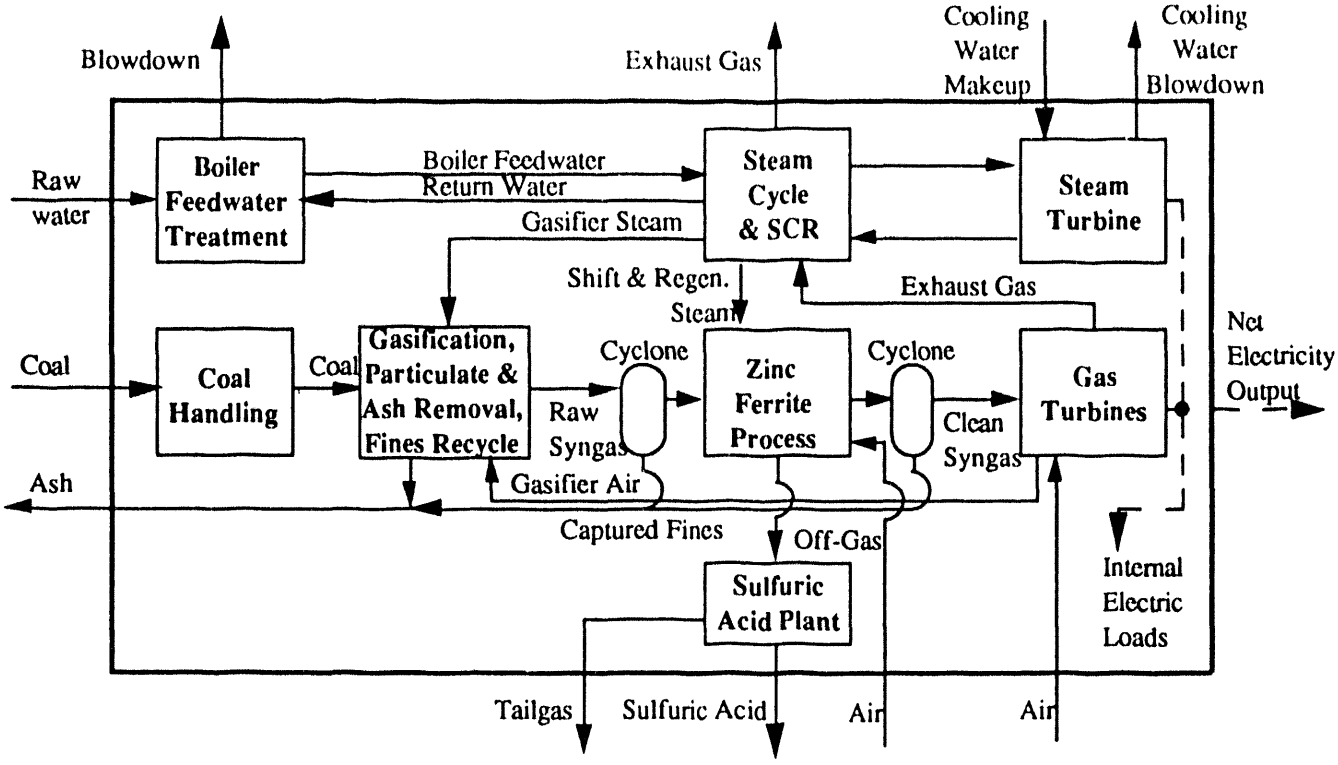

Figure 8: Schematic of the Lurgi Air-blown Dry Ash Gasifier IGCC System

bustors the DOE/METC performance model yields NO_x emissions nearly four times greater than federal New Source Performance Standards (NSPS) for coal-fired power plants.

To mitigate NO_x emissions, several approaches are possible. In the near term, the most likely approach is the use of post-combustion exhaust gas NO_x reduction technology. In the longer term, advanced staged combustion designs, featuring rich/lean combustion, may be commercialized and employed for fuels with high nitrogen content. In this study, we consider the use of selective catalytic reduction (SCR) for NO_x control. In a SCR system, ammonia is injected into the flue gas upstream of a catalytic reactor through a set of nozzles comprising an injection grid. Because of the temperature window required for typical SCR catalysts, the SCR reactor employed with gas-turbine combined cycle system are typically located in the heat recovery steam generator (HRSG). We employ a new performance and cost model of an SCR system (Frey, 1993) to explore the effects of two key design variables: the required NO_x removal efficiency, which has a substantial impact on the catalyst volume requirement, and the catalyst layer replacement interval, which can be varied to achieve trade-offs between initial capital cost and annual replacement costs for catalyst.

Key performance and cost parameters of the engineering models for the IGCC system were assigned probability distributions based on data analysis, literature review, and the elicitation of expert judgments.

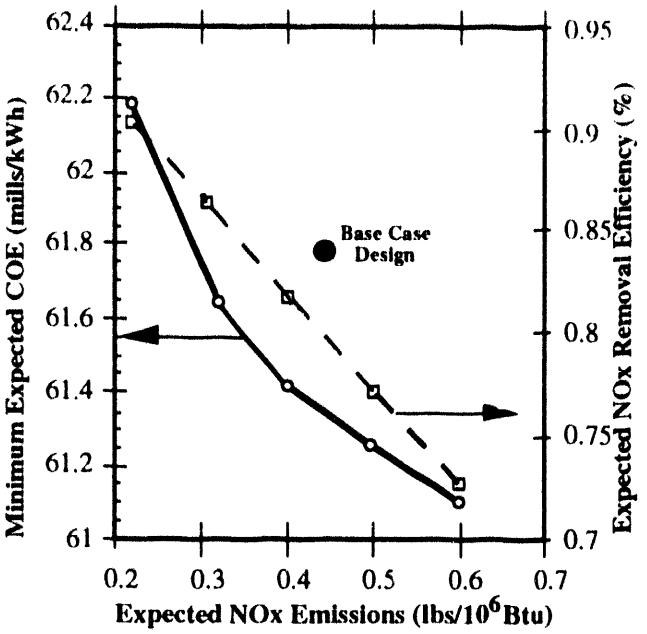

Figure 9: Minimization of Expected Cost of Electricity Subject to Expected Value of NOx Emission Constraints.

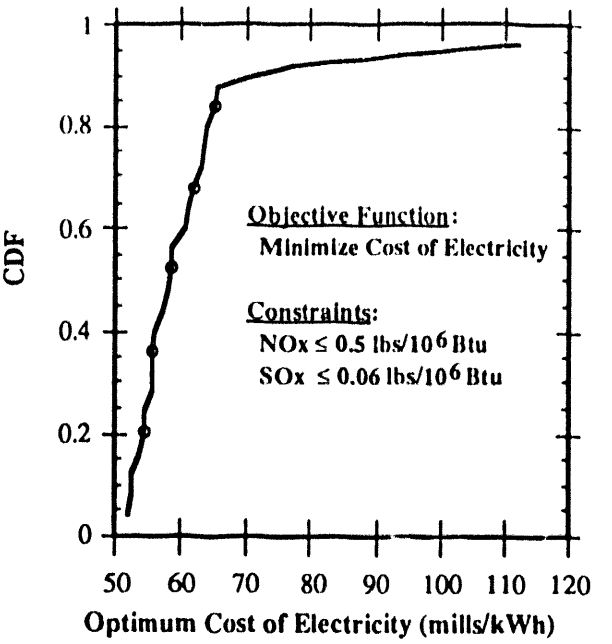

Figure 10: Effect of Uncertainties on Minimum Cost.

The characterization of performance uncertainties focused on four major process areas: gasification, zinc ferrite desulfurization, gas turbine, and SCR. Uncertainties in additional cost model parameters also were characterized, including direct and indirect capital costs, operating and maintenance costs, financial assumptions, and unit costs of consumables, byproducts, and wastes. Through an interactive screening process, the initial set of approximately 50 uncertain variables was narrowed to a set of 20 which most significantly affected uncertainty in plant efficiency, emissions, capital cost, and total levelized cost. These input uncertainty assumptions are given in Table 1. A sample size of 25 was used to illustrate the new capabilities. Figures 9 to 11 show the results of different stochastic optimization and stochastic programming problems applied to the IGCC flowsheet.

Figure 9 shows results of a stochastic optimization problem in which the expected cost of electricity (COE) is minimized for different levels of NO_x control. As the expected value of NO_x emissions is decreased, the cost of the optimal design increases, as does the expected value of NO_x removal efficiency in the SCR unit. As seen in Figure 9, the optimal design reduces the expected COE by 0.5 mills/kWh relative to the base case design achieving 0.44 lbs $NO_x/10^6$ Btu. For the 650 MW plant modeled in this example, this is equivalent to a total savings of approximately $2 million per year in plant costs resulting from the selection of optimal design parameters in the zinc ferrite and SCR units. Figure 9 also shows that the expected cost of the optimal design increases by 1.1 mills/kWh as NO_x is lowered from 0.6 to 0.2 lbs/10^6 Btu. Over this range, the optimal SCR removal efficiency increases from 73% to 90% (the maximum value established by the performance model). This limits the lowest achievable NO_x emissions to 0.22 lbs/10^6 Btu (expected value).

Table 1: Summary of Deterministic and Uncertainty Assumptions for the Illustrative Case Study.

DESCRIPTION AND UNITS (a)	DET VAL (b)	DISTRIBUTIONS AND THEIR PARAMETERS (c)			
		Type	Min	Max	Mode or Prob.
Gasifier Fines Carryover, wt-% of Coal Feed	5.0	F	0.0	1.0	5%
			1.0	3.5	20%
			3.5	5.0	25%
			5.0	8.0	25%
			8.0	15.0	15%
			15.0	20.0	5%
			20.0	30.0	5%
Fines Capture in Recycle Cyclone, wt-% of Fines Carryover	95	F	50	90	25%
			90	95	25%
			95	97	25%
			97	98	25%
Carbon Retention in the Bottom Ash, wt-%	2.5	T	0.75	10.0	2.5
Gasifier Coal Throughout, lb DAF coal/(h-ft2)	305	T	1.52	381	305
Gasifier NH3 Yield, % of coal-N converted	0.9	T	0.5	1.0	0.9
GAsifier Air/Coal Ratio, lb air/lb DAF coal	3.1	T	2.7	3.4	3.1
Steam/Coal Ratio, lb steam/lb DAF coal					
air/coal = 2.7	0.81	U	0.54	1.08	
air/coal = 3.1	1.55	U	1.24	1.86	
air/coal = 3.4	2.38	U	2.04	2.72	
Zinc Ferrite Sorbent Sulfur Loading, wt-% sulfur in sorbent	17.0	N	2.16	31.84	17.0
Zinc Ferrite Sorbent Attrition Rate, wt-% sorbent loss per absorption cycle	1.0	F	0.17	0.34	5%
			0.34	0.50	20%
			0.50	1.10	25%
			1.10	1.50	25%
			1.50	5.00	20%
			5.00	25.00	5%
Fuel NOx, % conversion of NH3 to NOx	90	T	50	100	90
Gasifier Direct Cost Uncertainty, % of estimated direct capital cost	20	U	10	30	
Sulfuric Acid Direct Cost Uncertainty, % of estimated direct capital cost	10	U	0	20	
Gas Turbine Direct Cost Uncertainty, % of estimated direct capital cost	25	U	0	50	
SCR Unit Catalyst Cost, $/ft3	840	U	250	840	
Standard Error of HRSG Direct Cost Model, $ Million	0	N	-17.3	17.3	
Maiintenance Cost Factor, Gasification, % of process area total cost	3	T	2	12	3
Maintenance Cost Factor, Combined Cycle, % of process area total cost	2	T	1.5	6	2
Unit Cost of Zic Ferrite Sorbent, $/lb	3.00	T	0.75	5.00	3.00
Indirect Construction Cost Factor, %	20	T	15	25	20
Project Contingency Factor, %	17.5	U	10	25	

(a) DAF = dry, ash free; SCR = selective catalytic reduction; HRSG = heat recovery steam generator

(b) DET. VAL. = deterministic (point-estimate) value.

(c) The first column indicates the type of distribution, where F = fractile, T = triangular, N = normal, and U = uniform. The remaining columns provide the parameters of the distribution.

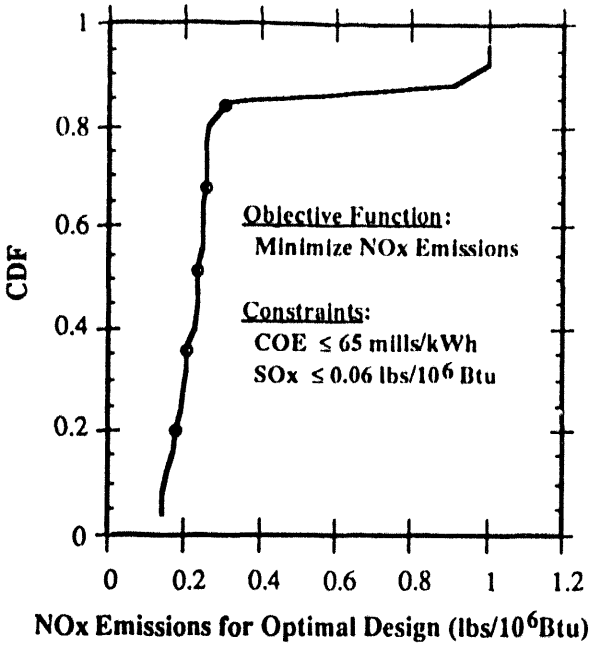

Figure 11: Effect of Uncertainties on Minimum NOx Emissions.

Figure 10 next shows the effect of uncertainties on the cost of an optimal design for the case of NO_x emissions constrained to 0.5 lbs/10^6 Btu or less, and SO_2 emissions to 0.06 lbs/10^6 Btu or less. The cost of electricity for the optimal design configuration varies by more than a factor of two due to the performance and cost uncertainties shown earlier in Table 1. An 80% confidence interval gives expected costs between 52.5 and 70.0 mills/kWh. Also there is a 5% probability of no feasible design able to meet the emission constraints with the assumed uncertainties.

Finally, Figure 11 shows an example in which NO_x emissions are minimized subject to a constraint on the maximum cost of electricity (in this case, 65 mills/kWh), representing an assumed upper bound on economic risk. The stochastic programming results for this case show a 50% probability of optimal designs achieving between 0.2 and 0.3 pounds $NO_x/10^6$ Btu. The mean value of the probabilistic results show a minimum NO_x emission rate of 0.32 lbs/10^6 Btu for this case. However, Figure 11 also shows a 15% chance of exceeding 0.6 lbs/10^6 Btu, which is the Federal New Source Performance Standard (NSPS) for coal-fired power plants. Thus, reducing process uncertainties or modifying process configuration to reduce the level of risk may be warranted.

These results are intended only to be illustrative of the new modeling capabilities now possible with stochastic optimization and stochastic programming. Additional case studies for other advanced power systems, including pressurized fluid bed combustion (PFBC) and externally fired combined cycle (EFCC) systems currently are in progress, and will be reported at a future date. In conjunction with these efforts, on-going work also is developing new or improved cost and performance models for selected process components and systems for IGCC, PFBC and EFCC designs.

5 Conclusions

This paper has presented new systems analysis tools and methodologies that can substantially improve the design and analysis of advanced coal-based energy systems of interest to DOE/METC. By combining existing process simulators with the mathematical methodologies presented here (i.e., probabilistic modeling, optimization, and MINLP synthesis) researchers and research managers now can tackle a wide range of system performance and cost analysis not heretofore possible. This new toolbox can be used in conjunction with new or existing process performance and cost models to insure that process design issues are more fully and rigorously considered in all phases of activity. These modeling tools also can be extended to a host of other technology applications where process design, cost minimization, risk analysis, environmental compliance, and R&D prioritization remain important issue.

6 References

Biegler L. T. (1983) Simultaneous Modular Simulation and Optimization, Proceeding of Second International Conference on Foundations of Computer Aided Process Design.

Biegler L.T. and J.E. Cuthrell (1985) Improved Infeasible Path Optimization for Sequential Modular Simulators, Part II, Computers and Chemical Engineering, 9:257-271.

Diwekar U. M., H. C. Frey, and E. S. Rubin (1992), Synthesizing optimal flowsheets: applications to IGCC system environmental control, *I&EC Res.*, **31**, 1927.

Diwekar U. M., I. E. Grossmann, and E. S. Rubin (1991), An MINLP process synthesizer for a sequential modular simulator, *I&EC Res.*, **31**, 313.

Diwekar U. M. and E. S. Rubin (1991), Stochastic Modeling of Chemical Processes, *Comput. chem. Engng.*, **15**, 105.

Diwekar U. M. and E. S. Rubin (1993), An Efficient Handling of the Implicit Constraints Problem in the ASPEN MINLP Process Synthesizer, *I&EC Res*, **32**, 2006.

Diwekar U. M. and E. S. Rubin (1994), Parameter Design Method using Stochastic Optimization with ASPEN, *I&EC Res*, **33**, 292.

Frey H. C. (1993), Performance Models of Selective Catalytic Reduction NO_x Control Systems, Quarterly report from Carnegie Mellon University to U.S. Department of Energy, Pittsburgh, PA 15213.

Frey H. C. and E. S. Rubin (1992a), Evaluation of Advanced Coal Gasification Combined-Cycle Systems under Uncertainty, *I&EC Res*, **31**, 1299.

Frey H. C. and E. S. Rubin (1992b), Integration of Coal Utilization and Environmental Control in Integrated Gasification Combined Cycle System, *Env. Sci. Tech.*, **26**, 1982.

Frey H. C., E. S. Rubin, and U. M. Diwekar (1994), Process Modeling of Advanced Technologies Under Uncertainty, *Energy*, **19 (4)**, 449.

Gill P.E., W. Murray, and M. H. Wright (1981), Practical Optimization, Academic Press, London.

Holt N. A., E. Clark, and A. Cohn (1989), NO_x Control in Coal Gasification Combined Cycle Systems, Symposium on Stationary Combustion Nitrogen Oxide Control Volume 1, GS-6453, Electric Power Research Institute, Palo Alto, CA, July 1989, 5A-17.

Kravanja Z. and I. E. Grossmann (1990), PROSYN-An MINLP synthesizer, *Comput. chem. Engng.*, **14**, 1363.

Lang Y. D. and L. T. Biegler (1987), A Unified Algorithm for Flowsheet Optimization, *Comput. chem. Engng.*, **11**, 143.

Marsten R. (1986), User's Manual for ZOOM/XMP, The Department of Management Information Systems, University of Arizona: Tucson.

Massachusetts Institute of Technology, ASPEN User's Manual, Vol. 1. Reports DOE/MC/16481-1203. NTIS/DE82020196 (1982).

P24 Development of a Radio Frequency Surface Contour Mapping System

CONTRACT INFORMATION

Contract Number W-7405-Eng-82 (Ames)
93MC30134.000 (METC)

Contractor Ames Laboratory
Iowa State University
Ames, IA 50011
(515) 294-3758

Contractor Project Manager William H. Buttermore

Principal Investigators Robert J. Weber
Warren E. Straszheim

METC Project Manager Margaret A. Kotzalas

Period of Performance January 1, 1993 to continuing

Schedule and Milestones

FY94 Program Schedule

	O	N	D	J	F	M	A	M	J	J	A	S
Design of a proof-of-concept RF-SCMS	———	———	———	———	———	———						
Fabrication of a proof-of-concept RF-SCMS and laboratory testing.							———	———	———			
Design of a phased array RF-SCMS system										———	———	———

OBJECTIVES

A radio-frequency based system is being developed for imaging the top surface of the contents of vessels used in coal processes including lockhoppers, gasifiers, and mixing chambers. The system will be designed to image a minimum of 25 pixels with a depth resolution

of ±1 inch over ranges of 4 to 30 feet. The system must tolerate harsh environments as found in coal gasifiers with temperatures up to 1800 F and pressures up to 600 psig). The system will provide both a visual readout of the contour of the upper surface of a vessel's contents via a computer monitor and a data interface to the process control system.

BACKGROUND INFORMATION

The capability to continuously monitor the contents of a vessel is important to many aspects of coal utilization. Vessels of concern include gasifiers, storage silos, lockhoppers, etc. Surface monitoring and mapping can be important since interruptions in the designed flow of materials can severely disrupt or shut down coal processes.

METC developed an acoustic-based surface contour monitoring system which used an array of transmitters and receivers to monitor multiple locations within a vessel. However, acoustic-based systems can be affected by the extreme conditions within many of these vessels, while RF-based systems are more immune to such interference.

PROJECT DESCRIPTION

Design of a radio frequency surface contour mapping system is building upon a similar surface contour mapping device developed by Morgantown Energy Technology Center (METC) which used acoustic signals. The first stages of work include assessment of the conceptual design for the radio frequency-based surface contour mapping system (RF-SCMS) developed at METC and development of a design for an RF-SCMS system. This will be followed by fabrication and laboratory testing of a proof-of-concept system utilizing mechanical scanning of a single-channel RF system. Following testing of the proof-of-concept system, a design will be developed for a multiple channel, phased array system. Following initial tests of that system in the laboratory, the system will be hardened as necessary to withstand harsh environments and then subjected to field tests under actual process conditions.

RESULTS

Work to date has focused on review of the METC design and engineering analysis of the radar-based system. Extensive simulations have been performed to determine the lateral and depth resolution of the system. Initial results indicate that a 4.3 GHz system using a 9-antenna array should be able to achieve a depth resolution of 1 inch and a beam size of 25 inches at 20 feet which could be used to image about 10 pixels within a 6-foot vessel. Work is also proceeding on development of delay-and-sum algorithms for steering the beam about the vessel.

Figures 1 and 2 below show the actual and reconstructed surface for one test arrangement. In this case, a 9-element antenna array was positioned 10 m (32.8 ft)above the floor of a vessel 2 m (6.6 ft) in diamter. The test surface was at a height of 3.0 m (9.8 ft) with a ridge of 3.5 m (11.5 ft) across the center of the vessel. The reconstructed surface clearly shows the ridge across the center of the vessel. Additional tests are in progress to determine the best possible resolution for a given number of antennas in the array.

A demonstration system built around a 4.3 GHz radar transmitter/receiver is being assembled for the proof-of-concept system, and laboratory facilities have been prepared. All equipment, including a data acquistion system, have been acquired and are being installed.

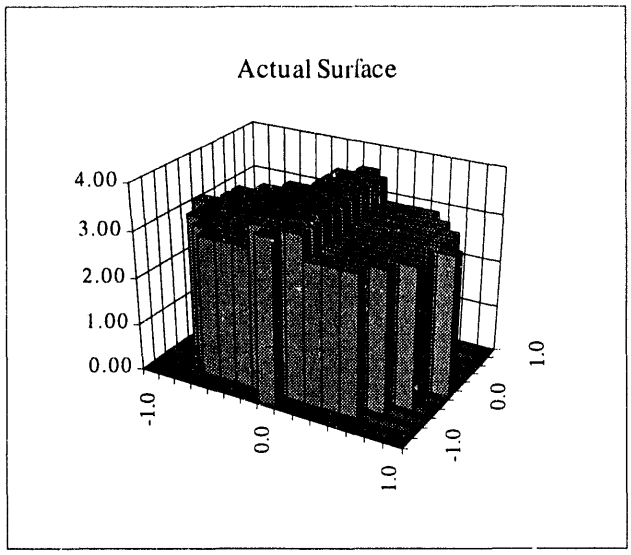

Figure 1. Original Test Surface

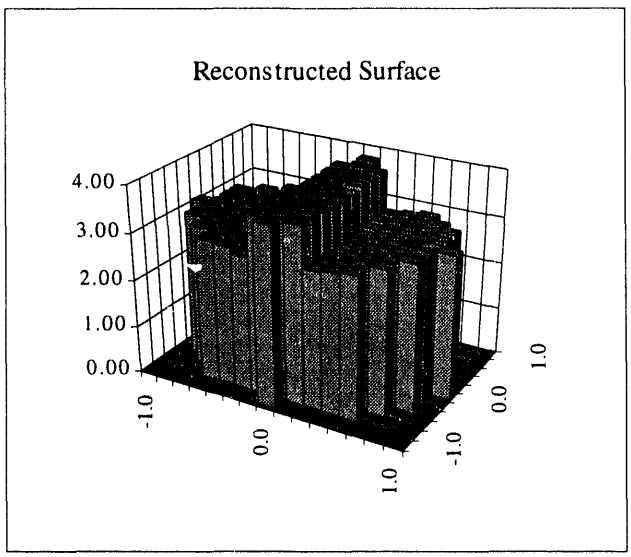

Figure 2. Surface Reconstructed from Calculated Data

Tests of the system will verify the computer simulations and data processing algorithms, and aid in the design of the actual SCMS which will utilize multiple antennas. Issues to be addressed include the size and placement of the antenna array and the operating frequency of the system. A higher frequency system operating at 35 GHz would provide improved resolution and will likely be adopted for the final design.

FUTURE WORK

In future work, the full SCMS will be constructed using multiple antennas and using electronic switching. The system will be hardened for testing on actual, operating structures and will be modified as needed to achieve the necessary performance.

DATE
FILMED
11/9/94

END